frontiers | Research Topics

Balancing alloantigen-induced immune responses and anti-tumor immunity in transplantation

Edited by
Rita Maccario, Luigi Nespoli and Marcello Maestri

Published in
Frontiers in Immunology

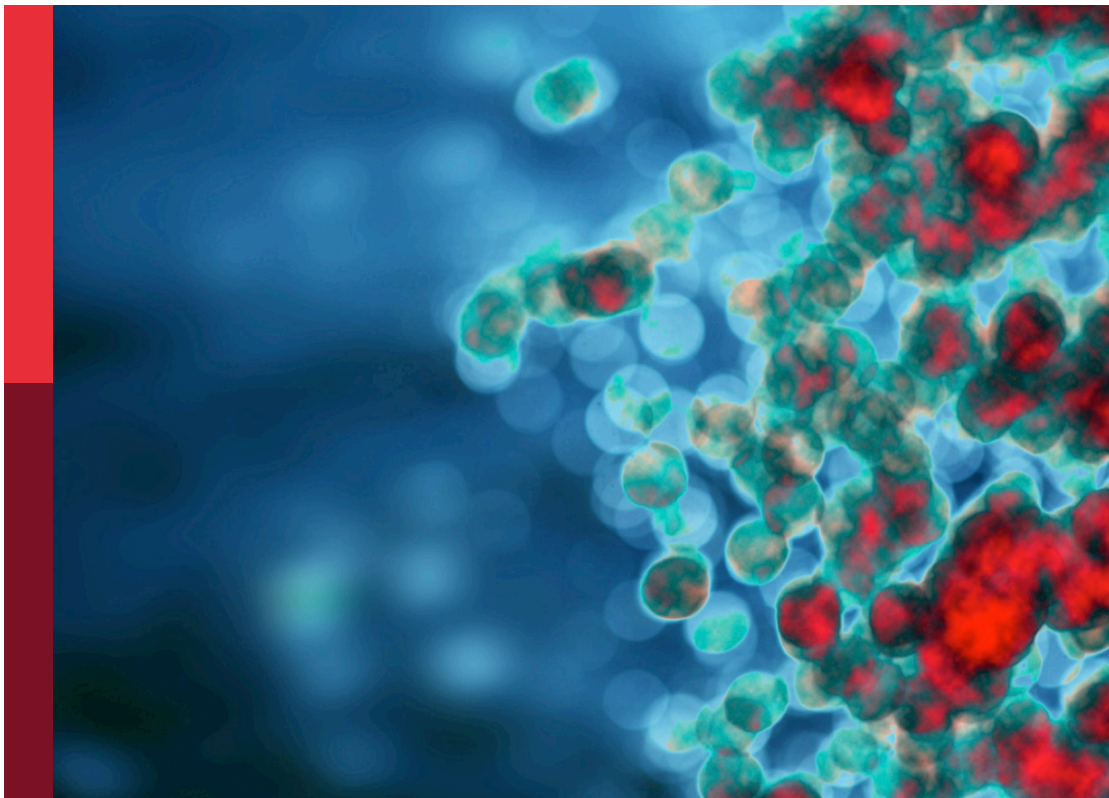

ISSN 1664-8714
ISBN 978-2-8325-6695-4
DOI 10.3389/978-2-8325-6695-4

Generative AI statement
Any alternative text (Alt text) provided alongside figures in the articles in this ebook has been generated by Frontiers with the support of artificial intelligence and reasonable efforts have been made to ensure accuracy, including review by the authors wherever possible. If you identify any issues, please contact us.

About Frontiers

Frontiers is more than just an open access publisher of scholarly articles: it is a pioneering approach to the world of academia, radically improving the way scholarly research is managed. The grand vision of Frontiers is a world where all people have an equal opportunity to seek, share and generate knowledge. Frontiers provides immediate and permanent online open access to all its publications, but this alone is not enough to realize our grand goals.

Frontiers journal series

The Frontiers journal series is a multi-tier and interdisciplinary set of open-access, online journals, promising a paradigm shift from the current review, selection and dissemination processes in academic publishing. All Frontiers journals are driven by researchers for researchers; therefore, they constitute a service to the scholarly community. At the same time, the *Frontiers journal series* operates on a revolutionary invention, the tiered publishing system, initially addressing specific communities of scholars, and gradually climbing up to broader public understanding, thus serving the interests of the lay society, too.

Dedication to quality

Each Frontiers article is a landmark of the highest quality, thanks to genuinely collaborative interactions between authors and review editors, who include some of the world's best academicians. Research must be certified by peers before entering a stream of knowledge that may eventually reach the public - and shape society; therefore, Frontiers only applies the most rigorous and unbiased reviews. Frontiers revolutionizes research publishing by freely delivering the most outstanding research, evaluated with no bias from both the academic and social point of view. By applying the most advanced information technologies, Frontiers is catapulting scholarly publishing into a new generation.

What are Frontiers Research Topics?

Frontiers Research Topics are very popular trademarks of the *Frontiers journals series*: they are collections of at least ten articles, all centered on a particular subject. With their unique mix of varied contributions from Original Research to Review Articles, Frontiers Research Topics unify the most influential researchers, the latest key findings and historical advances in a hot research area.

Find out more on how to host your own Frontiers Research Topic or contribute to one as an author by contacting the Frontiers editorial office: frontiersin.org/about/contact

Balancing alloantigen-induced immune responses and anti-tumor immunity in transplantation

Topic editors

Rita Maccario — San Matteo Hospital Foundation (IRCCS), Italy

Luigi Nespoli — University of Insubria, Italy

Marcello Maestri — San Matteo Hospital Foundation (IRCCS), Italy

Citation

Maccario, R., Nespoli, L., Maestri, M., eds. (2025). *Balancing alloantigen-induced immune responses and anti-tumor immunity in transplantation*.

Lausanne: Frontiers Media SA. doi: 10.3389/978-2-8325-6695-4

Table of contents

frontiers | Frontiers in Immunology

TYPE Editorial
PUBLISHED 28 July 2025
DOI 10.3389/fimmu.2025.1663706

OPEN ACCESS

EDITED AND REVIEWED BY
Antoine Toubert,
Université Paris Cité, France

*CORRESPONDENCE
Marcello Maestri
marcello.maestri@unipv.it

RECEIVED 10 July 2025
ACCEPTED 15 July 2025
PUBLISHED 28 July 2025

CITATION
Maccario R, Maestri M and Nespoli L (2025) Editorial: Balancing alloantigen-induced immune responses and anti-tumor immunity in transplantation.
Front. Immunol. 16:1663706.
doi: 10.3389/fimmu.2025.1663706

Editorial: Balancing alloantigen-induced immune responses and anti-tumor immunity in transplantation

Rita Maccario[1], Marcello Maestri[2*] and Luigi Nespoli[3]

[1]Cell Factory, Pediatric Hematology/Oncology Lab, Fondazione IRCCS Policlinico San Matteo, Pavia, Italy, [2]Department of Clinical-Surgical, Diagnostic and Pediatric Sciences, Universita di Pavia, Pavia, Italy, [3]Department of Pediatric Science, Universita degli Studi dell'Insubria, Varese, Italy

KEYWORDS

alloimmunity, transplantation, immune tolerance, immunosuppression, cell-based therapies, opportunistic infections

Editorial on the Research Topic
Balancing alloantigen-induced immune responses and anti-tumor immunity in transplantation

Introduction

Transplantation medicine has transformed from an experimental procedure with limited success to a life-saving intervention performed hundreds of thousands of times annually worldwide. Despite remarkable advances in unraveling the immune cascades and molecular interactions involved in solid organ and hematopoietic stem cells transplantation (HCT), alloimmune reactions remain the primary barrier to optimal long-term transplant outcomes.

Extensive research has established the pivotal role of T-cell-mediated and antibody-mediated adaptive immunity in alloimmune reactions. More recently, the critical role of innate immunity in early alloreactive response induction and maintenance of chronic organ rejection and chronic graft-versus-host disease (GVHD) has gained recognition (1, 2). The complexity of alloimmune reactions continues to challenge the transplant community. While acute solid organ rejection rates have declined significantly over the past three decades, improvements in long-term graft survival have plateaued. This disconnect underscores our incomplete understanding of the chronic alloimmune processes that ultimately lead to graft failure.

The allorecognition landscape metaphor proposed by Rinkevich bridges natural and clinical transplantation by conceptualizing self/non-self-recognition as dynamic continuum of evolving states that shift throughout a patient's lifespan. Rinkevich's innovative perspective suggests that immunity evolved not as a pathogen-driven mechanism but as a system to preserve individuality by preventing invasion from conspecific cells. This revolutionary concept provides valuable insight, advocating for reevaluation of fundamental immune tolerance principles derived from natural allorecognition mechanisms observed in marine invertebrates and humans, such as tolerogenic fetal-maternal immune interactions during successful fetal implantation.

These biological insights could inspire novel therapeutic strategies for achieving sustained graft acceptance.

Strategies to induce donor-recipient tolerance

Achieving long-lasting donor-recipient tolerance requires complex interventions before, during, and after transplantation. Primary considerations include identifying optimal donor-recipient matches regarding major and minor histocompatibility antigens, developing predictive biomarkers for post-transplant graft rejection or GVHD onset, and determining optimal immunosuppressive therapy to prevent or mitigate graft rejection or GVHD while preserving adequate anti-pathogen and anti-tumor immune surveillance.

Haider et al. addressed a critical need in transplantation immunology by achieving high-resolution HLA genotyping with enhanced accuracy and efficiency. This advancement is highly relevant for improving donor-recipient matching and reducing alloimmune complications.

Pasi et al. explored the underexamined role of recipient-specific anti-HLA antibodies (RSA) in HCT, investigating RSA-mediated damage mechanisms and their potential involvement in endothelial damage contributing to GVHD. Particular attention was directed toward RSA targeting non-inherited maternal or paternal antigens in haploidentical HCT (3).

Tao et al. provided detailed exploration of TIM proteins and miRNA in transplantation immunity, specifically focusing on liver, kidney, and heart transplantation. Their work examined immune response regulation by TIM proteins and highlighted miRNA influence on transplantation outcomes, including the miRNA-TIM network with potential for improving transplantation results.

Luo et al. identified two distinct MICA polymorphism types that differentially regulate NKG2D receptor activation on NK lymphocytes. Given NK alloreactivity's role in transplantation, these findings suggest that genetic variation in MICA may contribute to understanding individual differences in post-transplant alloreactive immune activation.

Naciri Bennani et al. explored innovative approaches to overcoming alloimmune barriers such as ABO incompatibility, reporting favorable outcomes in ABO-incompatible kidney transplant recipients, including those with exceptionally high baseline antibody titers. These successful outcomes required aggressive immunosuppression, indicating both feasibility and inherent challenges in extending transplant eligibility.

Opportunistic infections in transplantation

Achieving favorable long-term outcomes in HCT or solid organ transplantation depends critically on balancing effective prevention of severe GVHD and allograft rejection with risks of compromised anti-pathogen and anti-tumor immune surveillance. Powerful immunosuppressive drugs that substantially reduce rejection and GVHD incidence increase transplant recipient susceptibility to life-threatening opportunistic infections.

Addressing heightened infection risk from intensive immunosuppression, Zhong et al. evaluated prophylactic CMV hyperimmune globulin (CMV-Ig) effectiveness, demonstrating significant reductions in human CMV (HCMV) viremia and improved renal function preservation in ABO-incompatible transplant recipients. Their findings advocate incorporating passive immune prophylaxis in high-risk management protocols.

Cuesta-Martín de la Cámara et al. highlighted Epstein-Barr virus (EBV)-specific polyfunctional CD8 T lymphocyte profiles as predictive biomarkers for infection control following pediatric liver transplantation. Similarly, Zavaglio et al. linked robust HCMV-specific T cell responses to spontaneous HCMV clearance in kidney transplant recipients.

Mele et al. described proof-of-concept for a novel whole-blood interferon-γ release assay for detecting and evaluating HCMV-specific CD4 T lymphocytes to improve HCMV infection management in immunocompromised patients—a major concern in transplantation medicine.

Additional work by Cuesta-Martín de la Cámara et al. aimed to identify immunological biomarkers as risk factors for opportunistic infection in pediatric liver transplantation. While significant predictive immunological markers could not be identified for early post-transplant infections, late-onset infections appeared connected with T-cell lymphopenia and hypogammaglobulinemia.

These studies collectively underscore the potential of threatening opportunistic infections (4, 5).

Antibodies and cell-based advanced therapies

Anti-thymocyte globulin (ATG) is widely utilized in HCT for GVHD prophylaxis, available primarily as ATG-Fresenius (ATG-F) and ATG-Thymoglobulin (ATG-T). Determining optimal formulation and dosing remains challenging due to the need to balance effective GVHD prevention with associated infection risks. Falicovich et al. compared low-dose ATG-F to standard-dose ATG-T in unrelated HCT recipients, finding comparable GVHD incidence, overall survival, and non-relapse mortality. However, ATG-T recipients experienced significantly higher EBV reactivation rates, highlighting formulation-specific risks.

Mesenchymal stromal cells (MSCs) represent a promising therapeutic strategy due to their immunomodulatory capabilities (6). Liang et al. investigated human liver-derived MSCs (L-MSCs) in murine renal ischemia models, demonstrating their superiority in reducing inflammation and enhancing macrophage polarization toward anti-inflammatory and reparative phenotypes compared to bone marrow (BM-MSCs) and adipose MSC (A-MSCs). These findings highlight the importance of MSC source selection for maximizing therapeutic efficacy.

Clinical validation was provided by Hendriks et al., who conducted a phase Ib trial of allogeneic BM-MSC infusion in kidney transplant recipients. They reported MSC therapy safety

and identified minor immune cell changes post-infusion. Notably, MSC infusions induced distinct, transient B and T cell phenotypes ($CD11b^+CD11c^+Ki\text{-}67^+$), suggesting acute immune modulation. While the clinical relevance of these transient cells requires further investigation, their emergence underscores the rapid immunological influence of MSC treatments.

Wang et al. reviewed emerging biotechnological approaches, introducing the potential of allogeneic CAR virus-specific T cells (CAR-VST) designed to target both malignancy and infection without inducing GVHD.

Li et al. described a compelling strategy applied to a leukemia patient who relapsed after umbilical cord blood transplantation (UCBT) and was subsequently treated with CD19 CAR-T cells derived from the patient himself. The patient with refractory disease at CAR-T infusion is still in remission more than six years post-therapy.

Montagna et al. focused on establishing a Phase I/II clinical trial evaluating safety and preliminary efficacy of cell-based advanced therapy. Their proposed trial results from extensive preclinical studies investigating donor-derived cytotoxic T lymphocytes to prevent leukemia relapse in pediatric patients undergoing haploidentical HCT, a highly relevant and innovative concept addressing clear clinical needs.

Conclusion

This Research Topic captures the dynamic state of alloimmunity research, from fundamental mechanistic studies to innovative clinical applications. The contributions highlight how technological advances, including single-cell analytics, spatial biology, and computational modeling, provide unprecedented insights into alloimmune complexity. These developments promise to advance our understanding and treatment of transplant-related complications while improving long-term patient outcomes.

Author contributions

RM: Conceptualization, Supervision, Validation, Writing – original draft, Writing – review & editing. MM: Conceptualization, Data curation, Methodology, Supervision, Writing – original draft, Writing – review & editing. LN: Conceptualization, Data curation, Methodology, Supervision, Validation, Writing – original draft, Writing – review & editing.

Conflict of interest

The authors declare that the research was conducted in the absence of any commercial or financial relationships that could be construed as a potential conflict of interest.

Generative AI statement

The author(s) declare that no Generative AI was used in the creation of this manuscript.

Publisher's note

References

1. Velardi A, Ruggeri L, Moretta A, Moretta L. NK cells: a lesson from mismatched hematopoietic transplantation. *Trends Immunol.* (2002) 23:438–44. doi: 10.1016/s1471-4906(02)02284-6

2. Locatelli F, Pende D, Falco M, Della Chiesa M, Moretta A, Moretta L. NK cells mediate a crucial graft-versus-leukemia effect in haploidentical-HSCT to cure high-risk acute leukemia. *Trends Immunol.* (2018) 39:577–90. doi: 10.1016/j.it.2018.04.009

3. Van Rood JJ, Loberiza FR Jr, Zhang MJ, Oudshoorn M, Claas F, Cairo MS, et al. Effect of tolerance to noninherited maternal antigens on the occurrence of graft-versus-host disease after bone marrow transplantation from a parent or an HLA-haploidentical sibling. *Blood.* (2002) 99:1572–7. doi: 10.1182/blood.v99.5.1572

4. Fishman JA. Infection in solid-organ transplant recipients. *N Engl J Med.* (2007) 357:2601–14. doi: 10.1056/NEJMra064928

5. Baldanti F, Lilleri D, Gerna G. Monitoring human cytomegalovirus infection in transplant recipients. *J Clin Virol.* (2008) 41:237–41. doi: 10.1016/j.jcv.2007.12.001

6. Le Blanc K, Frassoni F, Ball L, Locatelli F, Roelofs H, Lewis I, et al. Mesenchymal stem cells for treatment of steroid-resistant, severe, acute graft-versus-host disease: a phase II study. *Lancet.* (2008) 371:1579–86. doi: 10.1016/S0140-6736(08)60690-X

frontiers | Frontiers in Immunology

TYPE Original Research
PUBLISHED 22 July 2024
DOI 10.3389/fimmu.2024.1448092

OPEN ACCESS

EDITED BY
Rita Maccario,
San Matteo Hospital Foundation (IRCCS), Italy

REVIEWED BY
Marcello Maestri,
University of Pavia, Italy
Maria Ester Bernardo,
San Raffaele Hospital (IRCCS), Italy

*CORRESPONDENCE
Timucin Taner
Taner.timucin@mayo.edu

†These authors have contributed equally to this work and share first authorship

RECEIVED 12 June 2024
ACCEPTED 04 July 2024
PUBLISHED 22 July 2024

CITATION
Liang Y, Ozdogan E, Hansen MJ, Tang H, Saadiq I, Jordan KL, Krier JD, Gandhi DB, Grande JP, Lerman LO and Taner T (2024) Human liver derived mesenchymal stromal cells ameliorate murine ischemia-induced inflammation through macrophage polarization. *Front. Immunol.* 15:1448092. doi: 10.3389/fimmu.2024.1448092

Human liver derived mesenchymal stromal cells ameliorate murine ischemia-induced inflammation through macrophage polarization

Yun Liang[1†], Elif Ozdogan[2†], Michael J. Hansen[3], Hui Tang[4], Ishran Saadiq[4], Kyra L. Jordan[4], James D. Krier[4], Deep B. Gandhi[4], Joseph P. Grande[5], Lilach O. Lerman[4] and Timucin Taner[1,3*]

[1]Department of Surgery, Mayo Clinic, Rochester, MN, United States, [2]Boston Children's Hospital, Harvard Medical School, Boston, MA, United States, [3]Department of Immunology, Mayo Clinic, Rochester, MN, United States, [4]Division of Nephrology and Hypertension, Mayo Clinic, Rochester, MN, United States, [5]Department of Laboratory Medicine and Pathology, Mayo Clinic, Rochester, MN, United States

Introduction: The immunomodulatory properties of mesenchymal stromal cells (MSC) have been well-characterized in *in-vitro* and *in-vivo* models. We have previously shown that liver MSC (L-MSC) are superior inhibitors of T-cell activation/proliferation, NK cell cytolytic function, and macrophage activation compared to adipose (A-MSC) and bone marrow MSC (BM-MSC) *in-vitro*.

Method: To test these observations *in-vivo*, we infused these types of MSC into mice with unilateral renal artery stenosis (RAS), an established model of kidney inflammation. Unilateral RAS was induced via laparotomy in 11-week-old, male 129-S1 mice under general anesthesia. Control mice had sham operations. Human L-MSC, AMSC, and BM-MSC (5x105 cells each) or PBS vehicle were injected intra-arterially 2 weeks after surgery. Kidney morphology was studied 2 weeks after infusion using micro-MRI imaging. Renal inflammation, apoptosis, fibrosis, and MSC retention were studied *ex-vivo* utilizing western blot, immunofluorescence, and immunohistological analyses.

Results: The stenotic kidney volume was smaller in all RAS mice, confirming significant injury, and was improved by infusion of all MSC types. All MSC-infused groups had lower levels of plasma renin and proteinuria compared to untreated RAS. Serum creatinine improved in micetreated with BM- and L-MSC. All types of MSC located to and were retained within the stenotic kidneys, but L-MSC retention was significantly higher than A- and BM-MSC. While all groups of MSC-treated mice displayed reduced overall inflammation and macrophage counts, L-MSC showed superior potency *in-vivo* at localizing to the site of inflammation and inducing M2 (reparative) macrophage polarization to reduce inflammatory changes.

Discussion: These *in-vivo* findings extend our *in-vitro* studies and suggest that L-MSC possess unique anti-inflammatory properties that may play a role in liver-induced tolerance and lend further support to their use as therapeutic agents for diseases with underlying inflammatory pathophysiology.

KEYWORDS

mesenchymal stromal cells, immunomodulation, renal artery stenosis, liver tolerance, inflammation

Introduction

Mesenchymal stromal cells (MSC) have been widely studied for their potential as therapeutic agents to treat a multitude of inflammatory pathologies due to their immunomodulatory capabilities. MSC have been derived from several types of tissues, but those isolated from adipose tissue and bone marrow are most often used in clinical trials. Guided by the liver's unique tolerogenic microenvironment and immunomodulatory properties, we postulate that liver-derived MSC (L-MSC) may have superior therapeutic potential. In fact, *in-vitro* studies that directly compared MSC isolated from healthy adult liver (L-MSC) to either those from adipose (A-MSC) or bone marrow (BM-MSC) demonstrate that L-MSC are superior at inhibiting the proliferation of alloreactive T cells, IFNy production by T cells (1), and the cytotoxic abilities of NK cells (2). Additionally, transcriptomic and proteomic analyses of A-, BM-, and L-MSC show significantly higher level of expression of several key immunomodulatory molecules in L-MSC (1).

Collectively, the *in-vitro* studies suggest that L-MSC possess a distinct genomic profile that may enhance their immunomodulatory capabilities compared to A- or BM-MSC. The goal of this study is to characterize the function of L-MSC *in-vivo* and evaluate if their superior immunomodulatory capabilities seen *in-vitro* translate into better function *in-vivo*. We examined the therapeutic and immunomodulatory function of L-MSC in the context of ischemic injury using the validated unilateral renal artery stenosis (RAS) mouse model and directly compared their effect to that of A- and BM-MSC. We hypothesized that L-MSC would be non-inferior in their ability to improve overall renal function in the stenotic kidney with greater influence on immunological changes compared to A- or BM-MSC.

Materials and methods

Cell culture

The collection of MSC from healthy adults are approved by Mayo Clinic Institutional Review Board (IRB #17-007379 (liver), IRB #11-009182 (adipose tissue) and IRB # 10-002572 (bone marrow). All tissues are collected as part of scheduled donation procedures and informed consent are obtained prior to collecting tissue samples for this study. MSC are isolated and passaged from human adipose, bone marrow, and liver tissue as previously described (1–3). Specifically, adipose tissue is obtained from the subcutaneous compartment during the abdominal incision for a living donor nephrectomy procedure. Bone marrow aspiration from the iliac crest is performed by specialized hematology team under general anesthesia as part of living donor nephrectomy procedure. A liver biopsy sample, measuring 1cm x 1cm, is obtained from donor organs (deceased or living donor) for isolation of MSC. After obtaining tissue samples, the source tissue is enzymatically digested, and the plastic-adherent cells from the resulting cell suspension are placed into MSC culture media and are allowed to proliferate for 2 weeks before first passage. The cell lines used to date represent both sexes (50% female), racial heterogeneity (>10% non-Caucasians), and a wide range of ages from 20 to 75. Their phenotype and trilineage differentiation capacity were confirmed with flow cytometry and MSC functional identification assay (R&D Systems, Minneapolis, MN, USA), respectively. Prior to administration into mice, MSC ($5x10^5$ cells in 200ul PBS) in Passage 3 were fluorescently labeled with CellTrace™ Far Red (CTFR, ThermoFisher Scientific, Waltham, MA, USA) to allow for detection after infusion.

Renal artery stenosis model

All protocols were approved by Mayo Clinic IRB and Institutional Animal Care and Use. As previously described (4), 11-week-old, male 129-S1 mice (Jackson laboratory, Bar Harbor, ME, USA) underwent open laparotomy under general anesthesia. After exposure of the right renal artery, a 0.15mm diameter arterial cuff was placed on the artery and secured with sutures to achieve partial occlusion of blood flow to the right kidney (i.e., stenotic kidney, STK). Two weeks following RAS surgery, fluorescently tagged MSC ($5x10^5$ cells in 200ul of PBS) derived from human adipose (A-MSC), bone marrow (BM-MSC), or liver (L-MSC) tissues, were given to RAS mice intra-arterially through direct cannulation of the carotid artery via vascular cut down. Mice that underwent surgery without cuff placement (n=4) served as negative controls (i.e. sham group). Mice that underwent RAS surgery but received an infusion of PBS (n=4) served as positive controls (i.e. untreated RAS group). Tail cuff blood pressures (Kent Scientific, Torrington, CT, USA) were also obtained at baseline, two weeks following RAS surgery, and two weeks following MSC

infusion. General anesthesia was achieved using 3% isoflurane inhalation for induction and 1.5% during RAS surgery and intra-arterial MSC injection. Mice were euthanized after MRI imaging. Briefly, mice underwent general anesthesia with isoflurane as stated above. A midline abdominal incision (approximately 1-2cm in length) was made to access the peritoneal cavity. Peritoneal organs were then reflected superiorly to expose the inferior vena cava in order to obtain blood samples. After exsanguination, the STKs were collected for tissue processing.

Imaging protocol

Two weeks after MSC or PBS injection, mice were scanned using MRI as previously described (5). Previously established imaging protocols were used to acquire the appropriate images to quantify the volume, perfusion, and oxygenation of the STKs (5, 6). All image analyses were performed using Analyze software (version 12.0; Biomedical Imaging Resource, Mayo Clinic, MN, USA) and Matlab (The MathWorks, Natick, MA, USA).

Serum and urinary biomarker measurements

Post MRI imaging, blood from the inferior vena cava and urine were collected at the time of euthanasia. Whole blood was centrifuged, and the resulting plasma was collected. Plasma renin concentration was measured by the Renin Assay Kit (Cat#MAK157, Millipore Sigma, St. Louis, MO, USA). Serum creatinine was measured using the Serum Creatinine Detection Kits (Cat# KB02-H, Arbor Assays, Ann Arbor, MI, USA). Urinary protein levels were measured using the Pierce™ Bradford Protein Assay kit (Cat#23200, ThermoFisher, Waltham, MA, USA). All kits were used per manufacturer's instructions.

Immunohistochemistry

Following imaging, mice were euthanized as described above, and the STKs were collected and divided into equal parts for both frozen and paraffin-embedded sectioning. Paraffin-embedded STK sections were stained with CD45 (overall inflammation, 1:200 dilution, Cat#ab10558, Abcam, Waltham, MA, USA); CD14 (overall macrophage, 1:200 dilution, Cat#ab182032, Abcam); F4/80 (1:100 dilution, Cat#ab6640, Abcam) and iNOS (M1, inflammatory macrophage: 1:100 dilution, Cat#sc-7271, Santa Cruz Biotechnology, Dallas, TX, USA); F4/80 and mannose receptor-1 (M2, reparative macrophage, 1:100 dilution, Cat#HPA004114, Sigma Aldrich, St. Louis, MO, USA); trichrome (fibrosis, Cat#NC9485545, ThermoFisher); TUNEL (apoptosis, Cat#G3250, Promega, Madison, WI, USA); and PAS (renal cortical tubular atrophy, Cat#395B-1KT, Sigma Aldrich). Frozen STK sections were stained with DHE (reactive oxygen species, Cat#D11347, ThermoFisher). All non-diluted antibodies were used per manufacturer instructions. Six images of each stain were captured with Zeiss® microscope for immunofluorescence stains and Nikon® microscope for immunohistochemistry stains. M1 (double positive for F4/80 and iNOS$^+$), M2 (double positive for F4/80 and mannose receptor-1$^+$), TUNEL$^+$, and MSC retention were quantified by manual counts per high power field. Cortical tubular atrophy was scored by adapting the Banff criteria by an independent pathologist who was blinded to the treatment groups using PAS-stained slides (7). All other stains were quantified based on the percentage of positive stain area using ImageJ (8).

RT-PCR

Frozen STK samples were homogenized in 350ul of ice-cold lysis buffer, supplied by mirVana PARIS total RNA isolation kit (Cat# AM1556, ThermoFisher Scientific). Total RNAs were then isolated from homogenized samples according to the kit protocol. Total RNA concentrations were measured by a NanoDrop Spectrophotometer (NanoDrop). First-strand cDNA was produced from 800ng of total RNA using SuperScript VILO cDNA Synthesis kit (Cat#11755-050, ThermoFisher Scientific). Relative quantitative PCR were performed using Taqman assays, containing 4ul of cDNA products. All primers were purchased from ThermoFisher Scientific with the following catalog numbers: CD45 (Mm01293577); IFNy (Mm01168134); TNFa (Mm00443258); and GAPDH (Mm99999915). PCR analysis was done on Applied Biosystems Quantstudio 7 using the following conditions: 50°C for 2 minutes, 95°C for 10 minutes and 40 cycles of 95°C for 15 seconds and 60°C for 1 minute. Fold changes of gene expressions were calculated using 2-ΔΔCT method.

Western blot

Frozen STK samples were homogenized, and protein expression was expressed by western blotting. Protein concentrations were measured using a BCA Protein Assay Kit (Cat# 23225, ThermoFisher Scientific) per manufacturer's instructions. The membranes were blocked with 5% BSA, incubated with primary antibodies, washed, and incubated with secondary antibodies at room temperature. Finally, the membranes were washed and incubated with ECL Western Blot Substrate (Cell Signaling Technology, Inc., Danvers, MA, USA) and were visualized on ImageQuant™ LAS4000. Anti-IFNy (Cat# BS-0480R, Bioss, Woburn, MA, USA) and anti-TNFa (Cat# ab6671, Abcam, Waltham, MA, USA) antibodies were used as primary antibodies. GAPDH antibody was used to normalize the results.

Statistical analysis

All statistical analyses were performed using GraphPad Prism version 10.2.2 (324) for Windows (GraphPad Software, Boston, Massachusetts USA, www.graphpad.com). All data are expressed as either mean ± SD for normally distributed data or median [IQR] for non-normally distributed data. Hypothesis testing was carried out using one-way ANOVA followed by a student t-test for normally distributed data. Data not following normal distribution were analyzed using Kruskal-Wallis followed by Wilcoxon test. All data were considered significant if $p<0.05$.

Results

Blood pressure

Initially, eight mice were randomly assigned to receive infusion of each type of MSC. At the conclusion of the study, two mice in the A-MSC group were lost due to total infarction of the STK, one mouse in the BM-MSC was lost due to hydronephrosis of the STK secondary to ureteral stricture, and one mouse in the L-MSC died just prior to MRI imaging, resulting in a final count of A-MSC (n=6), BM-MSC (n=7), and L-MSC (n=7) for analyses. Blood pressure using tail cuffs were obtained at baseline, post-RAS surgery, and post-MSC or PBS infusion. As expected, mean systolic (SBP) and diastolic blood pressure (DBP) measurements were higher than baseline after RAS surgery (Figure 1A). Injection of MSC did not show reduction of overall SBP or DBP nor in the amount of absolute or percent change in SBP or DBP from RAS surgery to post-MSC injection (data not shown).

Serum and urine biomarkers

RAS induced proteinuria (1795 ± 199ug/ml vs 938 ± 297ug/ml in sham, p= 0.002) and tended to elevate serum creatinine (0.27 ± 0.05mg/dL vs 0.16 ± 0.02mg/dL in sham, p= 0.062) compared to sham (Figure 1B). Compared to RAS, proteinuria (A-MSC: 717 ± 350ug/ml, p<0.001; BM-MSC: 986 ± 374ug/ml, p= 0.002; L-MSC: 1292 ± 624ug/ml, p= 0.047) and plasma renin (A-MSC: 205.5 ± 22.2ng/ml, p= 0.002; BM-MSC: 169.6 ± 24.7ng/ml, p< 0.001; L-MSC: 149.8 ± 47.2ng/ml, p< 0.001; RAS: 256.3 ± 21.0ng/ml) decreased with MSC treatment for all types. Mice treated with either BM-MSC or L-MSC also resulted in decreased mean serum creatinine (BM-MSC: 0.14 ± 0.09mg/dL, p= 0.024; L-MSC: 0.12 ± 0.14mg/dL, p= 0.009; all vs RAS). Compared to A-MSC, L-MSC treated mice had lower plasma renin levels (149.8 ± 47.2ng/ml vs A-MSC, p= 0.002) but higher proteinuria (1292 ± 624ug/ml vs A-MSC, p= 0.018). No differences were noted among the three MSC groups for serum creatinine (Figure 1B).

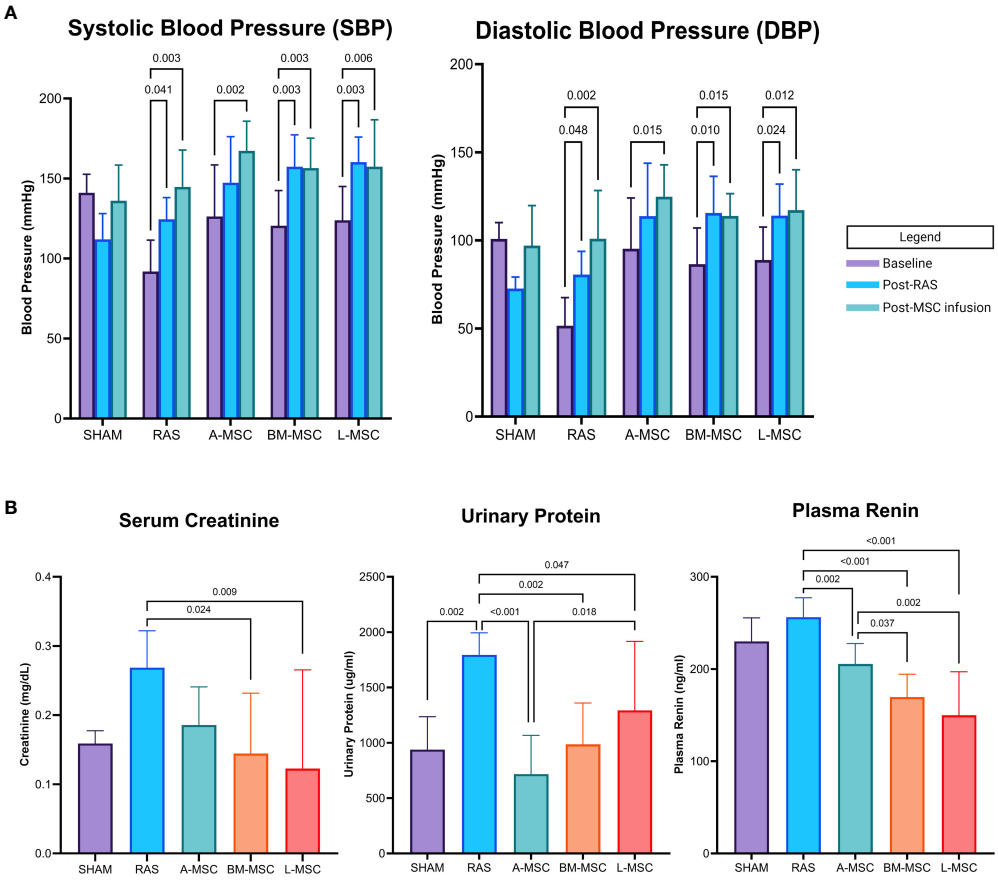

FIGURE 1
Blood pressure (mean ± SD) measured by tail cuff within each group at baseline, after RAS surgery, and after PBS or MSC infusion are shown in **(A)**. Serum creatinine, urinary protein, and plasma renin levels for each group are shown in **(B)**. All levels are expressed as mean ± SD. RAS, renal artery stenosis.

10.3389/fimmu.2024.1448092

Renal volume, perfusion, and oxygenation

Non-invasive evaluation of the volume, perfusion, and oxygenation of the STKs were performed using micro-MRI analysis. Compared to the sham group, untreated RAS mice had significant loss of volume in the STKs (94.18 ± 50.6mm^3 vs 266 ± 24.7mm^3 in sham, p< 0.001), suggestive of ischemic injury (Figures 2A, B). With MSC treatment, the volumes of the STKs significantly improved compared to the untreated RAS mice (A-MSC: 188.8 ± 17.6mm^3; BM-MSC: 226.1 ± 37.9mm^3; L-MSC: 181.9 ± 62mm^3; all vs RAS, p<0.001). No significant differences were noted in the volume of the STKs among the MSC treatment groups (Figure 2B). Cortical and medullary perfusion and oxygenation were also measured using micro-MRI. In this

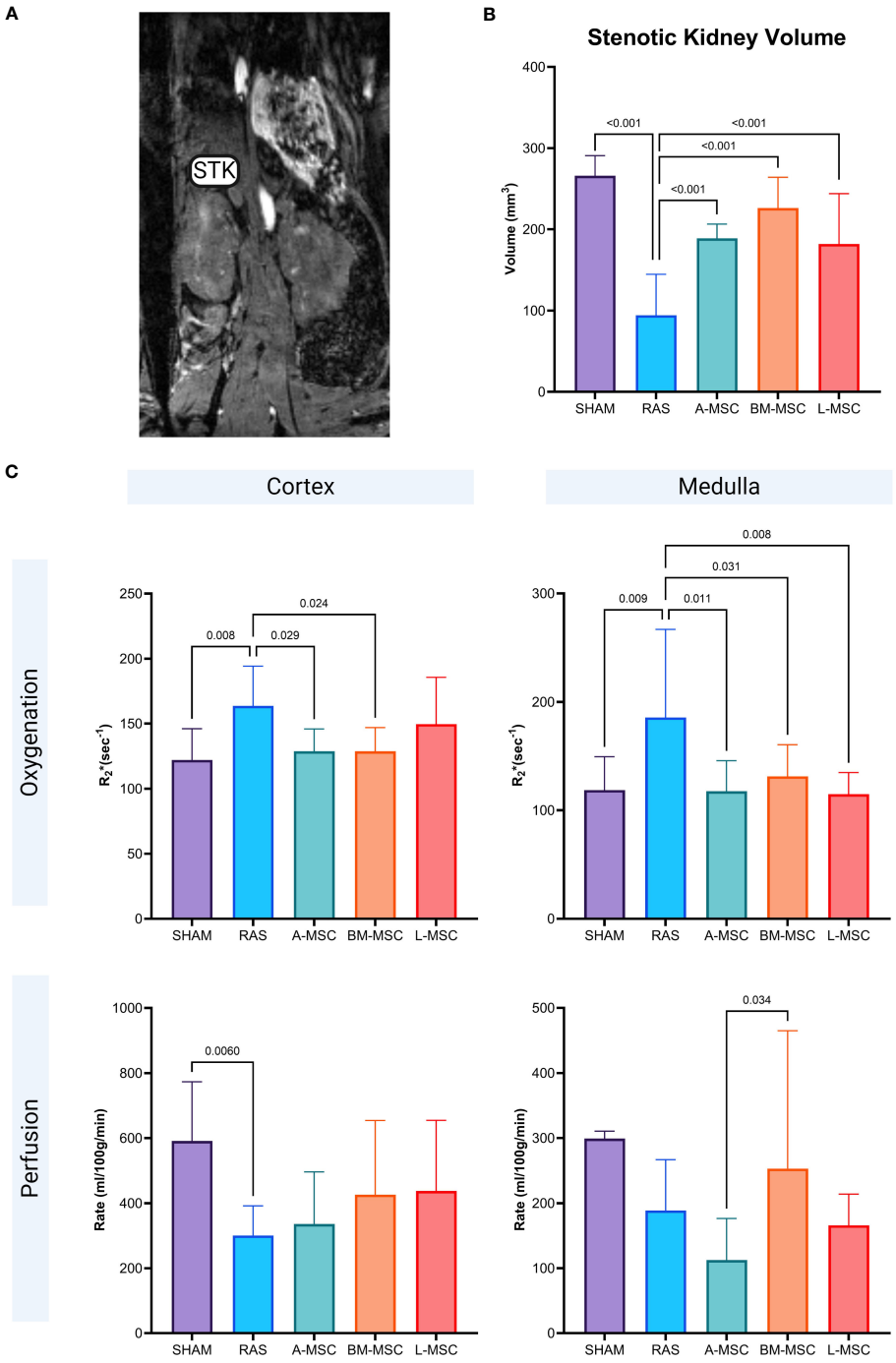

FIGURE 2
Representative MRI image of STK in coronal section **(A)**. Non-invasive measurement of volume in the STKs **(B)** and the oxygenation and perfusion to the cortex and medulla in the STKs **(C)** within each group. All measurements are expressed as mean ± SD. For oxygenation, R_2*(sec-1) reflects hypoxia with lower R_2* indicating better oxygenation. STK, stenotic kidney.

method, R_2*(sec^{-1}) reflects hypoxia, thus lower R_2* indicated better oxygenation. The untreated RAS group had decreased oxygenation to both the cortex (163.8 ± 30.5 sec^{-1} vs 122.1 ± 24.1sec^{-1} in sham, p= 0.008) and the medulla (186 ± 81.3 sec^{-1} vs 119 ± 30.8 sec^{-1} in sham, p= 0.009) and decreased mean perfusion to the cortex (301 ± 91.2ml/100g/min vs 591 ± 182ml/100g/min in sham, p= 0.006) when compared to the sham group. Mice treated with MSC had higher oxygenation to the medullary region compared to the RAS group (A-MSC: 118 ± 28.2 sec^{-1}, p= 0.011; BM-MSC: 131 ± 29.3 sec^{-1}, p= 0.031; L-MSC: 115 ± 20 sec^{-1}, p=0.008; all vs RAS), while those treated with A-MSC (128.8 ± 17.1 sec^{-1} vs 163.8 ± 30.5 sec^{-1} in RAS, p= 0.029) or BM-MSC (128.7 ± 18.2 sec^{-1} vs RAS, p= 0.024) had improved oxygenation in the cortex. No significant improvement was observed in perfusion to the cortex and medulla with MSC treatment (Figure 2C), but medullary perfusion in BM-MSC group was higher than in A-MSC group.

Inflammatory profiles

Untreated RAS mice had significantly higher gene expression of CD45 (27.8 ± 25.5 vs 1.02 ± 0.2 in sham, p< 0.001), IFNy (10.8 ± 10.3 vs 1.03 ± 0.27 in sham, p= 0.002), and TNFa (35.9 ± 34.4 vs 1 ± 0.2 in sham, p= 0.001). Treatment with MSC of all types resulted in decreased gene expression of CD45 (A-MSC: 0.55 ± 0.23; BM-MSC: 0.49 ± 0.26; L-MSC: 1.26 ± 1.12; all vs RAS, p< 0.001); IFNy (A-MSC: 0.67 ± 0.74; BM-MSC: 0.31 ± 0.21; L-MSC: 0.35 ± 0.28; all vs RAS, p≤ 0.001); and TNFa (A-MSC: 0.39 ± 0.17; BM-MSC: 0.30 ± 0.12; L-MSC: 0.63 ± 0.61; all vs RAS, p≤ 0.001) when compared to the untreated RAS group (Figure 3A). On western blot, the protein expression of IFNy was higher for A-MSC (0.8 ± 0.03 vs RAS, p< 0.001) and BM-MSC treated mice (0.76 ± 0.07 vs RAS, p= 0.002) compared to untreated RAS mice (0.52 ± 0.06). On the other hand, mice treated with L-MSC (0.43 ± 0.1) had lower protein expression of IFNy compared to A-MSC (p< 0.001) and BM-MSC (p< 0.001) and similar level of expression to the untreated RAS group. No significant differences were observed for TNFa protein expression among untreated and MSC-treated RAS mice (Figure 3B), but they were no longer lower than sham.

MSC were tagged with a fluorescent protein (CTFR, in pink) prior to administration to allow for evaluation of their retention in the STK on unstained frozen sections. Among the three types, L-MSC (8 [6.4] cells) had the highest retention in the STK compared to A-MSC (5 [2.7] cells vs L-MSC, p= 0.011) or BM-MSC (4 [1.3] cells vs L-MSC, p< 0.001) (Figures 4A, B). Untreated RAS mice displayed the highest level of overall inflammation (CD45 positivity: 7.4 ± 4.6% vs 0.9 ± 0.5% in sham, p< 0.001) and total macrophage expression (CD14 positivity: 18.4 [21.5] % vs 0.2 [1] % in sham, p<

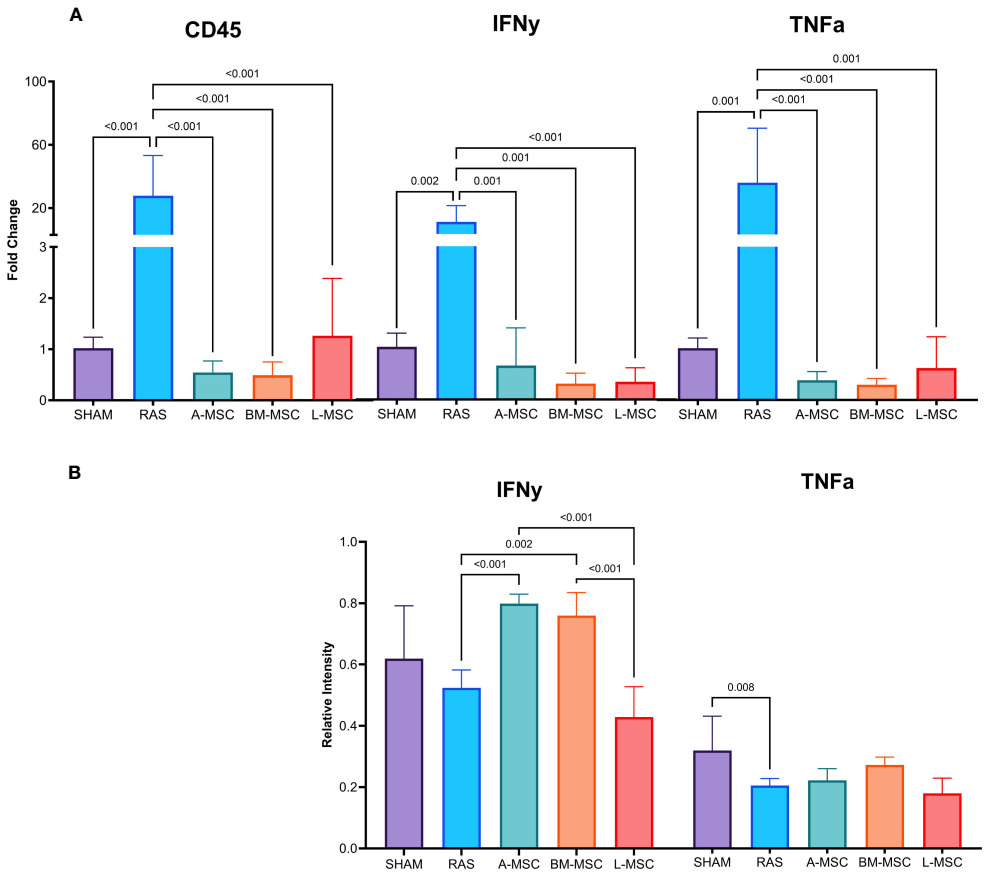

FIGURE 3
Levels of gene expression for overall inflammation (CD45), IFNy, and TNFa were measured using real-time PCR **(A)**. Protein expression of IFNy and TNFa were measured using western blot **(B)**. All measurements are expressed as mean ± SD. IFNy, interferon gamma; TNFa, tumor necrosis factor alpha.

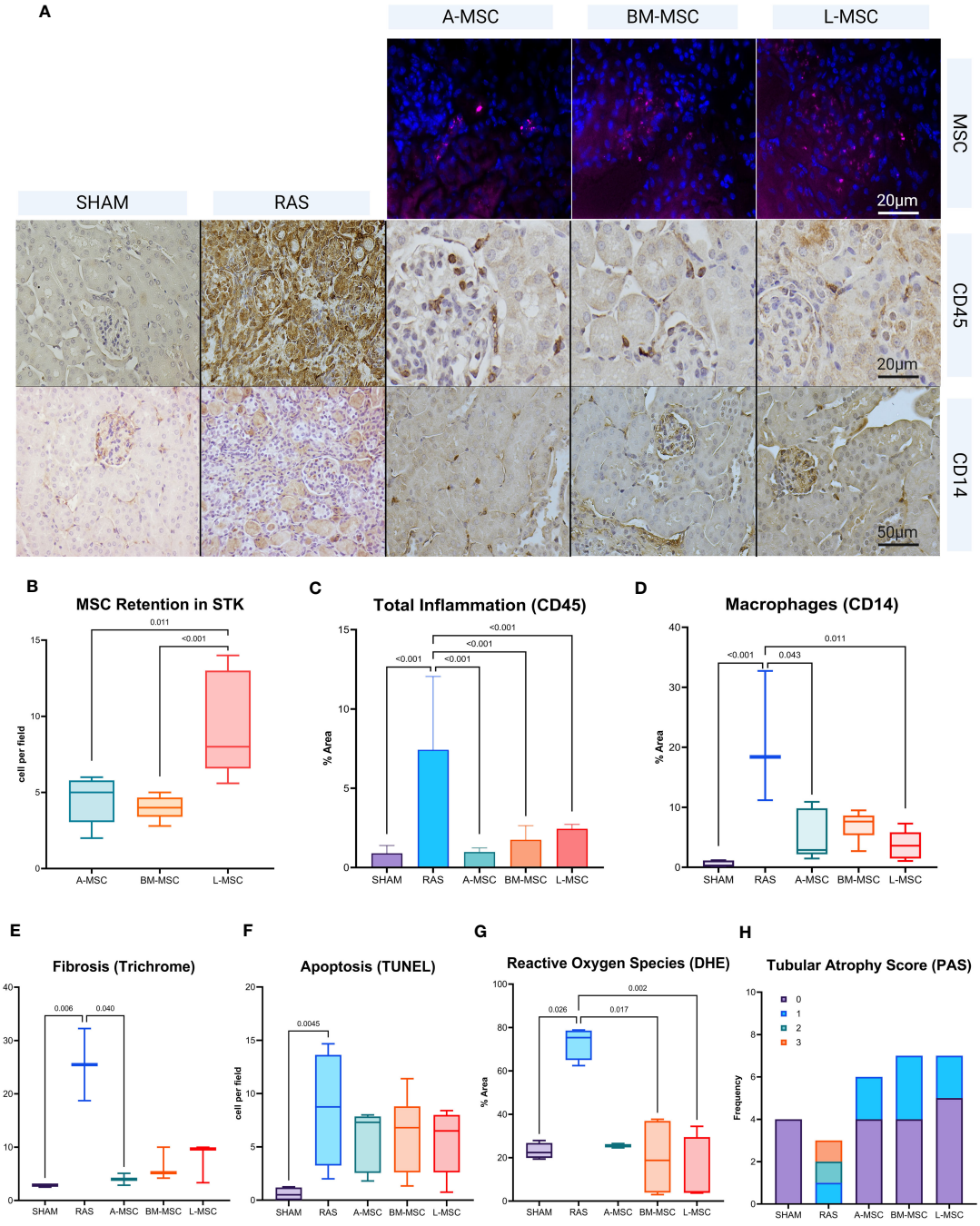

FIGURE 4
Representative histological images of MSC retention, CD45 stain, and CD14 stain. MSCs are labeled in pink. Positive staining for either CD45 or CD14 are in brown **(A)**. Manual counts (median ± IQR) of retained MSCs and TUNEL+ cells per high power field (40x) and percent area of positive stain for CD45 (mean ± SD), CD14 (median ± IQR), Trichrome (median ± IQR), DHE (median ± IQR), and PAS (counts in each score) in the STKs within each group are shown in **(B–H)**. MSC, mesenchymal stromal cells; TUNEL, Terminal deoxynucleotidyl transferase dUTP nick end labeling; DHE, Dihydroethidium; PAS, Periodic acid-Schiff.

0.001) on histology compared to the sham group (Figures 4A, C, D). Infusion of all MSC types led to reduction in overall inflammation (A-MSC: 1 ± 0.3%; BM-MSC: 1.8 ± 0.9%; L-MSC: 2.4 ± 0.3%; all vs RAS, p< 0.001). For overall macrophage expression, A-MSC (2.9 [7.7] % vs RAS, p= 0.044) and L-MSC (3.6 [4.4] % vs RAS, p= 0.011) treated mice resulted in lower expression compared to untreated RAS mice (Figures 4A, C, D).

Focusing specifically on M1 (inflammatory) and M2 (reparative) macrophage types, RAS led to significant increase in the frequency of M1 macrophages (6.4 [4.6] cells vs 0.1 [0.35] cells in sham, p= 0.002) in STKs (Figures 5A, C). L-MSC-treated mice had decreased frequency of M1 (3 [2.4] cells vs 6.4 [4.6] cells in RAS, p= 0.045) and markedly increased M2 macrophages (3.8 [4.4] cells vs 1.2 [1.3] cells in RAS, p= 0.048) in the STKs compared to untreated RAS mice

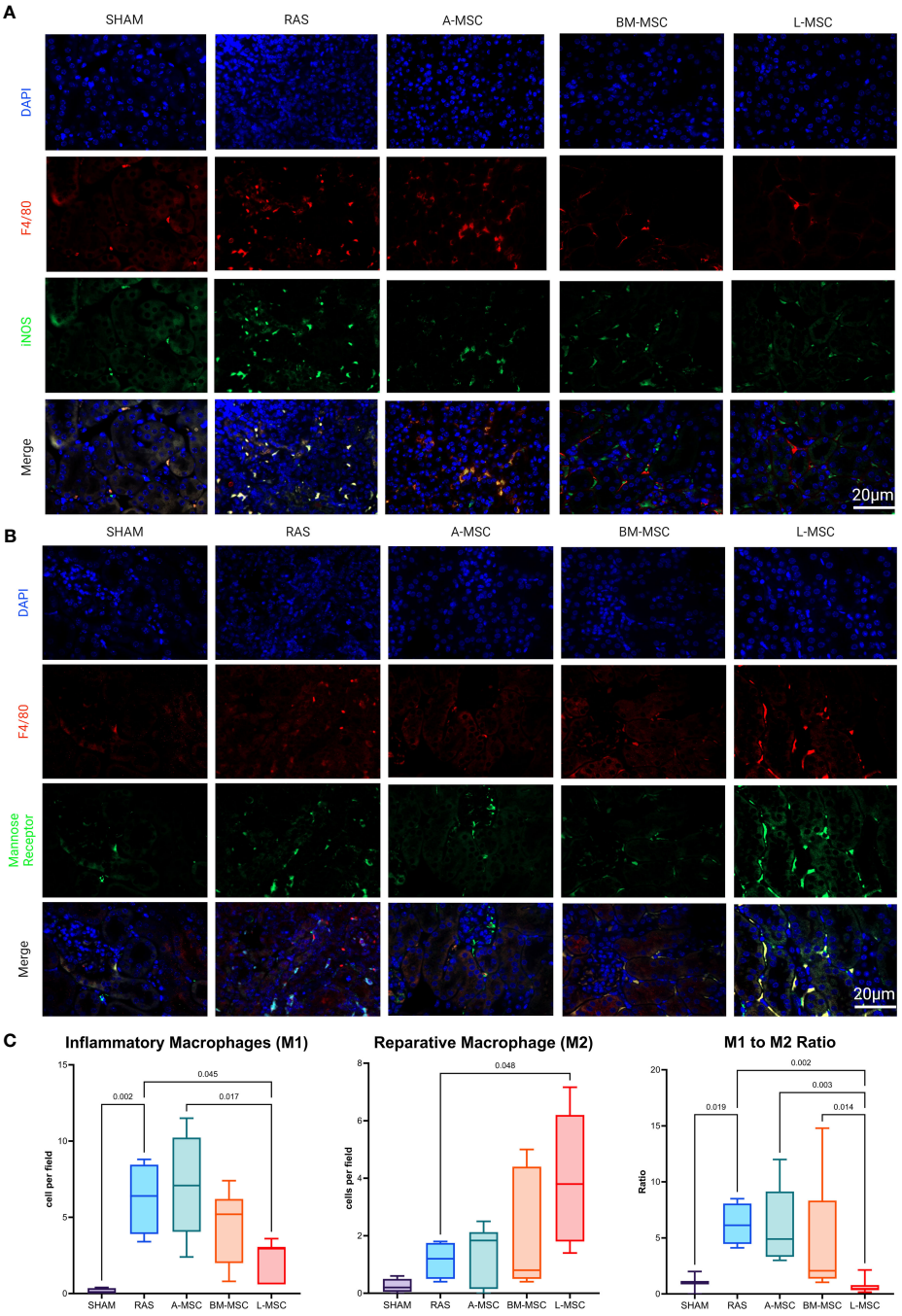

FIGURE 5
Representative images of inflammatory macrophages, M1 in **(A)** and reparative macrophages, M2 in **(B)** the STKs within each group. Manual counts of M1 and M2 per high power field (40x) and their ratio within the STKs are shown in **(C)** as median ± IQR. RAS, renal artery stenosis; A-MSC, Adipose mesenchymal stromal cells; BM-MSC, Bone Marrow mesenchymal stromal cells; L-MSC, Liver mesenchymal stromal cells.

(Figures 5A–C). Treatment with A-MSC or BM-MSC did not achieve significant reduction in M1 or elevation in M2 macrophages (Figure 5C). Looking at the ratio of M1 to M2 presence in the STKs, L-MSC-treated (ratio: 0.45 [0.46]) mice resulted in the lowest polarization toward the inflammatory M1 macrophage subtype compared to either untreated RAS (ratio: 6.13 [3.6] vs L-MSC, p= 0.002) or A-MSC (ratio: 4.9 [5.8] vs L-MSC, p= 0.003) and BM-MSC (ratio: 2.1 [7] vs L-MSC, p=0.014) treated mice (Figure 5C).

For non-immune related changes, significant reduction in fibrosis was noted for A-MSC (4 [2.3]% vs 25.5 [13.5]% RAS, p= 0.04) treated mice. Oxidative stress was also reduced for BM-MSC (18.8 [33.1]% vs RAS, p= 0.017) and L-MSC (4.3 [25.7]% vs RAS, p= 0.002) treated mice compared to untreated RAS group (75.3 [13.6]%). No significant differences were noted in apoptosis or tubular atrophy scores between untreated RAS and MSC treated groups (Figures 4E–H).

Discussion

In this study, we aimed to characterize the effect of the novel L-MSC *in-vivo* and to directly compare their impact on ischemic injury to the more established A- and BM-MSC. We demonstrated that L-MSC are equally as effective as A-MSC and BM-MSC at improving renal function, the volume, and oxygenation of the renal medulla in the STKs. Additionally, L-MSC-treated RAS mice achieved a similar reduction in inflammation in the STKs as those treated with A- and BM-MSC. However, significantly more L-MSC were retained in the STKs, and L-MSC-treated mice had greater polarization of macrophages toward a more reparative (M2) phenotype compared to A- and BM-MSC treated groups.

MSC have been extensively investigated as therapeutic agents for inflammatory conditions, classically in graft versus host disease and inflammatory bowel disease, but also in ischemic renal injury (9–12). Although the clinical efficacy of MSC treatments has been variable, data from experimental and human clinical trials support MSCs' immunomodulatory potential through intricate communications with both the innate and adaptive immune system via several proposed routes, including paracrine secretions, direct cell-to-cell contact, and release of exosomes. The downstream effect is the resolution of inflammation and the promotion of tissue regeneration through several mediatory pathways such as induction of M2 macrophage polarization (12, 13).

The source tissue of MSC and the microenvironment in which they are found impact MSC functions and properties. The liver is often considered to be an immunologically privileged organ that serves as a critical immune interface (14). Several clinical studies involving simultaneous liver and kidney transplant or simultaneous liver and heart transplant demonstrate that compared to solitary kidney or heart transplants, the presence of concomitant liver allograft was protective against both T cell and antibody-mediated rejection and overall improved graft survival (15–18). On a cellular level, simultaneous liver and kidney transplant recipients demonstrated lower frequency of circulating $CD8^+$, activated $CD4^+$, and effector memory T cells and had decreased alloreactivity to donor cells compared to solitary kidney transplant recipients (16). Likewise, secretome analysis of simultaneous liver and kidney transplant recipients showed downregulation of inflammatory pathways and upregulation of tissue integrity pathways (17). Taken together, the superior immunomodulatory properties of the MSC isolated from liver may be closely associated with the immune context surrounding the organ.

Our findings in this study underscore previous studies that demonstrated improvement in renal function, oxidative stress, and inflammation after MSC treatment (4, 19, 20) as well as the impact of MSC on macrophage polarization (12). However, the current study augments the previous bodies of literature in several ways. We directly determined and compared the positive impact of MSC isolated from liver tissue, which has not been explored in detail to our best knowledge as a therapeutic agent, to that of more established MSC isolated from adipose and bone marrow tissues. Additionally, we demonstrated that a significantly higher number of L-MSC homed to site of injury than A-MSC and BM-MSC and exhibited greater impact on macrophage phenotypes. Interestingly, for more structural related changes, only A-MSC treated group achieved reduction in fibrosis while BM- and L-MSC treated groups showed significant reduction in levels of reactive oxygen species. While MSCs generally share many similar characteristics, previous studies have demonstrated significant differences among A-, BM, and L-MSCs that may explain some of the differing effects we observed in this study. For example, *in-vitro* studies have shown that L-MSC have a more homogenous migration kinetics toward chemoattractants than A-MSC, while the latter have superior anti-fibrotic and pro-angiogenic properties (21–24). Macrophage polarization plays a major role in liver disease (25). M1 macrophages promote tissue injury in vast majority of the liver diseases (viral, alcohol-related and metabolic-associated), whereas M2 macrophages attenuate liver injury and inflammation (26). At steady state, the liver microenvironment favors M2 polarization (27) for homeostasis. Interestingly, here, we demonstrate that adoptive transfer of human L-MSC in a mouse model of inflammation also promotes M2 polarization. Thus, it is possible that L-MSC have a role in liver homeostasis, which will need to be investigated further in the future.

Our study is not without limitations. The MSC treated groups did not result in improvement in blood pressures and perfusion or decrease in apoptosis compared to untreated RAS group. Given our small sample size, it is possible that our study may not have been adequately powered to evaluate all these physiological and histological changes. We also found that despite L-MSC-treated RAS mice having lower plasma renin, the urinary protein level was higher compared to the A-MSC group. This might be due to differential impact of MSC types on cells in the juxtaglomerular apparatus. Additionally, we noted discordance between IFNy gene expression and protein expression for A- and BM-MSC treated mice. The elevated IFNy protein expression in the A- and BM-MSC groups, but not in L-MSC group, could be related to post-transcriptional regulation. Indeed, previous transcriptomic analysis comparing A-, BM-, and L-MSC demonstrated significant upregulation of INFy regulatory genes in L-MSC (1, 2), further supporting that L-MSC likely exert greater influence on the immune system than A- or BM-MSC. Additionally, while some of the superior effects on macrophages might have resulted from the engraftment of a larger number of L-MSC compared to A- and BM-MSC, such differences were not consistently observed in other parameters. Therefore, cell number may not have been the sole determinant of L-MSCs' effects. In our study, mice were also given a single infusion of MSC. Multiple infusions may be needed in order for MSC to exert maximal effect on the ischemic injury to the kidney (28). Additionally, more time than the allocated two weeks in this study may have been needed to see a more pronounced impact of reduced inflammation on renal function in the MSC-treated groups.

In summary, our study established the effect of L-MSC *in-vivo* on ischemic injury and directly compared their impact to that of A-MSC and BM-MSC. We showed that L-MSC are as effective as the commonly studied A- and BM-MSC at mitigating ischemic renal injuries. Furthermore, they are superior at homing to site of injury and at inducing polarization toward reparative macrophages when compared to A- and BM-MSC. Based on these findings, we are currently exploring the effect of local delivery of MSC on

alloimmune mediated damages through direct infusion into the allograft renal artery in our ongoing clinical trials with adult renal transplant recipients (NCT05456243). As part of the clinical trial, we are collaborating with the Mayo Clinic Center for Regenerative Biotherapeutics Laboratory (IRB 17-007379) to routinely generate and culture MSC cell lines from adipose, bone marrow, and liver tissue (1cm x 1cm biopsy sample) from healthy adult donors in a GMP facility and testing for MSC phenotypic markers and tri-lineage differentiation to meet the release criteria for clinical use. More work will need to be done to detail the mechanism(s) through which L-MSC interact with the immune system to effectuate their impact on the surrounding environment.

Data availability statement

The raw data supporting the conclusions of this article will be made available by the authors, without undue reservation.

Ethics statement

The studies involving humans were approved by Mayo Clinic Institutional Review Board. The studies were conducted in accordance with the local legislation and institutional requirements. The human samples used in this study were acquired from primarily isolated as part of your previous study for which ethical approval was obtained. Written informed consent for participation was not required from the participants or the participants' legal guardians/next of kin in accordance with the national legislation and institutional requirements. The animal study was approved by Institutional Animal Care and Use. The study was conducted in accordance with the local legislation and institutional requirements.

Author contributions

YL: Conceptualization, Data curation, Formal analysis, Investigation, Methodology, Writing – original draft, Writing – review & editing. EO: Conceptualization, Data curation, Formal analysis, Investigation, Methodology, Writing – review & editing. MH: Data curation, Formal analysis, Investigation, Writing – review & editing. HT: Data curation, Formal analysis, Investigation, Writing – review & editing. IS: Data curation, Formal analysis, Investigation, Writing – review & editing. KJ: Data curation, Formal analysis, Investigation, Writing – review & editing. JK: Data curation, Formal analysis, Investigation, Writing – review & editing. DG: Data curation, Formal analysis, Investigation, Writing – review & editing. JG: Data curation, Formal analysis, Investigation, Writing – review & editing. LL: Conceptualization, Formal analysis, Investigation, Methodology, Writing – review & editing. TT: Conceptualization, Data curation, Formal analysis, Investigation, Methodology, Writing – review & editing.

Funding

The author(s) declare financial support was received for the research, authorship, and/or publication of this article. This project was partly supported by National Institute of Health grants HL158691 and DK120292.

Conflict of interest

The authors declare that the research was conducted in the absence of any commercial or financial relationships that could be construed as a potential conflict of interest.

The author(s) declared that they were an editorial board member of Frontiers, at the time of submission. This had no impact on the peer review process and the final decision.

Publisher's note

References

1. Taner T, Abrol N, Park WD, Hansen MJ, Gustafson MP, Lerman LO, et al. Phenotypic, transcriptional, and functional analysis of liver mesenchymal stromal cells and their immunomodulatory properties. *Liver Transpl.* (2020) 26:549–63. doi: 10.1002/lt.25718

2. Yigitbilek F, Ozdogan E, Abrol N, Park WD, Hansen MJ, Dasari S, et al. Liver mesenchymal stem cells are superior inhibitors of NK cell functions through differences in their secretome compared to other mesenchymal stem cells. *Front Immunol.* (2022) 13:952262. doi: 10.3389/fimmu.2022.952262

3. Ramakrishnan A, Torok-Storb B, Pillai MM. Primary marrow-derived stromal cells: isolation and manipulation. *Methods Mol Biol.* (2013) 1035:75–101. doi: 10.1007/978-1-62703-508-8_8

4. Zou X, Jiang K, Puranik AS, Jordan KL, Tang H, Zhu X, et al. Targeting murine mesenchymal stem cells to kidney injury molecule-1 improves their therapeutic efficacy in chronic ischemic kidney injury. *Stem Cells Transl Med.* (2018) 7:394–403. doi: 10.1002/sctm.17-0186

5. Jiang K, Ferguson CM, Ebrahimi B, Tang H, Kline TL, Burningham TA, et al. Noninvasive assessment of renal fibrosis with magnetization transfer MR imaging: validation and evaluation in murine renal artery stenosis. *Radiology.* (2017) 283:77–86. doi: 10.1148/radiol.2016160566

6. Ebrahimi B, Crane JA, Knudsen BE, Macura SI, Grande JP, Lerman LO. Evolution of cardiac and renal impairment detected by high-field cardiovascular magnetic resonance in mice with renal artery stenosis. *J Cardiovasc Magn Reson.* (2013) 15:98. doi: 10.1186/1532-429X-15-98

7. Loupy A, Haas M, Roufosse C, Naesens M, Adam B, Afrouzian M, et al. The Banff 2019 Kidney Meeting Report (I): Updates on and clarification of criteria for T cell– and antibody-mediated rejection. *Am J Transplantation.* (2020) 20:2318–31. doi: 10.1111/ajt.15898

8. Schneider CA, Rasband WS, Eliceiri KW. NIH Image to ImageJ: 25 years of image analysis. *Nat Methods.* (2012) 9:671–5. doi: 10.1038/nmeth.2089

9. Alfarano C, Roubeix C, Chaaya R, Ceccaldi C, Calise D, Mias C, et al. Intraparenchymal injection of bone marrow mesenchymal stem cells reduces kidney fibrosis after ischemia-reperfusion in cyclosporine-immunosuppressed rats. *Cell Transplant*. (2012) 21:2009–19. doi: 10.3727/096368912X640448

10. Cheng K, Rai P, Plagov A, Lan X, Kumar D, Salhan D, et al. Transplantation of bone marrow-derived MSCs improves cisplatinum-induced renal injury through paracrine mechanisms. *Exp Mol Pathol*. (2013) 94:466–73. doi: 10.1016/j.yexmp.2013.03.002

11. Zhang X, Tao Y, Chopra M, Ahn M, Marcus KL, Choudhary N, et al. Differential reconstitution of T cell subsets following immunodepleting treatment with alemtuzumab (anti-CD52 monoclonal antibody) in patients with relapsing-remitting multiple sclerosis. *J Immunol*. (2013) 191:5867–74. doi: 10.4049/jimmunol.1301926

12. Planat-Benard V, Varin A, Casteilla L. MSCs and inflammatory cells crosstalk in regenerative medicine: concerted actions for optimized resolution driven by energy metabolism. *Front Immunol*. (2021) 12:626755. doi: 10.3389/fimmu.2021.626755

13. Cao W, Cao K, Cao J, Wang Y, Shi Y. Mesenchymal stem cells and adaptive immune responses. *Immunol Lett*. (2015) 168:147–53. doi: 10.1016/j.imlet.2015.06.003

14. Crispe IN, Giannandrea M, Klein I, John B, Sampson B, Wuensch S. Cellular and molecular mechanisms of liver tolerance. *Immunol Rev*. (2006) 213:101–18. doi: 10.1111/j.1600-065X.2006.00435.x

15. Taner T, Heimbach JK, Rosen CB, Nyberg SL, Park WD, Stegall MD. Decreased chronic cellular and antibody-mediated injury in the kidney following simultaneous liver-kidney transplantation. *Kidney Int*. (2016) 89:909–17. doi: 10.1016/j.kint.2015.10.016

16. Taner T, Gustafson MP, Hansen MJ, Park WD, Bornschlegl S, Dietz AB, et al. Donor-specific hypo-responsiveness occurs in simultaneous liver-kidney transplant recipients after the first year. *Kidney Int*. (2018) 93:1465–74. doi: 10.1016/j.kint.2018.01.022

17. Taner T, Park WD, Stegall MD. Unique molecular changes in kidney allografts after simultaneous liver-kidney compared with solitary kidney transplantation. *Kidney Int*. (2017) 91:1193–202. doi: 10.1016/j.kint.2016.12.016

18. Tracy KM, Matsuoka LK, Alexopoulos SP. Update on combined heart and liver transplantation: evolving patient selection, improving outcomes, and outstanding questions. *Curr Opin Organ Transplant*. (2023) 28:104–9. doi: 10.1097/MOT.0000000000001041

19. Kim SR, Jiang K, Chen X, Puranik AS, Zhu XY, Lerman A, et al. Selective kidney targeting increases the efficacy of mesenchymal stromal/stem cells for alleviation of murine stenotic-kidney senescence and damage. *J Tissue Eng Regener Med*. (2022) 16:550–8. doi: 10.1002/term.3299

20. Kim SR, Zou X, Tang H, Puranik AS, Abumoawad AM, Zhu XY, et al. Increased cellular senescence in the murine and human stenotic kidney: Effect of mesenchymal stem cells. *J Cell Physiol*. (2021) 236:1332–44. doi: 10.1002/jcp.29940

21. Yigitbilek F, Conley SM, Tang H, Saadiq IM, Jordan KL, Lerman LO, et al. Comparable *in vitro* function of human liver-derived and adipose tissue-derived mesenchymal stromal cells: implications for cell-based therapy. *Front Cell Dev Biol*. (2021) 9:641792. doi: 10.3389/fcell.2021.641792

22. Brennan MA, Renaud A, Guilloton F, Mebarki M, Trichet V, Sensebé L, et al. Inferior *in vivo* osteogenesis and superior angiogenesis of human adipose-derived stem cells compared with bone marrow-derived stem cells cultured in xeno-free conditions. *Stem Cells Transl Med*. (2017) 6:2160–72. doi: 10.1002/sctm.17-0133

23. Jervis M, Huaman O, Cahuascanco B, Bahamonde J, Cortez J, Arias JI, et al. Comparative analysis of *in vitro* proliferative, migratory and pro-angiogenic potentials of bovine fetal mesenchymal stem cells derived from bone marrow and adipose tissue. *Veterinary Res Commun*. (2019) 43:165–78. doi: 10.1007/s11259-019-09757-9

24. Yoshida M, Nakashima A, Ishiuchi N, Miyasako K, Morimoto K, Tanaka Y, et al. Comparison of the therapeutic effects of adipose- and bone marrow-derived mesenchymal stem cells on renal fibrosis. *Int J Mol Sci*. (2023) 24:16920. doi: 10.3390/ijms242316920

25. Wang C, Ma C, Gong L, Guo Y, Fu K, Zhang Y, et al. Macrophage polarization and its role in liver disease. *Front Immunol*. (2021) 12:803037. doi: 10.3389/fimmu.2021.803037

26. Stahl EC, Haschak MJ, Popovic B, Brown BN. Macrophages in the aging liver and age-related liver disease. *Front Immunol*. (2018) 9:2795. doi: 10.3389/fimmu.2018.02795

27. Wen Y, Lambrecht J, Ju C, Tacke F. Hepatic macrophages in liver homeostasis and diseases-diversity, plasticity and therapeutic opportunities. *Cell Mol Immunol*. (2021) 18:45–56. doi: 10.1038/s41423-020-00558-8

28. Oliveira-Sales EB, Maquigussa E, Semedo P, Pereira LG, Ferreira VM, Câmara NO, et al. Mesenchymal stem cells (MSC) prevented the progression of renovascular hypertension, improved renal function and architecture. *PloS One*. (2013) 8:e78464. doi: 10.1371/journal.pone.0078464

frontiers | Frontiers in Immunology

TYPE Brief Research Report
PUBLISHED 09 October 2024
DOI 10.3389/fimmu.2024.1455300

OPEN ACCESS

EDITED BY
Rita Maccario,
San Matteo Hospital Foundation (IRCCS), Italy

REVIEWED BY
Luigi Nespoli,
University of Insubria, Italy
Marcello Maestri,
University of Pavia, Italy

*CORRESPONDENCE
Cees van Kooten
c.van_kooten@lumc.nl

RECEIVED 26 June 2024
ACCEPTED 23 September 2024
PUBLISHED 09 October 2024

CITATION
Hendriks SH, Heidt S, Reinders MEJ, Koning F and van Kooten C (2024) Allogenic MSC infusion in kidney transplantation recipients promotes within 4 hours distinct B cell and T cell phenotypes.
Front. Immunol. 15:1455300.
doi: 10.3389/fimmu.2024.1455300

Allogenic MSC infusion in kidney transplantation recipients promotes within 4 hours distinct B cell and T cell phenotypes

Sanne H. Hendriks[1], Sebastiaan Heidt[1,2], Marlies E.J. Reinders[2,3], Frits Koning[1] and Cees van Kooten[3]*

[1]Department of Immunology, Leiden University Medical Center, Leiden University, Leiden, Netherlands, [2]Department of Internal Medicine, Nephrology and Transplantation, Erasmus MC Transplant Institute, Erasmus University Medical Center, Rotterdam, Netherlands, [3]Department of Internal Medicine (Nephrology) and Transplant Center, Leiden University Medical Center, Leiden University, Leiden, Netherlands

Background: Infusion of mesenchymal stromal cells (MSCs) has been proposed as immune-modulatory therapy in solid organ transplantation. The use of allogenic MSCs could improve standardization and allow for direct availability of the product.

Method: The nonrandomized phase Ib Neptune clinical trial provided safety and feasibility data on the use of allogenic bone-marrow-derived MSCs, infused in 10 patients at week 25 and 26 post kidney transplantation. Here, we performed detailed analysis on the peripheral blood immune cell composition of these patients up to 52 weeks post transplantation. We used a 40 marker antibody panel with mass cytometry to assess potential effects of MSC therapy on the immune system.

Results: We showed minor changes in major immune lineages at week 27, 34 and 52 post kidney transplantation after MSC infusion at week 25 and week 26, confirming previous data with regular flow cytometry. However, in a direct comparison between pre- and post MSC infusion, as soon as 4 hours after MSC infusion, we observed a significant increase in cell numbers of B cell and T cell subsets that shared a unique expression of CD11b, CD11c, CD38, CD39, and Ki-67.

Conclusion: Exploring these $CD11b^+CD11c^+CD38^+CD39^+Ki\text{-}67^+$ B cells and T cells in the context of MSC infusion after kidney transplantation may be a promising avenue to better understand the immunological effects of MSC therapy.

KEYWORDS

kidney transplantation, immunosuppression, mesenchymal stromal cells, immune regulation, mass cytometry, allogenic

Introduction

Kidney transplantation continues to be the treatment of choice for patients with end-stage kidney disease (1). Short-term kidney graft survival has improved due to, amongst others, the use of potent immunosuppressive agents. However, long-term graft survival has not followed this trend, partially due to long-term toxicity of these immunosuppressive drugs (2–4). For example, calcineurin inhibitors, the backbone of current immunosuppressive regimens, are nephrotoxic and may cause tubulointerstitial damage (5). Therefore, new strategies are being explored to reduce the use of immunosuppressive drugs without increasing the risk of allograft rejection.

The use of mesenchymal stromal cell (MSC) therapy could be such an approach. MSCs have been shown to exert anti-inflammatory, immune-regulatory and tissue repair properties (6, 7). Autologous MSCs have shown beneficial effects in clinical trials in the setting of solid organ transplantation (8–10). However, since *in vitro* expansion to obtain sufficient numbers of MSCs can take several weeks, autologous MSC are not readily available, which is often impractical in the clinical setting. Additionally, the per-patient nature of this process incurs considerable expenses. Alternatively, allogenic MSCs may be used for acute treatments and be beneficial due to standardized quality control and direct availability of the product. Yet, allogenic MSCs could potentially evoke a donor-specific alloimmune response, potentially harming the kidney allograft (11). In our recently published nonrandomized phase Ib Neptune clinical trial, allogenic bone-marrow-derived-MSCs were infused to assess safety and feasibility of administration of third-party MSCs after kidney transplantation (12). In view of safety, the MSCs were selected based on the absence of repeated Human Leukocyte Antigen (HLA) mismatches with the organ donor. The patients received MSCs at week 25 and 26 after transplantation in combination with alemtuzumab induction therapy at day 0 and day 1 and maintenance triple therapy consisting of prednisone, tacrolimus and everolimus. The study showed that the administration of allogenic MSCs was safe and feasible. Additionally, using a major immune lineage flow cytometry panel on freshly obtained blood samples, it was shown that, while monocytes, B cells, NK cells, and $CD8^+$ T cells remained stable after the two infusions, $CD4^+$ T cells increased upon the infusions. This could potentially be explained by lymphocyte repopulation after induction therapy (12).

Both direct and indirect interactions of MSCs with various immune cells have been described (6, 7, 13–15). However, indirect effects through the release of extracellular vesicles, membrane particles and by undergoing apoptosis are thought to be most relevant due to the short lifespan of MSCs *in vivo* (6, 7). Our recent work described cell death of MSC within 4 hours of infusion, as shown by the rapid and short-lived appearance of MSC-specific cell-free DNA in the circulation (16). MSC-derived vesicles, including exosomes, that occur during cell death may trigger monocytes and phagocytes to induce tolerogenic dendritic cells and regulatory T cells (Treg) (17, 18). The effects of the MSCs on the peripheral immune cells shortly after intravenous MSC infusion have not been elucidated yet.

Therefore, in the current study we applied mass cytometry to perform in-depth characterization of the peripheral blood immune composition of patients included in the Neptune trial. We exploited a metal-conjugated mass cytometry antibody panel containing 40 antibodies, previously used for a study with autologus MSC therapy (19), for the staining of bio-banked peripheral blood mononuclear cells (PBMCs). We report the influence of MSC therapy in kidney transplantation patients on major immune cell lineages up to 52 weeks after transplantation. Furthermore, we show the short-term effects 4 hours after each MSC infusion at week 25 and week 26 in an in-depth analysis of the immune cell subsets.

Abbreviations: APC, antigen presenting cell; B2M, β-2-microglobulin; HLA, human leukocyte antigen; LUMC, Leiden University Medical Center; MSC, mesenchymal stromal cell; PBMC, peripheral blood mononuclear cell; Treg, regulatory T cells.

Materials and methods

Study design

The Neptune clinical trial was a nonrandomized, prospective, single-center, phase Ib study in living-donor kidney transplant recipients in which allogenic bone marrow derived MSCs were infused 25 weeks and 26 weeks after transplantation (day 0) in 10 patients (Figure 1) (12). All patients received alemtuzumab induction therapy at day 0 and day 1 and maintenance triple therapy consisting of prednisone, tacrolimus (Advagraf), and everolimus (Certican). The study was performed at Leiden University Medical Center (LUMC), the Netherlands. The trial design and trial protocol have been previously described and were approved by the local ethics committee at the LUMC, Leiden, and by the Central Committee on Research involving Human Subjects in the Netherlands (12, 20). The trial was performed in accordance with the principles of the Declaration of Helsinki. Inclusion and exclusion criteria were described in the trial protocol (12, 20). Written informed consent was obtained from all participants.

Processing of the MSCs took place at the GMP Facility of the LUMC. The MSC product was infused via peripheral intra venous infusion within a period of 30 min, with a target dose of 1.5×10^6 cells per/kg body weight (range $1– 2 \times 10^6$ cells).

During the trial protocol 9 blood samples were obtained of each of the 10 patients; before transplantation (week 0), at week 24, at week 25 and 26 before infusion of MSCs and 4 hours after infusion of MSCs, at week 27, at week 34 and at week 52 (Figure 1). All patients received their allocated treatment. One patient had not enough PBMCs stored at 26 weeks.

Mass cytometry staining and data acquisition

Peripheral blood mononuclear cells (PBMCs) were isolated by Ficoll-Paque density-gradient centrifugation and cryopreserved in liquid nitrogen until time of analysis in 20%FCS, 10%DMSO RPMI.

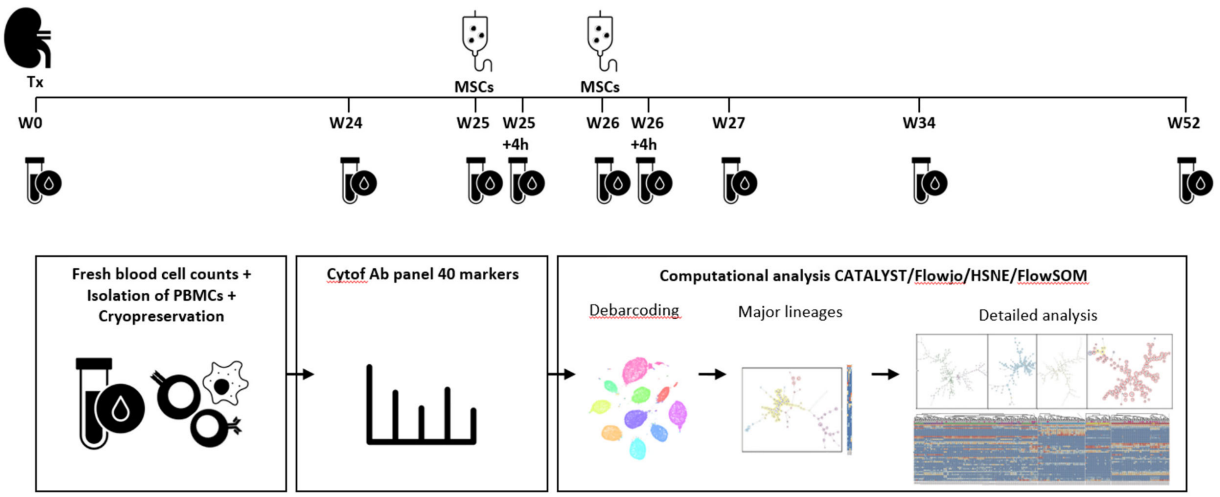

FIGURE 1
Identification of immune cell lineages in peripheral blood. Experimental setup. MSC infusion took place at week 25 and week 26 after kidney transplantation (Tx). Blood samples were taken at the following time points: week 0, week 24, week 25 before MSC infusion and 4 hours after MSC infusion, at week 26 before and 4 hours after MSC infusion, at week 27, week 34 and week 52. After fresh blood cell counts, isolation of PBMCs and cryopreservation the cells were stained and measured in one batch per patient. After debarcoding, the cells were split based on a first level FlowSOM, already showing a discrepancy between major immune lineages (CD19, CD3, CD16/CD56 and CD11b/CD11c), but a second step provides cleaner data (e.g. removed duplicates) and in-depth analysis which is used for further analysis in this paper.

A metal conjugated 40-antibody panel for mass cytometry was developed incorporating all major immune cell lineages. Heavy metal isotope-tagged monoclonal antibodies (mAbs) for mass cytometry are listed in Supplementary Table S1. Antibody conjugations and sample staining have been described previously (19). Samples were live-cell barcoded, stained and measured in batches of 9 time point samples and 1 reference sample (samples of each patient were kept within one batch). Barcoding of live cell samples was performed with α-B2M (anti-β-2-microglobulin) and α-CD298 mAbs using a protocol adapted from Mei et al (21). Cells were acquired within 48h of staining on a Helios mass cytometer (Fluidigm) at an event rate of <250 events/sec in Cell Acquisition Solution (Fluidigm) containing 10x diluted EQ Four Element Calibration Beads (Fluidigm). To make a compensation matrix, staining beads (eComp) were individually stained with the conjugated antibodies and incubated for 45 min at a volume of 100µl. After washing, the beads were pooled, washed and acquired in cell staining buffer. Experiments and acquisition were performed in a period of 65 days.

Mass cytometry data analysis

Data were normalized with EQ-normalization passport for each experiment. Followed by gating to remove debris, dead cells, and doublets with channels 89Y_CD45, 193Ir_DNA, Residual, 103Rh_DNA (life/dead), and 140Ce_bead (Flowjo v. 10.6.1.) Next, the data were compensated in R version 4.1.1 using the CATALYST package and automatic cutoffs. Data were debarcoded with HSNE in Cytosplore. Data were arcsin 5 transformed in R, and batch effects were corrected using the reference samples. The data were downsampled to a maximum of 50,000 cells/sample to both create similar numbers of cells per sample and minimize computational time, while keeping enough cells for in-depth analyzation, and analyzed using the FlowSOM package (22). The downsampled cells were clustered into 100 clusters and gathered in 30 metaclusters for the first overview FlowSOM. Metaclusters with similar phenotypes were then merged, resulting in four groups resembling the major lineages (Figure 1; Supplementary Figure S1). A separate FlowSOM was then performed for each group for in-depth analysis. This two step approach allowed for better in-depth phenotyping as there are less cells in the analysis and small differences can be visualised. For group 1, 2 and 3 a FlowSOM was created with 121 clusters and 100 metaclusters and for group 4, a FlowSOM with 225 clusters and 200 metaclusters was made. Metaclusters with similar phenotypes were merged. Clusters that contained over 500 cells and originated from different samples were included, while doublet clusters were removed (Supplementary Figure S1). Using the absolute cell counts obtained on fresh blood samples (BD Multitest kit, BD Biosciences) the absolute number of cells in each subset could be calculated. Graphs were generated using Graphpad prism version 8.4.2 by comparing the absolute number of cells at different time points. Any measurements with a value of zero were depicted as a dot on the X-axis. Selected subsets were gated for validation purposes using Flowjo v10.6.1.

Statistical analysis

For the discovery analysis, the comparisons within one cluster were performed with the Wilcoxon signed rank test in Graphpad prism version 8.4.2 and corrected for multiple testing with Bonferroni.

Results

Increase of B cells and CD8$^+$ T cells 9 weeks after MSC infusion at week 34

In the Neptune clinical trial allogenic bone marrow-derived MSCs were infused at 25 and 26 weeks post kidney transplantation in 10 patients (Figure 1). Notably, no adverse effects directly attributable to the MSC infusions were observed in these patients (age 24-68). All patients maintained a functioning kidney graft at the study's conclusion, with no occurrences of biopsy-proven acute rejection (BPAR). Detailed clinical information on the study population is available in Dreyer et al. (12).

Participants provided nine blood samples: pre-transplantation (week 0), at weeks 24, 25, and 26 (before and 4 hours after MSC infusion), and at weeks 27, 34, and 52. A 40-marker antibody panel was used with mass cytometry to analyze all samples. Acquired data were analyzed using the FlowSOM clustering method using two steps resulting in 368 phenotypically distinct clusters, as illustrated in Figure 1 and Supplementary Figure S1. For each cluster we determined to which major immune lineage it belonged (B cells, myeloid cells, CD3$^+$CD4$^-$CD8$^-$ (CD3$^+$DN) T cells, CD4$^+$ T cells, CD8$^+$ T cells or NK cells, Supplementary Figure S1). Next, the proportion of each cluster was assessed as percentage of the total CD45$^+$ population and as percentage of total lymphocytes at each of the time points (Figure 2A). Pre-transplantation (week 0) lymphocytes (49.0%) and myeloid cells (50.4%) each made up half of the total CD45$^+$ population. However, at week 24 till week 52 this distribution was skewed towards a dominance of myeloid cells (74.6%-83.4%). Within the lymphocytes, before transplantation (week 0) 54.6% lymphocytes were CD4$^+$ T cells, whereas at week 24 till 34 the NK cells made up 40.4%-48.8% of the lymphocytes. While at week 52 the percentage of both B cells and CD4$^+$ T cells were again increased, the CD4$^+$ T cells remained low compared to week 0 (Figure 2A). Due to alemtuzumab induced lymphodepletion these changes in the immune composition were expected and our results confirm that after one year the immune compartment is still not fully recovered.

Next, for each major immune lineage the absolute number of cells at week 25 after transplantation (before MSC infusion) was compared with the number of cells at the following timepoints; week 26 before second infusion of MSC, week 27, week 34 and week 52 (Figure 2B). This revealed no differences in the absolute cell numbers between those time points within the myeloid compartment, NK cells, CD3$^+$DN T cells and CD4$^+$ T cells. However, at week 34 the number of both CD8$^+$ T cells and B cells was increased compared to week 25 (both p=0.027). B cell numbers continued to be elevated at week 52 (p=0.027) while the CD8$^+$ T cells were not.

CD3$^+$CD4$^-$CD8$^-$ T cells were decreased 4 hours after first MSC infusion

Although infused MSC are only short lived, we hypothesized that this could still affect circulating immune cells early after MSC infusion. Therefore, we directly compared the absolute numbers of cells at week 25 and week 26 before and 4 hours after each MSC infusion at the major immune lineage level in all individual patients (Figure 3). We did not observe significant changes in the major lineages of myeloid cells, NK cells, B cells, CD4$^+$ T cells and CD8$^+$ T cells upon MSC infusion. However, the number of CD3$^+$DN T cells was decreased 4 hours after the first, but not the second, MSC infusion (p=0.010, Figure 3).

Lineage$^+$CD11b$^+$CD11c$^+$CD38$^+$CD39$^+$Ki-67$^+$ subsets are increased 4 hours after each MSC infusion

We next focused on a more detailed analysis of the 368 phenotypically distinct clusters resulting from the FlowSOM clustering. For this we compared the absolute cell numbers of these individual clusters at week 25 and week 26, before and 4 hours after each MSC infusion. This analysis revealed statistically significant differences for 75 clusters (Supplementary Table S2). Within these 75 cluster we next combined clusters that exhibited a similar phenotype, resulting in three B cell subsets, seven myeloid subsets, seven CD3$^+$DN T cell subsets, four CD8$^+$ T cell subsets, 14 CD4$^+$ T cell subsets and 14 NK cell subsets, showing a statistically significant increase or decrease when comparing the time points before MSC infusion with the time points 4 hours after MSC infusion (Supplementary Tables S3-S9).

Within both the B cells and the T cells we observed several subsets that all shared the expression of CD11b, CD11c, CD38, CD39, and Ki-67 (Supplementary Tables S3-S9, indicated in bold). Strikingly, all these subsets were significantly increased 4 hours after MSC infusion, at either one or both infusion moments (Table 1). To confirm the changes in these subsets derived from the FlowSOM analysis, we in addition manually gated for these CD11b$^+$CD11c$^+$CD38$^+$CD39$^+$Ki-67$^+$ phenotypes. Manual gating revealed similarly increased B cell and T cell subsets 4 hours after MSC infusion (Supplementary Figures S2, S3A). Significance was reached for the B cells with this phenotype at week 25, for the CD3$^+$DN T cells at both week 25 and week 26, for the CD4$^+$ T cells at week 25 and for the CD8$^+$ T cells both at week 25 and week 26 (Supplementary Figures S3B-E). To conclude, lineage$^+$CD11b$^+$CD11c$^+$CD38$^+$CD39$^+$Ki-67$^+$ subsets discovered in the FlowSOM analysis are increased 4 hours after each MSC infusion which was confirmed with manual gating of these subsets.

Discussion

In the current work we used mass cytometry to gain insight on the impact of MSC therapy on the immune compartment in kidney transplant recipients. In previous work we described the safety and feasibility of the allogenic MSC infusion (12). In the current study we used mass cytometry to visualize the composition of the immune compartment before and up to 52 weeks after kidney transplantation in MSC treated patients. We focused on the

10.3389/fimmu.2024.1455300

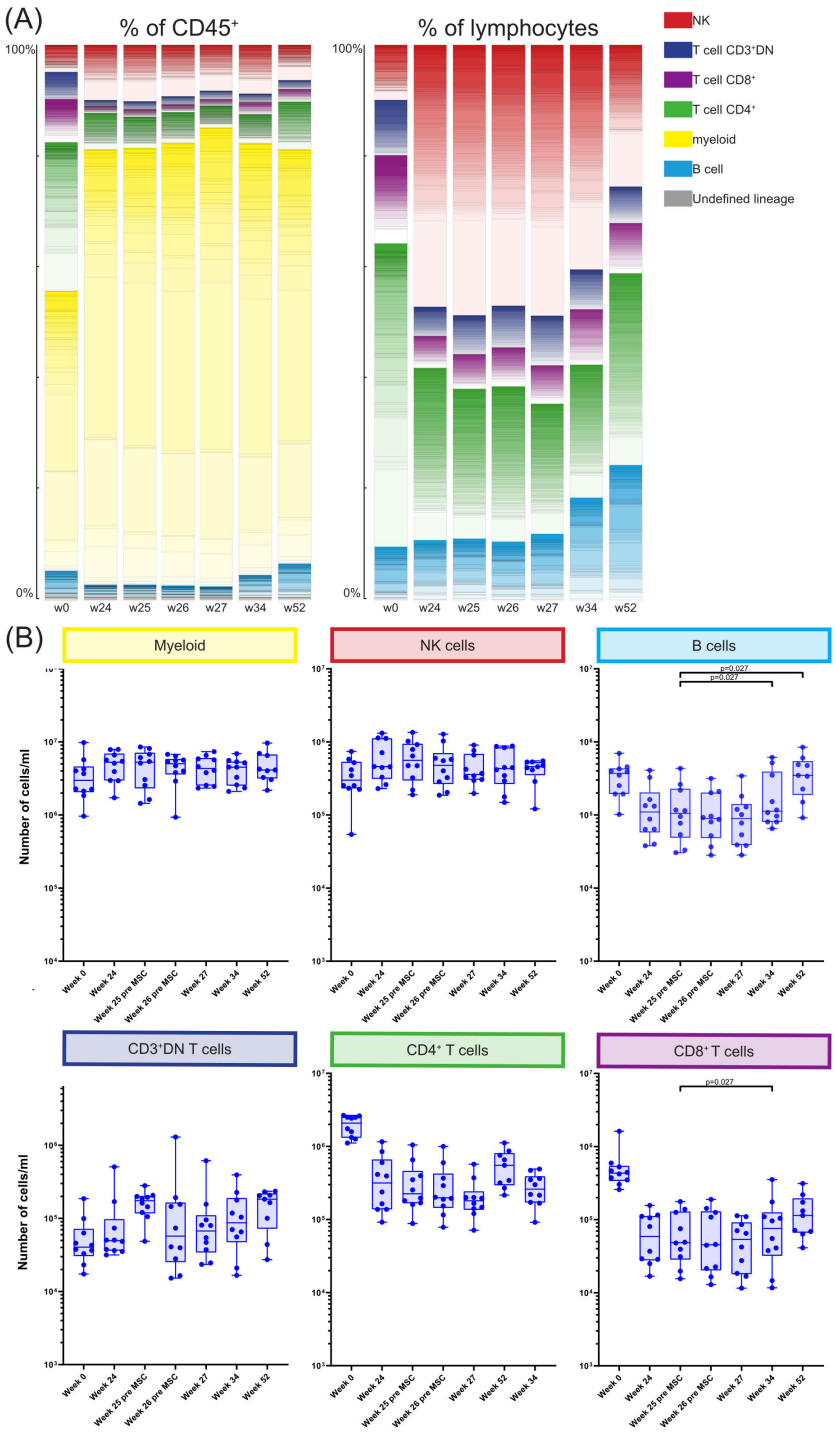

FIGURE 2
Longitudinal quantification and distribution of major immune cell lineages. **(A)** Graphs showing the number of cells/ml in the MSC treated patients at timepoint w0, w24, w25, w26, w27, w34 and w52, for the six major immune lineages, Myeloid, NK/ILC, B cells, $CD3^+$DN Tcells, $CD4^+$ T cells and $CD8^+$ T cells. Each dot represents an individual patient at the timepoint indicated. P-values were calculated using the Mann-Whitney U test and corrected within each cluster with Bonferroni. **(B)** The contribution of the different cell clusters and major lineages as percentage of $CD45^+$ cells (left panel) and as percentage of lymphocytes (right panel), in the MSC treated patients at timepoint w0, w24, w25, w26, w27, w34 and w52.

effects as soon as 4 hours post MSC transfusion and were able to show significant changes in specific B cell and T cell subsets shortly post MSC transfusion.

It is known that MSCs can impact various immune cell types such as dendritic cells, monocytes, macrophages, B cells, T cells including Treg/Th1/Th2 and Th17 helper cells, NK cells and NKT cells, ILCs, myeloid-derived suppressor cells, neutrophils, and mast cells (6, 7, 13–15). This effect can occur through direct cell-cell contact or indirectly by MSC-derived vesicles, including exosomes and apoptotic bodies, or soluble factors, as reported in studies by

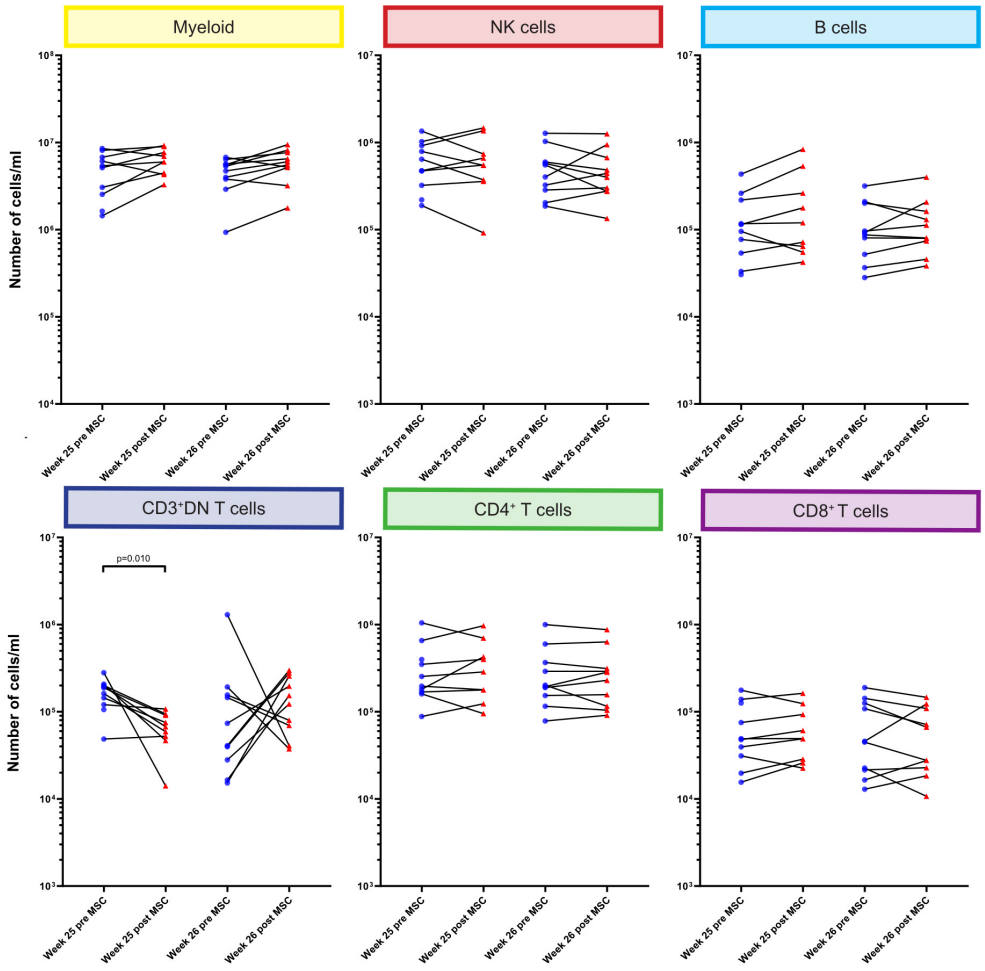

FIGURE 3
Quantification of major immune cell lineages pre and post MSC therapy. Graphs showing the number of cells/ml in the MSC treated patients at timepoint w25 pre and post MSC and w26 pre and post MSCs for the six major immune lineages, Myeloid, NK/ILC, B cells, $CD3^+$DN Tcells, $CD4^+$ T cells and $CD8^+$ T cells. Each dot represents an individual patient at the timepoint indicated connected with a line to the following timepoint. Blue: pre-MSC infusion, red: 4 hours after MSC infusion. P-values were calculated using the Mann-Whitney U test and corrected within each cluster with Bonferroni.

Weiss et al. and Jiang et al (23, 24). Upon intravenous infusion MSCs tend to accumulate in the lungs as they cannot pass through narrow capillaries due to their size (17, 25). We have recently shown the rapid death of MCSs upon infusion, determined by MSC-specific cell free DNA measured in plasma 4 hours after infusion (16). In the current study we focused on potential changes in the composition of immune cell subsets at this time point, since massive cell death of MSCs may affect immune cell composition. We showed that absolute cell numbers of three B cell subsets, seven myeloid subsets, seven $CD3^+$DN T cell subsets, four $CD8^+$ T cell subsets, 14 $CD4^+$ T cell subsets (2 Treg), and 14 NK cell subsets were significantly changed 4 hours after infusion compared to pre-infusion. Strikingly, we observed that several of these subsets exhibited an unusual $CD11b^+CD11c^+CD38^+CD39^+Ki\text{-}67^+$ phenotype. Manual gating confirmed the increased presence of CD11b/CD11c/CD38/CD39/Ki-67 positivity in B cells, $CD3^+$DN, $CD4^+$ and $CD8^+$ T cells 4 hours after MSC infusion.

CD38, CD39 and Ki-67 are commonly expressed by both B cells and T cells ($CD3^+$DN, $CD4^+$ and $CD8^+$). Both CD38 and CD39 suggest activation and Ki-67 can indicate proliferation (26, 27). CD38, CD39 and Ki-67 could be upregulated by B cells and T cells within the first hours of activation upon encounter with either the apoptotic MSCs or phagocytic cells. Alternatively, increase of these $CD38^+CD39^+Ki\text{-}67^+$ cells could indicate recruitment from adjacent tissues, like the lung, in response to the accumulation of dead MSCs. The integrins CD11b and CD11c are commonly expressed by dendritic cells, monocytes and macrophages. Although not typical, B and T cells can express both CD11b and CD11c (28–30). $CD11b^+CD11c^+$ B cells have been found to strongly stimulate T cells but produce modest levels of secreted antibody (29). While the exact role of $CD11c^+$ on T cells is unclear, it has been reported that CD11c may have a regulatory function on $CD8^+$ T cells and that these cells have a high migratory capacity (30, 31). While the infusion of MSCs may potentially trigger early and transient upregulation of CD11b and CD11c in B cells and T cells, this remains unexpected and warrants further study. The conduction of a kinetic study with closer intervals could track the marker expression on these cells and thus shed a light on the upregulation of these markers.

10.3389/fimmu.2024.1455300

TABLE 1 $CD11b^+CD11c^+CD38^+CD39^+Ki\text{-}67^+$ B cells and T cells from FLOWSOM analysis.

Lineage	Subset	Cell type	Cells/µl median (range) week 25			Cells/µl median (range) week 26		
			0h	+4h & MSC	p-value	0h	+4h & MSC	p-value
B cells	2	Proliferating $CD11b^+CD11c^+CD38^+CD39^+$ mature B cell	7962 (1767-13262)	14297 (6162-28367)	0.042	5789 (1048-13415)	8351 (2456-16642)	ns
$CD3^+$DN T cells	1	Proliferating $CD11b^+CD11c^+CD38^+CD39^+$ memory T cell	9979 (3506-14865)	14666 (6548-27992)	0.031	5683 (3432-12298)	12023 (4110-15663)	ns
$CD3^+$DN T cells	3	Proliferating $CD11b^+CD11c^+CD38^+CD39^+CD57^+$ effector T cell	381 (0-693)	848 (176-2095)	0.008	773 (373-2505)	578 (280-2220)	0.012
CD4+ T cells	11	Activated proliferating $CD11b^+CD11c^+CD38^+CD39^+Tigit^+$ memory $CD4^+$ T cell	1990 (562-4678)	3063 (1417-7482)	0.016	1321 (374-1666)	992 (685-2377)	ns
CD4+ T cells	12	Proliferating $CD11b^+CD11c^+CD38^+CD39^+$ $CD4^+$ T cell	5359 (1729-26545)	10234 (5410-28323)	0.039	3773 (1318-11496)	5312 (1979-15062)	0.008
CD8+ T cells	4	Proliferating $CD11b^+CD11c^+CD38^+CD39^+CD27^+CD127^+$ Tc1-like cytotoxic T cell	2545 (610-7857)	4858 (1708-12136)	ns	1848 (374-3702)	2844 (609-5068)	0.039

ns, not significant.

The identification of the unusual marker combinations made us consider the formation of doublets. While it is possible that cells stick together and form doublets during staining, doublets were excluded by gating on DNA, width, residual, center and offset excluding the vast majority of doublets. Furthermore, using the barcoding, cells with extra barcodes were also excluded, further mitigating this potential bias. While some cells could theoretically form doublets and contain a single barcode, this is unlikely and would occur equally for all 9 pooled samples of a patient. Therefore these cells would not be elevated specifically 4 hours after each MSC infusion. While limited, doublet formation could still introduce some bias in CyTOF studies, future studies are recommended to use the latest staining techniques to minimize these occurrences and up-to-date post-acquisition data analysis workflow to distinguish these cells.

An alternative explanation for the unusual marker combination can be trogocytosis, a process in which a cell acquires fragments from another living cell. The trogocytic cell has the capability to assimilate membrane proteins from other cells, which can then become integrated in its own plasma membrane (32, 33). While antigen presenting cells (APCs), B cells and T cells all have this ability, the transfer of membrane proteins from APCs to B cells and T cells is best described (34). One could envisage that during the process of trogocytosis, CD11b and CD11c may be transferred from myeloid cells to $CD38^+CD39^+Ki\text{-}67^+$ B cells or T cells, resulting in the $CD11b^+CD11c^+CD38^+CD39^+Ki\text{-}67^+$ B cell and T cell phenotype. Trogocytosis of the MSCs, or integration of extracellular vesicles or apoptotic blebs derived from the MSC, are unlikely to explain the observed phenotype as MSCs do not express CD45, CD11b, CD11c, CD38, CD19 or CD3, though they can express CD39 (35). How MSC would drive the increased interaction between myeloid cells and B or T cells, and thereby the process of trogocytosis, is currently unknown. In our previous work we tracked the response of 29 cytokines 4 hours after each MSC infusion (12). TNFα showed a significant decrease 4 hours after the first MSC infusion however this effect was not seen after the second infusion. Anti-inflammatory cytokine IL4 showed small though significant differences after both the first and second infusion. Anti-inflammatory cytokine IL10 was decreased after each infusion, which was significant after the second infusion. Proinflammatory cytokine IFNγ showed non-significant decrease at both time points. No major changes were observed 4 hours after MSC infusions for the other cytokines. The responses of these cytokines, anti-inflammatory as well as proinflammatory, are systemic in nature, and therefore a direct association with the identified cells cannot be definitively established.

In previous work we showed that while absolute numbers of monocytes, B cells, NK cells and $CD8^+$ T cells remained stable in the two weeks after infusion (week 26 and 27), $CD4^+$ T cells increased in the second week post MSC infusion (week 27). However, this could be due to the immune cell repopulation as a consequence of induction therapy with alemtuzumab (12). In the current study we could confirm that B cells, $CD4^+$ T cells and $CD8^+$ T cells did not reach their base line levels at week 25, the time of the first MSC infusion (12). Repopulation after induction therapy was still ongoing at 52 weeks, as the number of $CD4^+$ T cells and $CD8^+$ T

cells was still lower compared to baseline. Unexpectedly, our data show that the absolute number of $CD3^+$DN T cells was not decreased at 24 weeks compared to baseline. This double negative population was not studied in our previous report. These data indicate that either the $CD3^+$DN T cells are less efficiently depleted by the induction therapy or they repopulate quicker within 24 weeks compared to both $CD4^+$ and $CD8^+$ T cells.

The transient upregulation of markers such as CD11b, CD11c, CD38, CD39, and Ki-67 on B cells and T cells shortly after MSC infusion suggests early immune activation. However, it remains to be established whether this contributes to potential long-term beneficial clinical effects. Autologous MSC infusion has been exploited for a safe reduction in immunosuppressive drugs (9), and has been proposed to induce an immune regulatory milieu (10). Both CD38 and CD39 play key roles in the adenosine pathway, which is known to regulate immune responses by generating the immunosuppressive molecule adenosine (36, 37). The extracellular adenosine level normally kept low under physiological conditions, but it increases during inflammation and cell death which could be triggered by the massive cell death of MSCs (37). CD38, through its enzymatic activity, influences the metabolism of NAD^+, indirectly contributing to the generation of substrates such as ATP and ADP, which are crucial for the adenosine-producing activity of CD39. CD39 further catalyses the conversion of ATP and ADP into AMP, a precursor of adenosine. Unfortunately, we do not have information on CD73, a molecule required for the final conversion of AMP to adenosine. Future studies should incorporate CD73 to provide a more comprehensive view of adenosine regulation and its potential role in immune modulation via this pathway. This could reveal whether the transient increase in $CD11b^+CD11c^+CD38^+CD39^+$Ki-$67^+$ B cells and T cells contributes to a sustained immunosuppressive or regulatory environment, particularly through the adenosine pathway, and help clarify the longer-term effects of MSCs infusion on allograft survival in kidney transplantation.

The current research involved an unbiased discovery analysis of various immune cell markers, leading to the identification of numerous distinct clusters/subsets. As a result, a large number of comparisons were made. In this study we corrected with Bonferroni to account for multiple comparisons within a single cluster. Correcting for false positives across the entire study would require extremely low p-values to remain significant after correction. Therefore, we argue that the subsets discovered in this study should be validated and examined more closely in future studies to determine their potential role in MSC therapy. As the current study was a single center study with a limited number of patients, these future studies are recommended to involve multiple centers and include a larger number of patients.

In conclusion, we here report an extensive description of the immune cell composition in kidney transplantation patients 4 hours after receiving MSC therapy. While the mechanisms of action are still unclear, our results indicate that subsets of cells within all the immune cell lineages respond to MSC infusion as soon as 4 hours. We highlight the discovery of $CD11b^+CD11c^+CD38^+CD39^+$Ki-$67^+$ B and T cell subsets which increased consistently 4 hours after MSC infusion. Our findings may facilitate in the ongoing quest to understand the effect of MSC therapy on the immune system.

Data availability statement

The raw data supporting the conclusions of this article will be made available by the authors, without undue reservation.

Ethics statement

The studies involving humans were approved by Central Committee on Research involving Human Subjects in the Netherlands. The studies were conducted in accordance with the local legislation and institutional requirements. The participants provided their written informed consent to participate in this study.

Author contributions

SHH: Conceptualization, Formal analysis, Investigation, Methodology, Validation, Visualization, Writing – original draft, Writing – review & editing. SH: Conceptualization, Supervision, Writing – original draft, Writing – review & editing. MR: Methodology, Resources, Writing – review & editing. FK: Conceptualization, Supervision, Writing – original draft, Writing – review & editing. CK: Conceptualization, Supervision, Writing – original draft, Writing – review & editing.

Funding

The author(s) declare financial support was received for the research, authorship, and/or publication of this article. ZonMW-TAS, Grant/Award Number: 116004104.

Acknowledgments

We thank the research technicians from the Transplant Immunology lab for technical assistance with PBMC biobanking and absolute cell counts.

Conflict of interest

The authors declare that the research was conducted in the absence of any commercial or financial relationships that could be construed as a potential conflict of interest.

The author(s) declared that they were an editorial board member of Frontiers, at the time of submission. This had no impact on the peer review process and the final decision.

Publisher's note

All claims expressed in this article are solely those of the authors and do not necessarily represent those of their affiliated

Supplementary material

The Supplementary Material for this article can be found online at: https://www.frontiersin.org/articles/10.3389/fimmu.2024.1455300/full#supplementary-material.

References

1. Garcia GG, Harden P, Chapman J, Committee FtWKDS. The global role of kidney transplantation. *Curr Opin Organ transplantation*. (2012) 17:362–7. doi: 10.1097/mot.0b013e328354c277

2. Lamb KE, Lodhi S, Meier-Kriesche HU. Long-term renal allograft survival in the United States: a critical reappraisal. *Am J transplantation: Off J Am Soc Transplant Am Soc Transplant Surgeons*. (2011) 11:450–62. doi: 10.1111/j.1600-6143.2010.03283.x

3. Coemans M, Susal C, Dohler B, Anglicheau D, Giral M, Bestard O, et al. Analyses of the short- and long-term graft survival after kidney transplantation in Europe between 1986 and 2015. *Kidney Int*. (2018) 94:964–73. doi: 10.1016/j.kint.2018.05.018

4. Wekerle T, Segev D, Lechler R, Oberbauer R. Strategies for long-term preservation of kidney graft function. *Lancet*. (2017) 389:2152–62. doi: 10.1016/s0140-6736(17)31283-7

5. Nankivell BJ, P'Ng CH, O'Connell PJ, Chapman JR. Calcineurin inhibitor nephrotoxicity through the lens of longitudinal histology: comparison of cyclosporine and tacrolimus eras. *Transplantation*. (2016) 100:1723–31. doi: 10.1097/TP.0000000000001243

6. Aggarwal S, Pittenger MF. Human mesenchymal stem cells modulate allogeneic immune cell responses. *Blood*. (2005) 105:1815–22. doi: 10.1182/blood-2004-04-1559

7. Galleu A, Riffo-Vasquez Y, Trento C, Lomas C, Dolcetti L, Cheung TS, et al. Apoptosis in mesenchymal stromal cells induces in vivo recipient-mediated immunomodulation. *Sci Trans Med*. (2017) 9(416):eaam7828. doi: 10.1126/scitranslmed.aam7828

8. Stolzing A, Jones E, McGonagle D, Scutt A. Age-related changes in human bone marrow-derived mesenchymal stem cells: consequences for cell therapies. *Mech Ageing Dev*. (2008) 129:163–73. doi: 10.1016/j.mad.2007.12.002

9. Reinders MEJ, Groeneweg KE, Hendriks SH, Bank JR, Dreyer GJ, de Vries APJ, et al. Autologous bone marrow-derived mesenchymal stromal cell therapy with early tacrolimus withdrawal: The randomized prospective, single-center, open-label TRITON study. *Am J Transplantation*. (2021) 21:3055–65. doi: 10.1111/ajt.16528

10. Perico N, Casiraghi F, Gotti E, Introna M, Todeschini M, Cavinato RA, et al. Mesenchymal stromal cells and kidney transplantation: pretransplant infusion protects from graft dysfunction while fostering immunoregulation. *Transpl Int*. (2013) 26:867–78. doi: 10.1111/tri.12132

11. Avivar-Valderas A, Martin-Martin C, Ramirez C, Del Rio B, Menta R, Mancheno-Corvo P, et al. Dissecting allo-sensitization after local administration of human allogeneic adipose mesenchymal stem cells in perianal fistulas of crohn's disease patients. *Front Immunol*. (2019) 10:1244. doi: 10.3389/fimmu.2019.01244

12. Dreyer GJ, Groeneweg KE, Heidt S, Roelen DL, van Pel M, Roelofs H, et al. Human leukocyte antigen selected allogeneic mesenchymal stromal cell therapy in renal transplantation: The Neptune study, a phase I single-center study. *Am J transplantation: Off J Am Soc Transplant Am Soc Transplant Surgeons*. (2020) 20:2905–15. doi: 10.1111/ajt.15910

13. Li H, Rong P, Ma X, Nie W, Chen C, Yang C, et al. Paracrine effect of mesenchymal stem cell as a novel therapeutic strategy for diabetic nephropathy. *Life Sci*. (2018) 215:113–8. doi: 10.1016/j.lfs.2018.11.001

14. Liu S, Liu F, Zhou Y, Jin B, Sun Q, Guo S. Immunosuppressive property of MSCs mediated by cell surface receptors. *Front Immunol*. (2020) 11:1076. doi: 10.3389/fimmu.2020.01076

15. Merimi M, El-Majzoub R, Lagneaux L, Moussa Agha D, Bouhtit F, Meuleman N, et al. The therapeutic potential of mesenchymal stromal cells for regenerative medicine: current knowledge and future understandings. *Front Cell Dev Biol*. (2021) 9:661532. doi: 10.3389/fcell.2021.661532

16. Dreyer GJ, Drabbels JJ, de Fijter JW, van Kooten C, Reinders ME, Heidt S. Cell-free DNA measurement of three genomes after allogeneic MSC therapy in kidney transplant recipients indicates early cell death of infused MSC. *Front Immunol*. (2023) 14:1240347. doi: 10.3389/fimmu.2023.1240347

17. de Witte SFH, Luk F, Sierra Parraga JM, Gargesha M, Merino A, Korevaar SS, et al. Immunomodulation by therapeutic mesenchymal stromal cells (MSC) is triggered through phagocytosis of MSC by monocytic cells. *Stem Cells (Dayton Ohio)*. (2018) 36:602–15. doi: 10.1002/stem.2779

18. Consentius C, Akyuz L, Schmidt-Lucke JA, Tschope C, Pinzur L, Ofir R, et al. Mesenchymal stromal cells prevent allostimulation *in vivo* and control checkpoints of th1 priming: migration of human DC to lymph nodes and NK cell activation. *Stem Cells (Dayton Ohio)*. (2015) 33:3087–99. doi: 10.1002/stem.2104

19. Hendriks SH, Heidt S, Schulz AR, de Fijter JW, Reinders MEJ, Koning F, et al. Peripheral blood immune cell composition after autologous MSC infusion in kidney transplantation recipients. *Transpl Int*. (2023) 36:11329. doi: 10.3389/ti.2023.11329

20. Reinders ME, Dreyer GJ, Bank JR, Roelofs H, Heidt S, Roelen DL, et al. Safety of allogeneic bone marrow derived mesenchymal stromal cell therapy in renal transplant recipients: the neptune study. *J Trans Med*. (2015) 13:344. doi: 10.1186/s12967-015-0700-0

21. Mei HE, Leipold MD, Maecker HT. Platinum-conjugated antibodies for application in mass cytometry. *Cytometry Part A: J Int Soc Analytical Cytology*. (2016) 89:292–300. doi: 10.1002/cyto.a.22778

22. Van Gassen S, Callebaut B, Van Helden MJ, Lambrecht BN, Demeester P, Dhaene T, et al. FlowSOM: Using self-organizing maps for visualization and interpretation of cytometry data. *Cytometry Part A: J Int Soc Analytical Cytology*. (2015) 87:636–45. doi: 10.1002/cyto.a.22625

23. Weiss ARR, Dahlke MH. Immunomodulation by mesenchymal stem cells (MSCs): mechanisms of action of living, apoptotic, and dead MSCs. *Front Immunol*. (2019) 10:1191. doi: 10.3389/fimmu.2019.01191

24. Jiang W, Xu J. Immune modulation by mesenchymal stem cells. *Cell Prolif*. (2020) 53:e12712. doi: 10.1111/cpr.12712

25. Eggenhofer E, Benseler V, Kroemer A, Popp FC, Geissler EK, Schlitt HJ, et al. Mesenchymal stem cells are short-lived and do not migrate beyond the lungs after intravenous infusion. *Front Immunol*. (2012) 3:297. doi: 10.3389/fimmu.2012.00297

26. Kansas GS, Wood GS, Tedder TF. Expression, distribution, and biochemistry of human CD39. Role in activation-associated homotypic adhesion of lymphocytes. *J Immunol*. (1991) 146:2235–44. doi: 10.4049/jimmunol.146.7.2235

27. Stoeckler JD, Stoeckler HA, Kouttab N, Maizel AL. 1alpha,25-Dihydroxyvitamin D3 modulates CD38 expression on human lymphocytes. *J Immunol*. (1996) 157:4908–17. doi: 10.4049/jimmunol.157.11.4908

28. Gane P, Fain O, Mansour I, Roquin H, Rouger P. Expression of CD11b (Leu15) antigen on CD3+, CD4+, CD8+, CD16+ peripheral lymphocytes. Estimation of CD3 + 8+11b+ and CD3 + 4-8-11b+ T-cell subsets using a single laser flow cytometer. *Scand J Immunol*. (1992) 36:395–404. doi: 10.1111/j.1365-3083.1992.tb02953.x

29. Griffin DO, Rothstein TL. A small CD11b(+) human B1 cell subpopulation stimulates T cells and is expanded in lupus. *J Exp Med*. (2011) 208:2591–8. doi: 10.1084/jem.20110978

30. Qualai J, Li LX, Cantero J, Tarrats A, Fernandez MA, Sumoy L, et al. Expression of CD11c is associated with unconventional activated T cell subsets with high migratory potential. *PloS One*. (2016) 11:e0154253. doi: 10.1371/journal.pone.0154253

31. Vinay DS, Kim CH, Choi BK, Kwon BS. Origins and functional basis of regulatory CD11c+CD8+ T cells. *Eur J Immunol*. (2009) 39:1552–63. doi: 10.1002/eji.200839057

32. Schriek P, Villadangos JA. Trogocytosis and cross-dressing in antigen presentation. *Curr Opin Immunol*. (2023) 83:102331. doi: 10.1016/j.coi.2023.102331

33. Zeng F, Morelli AE. Extracellular vesicle-mediated MHC cross-dressing in immune homeostasis, transplantation, infectious diseases, and cancer. *Semin Immunopathol*. (2018) 40:477–90. doi: 10.1007/s00281-018-0679-8

34. Sprent J. Swapping molecules during cell-cell interactions. *Sci STKE*. (2005) 2005:pe8. doi: 10.1126/stke.2732005pe8

35. Saldanha-Araujo F, Ferreira FI, Palma PV, Araujo AG, Queiroz RH, Covas DT, et al. Mesenchymal stromal cells up-regulate CD39 and increase adenosine production to suppress activated T-lymphocytes. *Stem Cell Res*. (2011) 7:66–74. doi: 10.1016/j.scr.2011.04.001

36. Wang B, Zhou A, Pan Q, Li Y, Xi Z, He K, et al. Adenosinergic metabolism pathway: an emerging target for improving outcomes of solid organ transplantation. *Transl Res*. (2024) 263:93–101. doi: 10.1016/j.trsl.2023.09.002

37. Sitkovsky MV, Lukashev D, Apasov S, Kojima H, Koshiba M, Caldwell C, et al. Physiological control of immune response and inflammatory tissue damage by hypoxia-inducible factors and adenosine A2A receptors. *Annu Rev Immunol*. (2004) 22:657–82. doi: 10.1146/annurev.immunol.22.012703.104731

frontiers | Frontiers in Immunology

TYPE Original Research
PUBLISHED 24 October 2024
DOI 10.3389/fimmu.2024.1479472

OPEN ACCESS

EDITED BY
Rita Maccario,
San Matteo Hospital Foundation (IRCCS), Italy

REVIEWED BY
Daniela Montagna,
San Matteo Hospital Foundation (IRCCS), Italy
Mithil Soni,
Columbia University, United States

*CORRESPONDENCE
Ricardo Cuesta-Martín de la Cámara
ricardocuestamartin@gmail.com

†These authors have contributed equally to this work and share last authorship

RECEIVED 12 August 2024
ACCEPTED 07 October 2024
PUBLISHED 24 October 2024

CITATION
Cuesta-Martín de la Cámara R, Torices-Pajares A, Miguel-Berenguel L, Reche-Yebra K, Frauca-Remacha E, Hierro-Llanillo L, Muñoz-Bartolo G, Lledín-Barbacho MD, Gutiérrez-Arroyo A, Martínez-Feito A, López-Granados E and Sánchez-Zapardiel E (2024) Epstein-Barr virus-specific T-cell response in pediatric liver transplant recipients: a cross-sectional study by multiparametric flow cytometry. *Front. Immunol.* 15:1479472. doi: 10.3389/fimmu.2024.1479472

Epstein-Barr virus-specific T-cell response in pediatric liver transplant recipients: a cross-sectional study by multiparametric flow cytometry

Ricardo Cuesta-Martín de la Cámara[1,2,3]*, Andrea Torices-Pajares[2], Laura Miguel-Berenguel[1], Keren Reche-Yebra[2], Esteban Frauca-Remacha[4,5,6], Loreto Hierro-Llanillo[4,5,6], Gema Muñoz-Bartolo[4,5,6], María Dolores Lledín-Barbacho[4,5,6], Almudena Gutiérrez-Arroyo[7], Ana Martínez-Feito[1], Eduardo López-Granados[1,2,6,8†] and Elena Sánchez-Zapardiel[1,2,6†]

[1]Clinical Immunology Department, University Hospital La Paz, Madrid, Spain, [2]Lymphocyte Pathophysiology in Immunodeficiencies Group, La Paz Institute for Health Research (IdiPAZ), Madrid, Spain, [3]Medicine and surgery Department, Autonomous University of Madrid, Madrid, Spain, [4]Paediatric Hepatology Department, University Hospital La Paz, Madrid, Spain, [5]European Reference Network (ERN) RARE LIVER, Madrid, Spain, [6]European Reference Network (ERN) TransplantChild, Madrid, Spain, [7]Microbiology Department, University Hospital La Paz, Madrid, Spain, [8]Centre for Biomedical Network Research on rare diseases (CIBERER U767), Madrid, Spain

Background: Epstein-Barr virus (EBV) specific T-cell response measurement can help adjust immunosuppression in transplant patients with persistent infections. We aim to define T-cell responses against EBV in a cohort of pediatric liver-transplant patients.

Methods: Thirty-eight immunosuppressed pediatric liver-transplant patients (IP) and 25 EBV-seropositive healthy-adult controls (HC) were included in our cross-sectional study. Based on their EBV serological (S) and viral load (VL) status, patients were categorized into IP-S^{NEG}, IP-$S^{POS}VL^{NEG}$ and IP-$S^{POS}VL^{POS}$ groups. T-cell response was assessed at two timepoints by stimulating cells with EBV peptides (PepTivator®) and performing intracellular-cytokine and activation-induced marker staining. Background subtraction was used to determine EBV-specific T-lymphocyte frequency.

Results: Polyfunctional CD8+ T cells indicated previous EBV contact (IP-S^{NEG} 0.00% vs IP-S^{POS} 0.04% and HC 0.02%; p=0.001 and p=0.01, respectively). Polyfunctional CD8+CD107a+IFNɣ+IL2-TNFα- profile was increased in serology-positive (IP-S^{NEG} 0.01% vs IP-S_{POS} 0.13% and HC 0.03%; p=0.01 and p=0.50, respectively) and viral-load positive (IP-$S^{POS}VL^{POS}$ 0.43% vs IP-$S^{POS}VL^{NEG}$ 0.07% and HC 0.03%; p=0.03 and p=0.001, respectively) patients. Central-memory cells were increased among serology-positive adults (IP-S^{NEG} 0.00% vs IP-S^{POS} 0.13% and HC 4.33%; p=0.58 and p=0.002, respectively). At the second timepoint, IP-S^{NEG} patients remained negative (first visit 0.01% vs second visit 0.00%, p=0.44). On the other hand, IP-$S^{POS}VL^{POS}$ patients had cleared viral loads

and, subsequently, decreased polyfunctional CD8+CD107a+IFNɣ+IL2-TNFα- cells (first visit 0.43% vs second visit 0.10%, p=0.81).

Conclusion: Polyfunctional CD8+ EBV-specific T-cell response allows detecting EBV previous contact in liver-transplant children. %CD8+CD107a+IFNɣ+IL2-TNFα- is increased in patients with positive viral loads. Central memory CD4+ T-cell population more effectively determines prior EBV-exposure in adults.

KEYWORDS

liver transplantation, Epstein-Barr virus infections, cellular immunity, flow cytometry, cytokines, surface antigens

1 Introduction

The progressive improvement of immunosuppressive treatments to prevent graft rejection over the past few decades has contributed to the remarkable improvement in overall graft survival in children receiving liver transplants (1, 2). However, because of this effective immunosuppressive treatment, graft recipients experience a secondary state immunodeficiency, that renders them highly susceptible to infections (3, 4) and malignancies (5).

Most humans are infected with Epstein-Barr virus (EBV), which primarily targets epithelial and B cells, leading to both lytic and latent infections (6). Although EBV has oncogenic potential, it is usually controlled by the immune response. Adults are generally more competent in managing EBV than children, due to a more mature immune system and prior exposure to the virus.

However, in immunosuppressed recipients, EBV reactivation can lead to post-transplant lymphoproliferative disorder (PTLD) (1, 7), a condition characterized by uncontrolled proliferation of EBV-infected cells (8). In liver transplantation, the incidence of PTLD is remarkably higher in pediatric patients (6.3-15.0%) than adults (1.2-2.8%) (9, 10), partially due to their immunologically naïve status for the virus pre-transplantation (seroprevalence in children is approximately 50% vs. 90% in adults) (11) and the incidence of EBV primary infection under immunosuppression (12). In fact, several studies have reported that pre-transplant EBV-seronegative pediatric liver recipients are at higher risk (hazard ratio 12-18) (13) of developing PTLD (14–16).

The Healthcare Working Group of the European Reference Network on Pediatric Transplantation (ERN TransplantChild) has recently published the results of a cross-sectional survey evaluating PTLD strategies for diagnosis and treatment across several pediatric solid organ transplantation programs, from 9 different European countries (17). Over the 2012-2016 period, 1471 pediatric liver transplants were performed and 115 (7.8%) PTLD cases were diagnosed. PTLD preemptive strategies varied across different programs, but all of them included EBV DNA-load measurement by quantitative polymerase chain reaction (qPCR) as the main subrogated biomarker for EBV-specific immunity.

Although EBV-load informative capacity appears to be widely integrated into daily clinical practice, its interpretation for PTLD diagnosis and surveillance is still controversial (18). Actually, no specific EBV viremia cutoff value has been defined to initiate preemptive treatment of PTLD (17). Regarding pediatric liver recipients, the association between high viral load and risk of PTLD development seems to be very poor (19), highlighting the necessity of new biomarkers.

Several techniques have been previously validated in different transplantation settings to estimate T-cell EBV response, being the most standardize one the detection of interferon gamma (IFNɣ) by either enzyme-linked immunospot (ELISpot) (20–23) or enzyme-linked immunosorbent (ELISA)-based (QuantiFERON®) assays (24–29). Other promising techniques involve the identification by flow cytometry of antigen-specific cells using mayor histocompatibility complex class I and class II multimers (23, 30–32), intracellular cytokine staining (ICS) (30, 31, 33–42) or activation-induced marker staining (AIMS) (43, 44).

Research on the T-cell compartment against EBV in pediatric liver recipients is scarce and primarily utilizes ELISpot and tetramer assays. There seems to be a correlation between immunosuppression doses and frequency of EBV-specific cells by ELISpot (45–47). Similar results were reported prospectively, measuring cellular response by tetramers (46). Nevertheless, neither tetramers nor dextramers are apparently effective in discriminating transplanted patients according to EBV viral load (32, 48).

Ning et al. used ICS to measure specific T-cell response in two pediatric liver recipients with detectable viral loads and diagnosis of PTLD. Those patients presented a reduction in T-cell polyfunctionality, with an increment in the expression of CD107a and tumor necrosis factor alpha (TNFα) (49). Another study, examining 20 pediatric-transplanted patients (7 liver-graft recipients), presented findings on T-cell response by ICS. Authors reported a significant increment in EBV-specific T cells in PTLD patients during rituximab treatment, which correlated with a reduction in viral load and subsequent control of EBV by T-cell responses following B-cell recovery (50). To our knowledge, the use of AIMS in this field has never been reported, although OX40 (CD134) has been previously defined as a potential biomarker of T-cell activation status in various types of transplants (51, 52).

The aim of this cross-sectional study is to characterize the specific helper and cytotoxic T-cell response to EBV in a cohort of pediatric liver recipients by both ICS and AIMS flow-cytometry methods, and compare it with a cohort of EBV-seropositive healthy adult controls (HC). Furthermore, we aim to identify cellular profiles that allow the discrimination of liver recipients according to both their EBV serological and viral-load status. We hypothesize that pediatric liver recipients controlling EBV will exhibit higher percentages of EBV-specific T cells compared to non-controllers, while also displaying specific cellular profiles.

2 Materials and methods

2.1 Patients and samples

Our cross-sectional study included 38 immunosuppressed pediatric patients (IP) at University Hospital La Paz, who received a liver graft between March 2018 and November 2022, and 25 EBV seropositive HC. All patients gave informed consent, approved by the ethics committee of our institution (reference PI-4000).

Demographic and clinically relevant information from each patient were collected (Table 1). PTLD diagnosis was based on histopathologic criteria. Transplant indication was categorized in five groups (Table 1) (53).

Specific T-cell response against EBV was assessed at two different timepoints, determined by patient availability (median time 3.7 months interquartile range [IQR] 3.2-4.9 between visits). EBV serology and viral load were measured in parallel with each immune response assessment for every patient.

Based on their serological status at the first visit, patients were categorized into EBV seronegative (IP-S^{NEG}) and EBV seropositive (IP-S^{POS}) individuals; the latter group was further classified according to EBV viral load into negative (IP-$S^{POS}VL^{NEG}$) and positive (IP-$S^{POS}VL^{POS}$). At the time of the second visit, patients were reclassified based on their updated serological and viral load status at that time. Due to sample exclusions for technical reasons, the immune response was not measured in all samples. ICS was performed to 38/38 (100%) and 28/38 (74%) patients at first and second visit, respectively. AIMS was performed to 27/38 (71%) and 29/38 (76%) patients at first and second visit, respectively, although results for both timepoints were available for only 21 individuals. Among HC participants, ICS and AIMS were successfully performed to 24/25 (96%) and 20/25 (84%) samples, respectively.

Heparinized blood samples from all individuals were collected to isolate peripheral blood mononuclear cells (PBMCs) by density gradient.

2.2 Intracellular cytokine staining

Analysis of specific T-cell response to EBV by ICS was assessed as described by Lovelace and Maecker (54). Details of the method are provided in the Supplementary Material.

T-cell responses were further categorized as monofunctional, when only one response marker was displayed (CD107a, IFNɣ, Interleukin 2 [IL2] or TNFα), and polyfunctional, when more than one response marker was expressed. Integrated median fluorescence intensity (iMFI) was calculated for each response marker, multiplying MFI by the frequency of the corresponding specific population.

Unstimulated PBMCs background was subtracted from all test samples to obtain the frequency of EBV-specific T lymphocytes. Gating strategy is displayed in Supplementary Figure S1A.

2.3 Activation-induced cell marker staining

Analysis of AIMS was performed by flow cytometry. Details of the method are provided in the Supplementary Material.

CD4+ T lymphocytes were distributed in naïve (Tn, CD27+ CD45RO-), effector (Teff, CD27-CD45RO-), central memory (Tcm, CD27+CD45RO+) and effector memory (Tem, CD27-CD45RO+) subpopulations. Memory compartment was calculated by the sum of Tcm and Tem subpopulations.

Unstimulated PBMCs background was subtracted from all test samples to obtain the frequency of EBV-specific T lymphocytes. Gating strategy is displayed in Supplementary Figure S1B.

2.4 Immunophenotype analysis

Immunophenotype of T, B, natural killer (NK) and natural killer T (NKT) lymphocytes was performed by multiparametric flow cytometry. Details of the method are provided in the Supplementary Material.

2.5 EBV viral load measurement

EBV viral loads were quantified in whole blood by a specific qPCR assay following manufacturer's instructions (RealStar® EBV PCR-Kit 1.0, Altona). Results were informed in International Units per milliliter (IU/mL). The negative group for viral load comprised exclusively patients with zero IU/mL.

2.6 EBV serology

EBV serological status was determined by a chemiluminescent microparticle immunoassay. Presence of IgM antibodies against viral capsid antigen (VCA) and/or IgG antibodies against VCA and nuclear antigen (EBNA) were measured following manufacturer's instructions (Abbott, Germany). EBV seropositive status was defined by the positivity of at least one of the analyzed antibodies.

2.7 Statistics

Descriptive data are presented as median with IQR. Categorical data are presented as absolute number and proportion (%). The software package Prism 8 (GraphPad, USA) was used for statistical analysis. Significance of differences comparing frequencies was determined by Pearson $\chi 2$-test and by *t* test or analysis of variance (Mann Whitney or Kruskal-Wallis tests) when comparing median values. Median frequencies between timepoints were compared by

TABLE 1 Epidemiologic and clinical features in EBV-seropositive adult healthy controls (HC) and immunosuppressed pediatric liver-transplanted patients, categorized as positive/negative serology status (IP-S^{POS} and IP-S^{NEG}, respectively) or positive/negative viral load status (IP-$S^{POS}VL^{POS}$ and IP-$S^{POS}VL^{NEG}$, respectively).

Characteristics	HC (n=25)	IP-S^{POS} (n=32)	IP-S^{NEG} (n=6)	P-value	HC (n=25)	IP-$S^{POS}VL^{POS}$ (n=8)	IP-$S^{POS}VL^{NEG}$ (n=24)	P-value
Sex, n (%)				0.10				0.07
Male	17 (68)	13 (41)	4 (67)		17 (68)	2 (25)	11 (46)	
Female	8 (32)	19 (59)	2 (33)		8 (32)	6 (75)	13 (54)	
Age, years (IQR)	54 (41-62)	5 (3-9)	5 (3-6)	**<0.001**	54 (41-62)	3 (2-4)	5 (4-9)	**<0.001**
Donor sex, n (%)				0.62				0.34
Male		8 (25)	3 (50)			1 (13)	7 (29)	
Female		13 (41)	2 (33)			5 (63)	8 (33)	
Donor age, years (IQR)		28 (19-34)	27 (15-38)			30 (26-31)	27 (16-34)	
Type of donor, n (%)				0.25				0.52
Living donor		10 (31)	4 (67)			3 (38)	7 (29)	
Deceased donor - whole graft		9 (28)	1 (17)			1 (13)	8 (33)	
Deceased donor - split graft		13 (41)	1 (17)			4 (50)	9 (38)	
ABO compatibility, n (%)				>0.99				>0.99
Compatible		25 (78)	6 (100)			7 (88)	18 (75)	
Incompatible		3 (9)	0 (0)			1 (13)	2 (25)	
Indication for transplantation, n (%)				0.23				0.31
Cholestasis/biliary atresia		19 (59)	3 (50)			6 (75)	13 (54)	
Metabolic diseases		7 (22)	2 (33)			0 (0)	7 (29)	
Cirrhosis (other)		2 (6)	0 (0)			1 (13)	1 (4)	
Severe acute liver failure		2 (6)	0 (0)			1 (13)	1 (4)	
Liver tumours		2 (6)	0 (0)			0 (0)	2 (8)	
Metabolic diseases and liver tumours		0 (0)	1 (17)			0 (0)	0 (0)	
Time since transplantation, months (IQR)		40 (31-47)	48 (26-53)	0.47		32 (12-36)	44 (35-47)	**0.002**
Immunosuppressive treatment, n (%)				0.47				0.70
CE		5 (16)	0 (0)			2 (25)	3 (13)	
TAC		2 (6)	0 (0)			0 (0)	2 (8)	

(Continued)

10.3389/fimmu.2024.1479472

TABLE 1 Continued

Characteristics	HC (n=25)	IP-S^{POS} (n=32)	IP-S^{NEG} (n=6)	P-value	HC (n=25)	IP-S^{POS}VL^{POS} (n=8)	IP-S^{POS}VL^{NEG} (n=24)	P-value
CE+TAC		22 (69)	6 (100)			5 (63)	17 (71)	
CE+TAC+MMF		3 (9)	0 (0)			1 (13)	2 (88)	
TAC blood levels, ng/ml (IQR)		3.4 (2.7-4.5)	4.4 (3.8-6.7)	0.07		4.1 (3.3-6.5)	3.3 (2.4-4.4)	0.18
EVB-serology pre-transplantation, n (%)				**0.03**				0.65
Positive		14 (56)	0 (0)			4 (50)	10 (42)	
Negative		13 (52)	6 (100)			2 (25)	11 (46)	
CMV-serology pre-transplantation, n (%)				0.66				>0.99
Positive		15 (47)	2 (33)			4 (50)	11 (46)	
Negative		14 (44)	4 (67)			3 (38)	11 (46)	
PTLD diagnosis, n (%)		5 (16)	0 (0)	0.57		2(25)	3(13)	0.58
Time since diagnosis of PTLD, days (IQR)		35 (12-133)	NA	NA		8 (6-10)	133 (84-311)	0.20
Lymphocyte number x10^3, cells/µL (IQR)		3.0 (2.4-3.9)	4.0 (2.9-4.3)	0.24		2.7 (2.2-3.3)	3.0 (2.4-4.7)	0.48
Immune phenotype, % (IQR)								
CD3+ T lymphocytes		78 (72-85)	72 (65-76)	0.20		74 (69-76)	83 (75-87)	0.11
CD4+ T lymphocytes		45 (38-55)	42 (37-49)	0.55		46 (34-55)	43 (39-56)	>0.99
CD8+ T lymphocytes		22 (17-30)	21 (12-29)	0.41		18 (14-28)	24 (20-36)	0.20
B lymphocytes		8 (6-14)	11 (8-14)	0.55		15 (7-20)	7 (5-9)	0.11
NK lymphocytes		10 (6-16)	19 (10-23)	0.13		13 (8-17)	7 (5-16)	0.33
NKT lymphocytes		0.7 (0.6-1.8)	0.6 (0.5-0.9)	0.20		0.8 (0.5-2.5)	0.7 (0.6-1.8)	0.80

CE, corticosteroids; CMV, Cytomegalovirus; EVB, Epstein-Barr virus; HC, healthy controls; IQR, interquartile range; MMF, mycophenolate mofetil; NA, not applicable; NK, natural killer; NKT, natural killer T; PTLD, post-transplant lymphoproliferative disorder; TAC, tacrolimus.
Statistically significant p-values are indicated in bold.

10.3389/fimmu.2024.1479472

Wilcoxon signed-rank test. Correlation between ICS and AIMS results was assessed by linear regression. P-values under 0.05 were considered significant.

3 Results

3.1 Demographic and clinical characteristics

A first classification of our cohort (n=38) was performed according to EBV serological status: IP-S^{NEG} (6/38, 16%) and IP-S^{POS} (32/38, 84%). A second distribution of EBV-seropositive patients (n=32) was made according to EBV viral loads: IP-$S^{POS}VL^{POS}$ (8/32, 25%) and IP-$S^{POS}VL^{NEG}$ (24/32, 75%).

First analysis of our cohort (Table 1) showed statistically significant differences when comparing age (HC adults vs. IP) and EBV-serology pre-transplantation (seropositive vs. seronegative). Interestingly, 52% of post-transplant EBV seropositive patients were negative pre-transplantation. When time since transplantation was analyzed, we observed that IP with positive EBV viral loads had been more recently transplanted (IP-$S^{POS}VL^{POS}$ 32 months IQR 12-36 vs. IP-$S^{POS}VL^{NEG}$ 44 months IQR 35-47, p=0.002). Percentages of T, B and NK subpopulations were similar among groups (Table 1).

3.2 EBV-specific T-cell response by intracellular cytokine staining

At first visit, EBV-specific %CD3+ T cells by ICS was higher in HC than IP groups (IP-S^{NEG} 0.03% vs. IP-S^{POS} 0.04% and HC 0.06%; p=0.41 and p=0.24, respectively), but differences did not reach statistical signification. Nonetheless, all three groups showed similar positive-control stimulation (IP-S^{NEG} 0.75%, IP-S^{POS} 0.79% and HC 0.45%; p=0.08), indicating that cellular response *in vitro* was not impaired by immunosuppression. Positive-control responses remained comparable when dividing mono/polyfunctional CD4+ and CD8+ T-cell subpopulations (data not shown).

However, when splitting EBV-specific response between T-cell subpopulations (Figure 1A), statistically significant differences were observed. Median frequency of monofunctional CD4+ and CD8+ T cells was higher than polyfunctional cells in all groups (Figure 1A). Interestingly, although monofunctional responses were detected in higher frequencies, only polyfunctional CD8+ T cells significantly discriminated EBV seronegative patients from seropositive HC and IP groups (IP-S^{NEG} 0.00% vs. IP-S^{POS} 0.04% and HC 0.02%; p=0.01 and p<0.001, respectively; Figure 1A).

For a more detailed analysis, the different EBV-specific CD8+ T-cell profiles were analyzed (Figures 1B, C). Three different CD8+ polyfunctional profiles differentiated seronegative recipients from both HC and IP seropositive individuals: CD8+CD107a+IFNɣ+IL2+TNFα+, CD8+CD107a+IFNɣ+IL2-TNFα+ and CD8+CD107a-IFNɣ+IL2-TNFα+ (Figure 1B). Furthermore, seropositive IP had higher frequencies of EBV-specific CD8+ polyfunctional cells than seronegative IP in two other subsets: CD8+CD107a+IFNɣ+IL2-TNFα- and CD8+CD107a+IFNɣ-IL2-TNFα+. The profile CD8+CD107a+IFNɣ+IL2-TNFα- was the most frequent one (0.13%).

Precisely, this CD8+CD107a+IFNɣ+IL2-TNFα- subset significantly discriminated patients with positive viral loads from the rest of individuals (IP-$S^{POS}VL^{POS}$ 0.43% vs. IP-$S^{POS}VL^{NEG}$ 0.07% and HC 0.03%; p=0.03 and p=0.001, respectively; Figure 1C). IP-$S^{POS}VL^{POS}$ patients also showed higher %CD8+CD107a+IFNɣ-IL2+TNFα- compared to HC, but not to IP-$S^{POS}VL^{NEG}$ group (Figure 1C). Remarkably, polyfunctional response was more intense than monofunctional response in seropositive individuals (Supplementary Table S1). All three cytokine markers IFNɣ, IL2 and TNFα had significantly higher iMFI values in polyfunctional response, both in CD4+ and CD8+ T cells, whereas CD107a only showed higher intensity in polyfunctional CD8+ T cells (Supplementary Table S1). In line with our previous results, CD8+ polyfunctional subpopulation allowed discriminating seropositive from seronegative status, according to iMFI from all four response markers (Table 2). However, regarding EBV viral load, only total (mono and polyfunctional) CD107a iMFI on CD8+ T cells significantly differentiated IP with positive viral loads from the other groups (IP-$S^{POS}VL^{POS}$ 123,398 vs. IP-$S^{POS}VL^{NEG}$ 20,708 and HC 21,207; p=0.03 and p=0.01, respectively).

To simplify cytometry panels, we studied whether CD8+ T cells expressing only CD107a and IFNɣ markers could be distinctive, regardless of other cytokines. As expected, %CD8+CD107a+IFNɣ+ T cells were significantly higher among seropositive individuals compared to seronegative IP (IP-S^{NEG} 0.02% vs. IP-S^{POS} 0.37% and HC 0.12%; p=0.002 and p=0.04, respectively). However, considering EBV viral load, although the frequency of specific cells was also increased within positive IP group, differences were significant compared to controls, but not to negative patients (IP-$S^{POS}VL^{POS}$ 0.70% vs. IP-$S^{POS}VL^{NEG}$ 0.19% and HC 0.12%; p=0.10 and p=0.03, respectively).

Finally, we explored whether CD3+IFNɣ+ T cells, the main population targeted by other methods, allowed discrimination of serology and/or viral-load status. While frequency of CD3+IFNɣ+ T cells was insufficient for serology discrimination (IP-S^{NEG} 0.10% vs. IP-S^{POS} 0.31% and HC 0.12%; p=0.31 and p>0.99, respectively), iMFI was significantly higher in seropositive than seronegative individuals (IP-S^{NEG} 182 vs. IP-S^{POS} 3,628 and HC 1,380; p=0.003 and p=0.01, respectively). When comparing viral-load status no statistically differences were reached either with CD3+IFNɣ+ frequency (IP-$S^{POS}VL^{POS}$ 0.37% vs. IP-$S^{POS}VL^{NEG}$ 0.24% and HC 0.12%; p>0.99 and p=0.40, respectively) or iMFI (IP-$S^{POS}VL^{POS}$ 3,834 vs. IP-$S^{POS}VL^{NEG}$ 2,809 and HC 1,380; p=0.62 and p=0.82, respectively).

3.3 EBV-specific T cell response by activation-induced cell marker staining

At first visit, differences were found in EBV-specific T-cell frequencies by AIMS between HC and IP groups (Figures 2A, B). As expected, CD4+ Tn EBV-specific subset was the lowest within each group, compared to Teff and memory compartment (Figures 2A, B). On the other hand, seropositive groups (Figure 2A) had higher frequency of EBV-specific memory compartment than Teff cells (IP-S^{POS} memory compartment 0.99% vs. Teff 0.04%, p=0.12; HC memory compartment 8.24% vs. Teff 0.37%, p<0.001), although differences were statistically significant only within HC group. Interestingly,

10.3389/fimmu.2024.1479472

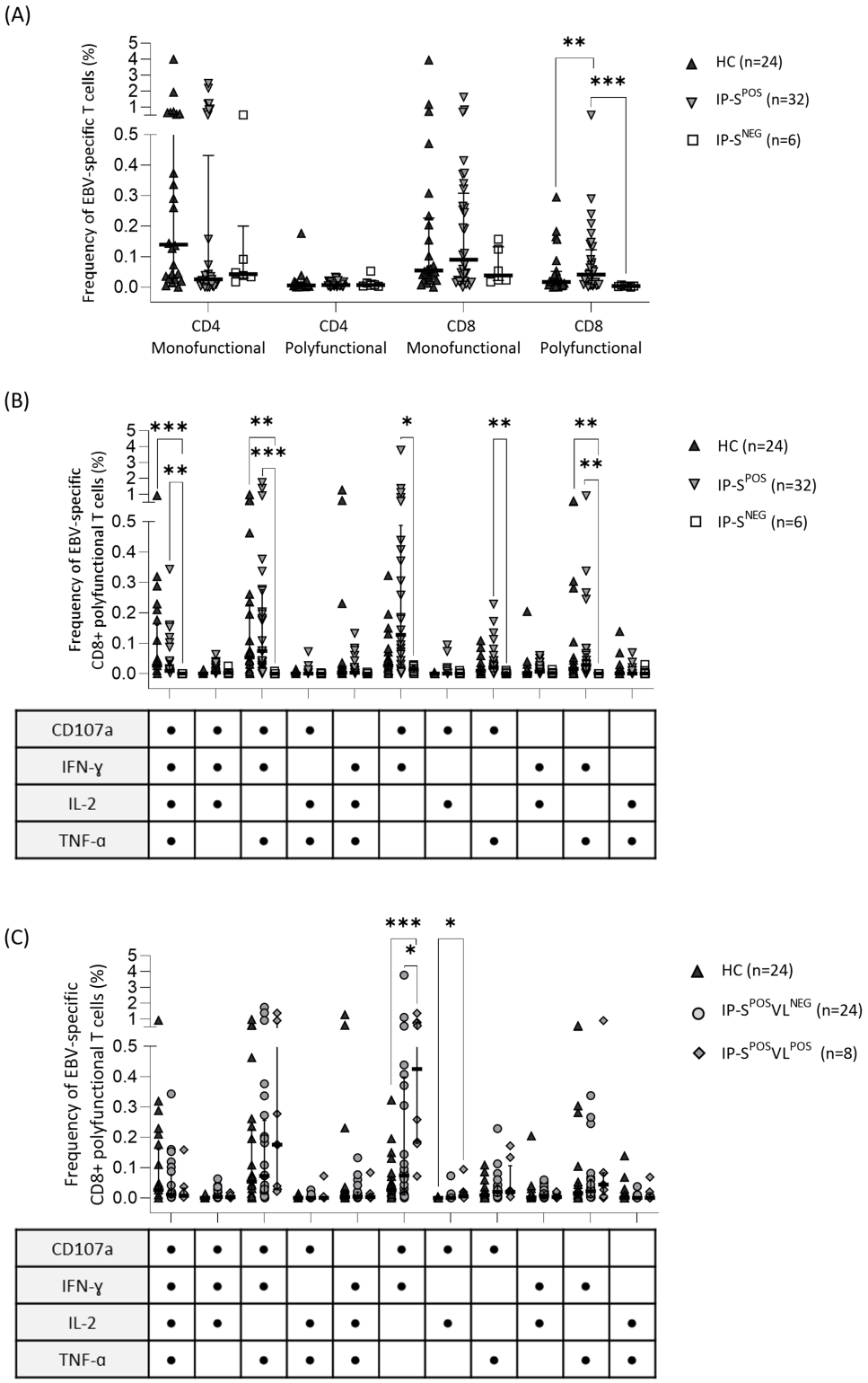

FIGURE 1
Specific T-cell response to Epstein-Barr virus (EBV) performed by intracellular cytokine staining of CD107a, IFNɣ, IL2 and TNFα markers in EBV seropositive healthy adult controls (HC) and immunosuppressed pediatric liver recipients (IP). **(A)** Median frequency of EBV-specific monofunctional (one response marker) or polyfunctional (more than one response markers) CD4+ and CD8+ T cells in HC and IP groups, the last one categorized according to their positive/negative serological status (IP-S^{POS} and IP-S^{NEG}, respectively). **(B)** Median frequency of EBV-specific polyfunctional CD8+ T-cell subpopulations according to the different response markers in HC, IP-S^{POS} and IP-S^{NEG} groups. **(C)** Median frequency of EBV-specific polyfunctional CD8+ T-cell subpopulations in HC and IP-S^{POS} groups, the last one segregated according to their positive/negative EBV viral-load status (IP-$S^{POS}VL^{POS}$ and IP-$S^{POS}VL^{NEG}$, respectively). The same HC group was used as the control group in panels **(A–C)**. Significance levels are denoted as *p-value<0.05, **p-value<0.01 and ***p-value<0.001.

10.3389/fimmu.2024.1479472

TABLE 2 Median of the integrated median fluorescence intensity (iMFI) for each marker (CD107a, IFNɣ, IL2 or TNFα) in both polyfunctional CD4+ and CD8+ T cells in EBV-seropositive adult healthy controls (HC) and immunosuppressed pediatric liver-transplanted patients, categorized as positive/negative serology status (IP-S^{POS} and IP-S^{NEG}, respectively) or positive/negative viral load status (IP-$S^{POS}VL^{POS}$ and IP-$S^{POS}VL^{NEG}$, respectively).

iMFI		HC (n=24)	IP-S^{POS} (n=32)	IP-S^{NEG} (n=6)	P-value	HC (n=24)	IP-$S^{POS}VL^{POS}$ (n=8)	IP-$S^{POS}VL^{NEG}$ (n=24)	P-value
T-cell subset	Parameter								
Polyfunctional CD4+ T cells	CD107a+	1,060	1,813	2,588	0.43	1,060	2,651	1,813	0.35
	IFNɣ+	475	179	49	0.07	475	181	179	0.13
	IL2+	122	93	237	0.69	122	95	93	0.93
	TNFα+	1,248	1,422	1,838	0.84	1,248	1,705	1422	0.85
Polyfunctional CD8+ T cells	CD107a+	17,538	42,771	373	**0.002**	17,538	105,001	18,628	**0.03**
	IFNɣ+	3,366	7,714	36	**0.002**	3,366	10,042	5,228	0.34
	IL2+	377	424	0	**0.001**	377	329	488	1.00
	TNFα+	7,370	8,307	0	**0.001**	7,370	11,509	7,391	0.86

Statistically significant p-values are indicated in bold.

seronegative IP showed higher frequencies of Teff than memory EBV-specific cells (memory compartment 0.00% vs. Teff 0.25%, p=0.14), although differences did not reach statistical signification.

Compared to IP seronegative group, percentages of EBV-specific cells were higher in HC group for Tn (0.14% vs. IP-S^{NEG} 0.00%, p=0.03), Tem (4.31% vs. IP-S^{NEG} 0.00%, p=0.01) and Tcm (4.33% vs. IP-S^{NEG} 0.00%, p=0.002) subpopulations (Figure 2A). However, comparing frequencies between seropositive and seronegative IP did not yield any statistically significant differences. Again, positive-control stimulation in CD4+ T cells was comparable by AIMS (IP-S^{NEG} 24.52%, IP-S^{POS} 32.67% and HC 26.42%; p=0.62).

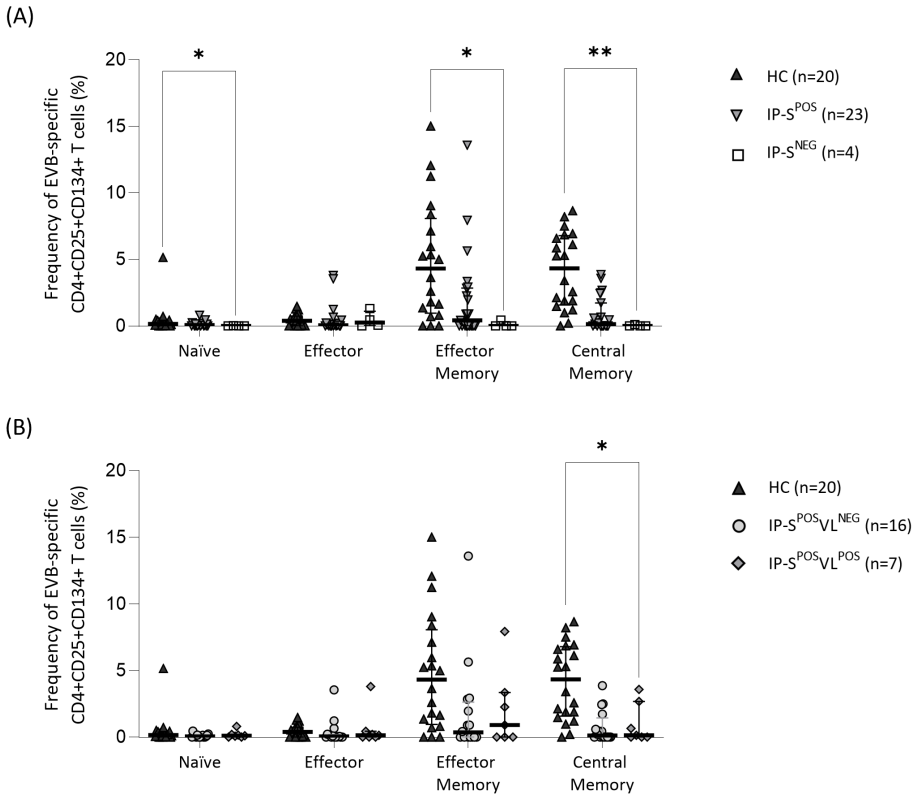

FIGURE 2
Specific T-cell response to Epstein-Barr virus (EBV) performed by activation-induced marker staining (CD4+CD25+CD134+) in EBV seropositive healthy adult controls (HC) and immunosuppressed pediatric liver recipients (IP). **(A)** Median frequency of EBV-specific CD4+CD25+CD134+ T cells in HC and IP groups, the last one categorized according to their positive/negative serological status (IP-S^{POS} and IP-S^{NEG}, respectively). **(B)** Median frequency of EBV-specific CD4+CD25+CD134+ cells in HC and IP-S^{POS} groups, the last one segregated according to positive/negative EBV viral-load status (IP-$S^{POS}VL^{POS}$ and IP-$S^{POS}VL^{NEG}$, respectively). The same HC group was used as the control group in both panels **(A, B)**. Significance levels are denoted as *p-value<0.05, **p-value<0.01 and ***p-value<0.001.

We next studied seropositive IP grouped by viral-load status (Figure 2B) and observed that %CD4+ Tcm cells was significantly higher in HC than seropositive IP with detectable EBV (IP-$S^{POS}VL^{POS}$ Tcm 0.13% vs. HC Tcm 4.32%, p=0.02). Interestingly, median %CD4+ Tem cells in seropositive IP-$S^{POS}VL^{POS}$ was higher than in IP-$S^{POS}VL^{NEG}$ (0.90% vs. 0.34%, respectively; p>0.99), although no significant differences were found.

Finally, we further investigated the potential correlation between the parameters defined by ICS (%CD8+CD107a+IFNɣ+IL2-TNFα-) and AIMS (%CD4+CD134+CD25+ Tcm), which effectively distinguished positive from negative individuals. We noted that those parameters exhibited no correlation (data not shown), likely due to the comparison involving distinct T-cell subpopulations. Thus, a potential correlation between EBV-specific CD4+ T cells by ICS (% and iMFI CD4+INFɣ) and AIMS (%CD4+CD134+CD25+ Tcm) techniques was next sought, although we did not observe any correlation, by either frequency or iMFI (data not shown). However, within HC group, after excluding the data from one individual lacking EBV-specific CD4+ CD134+CD25+ memory T cells, a significant correlation between iMFI CD4+INFɣ by ICS and %CD4+CD134+CD25+ by AIMS (r^2 = 0.24 and p=0.04, Figure 3) was found.

3.4 EBV-specific T cell response at two different timepoints

EBV-specific response was measured on a second visit by both techniques. Serological and viral-load status was re-evaluated and patients were reclassified accordingly. Tacrolimus blood levels remained similar at first and second timepoints in all three groups (data not shown).

At the second timepoint, identical results to those reported at the first visit were found when comparing frequencies of EBV-specific cells detected by ICS and AIMS. We confirmed that only polyfunctional CD8+ specific T cells significantly discriminated EBV seronegative patients from seropositive individuals (IP-S^{NEG} 0.00% vs. IP-S^{POS} 0.03% and HC 0.02%; p=0.01 and p=0.02, respectively). Likewise, %EBV-specific cells from HC were higher than those detected in seronegative patients for Tn (0.14% vs. 0.01%, p=0.05), Tem (4.31% vs. 0.00%, p=0.01) and Tcm (4.33% vs. 0.00%, p=0.003) subpopulations.

Regarding IP-$S^{POS}VL^{POS}$ group, all recipients with detectable EBV at first timepoint cleared viral loads at the second visit (median time 3.5 months IQR 2.2-5.3 between timepoints). Consequently, median % CD8+CD107a+IFNɣ+IL2-TNFα- (first visit 0.26% vs. second visit 0.10%, p=0.81; Figure 4A) and %CD4+CD25+CD134+ Tcm cells (first visit 0.39% vs. second visit 0.14%, p=0.88; Figure 4B) decreased at the second timepoint, although no significant differences were found.

On the other hand, only two IP-$S^{POS}VL^{NEG}$ patients at first timepoint had detectable EBV at the second visit (black arrows in Figures 4C, D) (median time 3.7 months IQR 3.3-4.8 between timepoints). Interestingly, significant differences were found by ICS (first visit 0.08% vs. second visit 0.06%, p=0.04; Figure 4C), but not by AIMS (first visit 0.00% vs. second visit 0.76%, p=0.31; Figure 4D). Frequency of CD8+CD107a+IFNɣ+IL2-TNFα- cells decreased or remained similar for all patients, except for the individual who tested positive for EBV at the second visit, whose frequency increased from 0.06% to 0.09% (black arrow in Figure 4C). This patient's frequency of specific CD4+CD25+CD134+ Tcm cells also increased from 0.00% to 1.06% (black arrow in Figure 4D). Nevertheless, that variation in the specific response by AIMS was not observed in the other patient who tested positive for viral load at the second timepoint (black arrow in Figure 4D). One IP-$S^{POS}VL^{NEG}$ patient had his immunosuppression regimen changed between visits, incorporating mycophenolate to his treatment with corticosteroids and tacrolimus. Interestingly, frequency

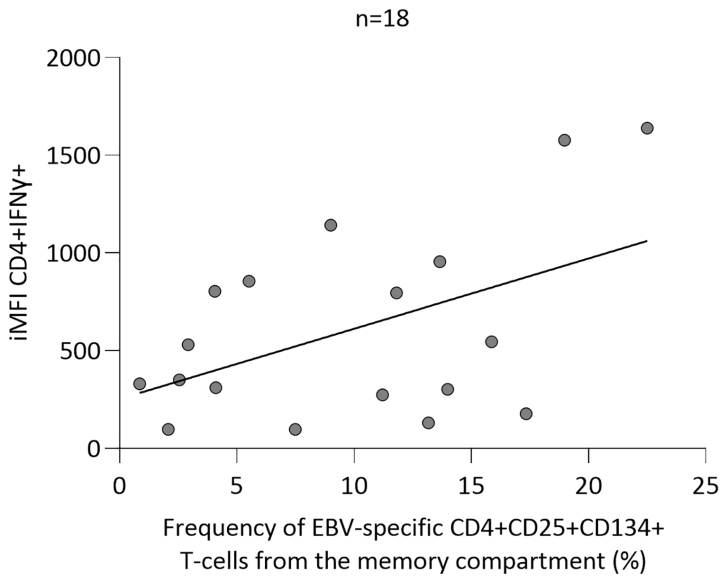

FIGURE 3
Linear regression analysis between integrated median fluorescence intensity (iMFI) of Epstein-Barr virus (EBV)-specific CD4+IFNɣ+ T cells measured by intracellular cytokine staining and EBV-specific CD4+CD25+CD134+ central memory T (Tcm) cells measured by activation-induced marker staining.

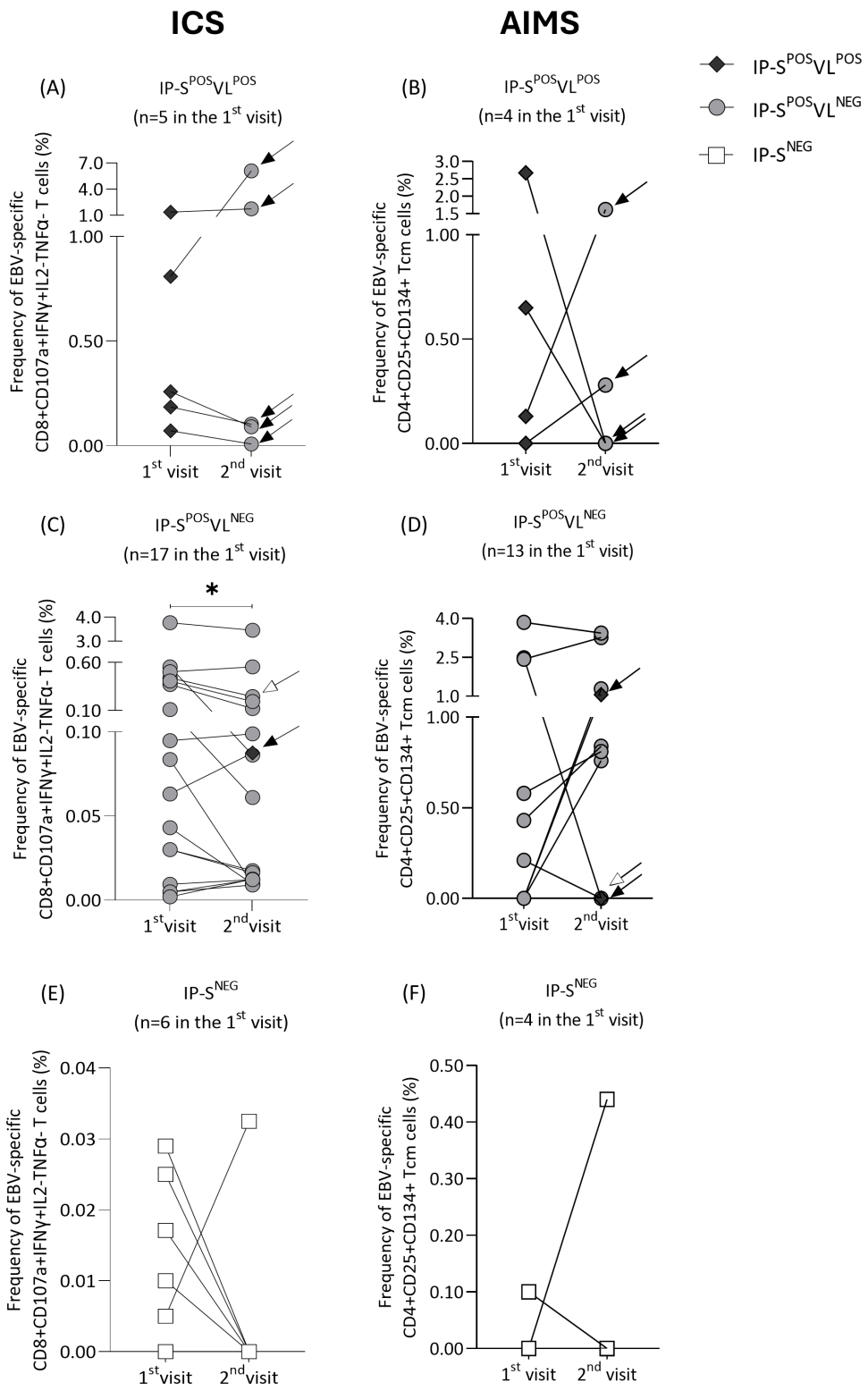

FIGURE 4
Frequency of Epstein-Barr virus (EBV)-specific CD8+CD107a+IFNɣ+IL2-TNFα- T cells **(A, C, E)** and CD4+CD25+CD134+ central memory T (Tcm) cells **(B, D, F)** measured at two different timepoints (1st and 2nd visit) in immunosuppressed pediatric liver recipients (IP). Patients were classified at their first visit according to their positive/negative EBV serological and viral-load status: IP-$S^{POS}VL^{POS}$ **(A, B)**, IP-$S^{POS}VL^{NEG}$ **(C, D)** and IP-S^{NEG} **(E, F)** groups. At the second visit, their updated serological and viral-load status is represented by rhomboid, circular or square markers, respectively. Changes in their classification at second visit are marked with a black arrow. Patients that suffered changes in his immunosuppression regimen at second visit are marked with a white arrow. Significance levels are denoted as *p-value<0.05, **p-value<0.01 and ***p-value<0.001.

of EBV-specific T cells by ICS decreased from 0.44% to 0.25%, while frequency of CD4+CD25+CD134+ Tcm cells remained at 0.00% (white arrows in Figures 4C, D).

Finally, all seronegative patients (Figures 4E, F) kept their negative serological status at the second visit (median time of 3.9 months IQR 3.6-4.0 between timepoints). Consequently, no differences in EBV-specific response were found, either by ICS (0.01% vs. 0.00%, p=0.44; Figure 4E) or AIMS (0.00% vs. 0.00%, p>0.99; Figure 4F).

4 Discussion

In our study, we have first explored EBV-specific T-cell response combining ICS and AIMS techniques in a cohort of pediatric liver transplanted recipients. We found significant differences in polyfunctional CD8+ T-cell response between EBV-seronegative and seropositive individuals, and among patients with positive and negative viral loads.

Firstly, we found higher percentages of monofunctional than polyfunctional EBV-specific T cells. This could be attributed to cross-reactivity resulting from heterologous immunity (55), although recent studies state that it is less generalized than previously reported (56). Since we have also confirmed that monofunctional responses showed lower iMFI (49), we can attribute this result to a potential unspecific bystander activation *in vitro*. The presence of monofunctional EBV-specific cells among seronegative patients provides additional support for that hypothesis.

The predominance of CD8+ over CD4+ T-cell responses in controlling EBV infection is well documented (49, 57). Although both CD4+ and CD8+ T cells show polyfunctional responses after primary infection, only the CD8+ polyfunctional subset increases over time (58). Accordingly, we observe that polyfunctional CD8+ T cells are significantly increased in seropositive individuals (Figure 1B). Remarkably, we expected a reduction in the frequency of this population in patients with detectable viral loads, in concordance with Ning et al., who demonstrated this in two pediatric liver recipients with PTLD (49). Conversely, IP-$S^{POS}VL^{POS}$ in our cohort showed high %CD8+ EBV-specific cells (Figure 1C), including 2 patients who were studied at the time of PTLD diagnosis.

The increment of CD8+CD107a+IFNɣ+IL2-TNFα- in recipients with detectable EBV viral loads reflects the critical role of cytotoxicity, as indicated by CD107a, and the antiviral function of IFNɣ in the response against EBV. Frequent EBV reactivation might inflate this cell compartment, exhausting and rendering cells dysfunctional, thus requiring larger numbers to control the virus (59). Previously suggested explanation for pediatric graft recipients carrying chronically high EBV loads involves an exhausted phenotype (23). We did not include exhaustion markers in our study, but we consider that they would be useful to better describe viral responses in future investigations. Other protocols, such as expanding T cells in the presence of EBV peptides for 7-10 days before analysis (60), could also be applied. However, we chose shorter incubation times (54), as this approach was more compatible with the workflow of our routine laboratory.

We further evaluated CD107a combined with IFNɣ, as exclusive response markers to distinguish patients with positive viral loads. While %CD8+CD107a+IFNɣ+ helped in serostatus discrimination, it did not show significant differences in EBV viral loads, likely due to our limited sample size. Similar results were reported by Wilsdorf et al., who measured intracellular IFNɣ after EBV-peptide stimulus in pediatric transplanted patients with PTLD (4/16 liver-graft recipients) or positive viral-loads (3/4 liver-graft recipients) and 18 HC. Median %CD4+IFNɣ+ and %CD8+IFNɣ+ was higher in recipients with EBV reactivation, yet they did not find significant differences either (50).

In our cohort, %CD3+IFNɣ+ cells do not differentiate seropositive from seronegative patients, contrary to prior studies using ELISpot (47). Instead, we found that the intensity of IFNɣ response in CD3+ T cells effectively differentiated these two groups. While no equivalent parameter to iMFI has been described in ELISpot assays, mean spot size could be comparable (61). Our findings may be influenced by the constraints of our sample size, but conducting additional studies to explore iMFI further would be valuable.

On the other hand, the use of AIMS to measure specific viral response is not extended, although it has been validated in HC for Varicella-Zoster Virus, Cytomegalovirus, EBV (44) and Hepatitis C (43). Regarding EBV, it seems feasible to distinguish seronegative from seropositive individuals measuring %CD4+CD134+CD25+ specific-cells (44). We confirmed these findings by examining Tcm and Tem CD4+ subsets, consistent with the predominant memory CD4+ response to EBV (62). Interestingly, we detected specific CD4+ Teff cells in seronegative individuals, probably reflecting antigen exposure in some patients (63), although we cannot exclude unspecific activation, since percentages were similar among groups. The increase of EBV-specific CD4+ Tn in HC (Figure 1A) has been previously reported as a genuine memory population transitioning to express naïve surface markers (62). This stem memory T-cell population (CCR7+CD27+CD45RO-) shares some features with Tn and requires staining with specific markers (CD95) for proper selection (64). These cells emerge rapidly post-antigen exposure, transitioning into effector cells, while retaining self-renewal and multipotent abilities, making them ideal for adoptive T-cell therapies, including EBV infection in transplant recipients (65, 66).

Due to the age gap, memory response in HC is the highest, reflecting repeated exposures to EBV antigens over their lifetimes, which expands the clonal repertoire against the virus (23). Interestingly, Tem specific subset is increased in patients with active viral replication, consistent with findings by Amyes et al. (67). They observed a primary burst of CD4+ Teff cells in response to EBV, persisting throughout the chronic phase of infection. However, our stimulation with a cocktail of lytic and latent EBV peptides does not differentiate between viral phases (58, 67).

Regarding correlation between ICS and AIMS, Sadler et al. demonstrated that EBV-specific production of IFNɣ significantly correlated with %CD4+CD134+CD25+ cells in HC (44). While we did not replicate this result, we found %CD4+CD134+CD25+ cells from memory compartment correlated with CD4+ response measured by IFNɣ iMFI, confirming AIMS reliability to infer specific CD4+ T-cell response. Further studies on CD8+ T-cell activation markers, such as CD38 and HLA-DR (44), are recommended.

At the second visit, we confirmed that polyfunctional CD8+ EBV-specific T-cell response detects serology and viral-load positive

individuals. Furthermore, we replicated our findings on CD4+ Tcm population in adults. Compared to first visit, we observed changes in EBV-specific cellular response among patients with viral-load status shifts, significant in the largest sample group (Figure 4C). Interestingly, tacrolimus blood levels remained similar between visits, questioning the effect of immunosuppression treatment. Positive control stimulus elicited a similar reaction in HC and immunosuppressed patients, suggesting that anti-CD3/28 beads override immunosuppression. Similarly, Arasaratnam et al. found comparable IFNɣ production by Staphylococcal enterotoxin B in pediatric liver recipients post-immunosuppression (45).

On the other hand, other authors observed that immunosuppression treatment modifications for PTLD management lead to changes in frequency of EBV-specific cells detected by ELISpot (45–47). Moreover, OX40 has been postulated as an indicator of the immunosuppressive status of patients after stem cell transplantation (68), although Lamb et al. reported a recipient of stem cell transplantation whose changes in the immunosuppressive treatment did not reflect differences in %CD4+CD134+ cells (69). To elucidate the potential use of ICS or AIMS in evaluating immunosuppressive status of transplanted patients further prospective studies are needed.

In conclusion, our study reveals significant insights into EBV-specific T-cell responses in pediatric liver transplant recipients. We demonstrated that polyfunctional CD8+ T cells were markedly increased in seropositive individuals, underscoring their role in controlling EBV infection. Despite a limited sample size, our findings support the utility of CD107a/IFNɣ response markers for distinguishing EBV serostatus and viral load. Additionally, OX40 proved reliable in assessing CD4+ memory responses, suggesting its potential for broader application in evaluating antiviral immunity. Further prospective research is recommended to refine our understanding of EBV-specific T-cell dynamics in transplant recipients.

Data availability statement

The original contributions presented in the study are included in the article/Supplementary Material. Further inquiries can be directed to the corresponding author.

Ethics statement

The studies involving humans were approved by University Hospital La Paz ethics committee. The studies were conducted in accordance with the local legislation and institutional requirements. Written informed consent for participation in this study was provided by the participants' legal guardians/next of kin.

Author contributions

RC: Conceptualization, Data curation, Investigation, Methodology, Writing – original draft, Writing – review & editing. AT: Investigation, Methodology, Writing – review & editing. LM: Investigation, Methodology, Writing – review & editing. KR: Investigation, Methodology, Writing – review & editing. EF: Writing – review & editing, Conceptualization, Investigation. LH: Writing – review & editing, Conceptualization, Investigation. GM: Writing – review & editing, Investigation. ML: Writing – review & editing, Investigation. AG: Writing – review & editing, Methodology. AM: Writing – review & editing, Investigation. EL: Supervision, Writing – original draft, Writing – review & editing, Conceptualization, Investigation. ES: Supervision, Writing – original draft, Writing – review & editing, Conceptualization, Investigation.

Funding

The author(s) declare financial support was received for the research, authorship, and/or publication of this article. This work was supported by FIS (ISCIII) grant no. PI19-01311.

Acknowledgments

The authors are grateful to all participating patients and their families. They would also like to express their appreciation to Teresa Plaza, Amaya Iturralde, Sergio Ruiz, Natividad Herraiz and Concepción Esteban, for their excellent technical assistance. This study has been funded by Instituto de Salud Carlos III (ISCIII) through the project "PI19-01311" and co-funded by the European Union.

Conflict of interest

The authors declare that the research was conducted in the absence of any commercial or financial relationships that could be construed as a potential conflict of interest.

The author(s) declared that they were an editorial board member of Frontiers, at the time of submission. This had no impact on the peer review process and the final decision.

Publisher's note

Supplementary material

The Supplementary Material for this article can be found online at: https://www.frontiersin.org/articles/10.3389/fimmu.2024.1479472/full#supplementary-material

SUPPLEMENTARY FIGURE 1
Flow-cytometry gating strategy for **(A)** intracellular cytokine staining or **(B)** activation-induced marker staining in a representative healthy control. Cells were left unstimulated (NC) or stimulated using a positive control (PC) or Epstein-Barr virus peptides (EBV).

References

1. Jain A, Mazariegos G, Kashyap R, Kosmach-Park B, Starzl TE, Fung J, et al. Pediatric liver transplantation. A single center experience spanning 20 years. *Transplant*. (2002) 73:941–7. doi: 10.1097/00007890-200203270-00020

2. Jara P, Hierro L. Trasplante hepático infantil. Resultados a largo plazo. *Gastroenterol Hepatol*. (2010) 33:398–410. doi: 10.1016/j.gastrohep.2009.11.004

3. Fishman JA. Infection in organ transplantation. *Am J Transplant*. (2017) 17:856–79. doi: 10.1111/ajt.14208

4. Roberts MB, Fishman JA. Immunosuppressive agents and infectious risk in transplantation: managing the "Net state of immunosuppression. *Clin Infect Dis*. (2021) 73:e1302–17. doi: 10.1093/cid/ciaa1189

5. Domhan S, Zeier M, Abdollahi A. Immunosuppressive therapy and post-transplant Malignancy. *Nephrol Dial Transplant*. (2008) 24:1097–103. doi: 10.1093/ndt/gfn605

6. Huang W, Bai L, Tang H. Epstein-Barr virus infection: the micro and macro worlds. *Virol J*. (2023) 20:220. doi: 10.1186/s12985-023-02187-9

7. Green M, Webber S. Posttransplantation lymphoproliferative disorders. *Pediatr Clin North Am*. (2003) 50:1471–91. doi: 10.1016/S0031-3955(03)00127-5

8. Martinez OM, Krams SM. The immune response to epstein barr virus and implications for posttransplant lymphoproliferative disorder. *Transplant*. (2017) 101:2009–16. doi: 10.1097/TP.0000000000001767

9. Eshraghian A, Imanieh MH, Dehghani SM, Nikeghbalian S, Shamsaeefar A, Barshans F, et al. Post-transplant lymphoproliferative disorder after liver transplantation: Incidence, long-term survival and impact of serum tacrolimus level. *WJG*. (2017) 23:1224. doi: 10.3748/wjg.v23.i7.1224

10. Taylor AL, Marcus R, Bradley JA. Post-transplant lymphoproliferative disorders (PTLD) after solid organ transplantation. *Crit Rev Oncol/Hematol*. (2005) 56:155–67. doi: 10.1016/j.critrevonc.2005.03.015

11. Trottier H, Buteau C, Robitaille N, Duval M, Tucci M, Lacroix J, et al. Transfusion-related Epstein-Barr virus infection among stem cell transplant recipients: a retrospective cohort study in children. *Transfusion*. (2012) 52:2653–63. doi: 10.1111/j.1537-2995.2012.03611.x

12. Green M, Michaels MG. Epstein–barr virus infection and posttransplant lymphoproliferative disorder. *Am J Transplant*. (2013) 13:41–54. doi: 10.1111/ajt.12004

13. San-Juan R, Comoli P, Caillard S, Moulin B, Hirsch HH, Meylan P. Epstein-Barr virus-related post-transplant lymphoproliferative disorder in solid organ transplant recipients. *Clin Microbiol Infect*. (2014) 20:109–18. doi: 10.1111/1469-0691.12534

14. Barış Z, Özçay F, Yılmaz Özbek Ö, Haberal N, Sarıalioğlu F, Haberal M. A single-center experience of post-transplant lymphoproliferative disorder (PTLD) cases after pediatric liver transplantation: Incidence, outcomes, and association with food allergy. *Turk J Gastroenterol*. (2018) 29:354–60. doi: 10.5152/tjg.2018.17731

15. Quintero Bernabeu J, Juamperez J, Mercadal-Hally M, Larrarte King M, Gallego Melcon S, Gros Subias L, et al. Epstein–Barr virus-associated risk factors for post-transplant lymphoproliferative disease in pediatric liver transplant recipients. *Pediatr Transplant*. (2022) 26(6):e14292. doi: 10.1111/petr.14292

16. Wu JF, Ho MC, Ni YH, Chen HL, Lu CY, Hsu HY, et al. Timing of epstein-barr virus acquisition and the course of posttransplantation lymphoproliferative disorder in children. *Transplant*. (2009) 87:758–62. doi: 10.1097/TP.0b013e318198d645

17. Baker A, Frauca Remacha E, Torres Canizales J, Bravo-Gallego LY, Fitzpatrick E, Alonso Melgar A, et al. Current practices on diagnosis, prevention and treatment of post-transplant lymphoproliferative disorder in pediatric patients after solid organ transplantation: results of ERN transplant Child healthcare working group survey. *Children*. (2021) 8:661. doi: 10.3390/children8080661

18. Allen UD, Preiksaitis JK. The AST Infectious Diseases Community of Practice. Post-transplant lymphoproliferative disorders, Epstein-Barr virus infection, and disease in solid organ transplantation: Guidelines from the American Society of Transplantation Infectious Diseases Community of Practice. *Clin Transplant*. (2019) 33(9):e13652. doi: 10.1111/ctr.13652

19. Green M, Soltys K, Rowe DT, Webber SA, Mazareigos G. Chronic high Epstein-Barr viral load carriage in pediatric liver transplant recipients. *Pediatr Transplant*. (2009) 13:319–23. doi: 10.1111/j.1399-3046.2008.00926.x

20. Abate D, Saldan A, Fiscon M, Cofano S, Paciolla A, Furian L, et al. Evaluation of Cytomegalovirus (CMV)–Specific T Cell Immune Reconstitution Revealed That Baseline Antiviral Immunity, Prophylaxis, or Preemptive Therapy but not Antithymocyte Globulin Treatment Contribute to CMV-Specific T Cell Reconstitution in Kidney Transplant Recipients. *J Infect Dis*. (2010) 202:585–94. doi: 10.1086/654931

21. Calarota SA, Chiesa A, Zelini P, Comolli G, Minoli L, Baldanti F. Detection of Epstein-Barr virus-specific memory CD4 $^{+}$ T cells using a peptide-based cultured enzyme-linked immunospot assay. *Immunology*. (2013) 139:533–44. doi: 10.1111/imm.2013.139.issue-4

22. Jarque M, Crespo E, Melilli E, Gutiérrez A, Moreso F, Guirado L, et al. Cellular immunity to predict the risk of cytomegalovirus infection in kidney transplantation: A prospective, interventional, multicenter clinical trial. *Clin Infect Dis*. (2020) 71(9):2375–85. doi: 10.1093/cid/ciz1209

23. Macedo C, Webber SA, Donnenberg AD, Popescu I, Hua Y, Green M, et al. EBV-specific CD8+ T cells from asymptomatic pediatric thoracic transplant patients carrying chronic high EBV loads display contrasting features: activated phenotype and exhausted function. *J Immunol*. (2011) 186:5854–62. doi: 10.4049/jimmunol.1001024

24. Kumar D, Chernenko S, Moussa G, Cobas I, Manuel O, Preiksaitis J, et al. Cell-mediated immunity to predict cytomegalovirus disease in high-risk solid organ transplant recipients. *Am J Transplant*. (2009) 9:1214–22. doi: 10.1111/j.1600-6143.2009.02618.x

25. Kumar D, Mian M, Singer L, Humar A. An interventional study using cell-mediated immunity to personalize therapy for cytomegalovirus infection after transplantation. *Am J Transplant*. (2017) 17:2468–73. doi: 10.1111/ajt.14347

26. Lisboa LF, Kumar D, Wilson LE, Humar A. Clinical utility of cytomegalovirus cell-mediated immunity in transplant recipients with cytomegalovirus viremia. *Transplant*. (2012) 93:195–200. doi: 10.1097/TP.0b013e31823c1cd4

27. Manuel O, Husain S, Kumar D, Zayas C, Mawhorter S, Levi ME, et al. Assessment of cytomegalovirus-specific cell-mediated immunity for the prediction of cytomegalovirus disease in high-risk solid-organ transplant recipients: A multicenter cohort study. *Clin Infect Dis*. (2013) 56:817–24. doi: 10.1093/cid/cis993

28. Poglajen G, Zemljic G, Frljak S, Okrajšek R, Šebeštjen M, Cerar A, et al. Quantiferon-CMV guided virostatic prophylaxis after heart transplantation. *J Heart Lung Transplant*. (2019) 38:S119. doi: 10.1016/j.healun.2019.01.279

29. Westall GP, Cristiano Y, Levvey BJ, Whitford H, Paraskeva MA, Paul E, et al. A randomized study of quantiferon CMV-directed versus fixed-duration valganciclovir prophylaxis to reduce late CMV after lung transplantation. *Transplant*. (2019) 103:1005–13. doi: 10.1097/TP.0000000000002454

30. Benz C, Utermöhlen O, Wulf A, Villmow B, Dries V, Goeser T, et al. Activated virus-specific T cells are early indicators of anti-CMV immune reactions in liver transplant patients. *Gastroenterology*. (2002) 122:1201–15. doi: 10.1053/gast.2002.33021

31. Sund F, Lidehäll AK, Claesson K, Foss A, Tötterman TH, Korsgren O, et al. CMV-specific T-cell immunity, viral load, and clinical outcome in seropositive renal transplant recipients: a pilot study: CMV-specific immunity in renal transplant patients. *Clin Transplant*. (2009) 24:401–9. doi: 10.1111/j.1399-0012.2009.00976.x

32. Yamada M, Macedo C, Louis K, Shi T, Landsittel D, Nguyen C, et al. Distinct association between chronic Epstein-Barr virus infection and T cell compartments from pediatric heart, kidney, and liver transplant recipients. *Am J Transplant*. (2023) 23(8):1145–58. doi: 10.1016/j.ajt.2023.05.007

33. Egli A, Binet I, Binggeli S, Jäger C, Dumoulin A, Schaub S, et al. Cytomegalovirus-specific T-cell responses and viral replication in kidney transplant recipients. *J Transl Med*. (2008) 6:29. doi: 10.1186/1479-5876-6-29

34. Eid AJ, Brown RA, Arthurs SK, Lahr BD, Eckel-Passow JE, Larson TS, et al. A prospective longitudinal analysis of cytomegalovirus (CMV)-specific CD4+ and CD8+ T cells in kidney allograft recipients at risk of CMV infection: CMV-specific T-cell immunity after kidney transplant. *Transplant Int*. (2010) 23:506–13. doi: 10.1111/j.1432-2277.2009.01017.x

35. Gerna G, Lilleri D, Fornara C, Comolli G, Lozza L, Campana C, et al. Monitoring of human cytomegalovirus-specific CD4+ and CD8+ T-cell immunity in patients receiving solid organ transplantation. *Am J Transplant*. (2006) 6:2356–64. doi: 10.1111/j.1600-6143.2006.01488.x

36. Gerna G, Lilleri D, Chiesa A, Zelini P, Furione M, Comolli G, et al. Virologic and immunologic monitoring of cytomegalovirus to guide preemptive therapy in solid-organ transplantation. *Am J Transplant*. (2011) 11:2463–71. doi: 10.1111/j.1600-6143.2011.03636.x

37. La Rosa C, Limaye AP, Krishnan A, Longmate J, Diamond DJ. Longitudinal assessment of cytomegalovirus (CMV)–specific immune responses in liver transplant recipients at high risk for late CMV disease. *J Infect Dis*. (2007) 195:633–44. doi: 10.1086/511307

38. Radha R, Jordan S, Puliyanda D, Bunnapradist S, Petrosyan A, Amet N, et al. Cellular immune responses to cytomegalovirus in renal transplant recipients. *Am J Transplant*. (2005) 5:110–7. doi: 10.1111/j.1600-6143.2003.00647.x

39. Rogers R, Saharia K, Chandorkar A, Weiss ZF, Vieira K, Koo S, et al. Clinical experience with a novel assay measuring cytomegalovirus (CMV)-specific CD4+ and CD8+ T-cell immunity by flow cytometry and intracellular cytokine staining to predict clinically significant CMV events. *BMC Infect Dis*. (2020) 20:58. doi: 10.1186/s12879-020-4787-4

40. Sester M, Sester U, Gärtner B, Heine G, Girndt M, Mueller-Lantzsch N, et al. Levels of virus-specific CD4 T cells correlate with cytomegalovirus control and predict virus-induced disease after renal transplantation. *Transplant*. (2001) 71:1287–94. doi: 10.1097/00007890-200105150-00018

41. Sester U, Gärtner BC, Wilkens H, Schwaab B, Wössner R, Kindermann I, et al. Differences in CMV-specific T-cell levels and long-term susceptibility to CMV infection after kidney, heart and lung transplantation. *Am J Transplant*. (2005) 5:1483–9. doi: 10.1111/j.1600-6143.2005.00871.x

42. Snyder LD, Chan C, Kwon D, Yi JS, Martissa JA, Copeland CAF, et al. Polyfunctional T-cell signatures to predict protection from cytomegalovirus after lung transplantation. *Am J Respir Crit Care Med*. (2016) 193:78–85. doi: 10.1164/rccm.201504-0733OC

43. Keoshkerian E, Helbig K, Beard M, Zaunders J, Seddiki N, Kelleher A, et al. A novel assay for detection of hepatitis C virus-specific effector CD4+ T cells via co-expression of CD25 and CD134. *J Immunol Methods*. (2012) 375:148–58. doi: 10.1016/j.jim.2011.10.004

44. Sadler R, Bateman EA, Heath V, Patel SY, Schwingshackl PP, Cullinane AC, et al. Establishment of a healthy human range for the whole blood 'OX40' assay for the detection of antigen-specific CD4+ T cells by flow cytometry: Clinical validation of the 'OX40' assay for antigen-specifc CD4+ T cells. *Cytometry*. (2014) 86(5):350–61. doi: 10.1002/cytob.21165

45. Arasaratnam RJ, Tzannou I, Gray T, Aguayo-Hiraldo PI, Kuvalekar M, Naik S, et al. Dynamics of virus-specific T cell immunity in pediatric liver transplant recipients. *Am J Transplant*. (2018) 18:2238–49. doi: 10.1111/ajt.14967

46. Imadome Ki, Fukuda A, Kawano F, Imai Y, Ichikawa S, Mochizuki M, et al. Effective control of Epstein-Barr virus infection following pediatric liver transplantation by monitoring of viral DNA load and lymphocyte surface markers. *Pediatr Transplant*. (2012) 16:748–57. doi: 10.1111/j.1399-3046.2012.01750.x

47. Smets F, Latinne D, Bazin H, Reding R, Otte JB, Buts JP, et al. Ratio between Epstein-Barr viral load and anti-Epstein-Barr virus specific T-cell response as a predictive marker of posttransplant lymphoproliferative disease. *Transplant*. (2002) 73:1603–10. doi: 10.1097/00007890-200205270-00014

48. Gotoh K, Ito Y, Ohta R, Iwata S, Nishiyama Y, Nakamura T, et al. Immunologic and virologic analyses in pediatric liver transplant recipients with chronic high Epstein-Barr virus loads. *J Infect Dis*. (2010) 202:461–9. doi: 10.1086/653737

49. Ning RJ, Xu XQ, Chan KH, Chiang AKS. Long-term carriers generate Epstein-Barr virus (EBV)-specific CD4(+) and CD8(+) polyfunctional T-cell responses which show immunodominance hierarchies of EBV proteins. *Immunology*. (2011) 134:161–71. doi: 10.1111/j.1365-2567.2011.03476.x

50. Wilsdorf N, Eiz-Vesper B, Henke-Gendo C, Diestelhorst J, Oschlies I, Hussein K, et al. EBV-specific T-cell immunity in pediatric solid organ graft recipients with posttransplantation lymphoproliferative disease. *Transplant*. (2013) 95:247–55. doi: 10.1097/TP.0b013e318279968d

51. Nagamata S, Nagasaka M, Kawabata A, Kishimoto K, Hasegawa D, Kosaka Y, et al. Human CD134 (OX40) expressed on T cells plays a key role for human herpesvirus 6B replication after allogeneic hematopoietic stem cell transplantation. *J Clin Virol*. (2018) 102:50–5. doi: 10.1016/j.jcv.2018.02.011

52. Wang YL, Fu YX, Zhu ZJ, Wang H, Shen ZY. OX40 mRNA in peripheral blood as a biomarker of acute renal allograft rejection. *Chin Med J (Engl)*. (2012) 125:3786–90.

53. Díaz Fernández C, Gámez Arance M, de la Vega Bueno A, Frauca Remacha E. Trasplante hepático pediátrico: indicaciones, técnicas quirúrgicas, complicaciones y tratamiento. *Anales Pediatría*. (2004) 60:42–55. doi: 10.1016/s1695-4033(04)78216-8

54. Lovelace P, Maecker HT. Multiparameter intracellular cytokine staining. In: Hawley TS, Hawley RG, editors. *Flow Cytometry Protocols*, vol. 699 . Humana Press, Totowa, NJ (2011). p. 165–78. doi: 10.1007/978-1-61737-950-5_8

55. Welsh RM, Selin LK. No one is naive: the significance of heterologous T-cell immunity. *Nat Rev Immunol*. (2002) 2:417–26. doi: 10.1038/nri820

56. Rowntree LC, Nguyen THO, Halim H, Purcell AW, Rossjohn J, Gras S, et al. Inability to detect cross-reactive memory T cells challenges the frequency of heterologous immunity among common viruses. *J Immunol*. (2018) 200:3993–4003. doi: 10.4049/jimmunol.1800010

57. Callan MF, Tan L, Annels N, Ogg GS, Wilson JD, O'Callaghan CA, et al. Direct visualization of antigen-specific CD8+ T cells during the primary immune response to Epstein-Barr virus In vivo. *J Exp Med*. (1998) 187:1395–402. doi: 10.1084/jem.187.9.1395

58. Lam JKP, Hui KF, Ning RJ, Xu XQ, Chan KH, Chiang AKS. Emergence of CD4+ and CD8+ Polyfunctional T cell responses against immunodominant lytic and latent EBV antigens in children with primary EBV infection. *Front Microbiol*. (2018) 9:416. doi: 10.3389/fmicb.2018.00416

59. Lachmann R, Bajwa M, Vita S, Smith H, Cheek E, Akbar A, et al. Polyfunctional T cells accumulate in large human cytomegalovirus-specific T cell responses. *J Virol*. (2012) 86:1001–9. doi: 10.1128/JVI.00873-11

60. Soni MK, Migliori E, Fu J, Assal A, Chan HT, Pan J, et al. The prospect of universal coronavirus immunity: characterization of reciprocal and non-reciprocal T cell responses against SARS-CoV2 and common human coronaviruses. *Front Immunol*. (2023) 14:1212203. doi: 10.3389/fimmu.2023.1212203

61. Darrah PA, Patel DT, De Luca PM, Lindsay RWB, Davey DF, Flynn BJ, et al. Multifunctional TH1 cells define a correlate of vaccine-mediated protection against Leishmania major. *Nat Med*. (2007) 13:843–50. doi: 10.1038/nm1592

62. Long HM, Chagoury OL, Leese AM, Ryan GB, James E, Morton LT, et al. MHC II tetramers visualize human CD4+ T cell responses to Epstein–Barr virus infection and demonstrate atypical kinetics of the nuclear antigen EBNA1 response. *J Exp Med*. (2013) 210:933–49. doi: 10.1084/jem.20121437

63. Gasper DJ, Tejera MM, Suresh M. CD4 T-cell memory generation and maintenance. *Crit Rev Immunol*. (2014) 34:121–46. doi: 10.1615/CritRevImmunol.2014010373

64. Mahnke YD, Brodie TM, Sallusto F, Roederer M, Lugli E. The who's who of T -cell differentiation: Human memory T -cell subsets. *Eur J Immunol*. (2013) 43:2797–809. doi: 10.1002/eji.201343751

65. Wang Y, Qiu F, Xu Y, Hou X, Zhang Z, Huang L, et al. Stem cell-like memory T cells: The generation and application. *J Leukocyte Biol*. (2021) 110:1209–23. doi: 10.1002/JLB.5MR0321-145R

66. Palianina D, Mietz J, Stühler C, Arnold B, Bantug G, Münz C, et al. Stem cell memory EBV-specific T cells control post-transplant lymphoproliferative disease and persist in *vivo*. *Immunology*. (2023) 10(34):eado2048. doi: 10.1101/2023.05.30.542809

67. Amyes E, Hatton C, Montamat-Sicotte D, Gudgeon N, Rickinson AB, McMichael AJ, et al. Characterization of the CD4+ T cell response to epstein-barr virus during primary and persistent infection. *J Exp Med*. (2003) 198:903–11. doi: 10.1084/jem.20022058

68. Liu L, Cui J, You Y, Shi W, Zou P, Chen L, et al. Expression of CD134 on CD4+ T cells reflects the immunosuppressive state after allo-HCT by revealing the intensity of T cell activation. *Int J Clin Exp Med*. (2016) 9:17782–91.

69. Lamb LS, Abhyankar SA, Hazlett L, O'Neal W, Folk RS, Vogt S, et al. Expression of CD134 (0X-40) on T cells during the first 100 days following allogeneic bone marrow transplantation as a marker for lymphocyte activation and therapy-resistant graft-versus-host disease. *Cytometry*. (1999) 38:238–43. doi: 10.1002/(SICI)1097-0320(19991015)38:5<238::AID-CYTO6>3.0.CO;2-O

frontiers | Frontiers in Immunology

TYPE Review
PUBLISHED 22 November 2024
DOI 10.3389/fimmu.2024.1500228

OPEN ACCESS

EDITED BY
Rita Maccario,
San Matteo Hospital Foundation (IRCCS), Italy

REVIEWED BY
Baptiste Lamarthée,
Université de Franche-Comté, France
Marcello Maestri,
University of Pavia, Italy

*CORRESPONDENCE
Qing Ding
dingq@upmc.edu
Lihong Wang
zjgzywlh@njucm.edu.cn

RECEIVED 23 September 2024
ACCEPTED 06 November 2024
PUBLISHED 22 November 2024

CITATION
Tao J, Shen X, Qian H, Ding Q and Wang L (2024) TIM proteins and microRNAs: distinct impact and promising interactions on transplantation immunity.
Front. Immunol. 15:1500228.
doi: 10.3389/fimmu.2024.1500228

TIM proteins and microRNAs: distinct impact and promising interactions on transplantation immunity

Jialing Tao[1], Xiaoxuan Shen[2], Haiqing Qian[3], Qing Ding[4]* and Lihong Wang[3]*

[1]Translational Medical Innovation Center, Zhangjiagang TCM Hospital Affiliated to Nanjing University of Chinese Medicine, Zhangjiagang, Jiangsu, China, [2]Department of Endocrinology, Zhangjiagang TCM Hospital Affiliated to Nanjing University of Chinese Medicine, Zhangjiagang, Jiangsu, China, [3]Department of Reproduction, Zhangjiagang TCM Hospital Affiliated to Nanjing University of Chinese Medicine, Jiangsu, Zhangjiagang, China, [4]Department of Surgery, Thomas E. Starzl Transplantation Institute, University of Pittsburgh School of Medicine, Pittsburgh, PA, United States

Achieving sustained activity and tolerance in of allogeneic grafts after post-transplantation remains a substantial challenge. The response of the immune system to "non-self" MHC-antigenic peptides initiates a crucial phase, wherein blocking positive co-stimulatory signals becomes imperative to ensure graft survival and tolerance. MicroRNAs (miRNAs) inhibit mRNA translation or promote mRNA degradation by complementary binding of mRNA seed sequences, which ultimately affects protein synthesis. These miRNAs exhibit substantial promise as diagnostic, prognostic, and therapeutic candidates for within the realm of solid organ transplantations. Current research has highlighted three members of the T cell immunoglobulin and mucin domain (TIM) family as a novel therapeutic avenue in transplantation medicine and alloimmunization. The interplay between miRNAs and TIM proteins has been extensively explored in viral infections, inflammatory responses, and post-transplantation ischemia-reperfusion injuries. This review aims to elucidate the distinct roles of miRNAs and TIM in transplantation immunity and delineate their interdependent relationships in terms of targeted regulation. Specifically, this investigation sought seeks to uncover the potential of miRNA interaction with TIM, aiming to induce immune tolerance and bolster allograft survival after transplantation. This innovative strategy holds substantial promise in for the future of transplantation science and practice.

KEYWORDS

T cell immunoglobulin and mucin domain, microRNAs, transplantation, allograft rejection, allograft tolerance

1 Introduction

Allogeneic transplantation is the primary treatment for patients with end-stage diseases and severe trauma. Imbalances in the activation and suppression of the immune system, systemic dysfunction of the transplanted organ, and infections all contribute to the failure of allogeneic transplantations (1–3). In many cases, autologous transplantation is not feasible due to physiological restrictions (4, 5). Consequently, allogeneic transplantation remains the only viable solution in such scenarios. However, graft rejection remains a major obstacle leading to graft loss (6).

The T cell immunoglobulin and mucin domain (*TIM*) gene family comprises a series of genes encoding type 1 glycoprotein-like structural domains expressed on cell membranes that crucially regulate immune responses (7). Members of the *TIM* gene family, such as TIM-1, TIM-3, and TIM-4, exhibit structural characteristics that are conserved in both mice and humans (8). Initially identified as a susceptibility gene for asthma and allergy, TIM-1 is preferentially expressed on Th2 cells and linked to atopic and autoimmune diseases (9). TIM-3 is expressed on innate and adaptive immune cells, including mast cells, dendritic cells (DCs), macrophages, and Th1 and Tc1 cells, and acts as an inhibitory receptor that promotes Th1 apoptosis and reduces the production of inflammatory factors (10–12). TIM-4 is solely expressed on the surface of antigen-presenting cells (APCs), facilitating phagocytosis of apoptotic cells and modulating T cell responses (7, 13). Ongoing research underscores the extensive role of TIM proteins in immune tolerance and transplant rejection (14–16).

MicroRNAs (miRNAs), single-stranded RNAs approximately 22 nucleotides long, selectively and specifically regulate post-transcriptional gene expression (17). Recently, miRNAs have demonstrated specific and impactful biological effects, serving to establish immune tolerance following solid organ transplantation (18). Thus, miRNAs exhibit potential as diagnostic, predictive, and therapeutic markers for allograft rejection (19).

Both miRNAs and TIM proteins have wide applications in immune tolerance induction and transplantation (20). The interaction between miRNAs and TIM proteins in cancer therapy has been extensively studied (21, 22) (Table 1). However, their effects on allograft rejection models remain unclear. Thus, this review aims to discuss recent advancements in understanding the TIM–miRNA network and explore its potential applications in solid organ transplantation and immune tolerance.

2 *TIM* gene family

The *TIM* genes are located on mouse chromosome 11B1.1 and human chromosome 5q33.5, which are regions associated with various atopic/autoimmune diseases such as asthma and allergies (40). The TIM family comprises eight murine members (four coding genes, TIM-1–TIM-4, and four noncoding genes, TIM-5–

TABLE 1 TIM–miRNA interactions in diseases.

TIM	miRNA	Effect	Reference
TIM-1	miR-133a	Targeted regulation of glioblastoma cell proliferation, migration, and infiltration.	(21)
	miR-142	Alteration of endothelial cell permeability.	(23)
TIM-3	miR-330	Inhibition of NLRP3 inflammasome-mediated myocardial ischemia-reperfusion injury. Insulin resistance downregulated by enhancing M2 macrophage polarization. Mediation of anti-tumor immunity in AML.	(24–26)
	miR-125a-3p	Negative effect on AML progression.	(27)
	miR-498	Potential approaches for the treatment of AML.	(22)
	miR-18b	Improved pre-eclampsia by promoting trophoblast proliferation and migration.	(28)
	miR-34a	Modulates the degree of malignancy in AML	(29)
	miR-155	Regulation of CD8 T cell apoptosis and improved immunotherapy efficacy in hepatocellular carcinoma. Blocks macrophage transformation to prevent the development of atherosclerosis. Predicts colorectal cancer progression by targeting macrophage polarization. Accelerates cervical cancer progression by modifying the macrophage microenvironment.	(30–33)
	miR-455-5p	Predicts clinical regression in patients with skull base chordoma.	(34)
	miR-545-5p	Modulates the anti-tumor activity of CD8 T cells	(35)
	miR-149-3p	Anti-tumor immunity in breast cancer by reversing CD8 T cell depletion.	(36)
	miR-133a	A future therapeutic target in AML.	(37)
	miR-146a	A predictor of cellular immune failure following HIV infection.	(38)
TIM-4	miR-202	Acceleration of EC cell migration and invasion by targeting the miR-202–TIM-4 axis.	(39)

AML, acute myeloid leukemia; IL, interleukin; miRNA, microRNA; TIM, T cell immunoglobulin and mucin domain.

TIM-8) and three human members (TIM-1, TIM-3, and TIM-4) (41). TIM proteins share a similar structure, encompassing an immunoglobulin domain, mucin-like domain, transmembrane region, and cytoplasmic domain containing tyrosine-phosphorylated motifs (except for TIM-4) (12) (Figure 1). Based on gene sequence similarity, murine TIM-2 shares structural and functional similarities with murine TIM-1, and is considered a direct homolog of human TIM-1 (42).

2.1 Functional characteristics of TIM-1

Initially identified as the hepatitis A virus receptor (*HAVCR1*) and later as a human kidney injury molecule, TIM-1 is found on B cells, DCs, mast cells, and invariant natural killer T (iNKT) cells, playing a crucial role in immune activation (43–45). As a potential co-stimulatory molecule, it is well established that TIM-1 exerts immune effects by maintaining Breg suppression and stimulating effector T cell activity and homeostasis (8, 46). The diverse biological roles of TIM-1 open up new avenues for the treatment of autoimmune diseases, viral infections and tumors (47–49). Previous studies have suggested the potentially diverse roles of TIM-1 in inducing immune tolerance in transplantation.

2.2 Role of TIM-1 in transplantation

Recent studies have highlighted the pivotal role of TIM-1 in preventing and mitigating allograft rejection. The agonistic TIM-1-specific mAb 3B3 disrupts mouse allograft tolerance by interacting with effector T cells and Tregs (50). Additionally, TIM-1 not only serves as a surface marker but also as a crucial surface molecule that induces and maintains regulatory B cell (Breg) function in mice (51, 52). In a model of islet transplantation, anti-CD45RB and anti-TIM-1 (RMT1-10) antibodies increased interleukin (IL)-10 expression in TIM-1$^+$ Bregs and antigen-specific transplantation tolerance (52, 53). This combined antibody therapy relies on TIM-1 expression, IL-10-producing Bregs, and Tregs (54). Altered IL-10 levels and accelerated allograft rejection have been observed in TIM-1 knockout and mutant mice (46). Recent findings indicate that the inhibitory function of ex vivo expansion of human B cells partly relies on TIM-1, which maintains long-term regulatory function and human allogeneic skin graft survival by positively regulating STAT3 phosphorylation (55). The TIM-1 signaling pathway is not only targeted after allogeneic transplantation, but also as a new therapeutic strategy to improve post-transplant complications (56).

2.3 Functional characteristics of TIM-3

TIM-3 serves as a suppressor molecule involved in T cell activation and is a marker of T cell depletion in tumors and chronic viral infections (57). Subsequently, TIM-3 was found to accelerate tumor progression and support maternal-fetal tolerance (58, 59). Galectin-9 (Gal-9), the first ligand identified for TIM-3, eliminates interferon γ-producing Th1 cells, thereby reducing the severity and mortality of experimental autoimmune encephalomyelitis (60) (Table 2). TIM-3 interacts with different ligands and mediates various immune responses, making it a promising target for immunotherapy.

2.4 Role of TIM-3 in transplantation

Initially considered as a marker for terminally differentiated effector T cells, TIM-3 has been found to influence Treg acquisition and function, providing new insights into the mechanisms of transplant rejection (94). The natural TIM-3 ligand Gal-9 limits Th1 activation, thereby protecting specific Treg responses and

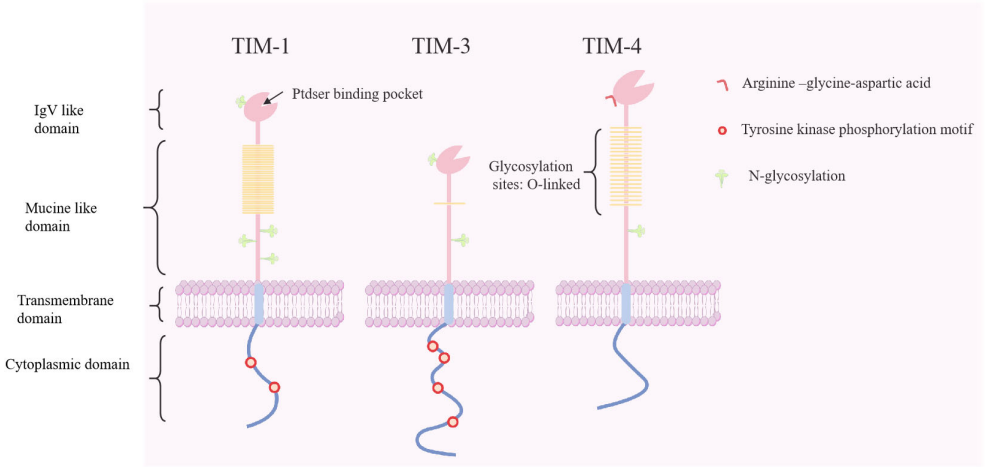

FIGURE 1
Molecular structure of human T cell immunoglobulin and mucin proteins (TIM-1, -3, and -4). The *TIM* genes encode type I membrane proteins that contain an Ig V-like domain, an O-linked glycosylated mucin domain, a transmembrane domain, and a cytoplasmic domain with tyrosine-phosphorylated motifs. TIM-4 contains RGD motifs that can interact with integrins and participate in intercellular adhesion. Ptdser, phosphatidylserine; RGD, arginine–glycine –aspartic acid.

TABLE 2 Expression and function of TIM proteins.

TIM	Ligand	Expression	Function	Reference
TIM-1	TIM-4	Activated $CD4^+$ T cells	Inhibition of interactions that modulate Th1/Th2 cytokine balance and attenuate renal IRI. Modulation of helper T cell activation and proliferation. Amelioration of Behcet's disease-like symptoms. Suppression of interactions inhibiting DC maturation and $CD4^+$ T cell proliferation, thereby inducing immune tolerance.	(61) (62, 63) (64)
		Th2	Exacerbates allergies/asthma.	(65)
	Ptdser	T cells	Enhanced viral cell attachment and infection.	(66, 67)
		iNKT cells	Inhibition of IL-17A production by γδ T cells via PD-1/PD-L1 signaling.	(68)
	P-/E-/S-selectin	Th1/Th17 cells	Binding, rolling, and accumulation of Th1 and Th17 cells in the local microenvironment during inflammatory disease.	(69)
	HAV	Proximal tubule cells	A marker of renal injury. Mediate fatty acid uptake; exacerbates inflammation and renal fibrosis, and accelerates the progression of diabetic nephropathy.	(70)
	LMIR5/CD300b	Epithelial tubular cells	Promote neutrophil recruitment to kidneys with IRI, thereby facilitating renal injury.	(71)
TIM-3	Gal-9	Th1, Tc1, and NK cells	Negative regulation of Th1 and CD8 T cell responses, promotion of Treg development to rescue inflammatory injuries after transplantation, and induction of immune tolerance. Modifies NK function, balances the Th1/Th2 ratio, and promotes maternal and fetal tolerance to prevent abortion.	(72) (73)
		T cells	PD-1 attenuates Gal-9/TIM-3-induced T cell apoptosis by binding to Gal-9, providing a novel target for anti-tumor immunity.	(74)
		Macrophages	Prevent macrophage M2 polarization by blocking Gal-9/TIM-3 signaling in *PTEN*-deficient gliomas, thereby attenuating glioma progression.	(75)
		NK	Drives NK cell dysfunction and immune escape in AML.	(76, 77)
	HMGB1	CD8 T cells/DCs	Accelerate viral infection by limiting effector T cell activation and amplification	(78)
		T cells	Promote AML progression.	(79)
			Block NF-KB activation, modulates immunosuppression, and increases mortality in sepsis.	(80)
	CEACAM1	T cells	T cell depletion and inhibited signaling	(57)
		CD4 T cells	Reduces= stress-induced tissue damage, inhibits Kupffer cell activation, and improves outcomes in liver transplantation.	(81)
		CD8 T cells	Regulation of premature restimulation-induced cell death of effector CD8 T cells and stabilization of T cell populations.	(82)
		T/NK/B cells	A potential target for anti-tumor immunity/autoimmune diseases.	(83–85)
	Ptdser	NK/CTL cells	Influence cell toxicity and mediates immune escape from malignant tumors.	(86, 87)
TIM-4	TIM-1	PMBCs	Possible involvement in the pathogenesis of systemic lupus erythematosus.	(88)
		B cells	Promote tumor and graft rejection.	(89)
			Promote Th2 proliferation and exacerbates allergic rhinitis.	(90)
	Ptdser	Macrophages	Facilitate viral entry into target cells	(91, 92)
			Scavenges apoptotic cells to avoid autoimmunity.	(93)

AML, acute myeloid leukemia; AHR, airway hyperreactivity; CEACAM1, carcinoembryonic antigen cell adhesion molecule 1; CTL, cytotoxic T cell; DC, dendritic cell; HAV, hepatitis A virus; Gal-9, galectin-9; HMGB1, high-mobility group protein B1; IL, interleukin; iNKT, invariant natural killer T; IRI, ischemia-reperfusion injury; NK, natural killer; PBMC, peripheral blood mononuclear cell; PD-1, programmed cell death protein 1; Ptdser, phosphatidylserine; TIM, T cell immunoglobulin and mucin domain.

attenuating allograft rejection (95). When allograft rejection occurs, increased expression of TIM-3 on the recipient's NK cells stimulates IFN-γ production through interaction with Gal-9 (96). Therefore, high serum levels of soluble TIM-3 and sGal-9 serve as prospective biomarkers for diagnosing and predicting renal transplant dysfunction (97, 98). Additionally, hepatocytic Gal-9 signaling via TIM-3$^+$CD4$^+$ T cells mitigate ischemia-reperfusion injury (IRI) during orthotopic liver transplantation in recipient mice (72). TIM-3$^+$CD4$^+$ and TIM-3$^+$CD8$^+$ T cells in allogeneic transplantation models exhibit a depleted dysfunctional phenotype owing to continuous stimulation by allogeneic antigens (99). This early induction and establishment of T cell dysfunction ultimately mediate and maintain the phenotypic and functional characteristics of self-tolerance or exhaustion (100). Moreover, inhibitory receptors such as TIM-3 and PD-1 ensure that Treg are depleted after graft rejection to prevent microbial and tumor unresponsiveness and to balance immunomodulatory functions (16). High pretransplant T-cell expression of PD-1 and Tim-3 co-suppressor receptors correlated positively with the incidence of posttransplant infection (101). Clinical studies have shown that elevated CEACAM1 levels are associated with a favorable outcome in orthotopic liver transplantation. Recent evidence confirms that T cell CEACAM1 - TIM-3 crosstalk inhibits Kupffer cell NF-KB phosphorylation, attenuates post-transplant liver injury and promotes T cell homeostasis (81). Overall, TIM-3 has shown potential applications in transplantation, but more thorough mechanisms of action need to be explored.

2.5 Functional characteristics of TIM-4

Traditionally known to be primarily expressed on the surface of APCs, including macrophages, mature DCs, B1 cells, and iNKT cells, recent studies have also identified TIM-4 expression in fibroblasts (13, 102). This diverse expression profile suggests potential multifaceted roles of TIM-4 in immune regulation and cellular interactions. Structurally, despite the lack of a cytoplasmic tail for intracellular signaling, the TIM-4 extracellular IgV domain contains arginine-glycine-aspartate (RGD) motifs, which predominantly facilitates APC-T cell adhesion (7, 103).

Initial studies have suggested that TIM-4 acts as a natural ligand for TIM-1, contributing to helper T cell proliferation and favoring Th2 immune responses (104). However, further investigations have revealed the nuanced effects of TIM-4 on T cell responses. Depending on the concentration of TIM-4 stimulation and the state of T cell activation, TIM-4 has contrasting effects on T cell proliferation (62, 105). These findings suggest that the influence of TIM-4 on T cells may involve receptors other than the known TIM-1 receptor, especially during the initial T cell surface expression.

As a phosphatidylserine receptor, TIM-4 contributes to the creation of an environment of immune tolerance by clearing apoptotic cells and debris, simultaneously suggesting potential risks associated with infection and tumorigenesis (91, 106). Overall, the function of TIM-4 as a potent co-stimulatory signal in APCs revealed its diverse and context-dependent biological activities. Its precise biological effects seem to be closely linked to the type of ligands it interacts with and the specific sites of T cell activation. Understanding the intricate interactions of TIM-4 with various receptors and their dual roles in immune tolerance and potential pathogenic processes remains an area of active research in immunology.

2.6 Role of TIM-4 in transplantation

Few studies have investigated TIM-4 in the context of transplantation. Researchers have focused on understanding TIM-4 expression in specific immune cells, particularly macrophages and DCs, as these cells play crucial roles in the modulation of TIM-4 to promote tolerance in human transplantation (107, 108).

Prior to 2010, studies exploring the direct relationship between TIM-4 and transplantation immunity were lacking. However, in 2010, Uchida et al. hypothesized that blocking the TIM-1–TIM-4 signaling pathway might alleviate hepatic IRI. The proposed intervention presented a novel approach aimed at extending the survival and success of transplanted organs (109). In the following year, Rong et al. provided initial evidence supporting this hypothesis by demonstrating that disrupting the TIM-1–TIM-4 pathway could inhibit CD4 T cell activation. This inhibition protected renal function and reduced local leukocyte recruitment and activation, offering a promising novel target for the treatment of acute kidney injury (61).

Subsequent studies further reinforced these initial findings, consistently showing that blocking TIM-4 signaling conferred protection against hepatic IRI. Notably, these studies highlight the significance of TIM-4-mediated phagocytosis, which is involved in activating the innate immune system and represents a crucial aspect of this process (110, 111). Indeed, these studies underscore the potential therapeutic implications of targeting TIM-4 in mitigating transplantation-related complications, and hold promise for developing novel strategies to enhance the success of organ transplantation.

Macrophages, particularly tissue-resident macrophages such as CD169$^+$ macrophages, play a critical role in modulating immune responses and influencing transplant outcomes. For instance, genetic ablation of TIM-4 in CD169$^+$ tissue-resident macrophages improve their survival. However, this alteration does not seem to affect the effective stimulation of Treg production or promote the prolonged survival of cardiac allografts (15).

Kupffer cells (KCs), the dominant macrophages in the liver, have been identified as critical mediators of tolerance following liver transplantation. KCs promote tolerance through mechanisms involving upregulation of FasL-induced apoptosis and cytokine secretion in T cells (112, 113). Disrupting TIM-4 signaling in KCs in combination with transforming growth factor (TGF)-B treatment significantly induces the transformation of inducible Tregs and ameliorates acute rejection after liver transplantation. This effect occurs via inhibition of the IL-4–STAT6–Gata3 signaling pathway, thereby modulating immune responses and improving tolerance induction (114).

However, studies on mice with congenital TIM-4 deficiency have reported an autoimmune response due to nonspecific immune activation. This is because of defects in the ability to eliminate

apoptotic cells, suggesting a crucial role for TIM-4 in maintaining immune homeostasis and preventing autoimmunity (115). Moreover, DCs, which are highly specialized APCs, are key players in the induction of inflammation and immune tolerance (116). In a skin transplantation model, disruption of TIM-4 co-stimulatory signaling on DCs enhanced the transfer of naïve CD4 cells to inducible Tregs, while limiting the transfer of IL-4/STAT-6 signaling. This modulation attenuates the Th2 response and effectively prolongs graft survival, highlighting the potential of targeting TIM-4 on DCs to modulate immune responses in transplantation scenarios (117).

Collectively, these findings emphasize the intricate role of TIM-4 in regulating immune responses involving macrophages, KCs, and DCs in transplantation scenarios, suggesting its potential as a target for therapeutic interventions to modulate immune tolerance and improve graft survival.

2.7 TIM proteins as phosphatidylserine receptors

Structurally, TIM proteins create a cavity with a distinctive "pocket" structure in the immunoglobulin variable region, securely binding to phosphatidylserine (93, 118) (Figure 2). During apoptosis, phosphatidylserine exposure to the plasma membrane triggers phagocytosis, which is essential for tissue homeostasis and immune regulation (119, 120). TIM-1 signaling by T and iNKT cells prevents recipient survival by inhibiting acute graft-versus-host disease after hematopoietic cell transplantation (20). TIM-1-expressing renal epithelial cells aid in phagocytosis of damaged cells, thereby limiting inflammation (121, 122). In addition to its role in phagocytosis, TIM-3 utilizes functional antibodies with phosphatidylserine to enhance T cell activation and anti-tumor activity (123). TIM-4, as a surface receptor, indirectly modulates inflammation and tumor progression through immune cell clearance (43, 106).

3 Expression and functions of miRNAs

3.1 Biogenesis of miRNAs

miRNAs are a class of small noncoding RNAs present in animals, plants, and some viruses that play a crucial regulatory role in transcription by either cleaving target mRNAs or inhibiting their translation (124). The gene sequences encoding miRNAs are arranged differently within the genome. Some miRNAs are organized as mono-cis-parallels with autonomous promoters, whereas others are arranged in multi-cis-parallels, sharing a common promoter and being transcribed into multiple miRNA clusters (125, 126). In certain cases, miRNA genes are located within the exons (Figure 3). RNA polymerase II is typically responsible for miRNA transcription. This process generates primary precursors known as pri-miRNAs, which adopt a typical hairpin structure and

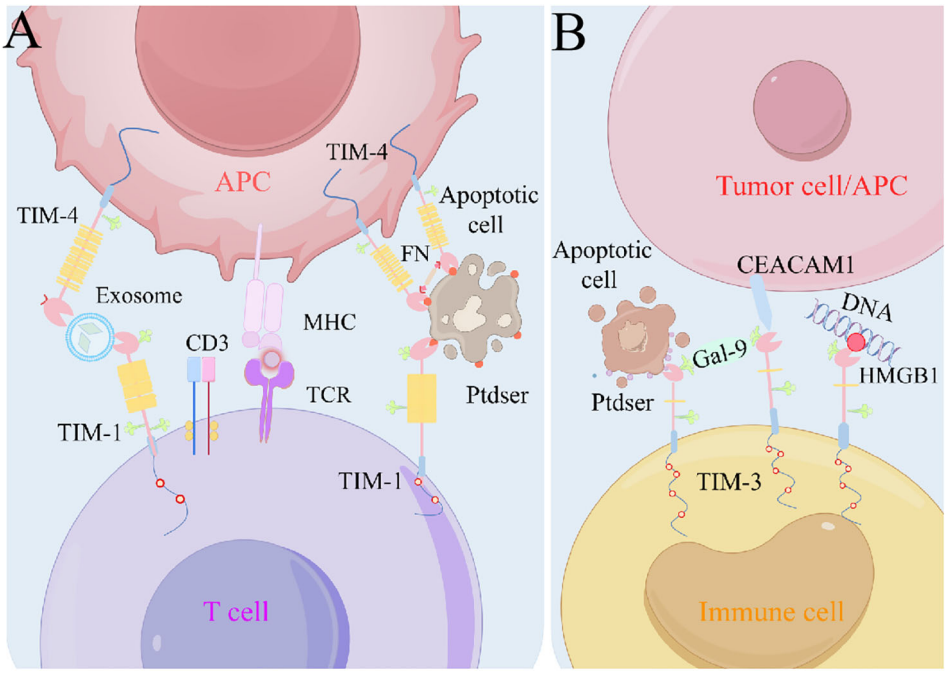

FIGURE 2
Models of TIM-ligand interactions. **(A)** TIM-1 can interact with Ptdser on the surface of apoptotic cells, or TIM-1 and TIM-4 interact via exosome bridging. TIM-4 is used as a bolus molecule to immobilize apoptotic cells near phagocytes to initiate efferocytosis. **(B)** Gal-9 can promote TIM-3 oligomerization and thus the interaction with other TIM-3 ligands, such as CEACAM1–TIM-3. Ptdser released from apoptotic cells can bind the FG-CC′ cleavage site of TIM-3. In addition, TIM-3 can bind HMGB1 and thus inhibit nucleic acid-mediated anti-tumor immunity. APC, antigen-presenting cell; CEACAM1, carcinoembryonic antigen cell adhesion molecule 1; Gal-9, galectin-9; HMGB1, high-mobility group protein B1; MHC, major histocompatibility complex; Ptdser, phosphatidylserine; TCR, T cell receptor; TIM, T cell immunoglobulin and mucin domain.

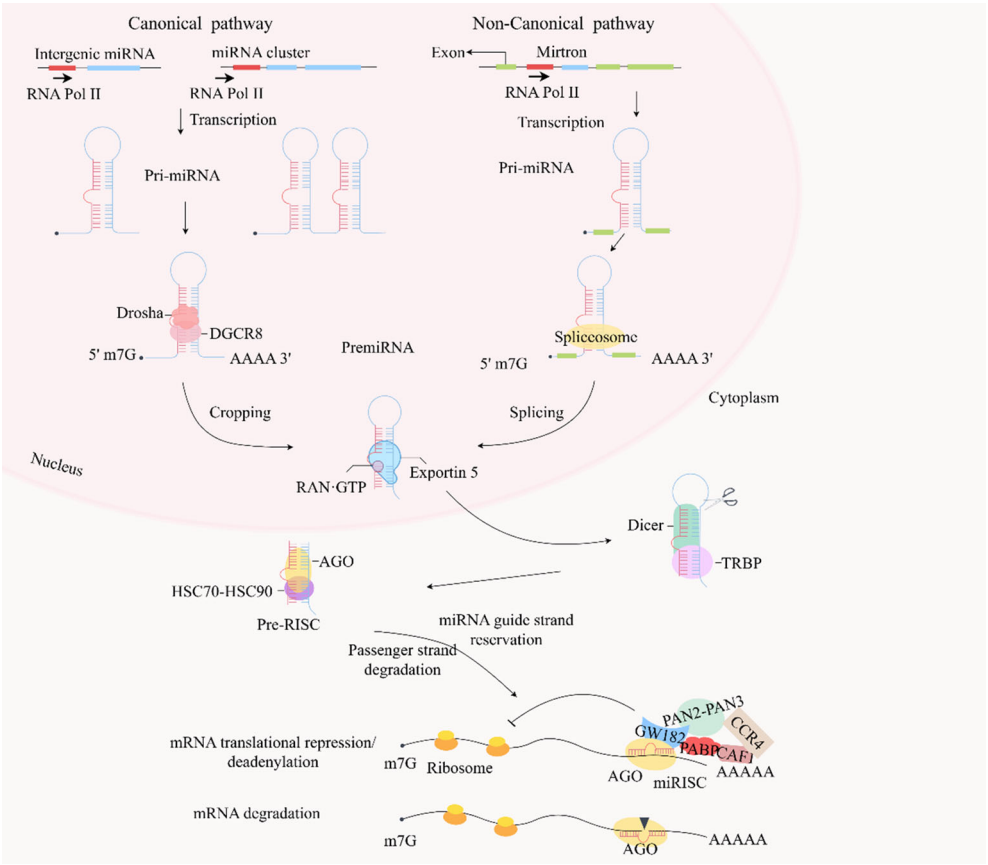

FIGURE 3
In the canonical pathway, typical miRNA genes are encoded by introns in the transcript, generating single or multiple cis-transcripts, but some miRNAs are encoded by exonic regions. miRNAs in the same cluster are co-transcribed and undergo additional post-transcriptional regulation. Most miRNAs generate primary transcription products (pri-miRNAs) in response to RNA polymerase II, which have the original hairpin structure of the embedded miRNA sequence. The primary precursor (pri-miRNA) is cleaved by the microprocessor complex (including Drosha and DGCR8) into a stem-loop structure of about 70 nucleotides called pre-miRNA. Drosha is an endonuclease responsible for processing and cropping the pri-miRNA, whereas DGCR8 is a protein that binds the pri-miRNA to Drosha. Furthermore, some pre-miRNAs are produced in the nucleus in very short introns (mirtrons) by splicing and debranching without Drosha/DGCR8 processing. The pre-miRNAs are then exported to the cytoplasm via Exportin 5 and RAN-GTP. Dicer in the cytoplasm cleaves the pre-miRNA by TRBP-assisted cleavage of the pre-miRNA, releasing a dsRNA of about 20 bp. The dsRNA is then loaded onto the AGO protein and the HSC70-HSC90 complex. The passenger strand is degraded, and the guide strand is retained in the AGO protein, ultimately forming a RISC. This RISC prevents the initiation of translation by inhibiting ribosome elongation and facilitates de-adenylation of poly(A) by recruiting GW182, PABP, CCR4-CAF1, and PAN2-PAN3 to promote mRNA attenuation. These mRNAs are cleaved and degraded when the RISC can target mRNAs that are nearly fully complementary. dsRNA, double-stranded RNA; miRNA, microRNA; RISC, RNA-induced silencing complex; TRBP, TAR RNA-binding protein.

contain a 5′- and a 3′-polyadenylated tail. Subsequently, pri-miRNA undergoes precise cleavage in the nucleus by Drosha and DiGeorge Syndrome Critical Region 8(DGCR8), a nucleic acid endonuclease of the RNase III family, producing pre-miRNAs with stem-loop structures (127).

The pre-miRNA, approximately 70 nucleotides in length, is formed by the Drosha enzyme and exported from the nucleus to the cytoplasm via Exportin 5. In the cytoplasm, it is further processed by Dicer/TAR RNA-binding protein (TRBP)/AGO into double-stranded RNA (dsRNA) consisting of a guide strand and a passenger strand. The guide strand, typically around 22 nucleotides long, enters the miRNA-induced silencing complex (RISC), leading to translational repression or degradation of the target mRNA, whereas the passenger strand is released and subsequently degraded (124, 128, 129). More recently, it was discovered that miRNA biogenesis can occur independently of the conventional Drosha–DGCR8 pathway. Some pre-miRNAs are produced in the nucleus in very short introns by splicing and debranching (130).

3.2 Clustered miRNAs

Approximately 25% of human miRNA genes are organized into clusters, wherein a single cluster contains two or more miRNA genes (131). Although multiple miRNA primary transcripts are generated from the same gene cluster, differential expression arises because of complex regulatory mechanisms. For instance, the 23a–27a–24-2 cluster, comprising three miRNAs, exhibits dysregulation in specific tumors and leukemias, where sometimes only one or two

miRNAs are expressed (132). Conversely, some clustered miRNAs show coordinated expression, with a change in a single miRNA gene within the cluster, triggering a chain reaction that affects the other pri/mature miRNAs (133). Current research supports the idea that miRNAs within the same cluster often target overlapping sets of genes, implying enhanced specificity in targeting and increased interconnectedness within the regulatory network (134). miRNA clusters display homogeneity, multiplicity, and paradoxical functions with respect to the roles of individual miRNAs.

3.3 Modes of miRNA regulation

miRNAs serve as fundamental components in RISC, which comprises AGO proteins along with certain cofactors (127). Initially, it was believed that miRNAs exert post-transcriptional control over their targets by regulating processes such as translation elongation, protein degradation, and ribosomal release (135). In mammals, the seed sequence at the 5′ end of the miRNA (nucleotides 2-8) recognizes the 3′ or 5′ UTR of the target mRNA (126). Typically, this recognition involves incomplete base pairing, ultimately leading to cleavage and degradation of the target mRNA. In addition, miRNA-mediated target decay and deadenylation ultimately lead to reduced protein production and fine-tuned gene expression (136).

3.4 Role of miRNAs in transplantation

The use of miRNAs as noninvasive biomarkers has shown promising potential for the diagnosis, prognosis, and treatment of various aspects of organ transplantation, particularly liver transplantation (137).

3.4.1 Liver transplantation

Reperfusion injury is a major concern after liver transplantation and a leading cause of graft failure and rejection (138). Serum miR-122 levels have been proposed as independent markers of persistent liver injury and early liver allograft dysfunction (139). Hepatocyte-derived miR-122 triggers M1 polarization of KCs, exacerbating hepatic IRI by modulating specific pathways (140). The early elevation of serum levels of miRNAs, including miR-122, miR-146a, and miR-192, has shown potential as powerful markers for predicting graft injury and acute rejection after liver transplantation, often preceding changes in transaminase levels (141).

miR-155 plays a role in inflammation, immunity, and tumorigenesis in liver disease. Inhibition of miR-155 expression in KCs results in positive outcomes by activating anti-inflammatory pathways, enhancing the survival of liver allografts, and attenuating inflammatory injury and apoptosis after IRI (142, 143). MiRNAs such as miR-155 and miR-181a may also serve as potential noninvasive biomarkers. Pre-transplant miR-155 levels identified patients at low immunological risk, and the combination of miR-181a and miR-155 levels acted as an early and noninvasive biomarker for preventing acute T cell-mediated rejection (TCMR) and subclinical rejection (144).

These findings suggest that specific miRNAs hold promise as reliable and early markers for assessing graft injury, predicting rejection episodes, and monitoring complications, such as HCC recurrence after liver transplantation. Further research and validation studies could enhance their clinical utility for improving patient outcomes and graft survival.

3.4.2 Renal transplantation

The use of miRNAs as diagnostic and prognostic markers in renal transplantation has shown considerable potential for addressing various aspects of graft health, rejection, and long-term dysfunction.

Recent validation studies have highlighted that miRNAs, including miR-142-5p, miR-142-3p, miR-155 and miR-223, have high specificity in biopsy specimens and help predict TCMR in allogeneic kidney transplantation (145). Interestingly, Pierre's group identified a variety of miRNAs that interact with the TIM gene, including miR-142-3p and miR-142-5p by analyzing miRNA profiles in kidney allograft samples. However, alloimmune injury pathways are often not unique or specific, and miRNAs such as miR-142-3p or miR-155-5p have been associated not only with IFTA but also with acute rejection or TCMR (146).

miR-21 is a crucial marker of chronic renal dysfunction after transplantation. Silencing miR-21 directly activates Notch2, inhibits the development of renal fibrosis and inflammation, and ultimately prevents chronic allograft dysfunction (147). Changes in miR-21 expression levels in plasma, urine, and graft tissue serve as diagnostic markers for identifying renal injury and dysfunction over time (148).

Moreover, miRNAs, including miR-19a, miR-886-5p, miR-126, miR-223, and miR-24, have been validated as independent predictors of HCC recurrence within the Milan criteria after liver transplantation, aiding the prognosis and management of HCC after transplantation (149).

Richard and colleagues conducted an analysis of microRNA expression in peripheral blood mononuclear cells (PBMC) from patients with chronic antibody-mediated rejection (CAMR) and those with stable graft function, revealing a significant upregulation of miR-142-5p in CAMR (150). This finding was validated and analyzed, indicating that miR-142-5p functions not only as a potential biomarker for CAMR but also plays a role in regulating the immune status of patients.

TCMR, treatable without causing graft failure but associated with chronic or progressive renal dysfunction, has been associated with specific miRNA profiles, aiding in the prediction and understanding of this type of rejection (151).

These findings underscore the potential of miRNAs as noninvasive and specific biomarkers for diagnosing rejection types, monitoring graft health, and predicting chronic dysfunction in renal transplantation. Continued research and validation are essential to refine their clinical utility and enhance their role in improving patient outcomes after transplantation.

3.4.3 Heart transplantation

The role of miRNAs in heart transplantation has emerged as a promising avenue for diagnosing graft rejection, understanding immune responses, and improving outcomes. Recent studies have shed light on the specific miRNAs associated with acute cellular rejection (ACR) and ABMR after heart transplantation.

Identified and validated in 2020, miR-181a-5p showed promise as a marker for ACR in heart transplantation (152). Its specificity and high negative predictive value render it a potential diagnostic tool. A 2021 study identified miR-139-5p, miR-151a-5p, and miR-186-5p as predictive markers for the subsequent development of rejection after heart transplantation (153).

T cell-derived exosomal miR-142-3p is elevated during cardiac allograft rejection, contributing to increased vascular permeability by downregulating the expression of the endothelial Rab11 family of interacting proteins 2 (RAB11FIP2) (154).

miR-146a and miR-155 are involved in the regulation of immune response and rejection mechanisms. Deletion of miR-146a in Tregs exerts tissue-protective effects and transiently prolongs cardiac survival in transplanted mice (155). miR-155 serves as a regulator of allograft rejection by affecting T cell proliferation and macrophage function (142, 156, 157).

Inhibition of miR-155 has shown promising results in suppressing macrophage maturation, downregulating T cell responses, and inducing graft immune tolerance. Using antagomiR-155 delivered through ultrasound-targeted microbubble destruction technology reduces the degree of ACR and improves allogeneic heart survival (158). Ultrasound-guided microbubble disruption technology, capable of delivering cationic microbubbles with miRNA155 silencers to target tissues, is considered a more desirable immunosuppressive therapy for ACR (159).

While these studies highlight the potential of miRNAs as diagnostic markers and therapeutic targets in heart transplantation, further research is necessary to validate these findings in larger cohorts and to standardize diagnostic approaches, considering the heterogeneity of treatment protocols across transplant centers. Developing miRNA-based interventions holds promise for improving rejection detection and for managing post-transplantation outcomes in heart transplantation.

4 Potential associations of TIM proteins with miRNAs

The relationship between miRNAs, specifically miR-155, and the TIM-3 pathway has been extensively studied in the context of various inflammatory and immune responses, including chronic infections and transplantation. However, the direct implications and specific roles of miR-155 and TIM-3 in allograft tolerance and transplantation immunity need to be further elucidated.

miR-155 is a crucial regulator of inflammation and immunity, affecting various immune cell activities such as macrophage polarization, differentiation of T helper cell subsets such as Th17 and Tregs, and cytokine production (160). miR-155 modulates the expression of suppressor of cytokine signaling 1 (SOCS1), a key negative regulator of the JAK–STAT pathway (161). This miRNA can influence macrophage phenotypes, including the M1/M2 balance, and affect the local inflammatory response in certain contexts, such as liver transplantation and hepatic IRI (32, 162, 163).

TIM-3, an inhibitory co-receptor expressed on immune cells, interacts with different ligands such as Gal-9 and plays a role in regulating immune responses (164, 165). Through its interactions, TIM-3 affects T cell polarization, cytokine production, DC maturation, and other immune activities (166, 167). The interplay between TIM-3 and miR-155 has been studied in inflammation and immune regulation, particularly in controlling adaptive and innate immune cell activation. However, direct evidence regarding their roles in allograft tolerance, specifically in transplantation immunity, is yet to be thoroughly investigated. Understanding the specific contributions of miR-155 and TIM-3 in allograft tolerance might offer potential therapeutic avenues for modulating immune responses and improving transplantation outcomes.

The interactions between other miRNAs (miR-142 and miR-330) and members of the TIM family (TIM-1 and TIM-3) have been studied in various contexts, shedding light on their roles in immune regulation, inflammatory responses, and tolerance induction in different physiological settings, including transplantation and maternal-fetal tolerance (23, 26, 59, 168). Studies have shown that miR-142-3p plays a role in modulating TIM-1 transcription, influencing endothelial cell permeability, and reducing systemic inflammatory responses during viral infections (169, 170). It reports that miR-142-3p are upregulated in biopsies from patients with microvascular inflammation typical of Antibody-mediated rejection (ABMR) (171). Elevated miR-142 levels have been observed in patients with cardiac and renal transplant rejection, indicating its potential as a biomarker for monitoring graft rejection. The regulatory function of miR-142 in targeting TGF-B sensitivity and enhancing Treg development has been linked to promoting cardiac allograft tolerance by targeting *Tgfbr1* (168). Contradictory findings have been reported regarding the effects of miR-142 knockdown in specific cells. While Treg-specific knockdown led to severe autoimmune disease, transient knockdown enhanced Treg survival and improved skin graft survival (172). After *in situ* liver transplantation, TIM-1 blockade not only inhibits macrophage recruitment and infiltration, but also enhances Th2/Treg differentiation and improves IRI (173). TIM-1 signaling, in turn, can maintain and induce baseline levels of Bregs and clear apoptotic cells during transplantation to produce IL-10, which promotes immune tolerance and survival (46). Even TIM-1$^+$ Bregs affect Th differentiation, thereby inhibiting Th1/Th17 cells and promoting Th2 cells and Foxp3$^+$ Tregs, which are dependent on IL-10 expression (174).

miR-330-5p protects against myocardial IRI and apoptosis by modulating TIM-3 transcription and translation, thereby reducing the expression of the inflammatory mediator NLRP3 (24). In a model of myocardial IRI, downregulation of miR-330 inhibited left ventricular remodeling via the TGF-B1–Smad3 pathway (175). miR-330–TIM-3 interactions promote macrophage M2 polarization, inhibiting local inflammation and insulin resistance (26). TIM-3 activity in innate immune cells, facilitated by miR-330, contributes to trophoblast invasion and angiogenesis, essential for maintaining maternal-fetal tolerance (176).

5 Hypothetical insights from the mechanism process

Although there is no direct evidence in the literature suggesting that miRNA and TIM may play an emerging role in transplantation immunity. However, we seem to be able to propose a plausible hypothesis for such an interaction mechanism through the signaling axis they share.

The miRNA/TIM/TLR signaling axis: In a model of lung transplantation, miR-21 and miR-122 ameliorate graft dysfunction and ischemia-reperfusion injury by negatively regulating the TLR signaling (177). Activation of the TLR signaling pathway alters macrophage miR-21 expression, which influences macrophage polarization status and inflammatory responses (178). The interaction between the two acts as a feedback regulator that modulates the initiation and termination of inflammation, providing a fundamental argument for post-transplant immune regulation (179). Furthermore, in addition to TLRs themselves, miRNAs also regulate TLR-related signaling proteins that regulate related pathways. For example, in Kupffer's disease, miR-146a/b can act as a negative regulator to control the TLR4 pathway to prevent liver transplant injury by down-regulating IRAK1 and TRAF6 (180). TIM-3 inhibits the production of inflammatory factors associated with the TLR pathway by suppressing NF-KB to create an immune-tolerant microenvironment (181). Interestingly, HMGB1 promotes TIM-1Breg cell expansion through TLR2/4 and mitogen-activated protein kinase (MAPK) signaling pathways, providing new evidence for immune tolerance (182). Surprisingly, miRNAs were able to attenuate inflammatory and oxidative responses through the HMGB1/TLR4/NF-KB axis (183). Although the relationship between miRNAs and TIM-targeted regulation has long been clear. However, data show that miRNAs bind to mRNAs encoding the 3'-UTR of TIM-3 (36). All these data are sufficient to suggest that the miRNA/TIM/TLR may become a new signaling axis for immune regulation before and after transplantation.

miRNA/TIM/PI3K/AKT signaling axis: The ability of miRNAs to make early prediction and intervention of post-transplantation acute kidney injury through PI3K/AKT signaling pathway was found by prediction (184). miR-21 accelerates wound healing and angiogenesis in grafted skin by activating PI3K/AKT and ERK1/2 signaling (185). Upregulation of miR-221 was able to target PTEN to activate PI3K/AKT to restore contractile function and ameliorate myocardial injury in transplanted myocardium (186). Binding of Gal-9 to Tim-3 can inhibit activation of the PI3K/AKT pathway and enhance the function of Treg cells, thereby attenuating acute GVHD and inducing immune tolerance (187). In the AML model, elevated TIM-3 promotes M2 macrophage polarization, leading to elevated PI3K and AKT levels to accelerate tumor immune escape (188). Through PI3K/AKT signaling, it has long been clear that miRNAs can promote tumor metastasis, immune escape and microenvironmental remodeling (189). MiRNAs have a novel mechanism to balance immune injury and tolerance in viral infection and anti-tumor with respect to TIM signaling capacity in T/NK cells (190). In summary, we believe that induction of immune tolerance and improvement of graft function in the transplant microenvironment are the main themes of this pathway.

TIM/miR/SOCS1 signaling axis: Recent literature suggests that miR-142 and miR-155 exhibit differential expression patterns in the miRNA profiles of kidney transplant samples, with both being upregulated in biopsies from patients exhibiting microvascular inflammation characteristic of rejection (146, 171). Furthermore, it has been demonstrated that miR-155 directly targets SOCS1, thereby promoting immune cell activation and enhancing the immune response (161, 191). Collectively, these findings indicate that modulation of the miR-155/SOCS1 axis may offer novel insights into the mechanisms underlying transplantation immunity. In a similar vein, the miR-142/SOCS1 axis may play a significant role in disease pathogenesis by influencing T cell differentiation and enhancing the secretion of specific cytokines, including IL-6 and IL-8 (192, 193). These effects can adversely impact transplanted organs and elevate the risk of graft rejection. As illustrated in Table 1, existing studies have validated the regulatory roles of miR-142 and miR-155 in the modulation of TIM-1 and TIM-3, respectively.

These findings suggest that intricate interactions between miRNAs and members of the TIM family modulate immune responses, regulate inflammatory processes, and influence tissue-specific responses. These interactions can have diverse effects on various immune cells, leading to implications in transplantation tolerance, inflammation modulation, and maternal-fetal immune regulation. Further studies are required to better understand the precise mechanisms and outcomes of miRNA–TIM interactions in transplantation settings and harness their potential for therapeutic interventions aimed at promoting immune tolerance and mitigating transplant rejection.

6 Discussion

The field of transplantation medicine has evolved substantially over the years, offering life-saving treatments for individuals with organ failure or tissue damage. Despite these advancements, post-transplantation complications remain a considerable challenge. Issues such as graft rejection, IRI, allograft dysfunction, and infections can jeopardize successful organ transplantation. Enhancing long-term graft function and survival outcomes requires a personalized treatment approach tailored to individual immune responses.

The TIM family of proteins is a focal point of transplantation research. Modulation of the TIM pathways using blocking antibodies or soluble proteins has shown promise in altering immune responses. These approaches aim to tilt the balance toward tolerance by providing co-inhibitory signals to T and B cells or suppressing innate immune cells. However, varying affinities and epitopes of TIM antibodies can lead to different T cell effects, resulting in immune cell dysfunction. Moreover, TIM proteins act as receptors for phosphatidylserine, contributing not only to the regulation of innate immunity but also to the control of adaptive immune responses, adding complexity to their roles in transplantation.

miRNAs are key regulators of gene expression and have shown promise in transplantation immunology. Analysis of circulating and tissue-specific miRNAs has suggested them as diagnostic and prognostic biomarkers, offering insights into efficacy and predicting transplantation outcomes. These miRNAs hold the potential as the specific markers for assessing immune responses and status of transplanted organs.

Importantly, a reciprocal regulatory relationship exists between the TIM proteins and miRNAs. TIM proteins can regulate miRNAs through various mechanisms; conversely, miRNAs can influence the expression of TIM proteins. This intricate interplay has been observed in various contexts, including tumorigenesis, viral infections, and metabolic disorders, such as insulin resistance in diabetes mellitus. Exploring and understanding this reciprocal regulation in the context of transplant immune tolerance can offer new avenues for clinical studies and potential therapeutic interventions.

In the realm of future transplantation research in miRNA and TIM, several promising avenues beckon our exploration. Initially, we should focus on the study of specific miRNAs, such as miR-21, miR-155, and miR-133a-5p. Utilizing databases and software like miRWalk and TargetScan, we can predict potential binding sites for these miRNAs. Concurrently, in the context of transplantation, it's imperative to collect plasma, urine, or tissue samples from patients before and after transplantation or drug administration. These samples can undergo miRNA sequencing, followed by screening and validation of differentially expressed genes. To investigate downstream signaling molecule alterations, protein microarrays can be employed to identify differential proteins, which can then be verified using luciferase reporter genes for miRNA binding to the 3'UTR of genes.

Furthermore, the expression patterns of miRNAs may vary between different transplanted organs, indicating tissue-specific regulatory mechanisms. Hence, we should prioritize the study of post-transplantation immunomodulatory capacity on miRNA. This includes the regulation of immune cell function and response strength in adaptive immunity (T/B cells) and innate immunity (NK and macrophages). In terms of signaling pathways, our focus should be on influencing cell differentiation/activation/effector function, integrating transcriptomic, proteomic, and other multi-omics data with experimental validation for comprehensive analysis and screening.

Ultimately, leveraging the regulatory role of miRNAs, it's crucial to devise novel therapeutic strategies for a safe and effective approach to the transplantation site. Nanoparticle delivery technology can be utilized to transport specific immunomodulatory genes to transplanted tissues, thereby inducing local immunosuppressive cytokine production and fostering immune tolerance. Additionally, considering the fragility of miRNAs, Ultrasound Targeted Microbubbles Destruction offers a non-invasive, targeted gene delivery technique that is safe, efficient, and specific.

In summary, the intersection between TIM proteins and miRNAs represents a promising area for further investigation of transplantation immune tolerance. Understanding the complex interplay between these molecules and their regulatory roles may lead to innovative therapeutic strategies aimed at promoting immune tolerance and improving long-term outcomes in transplant recipients.

Author contributions

JT: Writing – original draft. XS: Software, Writing – original draft. HQ: Data curation, Writing – original draft. QD: Writing – review & editing. LW: Funding acquisition, Writing – review & editing.

Funding

The author(s) declare financial support was received for the research, authorship, and/or publication of this article. This work was supported by the National Natural Science Foundation of China (82305289), Science and Technology Development Plan of Suzhou (SKY2023078), Zhangjiagang Science and Technology Bureau Healthcare Guidance Project (ZKYL2313), and Zhangjiagang Health Youth Science and Technology Project (ZJGQNKJ202208), and Science and Technology Development Plan of Suzhou(KJXW2021066).

Acknowledgments

This is a short text to acknowledge the contributions of Zhangjiagang TCM Hospital Affiliated to Nanjing University of Chinese Medicine and QD that aided the efforts of the authors.

Conflict of interest

The authors declare that the research was conducted in the absence of any commercial or financial relationships that could be construed as a potential conflict of interest.

Publisher's note

References

1. Duneton C, Winterberg PD, Ford ML. Activation and regulation of alloreactive T cell immunity in solid organ transplantation. *Nat Rev Nephrol*. (2022) 18:663–76. doi: 10.1038/s41581-022-00600-0

2. Griffith BP, Shah A, Awad MA. Current status and outcomes in heart transplantation: A narrative review. *Rev Cardiovasc Med*. (2022) 23:11. doi: 10.31083/j.rcm2301011

3. Roberts MB, Fishman JA. Immunosuppressive agents and infectious risk in transplantation: managing the "Net state of immunosuppression. *Clin Infect Dis*. (2021) 73:e1302–e17. doi: 10.1093/cid/ciaa1189

4. Jane-Wit D, Fang C, Goldstein DR. Innate immune mechanisms in transplant allograft vasculopathy. *Curr Opin Organ Transplant*. (2016) 21:253–7. doi: 10.1097/MOT.0000000000000314

5. Dreyer CH, Rasmussen M, Pedersen RH, Overgaard S, Ding M. Comparisons of efficacy between autograft and allograft on defect repair in vivo in normal and osteoporotic rats. *BioMed Res Int*. (2020) 2020:9358989. doi: 10.1155/2020/9358989

6. Loupy A, Lefaucheur C. Antibody-mediated rejection of solid-organ allografts. *N Engl J Med*. (2018) 379:1150–60. doi: 10.1056/NEJMra1802677

7. Rodriguez-Manzanet R, DeKruyff R, Kuchroo VK, Umetsu DT. The costimulatory role of tim molecules. *Immunol Rev*. (2009) 229:259–70. doi: 10.1111/j.1600-065X.2009.00772.x

8. Du P, Xiong R, Li X, Jiang J. Immune regulation and antitumor effect of tim-1. *J Immunol Res*. (2016) 2016:8605134. doi: 10.1155/2016/8605134

9. Freeman GJ, Casasnovas JM, Umetsu DT, DeKruyff RH. Tim genes: A family of cell surface phosphatidylserine receptors that regulate innate and adaptive immunity. *Immunol Rev*. (2010) 235:172–89. doi: 10.1111/j.0105-2896.2010.00903.x

10. Tang R, Rangachari M, Kuchroo VK. Tim-3: A co-receptor with diverse roles in T cell exhaustion and tolerance. *Semin Immunol*. (2019) 42:101302. doi: 10.1016/j.smim.2019.101302

11. Banerjee H, Kane LP. Immune regulation by tim-3. *F1000Res*. (2018) 7:316. doi: 10.12688/f1000research.13446.1

12. Liu Y, Chen H, Chen Z, Qiu J, Pang H, Zhou Z. Novel roles of the tim family in immune regulation and autoimmune diseases. *Front Immunol*. (2021) 12:748787. doi: 10.3389/fimmu.2021.748787

13. Liu W, Xu L, Liang X, Liu X, Zhao Y, Ma C, et al. Tim-4 in health and disease: friend or foe? *Front Immunol*. (2020) 11:537. doi: 10.3389/fimmu.2020.00537

14. Ueno T, Habicht A, Clarkson MR, Albin MJ, Yamaura K, Boenisch O, et al. The emerging role of T cell ig mucin 1 in alloimmune responses in an experimental mouse transplant model. *J Clin Invest*. (2008) 118:742–51. doi: 10.1172/JCI32451

15. Thornley TB, Fang Z, Balasubramanian S, Larocca RA, Gong W, Gupta S, et al. Fragile tim-4-expressing tissue resident macrophages are migratory and immunoregulatory. *J Clin Invest*. (2014) 124:3443–54. doi: 10.1172/JCI73527

16. Gupta S, Thornley TB, Gao W, Larocca R, Turka LA, Kuchroo VK, et al. Allograft rejection is restrained by short-lived tim-3+Pd-1+Foxp3+ Tregs. *J Clin Invest*. (2012) 122:2395–404. doi: 10.1172/JCI45138

17. Hill M, Tran N. Mirna interplay: mechanisms and consequences in cancer. *Dis Model Mech*. (2021) 14:dmm047662. doi: 10.1242/dmm.047662

18. Harden JT, Krams SM. Micro-rnas in transplant tolerance. *Curr Opin Organ Transplant*. (2018) 23:66–72. doi: 10.1097/mot.0000000000000479

19. Hamdorf M, Kawakita S, Everly M. The potential of micrornas as novel biomarkers for transplant rejection. *J Immunol Res*. (2017) 2017:4072364. doi: 10.1155/2017/4072364

20. Iliopoulou BP, Hsu K, Perez-Cruz M, Tang SW, Pang WW, Erkers T, et al. Blockade of tim-1 on the donor graft ameliorates graft-versus-host disease following hematopoietic cell transplantation. *Blood Adv*. (2019) 3:3419–31. doi: 10.1182/bloodadvances.2019000286

21. Wei L, Peng Y, Shao N, Zhou P. Downregulation of tim-1 inhibits the proliferation, migration and invasion of glioblastoma cells via the mir-133a/tgfbr1 axis and the restriction of wnt/beta-catenin pathway. *Cancer Cell Int*. (2021) 21:347. doi: 10.1186/s12935-021-02036-1

22. Moghaddam Y, Andalib A, Mohammad-Ganji M, Homayouni V, Sharifi M, Ganjalikhani-Hakemi M. Evaluation of the effect of tim-3 suppression by mir-498 and its effect on apoptosis and proliferation rate of hl-60 cell line. *Pathol Res Pract*. (2018) 214:1482–8. doi: 10.1016/j.prp.2018.07.019

23. Kansakar U, Gambardella J, Varzideh F, Avvisato R, Jankauskas SS, Mone P, et al. Mir-142 targets tim-1 in human endothelial cells: potential implications for stroke, Covid-19, zika, ebola, dengue, and other viral infections. *Int J Mol Sci*. (2022) 23:10242. doi: 10.3390/ijms231810242

24. Zuo W, Tian R, Chen Q, Wang L, Gu Q, Zhao H, et al. Mir-330-5p inhibits nlrp3 inflammasome-mediated myocardial ischemia–reperfusion injury by targeting tim3. *Cardiovasc Drugs Ther*. (2020) 35:691–705. doi: 10.1007/s10557-020-07104-8

25. Fooladinezhad H, Khanahmad H, Ganjalikhani-Hakemi M, Doosti A. Negative regulation of tim-3 expression in aml cell line (Hl-60) using mir-330-5p. *Br J Biomed Sci*. (2016) 73:129–33. doi: 10.1080/09674845.2016.1194564

26. Sun J, Huang Q, Li S, Meng F, Li X, Gong X. Mir-330-5p/tim-3 axis regulates macrophage M2 polarization and insulin resistance in diabetes mice. *Mol Immunol*. (2018) 95:107–13. doi: 10.1016/j.molimm.2018.02.006

27. Emamdoost F, Khanahmad H, Ganjalikhani-hakemi M, Doosti A. The mir-125a-3p inhibits tim-3 expression in aml cell line hl-60 in vitro. *Indian J Hematol Blood Transfusion*. (2016) 33:342–7. doi: 10.1007/s12288-016-0733-4

28. Yang Z, Shan N, Deng Q, Wang Y, Hou Y, Mei J, et al. Extracellular vesicle-derived microrna-18b ameliorates preeclampsia by enhancing trophoblast proliferation and migration via notch2/tim3/mtorc1 axis. *J Cell Mol Med*. (2021) 25:4583–95. doi: 10.1111/jcmm.16234

29. Wang Y, Cheng Q, Liu J, Dong M. Leukemia stem cell-released microvesicles promote the survival and migration of myeloid leukemia cells and these effects can be inhibited by microrna34a overexpression. *Stem Cells Int*. (2016) 2016:1–8. doi: 10.1155/2016/9313425

30. Yan K, Fu Y, Zhu N, Wang Z, Hong J-L, Li Y, et al. Repression of lncrna neat1 enhances the antitumor activity of cd8+T cells against hepatocellular carcinoma via regulating mir-155/tim-3. *Int J Biochem Cell Biol*. (2019) 110:1–8. doi: 10.1016/j.biocel.2019.01.019

31. Zhang F, Zhao J, Sun D, Wei N. Mir-155 inhibits transformation of macrophages into foam cells via regulating ceh expression. *Biomedicine Pharmacotherapy*. (2018) 104:645–51. doi: 10.1016/j.biopha.2018.05.068

32. Jiang X, Zhou T, Xiao Y, Yu J, Dou S, Chen G, et al. Tim-3 promotes tumor-promoting M2 macrophage polarization by binding to stat1 and suppressing the stat1-mir-155 signaling axis. *OncoImmunology*. (2016) 5:1850–7. doi: 10.1080/2162402x.2016.1211219

33. Yan M, Zhang Y, Chang S. Chitosan nanoparticles loaded with tgf-B1 inhibit cervical cancer cell progression through down-regulation of microrna-155 and activation of tim-3 pathway. *J Biomed Nanotechnology*. (2021) 17:1850–7. doi: 10.1166/jbn.2021.3146

34. Zhou J, Jiang Y, Zhang H, Chen L, Luo P, Li L, et al. Clinicopathological implications of tim3+ Tumor-infiltrating lymphocytes and the mir-455-5p/galectin-9 axis in skull base chordoma patients. *Cancer Immunology Immunotherapy*. (2019) 68:1157–69. doi: 10.1007/s00262-019-02349-1

35. Ai Y, Wu S, Gao H, Wei H, Tang Z, Li X, et al. Repression of Crnde Enhances the Anti-Tumor Activity of Cd8 + t Cells against Oral Squamous Cell Carcinoma through Regulating Mir-545-5p and Tim-3. *J Cell Mol Med*. (2021) 25:10857–68. doi: 10.1111/jcmm.16909

36. Zhang M, Gao D, Shi Y, Wang Y, Joshi R, Yu Q, et al. Mir-149-3p reverses cd8 +T-cell exhaustion by reducing inhibitory receptors and promoting cytokine secretion in breast cancer cells. *Open Biol*. (2019) 9:190061. doi: 10.1098/rsob.190061

37. Hojati Z, Ganjalikhani-Hakemi M, Ameri M, Alimohammadi-Jelodar SF, Dehbashi M, Mohammad Ganji M, et al. Evaluation of silencing effect of mir-133a-5p mimic on tim-3 expression in aml (Hl-60) cell line. *Indian J Clin Biochem*. (2019) 35:359–66. doi: 10.1007/s12291-019-00834-z

38. Yu T, Ju Z, Luo M, Hu R, Teng Y, Xie L, et al. Elevated expression of mir-146a correlates with high levels of immune cell exhaustion markers and suppresses cellular immune function in chronic hiv-1-infected patients. *Sci Rep*. (2019) 9:18829. doi: 10.1038/s41598-019-55100-2

39. Xu C, Zhai J, Fu Y. Overexpression of nuclear enriched autosomal transcript 1 facilitates cell proliferation, migration invasion, and suppresses apoptosis in endometrial cancer by targeting microrna-202-3p/T cell immunoglobulin and mucin domain 4 axis. *Cancer Biotherapy Radiopharmaceuticals*. (2022) 37:815–23. doi: 10.1089/cbr.2020.3902

40. Kuchroo VK, Umetsu DT, DeKruyff RH, Freeman GJ. The tim gene family: emerging roles in immunity and disease. *Nat Rev Immunol*. (2003) 3:454–62. doi: 10.1038/nri1111

41. Kane LP. Tim family proteins and autoimmunity. *Autoimmunity*. (2007) 40:405–8. doi: 10.1080/08916930701464871

42. Meyers JH, Sabatos CA, Chakravarti S, Kuchroo VK. The tim gene family regulates autoimmune and allergic diseases. *Trends Mol Med*. (2005) 11:362–9. doi: 10.1016/j.molmed.2005.06.008

43. McGrath MM. Diverse roles of tim4 in immune activation: implications for alloimmunity. *Curr Opin Organ Transplant*. (2018) 23:44–50. doi: 10.1097/MOT.0000000000000487

44. Tami C, Silberstein E, Manangeeswaran M, Freeman GJ, Umetsu SE, DeKruyff RH, et al. Immunoglobulin a (Iga) is a natural ligand of hepatitis a virus cellular receptor 1 (Havcr1), and the association of iga with havcr1 enhances virus-receptor interactions. *J Virol*. (2007) 81:3437–46. doi: 10.1128/JVI.01585-06

45. Angiari S, Constantin G. Regulation of T cell trafficking by the T cell immunoglobulin and mucin domain 1 glycoprotein. *Trends Mol Med*. (2014) 20:675–84. doi: 10.1016/j.molmed.2014.10.003

46. Yeung MY, Ding Q, Brooks CR, Xiao S, Workman CJ, Vignali DA, et al. Tim-1 signaling is required for maintenance and induction of regulatory B cells. *Am J Transplant*. (2015) 15:942–53. doi: 10.1111/ajt.13087

47. Bod L, Kye Y-C, Shi J, Torlai Triglia E, Schnell A, Fessler J, et al. B-cell-specific checkpoint molecules that regulate anti-tumor immunity. *Nature*. (2023) 619:348–56. doi: 10.1038/s41586-023-06231-0

48. Wang J, Qiao L, Hou Z, Luo G, Ou JHJ. Tim-1 promotes hepatitis C virus cell attachment and infection. *J Virol*. (2017) 91:e01583-16. doi: 10.1128/jvi.01583-16

49. Liu Y, Chen Z, Qiu J, Chen H, Zhou Z. Altered tim-1 and il-10 expression in regulatory B cell subsets in type 1 diabetes. *Front Immunol*. (2021) 12:773896. doi: 10.3389/fimmu.2021.773896

50. Degauque N, Mariat C, Kenny J, Zhang D, Gao W, Vu MD, et al. Immunostimulatory tim-1–specific antibody deprograms tregs and prevents transplant tolerance in mice. *J Clin Invest*. (2008) 118:735–41. doi: 10.1172/jci32562

51. Cherukuri A, Rothstein DM. Regulatory and transitional B cells: potential biomarkers and therapeutic targets in organ transplantation. *Curr Opin Organ Transplant*. (2022) 27:385–91. doi: 10.1097/MOT.0000000000001010

52. Ding Q, Yeung M, Camirand G, Zeng Q, Akiba H, Yagita H, et al. Regulatory B cells are identified by expression of tim-1 and can be induced through tim-1 ligation to promote tolerance in mice. *J Clin Invest*. (2011) 121:3645–56. doi: 10.1172/jci46274

53. Li S, Li X, Yang M, Wei L, Wei L, Deng S, et al. Identification of the subsets of il-10-producing regulatory B cells in the course of tolerance induction and maintenance in islet allotransplantation. *Transplant Proc*. (2018) 50:3900–5. doi: 10.1016/j.transproceed.2018.04.065

54. Lee KM, Kim JI, Stott R, Soohoo J, O'Connor MR, Yeh H, et al. Anti-cd45rb/anti-tim-1-induced tolerance requires regulatory B cells. *Am J Transplant*. (2012) 12:2072–8. doi: 10.1111/j.1600-6143.2012.04055.x

55. Shankar S, Stolp J, Juvet SC, Beckett J, Macklin PS, Issa F, et al. Ex vivo-expanded human cd19+Tim-1+ Regulatory B cells suppress immune responses in vivo and are dependent upon the tim-1/stat3 axis. *Nat Commun*. (2022) 13:3121. doi: 10.1038/s41467-022-30613-z

56. Zheng Y, Wang L, Chen M, Liu L, Pei A, Zhang R, et al. Inhibition of T cell immunoglobulin and mucin-1 (Tim-1) protects against cerebral ischemia-reperfusion injury. *Cell Communication Signaling*. (2019) 17:112. doi: 10.1186/s12964-019-0417-4

57. Huang YH, Zhu C, Kondo Y, Anderson AC, Gandhi A, Russell A, et al. Ceacam1 regulates tim-3-mediated tolerance and exhaustion. *Nature*. (2015) 517:386–90. doi: 10.1038/nature13848

58. Zhao L, Cheng S, Fan L, Zhang B, Xu S. Tim-3: an update on immunotherapy. *Int Immunopharmacol*. (2021) 99:107933. doi: 10.1016/j.intimp.2021.107933

59. Li M, Sun F, Xu Y, Chen L, Chen C, Cui L, et al. Tim-3(+) decidual mphis induced th2 and treg bias in decidual cd4(+)T cells and promoted pregnancy maintenance via cd132. *Cell Death Dis*. (2022) 13:454. doi: 10.1038/s41419-022-04899-2

60. Zhu C, Anderson AC, Schubart A, Xiong H, Imitola J, Khoury SJ, et al. The tim-3 ligand galectin-9 negatively regulates T helper type 1 immunity. *Nat Immunol*. (2005) 6:1245–52. doi: 10.1038/ni1271

61. Rong S, Park JK, Kirsch T, Yagita H, Akiba H, Boenisch O, et al. The tim-1:Tim-4 pathway enhances renal ischemia-reperfusion injury. *J Am Soc Nephrol*. (2011) 22:484–95. doi: 10.1681/ASN.2010030321

62. Meyers JH, Chakravarti S, Schlesinger D, Illes Z, Waldner H, Umetsu SE, et al. Tim-4 is the ligand for tim-1, and the tim-1-tim-4 interaction regulates T cell proliferation. *Nat Immunol*. (2005) 6:455–64. doi: 10.1038/ni1185

63. Shim JA, Lee E-S, Choi B, Sohn S. The role of T cell immunoglobulin mucin domains 1 and 4 in a herpes simplex virus-induced behçet's disease mouse model. *Mediators Inflammation*. (2013) 2013:1–13. doi: 10.1155/2013/903948

64. Guo Y-Y, Yin C-J, Zhao M, Guo L-T, Su R-F, Fu X-X, et al. Effect of rmt1-10 on the immunological characteristics of dendritic cells cultured in vitro and corneal european review for medical and pharmacological sciences. *Eur Rev Med Pharmacol Sci*. (2019) 23:9150–62. doi: 10.26355/eurrev_201911_19405

65. Feng B-S, Chen X, He S-H, Zheng P-Y, Foster J, Xing Z, et al. Disruption of T-cell immunoglobulin and mucin domain molecule (Tim)–1/tim4 interaction as a therapeutic strategy in a dendritic cell–induced peanut allergy model. *J Allergy Clin Immunol*. (2008) 122:55–61.e7. doi: 10.1016/j.jaci.2008.04.036

66. Corneillie L, Lemmens I, Montpellier C, Ferrie M, Weening K, Van Houtte F, et al. The phosphatidylserine receptor tim1 promotes infection of enveloped hepatitis E virus. *Cell Mol Life Sci*. (2023) 80:326. doi: 10.1007/s00018-023-04977-4

67. Jayasinghe MK, Gao C, Yap G, Yeo BZJ, Vu LT, Tay DJW, et al. Red blood cell-derived extracellular vesicles display endogenous antiviral effects and enhance the efficacy of antiviral oligonucleotide therapy. *ACS Nano*. (2023) 17:21639–61. doi: 10.1021/acsnano.3c06803

68. Thio CL-P, Lai AC-Y, Wang J-C, Chi P-Y, Chang Y-L, Ting Y-T, et al. Identification of a pd-L1+Tim-1+ Inkt subset that protects against fine particulate matter–induced airway inflammation. *JCI Insight*. (2022) 7:e164157. doi: 10.1172/jci.insight.164157

69. Angiari S, Donnarumma T, Rossi B, Dusi S, Pietronigro E, Zenaro E, et al. Tim-1 glycoprotein binds the adhesion receptor P-selectin and mediates T cell trafficking during inflammation and autoimmunity. *Immunity*. (2014) 40:542–53. doi: 10.1016/j.immuni.2014.03.004

70. Mori Y, Ajay AK, Chang JH, Mou S, Zhao H, Kishi S, et al. Kim-1 mediates fatty acid uptake by renal tubular cells to promote progressive diabetic kidney disease. *Cell Metab*. (2021) 33:1042–61.e7. doi: 10.1016/j.cmet.2021.04.004

71. Yamanishi Y, Kitaura J, Izawa K, Kaitani A, Komeno Y, Nakamura M, et al. Tim1 is an endogenous ligand for lmir5/cd300b: lmir5 deficiency ameliorates mouse kidney ischemia/reperfusion injury. *J Exp Med*. (2010) 207:1501–11. doi: 10.1084/jem.20090581

72. Liu Y, Ji H, Zhang Y, Shen X, Gao F, He X, et al. Recipient T cell tim-3 and hepatocyte galectin-9 signaling protects mouse liver transplants against ischemia-reperfusion injury. *J Hepatol*. (2015) 62:563–72. doi: 10.1016/j.jhep.2014.10.034

73. Li YH, Zhou WH, Tao Y, Wang SC, Jiang YL, Zhang D, et al. The galectin-9/tim-3 pathway is involved in the regulation of nk cell function at the maternal-fetal interface in early pregnancy. *Cell Mol Immunol*. (2016) 13:73–81. doi: 10.1038/cmi.2014.126

74. Yang R, Sun L, Li CF, Wang YH, Yao J, Li H, et al. Galectin-9 interacts with pd-1 and tim-3 to regulate T cell death and is a target for cancer immunotherapy. *Nat Commun*. (2021) 12:832. doi: 10.1038/s41467-021-21099-2

75. Ni X, Wu W, Sun X, Ma J, Yu Z, He X, et al. Interrogating glioma-M2 macrophage interactions identifies gal-9/tim-3 as a viable target against pten-null glioblastoma. *Sci Adv*. (2022) 27:eabl5165. doi: 10.14791/btrt.2022.10.Suppl

76. Folgiero V, Cifaldi L, Li Pira G, Goffredo BM, Vinti L, Locatelli F. Tim-3/gal-9 interaction induces ifngamma-dependent ido1 expression in acute myeloid leukemia blast cells. *J Hematol Oncol*. (2015) 8:36. doi: 10.1186/s13045-015-0134-4

77. Goncalves Silva I, Yasinska IM, Sakhnevych SS, Fiedler W, Wellbrock J, Bardelli M, et al. The tim-3-galectin-9 secretory pathway is involved in the immune escape of human acute myeloid leukemia cells. *EBioMedicine*. (2017) 22:44–57. doi: 10.1016/j.ebiom.2017.07.018

78. Dolina JS, Braciale TJ, Hahn YS. Liver-primed cd8+ T cells suppress antiviral adaptive immunity through galectin-9-independent T-cell immunoglobulin and mucin 3 engagement of high-mobility group box 1 in mice. *Hepatology*. (2014) 59:1351–65. doi: 10.1002/hep.26938

79. Yasinska IM, Goncalves Silva I, Sakhnevych SS, Ruegg L, Hussain R, Siligardi G, et al. High mobility group box 1 (Hmgb1) acts as an "Alarmin" to promote acute myeloid leukemia progression. *Oncoimmunology*. (2018) 7:e1438109. doi: 10.1080/2162402X.2018.1438109

80. Huang S, Liu D, Sun J, Zhang H, Zhang J, Wang Q, et al. Tim-3 regulates sepsis-induced immunosuppression by inhibiting the nf-kappab signaling pathway in cd4 T cells. *Mol Ther*. (2022) 30:1227–38. doi: 10.1016/j.ymthe.2021.12.013

81. Kojima H, Kadono K, Hirao H, Dery KJ, Torgerson T, Yao S, et al. T cell ceacam1-tim-3 crosstalk alleviates liver transplant injury in mice and humans. *Gastroenterology*. (2023) 165:1233–48.e9. doi: 10.1053/j.gastro.2023.07.004

82. Lake CM, Voss K, Bauman BM, Pohida K, Jiang T, Dveksler G, et al. Tim-3 drives temporal differences in restimulation-induced cell death sensitivity in effector cd8(+) T cells in conjunction with ceacam1. *Cell Death Dis*. (2021) 12:400. doi: 10.1038/s41419-021-03689-6

83. Wu M, Wu A, Zhang X, Li Y, Li B, Jin S, et al. Identification of a novel small-molecule inhibitor targeting tim-3 for cancer immunotherapy. *Biochem Pharmacol*. (2023) 212:115583. doi: 10.1016/j.bcp.2023.115583

84. Jiang W, Li F, Jiang Y, Li S, Liu X, Xu Y, et al. Tim-3 blockade elicits potent anti-multiple myeloma immunity of natural killer cells. *Front Oncol*. (2022) 12:739976. doi: 10.3389/fonc.2022.739976

85. Matsumoto H, Fujita Y, Onizawa M, Saito K, Sumichika Y, Yoshida S, et al. Increased ceacam1 expression on peripheral blood neutrophils in patients with rheumatoid arthritis. *Front Immunol*. (2022) 13:978435. doi: 10.3389/fimmu.2022.978435

86. Kristenson L, Badami C, Ljungberg A, Islamagic E, Tian Y, Xie G, et al. Deletion of the tmem30a gene enables leukemic cell evasion of nk cell cytotoxicity. *Proc Natl Acad Sci U.S.A*. (2024) 121:e2316447121. doi: 10.1073/pnas.2316447121

87. Ma S, Tian Y, Peng J, Chen C, Peng X, Zhao F, et al. Identification of a small-molecule tim-3 inhibitor to potentiate T cell–mediated antitumor immunotherapy in preclinical mouse models. *Sci Transl Med*. (2023) 15:6752. doi: 10.1126/scitranslmed.adg6752

88. Zhao P, Xu L, Wang P, Liang X, Qi J, Liu P, et al. Increased expression of human T-cell immunoglobulin- and mucin-domain-containing molecule-4 in peripheral blood mononuclear cells from patients with system lupus erythematosus. *Cell Mol Immunol*. (2010) 7:152–6. doi: 10.1038/cmi.2009.118

89. Ding Q, Mohib K, Kuchroo VK, Rothstein DM. Tim-4 identifies ifn-Γ–expressing proinflammatory B effector 1 cells that promote tumor and allograft rejection. *J Immunol*. (2017) 199:2585–95. doi: 10.4049/jimmunol.1602107

90. Hu T, Fan X, Ma L, Liu J, Chang Y, Yang P, et al. Tim4-tim1 interaction modulates th2 pattern inflammation through enhancing sirt1 expression. *Int J Mol Med*. (2017) 40:1504–10. doi: 10.3892/ijmm.2017.3150

91. Rhein BA, Brouillette RB, Schaack GA, Chiorini JA, Maury W. Characterization of human and murine T-cell immunoglobulin mucin domain 4 (Tim-4) igv domain residues critical for ebola virus entry. *J Virol*. (2016) 90:6097–111. doi: 10.1128/JVI.00100-16

92. Sims B, Farrow A, Williams S, Bansal A, Krendelchtchikov A, Gu L, et al. Role of tim-4 in exosome-dependent entry of hiv-1 into human immune cells. *Int J Nanomedicine*. (2017) 12:4823–33. doi: 10.2147/ijn.S132762

93. Kobayashi N, Karisola P, Pena-Cruz V, Dorfman DM, Jinushi M, Umetsu SE, et al. Tim-1 and tim-4 glycoproteins bind phosphatidylserine and mediate uptake of apoptotic cells. *Immunity*. (2007) 27:927–40. doi: 10.1016/j.immuni.2007.11.011

94. Sanchez-Fueyo A, Tian J, Picarella D, Domenig C, Zheng XX, Sabatos CA, et al. Tim-3 inhibits T helper type 1-mediated auto- and alloimmune responses and promotes immunological tolerance. *Nat Immunol*. (2003) 4:1093–101. doi: 10.1038/ni987

95. Chou F-C, Kuo C-C, Wang Y-L, Lin M-H, Yen BL, Chang D-M, et al. Overexpression of galectin-9 in islets prolongs grafts survival via downregulation of th1 responses. *Cell Transplant*. (2013) 22:2135–45. doi: 10.3727/096368912x657891

96. Gleason MK, Lenvik TR, McCullar V, Felices M, O'Brien MS, Cooley SA, et al. Tim-3 is an inducible human natural killer cell receptor that enhances interferon gamma production in response to galectin-9. *Blood*. (2012) 119:3064–72. doi: 10.1182/blood-2011-06-360321

97. Li YM, Shi YY, Li Y, Yan L, Tang JT, Bai YJ, et al. Soluble tim-3 and gal-9 are associated with renal allograft dysfunction in kidney transplant recipients: A cross-sectional study. *Int Immunopharmacol*. (2018) 55:330–5. doi: 10.1016/j.intimp.2018.01.008

98. Shahbaz SK, Barabadi M, Ahmadpour P, Pourrezagholi F, Nafar M, Foroughi F, et al. Sequential monitoring of tim-3 mrna expression in blood and urine samples of renal transplant recipients. *Transplant Immunol*. (2019) 54:9–16. doi: 10.1016/j.trim.2018.10.007

99. Schietinger A, Greenberg PD. Tolerance and exhaustion: defining mechanisms of T cell dysfunction. *Trends Immunol*. (2014) 35:51–60. doi: 10.1016/j.it.2013.10.001

100. Sakuishi K, Apetoh L, Sullivan JM, Blazar BR, Kuchroo VK, Anderson AC. Targeting tim-3 and pd-1 pathways to reverse T cell exhaustion and restore anti-tumor immunity. *J Exp Med*. (2010) 207:2187–94. doi: 10.1084/jem.20100643

101. Mysore KR, Ghobrial RM, Kannanganat S, Minze LJ, Graviss EA, Nguyen DT, et al. Longitudinal assessment of T cell inhibitory receptors in liver transplant recipients and their association with posttransplant infections. *Am J Transplant*. (2018) 18:351–63. doi: 10.1111/ajt.14546

102. Savill J, Gregory C. Apoptotic ps to phagocyte tim-4: eat me. *Immunity*. (2007) 27:830–2. doi: 10.1016/j.immuni.2007.12.002

103. Park D, Hochreiter-Hufford A, Ravichandran KS. The phosphatidylserine receptor tim-4 does not mediate direct signaling. *Curr Biol*. (2009) 19:346–51. doi: 10.1016/j.cub.2009.01.042

104. Foks AC, Engelbertsen D, Kuperwaser F, Alberts-Grill N, Gonen A, Witztum JL, et al. Blockade of tim-1 and tim-4 enhances atherosclerosis in low-density lipoprotein receptor–deficient mice. *Arterioscler Thromb Vasc Biol*. (2016) 36:456–65. doi: 10.1161/atvbaha.115.306860

105. Rodriguez-Manzanet. R, Meyers. JH, Balasubramanian. S, Slavik. J, Kassam. N, Dardalhon. V, et al. Tim-4 expressed on antigen-presenting cells induces T cell expansion and survival. *J Immunol*. (2008) 180:4706–13. doi: 10.4049/jimmunol.180.7.4706

106. Chow A, SChad S, Green MD, Hellmann MD, Allaj V, Ceglia N, et al. Tim-4(+) cavity-resident macrophages impair anti-tumor cd8(+) T cell immunity. *Cancer Cell*. (2021) 39:973–88.e9. doi: 10.1016/j.ccell.2021.05.006

107. Locati M, Curtale G, Mantovani A. Diversity, mechanisms, and significance of macrophage plasticity. *Annu Rev Pathol*. (2020) 15:123–47. doi: 10.1146/annurev-pathmechdis-012418-012718

108. Ezzelarab M, Thomson AW. Tolerogenic dendritic cells and their role in transplantation. *Semin Immunol*. (2011) 23:252–63. doi: 10.1016/j.smim.2011.06.007

109. Uchida Y, Ke B, Freitas MC, Ji H, Zhao D, Benjamin ER, et al. The emerging role of T cell immunoglobulin mucin-1 in the mechanism of liver ischemia and reperfusion injury in the mouse. *Hepatology*. (2010) 51:1363–72. doi: 10.1002/hep.23442

110. Ni M, Zhang J, Sosa R, Zhang H, Wang H, Jin D, et al. T-cell immunoglobulin and mucin domain-containing protein-4 is critical for kupffer cell homeostatic function in the activation and resolution of liver ischemia reperfusion injury. *Hepatology*. (2021) 74:2118–32. doi: 10.1002/hep.31906

111. Zhang Y, Shen Q, Liu Y, Chen H, Zheng X, Xie S, et al. Hepatic ischemic preconditioning alleviates ischemia-reperfusion injury by decreasing tim4 expression. *Int J Biol Sci*. (2018) 14:1186–95. doi: 10.7150/ijbs.24898

112. Chen Y, Liu Z, Liang S, Luan X, Long F, Chen J, et al. Role of kupffer cells in the induction of tolerance of orthotopic liver transplantation in rats. *Liver Transpl*. (2008) 14:823–36. doi: 10.1002/lt.21450

113. Chen GS, Qi HZ. Effect of kupffer cells on immune tolerance in liver transplantation. *Asian Pac J Trop Med*. (2012) 5:970–2. doi: 10.1016/S1995-7645(12)60184-9

114. Wu H, Xu X, Li J, Gong J, Li M. Tim−4 blockade of kcs combined with exogenous tgf−B Injection helps to reverse acute rejection and prolong the survival rate of mice receiving liver allografts. *Int J Mol Med*. (2018) 42:346–58. doi: 10.3892/ijmm.2018.3606

115. Rodriguez-Manzanet R, Sanjuan MA, Wu HY, Quintana FJ, Xiao S, Anderson AC, et al. T and B cell hyperactivity and autoimmunity associated with niche-specific defects in apoptotic body clearance in tim-4-deficient mice. *Proc Natl Acad Sci U.S.A*. (2010) 107:8706–11. doi: 10.1073/pnas.0910359107

116. Waisman A, Lukas D, Clausen BE, Yogev N. Dendritic cells as gatekeepers of tolerance. *Semin Immunopathol*. (2017) 39:153–63. doi: 10.1007/s00281-016-0583-z

117. Yeung MY, McGrath MM, Nakayama M, Shimizu T, Boenisch O, Magee CN, et al. Interruption of dendritic cell-mediated tim-4 signaling induces regulatory T cells and promotes skin allograft survival. *J Immunol*. (2013) 191:4447–55. doi: 10.4049/jimmunol.1300992

118. Kerr D, Tietjen GT, Gong Z, Tajkhorshid E, Adams EJ, Lee KYC. Sensitivity of peripheral membrane proteins to the membrane context: A case study of phosphatidylserine and the tim proteins. *Biochim Biophys Acta Biomembranes*. (2018) 1860:2126–33. doi: 10.1016/j.bbamem.2018.06.010

119. Leventis PA, Grinstein S. The distribution and function of phosphatidylserine in cellular membranes. *Annu Rev Biophys*. (2010) 39:407–27. doi: 10.1146/annurev.biophys.093008.131234

120. Uribe-Querol E, Rosales C. Phagocytosis: our current understanding of a universal biological process. *Front Immunol*. (2020) 11:1066. doi: 10.3389/fimmu.2020.01066

121. Ichimura T, Asseldonk EJ, Humphreys BD, Gunaratnam L, Duffield JS, Bonventre JV. Kidney injury molecule-1 is a phosphatidylserine receptor that confers a phagocytic phenotype on epithelial cells. *J Clin Invest*. (2008) 118:1657–68. doi: 10.1172/JCI34487

122. Yang L, Brooks CR, Xiao S, Sabbisetti V, Yeung MY, Hsiao LL, et al. Kim-1-mediated phagocytosis reduces acute injury to the kidney. *J Clin Invest*. (2015) 125:1620–36. doi: 10.1172/JCI75417

123. Zhang D, Jiang F, Zaynagetdinov R, Huang H, Sood VD, Wang H, et al. Identification and characterization of M6903, an antagonistic anti-tim-3 monoclonal antibody. *Oncoimmunology*. (2020) 9:1744921. doi: 10.1080/2162402X.2020.1744921

124. Krol J, Loedige I, Filipowicz W. The widespread regulation of microrna biogenesis, function and decay. *Nat Rev Genet*. (2010) 11:597–610. doi: 10.1038/nrg2843

125. Saliminejad K, Khorram Khorshid HR, Soleymani Fard S, Ghaffari SH. An overview of micrornas: biology, functions, therapeutics, and analysis methods. *J Cell Physiol*. (2019) 234:5451–65. doi: 10.1002/jcp.27486

126. Khan Z, Suthanthiran M, Muthukumar T. Micrornas and transplantation. *Clin Lab Med*. (2019) 39:125–43. doi: 10.1016/j.cll.2018.10.003

127. Li S, Le TN, Nguyen TD, Trinh TA, Nguyen TA. Bulges control pri-mirna processing in a position and strand-dependent manner. *RNA Biol*. (2021) 18:1716–26. doi: 10.1080/15476286.2020.1868139

128. Cai Y, Yu X, Hu S, Yu J. A brief review on the mechanisms of mirna regulation. *Genomics Proteomics Bioinf*. (2009) 7:147–54. doi: 10.1016/S1672-0229(08)60044-3

129. Harris A, Krams SM, Martinez OM. Micrornas as immune regulators: implications for transplantation. *Am J Transplant*. (2010) 10:713–9. doi: 10.1111/j.1600-6143.2010.03032.x

130. Okamura K, Hagen JW, Duan H, Tyler DM, Lai EC. The mirtron pathway generates microrna-class regulatory rnas in drosophila. *Cell*. (2007) 130:89–100. doi: 10.1016/j.cell.2007.06.028

131. Kabekkodu SP, Shukla V, Varghese VK, DS J, Chakrabarty S, Satyamoorthy K. Clustered mirnas and their role in biological functions and diseases. *Biol Rev Camb Philos Soc*. (2018) 93:1955–86. doi: 10.1111/brv.12428

132. Chhabra R, Dubey R, Saini N. Cooperative and individualistic functions of the micrornas in the mir-23a~27a~24-2 cluster and its implication in human diseases. *Mol Cancer*. (2010) 9:232. doi: 10.1186/1476-4598-9-232

133. Lataniotis L, Albrecht A, Kok FO, Monfries CAL, Benedetti L, Lawson ND, et al. Crispr/cas9 editing reveals novel mechanisms of clustered microrna regulation and function. *Sci Rep*. (2017) 7:8585. doi: 10.1038/s41598-017-09268-0

134. Wang Y, Luo J, Zhang H, Lu J. Micrornas in the same clusters evolve to coordinately regulate functionally related genes. *Mol Biol Evol*. (2016) 33:2232–47. doi: 10.1093/molbev/msw089

135. Catalanotto C, Cogoni C, Zardo G. Microrna in control of gene expression: an overview of nuclear functions. *Int J Mol Sci*. (2016) 17:1712. doi: 10.3390/ijms17101712

136. Westholm JO, Lai EC. Mirtrons: microrna biogenesis via splicing. *Biochimie*. (2011) 93:1897–904. doi: 10.1016/j.biochi.2011.06.017

137. Zhou M, Hara H, Dai Y, Mou L, Cooper DK, Wu C, et al. Circulating organ-specific micrornas serve as biomarkers in organ-specific diseases: implications for organ allo- and xeno-transplantation. *Int J Mol Sci*. (2016) 17:1232. doi: 10.3390/ijms17081232

138. Hu ZQ, Lu Y, Cui D, Ma CY, Shao S, Chen P, et al. Micrornas and long non-coding rnas in liver surgery: diagnostic and therapeutic merits. *Hepatobiliary Pancreat Dis Int*. (2020) 19:218–28. doi: 10.1016/j.hbpd.2020.04.002

139. Roderburg C, Benz F, Vargas Cardenas D, Koch A, Janssen J, Vucur M, et al. Elevated mir-122 serum levels are an independent marker of liver injury in inflammatory diseases. *Liver Int*. (2015) 35:1172–84. doi: 10.1111/liv.12627

140. Liu L, Xiao F, Sun J, Wang Q, Wang A, Zhang F, et al. Hepatocyte-derived extracellular vesicles mir-122-5p promotes hepatic ischemia reperfusion injury by regulating kupffer cell polarization. *Int Immunopharmacol*. (2023) 119:110060. doi: 10.1016/j.intimp.2023.110060

141. Farid WR, Verhoeven CJ, de Jonge J, Metselaar HJ, Kazemier G, van der Laan LJ. The ins and outs of micrornas as biomarkers in liver disease and transplantation. *Transpl Int*. (2014) 27:1222–32. doi: 10.1111/tri.12379

142. Li J, Gong J, Li P, Li M, Liu Y, Liang S, et al. Knockdown of microrna-155 in kupffer cells results in immunosuppressive effects and prolongs survival of mouse liver allografts. *Transplantation*. (2014) 97:626–35. doi: 10.1097/TP.0000000000000061

143. Xiao Q, Ye QF, Wang W, Fu BQ, Xia ZP, Liu ZZ, et al. Mild hypothermia pretreatment protects hepatocytes against ischemia reperfusion injury via down-regulating mir-122 and igf-1r/akt pathway. *Cryobiology*. (2017) 75:100–5. doi: 10.1016/j.cryobiol.2017.01.005

144. Millan O, Ruiz P, Orts L, Ferre P, Crespo G, Santana M, et al. Monitoring of mir-181a-5p and mir-155-5p plasmatic expression as prognostic biomarkers for acute and subclinical rejection in *de novo* adult liver transplant recipients. *Front Immunol*. (2019) 10:873. doi: 10.3389/fimmu.2019.00873

145. Soltaninejad E, Nicknam MH, Nafar M, Ahmadpoor P, Pourrezagholi F, Sharbafi MH, et al. Differential expression of micrornas in renal transplant patients with acute T-cell mediated rejection. *Transpl Immunol*. (2015) 33:1–6. doi: 10.1016/j.trim.2015.05.002

146. Mahtal N, Lenoir O, Tinel C, Anglicheau D, Tharaux P-L. Micrornas in kidney injury and disease. *Nat Rev Nephrol*. (2022) 18:643–62. doi: 10.1038/s41581-022-00608-6

147. Schauerte C, Hübner A, Rong S, Wang S, Shushakova N, Mengel M, et al. Antagonism of profibrotic microrna-21 improves outcome of murine chronic renal allograft dysfunction. *Kidney Int*. (2017) 92:646–56. doi: 10.1016/j.kint.2017.02.012

148. Chen Y-J, Hsu C-T, Tsai S-F, Chen C-H. Association between circulating micrornas (Mir-21-5p, mir-20a-5p, mir-29b-3p, mir-126-3p and mir-101-3p) and chronic allograft dysfunction in renal transplant recipients. *Int J Mol Sci*. (2022) 23:12253. doi: 10.3390/ijms232012253

149. Han ZB, Zhong L, Teng MJ, Fan JW, Tang HM, Wu JY, et al. Identification of recurrence-related micrornas in hepatocellular carcinoma following liver transplantation. *Mol Oncol*. (2012) 6:445–57. doi: 10.1016/j.molonc.2012.04.001

150. Mari B, Danger R, Paul C, Giral M, Lavault A, Foucher Y, et al. Expression of mir-142-5p in peripheral blood mononuclear cells from renal transplant patients with chronic antibody-mediated rejection. *PLoS One*. (2013) 8:e60702. doi: 10.1371/journal.pone.0060702

151. Kim MY, Brennan DC. Therapies for chronic allograft rejection. *Front Pharmacol*. (2021) 12:651222. doi: 10.3389/fphar.2021.651222

152. Constanso-Conde I, Hermida-Prieto M, Barge-Caballero E, Núñez L, Pombo-Otero J, Suárez-Fuentetaja N, et al. Circulating mir-181a-5p as a new biomarker for acute cellular rejection in heart transplantation. *J Heart Lung Transplant*. (2020) 39:1100–8. doi: 10.1016/j.healun.2020.05.018

153. Kennel PJ, Yahi A, Naka Y, Mancini DM, Marboe CC, Max K, et al. Longitudinal profiling of circulating mirna during cardiac allograft rejection: A proof-of-concept study. *ESC Heart Failure*. (2021) 8:1840–9. doi: 10.1002/ehf2.13238

154. Sukma Dewi I, Celik S, Karlsson A, Hollander Z, Lam K, McManus J-W, et al. Exosomal mir-142-3p is increased during cardiac allograft rejection and augments vascular permeability through down-regulation of endothelial rab11fip2 expression. *Cardiovasc Res*. (2017) 113:440–52. doi: 10.1093/cvr/cvw244

155. Lu J, Wang W, Li P, Wang X, Gao C, Zhang B, et al. Mir-146a regulates regulatory T cells to suppress heart transplant rejection in mice. *Cell Death Discovery*. (2021) 7:165. doi: 10.1038/s41420-021-00534-9

156. Van Aelst LNL, Summer G, Li S, Gupta SK, Heggermont W, De Vusser K, et al. Rna profiling in human and murine transplanted hearts: identification and validation of therapeutic targets for acute cardiac and renal allograft rejection. *Am J Transplant*. (2016) 16:99–110. doi: 10.1111/ajt.13421

157. Feng Z, Xia Y, Zhang M, Zheng J. Microrna-155 regulates T cell proliferation through targeting gsk3B in cardiac allograft rejection in a murine transplantation model. *Cell Immunol*. (2013) 281:141–9. doi: 10.1016/j.cellimm.2013.04.001

158. He M, Jin Q, Deng C, Fu W, Xu J, Xu L, et al. Amplification of plasma micrornas for non-invasive early detection of acute rejection after heart transplantation with ultrasound-targeted microbubble destruction. *Ultrasound Med Biol*. (2023) 49:1647–57. doi: 10.1016/j.ultrasmedbio.2023.03.020

159. Yi L, Chen Y, Jin Q, Deng C, Wu Y, Li H, et al. Antagomir-155 attenuates acute cardiac rejection using ultrasound targeted microbubbles destruction. *Advanced Healthcare Materials*. (2020) 9:e2000189. doi: 10.1002/adhm.202000189

160. Hu J, Huang S, Liu X, Zhang Y, Wei S, Hu X, et al. Mir-155: an important role in inflammation response. *J Immunol Res*. (2022) 2022:1–13. doi: 10.1155/2022/7437281

161. Nie M, Liu J, Yang Q, Seok HY, Hu X, Deng ZL, et al. Microrna-155 facilitates skeletal muscle regeneration by balancing pro- and anti-inflammatory macrophages. *Cell Death Dis*. (2016) 7:e2261–e. doi: 10.1038/cddis.2016.165

162. Tang B, Wang Z, Qi G, Yuan S, Yu S, Li B, et al. Microrna-155 deficiency attenuates ischemia-reperfusion injury after liver transplantation in mice. *Transplant Int*. (2015) 28:751–60. doi: 10.1111/tri.12528

163. Song C, Wang G, Ma X, Mao P, Lu W, Zhang H, et al. The effect of mir-155–5p on M1 polarization of kupffer cells and immune response during liver transplantation through regulating the expression of kdm5d. *Mol Immunol*. (2023) 155:17–26. doi: 10.1016/j.molimm.2023.01.003

164. Wang Y, Feng T, Li H, Xiong Y, Tao Y. Gal-9/tim-3 signaling pathway activation suppresses the generation of th17 cells and promotes the induction of foxp3+ Regulatory T cells in renal ischemia-reperfusion injury. *Mol Immunol*. (2023) 156:136–47. doi: 10.1016/j.molimm.2023.03.008

165. Lamarthée B, Callemeyn J, Van Herck Y, Antoranz A, Anglicheau D, Boada P, et al. Transcriptional and spatial profiling of the kidney allograft unravels a central role for fcyriii+ Innate immune cells in rejection. *Nat Commun*. (2023) 14:4359. doi: 10.1038/s41467-023-39859-7

166. Li M, Peng X, Qian J, Sun F, Chen C, Wang S, et al. Galectin-9 regulates htr8/svneo function via jnk signaling. *Reproduction*. (2021) 161:1–10. doi: 10.1530/rep

167. Cai L, Zhou H, Fang Z, Yuan J, Niki T, Hirashima M, et al. Galectin-9 in combination with rapamycin induces cardiac allograft tolerance in mice. *Transplantation*. (2013) 96:379–86. doi: 10.1097/TP.0b013e31829b07b5

168. Anandagoda N, Roberts LB, Willis JCD, Sarathchandra P, Xiao F, Jackson I, et al. Dominant regulation of long-term allograft survival is mediated by microrna-142. *Am J Transplant*. (2020) 20:2715–27. doi: 10.1111/ajt.15907

169. Iwasaki K, Yamamoto T, Inanaga Y, Hiramitsu T, Miwa Y, Murotani K, et al. Mir-142-5p and mir-486-5p as biomarkers for early detection of chronic antibody-mediated rejection in kidney transplantation. *Biomarkers*. (2017) 22:45–54. doi: 10.1080/1354750X.2016.1204000

170. Mari B, Sukma Dewi I, Hollander Z, Lam KK, McManus J-W, Tebbutt SJ, et al. Association of serum mir-142-3p and mir-101-3p levels with acute cellular rejection after heart transplantation. *PLoS One*. (2017) 12:e0170842. doi: 10.1371/journal.pone.0170842

171. Tinel C, Lamarthée B, Callemeyn J, Van Loon E, Sauvaget V, Morin L, et al. Integrative omics analysis unravels microvascular inflammation-related pathways in kidney allograft biopsies. *Front Immunol*. (2021) 12:738795. doi: 10.3389/fimmu.2021.738795

172. Anandagoda N, Willis JCD, Hertweck A, Roberts LB, Jackson I, Gökmen MR, et al. Microrna-142–mediated repression of phosphodiesterase 3b critically regulates peripheral immune tolerance. *J Clin Invest*. (2019) 129:1257–71. doi: 10.1172/jci124725

173. Zhang Y, Ji H, Shen X, Cai J, Gao F, Koenig KM, et al. Targeting tim-1 on cd4 T cells depresses macrophage activation and overcomes ischemia-reperfusion injury in mouse orthotopic liver transplantation. *Am J Transplant*. (2013) 13:56–66. doi: 10.1111/j.1600-6143.2012.04316.x

174. Cherukuri A, Mohib K, Rothstein DM. Regulatory B cells: tim-1, transplant tolerance, and rejection. *Immunol Rev*. (2021) 299:31–44. doi: 10.1111/imr.12933

175. Liu ZY, Pan HW, Cao Y, Zheng J, Zhang Y, Tang Y, et al. Downregulated microrna-330 suppresses left ventricular remodeling via the tgf-beta1/smad3 signaling pathway by targeting sry in mice with myocardial ischemia-reperfusion injury. *J Cell Physiol*. (2019) 234:11440–50. doi: 10.1002/jcp.27800

176. Cui L, Sun F, Xu Y, Li M, Chen L, Chen C, et al. Tim-3 coordinates macrophage-trophoblast crosstalk via angiogenic growth factors to promote pregnancy maintenance. *Int J Mol Sci*. (2023) 24:1538. doi: 10.3390/ijms24021538

177. Lu Y, Wang Y-L, Liu Q, Zhou P, Mei P-Y, Li J-S, et al. Mirna-122 promotes ischemia-reperfusion injury after lung transplantation via the toll-like receptor signaling pathway. *Curr Med Sci*. (2021) 41:1231–8. doi: 10.1007/s11596-021-2487-y

178. Riechert G, Maucher D, Schmidt B, Schumann J. Mirna-mediated priming of macrophage M1 differentiation differs in gram-positive and gram-negative settings. *Genes*. (2022) 13:211. doi: 10.3390/genes13020211

179. Li Y, Shi X. Micrornas in the regulation of tlr and rig-I pathways. *Cell Mol Immunol*. (2012) 10:65–71. doi: 10.1038/cmi.2012.55

180. Jiang W, Ni Q, Tan L, Kong L, Lu Y, Xu X, et al. The microrna-146a/B attenuates acute small-for-size liver graft injury in rats. *Liver Int*. (2014) 35:914–24. doi: 10.1111/liv.12674

181. Wang S, Cao C, Piao H, Li Y, Tao Y, Zhang X, et al. Tim-3 protects decidual stromal cells from toll-like receptor-mediated apoptosis and inflammatory reactions and promotes th2 bias at the maternal-fetal interface. *Sci Rep*. (2015) 5:9013. doi: 10.1038/srep09013

182. Ye L, Zhang Q, Cheng Y, Chen X, Wang G, Shi M, et al. Tumor-derived exosomal hmgb1 fosters hepatocellular carcinoma immune evasion by promoting tim-1+ Regulatory B cell expansion. *J ImmunoTherapy Cancer*. (2018) 6:145. doi: 10.1186/s40425-018-0451-6

183. Xia H, Wang D, Guo X, Wu K, Huang F, Feng Y. Catalpol Protects against Spinal Cord Injury in Mice through Regulating Microrna-142-Mediated Hmgb1/Tlr4/Nf-Kb Signaling Pathway. *Front Pharmacol*. (2021) 11:630222. doi: 10.3389/fphar.2020.630222

184. Guo D, Fan Y, Yue J-R, Lin T. A regulatory mirna–mrna network is associated with transplantation response in acute kidney injury. *Hum Genomics*. (2021) 15:69. doi: 10.1186/s40246-021-00363-y

185. Wu D, Kang L, Tian J, Wu Y, Liu J, Li Z, et al. Exosomes derived from bone mesenchymal stem cells with the stimulation of fe3o4 nanoparticles and static magnetic field enhance wound healing through upregulated mir-21-5p. *Int J Nanomedicine*. (2020) 15:7979–93. doi: 10.2147/ijn.S275650

186. Hao C, Lu Z, Zhao Y, Chen Z, Shen C, Ma G, et al. Overexpression of gata4 enhances the antiapoptotic effect of exosomes secreted from cardiac colony-forming unit fibroblasts via mirna221-mediated targeting of the pten/pi3k/akt signaling pathway. *Stem Cell Res Ther*. (2020) 11:251. doi: 10.1186/s13287-020-01759-8

187. Pang N, Tudahong S, Zhu Y, He J, Han C, Chen G, et al. Galectin-9 alleviates acute graft-versus-host disease after haplo-hematopoietic stem cell transplantation by regulating regulatory T cell/effector T cell imbalance. *Immunity Inflammation Dis*. (2024) 12:e1177. doi: 10.1002/iid3.1177

188. Ning Q, Jian T, Cui S, Shi L, Jian X, He X, et al. Tim-3 facilitates immune escape in benzene-induced acute myeloid leukemia mouse model by promoting macrophage

M2 polarization. *Ecotoxicology Environ Saf*. (2023) 266:115532. doi: 10.1016/j.ecoenv.2023.115532

189. Hong BS, Ryu HS, Kim N, Kim J, Lee E, Moon H, et al. Tumor suppressor mirna-204-5p regulates growth, metastasis, and immune microenvironment remodeling in breast cancer. *Cancer Res*. (2019) 79:1520–34. doi: 10.1158/0008-5472.Can-18-0891

190. Cheng YQ, Ren JP, Zhao J, Wang JM, Zhou Y, Li GY, et al. Microrna-155 regulates interferon-Γproduction in natural killer cells via tim-3 signaling in chronic hepatitis C virus infection. *Immunology*. (2015) 145:485–97. doi: 10.1111/imm.12463

191. Prieto I, Kavanagh M, Jimenez-Castilla L, Pardines M, Lazaro I, Herrero del Real I, et al. A mutual regulatory loop between mir-155 and socs1 influences renal inflammation and diabetic kidney disease. *Mol Ther - Nucleic Acids*. (2023) 34:102041. doi: 10.1016/j.omtn.2023.102041

192. Talebi F, Ghorbani S, Chan WF, Boghozian R, Masoumi F, Ghasemi S, et al. Microrna-142 regulates inflammation and T cell differentiation in an animal model of multiple sclerosis. *J Neuroinflamm*. (2017) 14:55. doi: 10.1186/s12974-017-0832-7

193. Han J, Li Y, Zhang H, Guo J, Wang X, Kang Y, et al. Microrna-142-5p facilitates the pathogenesis of ulcerative colitis by regulating socs1. *Int J Clin Exp Pathol*. (2018) 11:5735–44.

frontiers | Frontiers in Immunology

TYPE Original Research
PUBLISHED 02 December 2024
DOI 10.3389/fimmu.2024.1504495

OPEN ACCESS

EDITED BY
Rita Maccario,
San Matteo Hospital Foundation (IRCCS), Italy

REVIEWED BY
Josefina M. Alberu,
Tecnológico de Monterrey, Mexico
Paul Schroder,
Houston Methodist Hospital, United States

*CORRESPONDENCE
Lionel Rostaing
lrostaing@chu-grenoble.fr

RECEIVED 30 September 2024
ACCEPTED 13 November 2024
PUBLISHED 02 December 2024

CITATION
Naciri Bennani H, Bobo Barry KM, Noble J, Malvezzi P, Jouve T and Rostaing L (2024) Outcomes of ABO-incompatible kidney transplants with very high isoagglutinin titers: a single-center experience and literature review.
Front. Immunol. 15:1504495.
doi: 10.3389/fimmu.2024.1504495

Outcomes of ABO-incompatible kidney transplants with very high isoagglutinin titers: a single-center experience and literature review

Hamza Naciri Bennani[1], Kadiatou Mamadou Bobo Barry[1], Johan Noble[1], Paolo Malvezzi[1], Thomas Jouve[1,2] and Lionel Rostaing[1,2*]

[1]Nephrology, Hemodialysis, Apheresis and Kidney Transplantation Department, Grenoble University Hospital, Grenoble, France, [2]Grenoble-Alpes University, Grenoble, France

Background: ABO-incompatible kidney transplantation (ABOi-KTx) represents a possible solution to address the shortage of kidney donors. However, these transplants present immunological challenges, particularly when isoagglutinin titers are elevated pretransplant.

Methods: Single-center retrospective study describing clinical and biological outcomes of 8 patients who underwent ABOi-KTx with initial isoagglutinin titers ≥ 1/512. All patients followed a desensitization protocol combining immunosuppression (rituximab, tacrolimus, mycophenolate mofetil, steroids), and specific or semi-specific apheresis sessions. Clinical and biological data were extracted from electronic medical records.

Results: There were 5 males; median age of 62 years [34-82 years]; all achieved an isoagglutinin titer of ≤1/8 before transplantation after a median of 13 (range: 9-15) apheresis sessions. Three patients (37%) experienced acute humoral rejection, which required additional plasmapheresis sessions. Two patients developed chronic active rejection, successfully treated. On the infectious side, three patients developed BK-virus reactivation. Two patients developed cytomegalovirus viremia, and two others presented with bacterial infections. Surgically, two patients developed a lymphocele, and one had a perirenal hematoma. All patients survived the transplant with stable renal function: mean serum creatinine was 138 ± 15 µmol/L after four years of follow-up.

Conclusion: ABO-incompatible kidney transplantation, even in patients with high isoagglutinin titers, is feasible and can achieve favorable long-term graft and patient survival outcomes. However, these procedures require substantial clinical expertise and close follow-up to monitor and manage the elevated risks of infection and rejection in this population.

KEYWORDS

kidney transplantation, isoagglutinins, ABO incompatible transplant, desensitization, apheresis, antibody-mediated rejection

1 Introduction

The number of living donor kidney transplants is increasing due to the shortage of kidneys from deceased donors and the growing number of patients on transplant waiting lists. In France, this shortage is exacerbated by increasing organ donation refusals, resulting in prolonged and variable wait times. ABO-incompatible (ABOi) kidney transplantation offers an opportunity to expand the donor pool and improve the survival prospects of patients awaiting a transplant (1, 2) especially in the absence of a national kidney paired donation program.

However, ABO incompatibility typically necessitates pre-transplant desensitization, involving apheresis and immunosuppression with rituximab, to reduce the risk of acute antibody-mediated rejection. Numerous studies have demonstrated that the long-term survival rates of patients and kidney allografts in ABOi transplants are comparable to those receiving ABO-compatible (ABOc) living donor transplants (1–15). Nevertheless, ABOi recipients are more prone to complications, such as hemorrhagic episodes related to apheresis, lymphocele, and BK virus infection (12, 16–22).

The presence of high isoagglutinin titers presents a significant challenge, increasing the risk of acute rejection and jeopardizing graft viability. This study aims to describe the clinical and biological outcomes of patients who underwent ABOi kidney transplantation with high isoagglutinin titers at a single center, with a particular focus on desensitization outcomes and related complications.

2 Patients and method

We conducted a retrospective, single-center observational study from January 2015 to July 2024; during that period there were 65 ABO incompatible kidney transplants of which eight had an initial isoagglutinin titer greater than 512. The objective of our study was to describe the clinical and biological outcomes of ABO-incompatible kidney transplant patients with high isoagglutinin titers following desensitization combining rituximab and apheresis.

2.1 Immunosuppression

Immunosuppression was initiated prior to transplantation. Rituximab (375 mg/m²) was administered 30 days before transplantation, and conventional immunosuppression began 15 days prior to transplantation, consisting of tacrolimus (0.05 mg/kg every 12 hours, targeting trough levels of 8-10 ng/mL), mycophenolic acid (MPA) (360 mg twice daily) or mycophenolate mofetil (MMF) (500 mg twice daily), and prednisone (0.5 mg/kg/day). In addition to these treatments, patients underwent apheresis sessions. Based on the initial isoagglutinin titers (IgM and IgG), and clinical profile, patients received one or more of the following:

- Semi-specific immunoadsorption (Globaffin® column, Fresenius, Bad Homburg, Germany) with or without membrane filtration (Monet®, Fresenius Medical Care),
- Double filtration plasmapheresis (DFPP) performed on a PlasautoΣ with a Plasmaflo® OP-08W and Cascadeflo® EC-30W for the first session, followed by Cascadeflo® EC-20W (Asahi Kasei Medical, Tokyo, Japan),
- Specific immunoadsorption (Glycorex® column, Lund, Sweden, or ABO Adsopak® column, Pocard, Russia),
- Plasma exchange using the Optia® or Comtec® monitor with fresh frozen plasma (FFP) the day before kidney transplantation.

Table 1 compares the different apheresis techniques used.

Apheresis sessions begin three weeks prior to the planned transplant date. Most patients initially undergo DFPP sessions, and, depending upon the decrease of isoagglutinin titers, specific immunoadsorption (IA) sessions may be used to achieve a more significant reduction in titers, with up to 15 liters of plasma treated in a single IA session (23). Semi-specific immunoadsorption is preferred for patients at risk of hypotension during sessions. The addition of a Monet® filtration membrane, at least once a week depending on the IgM level, is essential for eliminating IgM isoagglutinin's not removed by semi-specific IA (24). Each patient benefits from a personalized approach based on the kinetics of isoagglutinins measured before and after each apheresis session.

All patients underwent within 12 hours pretransplant a plasma exchange, which treated 1.5 times the plasma volume with 100% plasma replacement to mitigate the loss of coagulation factors during previous apheresis session (particularly DFPP ones) (25–28).

Extracorporeal circuit anticoagulation was performed using regional citrate anticoagulation during immunoadsorption, plasma exchange, or DFPP not coupled with hemodialysis. For DFPP coupled with hemodialysis, anticoagulation of the extracorporeal circuit was achieved with intravenous sodium heparin.

The goal was to achieve an isoagglutinin titer (IgG and IgM) of ≤ 1/8 on the day of transplantation.

In the posttransplant period we do not monitor isoagglutinin titers except when clinically necessary (i.e., drop in urine output or rise in serum creatinine level).

Induction therapy included basiliximab (20 mg on days 0 and 4). In cases where donor-specific antibodies (DSAs) were present, antithymocyte globulin (1 mg/kg daily for five days) was used instead of basiliximab. Post-transplant immunosuppression included tacrolimus (0.05 mg/kg every 12 hours, targeting trough levels of 8-10 ng/mL until day 30, then reducing to 5-8 ng/mL), MPA (720 mg twice daily) or MMF (1 g twice daily), administered until day 15, after which doses were halved, and steroids (methylprednisolone 10 mg/kg on day 0, with a maximum of 500 mg, 6 mg/kg on day 1, 4 mg/kg on day 2, 2 mg/kg on day 3, 1 mg/kg on day 4, followed by prednisone at 0.5 mg/kg on day 5, 0.25 mg/kg on day 6, then 10 mg daily until day 90, and finally 5 mg daily).

A systematic kidney biopsy is performed at three- and twelve-months post-transplant. Otherwise, the indications for kidney biopsy remain the same as for ABO-compatible transplants.

TABLE 1 Apheresis techniques.

Technique	Description	Indications	Prescription	Advantages and Disadvantages
DFPP	Utilizes a two-step filtration system: - the first filter separates cellular elements from blood plasma. - the second filter removes plasma substances based on membrane pore size and molecular weight of the substance.	Purification role: IgG, IgM, Fibrinogen, alpha2-macroglobulin, LDL cholesterol, etc.	Treated PV = 1.5 x the patient's PV Blood flow rate = 150 ml/min	Advantages: Semi-specific technique Low amount of substitution products Disadvantages: Hemorrhagic risk due to loss of coagulation factors Variable hemodynamic tolerance
Specific IA	Utilizes adsorption columns specifically targeting blood group antibodies (A or B).	Purification role: Isoagglutinins of IgG and IgM	Treated PV = 3 to 6 x the patient's PV Blood flow rate = 50 ml/min	Advantages: Specific technique No hemorrhagic risk Good hemodynamic tolerance No substitution products Disadvantages: None noted
Semi-specific IA	Utilizes adsorption columns that remove IgG.	Purification role: IgG Addition of a Monet® filter to remove IgM.	Treated PV = 100 ml/kg with a maximum of 10 liters Blood flow rate = 80 ml/min	Advantages: Semi-specific technique No hemorrhagic risk Good hemodynamic tolerance No substitution products Disadvantages: None noted
Plasma Exchange	Broadly removes plasma components, including isoagglutinins, by replacing the patient's plasma with substitution product.	Purification and Transfusion roles: replacement with plasma providing coagulation factors.	Treated PV = 1.5 x the patient's PV Blood flow rate = 80 ml/min if centrifugation and 150 ml/min if filtration Substitution = Plasma of the same blood group as the recipient (except if donor A and recipient B or vice versa) or AB plasma.	Advantages: Good hemodynamic tolerance Disadvantages: Non-specific Hemorrhagic risk unless plasma substitution prevents loss of coagulation factors Requires a substitution product

PV, Plasma Volume; DFPP, Double filtration plasmapheresis; IA, Immunoadsorption.

2.2 Prophylaxes

If the donor was CMV-seropositive and the recipient was CMV-seronegative, or if the recipient was CMV-seropositive, valganciclovir (900 mg daily, adjusted for estimated glomerular filtration rate [eGFR]) was administered for six or 3 months, respectively. For Pneumocystis jirovecii prophylaxis, sulfamethoxazole/trimethoprim (400 mg/80 mg every day) was given for six months.

2.3 Collected data and statistical analyses

Clinical and biological data were collected from electronic medical records using the CristalNet and Easily software systems. Statistical analyses were performed using Excel 2016 and R statistical software. Quantitative variables are presented as means ± standard deviations (SD) or medians with quartiles (Q1–Q3), while qualitative variables are presented as numbers and percentages.

The study was conducted in accordance with the guidelines of the Declaration of Helsinki and was approved by the French National Committee for Data Protection (CNIL; approval number 1987785v0). The biobank collection number is BRIF BB-0033-00069. Informed consent was obtained from all participants in the study.

3 Results

We included eight patients, i.e., 12.3% of our ABO incompatible cohort with a male-to-female ratio of 5:3. The median age at transplantation was 62 years (range: 34-82 years). The median posttransplant follow-up duration was 60 (range: 4-96) months. All patients were undergoing their first kidney transplant. Rituximab was administered at a dose of 375 mg/m² on day -30 to all patients, except two who received an additional rituximab infusion on day -15 (375 mg/m²) due to the presence of donor-specific antibodies prior to transplantation. The characteristics of the patients are presented in Tables 2, 3.

Isoagglutinin levels decreased significantly following the rituximab infusion and prior to the initiation of apheresis, as shown in Table 2 and Figure 1. The target isoagglutinin level of less than 1/8 was achieved in all patients before kidney

10.3389/fimmu.2024.1504495

TABLE 2 Characteristics of Patients.

	Patients (n=8)
Donor Age (years)	60 ± 13
Donor measured GFR (mL/min)	79 ± 15
Etiology of ESKD	
Vascular nephropathy (%)	4 (50%)
ADPKD (n)	3 (37%)
Diabetes nephropathy (n)	1 (13%)
ABO incompatibility	
A → O	7 (87%)
AB → O	1 (13%)
Isoagglutinin titers (medians)	
Before Rituximab	
Anti-A IgM	64 [32;512]
Anti-A IgG	1024 [256;2048]
Anti-B IgM	128
Anti-B IgG	1024
Before apheresis	
Anti-A IgM	64 [16;128]
Anti-A IgG	512 [32;1024]
Anti-B IgM	128
Anti-B IgG	256
After kidney transplantation	
Anti-A IgM	
M+1	8 [2;32]
M+3	8 [2;64]
M+6	4 [2;8]
M+12	4 [1;8]
Anti-A IgG	
M+1	32 [4;512]
M+3	32 [4;2048]
M+6	16 [4;128]
M+12	32 [2;64]
Anti-B IgM	
M+1	2
M+6	2
Anti-B IgG	
M+1	4
M+6	4
HLA mismatches	
Class I (A/B/C)	3.7 ± 1.8
Class II (DR/DQ/DP)	4 ± 2
Anti-HLA antibodies (n ;%)	4 (50%)
Blood transfusion	2 (25%)
Pregnancy	2 (25%)
DSA (%)	2 (25%)
MFI	DQ2 at 800 and A32 at 4600
Cold ischemia time (min)	78 ± 20
Induction Therapy (n; %)	
ATG	2 (25%)
Basiliximab	6 (75%)
Preemptive kidney transplantation	1 (13%)

ESKD, end-stage kidney disease; CGN, chronic glomerulonephritis, HLA, human leukocyte antigen; GFR, glomerular-filtration rate; ATG, antithymocyte globulins; ADPKD, Autosomal dominant polycystic kidney disease; MFI, mean fluorescent intensity; DSA, Donor-specific antibodies.

transplantation after a median of 13 (range: 9-15) apheresis sessions (Figure 2).

All the patients experienced immediate graft function; however, in 3 of them as of postoperative day (POD) 2 there was a decrease in urine output while serum creatinine was plateauing at > 250 µmol/L. This was highly suggestive of acute humoral rejection because the allograft doppler ultrasound analyses were normal. For these three patients, the anti-A IgG isoagglutinin level had risen to 1/32 in two patients and 1/16 in the third (i.e., rebounds), while anti-A IgM levels remained below 1/8. This required resumption of plasma exchange (4, 5, and 8 sessions, respectively), leading to an immediate increase of diuresis and improvement in renal function (Patient 4, 5 and 8 in Table 3 and Figures 3, 4). One of these patients also presented with elevated creatinine (280 µmol/L) at the 1-month follow-up, which prompted a graft biopsy. The biopsy revealed mixed humoral and cellular rejection (grade 3), which was successfully treated with methylprednisolone boluses, four plasma exchange sessions, and a single dose intravenous immunoglobulin (IVIg) -20 gr- after the last apheresis session.

During follow-up, two other patients (2 women, each having her husband as a donor) developed chronic active humoral rejection at 6 and 12 months, respectively, confirmed by graft biopsy after observing a rise in plasma creatinine. Both of them had very low isoagglutinin titers at posttransplant and did not experience any episodes of acute rejection. One patient was ABOi plus HLA incompatible (DSA at pretransplant: anti-A32 with MFI of 1,200): the 6-month protocol biopsy showed evidence for chronic active antibody-mediated rejection: she was therefore placed on

TABLE 3 Individualized characteristics of patient.

Patient	Donor/Recipient ABO incompatibility	Isoagglutinin titers (anti-A IgG; anti-A IgM; anti-B IgG; anti-B IgM)							Number of apheresis sessions	Acute rejection	Serum creatinine and eGFR at the last follow-up (µmol/L; ml/min/1,73m²)	Follow-up duration in months
		Before rituximab	Before apheresis	The day of kidney transplantation	After Kidney transplantation							
					M1	M3	M6	M12				
1	A/O	2048; 512	2048; 128	4; 1	512; 32	2048; 64	NA	NA	15 (11 IAss, 3 IAs,1 PE)	No	130; 59	3
2	A/O	2048; 256	512; 64	4; 1	64; 4	128; 8	128; 8	64; 8	15 (13 DFPP, 1 IAs, 1 PE)	No	117; 70	12
3	AB/O	256; 32; 1024; 128	32; 16; 256; 128	2; 1; 4; 2	32; 8; 4; 2	NA	32; 8; 4; 2	NA	14 (8 IAss, 5 IAss + Monet®, 1 PE)	No	100; 53	30
4	A/O	1024; 32	512; 16	8; 1	32; 16	32; 2	16; 4	32; 4	9 (6 DFPP, 2 IAs, 1 PE)	Yes	134; 35	48
5	A/O	1024; 256	256; 128	8; 2	16; 8	64; 8	32; 8	16; 2	12 (11 DFPP, 1 PE)	Yes	147; 41	60
6	A/O	1024; 64	1024; 128	8; 2	4; 2	8; 4	4; 4	4; 2	10 (9 DFPP, 1 PE)	No	122; 42	72
7	A/O	512; 64	256; 32	4; 1	4; 2	8; 4	4; 2	2; 1	10 (7 DFPP, 2 IAs, 1 PE)	No	150; 30	72
8	A/O	1024; 64	1024; 64	2; 1	16; 4	8; 4	16; 4	32; 8	14 (10 DFPP, 3 IAs, 1 PE)	Yes	113; 71	12

GFR, glomerular-filtration rate; IAss, semi-specific immunoadsorption; IAs, specific immunoadsorption; DFPP, Double filtration plasmapheresis; PE, plasma exchange; NA, Not available.

10.3389/fimmu.2024.1504495

10.3389/fimmu.2024.1504495

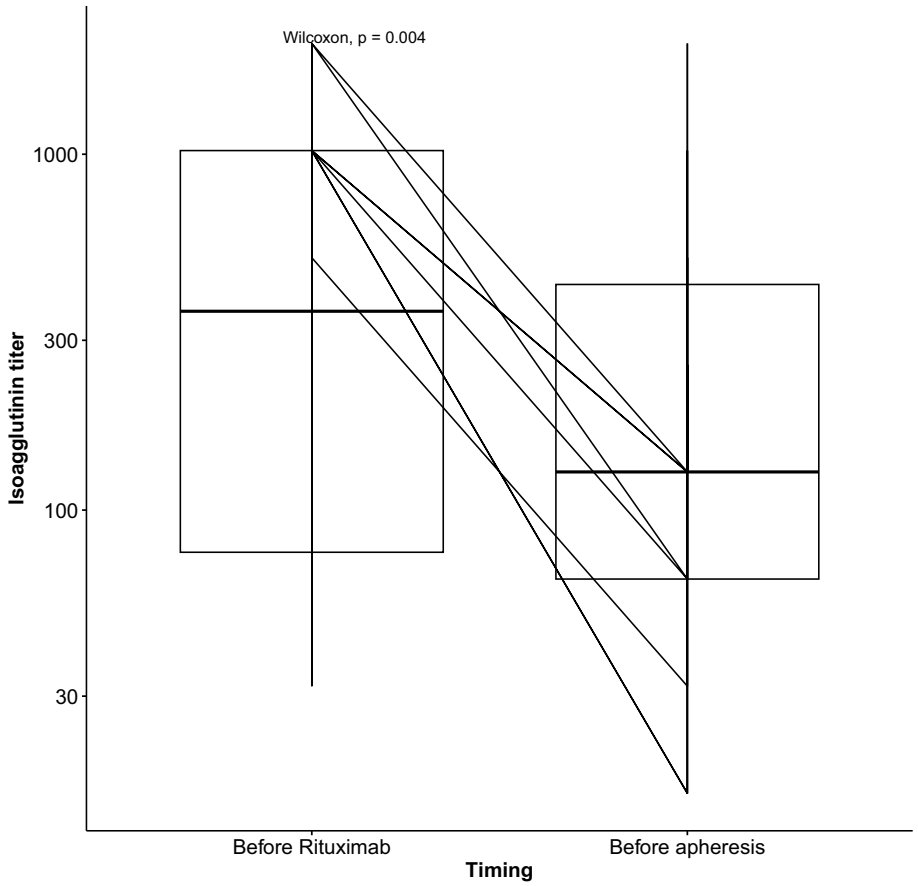

FIGURE 1
Outcomes of isoagglutinin titers after rituximab infusion.

tocilizumab therapy (162 mg/week subcutaneously for one year). The second patient developed a *de novo* DSA by 12 months posttransplant (anti-DQ7 with MFI at 2,000). She was treated by a single dose of Rituximab (1gr).

The outcomes for serum creatinine, estimated glomerular filtration rate (eGFR), albuminuria, and tacrolimus trough levels are illustrated in Figure 4.

Regarding infectious complications, three patients developed BK virus viruria at months 1, 5, and 6, with two showing positive BK viremia and one presenting with BK virus nephropathy on a graft biopsy at month 3 (Table 4). Management involved reducing immunosuppression by lowering tacrolimus target trough levels, substituting mycophenolate mofetil with everolimus, and administering every two weeks IVIg (20 gr) for three months. The outcome was favorable, with resolution of BK viremia and viruria, and disappearance of BK virus nephropathy on follow-up biopsy at month 12. Among these three patients, one also developed concurrent CMV viremia and acute pyelonephritis; both conditions were successfully managed with valganciclovir and antibiotics with favorable outcomes. An additional patient developed CMV viremia, which also responded well to a three-week course of valganciclovir. Lastly, one patient developed a bacterial infection (community-acquired pneumonia) which resolved with antibiotic therapy. None of the patients developed hypogammaglobulinemia secondary to rituximab after one year of follow-up (Figure 5).

Surgically, two patients developed lymphocele, which resolved spontaneously. One patient presented with a compressive perirenal graft hematoma and required surgical revision on day 14 post-transplantation. Additionally, two patients required transfusion with two units of red blood cells (RBCs) immediately post-transplant due to low hemoglobin level without external bleeding (Table 4). Hemoglobin levels during the first year posttransplant are depicted in Figure 4.

4 Discussion

In this study we demonstrate that it is feasible to perform ABO incompatible kidney transplantation even when isoagglutinin titers are very high after a median of 13 (range: 9-15) apheresis sessions pretransplant; it resulted with 100% patient and graft survival in the long term. However, in such situations the risk of antibody (isoagglutinin)-mediated rejection and infectious complications remains high and therefore such hazardeous transplant should only be performed in well-experienced centers.

Chung et al. (29), in a comparative study of ABOi KTx patients with either high titers (≥1:256, n=8) or low titers (≤1:128, n=6), found

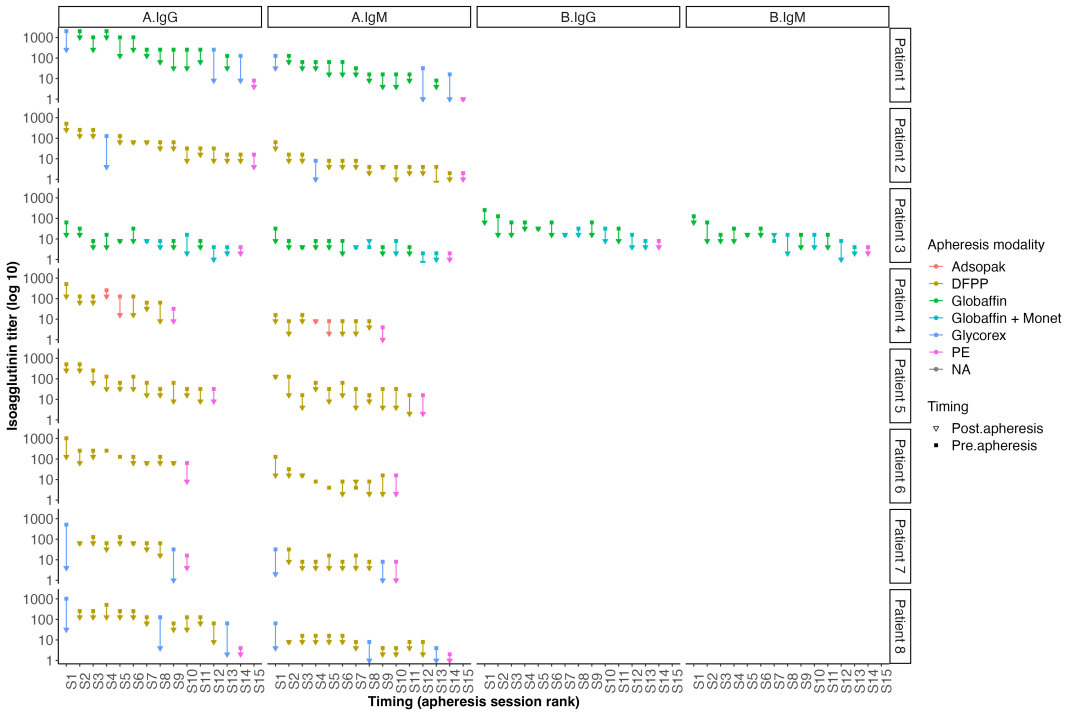

FIGURE 2
Outcomes of isoagglutinin titers after each apheresis session according to the technique used.

that the high-titer group required more i) pre-transplant apheresis sessions (10.5 ± 3.5 vs. 6.0 ± 1.3; p = 0.01) to achieve an acceptable titer before transplantation, and ii) post-transplant sessions (1.6 ± 1.8 vs. 0 ± 0) due to a rebound in isoagglutinin levels compared to the low-titer group. Indeed, the rebound of isoagglutinin titers within the first two weeks after kidney transplantation can be a risk factor for rejection, as demonstrated by Süsal et al. (30) in a case of ABOi kidney transplantation (A donor, O recipient) with initial

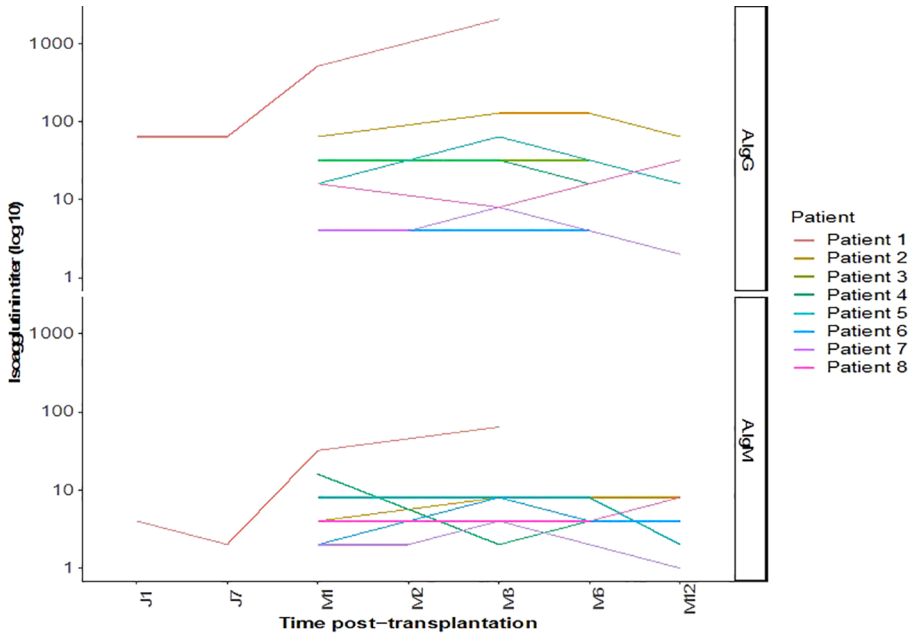

FIGURE 3
Outcomes of isoagglutinin titers after kidney transplantation.

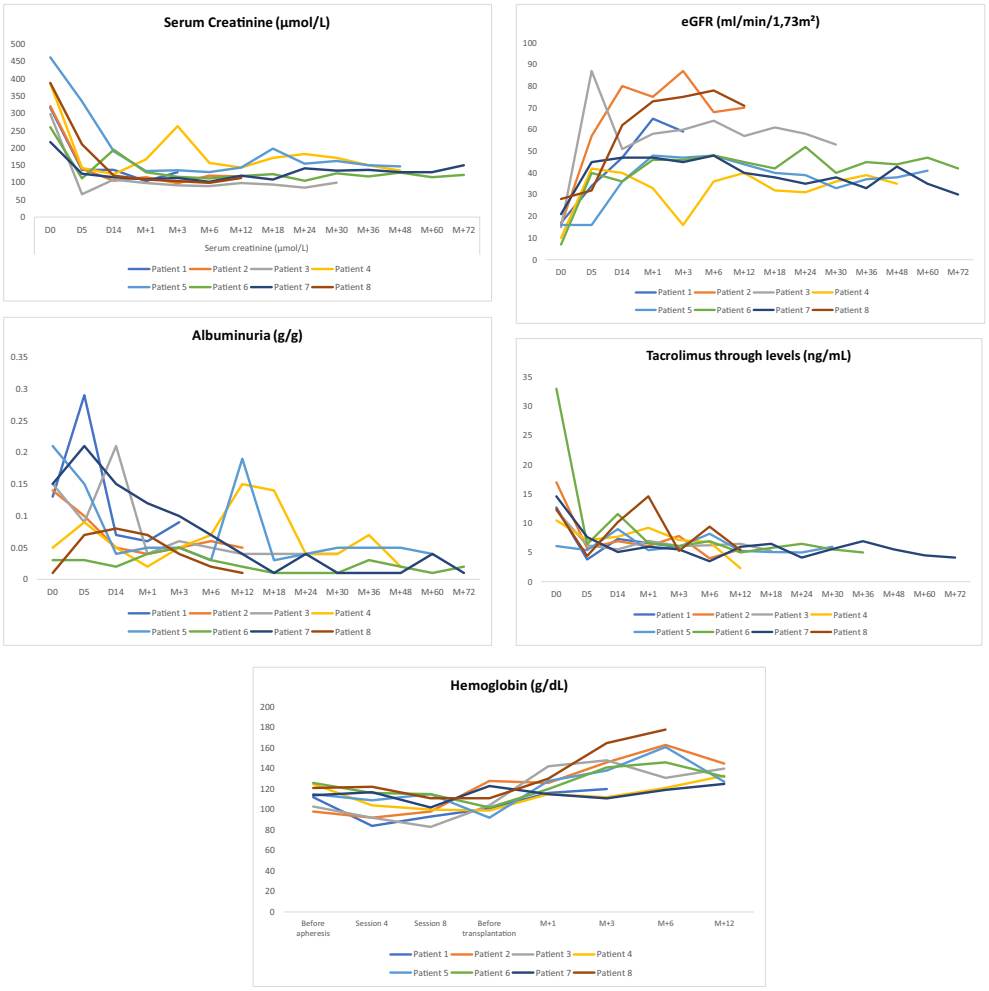

FIGURE 4
Outcomes of Albuminuria (g/g), eGFR(ml/min/1,73m^2), tacrolimus through levels (ng/mL), Serum creatinine (µmol/L) and Homoglobin (g/dL) during follow-up.

isoagglutinin titers of 1/124 for IgM and 1/1024 for IgG, which were reduced to <1/8 after desensitization. However, she presented a typical humoral rejection with a rebound of IgG titers to 1/36 and of IgM to 1/8 on POD5; she did not respond to methylprednisolone pulses and plasmapheresis. Nonetheless, the acute rejection was controlled by IV daratumumab combined with four specific immunoadsorption sessions.

Won et al. (31) showed that predictive factors for the rebound of isoagglutinin titers after kidney transplantation included a short interval (<7 days) between rituximab administration and the first plasmapheresis, a high initial titer (≥256), low rate of titer reduction, and blood group O. They also demonstrated that low-dose rituximab (200 mg) had no significant effect on isoagglutinin rebound titers but allowed for a reduction in infection rates. Rarely, despite intensifying apheresis sessions, kidney transplantation may fail due to incomplete reduction of isoagglutinin titers, as shown by Wilpert et al. (32), who were unable to transplant 4 out of 11 patients with initial titers ≥ 1/256.

ABO-incompatible kidney transplantation represents a major advancement in transplant medicine, and should no longer be viewed as a barrier to expanding the organ donor pool (1, 2, 13). Theoretically, the number of kidney transplants from living donors can be increased by up to **30%** when patients are transplanted across the ABO antibody barrier (33). Nevertheless, it poses significant immunological and infectious challenges, particularly in patients with elevated isoagglutinin titers, as demonstrated by our study. This underscores the importance of rigorous long-term monitoring and individualized therapeutic adjustments to ensure optimal outcomes.

4.1 Desensitization protocol and management of isoagglutinin titers

Pre-transplant desensitization is essential for the success of ABO-incompatible transplantation. In our cohort, Apheresis sessions begin three weeks prior to the planned transplant date. Isoagglutinins measured before and after each apheresis session. All patients achieved an isoagglutinin titer below 1/8 prior to transplantation, demonstrating the effectiveness of the desensitization protocol combining rituximab and apheresis (3). However, 37% of them developed acute antibody-mediated

10.3389/fimmu.2024.1504495

TABLE 4 Outcomes and complications of patient and allograft post-transplantation.

	Patients (n=8)
Patient Survival at last follow-up	8 (100%)
Graft survival at last follow-up	8 (100%)
Delayed graft function (serum creatinine > 250 µmol/L at D5)	2 (25%)
Hemodialysis at posttransplant	0
Serum creatinine (µmol/L) D0 D5 D14 M+1 M+3 M+6 M+12 M+18 M+24 M+36 M+48	 331 ± 78 158 ± 81 136 ± 35 120 ± 22 131 ± 55 115 ± 22 121 ± 16 139 ± 43 133 ± 38 138 ± 28 138 ± 15
Acute humoral rejection	3 (37,5%)
Acute cellular rejection	1 (12,5%)
Chronic humoral rejection	2 (25%)
Lymphocele (n; %)	2 (25%)
Hematoma requiring surgical revision (n; %)	1 (12,5%)
Patients requiring red-blood cell transfusion between D0 and D5 (n; %)	2 (25%)
BKV viruria (n; %) BKV viremia (n; %) BKV nephropathy (n; %)	3 (37,5%) 2 (25%) 1 (12,5%)
CMV viremia (n; %)	2 (25%)
Acute pyelonephritis (n; %)	1 (12,5%)
Bacterial pneumopathy (n; %)	1 (12,5%)

BKV, BK virus; CMV, cytomegalovirus.

rejection (AMR), which coincided with a rise in isoagglutinin titers, necessitating additional plasmapheresis. These interventions resulted in a favorable outcome.

In the posttransplant period we typically do not monitor isoagglutinin titers unless clinically necessary (i.e., drop in urine output or rise in serum creatinine level). If there are no complications, patients typically remain hospitalized for seven days post-transplant.

4.2 Acute and chronic rejections: immunological challenges

Humoral and cellular rejections pose significant threats to graft survival in ABO-incompatible (ABOi) transplant patients. Despite achieving acceptable isoagglutinin titers pre-transplant, 37% of patients in our cohort developed acute antibody-mediated rejection (AMR) post-transplant, while 25% experienced active chronic AMR during follow-up. These cases required additional treatments, such as tocilizumab (a monoclonal antibody that blocks IL-6 receptor) in one patient and a second rituximab infusion in another, which stabilized graft function.

These findings are consistent with those of Gan et al. (3), who reported a high incidence of acute cellular rejection (12.5%) and acute humoral rejection (8.3%) in a cohort of 26 ABOi kidney transplant patients with pre-desensitization IgG titers ranging from 2 to 2048. Similarly, Hew et al. (4) reported that 18.2% of pediatric ABOi kidney transplant recipients experienced acute cellular rejection within the first 12 months post-transplant. In addition, Chung et al. (29), in a comparative study of ABOi patients with high titers (≥1:256, n=8) and those with low titers (≤1:128, n=6), found a higher incidence of acute cellular rejection in the high-titer group (37% vs. 0%).

The overall incidence of acute rejections appears to be higher in ABOi transplants compared to ABO-compatible (ABOc) transplants. De Weerd et al. (13), in a study comparing 296 ABOi kidney transplant recipients with 1184 ABOc living donor and 1184 ABOc deceased donor kidney transplant (KTx) recipients, found acute rejection rates of 29%, 18%, and 19%, respectively ($p = 0.001$). However, this did not significantly impact graft or patient survival. In support of this, Deng et al. (8) demonstrated that the presence of pre-transplant donor-specific antibodies (DSA) significantly increased the risk of acute antibody-mediated rejection and graft loss in both ABOi and ABOc kidney transplants (8).

The use of B-cell depleting agents like rituximab plays a crucial role in reducing the risk of humoral rejection, as shown in a study by Bleasel et al. (34). They compared 66 ABOi KTx patients who did not receive B-cell depletion to 18 ABOi KTx patients treated with rituximab. They observed humoral rejection in 39% of patients without rituximab versus in only 6% of patients who received rituximab within the first 3 months posttransplant. Additionally, 6 patients without rituximab required splenectomy for refractory rejection, with two cases of early graft loss due to humoral rejection on POD 6 and extensive graft necrosis. By comparison, in our series of 44 ABOi KTx recipients in which all have had received before transplantation rituximab infusion we did not observe a single graft loss (6, 7).

Long-term management of ABOi kidney transplants remains challenging due to the risk of chronic rejection. Chronic rejection remains a leading cause of graft loss, particularly in HLA-incompatible transplants, even in the presence of residual antibody titers (4). In our cohort, we observed two cases of chronic rejection.

Guy et al. (5) reported that long-term histological lesions, i.e., after 5 years of follow-up were similar between ABOi and ABOc KTx patients. They also found that microvascular inflammation was less severe in ABOi KTx patients without DSA compared to both ABOi and ABOc KTx patients with DSA, supporting the theory that accommodation may mitigate the harmful effects of residual isoagglutinins and prevent chronic lesions. Tasaki et al. (35) demonstrated that ABOi patients exhibited downregulation of donor-specific blood group antibodies while continuing to produce antibodies against other antigens. Finally, Heo et al. (15), in a study of 1292 ABOc and 347 ABOi kidney transplants, showed that ABOi transplants are associated with a lower risk of *de novo* DSA production and chronic AMR.

These data confirm that ABOi kidney transplants can be safely performed, although they require both short-term (particularly during the first six months, when most acute rejections occur) and long-term follow-up strategies. Personalized immunosuppressive adjustments are critical to preventing post-transplant immunological complications.

4.3 Infectious complications: impact of immunosuppression

Infectious complications represent a major challenge in the management of ABO-incompatible (ABOi) transplant patients. In our cohort, three patients developed BK virus (BKV) viruria, two of whom had positive BKV viremia, and one case of BKV-associated nephropathy (BKVAN) was confirmed by biopsy. The management of these infections required a reduction in immunosuppression, including lowering the target tacrolimus levels to *between 3 and 4 ng/mL*, substituting mycophenolate mofetil with everolimus (*target trough level of 6 to 7 ng/mL*), and administering intravenous immunoglobulins (IVIg), i.e., it has been shown that IVIg do contain specific anti-BKV antibodies (36). These approaches are consistent with recommendations in the literature (37). In our three patients the outcome was favorable, with BKV viremia and viruria resolving and BKVAN disappearing in the graft biopsy performed 12 months after initial diagnosis.

The incidence of viral infections, particularly BKV, is well-documented in ABOi kidney transplants. Sharif et al. (21) found that ABOi KTx patients had a significantly higher incidence of BKVAN compared to HLA-incompatible (HLAi) KTx patients (17.7% vs. 5.9%, p = 0.008). Eder et al. (12), in a study of 465 patients (42 ABOi, 106 HLAi, and 317 ABOc/HLAc controls), showed that ABOi patients had significantly higher Torque Teno Virus (TTV) loads than HLAi KTx patients and controls at 3- and 6-months post-transplant, reflecting the degree of immunosuppression. As a result, biopsy-proven BKVAN was more frequent in ABOi patients compared to HLAi and control patients (11.9% vs. 2.8% vs. 4.1%; p = 0.046). Moreover, ABOi patients treated with rituximab had higher TTV viral loads at 3 months compared to those who did not receive rituximab. This suggests that rituximab significantly increases the risk of BKV infection, as confirmed by a meta-analysis of 4256 ABOi patients conducted by Lee et al. (38). The study found that higher doses of rituximab (>500 mg) were associated with a higher risk of BKV infections compared to lower doses (200 mg), with no significant differences in rejection rates or graft function.

Intense immunosuppression, rather than an intrinsic characteristic of ABOi transplants, likely contributes to the increased risk of infections. In a 2018 study (39), rituximab was responsible for severe hypogammaglobulinemia (IgG < 4 g/L) in 25% of ABOi patients within the first-year post-transplant, necessitating IVIg infusions. However, the use of IVIg led to an infection rate comparable to that of ABOi patients with mild to moderate hypogammaglobulinemia who did not receive IVIg, highlighting the importance of regular IgG monitoring.

Pre-transplant isoagglutinin titers also seem to influence infection risk. In a study of 48 ABOi KTx recipients (19% with titers ≥ 1/256) compared to 96 ABO-compatible (ABOc) KTx recipients, Speer et al. (40) found that ABOi patients with high titers (≥1:256) had a higher incidence of BKV replication than those with low titers or ABOc patients. Koo et al. (1) similarly observed that ABOi patients with low titers (≤1:64) had fewer bacterial infections than those with high titers (≥1:128; p = 0.022), likely because patients with high titers require more aggressive desensitization and immunosuppression.

Interestingly, bacterial infections were less common, likely due to systematic antibiotic prophylaxis with sulfamethoxazole/trimethoprim and/or phenoxymethylpenicillin during the first 6 months post-transplant. We observed, in our series, only one case of bacterial pneumonia and one case of urinary tract infection (UTI) during the follow-up period. However, Speer et al. (40) reported that ABOi KTx recipients developed UTIs (22.9% vs. 8.5%; p = 0.019) and pneumonia (8.3% vs. 1.0%; p = 0.025) more frequently than ABOc KTx patients.

To mitigate infection risk, selective apheresis may offer some protection, as shown by Matuschik et al. (41). Their study comparing ABOi patients desensitized using specific immunoadsorption (IA) with Glycosorb® versus non-specific IA with Immunosorba® found that non-specific IA significantly increased the risk of severe postoperative infections, mainly of urinary origin (adjusted HR 3.08, 95% CI: 1.3–8.1).

These findings emphasize the need to strike a delicate balance between immunosuppression to prevent rejection and minimizing infection risk. Continuous optimization of prophylaxis protocols and individualized immunosuppression management are crucial to achieving this balance.

4.4 Surgical complications and hemorrhage management

Although less common, surgical complications can still pose challenges in the management of ABO-incompatible (ABOi) kidney transplants. In our study, two patients (25%) developed a lymphocele. The significantly higher incidence of lymphoceles among ABOi KTx patients, compared to ABO-compatible (ABOc) recipients, has been supported by Habicht et al. (20) and corroborated by a study we conducted in 2016, which included 44 ABOi and 44 ABOc KTx patients (6, 7), where 19% of ABOi patients developed a lymphocele.

One potential explanation for the increased incidence of lymphocele is the impact of mycophenolate mofetil (MMF), as demonstrated by Lopau et al. (42). It is hypothesized that the use of MMF one to two weeks prior to kidney transplantation surgery in ABO-incompatible patients may heighten the risk of lymphocele formation. Another hypothesis pertains to the necessity of preoperative apheresis sessions. Jänigen et al. (43) found that undergoing eight or more sessions of immunoadsorption/plasmapheresis preoperatively significantly increases the risk of developing a lymphocele.

From a hemorrhagic standpoint, one patient (12.5%) in our study required surgical revision due to a perirenal hematoma. The

10.3389/fimmu.2024.1504495

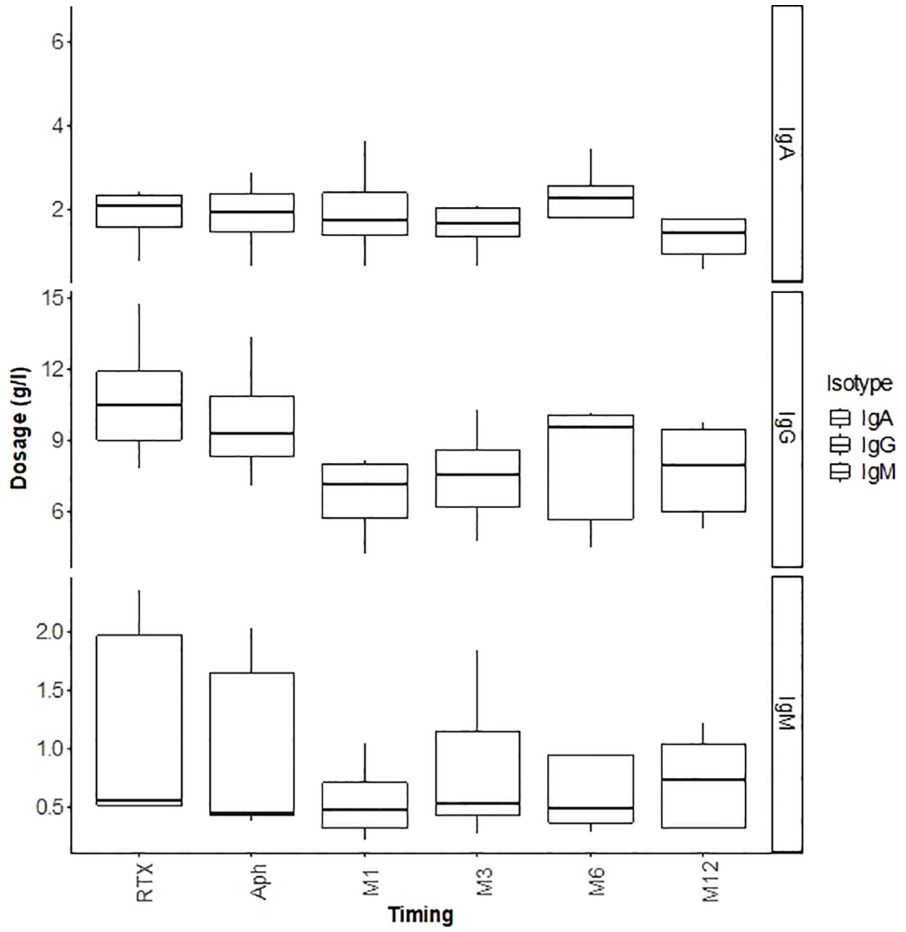

FIGURE 5
Outcomes of immunoglobulins (IgG, IgM, IgA) in g/L during the first 12 months post-transplant.

literature shows a higher risk of bleeding complications in ABO-incompatible (ABOi) kidney transplant (KTx) recipients compared to ABO-compatible (ABOc) recipients. For instance, a meta-analysis by de Weerd et al. (44) found a significantly higher incidence of postoperative hemorrhagic complications in ABOi patients (11%) vs. ABOc patients (4%) ($p < 0.001$). Similarly, a study by Zschiedrich et al. (45) comparing 97 ABOi KTx to 107 ABOc KTx identified bleeding complications in 21% of ABOi patients compared to 13% of ABOc patients ($p = 0.19$). Lastly, Habicht et al. (20) reported bleeding events in 9.5% of ABOi recipients vs. 2% in ABOc recipients.

These hemorrhagic events are often linked to the depletion of coagulation factors during apheresis sessions (17–19, 29), a process required for ABOi desensitization, particularly for patients with high antibody titers (≥1:256), which necessitates more intensive apheresis. To counteract coagulation factor loss (25–28), our protocol involved a pre-transplant plasma exchange, where 1.5 times the plasma volume was treated with 100% plasma replacement to replenish coagulation factors. Although our study sample size limits robust conclusions, the data suggest that targeted plasma exchange could play a role in managing bleeding risks in ABOi patients. However, further research is necessary to confirm its efficacy and safety across larger patient cohorts.

4.5 Graft and patient survival: long-term outcomes

Long-term outcomes for ABO-incompatible kidney transplants in terms of graft survival are generally promising, although some studies suggest that ABOi kidney grafts exhibit slightly lower survival rates compared to ABO-compatible (ABOc) grafts, particularly in the early post-transplant years. In our study, graft survival in ABOi patients was 100% after a mean follow-up of 4.6 ± 3 years. Similarly, Koo et al. (1) reported a graft survival rate of 92% in a cohort of 426 ABOi KTx patients after five years of follow-up, with no statistically significant difference observed between the low-titer ABOi group (≤1:64, n = 300) and the high-titer group (≥1:128, n = 126). These findings are further supported by Chung et al. (29), who found no significant difference in graft survival at one-year post-transplantation between ABOi KTx patients with high isoagglutinin titers (≥1:256) and those with low titers (≤1:128).

In our study, most ABOi grafts demonstrated stable renal function, with an average creatinine level of 121 ± 16 µmol/L after one year, and 138 ± 15 µmol/L after four years of follow-up. These results are consistent with those reported by Gan et al. (3), who observed an average creatinine level of 115 ± 37 µmol/L at one year and 143.8 ± 99 µmol/L after five years, alongside a graft

survival rate of 90%. Similarly, a Spanish study by Oppenheimer et al. (14) found an average creatinine level of 115.8 ± 8.0 µmol/L at one year.

Despite these favorable outcomes, ABOi graft survival remains somewhat lower than that of ABOc grafts, particularly during the early post-transplant period. A meta-analysis by Scurt et al. (46), which included 65,063 transplant recipients, 7,098 of whom were ABOi patients, showed that three-year graft survival rates in ABOi kidney recipients were significantly lower compared to ABOc recipients. However, this difference diminishes after five years of follow-up, likely due to the elevated risk of acute rejection and infection in the early post-transplant phase. De Weerd et al. (13) also reported that ABOi graft survival was comparable to that of ABOc grafts from deceased donors, but slightly lower than that of ABOc grafts from living donors, especially in patients with isoagglutinin titers ≥ 1:128. The estimated glomerular filtration rate (GFR) at one year was, on average, 49.7 mL/min/1.73 m^2 in the ABOi group, compared to 55.1 mL/min/1.73 m^2 in the ABOc living donor group and 48.9 mL/min/1.73 m^2 in the ABOc deceased donor group. These results are consistent with those of Massie et al. (2), who demonstrated that ABOi kidney recipients experienced superior survival beyond 180 days post-transplant compared to matched candidates on the waiting list, although the mortality risk remained higher within the first 30 days post-transplantation.

In terms of patient survival, the outcomes of our study were equally favorable, with a long-term survival rate of 100% after a mean follow-up of 4.6 ± 3 years. In a previous study involving 44 ABOi and 44 ABOc KTx patients (6, 7), we also observed a 100% patient survival rate after a mean follow-up of 18 ± 14.8 months. These findings align with those of Gan et al. (3) and Koo et al. (1), who reported patient survival rates of 90% and 96%, respectively, in ABOi patients after five years of follow-up. In comparison, ABOc patients receiving a kidney graft from a deceased donor had a one-year survival rate of 97.3% and a five-year survival rate of 93%, while patients remaining on the waiting list exhibited survival rates of 97.6% and 90%, respectively (1). Thus, KTx ABOi patients benefit from superior survival compared to those on the transplant waiting list or those receiving ABOc grafts from deceased donors. These findings are corroborated by de Weerd et al. (13), who found that ABOi KTx patient survival was higher than that of ABOc recipients of deceased donor transplants [HR 0.69 (0.49-0.96)], and comparable to ABOc recipients of living donor transplants [HR 1.28 (0.90-1.81)]. The cumulative incidence of mortality with a functioning graft in ABOi patients was 3.0%, 6.4%, and 13.5% at 1, 5, and 10 years, compared to 1.6%, 7.0%, and 10.4% at 1, 5, and 10 years for ABOc transplant recipients.

5 Conclusion

The presence of elevated isoagglutinin titers should no longer be considered a barrier to ABO-incompatible (ABOi) kidney transplantation, thanks to advancements in desensitization protocols involving rituximab and apheresis. Our findings, alongside evidence from the literature, confirm that ABOi kidney transplants can achieve long-term patient survival rates comparable to, or even surpassing, those of ABO-compatible (ABOc) recipients of deceased donor grafts or patients remaining on the transplant waiting list. However, achieving these outcomes requires substantial expertise and resources, as effective management of ABOi transplants demands rigorous desensitization protocols, highly trained personnel in apheresis and immunology, and vigilant postoperative monitoring.

Data availability statement

The raw data supporting the conclusions of this article will be made available by the authors, without undue reservation.

Ethics statement

The studies were conducted in accordance with the local legislation and institutional requirements. Written informed consent for participation was not required from the participants or the participants' legal guardians/next of kin because It was standard of care procedures.

Author contributions

HNB: Data curation, Writing – original draft. KB: Data curation, Writing – original draft. JN: Writing – review & editing. PM: Methodology, Writing – original draft. TJ: Writing – original draft. LR: Writing – review & editing.

Funding

The author(s) declare that no financial support was received for the research, authorship, and/or publication of this article.

Conflict of interest

The authors declare that the research was conducted in the absence of any commercial or financial relationships that could be construed as a potential conflict of interest.

Generative AI statement

The author(s) declare that no Generative AI was used in the creation of this manuscript.

Publisher's note

References

1. Koo TY, Lee J, Lee Y, Kim HW, Kim BS, Huh KH, et al. Outcomes of ABO-incompatible living donor kidney transplantation compared to waiting or deceased donor kidney transplantation. *Am J Nephrol*. (2024) 55:235–44. doi: 10.1159/000535583

2. Massie AB, Orandi BJ, Waldram MM, Luo X, Nguyen AQ, Montgomery RA, et al. Impact of ABO-incompatible living donor kidney transplantation on patient survival. *Am J Kidney Dis*. (2020) 76:616–23. doi: 10.1053/j.ajkd.2020.03.029

3. Gan CC, Jalalonmuhali M, Nordin NZ, Abdul Wahab MZ, Yahya R, Ng KP, et al. ABO-incompatible living-donor kidney transplantation in a developing country: A multicenter experience in Malaysia. *Transplant Proc*. (2021) 53:856–64. doi: 10.1016/j.transproceed.2020.10.038

4. Hew EY, Kessaris N, Stojanovic J, Jones H, Christian M, Edwards A, et al. Successful ABO and HLA incompatible kidney transplantation in children in the UK. *Pediatr Nephrol*. (2023) 38:529–35. doi: 10.1007/s00467-022-05583-5

5. Guy P, Delas A, Esposito L, Cointault O, Colombat M, Congy-Jolivet N, et al. Progression of histological lesions after ABO incompatible kidney transplantation. *Front Immunol*. (2022) 13:969998. doi: 10.3389/fimmu.2022.969998

6. Naciri Bennani H, Abdulrahman Z, Allal A, Sallusto F, Delarche A, Game X, et al. Early post-transplant complications following ABO-incompatible kidney transplantation. *J Nephropathol*. (2016) 5:19–27. doi: 10.15171/jnp.2016.04

7. Abdulrahman Z, Bennani Naciri H, Allal A, Sallusto F, Debiol B, Esposito L. Long-term outcomes after ABO-incompatible kidney transplantation; a single-center French study. *J Nephropathol*. (2017) 6:290–303. doi: 10.15171/jnp.2017.48

8. Deng Y, Frischnknecht L, Wehmeier C, de Rougemont O, Villard J, Ferrari-Lacraz S, et al. Pre-transplant donor specific antibodies in ABO incompatible kidney transplantation - data from the Swiss transplant cohort study. *Front Immunol*. (2024) 15:1355128. doi: 10.3389/fimmu.2024.1355128

9. Prabhakar A, Gang S, Hegde U, Konnur A, Patel H, Rajapurkar M. Kidney transplantation with ABO-incompatible donors: A comparison with matched ABO compatible donor transplants. *Indian J Nephrol*. (2021) 31:358–64. doi: 10.4103/ijn.IJN_206_20

10. Lee JY, Cha SH, Kim SH, Jeong KH, Chung KY, Cho HR, et al. Risk due to ABO incompatibility and donor-recipient weight mismatch in living donor kidney transplantation: A national cohort study. *J Clin Med*. (2021) 10:5674. doi: 10.3390/jcm10235674

11. Begum NAS, Kashem TS, Nobi F, Arefin SU, Rashid HU. Experiences of performing ABO-incompatible kidney transplantation in Bangladesh. *Korean J Transplant*. (2022) 36:111–8. doi: 10.4285/kjt.22.0014

12. Eder M, Schrag TA, Havel EF, Kainz A, Omic H, Doberer K, et al. Polyomavirus nephropathy in ABO blood group-incompatible kidney transplantation: Torque Teno virus and immunosuppressive burden as an approximation to the problem. *Kidney Int Rep*. (2024) 9:1730–41. doi: 10.1016/j.ekir.2024.04.003

13. de Weerd AE, van den Brand JAJG, Bouwsma H, de Vries APJ, Dooper IPMM, Sanders JF, et al. ABO-incompatible kidney transplantation in perspective of deceased donor transplantation and induction strategies: a propensity-matched analysis. *Transpl Int*. (2021) 34:2706–19. doi: 10.1111/tri.14145

14. Oppenheimer F, Revuelta I, Serra N, Lozano M, Gutiérrez-Dalmau A, Esforzado N, et al. Trasplante renal ABO incompatible: de un sueño a una realidad. Experiencia del Hospital Clínic de Barcelona [ABO incompatible living donor kidney transplantation: a dream come true. Experience of Hospital Clínic of Barcelona. *Nefrologia*. (2010) 30:54–63. doi: 10.3265/Nefrologia.pre2009.Dic.5695

15. Heo GY, Jang Y, Choi H, Kim YC, Han SS, Kim HW, et al. Impact of ABO incompatibility and early antibody-mediated rejection on chronic antibody-mediated rejection in kidney transplant patients. *J Nephrol*. (2023) 36:2571–80. doi: 10.1007/s40620-023-01643-7

16. Lentine KL, Axelrod D, Klein C, Simpkins C, Xiao H, Schnitzler MA, et al. Early clinical complications after ABO-incompatible live-donor kidney transplantation: a national study of Medicare- insured recipients. *Transplantation*. (2014) 98:54–65. doi: 10.1097/TP.0000000000000029

17. Kim MH, Jun KW, Hwang JK, Kim JI, Chung BH, Choi BS, et al. Risk factors for postoperative bleeding in ABO-incompatible kidney transplantation. *Clin Transplant*. (2015) 29:365–72. doi: 10.1111/ctr.12525

18. de Weerd AE, van Agteren M, Leebeek FW, Ijzermans JN, Weimar W, Betjes MG. ABO- incompatible kidney transplant recipients have a higher bleeding risk after antigen-specific immunoadsorption. *Transpl Int*. (2015) 28:25–33. doi: 10.1111/tri.12412

19. Ohdan H. How can we minimize bleeding complications in ABO-incompatible kidney transplant recipients? *Transpl Int*. (2015) 28:22–4. doi: 10.1111/tri.12447

20. Habicht A, Bröker V, Blume C, Lorenzen J, Schiffer M, Richter N, et al. Increase of infectious complications in ABO-incompatible kidney transplant recipients–a single centre experience. *Nephrol Dial Transplant*. (2011) 26:4124–31. doi: 10.1093/ndt/gfr215

21. Sharif A, Alachkar N, Bagnasco S, Geetha D, Gupta G, Womer K, et al. Incidence and outcomes of BK virus allograft nephropathy among ABO- and HLA-incompatible kidney transplant recipients. *Clin J Am Soc Nephrol*. (2012) 7:1320–7. doi: 10.2215/CJN.00770112

22. Bentall A, Neil D, Sharif A, Ball S. ABO- incompatible kidney transplantation is a novel risk factor for BK nephropathy. *Transplantation*. (2015) 99:e8–9. doi: 10.1097/TP.0000000000000483

23. Rostaing L, Allal A, Del Bello A, Sallusto F, Esposito L, Doumerc N, et al. Treatment of large plasma volumes using specific immunoadsorption to desensitize ABO-incompatible kidney-transplant candidates. *J Nephropathol*. (2016) 5:90–7. doi: 10.15171/jnp.2016.17

24. Eskandary F, Wahrmann M, Biesenbach P, Sandurkov C, König F, Schwaiger E, et al. ABO antibody and complement depletion by immunoadsorption combined with membrane filtration–a randomized, controlled, cross-over trial. *Nephrol Dial Transplant*. (2014) 29:706–14. doi: 10.1093/ndt/gft502

25. Naciri Bennani H, Marlu R, Terrec F, Motte L, Seyve L, Chevallier E, et al. How to improve clotting factors depletion in double-filtration plasmapheresis. *J Clin Apher*. (2021) 36:766–74. doi: 10.1002/jca.21928

26. Marlu R, Naciri Bennani H, Seyve L, Noble J, Chevallier E, Motte L, et al. Comparison of three modalities of plasmapheresis on coagulation: Centrifugal, single-membrane filtration, and double-filtration plasmapheresis. *J Clin Apher*. (2021) 36:408–19. doi: 10.1002/jca.21879

27. Marlu R, Bennani HN, Seyve L, Malvezzi P, Janbon B, Noble J, et al. Effect of immunoadsorption alone or combined with membrane filtration on hemostasis parameters. *J Clin Apher*. (2020) 35:444–52. doi: 10.1002/jca.21825

28. Marlu R, Malvezzi P, Seyve L, Jouve T, Maurizi J, Defendi F, et al. Effect of double-filtration plasmapheresis for antibody-mediated rejection on hemostasis parameters and thrombin generation. *Thromb Res*. (2018) 166:113–21. doi: 10.1016/j.thromres.2018.04.018

29. Chung BH, Lee JY, Kang SH, Sun IO, Choi SR, Park HS, et al. Comparison of clinical outcome between high and low baseline anti-ABO antibody titers in ABO-incompatible kidney transplantation. *Ren Fail*. (2011) 33:150–8. doi: 10.3109/0886022X.2011.552149

30. Süsal CC, Kraft L, Ender A, Süsal C, Schwenger A, Amann K, et al. Blood group-specific apheresis in combination with daratumumab as a rescue therapy of acute antibody-mediated rejection in a case of ABO- and human leukocyte antigen-incompatible kidney transplantation. *SAGE Open Med Case Rep*. (2023) 11:2050313X231211050. doi: 10.1177/2050313X231211050

31. Won D, Choe W, Kim HJ, Kwon SW, Han DJ, Park SK. Significance of isoagglutinin titer in ABO-incompatible kidney transplantation. *J Clin Apher*. (2014) 29:243–50. doi: 10.1002/jca.21312

32. Wilpert J, Geyer M, Teschner S, Schaefer T, Pisarski P, Schulz-Huotari C, et al. ABO-incompatible kidney transplantation-proposal of an intensified apheresis strategy for patients with high initial isoagglutinine titers. *J Clin Apher*. (2007) 22:314–22. doi: 10.1002/jca.20153

33. Morath C, Zeier M, Döhler B, Opelz G, Süsal C. ABO-incompatible kidney transplantation. *Front Immunol*. (2017) 8:234. doi: 10.3389/fimmu.2017.00234

34. Bleasel JM, Wan SS, Chadban SJ, Ying T, Gracey DM, Aouad LJ, et al. ABO incompatible kidney transplantation without B-cell depletion is associated with increased early acute rejection: A single-center Australian experience. *Transpl Int*. (2023) 36:11567. doi: 10.3389/ti.2023.11567

35. Tasaki M, Saito K, Nakagawa Y, Imai N, Ito Y, Aoki T, et al. Acquired downregulation of donor-specific antibody production after ABO-incompatible kidney transplantation. *Am J Transplant*. (2017) 17:115–28. doi: 10.1111/AJT.13937

36. Randhawa P, Pastrana DV, Zeng G, Huang Y, Shapiro R, Sood P, et al. Commercially available immunoglobulins contain virus neutralizing antibodies against all major genotypes of polyomavirus BK. *Am J Transplant*. (2015) 15:1014–20. doi: 10.1111/ajt.13083

37. Genberg H, Kumlien G, Wennberg L, Tydén G. Long-term results of ABO-incompatible kidney transplantation with antigen-specific immunoadsorption and rituximab. *Transplantation*. (2007) 84:S44–7. doi: 10.1097/01.tp.0000296031.41424.f8

38. Lee HR, Kim K, Lee SW, Song JH, Lee JH, Hwang SD. Effect of rituximab dose on induction therapy in ABO-incompatible living kidney transplantation: A network meta-analysis. *Med (Baltimore)*. (2021) 100:e24853. doi: 10.1097/MD.0000000000024853

39. Naciri Bennani H, Abdulraham Z, Puissant-Lubrano B, Allal A, Rostaing L. Rituximab and hypogammaglobulinemia in the setting of ABO-incompatible kidney transplantation. *J Nephropathol*. (2018) 7:151–7. doi: 10.15171/jnp.2018.34

40. Speer C, Kälble F, Nusshag C, Pego da Silva L, Schaier M, Becker LE, et al. Outcomes and complications following ABO-incompatible kidney transplantation performed after desensitization by semi-selective immunoadsorption - a retrospective study. *Transpl Int*. (2019) 32:1286–96. doi: 10.1111/tri.13482

41. Matuschik L, Seifert G, Lammich K, Holzner P, Tanriver Y, Fichtner-, et al. Non-antigen-specific immunoadsorption is a risk factor for severe postoperative infections in ABO-incompatible kidney transplant recipients. *Transpl Int*. (2024) 37:12263. doi: 10.3389/ti.2024.12263

42. Lopau K, Syamken K, Rubenwolf P, Riedmiller H, Wanner C. Impact of mycophenolate mofetil on wound complications and lymphoceles after kidney transplantation. *Kidney Blood Press Res*. (2010) 33:52–9. doi: 10.1159/000289573

43. Jänigen BM, Salabè C, Glatz T, Thomusch O, Lässle C, Fichtner-, et al. Single cohort study: ABO-incompatible kidney transplant recipients have a higher risk of lymphocele formation. *Langenbecks Arch Surg*. (2019) 404:999–1007. doi: 10.1007/s00423-019-01812-y

44. de Weerd AE, Betjes MGH. ABO-incompatible kidney transplant outcomes: A meta-analysis. *Clin J Am Soc Nephrol*. (2018) 13:1234–43. doi: 10.2215/CJN.00540118

45. Zschiedrich S, Jänigen B, Dimova D, Neumann A, Seidl M, Hils S, et al. One hundred ABO-incompatible kidney transplantations between 2004 and 2014: a single-centre experience. *Nephrol Dial Transplant*. (2016) 31:663–71. doi: 10.1093/ndt/gfv388

46. Scurt FG, Ewert L, Mertens PR, Haller H, Schmidt BMW, Chatzikyrkou C. Clinical outcomes after ABO-incompatible renal transplantation: a systematic review and meta-analysis. *Lancet*. (2019) 393:2059–72. doi: 10.1016/S0140-6736(18)32091-9

frontiers | Frontiers in Immunology

TYPE Review
PUBLISHED 15 January 2025
DOI 10.3389/fimmu.2024.1527648

OPEN ACCESS

EDITED BY
Rita Maccario,
San Matteo Hospital Foundation (IRCCS), Italy

REVIEWED BY
Gaurav Sutrave,
The University of Sydney, Australia
Luigi Nespoli,
University of Insubria, Italy

*CORRESPONDENCE
Danièle Bensoussan
d.bensoussan@chru-nancy.fr

RECEIVED 13 November 2024
ACCEPTED 30 December 2024
PUBLISHED 15 January 2025

CITATION
Wang V, Savoldo B, Guimaraes J-A, Dotti G, Reppel L and Bensoussan D (2025) Alloreactive-free CAR-VST therapy: a step forward in long-term tumor control in viral context. *Front. Immunol.* 15:1527648. doi: 10.3389/fimmu.2024.1527648

Alloreactive-free CAR-VST therapy: a step forward in long-term tumor control in viral context

Valentine Wang[1], Barbara Savoldo[2], José-Arthur Guimaraes[1], Gianpietro Dotti[2], Loïc Reppel[1,3] and Danièle Bensoussan[1,3]*

[1]Unité Mixte de Recherche (UMR) 7365 Centre National de la Recherche Scientifique (CNRS), Ingénierie Moléculaire, Cellulaire et Physiopathologie (IMoPA), Université de Lorraine, Nancy, France, [2]Lineberger Comprehensive Cancer Center, University of North Carolina, Chapel Hill, NC, United States, [3]Centre Hospitalier Régional Universitaire (CHRU) Nancy, Cell Therapy and Tissue Bank Unit, MTInov Bioproduction and Biotherapy Integrator, Nancy, France

CAR-T cell therapy has revolutionized immunotherapy but its allogeneic application, using various strategies, faces significant challenges including graft-versus-host disease and graft rejection. Recent advances using Virus Specific T cells to generate CAR-VST have demonstrated potential for enhanced persistence and antitumor efficacy, positioning CAR-VSTs as a promising alternative to conventional CAR-T cells in an allogeneic setting. This review provides a comprehensive overview of CAR-VST development, emphasizing strategies to mitigate immunogenicity, such as using a specialized TCR, and approaches to improve therapeutic persistence against host immune responses. In this review, we discuss the production methods of CAR-VSTs and explore optimization strategies to enhance their functionality, activation profiles, memory persistence, and exhaustion resistance. Emphasis is placed on their unique dual specificity for both antitumor and antiviral responses, along with an in-depth examination of preclinical and clinical outcomes. We highlight how these advances contribute to the efficacy and durability of CAR-VSTs in therapeutic settings, offering new perspectives for broad clinical applications. By focusing on the key mechanisms that enable CAR-VSTs to address autologous CAR-T cell challenges, this review highlights their potential as a promising strategy for developing effective allogeneic CAR-T therapies.

KEYWORDS

CAR-T, virus specific T cell, CAR-VST, allogeneic, GvHD, graft rejection

1 Introduction

Autologous Chimeric Antigen Receptor T cell (CAR-T cell) therapy, while highly personalized and effective, faces several significant limitations. The manufacturing process is complex and time-consuming, often taking weeks to harvest, engineer, and expand the patient's own T cells (1). This delay can be critical for patients with rapidly progressing diseases. Additionally, the quality of autologous T cells can be compromised in heavily pretreated or immunocompromised patients, potentially reducing the efficacy of the therapy (2). The cost associated with the individualized production of autologous CAR-T cells is also substantial, making it less accessible to a broader patient population (between 300 000-400 000$).

In contrast, allogeneic CAR-T cells represent a promising solution to overcome these challenges. Allogeneic CAR-T are derived from "treatment naïve" healthy donors, allowing for the generation of "off-the-shelf" products that can be prepared in advance and made readily available, with a significant reduction of the time from diagnosis to treatment (3). By using a restricted number of donors, production costs are lowered through large-scale manufacturing, making the treatment more accessible. Despite these ideal characteristics, the potential for graft-versus-host disease (GvHD) and the risk of rejection, which limits the efficiency and persistence of allogeneic CAR-T cells, remain significant hurdles. Lymphodepletion and various sophisticated gene modifications have been explored to prevent such complications. However, the alloreactivity of allogeneic CAR-T cells can lead to life-threatening complications, limiting their widespread use (4).

Using virus specific T cells (VST) as a raw material to generate CAR-T cells is an effective way to mitigate some of these drawbacks. Indeed, VST are associated with a low risk of GvHD (5, 6). Moreover, their anti-viral TCR contributes to their prolonged persistence through repeated virus reactivations or restimulations, enhancing the durability and efficacy of the therapy.

After a brief state of the art about allogeneic CAR-T cells, we will describe in the current review, the potential of VST then achievements of CAR-VST therapy, focusing on its development, preclinical research, and clinical applications.

2 Allogeneic CAR-T cells

Understanding alloreactivity mechanisms like graft-versus-host disease (GvHD) and graft rejection (GR) is crucial to develop strategies to develop allogeneic CAR-T cells.

2.1 Strategies for allogeneic CAR-T cells

To mitigate rejection of infused allogeneic VSTs by recipient-derived immune responses, lymphodepleting chemotherapy or radiotherapy is typically employed to reduce the host's immune response. Enhancing lymphodepletion prior to CAR-T cell infusion further reduces recipient T cell numbers, creating a more favorable environment for graft acceptance. Another approach involves creating Human Leukocyte Antigen (HLA)-matched cell banks to reduce immunogenicity (7), while gene-editing techniques, such as Clustered Regularly Interspaced Short Palindromic repeats (CRISPR) or Transcription Activator-Like Effector Nuclease (TALEN), are used to knock out HLA class I molecules, thus decreasing T-cell-mediated rejection (8–10). However, since Natural Killer (NK) cells can target cells lacking HLA class I through "missing-self" recognition, overexpressing non-classical HLA molecules, like HLA-E or HLA-G, can protect CAR-T cells from NK cell-mediated lysis (11–14).

To reduce GvHD, researchers have focused on preventing alloreactivity by modifying T cells to minimize their interaction with the recipient's immune system. Gene editing to knock out the TCR, particularly the TRAC gene, prevents T cells from recognizing and attacking recipient tissues, thus reducing GvHD risk. Technologies like CRISPR/Cas9, Zinc Finger Nucleases (ZFN), and TALEN are instrumental in achieving precise TCR knock-out (4, 15–19). Another approach consists in using non-T cell types-such as Natural Killer cells (20, 21), γδ T cells (22–24), Mucosal-Associated Invariant T (MAIT) cells (25–27), Double Negative T cells (DNTs) (28–31), Cytokine-Induced Killer cells (CIK) (32, 33), invariant NKT (iNKT) cells (34–37), inducible Pluripotent Stem Cell (iPSC) (38–40) and Virus Specific T cells (VST) cells-, as they have less alloreactivity leading to a reduced risk of inducing GvHD. For instance, NK cells provide a potent cytotoxic response regardless TCR involvement, while VST cells leverage prior viral specificity to reduce alloreactivity and minimize GvHD.

With these strategies in place to prevent GvHD risk, the focus now shifts to evaluating the clinical outcomes of allogeneic CAR-T cell therapies and their potential benefits across patient populations.

2.2 Clinical outcomes

Recent reviews highlight various strategies for producing allogeneic CAR-T cells using previous cited strategies to disrupt TCR and CD52 genes, minimizing GvHD and rejection risks (41–44). Many *off-the-shelf* products, such as UCART19/ALLO-501, have shown encouraging outcomes, achieving a 48% overall response rate (ORR) in B-ALL and lymphoma with manageable GvHD (45). Advanced trials, like ALLO-501A, report a 67% ORR without GvHD (ALPHA2 (NCT04416984), EXPAND (NCT05714345)) (46). Other candidates targeting CD123, CD22, and BCMA have achieved ORRs around 70% without GvHD (47–49). PBCAR0191 and CTX110 showed high efficacy (up to 83%) in lymphoma and B-ALL even after prior CAR-T failure (50). Innovative approaches, including shRNA-based CYAD-101 and iPSC-derived FT819, have shown good tolerability and stable outcomes (51–53). To address rejection without excessive immunosuppression, gene-editing strategies aim to reduce CAR-T cell immunogenicity. For instance, knocking out β2-microglobulin (β2M) prevents expression of HLA class I molecules, limiting recognition by host T cells. Some products, like PBCAR19B, also express HLA-E, which binds inhibitory receptors on NK cells, reducing NK-mediated lysis (54). Other approaches, such as

deleting both β2M and CD70 (as in CTX-130), aim to reduce recognition by both T and NK cells, improving CAR-T persistence in the host.

Building on the advances and challenges of allogeneic CAR-T cell development, we will focus on the strategy of using VST cells as a primary source for CAR-T cells, leveraging their unique immunological properties to improve the safety, persistence, and efficacy of allogeneic CAR-T therapies.

3 Virus specific T cells: state of the art

Viral infections, reactivations or diseases remain major complications in immunocompromised patients, including those with primary immunodeficiency or secondary immunodeficiency due to (i) allogeneic hematopoietic stem cell transplantation (allo-SCT), (ii) solid organ transplantation (SOT), (iii) immunosuppressive treatment, or (iv) human immunodeficiency virus infection. Although improvements in the management of viral infections have been made thanks to the implementation of new antiviral drugs, prophylactic and pre-emptive administration and viral load monitoring, in the absence of specific antiviral immunity, antiviral strategies are often ineffective, leading to treatment failure. To address this major limitation, adoptive transfer of virus specific T cells (VST) has been explored.

VST are isolated from a donor's lymphocyte pool and require prior immunization of the donor to the target viruses. For example, about 90% of the adult population has prior immunity to Epstein-Barr virus (EBV), while nearly 100% of the adult population in Asia and about 50% in Europe have immunity to cytomegalovirus (CMV) (55). After infusion into the patient, VST proliferate upon encounter with the specific viral antigens presented by the recipient's HLA molecules, and generate an antiviral immune response. The source of these VSTs can be the allo-SCT donor or a different donor, known as a third-party donor, which can overcome issues associated with the lack of availability of an allogeneic HPC donor for the generation of donor-derived VSTs. In the context of allo-HCT, the use of third-party VSTs allows for immediate access to an antiviral therapeutic product, which can overcome issues associated with limited access to the allo-SCT donor (e.g., lack of donor availability or prolonged manufacturing times in the event of a seronegative donor) (56). Additionally, it can expedite the process in SOT or in case of immunodeficiency, by using a readily available donor or ready-to-use HLA-typed antiviral VST from a bank (Figure 1). The qualitative characteristics of generated VST vary depending on the type of donor, the production method and the targeted virus. Currently, two major production strategies are commonly implemented: *ex vivo* expansion of specific VST by cell culture or direct immunomagnetic isolation of VST.

Ex vivo expansion relies on the co-culture of peripheral blood mononuclear cells (PBMC) with autologous antigen-presenting cells (APC), such as EBV-transformed lymphoblastoid cell lines (LCL) (57), antigen-pulsed dendritic cells (DC) or, more recently, peptide-loaded APC (58). This method, which requires a minimum of 10 days, allows for the expansion of large numbers of polyclonal VST, containing both CD8 and CD4 T cells.

Immunomagnetic isolation of VST requires the use of a device like the CliniMACS or its automated counterpart, the Prodigy (Miltenyi Biotec, Bergisch-Gladbach, Germany). Enrichment of VST based on IFN-γ secretion involves stimulating PBMC with one or more synthetic peptide pools, and subsequently isolation using the IFN-γ Catchmatrix reagent (Cytokine Capture System, Miltenyi Biotec). This procedure can be completed in 2 days including leukapheresis. Although a very small number of cells is often obtained through this process, VST are polyclonal and contain both CD8 and CD4 T cells (59). Another way to target VST before immunomagnetic sorting consists in using HLA restricted-multimers, which offers a highly specific approach by binding the TCR on specific T cells. However, isolated VST are usually composed either of a CD8 or a CD4 T-cell clone, depending on the MHC molecule used in the multimer (MHC class II multimers are still rarely available), leading to a very low number of VST, often lacking CD4 T cell support over time (60).

The use of *ex-vivo* expanded specific CD8+ T-cells from the initial donor was first proposed Riddell et al. in 1992 as a VST strategy to treat CMV reactivation after allo-SCT (61). Subsequently EBVST generated from donor derived PBMC stimulated with irradiated autologous LCL were utilized to prevent EBV reactivation (62, 63). In 2006, freshly immunomagnetically-isolated AdV-VST from allo-SCT donor leukapheresis without any prior expansion, successfully control in 4 out of 5 evaluable patients with AdV infection-related complications (59). The need for a fast, efficient and safe treatment for early post-transplant viral infections prompted the generation of VST from third-party donors. This development broadened the applicability of VST due to their low capacity to induce alloreactivity even when using HLA-mismatched donors (5, 6, 64). Currently, off-the-shelf, potentially multi-target VSTs represent a promising therapy for both early and late-stage viral infections in immunocompromised patients, provided that a compatible VST cell line is available (58, 65, 66).

To date, data from more than 50 clinical studies (phase I, I/II and II) currently available provide encouraging results, both regarding antiviral efficiency and tolerance (67). Safety studies reported that a minority of patients experienced no to low side effects related to VST therapy -specifically GvHD, Cytokine Release Syndrome (CRS), infusion toxicity, transplant-associated thrombotic microangiopathy, graft failure, and genitourinary complications- none of which were serious (grade I/II), allowing for a short monitoring period of one hour after VST infusion (68, 69).

The reported risk of post-administration GvHD is relatively low, around 10%, regardless of the antiviral VST type and donors, including third parties with partial HLA compatibility (70). Among the reported cases of GvHD, it appears that most of them are reactivations (2/3). However, it remains impossible to discriminate between the effects of the VST themselves and modulation of immunosuppressive drugs in patients waiting VST infusion (5). Nevertheless, heterologous immunity, which refers to the cross-reactivity of VST with allo-antigens in an allogeneic context, remains rarely observed, despite

10.3389/fimmu.2024.1527648

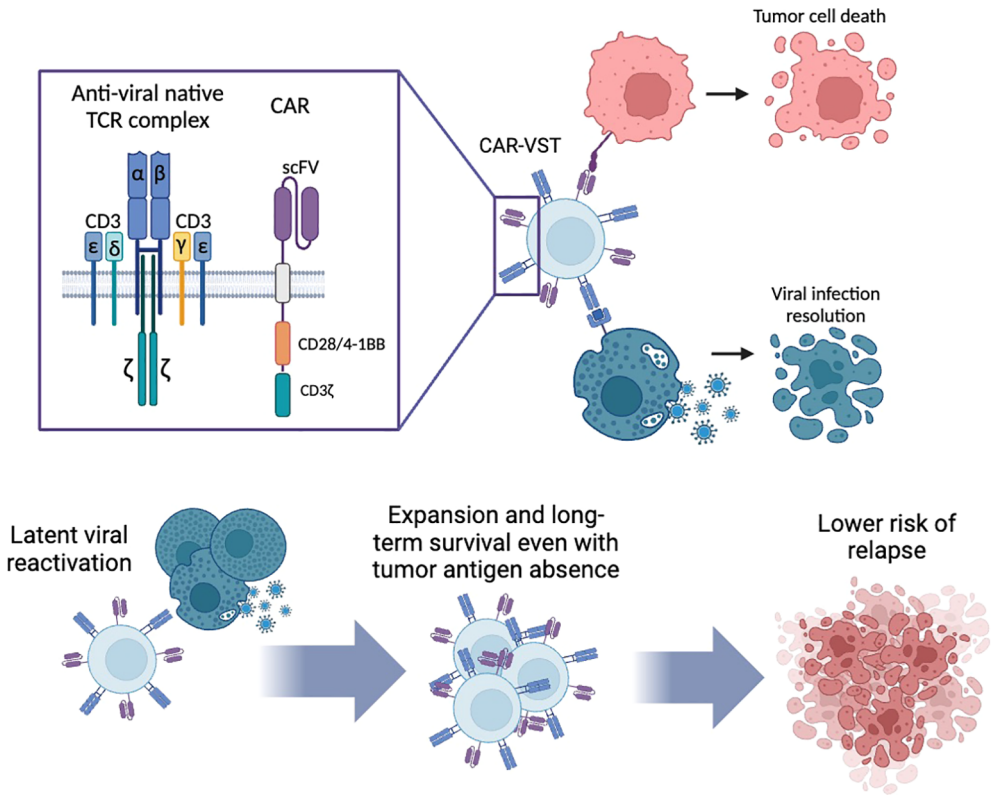

FIGURE 1
Dual specificity of CAR-VST: antitumoral lysis by the CAR and antiviral lysis via their native TCR. Long-term survival of CAR-VST is expected through the restimulation of the TCR by latent virus reactivation. CAR, Chimeric Antigen Receptor; CD, Cluster of differentiation; VST, Virus Specific T cell. Created with Biorender.com.

being a theoretical concern. This was first reported in the context of allo-SCT, with low GvHD incidence, whereas VST presented cross-reactivity with recipient HLA molecules *in vitro* (71). More recently, a lack of association between the presence of cross-reactive VST and decreased graft survival has been systematically observed in SOT patients (72). Several explanations have been proposed, including a lower avidity of VST TCR for the allogeneic epitope compared to the viral epitope, and the role of immunosuppressive regimens in transplanted patients.

Regarding antiviral efficacy, 65-90% of patients achieved a partial or complete antiviral response across various clinical studies (73). Different reasons have been suggested to explain this range. First, the delay between viral infection and VST infusion. In line with this assessment, our team observed a strong impact of a high viral load (>5 log) on overall survival, regardless of the involved virus, suggesting that VST should be considered as soon as a patient experience a chemo-refractory viral infection following allo-SCT (6). Moreover, the matching between VST and the patient appears to be more critical for the viral restricting alleles than for the overall degree of match *per se* (74). Last but not least, a specific antiviral immune reconstitution was frequently associated to the decrease or clearance of the viral load (59). This means that all the conditions must be met for *in vivo* VST expansion, particularly a moderate immunosuppression, given the role played by corticosteroids as previously reported in an *in vitro* study (75).

However, up to now, no phase III clinical efficacy study has been published. A randomized, controlled study in a large cohort of patients comparing antiviral treatment alone to antiviral treatment combined with VST will be helpful to confirm safety and efficacy. To this end, the results from Trace (TRansfer of Adenovirus, Cytomegalovirus and Epstein-Barr virus specific-T cells -NCT04832607), a European comparative study, are highly anticipated.

The persistence for up to 9 years of functional VST has been reported (57). Current data suggest that, rather than the total amount of VST infused, the frequency of different lymphocyte subpopulations (especially memory T stem cells (Tscm)) (5) is crucial for the *in vivo* expansion of VST and the persistence of the antiviral response (76),. Indeed, Gattinoni and colleagues identified distinct T cell subsets with differing potential for persistence and therapeutic efficacy in adoptive immunotherapy (77). These subsets include naive T cells (Tn), central memory T cells (Tcm), effector memory T cells (Tem), and stem cell memory T cells (Tscm). Tscm are of significant interest due to their superior longevity, self-renewal capacity, and ability to differentiate into other T cell subsets, making them ideal for adoptive cell therapies. Our team reported that immunomagnetic sorted VST contained Tscm, although poorly represented (around 1%), which could be sufficient to allow for (i) differentiation into Tcm, Tem and Teff subsets according to the linear developmental model, and (ii) maintenance of the proportion of IFN-γ+ cells among Tscm (78).

4 Development of CAR-VST as an alternative for allogeneic CAR-T cell products

4.1 Virus specific T cells advantages

The generation of VST opens avenues for the development of CAR-VST, offering distinct advantages in terms of quantity and subpopulation diversity. The development of CAR-VST presents a promising alternative to conventional allogeneic CAR-T cell therapy, offering a versatile and potentially more accessible therapeutic option. Moreover, CAR-VSTs may provide additional regulatory and safety benefits compared to TCR knockdown strategies using CRISPR-Cas9 or other gene modification techniques, as these approaches carry a potentially increased risk of genotoxicity and malignant transformation (79, 80). The different methods to generate VST influence the characteristics of the resulting CAR-VST.

CAR-VST maintain robust antitumor efficacy due to their dual specificity. They are capable of targeting both tumor cells through their CAR and viral infected cells *via* their native TCR. This dual targeting is particularly beneficial for sustained and targeted therapeutic responses.

One of the major advantages VST can provide is the long-term persistence by the restimulation of their native TCR. This can occur through the spontaneous reactivation of latent viruses, making VST against latent viruses such as EBV, CMV and AdV ideal candidates. Alternatively, CAR-VST can be restimulated on demand using existing or manufactured vaccines against viruses like VZV or CMV, ensuring continuous expansion and activity. Unlike traditional CAR-T cells, which often suffer from limited efficiency and persistence, CAR-VST are expected to benefit from the continued expression of a functioning TCR.

Moreover CAR-VST are associated with a low incidence of GvHD, a common complication expected with traditional allogeneic CAR-T cells. As mentioned previously, the low or absence of alloreactivity is due to inherent properties of VST, which have been amply demonstrated in clinical trials (71, 72).

However, the risk of rejection remains a challenge. Different strategies can be employed to address this drawback. One approach involves the engineering of these cells to limit their expression of HLA molecules, thereby reducing their immunogenicity. However, this strategy makes CAR-T cells susceptible to NK killing. An alternative strategy is based on selecting an intrafamilial third-party donor to provide high-quality cells with reduced rejection risks. While this option is not suitable for *off-the-shelf* production and does not lower costs, it offers a reliable source of at least semi-compatible cells.

4.2 VST investigated to produce CAR-VST

Clinical trials involving VST began to emerge significantly in the early 2000s (Figure 2). Initially, research on VST primarily focused on treating viral infections and their role in the context of transplantation. The introduction of CAR-VST into clinical research was initially relatively slow, with only a few pioneering studies before 2010. However, beginning in the 2010s, there has been a notable increase in the number of clinical trials. Simultaneously, there has been a progressive increase in research publications on CAR-VST, reflecting a growing interest in this promising therapy.

Several leading institutions are advancing the research and development of CAR-VST therapies, primarily in the USA.

The Center for Cell and Gene Therapy at Baylor College of Medicine in Houston, USA, has been extensively investigating CAR-VSTs targeting antigens such as GD2, CD19, CD30, and HER2. Their work involves the use of various cytokines and transduction methods to enhance the expansion and persistence of these cells. Collaborating with other institutions, they focused on improving both *in vitro* and *in vivo* antitumor activity. At the City of Hope in Duarte, California, researchers have used CD19-targeting CAR-VSTs, employing innovative vaccination strategies to boost efficacy and persistence.

In Europe, the University Children's Hospital Münster in Germany is working on GD2.CAR-VST, addressing challenges in CAR-VST expansion and co-stimulation requirements. INSERM U590 at Centre Léon Bérard in Lyon, France, is developing CD33.CAR-VST, maintaining a memory effector phenotype with demonstrated functional antitumor and antiviral activities. These institutions collectively contribute to the evolving field of CAR-VST therapy, aiming to enhance the safety, specificity, and therapeutic efficacy of cancer immunotherapies. These studies are summarized in Tables 1, 2.

5 Pre-clinical research on CAR-VST

5.1 Cell manufacturing

All the characteristics are summarized in Table 1.

5.1.1 VST manufacturing

The manufacturing of CAR-VST involves several critical steps to ensure the effective generation and expansion of these therapeutic cells (Figure 3). As mentioned in section 1, two approaches are consistently used to generate VSTs, which we will briefly summarize here.

5.1.1.1 Coculture methods

Most of the CAR-VST reported in the literature are generated from VST obtained in co-culture of PBMC with autologous APC. This approach has proven effective for manufacturing large quantities of VST, which is advantageous for producing multiple batches. However, this method requires long expansion periods, often taking at least three weeks with repeated restimulations, which can also lead to more differentiated and exhausted T cells. As autologous antigen presenting cells LCL (81, 94, 96), dendritic cells (83, 90) or PBMC loaded with viral antigens like VZV have been used (95). Alternatively, Quach et al. directly stimulated CD45RA-depleted PBMC with pepmixes specific to EBV antigens (87), resulting in a robust expansion of VST that showed response to

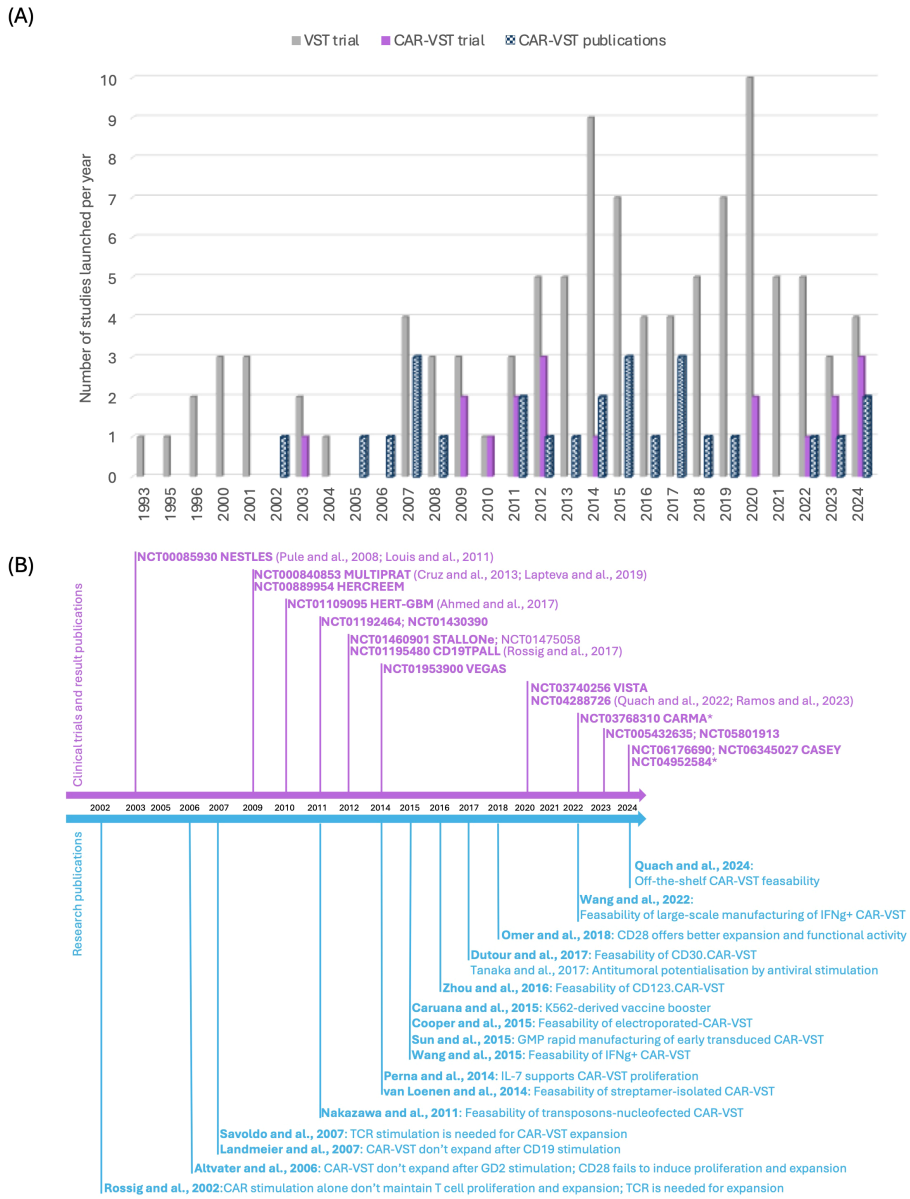

FIGURE 2
State of the art of CAR-VST in pre-clinical and clinical studies. **(A)** Publications on pre-clinical and clinical trials on CAR-VST and start year of clinical trials by year (clinicaltrial.gov, May 2024); **(B)** Relevant articles on CAR-VST pre-clinical results (blue) and clinical results (purple) by year. CAR, Chimeric Antigen Receptor; CD, Cluster of differentiation; GMP, good manufacturing practice; IFNγ, Interferon gamma; TCR, T cell receptor; VST, Virus Specific T cell.

EBV stimulation. Recombinant human interleukine-2 (IL-2) is the most common cytokine promoting T cell survival and proliferation. However, IL-2 is also known to induce a terminal effector phenotype which is correlated with strong cytotoxicity but short-term lifespan (77). Other cytokines like IL-4, IL-7 and/or IL-15 are currently under investigations to promote VST expansion and a more naïve phenotype (84, 87).

5.1.1.2 Immunomagnetic isolation

Immunomagnetic selection is used as an alternative method. In their studies, Wang and colleagues performed nine selection processes using PBMC from eight healthy CMV-seropositive donors. They successfully enriched IFN-γ+ T cells from pre-enrichment levels of 0.8 ± 0.5% to post-selection levels of 76.3% ± 11.6% (92, 93). The freshly isolated IFN-γ+, CMVST consisted in polyclonal CD8+ (44.0% ± 21.0%) and CD4+ T cells (49.8% ± 21.2%). The small number of sorted cells required an additional expansion phase, and further research is urged to enrich for naive and memory cells, rather than the effector phenotype so far obtained.

Overall, each procedure has distinct advantages and limitations. Coculture with LCL, DC or APC is time-consuming and often labor-intensive but produces high cell numbers with robust expansion. Immunomagnetic sorting is a rapid method enriching for highly specific VSTs; however, it leads to a low number of VST, requiring an additional expansion phase. Each method impacts the

TABLE 1 Pre-clinical studies on CAR-VST.

Team	Cells	VST sorting	Transduction	References
Center for Cell and Gene Therapy, Baylor College of Medicine, Houston, USA.	GD2.CAR-EBVST	Three stimulations by irradiated autologous EBV-LCL	Anti-OKT3 anti-CD28 antibodies After the third stimulation of irradiated LCL Retrovirus, retronectin	(81)
	CD30.CAR-VST CD28	Three stimulations by irradiated autologous EBV-LCL+IL-2 ADV or CMV	After the third stimulation of irradiated LCL Retrovirus, retronectin	(82)
	iCas9.GD2.CAR-CMVST CD28	Stimulation with autologous DC loaded with pp65 pepmix	After the second stimulation of irradiated LCL Retrovirus, retronectin	(83)
	GD2.CAR-EBVST	Three stimulations by irradiated autologous EBV-LCL	Early and late transduction Retrovirus, retronectin	(84)
	HER2-EBVST HER2-EBVST.iCD19 CD28	Stimulation with irradiated autologous EBV-LCL	Nucleofection with transposons	(85)
	GD2.CAR-VST CD19.CAR-VST Either CD28 or 41BB	Stimulation with autologous DC, PBMC and peptide-loaded-K562 (VZV or EBV)	Retrovirus, retronectin	(86)
	CD30.CAR-EBVST 2nd generation CD28	PBMCs were depleted of CD45RA positive cells by magnetic column separation, then stimulated with EBV pepmixes	Retrovirus, retronectin	(87)
Center for Cell and Gene Therapy, Baylor College of Medicine, Houston, USA + collaborators	GD2.CAR-EBVST GD2.CAR-EBVST.IL7R CD28	Stimulation with irradiated autologous EBV-LCL	Retrovirus, retronectin	(88)
	GD2.CAR-VZVST 3rd generation	PBMCs pulsed with overlapping peptide libraries spanning selected VZV antigens	Retrovirus, retronectin	(89)
	CD123.CAR-VST (AdV, CMV or EBV) CD28	Stimulation with autologous peptide-pulsed-DC+CD3/CD28 antibodies 1 µg/ml	Retrovirus, retronectin	(90)
Departments of Hematology and Hemamiddleoietic Cell Transplantation, City of Hope, Duarte, California	CD19.CAR.CD8- MP1.VST (Influenza) 1st generation	Stimulations by irradiated autologous LCL	Electroporation	(91)
	CD19.CAR-CMVST CD28	IFN-γ immunomagnetic selection after pp65 stimulation	Lentivirus (MOI=3), protamine sulfate	(92)
	CD19.CAR-CMVST CD28			(93)
University Children's Hospital Münster, Department of Paediatric Haematology and Oncology, Münster, Germany.	GD2.CAR-EBVST With or without CD28	Stimulation with irradiated autologous EBV-LCL	Retrovirus, retronectin	(94)
	GD2.CAR-VZVST CD19.CAR-VZVST With or without CD28	Stimulation with VZV lysates +irradiated autologous PBMC	Retrovirus, retronectin	(95)
INSERM U590/Equipe Cytokines et Cancer, Centre Léon Bérard, 69373 Lyon Cedex 08, France.	CD33.CAR-EBVST CD28	Stimulation with irradiated autologous EBV-LCL	Retrovirus	(96)

CAR, Chimeric Antigen Receptor; CD, Cluster of differentiation; CMV, Cytomegalovirus; CMVST, Cytomegalovirus Virus Specific T cell; DC, Dendritic Cell; EBV, Epstein-barr virus; EBVST, Epstein-barr Virus Specific T cell; GD2, disialoganglioside; HER2, Human Epidermal Growth Factor Receptor 2; IFNγ, Interferon gamma; IL, Interleukin; LCL, Lymphoblastoid Cell Line; MP-1, influenza A Matrix Protein 1; PBMC, Peripheral Blood Mononuclear Cell; TCR, T cell receptor; VST, Virus Specific T cell; VZV, Varicella Zoster Virus.

TABLE 2 Clinical trials and published results about CAR-VST (clinicaltrial.gov).

Team	Target and conditions	Virus specificity	Cell source	Additional treatment	Status	Phase	References; acronym	Start year
Baylor College of Medicine, Houston, USA	CD19 B-cell malignancies	EBV CMV, EBV, Adv, BKV and HHV-6	Allogeneic Allogeneic	Following allogeneic HSCT	Ongoing Withdrawn	1	NCT00840853; MULTIPRAT (68) NCT03768310; CARMA* NCT unknown (97);	2009 2022*
	CD30 Lymphoma	EBV	Allogeneic Autologous Allogeneic Allogeneic	bank of 7 lines from healthy donors IL7 receptor overexpressed	Recruiting Ongoing Withdrawn Not yet recruiting	1	NCT04288726 (98) NCT01192464 NCT04952584* NCT06176690	2020 2011 2024* 2024
	HER2 solid tumors	EBV ADV	Autologous Autologous	TGF-B resistance Oncolytic viruses	Completed Recruiting	1	NCT00889954; HERCREEM (no results so far) NCT03740256; VISTA	2009 2020
	CD70 B-cell malignancies	EBV	Autologous		Not yet recruiting	1	NCT06345027; CASEY	2024
Baylor College of Medicine, Houston, USA & collaborators	GD2 sarcoma Neuroblastoma	VZV EBV	Autologous Autologous	Vaccine	Ongoing Ongoing	1	NCT01953900; VEGAS NCT00085930; NESTLES (99, 100)	2014 2003
	HER2 Glioblastoma	CMV	Autologous		Completed	1	NCT01109095; HERT-GBM (101)	2010
Children's Mercy Hospital Kansas City and Baylor College of Medicine	GD2 Neuroblastoma	CMV ADV EBV	Allogeneic		Completed	1	NCT01460901; STALLONe	2012
Memorial Sloan Kettering Cancer Center	CD19 B-cell malignancies	EBV	Allogeneic		Ongoing	1	NCT01430390	2011
City of Hope Medical Center, California	CD19 B-cell malignancies	CMV (vaccine) CMV (vaccine)	Autologous Autologous	Vaccine Vaccine	Recruiting Recruiting	1	NCT05432635 NCT05801913	2023 2023
NCI et Fred Hutchinson Cancer Research Center	CD19 B-cell malignancies	CMV EBV	Allogeneic	Following allogeneic HCST	Completed	1/2	NCT01475058 (unpublished data)	2012
University College, London	CD19 B-cell malignancies	EBV (vaccine)	Allogeneic		Unknown	1/2	NCT01195480; CD19TPALL (102)	2012

*withdrawn clinical trials; AdV, Adenovirus; BKV, Bk virus or John Cunningham virus; CMV, Cytomegalovirus; EBV, Epstein-Barr virus; HHV, human herpesvirus; HSCT, Hemamiddleoietic stem cell transplantation; IL, Interleukine; TGF, Transforming growth factor-beta; VZV, Varicella Zona Virus.

10.3389/fimmu.2024.1527648

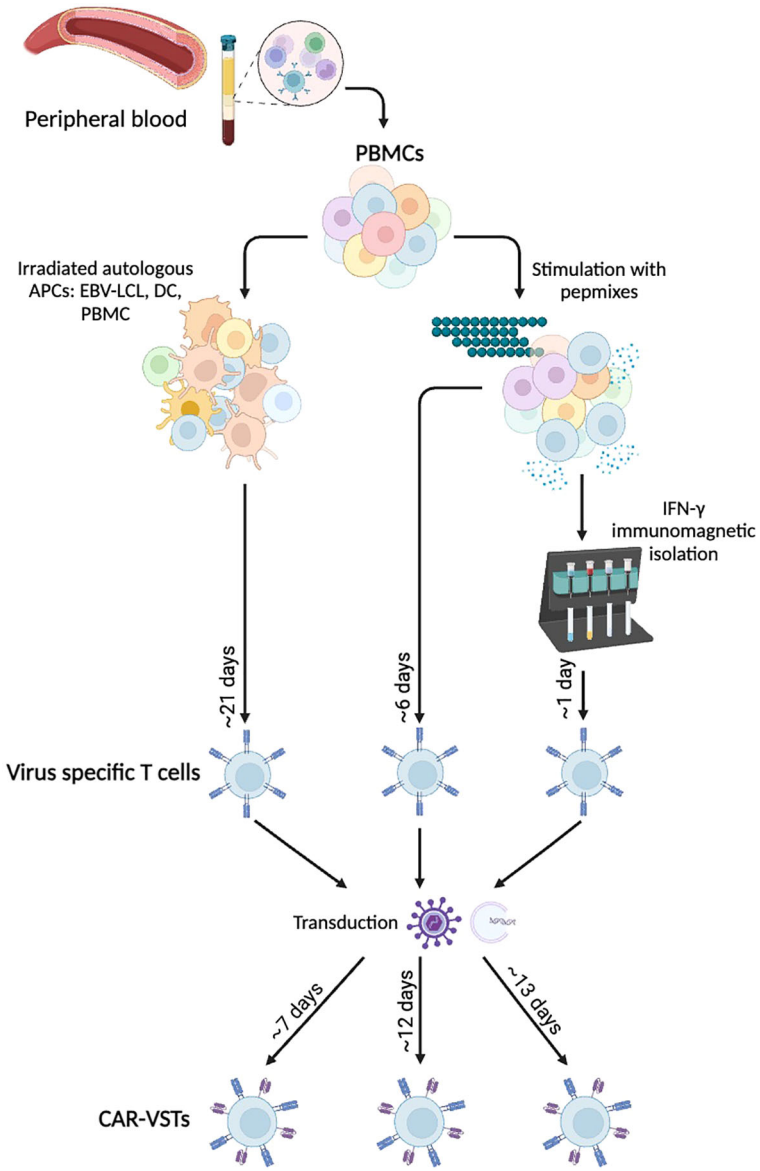

FIGURE 3
Manufacturing methods for *ex vivo* CAR-VST: VSTs are mainly produce either by coculture with Antigen Presenting Cells (APCs) or after peptide pool stimulation with or without immunomagnetic IFN-γ selection. Viral transduction or electroporation are performed to express the CAR transgene, leading to bi-specific CAR-VSTs. APC, Antigen Presenting Cell; CAR, Chimeric Antigen Receptor; DC, Dendritic Cell; EBV, Epstein-barr virus; IFNγ, Interferon gamma; LCL, Lymphoblastoid Cell Line; PBMC, Peripheral Blood Mononuclear Cell; VST, Virus Specific T cell. Created with BioRender.com.

final VST product's characteristics, balancing the trade-offs between efficiency, specificity, and scalability to optimize therapeutic efficacy against viral infections and malignancies.

5.1.2 CAR-VST manufacturing

The diversity in CAR sequences, costimulatory molecules and the inclusion of transgenes for cytokine production contributes to the significant variability in CAR expression levels, the extent of CAR-VST activation and their overall functionality. We will report hereafter the targets and the vectors that have been studied up to now in CAR-VST and will discuss later the different improvements in the construct.

Regarding the targets, both well-established and innovative targets are investigated in CAR-VST studies. The CD19 target was the most widely studied to treat B-cell malignancies (3, 91, 92). Several other targets have been investigated including: (i) the disialoganglioside GD2 in solid tumors, especially in glioblastoma and neuroblastoma (81, 83, 84, 86, 88, 89, 94, 95), (ii) HER-2 an antigen expressed in a range of tumors such as breast cancer, lung cancer and ovarian cancer (85) (iii) CD30, a molecule highly and consistently expressed on malignant Hodgkin Reed-Sternberg cells (82, 87, 96), (iv) the CD33 molecule expressed on acute myeloid leukemia blasts (96), as well as (v) the CD123 molecule (90).

The transduction of VST is often the most critical step of the manufacturing process (Table 3). Retroviral vectors have been widely used because of their ability to integrate transgenes effectively into the host genome. Retronectin-coated-plates are

TABLE 3 CAR-VST manufacturing: transduction strategies.

Team	Cells	Transduction	Transduction efficiency and main results	References
Center for Cell and Gene Therapy, Baylor College of Medicine, Houston, USA.	GD2.CAR-EBVST	Anti-OKT3 anti-CD28 antibodies After the third stimulation of irradiated LCL Retrovirus, retronectin	16.5% CAR expression (N=4)	(81)
	CD30.CAR-VST CD28	After the third stimulation of irradiated LCL Retrovirus, retronectin	26 ± 11% CAR expression (N=8)	(82)
	iCas9.GD2.CAR-CMVST CD28	After the second stimulation of irradiated LCL Retrovirus, retronectin	35-65% CAR expression (N=9)	(83)
	GD2.CAR-EBVST	Early and late transduction Retrovirus, retronectin	Early-and late transduced VSTs was 55 ± 4% and 22 ± 5% respectively (N=6)	(84)
	HER2-EBVST HER2-EBVST.iCD19 CD28	Nucleofection with transposons	47.9 ± 15.5% for HER2.CAR-VST (N=3) 36.4 ± 12.6% for HER2.CAR-VST.iCD19 Long term and stable expression *in vitro* (120 days)	(85)
	GD2.CAR-VST CD19.CAR-VST Either CD28 or 41BB	Retrovirus, retronectin	52-75% CAR expression (N=7)	(86)
	CD30.CAR-EBVST 2nd generation CD28	Retrovirus, retronectin	CD30.CAR expression increased from 40.59% ± 15.76% on day 8, up to 87.25% ± 6.9% at the end of culture (N=3)	(87)
Center for Cell and Gene Therapy, Baylor College of Medicine, Houston, USA + collaborators	GD2.CAR-EBVST GD2.CAR-EBVST.IL7R CD28	Retrovirus, retronectin	64 ± 3% for GD2.CAR (N=5) 34 ± 9% for GD2.CAR.IL7	(88)
	GD2.CAR-VZVST 3rd generation	Retrovirus, retronectin	53.1% ± 7.7% of VZVSTs from naturally infected donors and 44.6% ± 14.8% of VZVSTs from immunized donors (N=3)	(89)
	CD123.CAR-VST (AdV, CMV or EBV) CD28	Retrovirus, retronectin	>30% CAR expression (data not shown)	(90)
Departments of Hematology and Hemamiddleoietic Cell Transplantation, City of Hope, Duarte, California	CD19.CAR.CD8- MP1.VST (Influenza) 1st generation	Electroporation	96% CAR expression (N not specified)	(91)
	CD19.CAR-CMVST CD28	Lentivirus (MOI=3), protamine sulfate	From 8% CAR expression post transduction to 46% after 2 rounds of stimulation (N=3)	(92)
	CD19.CAR-CMVST CD28		27.0 ± 14.2% CAR expression (N=9)	(93)
University Children's Hospital Münster, Department of Paediatric Haematology and Oncology, Münster, Germany.	GD2.CAR-EBVST With or without CD28	Retrovirus, retronectin	21-28% for GD2 (N=3) 26-40% For GD2.CD28	(94)
	GD2.CAR-VZVST CD19.CAR-VZVST With or without CD28	Retrovirus, retronectin	46 ± 14% CAR expression (N=4)	(95)
INSERM U590/Equipe Cytokines et Cancer, Centre Léon Bérard, 69373 Lyon Cedex 08, France.	CD33.CAR-EBVST CD28	Retrovirus	35 ± 4% CAR expression stable for 1month (N=6)	(96)

CAR, Chimeric Antigen Receptor; CD, Cluster of differentiation; CMV, Cytomegalovirus; CMVST, Cytomegalovirus Virus Specific T cell; DC, Dendritic Cell; EBV, Epstein-barr virus; EBVST, Epstein-barr Virus Specific T cell; GD2, disialoganglioside; HER2, Human Epidermal Growth Factor Receptor 2; IFNγ, Interferon gamma; IL, Interleukin; LCL, Lymphoblastoid Cell Line; OKT3, Orthoclone-muromonab-CD3; PBMC, Peripheral Blood Mononuclear Cell; VST, Virus Specific T cell; VZV, Varicella Zoster Virus.

usually employed to enhance virus and cells contacts, with spinoculation utilized to maintain virus adherence and contact. A large range of transduction efficiency is described in the literature, extending from 10.2% in the first studies to 75%. Increased transgene expressions are observed over time in culture, following restimulations (87), or when transduction is performed early (3 days) after the first stimulation of VST generated with coculture method (84). Lentiviral vectors have also been used and they offer the advantage of transducing both dividing and non-dividing cells, enhancing the flexibility and efficiency of CAR-VST manufacturing. Only one team has described results of CAR-VST produced thought a lentiviral transduction, with increased CAR expression from 8% to 46% after 2 rounds of stimulation (N=3) in a first study and 27.0 ± 14.2% CAR (N=9) in their second study (92, 93).

Transposon systems and electroporation have also been employed as virus-free transduction methods. Nakazawa et al. implemented the Piggy bac-transposon system for transducing EBVST, achieving 47.9% ± 15.5% transduction efficiency for HER2-CAR (N=3) (85). Electroporation, thought electric pulses to introduce DNA into cells, offers a rapid and versatile approach for CAR transduction. Cooper et al. also used electroporation to transduce MP1-specific T cells with a CD19.CAR plasmid, achieving 96% CAR expression (N not specified) (91).

In summary, each transduction method has its unique advantages and challenges. Retroviral and lentiviral vectors are highly efficient but can raise safety consideration related to insertional mutagenesis. Moreover, rare T-cell malignancies were reported from autologous marketed CAR-T cells without evidence of the correlation with integration of the CAR transgene (103, 104) or with derived clonal hematopoiesis (105).While transposon systems are of interest as they provide stable gene integration without the theoretical risks associated with viral vectors, it is important to note the potential risks of malignant transformation associated with both virally transduced and transposon-generated CAR T cells (106).

5.1.3 *In vitro* evidence of bi-specific functionality of CAR-VST

The functional activity of CAR-VST is critical for their therapeutic efficacy. This section summarizes the functional assays and outcomes across the previously mentioned studies, focusing on common results and comparable methodologies.

Preclinical studies show that CAR-VST efficiently lyse tumor cells expressing the targeted tumor antigen, underscoring specific MHC-independent killing. This is true across various CAR, including CD30, GD2 and HER2. Specific lysis rates can vary, but highly enhanced killing compared to non-transduced VST or those targeting irrelevant antigens is consistent. For example, Savoldo et al. and Tanaka et al. reported around 50-58% lysis rates at 20:1 E/T ratio against tumor cells expressing the CAR-targeted antigens and against virus infected cells (see below) (82, 89). Thus, CAR-VST exhibited the dual capacity to lyse both types of targets effectively in cytotoxicity assays. Blocking experiments with monoclonal antibodies against the CAR-targeted antigen confirmed the specificity of the CAR-mediated killing (81, 82, 96). In addition, these CAR-VST did not exhibit cytotoxicity against autologous healthy cells or "non infected" cells (82). Several studies reported that CAR-VST maintained their cytotoxic and cytokine-secreting capabilities over extended culture periods. For instance, Savoldo et al., and Landmeier et al., observed stable and potent antitumor activity in long-term co-cultures (45 days), with CAR-modified T cells effectively eliminating tumor cells and proliferating in response to antigen exposure (82, 95). In addition, it was demonstrated that CAR-VST retained the ability to secrete multiple effector molecules, such as IFNγ, granzyme B and TNF-α, upon activation. Studies by Quach et al., Dutour et al., and Landmeier et al., demonstrated that the poly-functionality of these CAR-VST is preserved post-transduction, indicating that CAR expression does not compromise their broader immune functions (87, 95).

CAR-VST also demonstrated effective lysis of virus-APC, comparable to non-transduced VST targeting the same viruses. For instance, EBVST transduced with CAR retained their ability to lyse EBV-infected cells, showing overall comparable efficiency compared to non-transduced VST. For example, in studies by Rossig et al., and Savoldo et al., CAR-VST lysed autologous LCL effectively, maintaining their MHC-restricted killing capacity (81, 82). This dual functionality of CAR-VST was confirmed by their ability to produce IFN-γ either in ELISPOT assays and intracellular cytokine staining and to proliferate either upon stimulation with specific viral peptides or CAR-targeted tumor cells (90, 93). However, this capability was not consistently observed across all studies. Rossig et al. and Savoldo et al. reported that CAR stimulation alone was inadequate to maintain T cell proliferation and expansion (81, 82). Similarly, Landmeier et al. observed that CD19-CAR-VST did not expand after stimulation with a CD19+ cell line (95).

Overall, CAR-modified VSTs exhibit robust dual functionality, effectively targeting both virus-infected and tumor cells through their TCR and CAR engagement, respectively. These cells maintain their cytotoxicity and cytokine production, making them safe and potent agents for adoptive immunotherapy. However, the proliferation of CAR-VSTs appears to be suboptimal after CAR engagement only, suggesting that their expansion may depend on additional factors, like the presence of adequate costimulatory molecules.

5.1.4 *In vivo* evidence of antitumor efficacy of CAR-VST

In vivo evidence of tumor lysis has been assessed in immunocompromised mice models like SCID mice (82, 85) and more recently in NOD SCID mice (96), usually, relying on a FFluc or GFP-FFluc labeled-tumor cell line expressing the antigen of interest. Tumors have been engrafted either intraperitoneally, intra-tumor or intra-venously, with mice receiving CAR-VST or non-transduced VST as a negative control at tumor progression, following the same delivery routes. A study showed that CAR-VST effectively controlled tumor progression for more than two weeks (82) and this protection was further enhanced when they received additional costimulation from autologous EBV-LCL. In contrast, mice receiving control EBVST showed increased tumor growth regardless of costimulation. Similar issues were observed in the other studies. For example mice treated with HER2.CAR-VST

had a significantly longer survival, in a brain tumor model (85). In another study, CAR-VST could also be identified by immunohistochemistry at the tumor site, indicating their ability to localize at the tumor and affect the tumor microenvironment (96). Similarly, Savoldo et al., used VST transduced with the GFP-FFluc vector for *in vivo* tracking and showed that both non-transduced (NT-) and CD30.CAR-EBVST localized at the tumor site by day 7 post-infusion and expanded significantly over the next two weeks. This expansion was confirmed to be antigen-dependent, as the bioluminescence signal was significantly lower in mice with EBV+ HLA-mismatched tumors. Although immunodeficient mice have limitations, such as not allowing the study of VST interactions with other immune cells, they offer strong evidence of the potency and dual potential of these cells when humanized.

5.2 Strategies to improve CAR-VST functions

5.2.1 Role of endogenous TCR signaling

Signaling through the native TCR/CD3 complex is crucial for the robust activation of CAR-VST. The engagement of the TCR with its specific antigenic peptide presented by MHC molecules on APCs provides a strong and physiologically relevant activation signal. This signaling pathway ensures that T cells, including CAR-VST, maintain their antigen specificity and effector functions. Moreover, some studies have demonstrated that activation of CAR-VST through the CAR alone, although promoting effective antitumor activity, does not fully recapitulate proliferation that occurs through the TCR engagement. In the following section, we will summarize these findings, highlighting the differences in signaling outcomes between CAR and TCR activation.

5.2.1.1 Importance of native TCR signaling for CAR-VST proliferation and expansion

Rossig et al., demonstrated that stimulation through the CAR alone was not sufficient to maintain proliferation and expansion of CAR-VST beyond four weeks (81). This proliferative deficit could however be overcome by stimulation with autologous EBV-LCL, highlighting the need for native TCR engagement for sustained CAR-VST activity. Savoldo et al., confirmed that VSTs stopped proliferating and progressively died when restimulation with LCL and IL-2 was halted, ruling out any potential for autonomous growth (82). Landmeier et al., reported that repeated stimulation with VZV lysates resulted in robust proliferation of CAR-VST whereas exposure to tumor target cells failed to induce similar proliferation (95). The requirement for continuous antigen and cytokine stimulations to maintain CAR-VST proliferation further emphasize the importance of the TCR signaling pathway.

5.2.1.2 Impact of native TCR signaling on CAR-VST functionality

Beyond proliferation, different functional improvements were observed secondary to viral triggering. Specifically studies with CAR-VST after TCR engagement have demonstrated: (i) an increased expression of the CAR (85), both in CD4+ and CD8+ populations (84), (ii) an enhanced anti-tumor activity (92, 93), and (iii) a rescue of anti-tumoral dysfunction (89). Specifically, Tanaka et al., showed that VZV pepmix-loaded DCs could restore the antitumor activity of GD2.CAR-VZVSTs rendered dysfunctional by the tumor, suggesting that VZV vaccination could be leveraged to recover the function of CAR-VST cells through TCR stimulation.

In conclusion, the CAR and native TCR cooperate in enhancing the therapeutic potential of CAR-VST by ensuring robust and sustained immune responses. Specifically, the native TCR signaling is essential for the providing survival, proliferation, and expansion of CAR-VST.

5.2.2 Use of costimulatory domains (CD28, 4-1BB)

The native TCR/CD3 complex, upon engagement with its cognate antigen, provides the primary activation signal (Signal 1). However, a second signal (Signal 2) mediated by costimulatory molecules such as CD28 or 4-1BB is required for full activation, and to avoid anergy or apoptosis. Cytokines production (Signal 3) is also crucial to maintain T cell proliferation and survival. Thus, the coordinated sequence of these signaling paths is pivotal for the function of T cells in general and of CAR T cells in particular.

The role played by signal 2 has been clearly demonstrated with VST. EBVST expressing the GD2-CAR (first generation) outperformed CAR T cells lacking costimulatory endodomains, highlighting the critical role of costimulation in enhancing T cells efficacy. With the incorporation of costimulatory endodomains into CARs for T cells becoming standard of practice, second generation CARs have also been used to transduce VST.

Altvater et al., formally compared in EBVST effector memory T cells first and second generation CARs, namely GD2.ζ and GD2.CD28ζ CAR (94) and observed similar dual cytotoxicity and comparable IFN-γ secretion. Interestingly no expansion of CAR-VST in response to antigen-expressing tumor cells was observed.

5.2.2.1 CD28 versus 4-1BB

While the optimal costimulatory signal remains a topic of discussion, the majority of CAR-VST reported to date include a single CD28 co-stimulatory molecule. The report by Omer et al. is currently the only study that compares CD28 and 41BB signals in CAR-VSTs (86). The study evaluated in VZVST and EBVST first and second-generation GD2.CAR containing costimulatory endodomains derived from 4-1BB or CD28. The team found that a GD2.CAR containing both CD28 and CD3ζ chain (GD2.CD28ζ) significantly enhanced the function of CAR-VST compared to GD2.CAR containing 4-1BB and ζ (GD2.4-1BBζ) or ζ alone (GD2.ζ). Specifically, GD2.CD28ζ CAR-VST exhibited higher proliferation and cytokine secretion in response to TCR stimulation, and better expansion when stimulated through the CAR. In contrast, transduction of EBVST and VZVST with GD2.4-1BBζ or GD2.ζ halted their proliferation and function. The frequency of viral antigen-reactive T cells decreased in GD2.ζ and GD2.41BBζ VSTs, indicating T cell dysfunction rather than a loss of antigen-specific T cells. GD2.ζ and GD2.41BBζ VSTs exhibited also higher frequencies

of apoptotic cells and increased Fas expression compared to NT controls and GD2.CD28ζ-transduced VST. Moreover, GD2.4-1BBζ VSTs displayed a marked downregulation of the TCR α/β-chains, associated with a decreased response to viral antigens. This downregulation was paralleled by an increased cell size and a higher CD25 expression, indicating activation. The study found a strong correlation between the expression of activation markers and TCR α/β downregulation. Similarly, CD28 co-stimulation appeared crucial for optimal expansion and function of VST transduced with a different CAR (CD19.CAR).

Regarding the choice of costimulation molecules for effective activation, it should be noted that authorized CAR-T cell therapies mainly use the 4-1BB costimulation domain rather than CD28. 4-1BB, featured in commercial CAR-T products like Kymriah® and Breyanzi®, is known for promoting T cell persistence and a long-term memory phenotype, which is crucial for sustained antitumor activity. Conversely, CD28, used in Yescarta® and Tecartus®, is associated with rapid, potent T cell activation and functional cytotoxicity that leads to immediate tumor reduction but may also result in quicker T cell exhaustion. Even if the choice seems to depend on balancing the need for immediate efficacy versus long-term durability, there is no consensus CD28 or 41BB being the best costimulatory molecule (107, 108). Preclinical studies suggest that CD28-based CARs induce greater cytokine release compared to 4-1BB-based CARs, both domains confer similar antitumor activity in mouse models. Clinically, CAR-T cells with either domain have shown high efficacy in treating relapsed hematological malignancies, with no significant differences in antitumor activity. However, large clinical trials have reported higher rates of neurological toxicities with CD28, likely due to other factors. Further investigations should focus on directly comparing these costimulatory domains while controlling for confounding variables.

5.2.3 Characterization of the final product

5.2.3.1 TCR repertoire

While CAR expression introduces a new antigen specificity to T cells, it does not alter their existing TCR repertoire. Thus, the TCR diversity originally present in the VST is maintained. The engineering process does not promote the expansion of a single clone; rather, it adds a new receptor to an already diverse set of T cells. Maintaining a polyclonal TCR repertoire in CAR-VST is essential for their effectiveness against diverse antigens.

Nakazawa et al., demonstrated that HER2.CAR-VSTs retained a polyclonal TCR repertoire, as shown by GeneScan analyses, which revealed typical polyclonal patterns for TCRβ and TCRγ regions (85). Similarly, Wang et al., showed that neither CMV-specific TCR isolation nor CD19.CAR engineering resulted in clonal expansion, thereby preserving their broad Vβ usage (92, 93). This diverse TCR repertoire ensures that CAR-VSTs can target a wide array of antigens, which is essential for maintaining an effective and versatile immune response.

5.2.3.2 CD4 and CD8 cells

As previously mentioned, VST generated through culture or sorting methods, typically consist in a polyclonal population that includes both CD4+ and CD8+ T cell subsets, which are important for the sustained antitumor and antiviral efficacy of the CAR-VST products. CD8+ T cells serve as the cytotoxic arm, directly eliminating target cells while CD4+ T cells provide essential helper functions, boosting the activation, proliferation, and survival of CD8+ T cells. In this way, authors showed important variations of the CD4+/CD8+ ratio in the final CAR-VST products, probably depending on the viral infection status of the donor. Furthermore, it is worth noting that some studies have demonstrated that a high CD4/CD8 CAR ratio, in autologous CD19 CAR T cell products, is associated with poorer post-CAR T outcomes (109). Interestingly, VST products for CMV and EBV are generally CD8 dominant (110, 111), which aligns with the potential therapeutic benefits of a lower CD4/CD8 ratio, supporting better outcomes in this context.

5.2.3.3 Inducing naive and memory cells

Multiple studies have shown that CAR-VSTs predominantly exhibit effector memory phenotype, which is linked to their capacity for rapid response upon antigen re-exposure (90, 94, 95). As mentioned previously, the methods used for the generation of VST (co-culture or isolation of IFNγ secreting cells) lead to the enrichment in mature T cells. Moreover, the expansion of CAR-VST after transduction, skew their maturation of T cell subsets. A study highlighted the differences in memory potential based on the timing of CAR transduction (84). Early-transduced VST (day 3) had a higher percentage of Tcm (CD62L+ CCR7+), suggesting greater memory potential and better therapeutic efficacy compared to late-transduced VST (day 19), which were more differentiated and potentially less effective in the long term. However, it was also suggested in another study that TCR stimulation promotes a more favorable phenotype for long-term function and persistence. Indeed, CD19.CAR-CMVST, when stimulated through their native TCR with pp65pepmix-loaded autologous PBMCs, exhibited higher expression of genes linked to persistence and memory, such as KLF2, TCF7, and Lef1, compared to CAR stimulation alone (93). Optimized expansion protocols must be developed to promote the growth of less mature subsets.

Two unexplored aspects of CAR-VST optimization deserve attention: modulating the effector-to-memory phenotype and adjusting cellular metabolism to support long-lived memory subsets. Currently, CAR-VST products predominantly exhibit a Tem phenotype, irrespective of the production approach. Investigating the shift of this phenotype toward more immature subsets (Tcm or even Tscm) could enhance therapeutic durability and efficacy. This approach has been little explored except by using IL7-IL15 cytokine-cocktail and only within the context of CAR-T cells (112–114). Additionally, favoring a metabolic profile that promotes oxidative phosphorylation could help maintaining a Tcm or Tscm profile, as it is under investigation for CAR-T cells, potentially supporting sustained persistence and antitumor functionality (115–117). While studies on these approaches are lacking within the CAR-VST framework, they offer promising directions for future research.

5.2.3.4 Exhaustion markers

In addition to an optimal memory phenotype, the expression of exhaustion markers is being evaluated to generate less exhausted cells, for a better long-term survival. Exhaustion markers such as PD-1, LAG-3, and TIM-3 are typically upregulated in T cells that have been exposed to chronic antigen stimulation, leading to a decline in their functional capacity. However, Wang et al., found that CD19.CAR-CMVST cells did not display elevated levels of exhaustion markers following TCR stimulation (93). Similarly, Landmeier et al., observed that expanded VZVST maintain a robust memory phenotype (95), further supporting the potentials of CAR-VST for prolonged therapeutic applications.

5.2.4 Suicide gene as a safety system

In efforts to manage the safety of allogeneic CAR-VST therapies and control unforeseen toxicities, several approaches to control and eliminate these cells have been tested. Two notable strategies include the use of the inducible caspase-9 (iCasp9) suicide gene and cetuximab-mediated antibody-dependent cellular cytotoxicity (ADCC).

The first strategy allows for the selective induction of apoptosis of transduced cells upon administration of a small molecule dimerizer, effectively eliminating the CAR-VST in the event of severe toxicity or off-target effects. Caruana et al., demonstrated the incorporation of the iCasp9 suicide gene in CAR-VST (83). The second strategy take advantage of expressing a truncated version of the epidermal growth factor receptor (EGFRt) for cells to be targeted and eliminated by cetuximab, a monoclonal antibody that induces ADCC. However, studies suggest that the truncated EGFR system may have limited efficiency as a safety switch in the context of neutropenia (118). Furthermore, alternative systems, such as those based on CD20 mimotopes, have also been explored as potential elimination markers, offering additional safety mechanisms (119, 120). Wang et al., explored the use of cetuximab-mediated ADCC as a safety mechanism for CAR-VST (93).

5.2.5 Vaccination

An added feature of CAR expressed on VST is the possibility to leverage on the naïve TCR for prolonged persistence. Restimulating CAR-VST with the appropriate vaccine represents a promising approach to control persistence and functionality of CAR-VST. Several groups have studied this synergy. By using home-made (i.e. influenza virus) or existing vaccines (CMV or VZV vaccines) to stimulate the native TCR, several teams showed continuous activation and expansion of CAR-VST, maintaining their expansion and effector functions while preventing exhaustion. Indeed, Wang et al. reported significant increase in the frequency of human T cells and CAR+ CMVpp65-tetramer+ bispecific T cells in vaccinated mice compared to controls (92). For instance, human T cells in pp65-challenged mice reached 5.6% ± 2.6%, compared to only 0.3% ± 0.1% in controls. These bispecific T cells were also more abundant in the spleen, indicating a potential homing property. Landmeier reported that CAR-VZVST re-expanded after re-exposure to booster doses of a VZV vaccine (95). Moreover, vaccine could sustain antitumor effects in a relapsed tumor model, indicating that the vaccine could maintain the efficacy even after initial tumor progression (92) and could lead to a higher rate of complete tumor clearance with improved survival outcomes of mice compared to the one treated with CAR-VST alone (91). Similarly, in the CMV-vaccine murine model of Caruana, 47% of mice were tumor-free in the vaccinated group, compared to only 12% in the control group (83). However, one study also highlighted a potential risk of cytokine release syndrome (CRS), evidenced by significantly elevated levels of human-specific IFN-γ and IL-6 in the serum of mice (92). In this study, Caruana et al., explored another way to enhance expansion and proliferation of CAR-VST. They investigated the role of CD40L and OX40L, ligands of 2 molecules, CD40 and OX40, expressed on activated T cells and implicated in the immunological synapse to boost APCs. They transduced K562 cells with lentiviral vectors encoding either human CD40L or OX40L or pp65/eGFP or the combination CD40L/pp65 and OX40L/pp65. They generated GD2.CAR-CMVST with CD28 co-stimulation molecule. They observed cooperation between CD40L, OX40L and pp65 antigen presentation, significantly enhancing the activation and antitumor responses of the CAR-VSTs *in vivo* (n=8) in a murine model of xenogenic tumor, thanks to the induction of APC maturation upon antigen processing.

5.2.6 Immunogenicity et alloreactivity

The limited alloreactive repertoire of VST is the base for CAR-VST to provide effective antitumor activity without inducing severe GvHD, even when derived from partially HLA-matched donors (6, 71, 72).

However, in an allogeneic context, CAR-VST remain targetable by the recipient cells, undermining the long-term persistence and thus efficacy of an infused product. A recent *in vitro* study has proposed an original strategy to prevent recipient T cell-mediated killing of CAR-VST (87). Because CD30, in addition to its expression by tumors cells in Hodgkin lymphoma, anaplastic large cell lymphoma and human T cell leukemia virus type 1 + T cell lymphoma, is an activation marker highly upregulated by alloreactive T cells its targeting through a CAR could promote an anti-tumoral effect while at the same time eliminate recipient alloreactive T cells. CD30.CAR-EBVST have been tested in a Mixed Lymphocyte Reaction (MLR) co-cultured with allogeneic PBMC or primed alloreactive T cells (p-ART) to simulate an alloreactive immune response. Non-transduced (NT) EBVST and CD30.CAR-EBVST were eliminated while CD30.CAR-EBVST persisted, expanded and prevented p-ART expansion.

6 Clinical translation of CAR-VST

The following section evaluates the feasibility, safety profile and efficacy of CAR-VST in clinical settings.

6.1 Feasibility

Clinical trials have demonstrated the feasibility of manufacturing CAR-VST products at clinical scale level. For

instance, in the MULTIPRAT clinical trial (NCT00840853) HLA compatible CAR-VST were generated in a GMP compliant grade from an allo-SCT donor and infused into patients with relapsed B-cell malignancies post-allo-SCT (N=8) (68). This first clinical trial ensured safety and reproducibility of the generation of CAR-VST for clinical applications.

In the study by Quach et al., a bank of seven CD30.CAR EBVST lines was successfully generated (66). Further research by Sun et al., optimized the production process by incorporating early transduction techniques (84). This optimization process ensured that a higher proportion of T cells maintained central memory phenotypes, crucial for long-term persistence and efficacy. This Good Manufacturing Practice manufacturing process is currently applied for two clinical trials (NCT00840853/MULTIPRAT and NCT01460901/STALLONe). The HERT-GBM trial also showed successful manufacturing of 16 products for all the treated patients.

Overall, studies showed that manufacturing process successfully generated CAR-VST that met all release criteria, including viability, transduction efficiency and sterility. However, the scalability of the CAR-VST manufacturing process remain a significant challenge, as current clinical trials have only been conducted with small cohorts of patients. Expanding production to treat larger patient populations will require overcoming substantial logistical and technical hurdles. Advances in cell therapy manufacturing, such as automated culture systems and standardized protocols, may mitigate these challenges.

6.2 Safety of CAR-VST

The safety of CAR-VST has been a central focus in clinical research, with early-phase trials such as NCT00840853 showing a favorable safety profile for donor-derived CD19.CAR-VST, with no reported infusion-related toxicities or cases of GvHD. The CAR-VSTs persisted in patients for a median of 8 weeks in the blood and up to 9 weeks at disease sites, all without inducing significant adverse events (68). In the trial NCT04288726, which investigated CD30.CAR-EBVST, the safety of allogeneic CAR-VSTs was further confirmed in 14 patients. The study observed minimal severe adverse effects, with only a few instances of reversible grade 4 cytopenia and mild CRS, which resolved without intervention. Importantly, no cases of GvHD were reported, even in patients who received multiple infusions, including those with HLA mismatches products (66). The absence of GvHD maybe attributed to the fact that alloreactive recipient T cells would upregulate the CD30 molecule, which would be also targeted by the CAR. Consequently, no immediate rejection of CAR-VST by recipient T cells was observed even after multiple infusions.

Overall, CAR-VST therapies have demonstrated a consistently favorable safety profile with minimal severe toxicities. Most of the trials reported no infusion-related toxicities, with manageable adverse effects resolving without treatment. A significant advantage of CAR-VST is their reduced risk of GvHD, as these VST are less likely to cause off-target effects. This safety profile makes CAR-VST a potentially safer alternative to conventional CAR-T, especially in allogeneic settings.

6.3 Efficacy of CAR-VST

The efficacy of CAR-VST has been investigated as secondary endpoint of few clinical trials. In the NCT00840853 reported by Cruz et al., efficacy of donor-derived CD19.CAR-VST in the treatment of B-cell malignancies that have relapsed post-allo-SCT (68). This Phase 1 study involved eight patients treated with escalating-doses of allogeneic CAR-VST infused 3 months to 13 years post-HSCT. Objective antitumor effects were observed in 2 out of 6 patients with active disease, and 2 additional patients remained disease-free after receiving the therapy while in remission. One patient relapsed after 4 months and a second developed a Richter syndrome after 8 weeks. The CD19.CAR-VST demonstrated a modest persistence of 8 weeks in the blood and transgene was detectable until 12 weeks. In cases of viral reactivation, CAR-VST expanded, highlighting the role of natural infection/virus reactivation as potential mechanism to boost CAR-T cell numbers *in vivo*. No expansion of CAR-VST was observed with AdV positive viremia for one patient. In this study, viral reactivation was less frequently observed because of the cell infusion occurring, for some patients, long after allo-SCT. In the study of Lapteva et al., the role of TCR stimulation in enhancing the expansion and function of single-dose CD19.CAR-VST was specifically investigated, particularly in the absence of prior cytoreductive chemotherapy, in patients in remission of B-cell ALL with no evidence of minimal residual disease (97). In absence of viral reactivation (N=5), CAR-VST did not expand. In contrast, in patients who experienced viral reactivation (N=3), there was an outstanding expansion of CAR-VST up to 30,000-fold. Interestingly, only EBV reactivated. This led to effective depletion of CD19+ B cells and suggests that viral reactivation plays the role of a potent trigger for CAR-T cell expansion, avoiding the need for cytoreductive chemotherapy in some cases and even in absence of MRD. Five out of 8 patients remained in remission 42 to 60 months post-treatment, with EBVST still detectable. A similar observation was reported by Rossig et al. in the CD19TPALL trial (NCT01195480) (102). The aim of this multi-center phase I/II study was to determine if EBV-directed vaccination could improve the persistence and efficacy of CD19.CAR-EBVST in pediatric ALL with molecular relapse post first allo-SCT, or prophylactically post-second allo-SCT. Overall, at one-month post-infusion, 5 out of 11 treated patients achieved CR, with 1 *de novo* CR and 4 in CR for a 12-months follow up. One patient achieved PR, demonstrating some degree of antitumor activity. Three patients maintained a stable disease (SD) for 8 weeks to 29 months while 3 patients showed no response to the treatment, highlighting variability in therapeutic efficacy. However, at a median follow-up of 12 months, 10 out of 11 patients relapsed, with three patients remaining alive (two with disease and one in CR for three years). Median persistence of CD19.CAR-EBVST was improved significantly with vaccination directed with EBV antigens: 0 day (range: 0-28) without vaccination compared to 56 days (range: 0-221) with vaccination (P=0.06).

As mentioned before, other targets than CD19 were also investigated in early phase clinical trial. Quach reported a trial studying CD30.CAR-EBVSTs in patients with CD30+ lymphomas. Fourteen patients with r/r Hodgkin's lymphoma were treated using escalating doses of CD30.CAR-EBVSTs. Thirteen patients among

fourteen were evaluable for responses. The overall response rate was 69.2%, with 5/10 patients achieving CR and 4 patients achieving PR. The efficacy appeared dose-dependent, with higher response rates observed at higher dose levels. This suggests that the therapeutic potential of these CAR-VSTs may be optimized by adjusting the dosing regimen (98). The durability of responses varied, with some patients achieving long-term remission. For instance, patient 10, who had bulky disease, responded to three separate infusions from the same donor line, indicating that repeated administrations can maintain or enhance therapeutic efficacy. The study proposed several explanations for the rapid disappearance of circulating cells, including elimination by alloreactive T cells, short-life cells or residency at the tumor sites.

As a summary, the clinical trials conducted on CAR-VST therapies have demonstrated both the feasibility and safety of this approach in treating various malignancies. These studies highlighted that CAR-VSTs can be successfully manufactured in early-phases to meet clinical-grade standards. Safety was attested by few adverse events of low grade and absence of GvHD. However, the efficacy of CAR-VST therapies has shown variability across different trials and patient populations. While some patients have achieved complete remission and long-term survival, others have experienced disease progression or relapse, indicating that the current efficacy of CAR-VST therapies is not uniform. Factors such as the persistence of CAR-VSTs in the blood, their expansion in response to viral reactivation, and their residency at tumor sites are critical to achieve sustained antitumor activity. Long-term efficacy was associated in some trials with the potential of combining TCR and CAR stimulation to enhance the durability of CAR-T cell responses, and the importance of concomitant TCR stimulated by viral antigens. The reported studies suggest that enhancing the durability and expansion of CAR-VSTs, particularly through strategies like viral reactivation or vaccination, could improve therapeutic outcomes.

Moving forward, optimizing the manufacturing process to ensure a higher proportion of Tcm, exploring vaccination strategies that enhance CAR-VST persistence and define dose regimens are key areas that could improve the efficacy of CAR-VST therapies. Additionally, expanding these trials to larger cohorts will be essential to fully understand the therapeutic potential and to refine the approach for broader clinical application.

7 Conclusion and perspectives

In recent years, VSTs have emerged as a promising platform for CAR-T cell therapy, following a period of reduced interest in the field. This resurgence is largely driven by the evolution of understanding of VST biology and the development of more refined techniques for their genetic modification and expansion. The use of CAR-VSTs offers a unique advantage due to the inherent antiviral properties of VSTs, which may enhance the persistence and functionality of the engineered T cells in a therapeutic setting. Although we reported academic experiences of CAR-VSTs, pharmaceutical companies are also developing their own program with CAR-VSTs. Indeed, Atara Biotherapeutics, under the guidance of Pierre Fabre, has been at the forefront of developing EBVSTs for treating EBV-associated malignancies. Their product, Ebvallo® (tabelecleucel), approved by EMA is the first allogeneic T-cell immunotherapy for EBV-positive post-transplant lymphoproliferative disease (EBV+ PTLD). This disease commonly affects transplanted patients who receive immunosuppressive drugs to prevent graft rejection or GvHD. Ebvallo® is used as a monotherapy for this rare lymphoproliferative disease, involving stored EBVSTs generated from immunized healthy donors. The therapy has an orphan drug status in Europe. According to recent studies, tabelecleucel has shown a clinical benefit in patients with r/r EBV+ PTLD, a population with few treatment options, while maintaining a favorable safety profile (121–123). Atara Biotherapeutics is currently developing an allogeneic CAR-EBVST incorporating CD28 and an additional costimulatory molecule. Future clinical investigations will give some insight about the long-term efficacy and safety of this promising therapy.

Despite these advances, the application of CAR-VSTs in an allogeneic setting presents significant challenges, particularly the risk of rejection. While CAR-VSTs have shown promise in a directed allogeneic context—where donor cells are partially matched to minimize immune incompatibility—*off-the-shelf* allogeneic CAR-VSTs face substantial hurdles due to the risk of rejection. To mitigate these risks, strategies such as targeting CD30, which is expressed on both tumor cells and activated immune cells, including alloreactive T cells, have been explored. This dual-targeting approach could potentially reduce the risk of rejection while maintaining antitumor efficacy. Another avenue being investigated is the genetic deletion of HLA molecules to make universal CAR-VSTs that are less likely to be rejected by the host immune system. Several studies have highlighted the feasibility of this approach, demonstrating that CAR-T cells with deleted HLA molecules can evade alloreactive immune responses, though this strategy is still in the early stages of development (4, 124).

In conclusion, CAR-VSTs are gaining renewed interest as a promising *off-the-shelf* immunotherapy option, primarily due to their ability to avoid GvHD and their potential for long-term persistence through viral restimulation. While these features make these cells particularly attractive, the challenge of rejection in HLA-incompatible settings remains a significant hurdle. Future research will need to focus on overcoming this barrier, potentially through innovative strategies like HLA deletion, to fully harness the therapeutic potential of CAR-VSTs in allogeneic contexts.

Author contributions

VW: Conceptualization, Data curation, Funding acquisition, Investigation, Writing – original draft, Writing – review & editing. BS: Validation, Writing – review & editing. J-AG: Data curation, Investigation, Visualization, Writing – original draft. GD: Validation, Writing – review & editing. LR: Investigation, Validation, Writing – review & editing. DB: Validation, Writing – review & editing, Conceptualization, Funding acquisition, Investigation, Project administration, Resources, Supervision, Writing – original draft.

Funding

The author(s) declare financial support was received for the research, authorship, and/or publication of this article. This work was supported by Laurette Fugain (Grant N°2019-12) for funding the materials used in this work and the French-American Fulbright Commission for providing a fellowship at the University of North Carolina (USA).

Conflict of interest

The authors declare that the research was conducted in the absence of any commercial or financial relationships that could be construed as a potential conflict of interest.

Generative AI statement

The author(s) declare that no Generative AI was used in the creation of this manuscript.

Publisher's note

All claims expressed in this article are solely those of the authors and do not necessarily represent those of their affiliated organizations, or those of the publisher, the editors and the reviewers. Any product that may be evaluated in this article, or claim that may be made by its manufacturer, is not guaranteed or endorsed by the publisher.

References

1. Schuster SJ, Bishop MR, Tam CS, Waller EK, Borchmann P, McGuirk JP, et al. Tisagenlecleucel in adult relapsed or refractory diffuse large B-cell lymphoma. *N Engl J Med*. (2019) 380:45–56. doi: 10.1056/NEJMoa1804980

2. Neelapu SS, Locke FL, Bartlett NL, Lekakis LJ, Miklos DB, Jacobson CA, et al. Axicabtagene ciloleucel CAR T-cell therapy in refractory large B-cell lymphoma. *N Engl J Med*. (2017) 377:2531–44. doi: 10.1056/NEJMoa1707447

3. Wang X, Diamond DJ, Forman SJ, Nakamura R. Development of CMV-CD19 bi-specific CAR T cells with post-infusion *in vivo* boost using an anti-CMV vaccine. *Int J Hematol*. (2021) 114:544–53. doi: 10.1007/s12185-021-03215-6

4. Depil S, Duchateau P, Grupp SA, Mufti G, Poirot L. [amp]]lsquo;Off-the-shelf' allogeneic CAR T cells: development and challenges. *Nat Rev Drug Discovery*. (2020) 19:185–99. doi: 10.1038/s41573-019-0051-2

5. Qian C, Campidelli A, Wang Y, Cai H, Venard V, Jeulin H, et al. Curative or pre-emptive adenovirus-specific T cell transfer from matched unrelated or third party haploidentical donors after HSCT, including UCB transplantations: a successful phase I/II multicenter clinical trial. *J Hematol Oncol*. (2017) 10:102. doi: 10.1186/s13045-017-0469-0

6. Leroyer EH, Petitpain N, Morisset S, Neven B, Castelle M, Winter S, et al. On behalf of the SFGM-TC: Real-life use of third-party virus-specific T-cell transfer in immunocompromised transplanted patients. *HemaSphere*. (2024) 8:e40. doi: 10.1002/hem3.v8.1

7. Alcazer V, Depil S. Développement des CAR-T allogéniques. *Bull du Cancer*. (2021) 108:S73–80. doi: 10.1016/j.bulcan.2021.01.025

8. Lanza R, Russell DW, Nagy A. Engineering universal cells that evade immune detection. *Nat Rev Immunol*. (2019) 19:723–33. doi: 10.1038/s41577-019-0200-1

9. Poirot L, Philip B, Schiffer-Mannioui C, Le Clerre D, Chion-Sotinel I, Derniame S, et al. Multiplex genome-edited T-cell manufacturing platform for "Off-the-shelf" Adoptive T-cell immunotherapies. *Cancer Res*. (2015) 75:3853–64. doi: 10.1158/0008-5472.CAN-14-3321

10. Valton J, Guyot V, Marechal A, Filhol JM, Juillerat A, Duclert A, et al. A multidrug-resistant engineered CAR T cell for allogeneic combination immunotherapy. *Mol Ther*. (2015) 23:1507–18. doi: 10.1038/mt.2015.104

11. Chen X, Tan B, Xing H, Zhao X, Ping Y, Zhang Z, et al. Allogeneic CAR-T cells with of HLA-A/B and TRAC disruption exhibit promising antitumor capacity against B cell Malignancies. *Cancer Immunol Immunother*. (2024) 73:13. doi: 10.1007/s00262-023-03586-1

12. Moretta L, Bottino C, Cantoni C, Mingari MC, Moretta A. Human natural killer cell function and receptors. *Curr Opin Pharmacol*. (2001) 1:387–91. doi: 10.1016/S1471-4892(01)00067-4

13. Huisman W, Leboux DAT, van der Maarel LE, Hageman L, Amsen D, Falkenburg JHF, et al. Magnitude of off-target allo-HLA reactivity by third-party donor-derived virus-specific T cells is dictated by HLA-restriction. *Front Immunol*. (2021) 12:630440. doi: 10.3389/fimmu.2021.630440

14. Liu L, Wang L, Zhao L, He C, Wang G. The role of HLA-G in tumor escape: manipulating the phenotype and function of immune cells. *Front Oncol*. (2020) 10:597468. doi: 10.3389/fonc.2020.597468

15. Brudno JN, Somerville RPT, Shi V, Rose JJ, Halverson DC, Fowler DH, et al. Allogeneic T cells that express an anti-CD19 chimeric antigen receptor induce remissions of B-cell Malignancies that progress after allogeneic hematopoietic stem-cell transplantation without causing graft-versus-host disease. *J Clin Oncol*. (2016) 34:1112–21. doi: 10.1200/JCO.2015.64.5929

16. Torikai H, Reik A, Liu PQ, Zhou Y, Zhang L, Maiti S, et al. A foundation for universal T-cell based immunotherapy: T cells engineered to express a CD19-specific chimeric-antigen-receptor and eliminate expression of endogenous TCR. *Blood*. (2012) 119:5697–705. doi: 10.1182/blood-2012-01-405365

17. Tipanee J, Samara-Kuko E, Gevaert T, Chuah MK, VandenDriessche T. Universal allogeneic CAR T cells engineered with Sleeping Beauty transposons and CRISPR-CAS9 for cancer immunotherapy. *Mol Ther*. (2022) 30:3155–75. doi: 10.1016/j.ymthe.2022.06.006

18. MacLeod DT, Antony J, Martin AJ, Moser RJ, Hekele A, Wetzel KJ, et al. Integration of a CD19 CAR into the TCR alpha chain locus streamlines production of allogeneic gene-edited CAR T cells. *Mol Ther*. (2017) 25:949–61. doi: 10.1016/j.ymthe.2017.02.005

19. Qasim W. Allogeneic CAR T cell therapies for leukemia. *Am J Hematology*. (2019) 94:S50–4. doi: 10.1002/ajh.v94.S1

20. Heipertz EL, Zynda ER, Stav-Noraas TE, Hungler AD, Boucher SE, Kaur N, et al. Current perspectives on "Off-the-shelf" Allogeneic NK and CAR-NK cell therapies. *Front Immunol*. (2021) 12. doi: 10.3389/fimmu.2021.732135

21. Fauriat C, Long EO, Ljunggren HG, Bryceson YT. Regulation of human NK-cell cytokine and chemokine production by target cell recognition. *Blood*. (2010) 115:2167–76. doi: 10.1182/blood-2009-08-238469

22. Ferry GM, Agbuduwe C, Forrester M, Dunlop S, Chester K, Fisher J, et al. A simple and robust single-step method for CAR-Vδ1 γδT cell expansion and transduction for cancer immunotherapy. *Front Immunol*. (2022) 13:863155. doi: 10.3389/fimmu.2022.863155

23. Rozenbaum M, Meir A, Aharony Y, Itzhaki O, Schachter J, Bank I, et al. Gamma-delta CAR-T cells show CAR-directed and independent activity against leukemia. *Front Immunol*. (2020) 11:1347. doi: 10.3389/fimmu.2020.01347

24. Makkouk A, Yang X, Barca T, Lucas A, Turkoz M, Wong JTS, et al. Off-the-shelf Vδ1 gamma delta T cells engineered with glypican-3 (GPC-3)-specific chimeric antigen receptor (CAR) and soluble IL-15 display robust antitumor efficacy against hepatocellular carcinoma. *J Immunother Cancer*. (2021) 9:e003441. doi: 10.1136/jitc-2021-003441

25. Li YR, Zhou K, Wilson M, Kramer A, Zhu Y, Dawson N, et al. Mucosal-associated invariant T cells for cancer immunotherapy. *Mol Ther*. (2023) 31:631–46. doi: 10.1016/j.ymthe.2022.11.019

26. Bohineust A, Tourret M, Derivry L, Caillat-Zucman S. Mucosal-associated invariant T (MAIT) cells, a new source of universal immune cells for chimeric antigen receptor (CAR)-cell therapy. *Bull du Cancer*. (2021) 108:S92–5. doi: 10.1016/j.bulcan.2021.07.003

27. Dogan M, Karhan E, Kozhaya L, Placek L, Chen X, Yigit M, et al. Engineering human MAIT cells with chimeric antigen receptors for cancer immunotherapy. *J Immunol*. (2022) 209:1523–31. doi: 10.4049/jimmunol.2100856

28. Chen B, Lee JB, Kang H, Minden MD, Zhang L. Targeting chemotherapy-resistant leukemia by combining DNT cellular therapy with conventional chemotherapy. *J Exp Clin Cancer Res*. (2018) 37:88. doi: 10.1186/s13046-018-0756-9

29. Chen X, Wang D, Zhu X. Application of double-negative T cells in haematological Malignancies: recent progress and future directions. *biomark Res*. (2022) 10:11. doi: 10.1186/s40364-022-00360-w

30. Xiao X, Liu H, Qiu X, Chen P, Li X, Wang D, et al. CD19-CAR-DNT cells (RJMty19) in patients with relapsed or refractory large B-cell lymphoma: a phase 1, first-in-human study. *eClinicalMedicine*. (2024) 70:102516. doi: 10.1016/j.eclinm.2024.102516

31. Yang Y, Jacoby E, Fry TJ. Challenges and opportunities of allogeneic donor-derived CAR T cells. *Curr Opin Hematol*. (2015) 22:509–15. doi: 10.1097/MOH.0000000000000181

32. Biondi M, Tettamanti S, Galimberti S, Cerina B, Tomasoni C, Piazza R, et al. Selective homing of CAR-CIK cells to the bone marrow niche enhances control of the acute myeloid leukemia burden. *Blood*. (2023) 141:2587–98. doi: 10.1182/blood.2022018330

33. Leuci V, Donini C, Grignani G, Rotolo R, Mesiano G, Fiorino E, et al. CSPG4-specific CAR.CIK lymphocytes as a novel therapy for the treatment of multiple soft-tissue sarcoma histotypes. *Clin Cancer Res*. (2020) 26:6321–34. doi: 10.1158/1078-0432.CCR-20-0357

34. Rotolo A, Caputo VS, Holubova M, Baxan N, Dubois O, Chaudhry MS, et al. Enhanced anti-lymphoma activity of CAR19-iNKT cells underpinned by dual CD19 and CD1d targeting. *Cancer Cell*. (2018) 34:596–610. doi: 10.1016/j.ccell.2018.08.017

35. Leveson-Gower DB, Olson JA, Sega EI, Luong RH, Baker J, Zeiser R, et al. Low doses of natural killer T cells provide protection from acute graft-versus-host disease via an IL-4–dependent mechanism. *Blood*. (2011) 117:3220–9. doi: 10.1182/blood-2010-08-303008

36. Landoni E, Woodcock MG, Barragan G, Casirati G, Cinella V, Stucchi S, et al. IL-12 reprograms CAR-expressing natural killer T cells to long-lived Th1-polarized cells with potent antitumor activity. *Nat Commun*. (2024) 15:89. doi: 10.1038/s41467-023-44310-y

37. Heczey A, Liu D, Tian G, Courtney AN, Wei J, Marinova E, et al. Invariant NKT cells with chimeric antigen receptor provide a novel platform for safe and effective cancer immunotherapy. *Blood*. (2014) 124:2824–33. doi: 10.1182/blood-2013-11-541235

38. Ueda T, Kaneko S. *In vitro* differentiation of T cell: from CAR-modified T-iPSC. In: Kaneko S, editor. In vitro *differentiation of T-cells: methods and protocols*. Springer, New York, NY (2019). p. 85–91. doi: 10.1007/978-1-4939-9728-2_10

39. Zhou Y, Li M, Zhou K, Brown J, Tsao T, Cen X, et al. Engineering induced pluripotent stem cells for cancer immunotherapy. *Cancers (Basel)*. (2022) 14:2266. doi: 10.3390/cancers14092266

40. van der Stegen SJC, Lindenbergh PL, Petrovic RM, Xie H, Diop MP, Alexeeva V, et al. Generation of T-cell-receptor-negative CD8αβ-positive CAR T cells from T cell-derived induced pluripotent stem cells. *Nat BioMed Eng*. (2022) 6:1284–97. doi: 10.1038/s41551-022-00915-0

41. Lonez C, Breman E. Allogeneic CAR-T therapy technologies: has the promise been met? *Cells*. (2024) 13:146. doi: 10.3390/cells13020146

42. Smirnov S, Petukhov A, Levchuk K, Kulemzin S, Staliarova A, Lepik K, et al. Strategies to circumvent the side-effects of immunotherapy using allogeneic CAR-T cells and boost its efficacy: results of recent clinical trials. *Front Immunol*. (2021) 12:780145. doi: 10.3389/fimmu.2021.780145

43. Moradi V, Omidkhoda A, Ahmadbeigi N. The paths and challenges of "off-the-shelf" CAR-T cell therapy: An overview of clinical trials. *Biomedicine Pharmacotherapy*. (2023) 169:115888. doi: 10.1016/j.biopha.2023.115888

44. Lv Z, Luo F, Chu Y. Strategies for overcoming bottlenecks in allogeneic CAR-T cell therapy. *Front Immunol*. (2023) 14:1199145. doi: 10.3389/fimmu.2023.1199145

45. Benjamin R, Jain N, Maus MV, Boissel N, Graham C, Jozwik A, et al. UCART19, a first-in-class allogeneic anti-CD19 chimeric antigen receptor T-cell therapy for adults with relapsed or refractory B-cell acute lymphoblastic leukaemia (CALM): a phase 1, dose-escalation trial. *Lancet Haematology*. (2022) 9:e833–43. doi: 10.1016/S2352-3026(22)00245-9

46. Neelapu SS, Nath R, Munoz J, Tees M, Miklos DB, Frank MJ, et al. ALPHA study: ALLO-501 produced deep and durable responses in patients with relapsed/refractory non-hodgkin's lymphoma comparable to autologous CAR T. *Blood*. (2021) 138:3878. doi: 10.1182/blood-2021-146038

47. Boissel N, Chevallier P, Curran K, Schiller G, Liu H, Larson R, et al. P1408: UPDATED RESULTS OF THE PHASE I BALLI-01 TRIAL OF UCART22, AN ANTI-CD22 ALLOGENEIC CAR-T CELL PRODUCT, IN PATIENTS WITH RELAPSED OR REFRACTORY (R/R) CD22+ B-CELL ACUTE LYMPHOBLASTIC LEUKEMIA (B-ALL). *Hemasphere*. (2023) 7:e323373f. doi: 10.1097/01.HS9.0000972520.32337.3f

48. Sallman DA, DeAngelo DJ, Pemmaraju N, Dinner S, Gill S, Olin RL, et al. Ameli-01: A phase I trial of UCART123v1.2, an anti-CD123 allogeneic CAR-T cell product, in adult patients with relapsed or refractory (R/R) CD123+ Acute myeloid leukemia (AML). *Blood*. (2022) 140:2371–3. doi: 10.1182/blood-2022-169928

49. Mailankody S, Matous JV, Chhabra S, Liedtke M, Sidana S, Oluwole OO, et al. Allogeneic BCMA-targeting CAR T cells in relapsed/refractory multiple myeloma: phase 1 UNIVERSAL trial interim results. *Nat Med*. (2023) 29:422–9. doi: 10.1038/s41591-022-02182-7

50. McGuirk JP, Tam CS, Kröger N, Riedell PA, Murthy HS, Ho PJ, et al. CTX110 allogeneic CRISPR-cas9-engineered CAR T cells in patients (Pts) with relapsed or refractory (R/R) large B-cell lymphoma (LBCL): results from the phase 1 dose escalation carbon study. *Blood*. (2022) 140:10303–6. doi: 10.1182/blood-2022-166432

51. Mehta A, Farooq U, Chen A, McGuirk JP, Ly T, Wong L, et al. Interim phase I clinical data of FT819-101, a study of the first-ever, off-the-shelf, iPSC-derived TCR-less CD19 CAR T-cell therapy for patients with relapsed/refractory B-cell Malignancies. *Blood*. (2022) 140:4577–8. doi: 10.1182/blood-2022-167194

52. Prenen H, Dekervel J, Hendlisz A, Anguille S, Awada A, Cerf E, et al. Updated data from alloSHRINK phase I first-in-human study evaluating CYAD-101, an innovative non-gene edited allogeneic CAR-T in mCRC. *JCO*. (2021) 39:74–4. doi: 10.1200/JCO.2021.39.3_suppl.74

53. Lonez C, Bolsee J, Huberty F, Nguyen T, Jacques-Hespel C, Demoulin B, et al. 285 Proof-of-concept of a non-gene editing technology using shRNA down-regulation to engineer and optimize CAR T-cell functionality. *J Imm Ther Cancer*. (2023) 11. doi: 10.1136/jitc-2023-SITC2023.0285

54. Iyer SP, Sica RA, Ho PJ, Hu B, Zain J, Prica A, et al. S262: the cobalt-lym study of ctx130: a phase 1 dose escalation study of cd70-targeted allogeneic crispr-cas9–engineered car t cells in patients with relapsed/refractory (r/r) t-cell malignancies. *HemaSphere*. (2022) 6:163. doi: 10.1097/01.HS9.0000843940.96598.e2

55. Zuhair M, Smit GSA, Wallis G, Jabbar F, Smith C, Devleesschauwer B, et al. Estimation of the worldwide seroprevalence of cytomegalovirus: A systematic review and meta-analysis. *Rev Med Virology*. (2019) 29:e2034. doi: 10.1002/rmv.v29.3

56. Abraham AA, John TD, Keller MD, Cruz CRN, Salem B, Roesch L, et al. Safety and feasibility of virus-specific T cells derived from umbilical cord blood in cord blood transplant recipients. *Blood Adv*. (2019) 3:2057–68. doi: 10.1182/bloodadvances.2019000201

57. Heslop HE, Slobod KS, Pule MA, Hale GA, Rousseau A, Smith CA, et al. Long-term outcome of EBV-specific T-cell infusions to prevent or treat EBV-related lymphoproliferative disease in transplant recipients. *Blood*. (2010) 115:925–35. doi: 10.1182/blood-2009-08-239186

58. Pfeiffer T, Tzannou I, Wu M, Ramos C, Sasa G, Martinez C, et al. Posoleucel, an allogeneic, off-the-shelf multivirus-specific T-cell therapy, for the treatment of refractory viral infections in the post-HCT setting. *Clin Cancer Res*. (2023) 29:324–30. doi: 10.1158/1078-0432.CCR-22-2415

59. Feuchtinger T, Matthes-Martin S, Richard C, Lion T, Fuhrer M, Hamprecht K, et al. Safe adoptive transfer of virus-specific T-cell immunity for the treatment of systemic adenovirus infection after allogeneic stem cell transplantation. *Br J Haematology*. (2006) 134:64–76. doi: 10.1111/j.1365-2141.2006.06108.x

60. Cobbold M, Khan N, Pourgheysari B, Tauro S, McDonald D, Osman H, et al. Adoptive transfer of cytomegalovirus-specific CTL to stem cell transplant patients after selection by HLA–peptide tetramers. *J Exp Med*. (2005) 202:379–86. doi: 10.1084/jem.20040613

61. Riddell SR, Watanabe KS, Goodrich JM, Li CR, Agha ME, Greenberg PD. Restoration of viral immunity in immunodeficient humans by the adoptive transfer of T cell clones. *Science*. (1992) 257:238–41. doi: 10.1126/science.1352912

62. Papadopoulos EB, Ladanyi M, Emanuel D, Mackinnon S, Boulad F, Carabasi MH, et al. Infusions of donor leukocytes to treat epstein-barr virus-associated lymphoproliferative disorders after allogeneic bone marrow transplantation. *New Engl J Med*. (1994) 330:1185–91. doi: 10.1056/NEJM199404283301703

63. Rooney CM, Ng CYC, Loftin S, Smith CA, Li C, Krance RA, et al. Use of gene-modified virus-specific T lymphocytes to control Epstein-Barr-virus-related lymphoproliferation. *Lancet*. (1995) 345:9–13. doi: 10.1016/S0140-6736(95)91150-2

64. Kállay K, Kassa C, Réti M, Karászi É, Sinkó J, Goda V, et al. Early experience with cliniMACS prodigy CCS (IFN-gamma) system in selection of virus-specific T cells from third-party donors for pediatric patients with severe viral infections after hematopoietic stem cell transplantation. *J Immunother*. (2018) 41:158. doi: 10.1097/CJI.0000000000000197

65. Prockop S, Doubrovina E, Suser S, Heller G, Barker J, Dahi P, et al. Off-the-shelf EBV-specific T cell immunotherapy for rituximab-refractory EBV-associated lymphoma following transplantation. *J Clin Invest*. (2020) 130:733–47. doi: 10.1172/JCI121127

66. Quach DH, Lulla P, Rooney CM. Banking on virus-specific T cells to fulfill the need for off-the-shelf cell therapies. *Blood*. (2023) 141:877–85. doi: 10.1182/blood.2022016202

67. Papadopoulou A, Alvanou M, Karavalakis G, Tzannou I, Yannaki E. Pathogen-specific T cells: targeting old enemies and new invaders in transplantation and beyond. *HemaSphere*. (2023) 7:e809. doi: 10.1097/HS9.0000000000000809

68. Cruz CRY, Micklethwaite KP, Savoldo B, Ramos CA, Lam S, Ku S, et al. Infusion of donor-derived CD19-redirected virus-specific T cells for B-cell Malignancies relapsed after allogeneic stem cell transplant: a phase 1 study. *Blood*. (2013) 122:2965–73. doi: 10.1182/blood-2013-06-506741

69. Simmons HZ, Bazzell AF, Dains JE. Adverse effects of virus-specific T-cell therapy: an integrative review. *J Adv Pract Oncol*. (2019) 10:120–31.

70. Qian C, Wang Y, Reppel L, D'aveni M, Campidelli A, Decot V, et al. Viral-specific T-cell transfer from HSCT donor for the treatment of viral infections or diseases after HSCT. *Bone Marrow Transplant*. (2018) 53:114–22. doi: 10.1038/bmt.2017.232

71. Melenhorst JJ, Leen AM, Bollard CM, Quigley MF, Price DA, Rooney CM, et al. Allogeneic virus-specific T cells with HLA alloreactivity do not produce GVHD in human subjects. *Blood*. (2010) 116:4700–2. doi: 10.1182/blood-2010-06-289991

72. Karahan GE, Claas FHJ, Heidt S. Heterologous immunity of virus-specific T cells leading to alloreactivity: possible implications for solid organ transplantation. *Viruses*. (2021) 13:2359. doi: 10.3390/v13122359

73. Kaeuferle T, Krauss R, Blaeschke F, Willier S, Feuchtinger T. Strategies of adoptive T -cell transfer to treat refractory viral infections post allogeneic stem cell transplantation. *J Hematol Oncol*. (2019) 12:13. doi: 10.1186/s13045-019-0701-1

74. Rubinstein JD, Zhu X, Leemhuis T, Pham G, Ray L, Emberesh S, et al. Virus-specific T cells for adenovirus infection after stem cell transplantation are highly

effective and class II HLA restricted. *Blood Adv*. (2021) 5:3309–21. doi: 10.1182/bloodadvances.2021004456

75. Campidelli A, Qian C, Laroye C, Decot V, Reppel L, D'aveni M, et al. Adenovirus-specific T-lymphocyte efficacy in the presence of methylprednisolone: An *in vitro* study. *Cytotherapy*. (2018) 20:524–31. doi: 10.1016/j.jcyt.2017.12.010

76. Busch DH, Fräßle SP, Sommermeyer D, Buchholz VR, Riddell SR. Role of memory T cell subsets for adoptive immunotherapy. *Semin Immunol*. (2016) 28:28–34. doi: 10.1016/j.smim.2016.02.001

77. Gattinoni L, Restifo NP. Moving T memory stem cells to the clinic. *Blood*. (2013) 121:567–8. doi: 10.1182/blood-2012-11-468660

78. Qian C, Wang Y, Cai H, Laroye C, De Carvalho Bittencourt M, Clement L, et al. Adenovirus-specific T-cell subsets in human peripheral blood and after IFN-γ Immunomagnetic selection. *J Immunother*. (2016) 39:27–35. doi: 10.1097/CJI.0000000000000105

79. Li D, Zhou H, Zeng X. Battling CRISPR-Cas9 off-target genome editing. *Cell Biol Toxicol*. (2019) 35:403–6. doi: 10.1007/s10565-019-09485-5

80. Guo C, Ma X, Gao F, Guo Y. Off-target effects in CRISPR/Cas9 gene editing. *Front Bioeng Biotechnol*. (2023) 11:1143157/full. doi: 10.3389/fbioe.2023.1143157/full

81. Rossig C, Bollard CM, Nuchtern JG, Rooney CM, Brenner MK. Epstein-Barr virus-specific human T lymphocytes expressing antitumor chimeric T-cell receptors: potential for improved immunotherapy. *Blood*. (2002) 99:2009–16. doi: 10.1182/blood.V99.6.2009

82. Savoldo B, Rooney CM, Di Stasi A, Abken H, Hombach A, Foster AE, et al. Epstein Barr virus–specific cytotoxic T lymphocytes expressing the anti-CD30ζ artificial chimeric T-cell receptor for immunotherapy of Hodgkin disease. *Blood*. (2007) 110:2620–30. doi: 10.1182/blood-2006-11-059139

83. Caruana I, Weber G, Ballard BC, Wood MS, Savoldo B, Dotti G. K562-derived whole-cell vaccine enhances antitumor responses of CAR-redirected virus-specific cytotoxic-T lymphocytes *in vivo*. *Clin Cancer Res*. (2015) 21:2952–62. doi: 10.1158/1078-0432.CCR-14-2998

84. Sun J, Huye LE, Lapteva N, Mamonkin M, Hiregange M, Ballard B, et al. Early transduction produces highly functional chimeric antigen receptor-modified virus-specific T-cells with central memory markers: a Production Assistant for Cell Therapy (PACT) translational application. *J Immunother Cancer*. (2015) 3:5. doi: 10.1186/s40425-015-0049-1

85. Nakazawa Y, Huye LE, Salsman VS, Leen AM, Ahmed N, Rollins L, et al. PiggyBac-mediated cancer immunotherapy using EBV-specific cytotoxic T-cells expressing HER2-specific chimeric antigen receptor. *Mol Ther*. (2011) 19:2133–43. doi: 10.1038/mt.2011.131

86. Omer B, Castillo PA, Tashiro H, Shum T, Huynh MTA, Cardenas M, et al. Chimeric antigen receptor signaling domains differentially regulate proliferation and native T cell receptor function in virus-specific T cells. *Front Med (Lausanne)*. (2018) 5:343. doi: 10.3389/fmed.2018.00343

87. Quach DH, Ganesh HR, Briones YD, Nouraee N, Ma A, Hadidi YF, et al. Rejection resistant CD30.CAR-modified Epstein-Barr virus-specific T cells as an off-the-shelf platform for CD30+ lymphoma. *Mol Ther Oncol*. (2024) 32:200814. doi: 10.1016/j.omton.2024.200814

88. Perna SK, Pagliara D, Mahendravada A, Liu H, Brenner MK, Savoldo B, et al. Interleukin-7 mediates selective expansion of tumor-redirected cytotoxic T lymphocytes (CTLs) without enhancement of regulatory T-cell inhibition. *Clin Cancer Res*. (2014) 20:131–9. doi: 10.1158/1078-0432.CCR-13-1016

89. Tanaka M, Tashiro H, Omer B, Lapteva N, Ando J, Ngo M, et al. Vaccination targeting native receptors to enhance the function and proliferation of chimeric antigen receptor (CAR)-modified T cells. *Clin Cancer Res*. (2017) 23:3499–509. doi: 10.1158/1078-0432.CCR-16-2138

90. Zhou L, Liu X, Wang X, Sun Z, Song XT. CD123 redirected multiple virus-specific T cells for acute myeloid leukemia. *Leukemia Res*. (2016) 41:76–84. doi: 10.1016/j.leukres.2015.12.003

91. Cooper LJN, Al-Kadhimi Z, Serrano LM, Pfeiffer T, Olivares S, Castro A, et al. Enhanced antilymphoma efficacy of CD19-redirected influenza MP1-specific CTLs by cotransfer of T cells modified to present influenza MP1. *Blood*. (2005) 105:1622–31. doi: 10.1182/blood-2004-03-1208

92. Wang X, Wong CW, Urak R, Mardiros A, Budde LE, Chang WC, et al. CMVpp65 vaccine enhances the antitumor efficacy of adoptively transferred CD19-redirected CMV-specific T cells. *Clin Cancer Res*. (2015) 21:2993–3002. doi: 10.1158/1078-0432.CCR-14-2920

93. Wang X, Urak R, Walter M, Guan M, Han T, Vyas V, et al. Large-scale manufacturing and characterization of CMV-CD19CAR T cells. *J Immunother Cancer*. (2022) 10:e003461. doi: 10.1136/jitc-2021-003461

94. Altvater B, Pscherer S, Landmeier S, Niggemeier V, Juergens H, Vormoor J, et al. CD28 co-stimulation via tumour-specific chimaeric receptors induces an incomplete activation response in Epstein-Barr virus-specific effector memory T cells. *Clin Exp Immunol*. (2006) 144:447–57. doi: 10.1111/j.1365-2249.2006.03095.x

95. Landmeier S, Altvater B, Pscherer S, Eing BR, Kuehn J, Rooney CM, et al. Gene-engineered varicella-zoster virus reactive CD4+ cytotoxic T cells exert tumor-specific effector function. *Cancer Res*. (2007) 67:8335–43. doi: 10.1158/0008-5472.CAN-06-4426

96. Dutour A, Marin V, Pizzitola I, Valsesia-Wittmann S, Lee D, Yvon E, et al. *In vitro* and *in vivo* antitumor effect of anti-CD33 chimeric receptor-expressing EBV-CTL against CD33 acute myeloid leukemia. *Adv Hematol*. (2012) 2012:683065. doi: 10.1155/2012/683065

97. Lapteva N, Gilbert M, Diaconu I, Rollins LA, Al-Sabbagh M, Naik S, et al. T-cell receptor stimulation enhances the expansion and function of CD19 chimeric antigen receptor–expressing T cells. *Clin Cancer Res*. (2019) 25:7340–50. doi: 10.1158/1078-0432.CCR-18-3199

98. Quach DH, Ramos CA, Lulla PD, Sharma S, Ganesh HR, Nouraee N, et al. CD30.CAR-modified epstein-barr virus-specific T cells (CD30.CAR EBVSTs) provide a safe and effective off-the-shelf therapy for patients with CD30-positive lymphoma. *Blood*. (2022) 140:412–4. doi: 10.1182/blood-2022-160244

99. Pule MA, Savoldo B, Myers GD, et al. Virus-specific T cells engineered to coexpress tumor-specific receptors: persistence and antitumor activity in individuals with neuroblastoma. *Nat Med*. (2008) 14(11):1264–1270. doi: 10.1038/nm.1882

100. Louis CU, Straathof K, Bollard CM, et al. Enhancing the in vivo expansion of adoptively transferred EBV-specific CTL with lymphodepleting CD45 monoclonal antibodies in NPC patients. *Blood*. (2009) 113(11):2442–2450. doi: 10.1182/blood-2008-05-157222

101. Ahmed N, Brawley V, Hegde M, et al. HER2-Specific Chimeric Antigen Receptor-Modified Virus-Specific T Cells for Progressive Glioblastoma: A Phase 1 Dose-Escalation Trial. *JAMA Oncol*. (2017) 3(8):1094–101. doi: 10.1001/jamaoncol.2017.0184

102. Rossig C, Pule M, Altvater B, Saiagh S, Wright G, Ghorashian S, et al. Vaccination to improve the persistence of CD19CAR gene-modified T cells in relapsed pediatric acute lymphoblastic leukemia. *Leukemia*. (2017) 31:1087–95. doi: 10.1038/leu.2017.39

103. FDA Investigating CAR-Related T-cell Malignancies. *Cancer Discov*. (2024) 14 (1):9–10. doi: 10.1158/2159-8290.CD-NB2023-0091

104. Martin LJ, Whitmore JB, Shen RR, Neumann F. T-cell Malignancies with anti-CD19 chimeric antigen receptor T-cell therapy. *Blood Adv*. (2024) 8:4144–8. doi: 10.1182/bloodadvances.2024013248

105. Hamilton MP, Sugio T, Noordenbos T, Shi S, Bulterys PL, Liu CL, et al. Risk of second Malignancies and T-cell lymphoma after chimeric antigen receptor T-cell therapy. *N Engl J Med*. (2024) 390:2047–60. doi: 10.1056/NEJMoa2401361

106. Micklethwaite KP, Gowrishankar K, Gloss BS, Li Z, Street JA, Moezzi L, et al. Investigation of product-derived lymphoma following infusion of piggyBac-modified CD19 chimeric antigen receptor T cells. *Blood*. (2021) 138:1391–405. doi: 10.1182/blood.2021010858

107. Smith R, Shen R. Complexities in comparing the impact of costimulatory domains on approved CD19 CAR functionality. *J Transl Med*. (2023) 21:515. doi: 10.1186/s12967-023-04372-4

108. Cappell KM, Kochenderfer JN. A comparison of chimeric antigen receptors containing CD28 versus 4-1BB costimulatory domains. *Nat Rev Clin Oncol*. (2021) 18:715–27. doi: 10.1038/s41571-021-00530-z

109. Galli E, Bellesi S, Pansini I, Di Cesare G, Iacovelli C, Malafronte R, et al. The CD4/CD8 ratio of infused CD19-CAR-T is a prognostic factor for efficacy and toxicity. *Br J Haematology*. (2023) 203:564–70. doi: 10.1111/bjh.v203.4

110. Prockop SE, Hasan A, Doubrovina E, Dahi PB, Rodriguez-Sanchez I, Curry M, et al. Third-party cytomegalovirus-specific T cells improved survival in refractory cytomegalovirus viremia after hematopoietic transplant. *J Clin Invest*. (2023) 133(10): e165476. doi: 10.1172/JCI165476

111. Jiang W, Clancy LE, Avdic S, Sutrave G, Street J, Simms R, et al. Third-party CMV- and EBV-specific T-cells for first viral reactivation after allogeneic stem cell transplant. *Blood Adv*. (2022) 6:4949–66. doi: 10.1182/bloodadvances.2022007103

112. Youngblood B, Hale JS, Kissick HT, Ahn E, Xu X, Wieland A, et al. Effector cd8 t cells dedifferentiate into long-lived memory cells. *Nature*. (2017) 552(10):404. doi: 10.1038/nature25144

113. Kaech SM, Tan JT, Wherry EJ, Konieczny BT, Surh CD, Ahmed R. Selective expression of the interleukin 7 receptor identifies effector CD8 T cells that give rise to long-lived memory cells. *Nat Immunol*. (2003) 4:1191–8. doi: 10.1038/ni1009

114. Rutishauser RL, Martins GA, Kalachikov S, Chandele A, Parish IA, Meffre E, et al. Blimp-1 promotes terminal differentiation of virus-specific CD8 T cells and represses the acquisition of central memory T cell properties. *Immunity*. (2009) 31:296.

115. Shen L, Xiao Y, Zhang C, Li S, Teng X, Cui L, et al. Metabolic reprogramming by ex vivo glutamine inhibition endows CAR-T cells with less-differentiated phenotype and persistent antitumor activity. *Cancer Letters*. (2022) 538:215710. doi: 10.1016/j.canlet.2022.215710

116. Rial Saborido J, Völkl S, Aigner M, Mackensen A, Mougiakakos D. Role of CAR T cell metabolism for therapeutic efficacy. *Cancers*. (2022) 14:5442. doi: 10.3390/cancers14215442

117. Ghorai SK, Pearson AN. Current strategies to improve chimeric antigen receptor T (CAR-T) cell persistence. *Cureus*. (2024) 16(7):e65291. doi: 10.7759/cureus.65291.

118. Frigault MJ, Graham CE, Berger TR, Ritchey J, Horick NK, El-Jawahri A, et al. Phase 1 study of CAR-37 T cells in patients with relapsed or refractory CD37+ lymphoid Malignancies. *Blood*. (2024) 144:1153–67. doi: 10.1182/blood.2024024104

119. Philip B, Kokalaki E, Mekkaoui L, Thomas S, Straathof K, Flutter B, et al. A highly compact epitope-based marker/suicide gene for easier and safer T-cell therapy. *Blood*. (2014) 124:1277–87. doi: 10.1182/blood-2014-01-545020

120. Xiong X, Yu Y, Jin X, Xie D, Sun R, Lu W, et al. Functional validation of the RQR8 suicide/marker gene in CD19 CAR-T cells and CLL1CAR-T cells. *Ann Hematol*. (2023) 102:1523–35. doi: 10.1007/s00277-023-05227-0

121. Mahadeo KM, Baiocchi R, Beitinjaneh A, Chaganti S, Choquet S, Dierickx D, et al. Tabelecleucel for allogeneic haematopoietic stem-cell or solid organ transplant recipients with Epstein–Barr virus-positive post-transplant lymphoproliferative disease after failure of rituximab or rituximab and chemotherapy (ALLELE): a phase 3, multicentre, open-label trial. *Lancet Oncol*. (2024) 25:376–87. doi: 10.1016/S1470-2045(23)00649-6

122. Barlev A, Zimmermann H, Guzman-Becerra N, Mehta A, Xing B, Macabeo B, et al. Comparative analysis of tabelecleucel and current treatment in patients with Epstein-Barr virus-positive post-transplant lymphoproliferative disease following hematopoietic cell transplant or solid organ transplant. *J Med Economics*. (2024) 27:789–95. doi: 10.1080/13696998.2024.2354150

123. Nikiforow S, Whangbo JS, Reshef R, Tsai DE, Bunin N, Abu-Arja R, et al. Tabelecleucel for EBV+ PTLD after allogeneic HCT or SOT in a multicenter expanded access protocol. *Blood Advances*. (2024) 8:3001. doi: 10.1182/bloodadvances.2023011626

124. Kagoya Y, Guo T, Yeung B, Saso K, Anczurowski M, Wang CH, et al. Genetic ablation of HLA class I, class II, and the T-cell receptor enables allogeneic T cells to be used for adoptive T-cell therapy. *Cancer Immunol Res*. (2020) 8:926–36. doi: 10.1158/2326-6066.CIR-18-0508

Glossary

AdV	Adenovirus
AdVST	Adenovirus specific T cell
AEMPS	Spanish Agency of Medicines and Medical Devices
ALL	Acute Lymphoblastic Leukemia
Allo-SCT	allogeneic hematopoietic stem cell transplantation
APC	Antigen Presenting Cell
ATMP	Advanced Therapy Medicinal Product
B2M	β-2-microglobulin
CAR	Chimeric Antigen Receptor
iCas9	inducible CRISPR associated protein 9
CD	Cluster of differentiation
CMV	Cytomegalovirus
CMVST	Cytomegalovirus Specific T cell
CIK	Cytokine-Induced killer
CRS	Cytokine release syndrome
CRISPR	clustered regularly interspaced short palindromic repeats
DC	Dendritic Cell
DNA	Deoxyribonucleic acid
DNT	Double Negative T cell
EBV	Eptein Barr Virus
EBVST	Eptein Barr Virus Specific T cell
EGFRt	truncated Epidermal growth factor receptor
EMA	European Medicine Agency
EU	European Union
FDA	Food and Drug Administration
GD2	disialoganglioside
GR	Graft Rejection
GvHD	Graft versus Host Disease
HGBL	high-grade B-cell lymphoma
HLA	Human Leukocyte Antigen
IFN-γ	Interferon gamma
iNKT	invariant Natural Killer T cell
iPSC	Induced pluripotent stem cell
KIR	Killer cell immunoglobulin-like receptor
KO	Knock-out
LAG-3	Lymphocyte-activation gene 3
LCL	Lymphoblastoid Cell Line
MAIT	Mucosal-Associated Invariant T cell
MHC	Major Histocompatibility Complex
MP-1	influenza A Matrix Protein 1
MRD	Minimal residual disease
NK	Natural Killer cell
ORR	Objective Response Rate
p-ART	primed Alloreactive T cells
PBMC	Peripheral Blood Mononuclear Cell
PD-1	Programmed cell death 1
PTLD	Post-transplant lymphoproliferative disorder
rhIL	recombinant human Interleukin
r/r	Refractory or relapse
scFv	Single Chain Fragment Variable
shRNA	Small hairpin RNA
SOT	Solid Organ Transplantation
TALEN	Transcription Activator-Like Effector Nuclease
Tcm	Central memory T subset
TCR	T Cell Receptor
Tem	Effector memory T subset
TIM-3	T cell immunoglobulin and mucin domain-containing protein 3
TNF-α	Tumor Necrosis factor-Alpha
TRAC	T cell Receptor Alpha Constant
Tscm	Stem cell memory T subset
UCB	Umbilical cord blood
VST	Virus Specific T cell
VZV	Varicella Zoster Virus
VZVST	Varicella Zoster Virus Specific T cell
ZAP70	Zeta Chain of T Cell Receptor Associated Protein Kinase 70
ZFN	Zinc Finger Nucleases

frontiers | Frontiers in Immunology

TYPE Original Research
PUBLISHED 27 January 2025
DOI 10.3389/fimmu.2025.1526513

OPEN ACCESS

EDITED BY
Rita Maccario,
San Matteo Hospital Foundation (IRCCS), Italy

REVIEWED BY
Kotaro Miyao,
Anjo Kosei Hospital, Japan
Marcello Maestri,
San Matteo Hospital Foundation (IRCCS), Italy

*CORRESPONDENCE
Boaz Nachmias
BoazN@Hadassah.org.il
Batia Avni
batiavni@gmail.com

†These authors share first authorship

‡These authors share last authorship

RECEIVED 11 November 2024
ACCEPTED 06 January 2025
PUBLISHED 27 January 2025

CITATION
Falicovich I, Nachmias B, Elias S, Zimran E, Shaulov A, Stepensky P, Avni B and Grisariu S (2025) Low dose ATG-Fresenius for GVHD prophylaxis: a comparative study with ATG-Thymoglobulin. *Front. Immunol.* 16:1526513. doi: 10.3389/fimmu.2025.1526513

Low dose ATG-Fresenius for GVHD prophylaxis: a comparative study with ATG-Thymoglobulin

Itai Falicovich[1†], Boaz Nachmias[2*†], Shlomo Elias[3], Eran Zimran[3], Adir Shaulov[2], Polina Stepensky[3], Batia Avni[3*‡] and Sigal Grisariu[3‡]

[1]Faculty of Medicine, The Hebrew University, Jerusalem, Israel, [2]Department of Hematology, Hadassah Medical Center and Faculty of Medicine, Hebrew University, Jerusalem, Israel, [3]Bone Marrow Transplantation and Cancer Immunotherapy Department, Hadassah University Medical Center and Faculty of Medicine, The Hebrew University, Jerusalem, Israel

Background: Anti-Thymocyte Globulin (ATG) is commonly used to prevent graft-versus-host disease (GVHD), but the optimal dosage and type of ATG remains to be determined.

Objective: We compared retrospectively the safety and efficacy outcomes of allogeneic transplantation using low-dose ATG-Fresenius (15mg/kg) and ATG-Thymoglobulin (10mg/kg) for GVHD prevention.

Study design: Ninety-eight patients were included, with 46 in the ATG-T group and 52 in the ATG-F group. The median age was 48 years in the ATG-T group (range 20-71) and 50 years in the ATG-F group (range 18-73). Baseline characteristics were similar, with slightly more HLA mismatched donors and single-agent cyclosporine GVHD prophylaxis use in the ATG-T group. Additionally, the ATG-F group had more myeloid leukemia and myelodysplastic syndrome patients, while the ATG-T group had more lymphoma patients.

Results: The cumulative incidence of acute GVHD (aGVHD) grade II-IV and chronic GVHD (cGVHD) showed no significant differences. Multivariate analysis indicated that donor HLA mismatch influenced aGVHD risk significantly (p=0.005), and myeloablative conditioning increased cGVHD risk. Bacteremia and CMV reactivation rates were similar, but EBV DNA viremia was higher in the ATG-T group (22% *vs.* 8%, p=0.047), with one case of Post-Transplant Lymphoproliferative Disorder (PTLD) in the ATG-T group. Cumulative incidence of overall survival (OS), relapse incidence, non-relapse mortality (NRM) and GVHD free, Relapse free Survival (GRFS) did not significantly differ.

Conclusions: This study highlights the safety and efficacy of low-dose ATG-F compared to a relatively high dose ATG-T. Prospective studies are necessary to validate the safety and efficacy of low dose ATG-F for GVHD prevention.

KEYWORDS

ATG Fresenius, ATG thymoglobulin, allogenic bone marrow transplantation, acute GVHD, chronic GVHD

Introduction

Anti-Thymocyte Globulin (ATG) is frequently employed in the prevention of Graft Versus Host Disease (GVHD) as well as graft failure. It functions as an immunoregulator by attaching to T-cells and various other immune system cells (1). Among available ATG sera are ATG-Thymoglubolin (ATG-T, Sanofi Genzyme, Cambridge MA), derived from rabbit vaccination with human thymocytes, and ATG-Fresenius (ATG-F, Neovii, Rapperswil, Switzerland, ATG Fresenius®), derived from the human Jurkat T-cell line. While numerous clinical studies have demonstrated the effectiveness of each of these agents individually (2–8), there is a paucity of studies directly comparing the two agents. Furthermore, the variability in dosing regimens adds complexity to the comparison between these treatments.

The optimal dosage of ATG for GVHD prophylaxis displays variability, as demonstrated in multiple studies. An in-depth analysis of ATG formulations has unveiled distinctions in the targeted antigens between ATG-Fresenius and Thymoglobulin, potentially contributing to variations in their immunomodulatory capabilities (9). Since ATG-F recognizes a more limited spectrum of antigens, higher doses are used to achieve adequate immunomodulation compared to ATG-T. Additionally, it has been observed that different ATG products exhibit differing clearance rates, further influencing their immunomodulatory effects (10). Furthermore, the significance of patient-specific factors, such as absolute lymphocyte counts (ALCs), has been underscored, with individuals possessing lower ALCs being susceptible to receiving excessive ATG doses, resulting in profound T-cell depletion and inferior outcomes (11). These findings shed light on just a subset of the factors contributing to differences in these two formulations and their respective dosing regimens.

Reported ATG-T doses ranges from 2.5 to 10mg/kg (12). High doses of ATG-T (15mg/kg) compared to no ATG have been shown to reduce the incidence of acute GVHD (aGVHD) (50% *vs.* 11%, p=0.001) and chronic GVHD (cGVHD) (62% *vs* 39%; P =.04), while exposing the patients to a higher incidence of lethal infections (30% *vs* 7%, p=0.02) [3]. Lower doses of 4.5 mg/kg (again compared to no ATG) in patients who underwent hematopoietic stem cell transplantation (HSCT) from an HLA matched unrelated donor (MUD) was associated with a reduction of acute and chronic GVHD incidence, reduced use of post-transplant immunosuppression therapy (IST), and reduced patients' symptoms burden, but with an increased incidence of EBV infections (5). Similar effects have been observed in larger prospective studies of HSCT from HLA matched sibling donors (MSD) (13) and MUD (6), demonstrating a reduced incidence of aGVHD and cGVHD, without significant differences in incidence of infections compared to control groups.

Similarly, ATG-F doses range widely between 15mg/kg to 60mg/kg (14). A phase 3 randomized study demonstrated that lower doses of ATG-F (15mg/kg compared to 30mg/kg) reduced relapse incidence and increased five-year overall survival (OS) in pediatric patients undergoing allogeneic HSCT from MUD with a myeloablative conditioning regimen (15). In adults, the optimal dose of ATG-F has not yet been defined. A phase 3 randomized controlled study assessed the efficacy and safety of prophylactic ATG-F (at a total dose of 60 mg/kg) in adult patients undergoing allogeneic HSCT compared with no ATG (4). In the group of patients receiving ATG-F there was a significant reduction in the incidence of grade II-IV aGVHD and extensive cGVHD, without an increase in relapse or non-relapse mortality. Others have reported a lower rate of cGVHD with low dose (15-30 mg/kg) of ATG-F (16, 17).

Recently, two retrospective studies compared transplant outcomes between the two agents. Both studies showed a statistically significant decline in the incidence of overall cGVHD and moderate-severe cGVHD in patients who received ATG-F (at a dosage of 30mg/kg and 20 mg/kg, respectively) compared to those who received ATG-T (7.5mg/kg and 10mg/kg, respectively). There was no significant difference in the rate of aGVHD or infectious complications (18, 19).

In our clinical practice, between the years 2011-2014, we administered ATG-T at a dosage of 10mg/kg. As safety data for ATG-F accumulated, suggesting lower incidence of infectious complication due to the narrower antigen spectrum, we switched to ATG-F at a dosage of 15mg/kg starting in 2014 onwards. Despite previous studies showing the efficacy of ATG-F (60mg/kg) (4), we have chosen a lower dose of ATG-F to mitigate concerns regarding an increased risk of infection and relapse (3, 5, 15). We conducted a retrospective study at our center comparing transplant outcomes using ATG-F 15mg/kg (from 2014 forward) to our earlier protocol using ATG-T 10mg/kg. Given the lack of outcome data comparing between these two agents at these dosages, this study aims to address the gap and provide valuable insights into their relative efficacy and toxicity.

Methods

The study cohort included all patients above the age of 18 years old who underwent HSCT with ATG-T or ATG-F as GVHD prophylaxis at Hadassah university medical center from 2011-2018. Patients with an underlying disease for which the choice of ATG type has remained ATG-T (i.e., aplastic anemia), were not included in the study population. Data collected included patients' demographics, diagnosis, treatment outcomes and infectious complications. Adverse events were graded according to the CTCAE 4.0. The follow-up period spanned two years.

Myeloablative regimens included: Total body irradiation (TBI) ≥ 500 cGy as a single fraction or ≥ 800cGy if fractionated, total busulfan ≥ 9mg/kg, total melphalan ≥ 150mg/m^2, total Thiotepa ≥ 10mg/kg and treosulfan ≥36g/m2/d. Any other conditioning regimen utilized was categorized under the reduced-intensity regimen. ATG was administered to patients transplanted for MDS regardless of donor type and those transplanted from unrelated donors (both HLA matched and HLA mismatched). ATG-T was administered at a dosage of 2.5mg/kg/d for four consecutive days (on days -4, -3, -2, -1). ATG-F was administered at a dosage of 5mg/kg/d for three consecutive days (on days -3, -2, -1). The initial target for cyclosporine trough levels was 200-300ng/ml during the first month, and it was subsequently lowered to a range of 100-150ng/ml thereafter. Mycophenolate Mofetil (MMF) was initially given at a

dose of 15mg/kg three times daily during the first month and then gradually tapered down. Neutrophil engraftment was defined as the first of three consecutive days with an absolute neutrophil count > 0.5 per microliter (mcL). Platelet engraftment was defined as the first of seven consecutive days with a platelet count > 20 per mcL, without platelet transfusion. Post-transplant donor chimerism was monitored using peripheral blood (PB) and bone marrow (BM) short tandem repeats (STR) analysis. Acute and chronic GVHD were graded according to Mount Sinai Acute GvHD International Consortium (MAGIC) criteria for acute GVHD (20) and the NIH 2014 criteria for chronic GvHD previously published criteria (21). cGVHD incidence was calculated for patients surviving more than 100 days. Overall survival (OS) was defined as time from transplant to death from any cause. Non- Relapse mortality (NRM) was defined as mortality without prior relapse. GVHD and relapse-free survival (GRFS) was evaluated as a composite end point of: absence of grades III–IV acute GVHD, moderate-severe chronic GVHD requiring systemic immunosuppressive therapy, relapse, or death from any cause, during any time point after allo-HSCT.

The study was approved by the Hadassah University Hospital review board and was performed in accordance with the principles of the Declaration of Helsinki. Informed consent was waived by the Hadassah University Hospital ethical committee (approval no. 0608-20-HMO).

Statistical analysis

To test the association between two categorical variables, the χ^2 test as well as the Fisher's exact test was used. The comparison of a quantitative variable between two independent groups was performed by using the two-sample t-test or the non-parametric Mann-Whitney test for variables which were not normally distributed. The Kaplan-Meier survival model was used for testing the effect of categorical variables on survival, with the log-rank test for the comparison of survival curves. The Cox regression model was applied for testing the effect of quantitative variables on survival. This model was also used as the multivariate model for survival. The multivariable model included 2 blocks. In the first block, ATG type was forced into the regression and in the second block using the stepwise, forward, likelihood ratio approach, only significant pre transplant risk factors (such as demographic, underlying disease and pre-transplant characteristics, including median recipient age, gender, disease status at transplantation entry and comorbidity index, donor type, donor age and gender matching, HLA matching, ABO and CMV serology matching, transplant source, conditioning regimen intensity and GVHD prophylaxis) identified in the univariate analysis were incorporated in the Cox regression model. Probabilities of NRM, relapse and GVHD were calculated using the cumulative incidence function, accounting for competing risks, and were compared using Gray's test. Relapse was the competing risk of NRM and vice versa, and death was the competing risk of GVHD. All statistical tests used were two-tailed, and a p-value of 0.05 or less was considered statistically significant. The statistical analysis was performed using SPSS 26 and NCSS 24 software.

Results

Patient characteristics

Ninety-eight patients were included in the study, 46 in the ATG-T group and 52 in the ATG-F group. Baseline clinical characteristics of the groups are summarized in Table 1. Median follow up was 7.26 months in the ATG-T group *vs.* 14.58 months in the ATG-F group (p=0.276). Demographic, underlying disease and pre-transplant characteristics, including median recipient age, gender, disease status at transplantation entry, calculated refined disease risk index (rDRI) (22) and comorbidity index of the two groups were mostly similar. There was a significant difference between the two groups regarding underlying disease leading to transplantation (p=0.038, Chi-Square test), stemming from a higher percentage of patients transplanted for MDS and secondary AML in the ATG-F compared to the ATG-T group (21% Vs. 11%, respectively) and a higher rate of lymphoproliferative diseases (other than acute lymphoblastic leukemia) in the ATG-T compared to the ATG-F group (15% Vs. none, respectively).

Addressing known risk factors for GVHD (Table 1), there was no significant difference between the two cohorts regarding the median donor age and conditioning regimen intensity. However, there was a borderline significant higher incidence of HLA mismatch in the ATG-T group compared to the ATG-F group (39.1% Vs. 21.2%; p=0.052, Chi-Square test). In addition, a significantly higher number of patients received single-agent cyclosporine in the ATG-T compared to the ATG-F group (30.4% *vs* 3.8%, respectively; p<0.01, Chi-Square test). This difference is primarily attributed to the use of ATG-T during an earlier (before 2014) timeframe.

Regarding risk factors for infections, there was a significantly higher incidence of positive IgG serology for CMV in both donors and recipients within the ATG-F compared to the ATG-T cohort (82.4% *vs* 60.9%, respectively, p=0.022, Fisher-Freeman-Halton Exact test).

GVHD

aGVHD grade II-IV occurred in 23 out of 46 patients in the ATG-T group versus 21 out of 52 patients in the ATG-F group (50% *vs* 40.4%, p=0.417, Chi-Square test). The proportions of disease grading (Grade II *vs.* Grade III-IV) did not show a significant difference between the two groups (p=0.266, Chi-Square test, Table 2). The cumulative incidence of grade II-IV aGVHD and grade III-IV aGVHD showed no significant difference between the two groups (p=0.089, p=0.228, Gray's test, Figures 1A, B, respectively).

Univariate analysis of the entire cohort did not show a statistically significant effect of type of ATG, GVHD prophylaxis (excluding ATG), type of donor, conditioning intensity, and patient's age on the risk of aGVHD. In contrast, only HLA mismatching was associated with an increased risk for aGVHD (p=0.009, Log Rank test). Multivariate analysis (using Cox Regression model), incorporating HLA mismatching, ATG type

10.3389/fimmu.2025.1526513

TABLE 1 Patient characteristics.

Variables		ATG-T (n=46)	ATG-F (n=52)	p-value
Gender	Male	30 (65.2%)	39 (75%)	0.29
	Female	16 (34.8%)	13 (25%)	
Age at transplant (median), years		48.09 (19.9-70.9)	50.51 (18.38-72.9)	0.258
Donor age (median), years		30 (16-77)	27 (15-66)	0.441
Underling Disease	AML	17 (37%)	18 (34.6%)	**0.038**
	SecAML	8 (17.4%)	14 (36.9%)	
	ALL	5 (10.9%)	7 (13.5%)	
	MDS	5 (10.9%)	11 (21.2%)	
	MPN	1 (2.2%)	1 (1.9%)	
	LPD	7 (15.2%)	0	
	Others	3 (6.5%)	1 (1.9%)	
Disease status at Tx	CR	21 (45.7)	30 (57.7%)	0.497
	PR	2 (4.3%)	2 (3.8%)	
	AD	23 (50%)	20 (38.5)	
HCT-CI	Low (0)	8 (17.4%)	8 (15.4%)	0.627
	Moderate (1-2)	24 (52.2%)	32 (65.1%)	
	High (≥3)	14 (30.4%)	12 (23.1%)	
rDRI	Low-Intermediate	28 (60.9%)	35 (67.3%)	0.533
	High-Very High	18 (39.1%)	17 (32.7%)	
Donor Type	Sibling	9 (19.6%)	13 (25%)	0.630
	Unrelated	37 (80.4%)	38 (73.1%)	
	Other related	0	1 (1.9%)	
Transplant source	PBSC	41 (89.1%)	49 (94.2%)	0.469
	BM	5 (10.9%)	3 (5.8%)	
HLA matching	Match	28 (60.9%)	41 (78.8%)	**0.052**
	Mismatch	18 (39.1%)	11 (21.2%)	
ABO incompatibility	Matched	16 (34.8%)	25 (49.0%)	0.438
	Minor	13 (28.3%)	14 (27.5%)	
	Major	12 (26.1%)	9 (17.6%)	
	Bidirectional	5 (10.9%)	3 (5.9%)	
Conditioning regimen				
	MA	29 (63%)	26 (50%)	
	RIC	17 (37%)	26 (50%)	
GVHD prophylaxis	CSA	14 (30.4%)	2 (3.8%)	**<0.01**
	CSA+MTX	0	2 (3.8%)	
	CSA+MMF	32 (69.6%)	48 (92.3%)	
Gender matching D/R	M/F	10 (21.7%)	8 (15.4%)	0.695
	F/F	6 (13.0%)	5 (9.6%)	
	M/M	18 (39.1%)	26 (50.0%)	

(Continued)

TABLE 1 Continued

Variables		ATG-T (n=46)	ATG-F (n=52)	p-value
	F/M	12 (26.1%)	13 (25.0%)	
CMV – D/R serology status	+/+	28 (60.9%)	42 (82.4%)	**0.022**
	+/-	1 (2.2%)	2 (3.9%)	
	-/+	14 (30.4%)	7 (13.7%)	
	-/-	3 (6.5%)	0	

AML, Acute Myeloid Leukemia; secAML, Secondary AML; ALL, Acute Lymphoid Leukemia; MDS, Myelodysplastic syndrome; MPN, myeloprolipherative Disorder; LPD, lymphroliferative Disorder; Tx, Treatment; CR, Complete Remission; PR, Partial Remission; AD, Active Disease; HCT, CI Hematopoietic Cell Transplantation Comorbidity Index; rDRI, Refined Disease Risk Index; PBSC, Peripheral Blood Stem Cell; BM, Bone Marrow; MA, myeloablative; RIC, reduced intensity; CSA, Cyclosporin A; MMF, Mycophenolate Mofetil; D/R, Donor/Recipient.
Bold p-values signify statistical significance.

and GVHD prophylaxis, revealed that donor HLA mismatching maintained its statistically significant effect on the risk for aGVHD (HR=2.118, 95% CI [1.119-4.010], p=0.021) while ATG type and GVHD prophylaxis were not statistically significant (Hazard ratios for all outcomes, incorporating ATG type into the Cox regression model, are summarized in Table 3).

cGVHD occurred in 10 (21.7%) and 15 (28.8%) patients in the ATG-T *vs.* ATG-F group, respectively (p=0.49, Fisher's Exact test). Moderate-severe disease occurred in 10 (21.7%) *vs.* 13 (25%) patients, respectively (p=0.25, Fisher's Exact test). No differences were found between the groups in the cumulative incidence for cGVHD (Figure 1C) and moderate-severe cGVHD (Figure 1D) (p=0.74 and p=0.965, respectively, Gray's test). Univariate analysis revealed that myeloablative conditioning regimen and younger age were associated with a significant increased risk for cGVHD, while a history of aGVHD was associated with a borderline increased risk (p=0.068, Log Rank test). Donor-recipient gender mismatch and transplant source did not significantly affect the risk of developing cGVHD. In multivariate analysis, using the Cox Regression model, incorporating the significant factors identified in the univariate analysis (conditioning regimen and age), only myeloablative conditioning regimen was associated with an increased risk for cGVHD (results compared to MA regimen – RIC: HR=0.217, 95%CI [0.064-0.74], p=0.015, NMA: HR=0.113, 95%CI [0.015-0.841], p=0.033).

Engraftment

There was no significant difference between the cohorts in the median time to neutrophil and platelet engraftment (Figures 2A, B,

TABLE 2 Transplant outcomes.

Variables		ATG-T (n=46)	ATG-F (n=52)	p-value
Median follow-up months (range)		7.26 (2.6-24)	14.58 (4-24)	0.276
Infectious complications				
	Bacteremia	20 (43.5%)	24 (46.2%)	0.790
	CMV reactivation	36 (78.3%)	39 (75.0%)	0.704
	CMV disease	0	3 (5.8%)	0.098
	EBV reactivation	10 (21.7%)	4 (7.7%)	0.047
Other complications				
	VOD	8 (17.4%)	12 (23.1%)	0.486
	HC	11 (23.9%)	8 (15.4%)	0.287
Hospitalization days (range)		32.5 (21-256)	32.5 (14-248)	0.820
Mortality Incidence (%)		23 (50%)	25 (48.1%)	0.849
Death Cause				
	Relapse	9 (19.5%)	9 (17.3%)	0.952
	Infection	8 (17.3%)	8 (15.3%)	
	GVHD	5 (10.9%)	6 (11.53%)	
	Other	1 (2.2%)	2 (3.8%)	

aGVHD, Acute Graft Versus Host Disease; cGVHD, Chronic Graft Versus Host Disease; ANC, Absolute Neutrophil Count; PLT, Platelets; CMV, Cytomegalovirus; EBV, Epstein-Barr Virus; VOD, Veno-occlusive Disease; HC, Hemorrhagic Cystitis; DFS, Disease-Free Survival; GVHD, Graft Versus Host Disease.

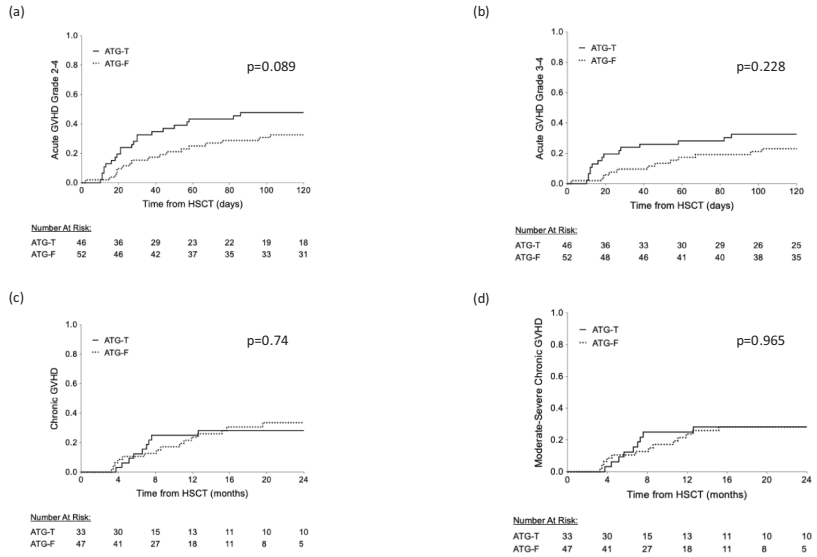

FIGURE 1
Cumulative rate of acute and chronic GVHD. **(A)** Acute GVHD grade II-IV **(B)** Acute GVHD grade III-IV **(C)** chronic GVHD **(D)** moderate-severe chronic GVHD.

respectively). Forty-five patients (98%) and 51 patients (98%) in the ATG-T group *vs*. ATG-F group, have achieved neutrophil engraftment with a median time of 15 *vs*. 14 days, respectively (p=0.913). Thirty-Eight patients (82.6%) *vs*. 51 patients (98%) in the ATG-T group *vs*. ATG-F group have achieved platelet engraftment with a median time of 16 *vs*.17 days, respectively (p=0.360).

Infections and other transplant related complications

No significant differences were observed in the incidence of bacteremia and CMV reactivation (Table 2). Bacteremia occurred in 43.5% *vs*. 46.2% (p=0.79), and CMV reactivation occurred in 78.3% *vs*. 75% (p=0.7, Chi-Square test) of patients in the ATG-T *vs*. ATG-F group, respectively. CMV disease, defined by the presence of clinical symptoms and/or signs together with documentation of CMV in tissue from the relevant organ [13], has occurred in three patients (5.8%) in the ATG-F group (CMV colitis and pneumonitis), with no documented cases in the ATG-T group (p=0.245, Fisher's Exact test). EBV DNA viremia (detected by PCR) was observed in 21.7% of patients in the ATG-T group and 7.7% in the ATG-F group (p=0.047, Chi-Square test), with a single case of Post-Transplant Lymphoproliferative Disorder (PTLD) in the ATG-T group, associated with EBV-DNA viremia.

No significant differences were observed in other transplant related complications including incidence of veno-occlusive disease (VOD) or hemorrhagic cystitis (Table 2).

TABLE 3 Hazard ratios of ATG type for different outcomes.

Outcome	HR	95% CI	P Value
Overall Survival	0.808	0.455-1.433	0.466
Relapse	0.579	0.258-1.299	0.185
NRM	0.912	0.452-1.842	0.798
AGVHD	0.729	0.398-1.338	0.308
CGVHD	1.137	0.500-2.585	0.760
GRFS	0.887	0.458-1.719	0.723

HR is given for ATG-F with ATG-T being the comparator.
Variables included in the model, determined by their significance in the univariate analysis (along with ATG type for each outcome), are as follows: OS, rDRI; HLA matching. Relapse, rDRI. NRM, HLA matching; demographics. AGVHD, HLA matching; GVHD prophylaxis type. CGVHD, Age, conditioning regimen. GRFS, rDRI, demographics.
NRM, Non-Relapse Mortality; aGVHD, Acute Graft Versus Host Disease; cGVHD, Chronic Graft Versus Host Disease; GRFS, cGVHD-free, relapse free survival.

Survival and relapse

Median follow up time of the surviving patients was 10.91 months (range 2.6-24 months). OS was not significantly affected by ATG type, gender matching, transplant source (peripheral stem cells versus bone marrow), disease status at entry to transplant and aGVHD occurrence. However, HLA mismatching and a higher rDRI had a statistically significant negative effect on OS (p=0.008, p=0.017, respectively, Log Rank test). The presence of cGVHD was correlated with a significant better OS (p<0.001, Log rank test) and with a significantly lower incidence of relapse (p=0.008, Fisher's Exact test). Using the Cox Regression model, incorporating ATG type as well as the significant pre transplant risk factors identified in the univariate analysis, donor HLA mismatching and rDRI were both associated with a significant hazard ratio for mortality (HR=1.997, 95% CI [1.120-3.562], p=0.019 and HR=1.899, 95% CI [1.070-3.372], p=0.028, respectively). Median follow up was 24 months in the ATG-T group *vs*. 21.5 months in the ATG-F group (p=0.485). At the end of follow-up, 23 patients (50%) in the ATG-T

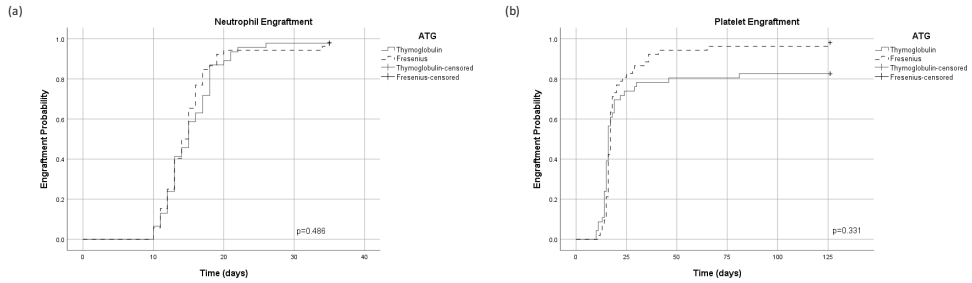

FIGURE 2
Cumulative incidence of engraftment. **(A)** Time dependent neutrophil engraftment. **(B)** Time dependent platelet engraftment.

group were alive *vs.* 27 patients (51.9%) in the ATG-F group (p=0.849). The most common cause of death in both groups was relapse, with no significant difference in the cumulative incidence of NRM (Figure 3A, p=0.854). The distribution of causes of death also did not differ between the groups (Table 2). Furthermore, there was no significant difference in the cumulative incidence of OS and relapse between the two groups (p=0.385, Figure 3B; p=0.343, Figure 3C; respectively, Log Rank and Gray's test).

No difference was found between the groups regarding overall GRFS and moderate severe cGVHD-free, Relapse free survival (p=0.108, Figure 4, p=0.919, respectively; Log Rank test).

Discussion

ATG-F has gained significant importance as GVHD prophylactic agent in patients undergoing HSCT in many centers. However, data regarding its optimal dose, as well as its efficacy and safety profile compared to ATG-T, is lacking. We present here a retrospective comparison of safety and efficacy outcomes between patients who were treated with ATG-T 10mg/kg and those who received ATG-F 15mg/kg at our medical center. We have found no significant difference in engraftment rates, cumulative risk for grade II-IV aGVHD and moderate-severe cGVHD, as well as DFS and OS. The two groups were highly comparable in demographic and baseline characteristics. However, there was a borderline significant higher incidence of HLA mismatch in the ATG-T group compared to the ATG-F group (p=0.052) and a significantly higher number of patients received single-agent cyclosporine in the ATG-T group (p<0.01). Notably, there was no difference in the rate of grade II-IV and III-IV aGVHD. Similarly to our results, other studies (as summarized in Table 4) comparing ATG-T and ATG-F at various dosing regimens did not report a disparity in GVHD incidence, either acute or chronic between the two agents (18, 23–25).

There are conflicting reports on the efficacy of ATG-T and ATG-F in cGVHD prophylaxis. The rate of moderate-severe cGVHD with low dose ATG-F in our study was similar to previous reports (16, 17). Similar to the study by Huang et al. (26), we found no difference in cGVHD between the groups. Others have reported a lower incidence of cGVHD (18, 27) and moderate-severe cGVHD (19) in the ATG-F group. The higher dosage of ATG-F (20-30mg/kg), usage of quadruple GVHD prophylaxis and a selected homogeneous donor type (MUD or haploidentical donors) in these studies may be the cause for this discrepancy.

Survival analysis showed no significant differences in the cumulative incidence of OS or relapse between the two ATG prophylactic groups (p=0.385, p=0.343). Our findings align with previous studies conducted by Huang et al., Polverelli et al. and Zhou et al. showing a similar OS in patients undergoing HSCT from MUD (in the two first studies) and Haploidentical donors (in the latter study) treated with ATG-T versus ATG-F at various doses (10mg/kg, 7.5mg/kg, 7.5mg/kg and ATG-F 20mg/kg, 30mg/kg, 20 mg/kg, respectively) (18, 19, 28). In accordance with previously reported cohorts (20, 26, 27), we have observed that HLA mismatching and a higher rDRI are associated with lower OS in the entire cohort. In addition, cGVHD was associated with a

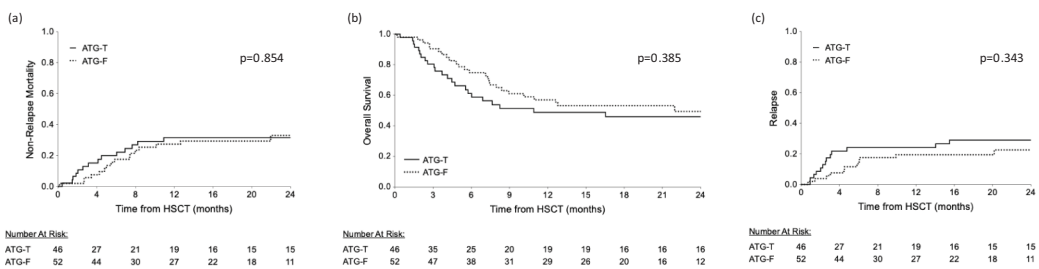

FIGURE 3
Cumulative survival rates. Similar survival rates are shown between the ATG-T and ATG-F groups. **(A)** relapse free survival and **(B)** overall survival and **(C)** relapse comparisons between the groups.

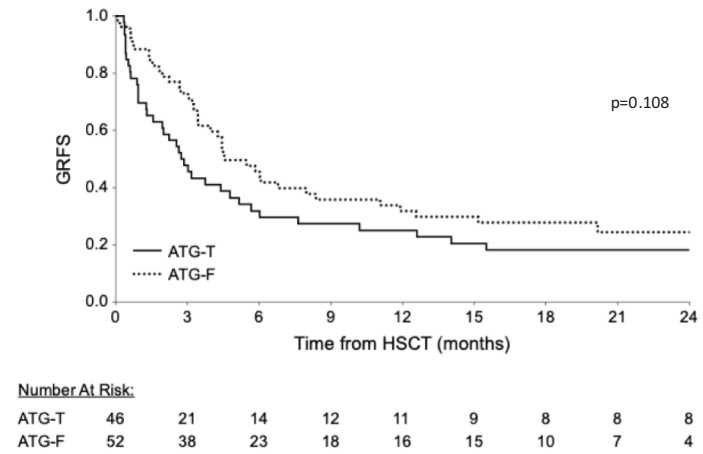

FIGURE 4
Cumulative GVHD Relapse Free Survival (GRFS). Similar cumulative GRFS are shown between the groups.

favorable effect on OS and with a reduced incidence of relapse, consistent with previous literature linking between the graft-versus-leukemia (GVL) effect and cGVHD (27, 29).

We did not observe any significant difference in NRM, in accordance with previous studies. GRFS and moderate-severe chronic GRFS did not differ, contrary to Polverelli et al. (19), who found a statistically significant advantage to ATG-F administered in higher doses, in moderate-severe cGVHD-relapse-free survival, (p=0.042). In our study, safety analysis signals were limited to a higher incidence of EBV DNA viremia in the ATG-T group. Use of ATG is a known risk factor for EBV viremia and PTLD (30, 31). However, similar to previous reports, we have observed an exceptionally low incidence of PTLD (1%), with only one patient in the ATG-T group developing PTLD. Studies have indicated a dose-dependent risk, with reported viremia rate of 31% and EBV-associated disease rate of 29% in ATG-T dose of 7-8mg/kg and up to 50% viremia in doses above 10mg/kg (32). Similar to our findings, others have also reported a trend towards a higher rate of EBV viremia with ATG-T (7.5mg/kg) compared with ATG-F (20mg/kg) (28). No significant differences in other infectious complications were found between the groups, including CMV reactivation and disease, and bacteremia, consistent with other studies comparing ATG-T and ATG-F (18, 19, 28).

This study is limited by its retrospective nature, a relatively small cohort size, variability in hematological underlying disorders, and the comparison between different time periods. The comparison of different ATG types inherently involves distinct time periods, during which transplant practices, supportive care measures, and outcomes may have evolved. While the follow-up period was standardized to ensure comparability, we acknowledge that changes over time in transplant protocols and patient care could have influenced outcomes.

The ATG dosing strategies in our study were based on institutional practices during the respective time periods, reflecting evolving evidence and clinical safety concerns. While lower-dose ATG-F (15 mg/kg) was chosen to mitigate the risk of infectious complications and relapse, it remains below the doses traditionally used in earlier studies. Furthermore, ATG dosing was not based on pharmacokinetics or absolute lymphocyte counts, as suggested by recent studies.

However, to the best of our knowledge this is the first report comparing low dose ATG-F (15mg/kg) with ATG-T at a dose of 10mg/kg. Moreover, there is a relatively high incidence of grade III-IV acute GVHD in both study groups. This can be attributed to the lower utilization of methotrexate (MTX) in our standard GVHD prophylaxis protocol during the documented years. Furthermore, donor lymphocyte exposure to ATG plays a pivotal role in GVHD risk. Unfortunately, our study did not encompass pharmacokinetic measurements, preventing us from investigating this critical factor thoroughly. Admiraal and colleagues' study suggested that customizing ATG dosing based on absolute lymphocyte counts may yield superior target achievement when compared to weight-based dosing (33). These limitations pose challenges on the generalizability of our findings.

Despite these limitations, the lack of adverse signals in our study is encouraging and suggests that the use of low dose ATG-F for GVHD prophylaxis, at a dose of 15mg/kg, is safe. Nonetheless, to draw definitive conclusions and establish the optimal type and dose of ATG for GVHD prophylaxis, a randomized controlled prospective study is needed. Such a study should incorporate MTX in MA GVHD prophylaxis protocols and include comprehensive pharmacokinetic assessments of ATG. This would allow for precise evaluation of the relationship between ATG exposure, absolute lymphocyte counts, and clinical outcomes such as GVHD incidence, relapse rate, and overall survival. Furthermore, post-transplant Cyclophosphamide (PT-Cy) has emerged as a promising agent for GVHD-prophylaxis. Retrospective studies have compared ATG to PT-Cy (34, 35) showing conflicting results. Strategies combining ATG and PT-Cy have been the subject of recent investigation (36). In haploidentical or unrelated donor settings, the addition of reduced doses of PT-Cy to ATG has shown promise. These findings suggest that the combination of ATG and PT-Cy can be a valuable strategy emphasizing the need to define the dosage and type of administered ATG.

TABLE 4 Summary of published data regarding ATG-T and ATG-F.

First author name	Type of paper (retrospective vs prospective; single Vs. multicenter: phase 1,2, or 3: randomized vs. nonrandomized)	PBSC vs. BM	Donor type (MSD vs. MUD vs. Haplo vs. cord blood)	ATG Thymo dosage and no. of patients	ATG Fresenius dosage And no. of patients	Non-relapse mortality results	Infections	Acute GVHD incidence	Ch GVHD incidence	Relapse Incidence	Event free surviva	Overall survival
Wang L 2023 (25)	Single center retrospective	PBSC	MUD and MMUD	10 mg/kg n=107	20 mg/kg N=79	Similar rates of NRM	Higher rate of CMV viremia in ATG-T group 64.6% vs. 29.9%, p<0.001	Similar rates of aGVHD	Lower incidence of extensive cGVHD with ATG-T (p=0.01, HR=0.41)	Similar cumulative incidence of relapse.	Similar recurrence-free survival	Similar OS
Zhou L. 2020 (28)	Single center retrospective	Mixed	Haplo	7.5 MG/ KG N=81	20 MG/ KG N=35	Similar rates of TRM	Similar incidence of EBV infections	Similar rates of aGVHD	The cumulative incidence of any grade and limited cGVHD was higher in the ATG-T group (66% vs. 56% p=0.002 and 61.4 vs. 53.5%, p=0.007, respectively)	Similar cumulative incidence of relapse mortality	-	Similar OS (p=0.421)
Polverelli N. 2018 (19)	Single center retrospective	Both	MUD	7.5 MG/ KG N=31	30 MG/ KG N=46	Similar cumulative incidence of TRM	Similar infection rates	Similar rates of aGVHD	Similar rates of overall cGVHD but higher incidence of moderate- severe cVVHD in ATG-T (23% vs 8% p=0.03)	Similar RI	Similar DFS	Similar OS (p=0.58)
Huang W. 2016 (18)	Single center retrospective	PBSC	MUD	10 MG/ KG N=56	20 MG/ KG N=54	No significant differences between the groups in the 100-day or 3-year TRM rate	Similar infection rates	similar rates of aGVHD	lower rate of cGVHD in the ATG-F group (15% VS 33% respectively: p = 0.04)	Non-significant lower relapse rates in the ATG-F group and 5 years follow-up (20% vs 35% p=0.08 and 20% vs 40%; p=0.07, respectively)	ATG-T:3-y and 5-y DFS were 48% and 45% ATG-F- 67% and 67% p = 0.07 and p = 0.06	Similar 3y and 5 OS 58 vs 68%
Huang W. 2015 (26)	Single center retrospective	PBSC	MMUD	10 mg/ kg N=23	20 mg/ kg N=28	Similar NRM	Similar infection rates	Similar rates of aGVHD	Similar rates of cGVHD	Similar RI	Non-significant higher DFS	3-year OS rate was similar.

(Continued)

10.3389/fimmu.2025.1526513

TABLE 4 Continued

First author name	Type of paper (retrospective vs prospective; single Vs. multicenter: phase 1,2, or 3: randomized vs. nonrandomized)	PBSC vs. BM	Donor type (MSD vs. MUD vs. Haplo vs. cord blood)	ATG Thymo dosage and no. of patients	ATG Fresenius dosage And no. of patients	Non-relapse mortality results	Infections	Acute GVHD incidence	Ch GVHD incidence	Relapse Incidence	Event free surviva	Overall survival
											rate in the ATG-F group, (45.7% vs 61.3%, p=0.08)	
Paiano S. 2015 (24)	Single center retrospective	Both	Related, MUD, MMUD	7.5 MG/ KG N=15	20 MG/ KG N=15	Similar rates of TRM	Similar infection rates	Similar rates of aGVHD	Similar rates of cGVHD	Similar cumulative relapse incidence	Similar DFS	Similar OS
Basara N 2005 (23)	Multicenter retrospective	Both	MUD and MMUD	15 mg/kg (n=3), 10 mg/ kg (n=28), 7.5 mg/kg (n=6), mg/kg (n=12)	45 mg/kg (n=11), 60 mg/ kg (n=27)	Similar rates of TRM	-	Similar rates of aGVHD	The use of ATG-F was associated with lower incidence of cGVHD (p=0.05) which was not confirmed in multivariate analysis.		Projected 3-year LFS was higher in the ATG-F group (38% vs 21%, p=0.003)	OS was not

MUD, matched unrelated donor; MSD, matched sibling donor; NRM, non-relapse mortality; TRM, treatment-related mortality; RI, relapse incidience; GVHD, graft vs host disease.

10.3389/fimmu.2025.1526513

In summary, while this study provides valuable insights into the safety and efficacy of low-dose ATG-F compared to ATG-T, further research is needed to validate these findings and guide clinical decision-making effectively. Prospective studies with larger patient cohorts and controlled designs will help to better understand the potential benefits and risks of different ATG dosing regimens for GVHD prophylaxis in hematopoietic stem cell transplantation.

Data availability statement

The original contributions presented in the study are included in the article/supplementary material. Further inquiries can be directed to the corresponding authors.

Ethics statement

The studies involving humans were approved by Hadassah University Hospital ethical committee (approval no. 0608-20-HMO). The studies were conducted in accordance with the local legislation and institutional requirements. The ethics committee/institutional review board waived the requirement of written informed consent for participation from the participants or the participants' legal guardians/next of kin because Retrospective analysis of standard of care, no identifiables.

Author contributions

IF: Formal analysis, Writing – original draft, Data curation. BN: Formal analysis, Writing – original draft, Methodology, Writing – review & editing. SE: Writing – review & editing. EZ: Writing – review & editing. AS: Writing – review & editing. PS: Writing – review & editing. BA: Conceptualization, Formal analysis, Writing – original draft, Writing – review & editing. SG: Conceptualization, Formal analysis, Writing – original draft, Writing – review & editing.

Funding

The author(s) declare that no financial support was received for the research, authorship, and/or publication of this article.

Conflict of interest

The authors declare that the research was conducted in the absence of any commercial or financial relationships that could be construed as a potential conflict of interest.

Generative AI statement

The author(s) declare that no Generative AI was used in the creation of this manuscript.

Publisher's note

References

1. Mohty M. Mechanisms of action of antithymocyte globulin: T-cell depletion and beyond. *Leukemia*. (2007) 21:1387–94. doi: 10.1038/sj.leu.2404683

2. Wolschke C, Zabelina T, Ayuk F, Alchalby H, Berger J, Klyuchnikov E, et al. Effective prevention of GVHD using *in vivo* T-cell depletion with anti-lymphocyte globulin in HLA-identical or -mismatched sibling peripheral blood stem cell transplantation. *Bone Marrow Transpl.* (2014) 49:126–30. doi: 10.1038/bmt.2013.143

3. Bacigalupo A, Lamparelli T, Bruzzi P, Guidi S, Alessandrino PE, di Bartolomeo P, et al. Antithymocyte globulin for graft-versus-host disease prophylaxis in transplants from unrelated donors: 2 randomized studies from Gruppo Italiano Trapianti Midollo Osseo (GITMO). *Blood*. (2001) 98:2942–7. doi: 10.1182/blood.V98.10.2942

4. Finke J, Bethge WA, Schmoor C, Ottinger HD, Stelljes M, Zander AR, et al. Standard graft-versus-host disease prophylaxis with or without anti-T-cell globulin in haematopoietic cell transplantation from matched unrelated donors: a randomised, open-label, multicentre phase 3 trial. *Lancet Oncol.* (2009) 10:855–64. doi: 10.1016/S1470-2045(09)70225-6

5. Walker I, Panzarella T, Couban S, Couture F, Devins G, Elemary M, et al. Pretreatment with anti-thymocyte globulin versus no anti-thymocyte globulin in patients with haematological Malignancies undergoing haemopoietic cell transplantation from unrelated donors: a randomised, controlled, open-label, phase 3, multicentre trial. *Lancet Oncol.* (2016) 17:164–73. doi: 10.1016/S1470-2045(15)00462-3

6. Socié G, Schmoor C, Bethge WA, Ottinger HD, Stelljes M, Zander AR, et al. Chronic graft-versus-host disease: long-term results from a randomized trial on graft-versus-host disease prophylaxis with or without anti–T-cell globulin ATG-Fresenius. *Blood*. (2011) 117:6375–82. doi: 10.1182/blood-2011-01-329821

7. Kröger N, Solano C, Wolschke C, Bandini G, Patriarca F, Pini M, et al. Antilymphocyte globulin for prevention of chronic graft-versus-host disease. *N Engl J Med*. (2016) 374:43–53. doi: 10.1056/NEJMoa1506002

8. Bacigalupo A, Lamparelli T, Barisione G, Bruzzi P, Guidi S, Alessandrino PE, et al. Thymoglobulin prevents chronic graft-versus-host disease, chronic lung dysfunction, and late transplant-related mortality: long-term follow-up of a randomized trial in patients undergoing unrelated donor transplantation. *Biol Blood Marrow Transpl.* (2006) 12:560–5. doi: 10.1016/j.bbmt.2005.12.034

9. Popow I, Leitner J, Grabmeier-Pfistershammer K, Majdic O, Zlabinger GJ, Kundi M, et al. A comprehensive and quantitative analysis of the major specificities in rabbit antithymocyte globulin preparations. *Am J Transpl.* (2013) 13:3103–13. doi: 10.1111/ajt.12514

10. Oostenbrink LVE, Jol-van Der Zijde CM, Kielsen K, Jansen-Hoogendijk AM, Ifversen M, Müller KG, et al. Differential elimination of anti-thymocyte globulin of fresenius and genzyme impacts T-cell reconstitution after hematopoietic stem cell transplantation. *Front Immunol.* (2019) 10:315. doi: 10.3389/fimmu.2019.00315

11. Seo J, Shin DY, Koh Y, Kim I, Yoon SS, Min Byun J, et al. Association between preconditioning absolute lymphocyte count and transplant outcomes in patients undergoing matched unrelated donor allogeneic hematopoietic stem cell transplantation with reduced-intensity conditioning and anti-thymocyte globulin. *Ther Adv Hematol.* (2021) 12:204062072110637. doi: 10.1177/20406207211063783

12. Baron F, Mohty M, Blaise D, Socié G, Labopin M, Esteve J, et al. Anti-thymocyte globulin as graft-versus-host disease prevention in the setting of allogeneic peripheral blood stem cell transplantation: a review from the Acute Leukemia Working Party of the European Society for Blood and Marrow Transplantation. *Haematologica*. (2017) 102:224–34. doi: 10.3324/haematol.2016.148510

13. Chang YJ, Wu DP, Lai YR, Liu QF, Sun YQ, Hu J, et al. Antithymocyte globulin for matched sibling donor transplantation in patients with hematologic Malignancies: A multicenter, open-label, randomized controlled study. *J Clin Oncol*. (2020) 38:3367–76. doi: 10.1200/JCO.20.00150

14. Bonifazi F, Rubio MT, Bacigalupo A, Boelens JJ, Finke J, Greinix H, et al. Rabbit ATG/ATLG in preventing graft-versus-host disease after allogeneic stem cell transplantation: consensus-based recommendations by an international expert panel. *Bone Marrow Transpl*. (2020) 55:1093–102. doi: 10.1038/s41409-020-0792-x

15. Locatelli F, Bernardo ME, Bertaina A, Rognoni C, Comoli P, Rovelli A, et al. Efficacy of two different doses of rabbit anti-T-lymphocyte globulin to prevent graft-versus-host disease in children with haematological Malignancies transplanted from an unrelated donor: a multicentre, randomised, open-label, phase 3 trial. *Lancet Oncol*. (2017) 18:1126–36. doi: 10.1016/S1470-2045(17)30417-5

16. Bonifazi F, Bandini G, Arpinati M, Tolomelli G, Stanzani M, Motta MR, et al. Intensification of GVHD prophylaxis with low-dose ATG-F before allogeneic PBSC transplantation from HLA-identical siblings in adult patients with hematological Malignancies: results from a retrospective analysis. *Bone Marrow Transpl*. (2012) 47:1105–11. doi: 10.1038/bmt.2011.225

17. Bonifazi F, Olivieri J, Sessa M, Dan E, Sinigaglia B, Rizzi S, et al. Low-dose anti-T lymphoglobulin as prophylaxis for graft-versus-host disease in unrelated donor transplantations for acute leukemias and myelodysplastic syndromes. *Biol Blood Marrow Transplant J Am Soc Blood Marrow Transpl*. (2018) 24:2450–8. doi: 10.1016/j.bbmt.2018.07.011

18. Huang W, Yu L, Cao T, Li Y, Liu Z, Li H, et al. The efficacy and safety of rabbit anti-thymocyte globulin vs rabbit anti-T-lymphocyte globulin in peripheral blood stem cell transplantation from unrelated donors. *Leuk Lymphoma*. (2016) 57:355–63. doi: 10.3109/10428194.2015.1045901

19. Polverelli N, Malagola M, Turra A, Skert C, Perucca S, Chiarini M, et al. Comparative study on ATG-thymoglobulin versus ATG-fresenius for the graft-versus-host disease (GVHD) prophylaxis in allogeneic stem cell transplantation from matched unrelated donor: a single-centre experience over the contemporary years. *Leuk Lymphoma*. (2018) 59:2700–5. doi: 10.1080/10428194.2018.1439584

20. Harris AC, Young R, Devine S, Hogan WJ, Ayuk F, Bunworasate U, et al. International, multicenter standardization of acute graft-versus-host disease clinical data collection: A report from the Mount Sinai acute GVHD international consortium. *Biol Blood Marrow Transplant J Am Soc Blood Marrow Transpl*. (2016) 22:4–10. doi: 10.1016/j.bbmt.2015.09.001

21. Schoemans HM, Lee SJ, Ferrara JL, Wolff D, Levine JE, Schultz KR, et al. EBMT-NIH-CIBMTR Task Force position statement on standardized terminology & guidance for graft-versus-host disease assessment. *Bone Marrow Transpl*. (2018) 53:1401–15. doi: 10.1038/s41409-018-0204-7

22. Armand P, Kim HT, Logan BR, Wang Z, Alyea EP, Kalaycio ME, et al. Validation and refinement of the Disease Risk Index for allogeneic stem cell transplantation. *Blood*. (2014) 123:3664–71. doi: 10.1182/blood-2014-01-552984

23. Basara N, Baurmann H, Kolbe K, Yaman A, Labopin M, Burchardt A, et al. Antithymocyte globulin for the prevention of graft-versus-host disease after unrelated hematopoietic stem cell transplantation for acute myeloid leukemia: results from the multicenter German cooperative study group. *Bone Marrow Transpl*. (2005) 35:1011–8. doi: 10.1038/sj.bmt.1704957

24. Paiano S, Roosnek E, Tirefort Y, Nagy-Hulliger M, Masouridi S, Levrat E, et al. Comparing two types of rabbit ATG prior to reduced intensity conditioning allogeneic hematopoietic SCT for hematologic Malignancies. *Bone Marrow Res*. (2015) 2015:980924. doi: 10.1155/2015/980924

25. Wang L, Kong P, Zhang C, Gao L, Zhu L, Liu J, et al. Outcomes of patients with hematological Malignancies who undergo unrelated donor hematopoietic stem cell transplantation with ATG-Fresenius versus ATG-Genzyme. *Ann Hematol*. (2023) 102:1569–79. doi: 10.1007/s00277-023-05220-7

26. Huang W, Zhao X, Tian Y, Cao T, Li Y, Liu Z, et al. Outcomes of peripheral blood stem cell transplantation patients from HLA-mismatched unrelated donor with antithymocyte globulin (ATG)-Thymoglobulin versus ATG-Fresenius: a single-center study. *Med Oncol*. (2015) 32:32. doi: 10.1007/s12032-014-0465-y

27. Baron F, Labopin M, Niederwieser D, Vigouroux S, Cornelissen JJ, Malm C, et al. Impact of graft-versus-host disease after reduced-intensity conditioning allogeneic stem cell transplantation for acute myeloid leukemia: a report from the Acute Leukemia Working Party of the European group for blood and marrow transplantation. *Leukemia*. (2012) 26:2462–8. doi: 10.1038/leu.2012.135

28. Zhou L, Gao Zy, Lu Dp. Comparison of ATG-thymoglobulin with ATG-Fresenius for Epstein-Barr virus infections and graft-versus-host-disease in patients with hematological Malignances after haploidentical hematopoietic stem cell transplantation: a single-center experience. *Ann Hematol*. (2020) 99:1389–400. doi: 10.1007/s00277-020-04014-5

29. Storb R, Gyurkocza B, Storer BE, Sorror ML, Blume K, Niederwieser D, et al. Graft-versus-host disease and graft-versus-tumor effects after allogeneic hematopoietic cell transplantation. *J Clin Oncol Off J Am Soc Clin Oncol*. (2013) 31:1530–8. doi: 10.1200/JCO.2012.45.0247

30. Lindsay J, Othman J, Yong MK, Ritchie D, Chee L, Tay K, et al. Dynamics of Epstein-Barr virus on post-transplant lymphoproliferative disorders after antithymocyte globulin-conditioned allogeneic hematopoietic cell transplant. *Transpl Infect Dis Off J Transplant Soc*. (2021) 23:e13719. doi: 10.1111/tid.13719

31. Landgren O, Gilbert ES, Rizzo JD, Socié G, Banks PM, Sobocinski KA, et al. Risk factors for lymphoproliferative disorders after allogeneic hematopoietic cell transplantation. *Blood*. (2009) 113:4992–5001. doi: 10.1182/blood-2008-09-178046

32. Yu Gp, Liu Q, Sun J, Xuan L, Wu M, Liu X, et al. Effect of antithymocyte globulin dosage for prophylactic Gvhd on Epstein-Barr virus reactivation and diseases in allogeneic hematopoietic stem cell transplantation. *Blood*. (2012) 120:4486–6. doi: 10.1182/blood.V120.21.4486.4486

33. Admiraal R, Nierkens S, de Witte MA, Petersen EJ, Fleurke GJ, Verrest L, et al. Association between anti-thymocyte globulin exposure and survival outcomes in adult unrelated haemopoietic cell transplantation: a multicentre, retrospective, pharmacodynamic cohort analysis. *Lancet Haematol*. (2017) 4:e183–91. doi: 10.1016/S2352-3026(17)30029-7

34. Brissot E, Labopin M, Moiseev I, Cornelissen JJ, Meijer E, Van Gorkom G, et al. Post-transplant cyclophosphamide versus antithymocyte globulin in patients with acute myeloid leukemia in first complete remission undergoing allogeneic stem cell transplantation from 10/10 HLA-matched unrelated donors. *J Hematol OncolJ Hematol Oncol*. (2020) 13:87. doi: 10.1186/s13045-020-00923-0

35. Nykolyszyn C, Granata A, Pagliardini T, Castagna L, Harbi S, Bouabdallah R, et al. Posttransplantation cyclophosphamide vs. antithymocyte globulin as GVHD prophylaxis for mismatched unrelated hematopoietic stem cell transplantation. *Bone Marrow Transpl*. (2020) 55:349–55. doi: 10.1038/s41409-019-0682-2

36. Duléry R, Brissot E, Mohty M. Combining post-transplant cyclophosphamide with antithymocyte globulin for graft-versus-host disease prophylaxis in hematological Malignancies. *Blood Rev*. (2023) 62:101080. doi: 10.1016/j.blre.2023.101080

frontiers | Frontiers in Immunology

TYPE Hypothesis and Theory
PUBLISHED 10 April 2025
DOI 10.3389/fimmu.2025.1563685

OPEN ACCESS

EDITED BY
Rita Maccario,
San Matteo Hospital Foundation (IRCCS), Italy

REVIEWED BY
Luigi Nespoli,
University of Insubria, Italy
CarloAlberto Redi,
University of Pavia, Italy

*CORRESPONDENCE
Baruch Rinkevich
buki@ocean.org.il

RECEIVED 20 January 2025
ACCEPTED 25 March 2025
PUBLISHED 10 April 2025

CITATION
Rinkevich B (2025) From seabed to sickbed: lessons gained from allorecognition in marine invertebrates.
Front. Immunol. 16:1563685.
doi: 10.3389/fimmu.2025.1563685

From seabed to sickbed: lessons gained from allorecognition in marine invertebrates

Baruch Rinkevich*

Department of Marine Biology, Israel Oceanographic & Limnological Research, National Institute of Oceanography, Haifa, Israel

Despite decades of progress, long-term outcomes in human organ transplantation remain challenging. Functional decline in transplanted organs has stagnated over the past two decades, with most patients requiring lifelong immunosuppression, therapies that overlook the principles of self/non-self recognition and natural transplantation events in humans. To address these discrepancies, this perspective proposes that immunity evolved not as pathogen-driven but as a mechanism to preserve individuality by preventing invasion from parasitic conspecific cells. It further reveals that the concept of "self/non-self" recognition encompasses multiple theories with complex and often ambiguous terminology, lacking precise definitions. In comparisons, natural historecognition reactions in sessile marine invertebrates are regulated by a wide spectrum of precise and specific allorecognition systems, with transitive and non-transitive hierarchies. Using the coral Stylophora pistillata and the ascidian Botryllus schlosseri as models, it is evident these organisms distinguish 'self' from 'non-self' with remarkable accuracy across various allogeneic combinations, identifying each non-self entity while simultaneously recognizing selfhood through transitive allogeneic hierarchies. Their allorecognition offers an improved explanation for post-transplant outcomes by accounting for the natural dynamic, spatiotemporal evolution of selfhood. To bridge natural (in invertebrates and humans alike) and clinical transplantation phenomena, the 'allorecognition landscape' (AL) metaphor is proposed. This unified framework conceptualizes self/non-self recognition as shaped by two dynamic continuums of 'self' and 'non-self' nature. Throughout the patient lifespan, the AL represents diverse and transient arrays of specific 'self' and 'non-self' states (including reciprocal states) that shift over time in either recognition direction, requiring adaptable clinical strategies to address their evolving nature.

KEYWORDS

marine invertebrates, fusion, allorecognition landscape, chimerism, corals, tunicates, self/non-self recognition, organ transplantation

1 Introduction

Human organ transplantation represents a pinnacle of modern medicine, integrating advancements in immunology, genetics, pharmacology, and surgery into a highly successful discipline. Driven by the goal of extending life and improving human well-being, this field focuses on restoring functions through the deliberate replacement of damaged organs. Started about seven decades ago (1), organ transplantation has become a routine part of medical practice worldwide, often celebrated in mainstream media for its advancements. Yet, despite significant progress in unraveling the complex immune cascades and molecular interactions involved in transplantation, major challenges remain. Long-term outcomes for transplanted organs have seen little improvement, with functional decline rates remaining largely unchanged over the past two decades (2, 3), while most patients depend on lifelong immunosuppressive therapy, as withdrawal typically leads to allograft rejection. Clearly, improving long-term graft survival necessitates a deeper understanding of transplant injury mechanisms, alongside innovative research approaches and fresh perspectives that could drive transformative advancements in knowledge, practices, and technologies. Here I emphasize the importance of exploring allogeneic mechanisms underlying 'self' vs. 'non-self' recognition, extending beyond the conventional focus on mammalian systems.

Historically, organ rejection has been attributed primarily to adaptive immunity, including T-cell-mediated and antibody-mediated rejection. However, recent studies have uncovered the critical role of innate immunity, such as missing-self activation of natural killer (NK) cells and monocyte-driven allorecognition (4, 5). These findings underscore the importance of innate immunity in initiating early immune responses to transplanted allografts and contributing to late-stage chronic rejection. Additionally, they challenge the long-standing immunological paradigm that regards innate immunity as merely a downstream effector mechanism activated by adaptive immune responses during graft rejection (5, 6). While the adaptive immune system, primarily evolved for infection defense, is both necessary and sufficient for transplant rejection, the specific pathways of innate immunity involved remain poorly understood. Notably, rejection-associated alloimmunity appears largely independent of the signaling mechanisms underlying antimicrobial immunity (7). A similar ambiguity surrounds the mechanisms of graft-versus-host disease (GVHD), a major contributor to morbidity and mortality following allogeneic hematopoietic stem cell transplantation (8).

Yet, current treatment approaches primarily target adaptive immune responses, with limited attention to innate immunity (6). This highlights the need for a deeper understanding of innate immunity in organ transplantation and the development of innovative approaches to address acute and chronic organ rejection effectively. A refined scholarly approach could shift focus from detailed molecular pathways and cellular mechanisms of rejection to exploring the fundamental processes of 'self/non-self' recognition. Adopting this view, studying the natural transplantation in marine invertebrates and the semi-allogeneic nature of vertebrate pregnancies offer promising avenues. Such studies may uncover universal principles, shed light on the evolutionary roots of alloimmunity, and reveal homologous kinships across species, ultimately transforming our understanding and approach to.

2 The evolutionary roots for the immune system

Defense against microbial pathogens is a universal trait among all metazoans. In invertebrates, innate immunity serves as the primary defense mechanism, and many of its features have been conserved, in various forms, within vertebrates (9, 10). The hallmark of innate immunity is its reliance on germline-encoded receptors to identify harmful elements, whereas vertebrate adaptive immunity depends on gene rearrangement to generate its repertoire. Despite their differences, both types of immune systems participate in a wide range of biological processes (9–11), while employing diverse tools to combat pathogens. This has led to the dominant paradigm, reflected in immunology textbooks, that immune recognition and its associated effector mechanisms evolved primarily to combat infectious agents. The adaptive immune system's effectiveness in neutralizing pathogens supports this view. However, evidence suggests that pathogens are not necessary to explain the high levels of polymorphism observed in immune systems (12). Additionally, all vertebrates and studied invertebrates exhibit allorecognition, using their immune systems to effectively reject allografts. Interestingly, this phenomenon does not naturally occur in adult vertebrates, presenting an intriguing evolutionary paradox (10).

To address this evolutionary paradox, we can explore alternative perspectives that challenge the prevailing view that vertebrate immunity evolved primarily to combat pathogens. One possibility is that vertebrate innate immunity may have originally served a different function in ancestral organisms. It may persist today as a relic or vestige of ancient systems that became redundant with the emergence of adaptive immunity (13, 14), or as an "evolutionary rudiment" whose sole role is to manage infections until the more robust adaptive immune response is activate (15). Another perspective suggests that vertebrate adaptive immunity may have co-opted an ancient polymorphic gene family encoding cell surface interaction molecules (16). For instance, molecules with multiple Ig-like domains, which emerged early in eukaryotic evolution, are present in yeast a-agglutinin cell wall proteins (17), in the extracellular domain of receptor tyrosine kinase in the marine sponge *Geodia cydonium* (18), or that marine invertebrates from disparate phyla reveal highly conserved immune machinery (19). A third perspective posits that the immune system's original function was to preserve individuality. This involved preventing the intrusion of conspecific alien cells into the soma and germline or eliminating newly introduced somatic mutations. An organism incapable of controlling the proliferation of somatic variants or alien conspecific cells could effectively be parasitized by these

lineages. In this framework, pathogen defense may have evolved later, giving rise to the diverse immune phenomena observed today (9, 10). This perspective, prioritizing individuality preservation, necessitates acknowledging naturally occurring transplantation events in vertebrates. It challenges the conventional view that vertebrate and human allograft reactions are purely artificial phenomena. Examples of natural transplantation in humans include fetal implantation, early fusions of dizygotic twins, and the persistence of fetal cells in the maternal bloodstream decades postpartum (9, 20, 21). I align with this third proposal.

Vertebrates robustly reject any allogeneic transplanted tissue, demonstrating strong defenses against events that do not occur naturally, yet fail to prevent the lifelong establishment of various natural transplantation events. Therefore, rather than the typical comparison of invertebrate and vertebrate immune systems based on innate versus adaptive responses to pathogens, greater focus should be placed on evaluating allorecognition as a potential shared foundational system underlying the evolution of diverse immune mechanisms. Organ transplantation, while not a natural phenomenon, should be considered within the broader context of innate allorecognition responses and their unresolved mysteries.

3 Self versus non-self recognition

A prominent perspective on the evolutionary pressures shaping the immune system is the concept of immunologic surveillance, introduced over six decades ago (22). This framework posits that host organisms are perpetually exposed to external pathogenic threats, driving the evolution of immune systems to distinguish and defend against harmful intruders. As a result, immunity is often framed as the ability to differentiate "self" from "non-self," serving as a foundational guideline in immunology. Yet, the "self/non-self" paradigm, while widely referenced, lacks inherent clarity and functions more as a guiding framework for exploring identity (23), at all levels of the 'units of selection' (24). Despite the precision of self–nonself recognition system (25), this concept remains entangled in semantic ambiguities, analogies, and complex theorizing, with limited clarity provided by scientific discourse (26).

The diverse expressions of "self/non-self" recognition in mammalian systems and the extensive study of this topic have led to years of detailed examination, resulting in numerous viewpoints and the emergence of complex terminology. Without delving into an historical account, the two decades following Burnet's (22) suggestion of self-recognition in marine invertebrates, saw a proliferation of perspectives on the "self/non-self" paradigm in vertebrates. These included Janeway's (27) theory that the immune system evolved to distinguish "infectious nonself" from "noninfectious self", the 'peptidic self model (28), the "liquid self" (29), the 'high determinant density' idea for alloreactivity (30), the Kärre's 'missing self' model (31) and Versteeg's (32) proposition that the immune system incorporates elements for recognizing both self and nonself. Other perspectives include Daunter's (33) distinction between "self-foreignness" and "foreignness per se" and Matzinger's (34) 'danger signals' theory, which suggests that immune responses are triggered not by "non-self" or "infectious non-self" but by the detection of "danger signals" by the host. These and other diverse ideas highlight the complexity and ongoing evolution of our understanding of immune system function. Additionally, popular yet often ambiguous terms such as 'pattern recognition receptors' (PRRs), 'pathogen-associated molecular patterns' (PAMPs), and 'damage-associated molecular patterns' (DAMPs) have emerged in discussions of self/non-self recognition. While widely adopted, these terms frequently lack precise definitions, reflecting the inherent ambiguity and implicit assumptions in scientific terminology. Moreover, in recent years, the traditional discussions on immune self versus non-self mechanisms have expanded to include processes such as the discrimination involved in spacer selection for palindromic repeats (CRISPR) and CRISPR-associated (Cas) proteins in prokaryotes (35, 36), to anti-cancer therapies (37–41), vaccine development (42), autoimmune diseases (43), the recognition of foreign nucleic acids (44, 45), and towards artificial immune systems (46).

Historecognition systems are well-documented across various marine invertebrate phyla, especially among sessile organisms like sponges, cnidarians, bryozoans, and tunicates. For sessile marine invertebrates, physical space is often limited. As these organisms expand, they may come into contact with specimens of other species as well as non-kin conspecifics. These tissue-to-tissue interactions are often regulated by self/non-self recognition systems, where high levels of label diversity improve recognition accuracy. The distinction between 'self' and 'non-self' is made either by detecting the presence or absence of self-defining attributes or by identifying nonself-specific attributes (47, 48). To confirm the existence of alloimmunity in invertebrates, Hildemann et al. (49) proposed three key criteria: the expression of antagonistic reactions, demonstration of specific responses, and the ability to induce memory, all of which should be interrelated. Building on this, Janeway (50) introduced three additional criteria for a biological system to be classified as an immune system: the ability to precisely distinguish between self and non-self, the targeted generation of effector responses against non-self molecules, and the capacity to regulate these responses effectively. These criteria have spurred numerous studies across a wide range of invertebrate species and phyla. However, the concept of immune "self" in these studies, as well as in the broader literature, remains undefined due to its conceptual and mechanistic ambiguity [but see some attempts (51, 52)].

Specific responses lead to allorecognition transitivity among conspecifics when more than two partners are involved. The simplest scenario reflects three conspecifics (A, B, C) that are tested for fusion/rejection phenomena. Transitivity is confirmed when (= for fusion; ≠for rejection): A = B and B = C, then A = C, or when A = B but A ≠ C, then B ≠ C. Nontransitive relationships occur when A = B, A = C, but B ≠ C. Specific hierarchies are established when A > B and B > C, leading to A > C for a linear hierarchy, or A < C for a circular hierarchy (Figure 1) (47, 53).

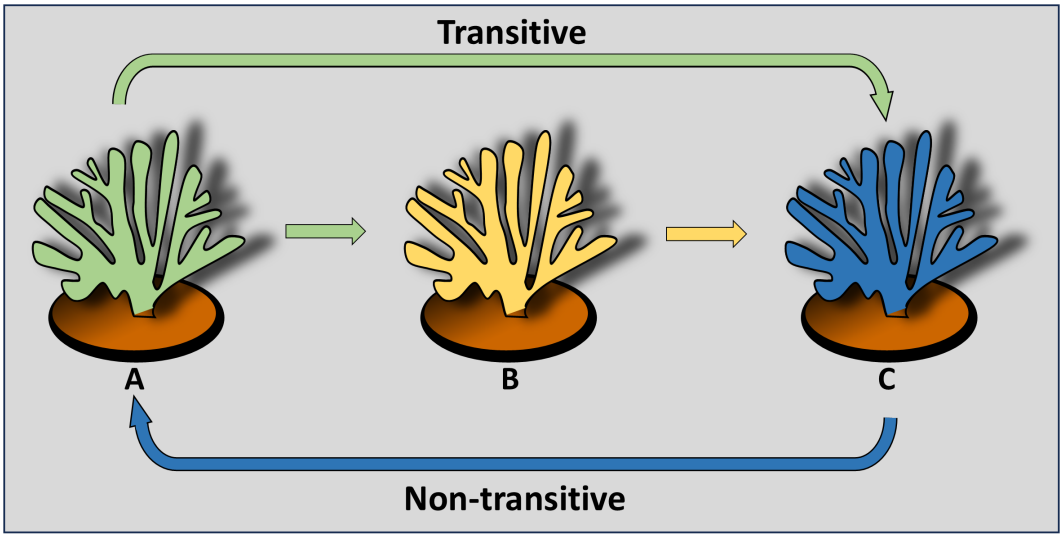

FIGURE 1
A cartoon depicting the simplest transitive (linear) and non-transitive (circular) allorecognition relationships among three conspecifics (the various colors) of the hermatypic coral *Stylophora pistillata* (Figure 2a). The colored arrows depict directionality and hierarchy of rejection outcomes.

4 What can allorecognition in marine invertebrates teach us?

To clarify the concept of allorecognition in marine invertebrates, I will elaborate alloimmunity in two representative species, one from the anthozoan basal phylum, the common Indo Pacific branching coral *Stylophora pistillata* (Figure 2a) (54) and the second from the highly evolved urochordates, the cosmopolitan colonial ascidian *Botryllus schlosseri* (Figure 2b) (55).

While the genetic background of *S. pistillata* has not yet been fully characterized, it is known that adult genotypes never fuse, and fusion occurs only during early life stages (0–4 months old spats). Juvenile colonies with shared parentage (kin) display higher fusion rates compared to unrelated colonies, emphasizing the role of genetic relatedness in fusion outcomes (56–58). Iso-grafts always fused where allografts resulted with a wide range of incompatible responses (Figure 3) (59–61). In *B. schlosseri*, both adults and young colonies can fuse. This allorecognition is genetically controlled by a single haplotype, called *BHF* (62), which determines compatibility and allows vascular fusion among individuals. Incompatibility, on the other hand, triggers inflammatory rejection responses. The *BHF* locus exhibits extraordinary polymorphism, with 100–300 codominantly expressed alleles per population. A colony can fuse with another colony that shares at least one of its two *BHF* alleles, even if the second allele or the rest of the genome differs. However,

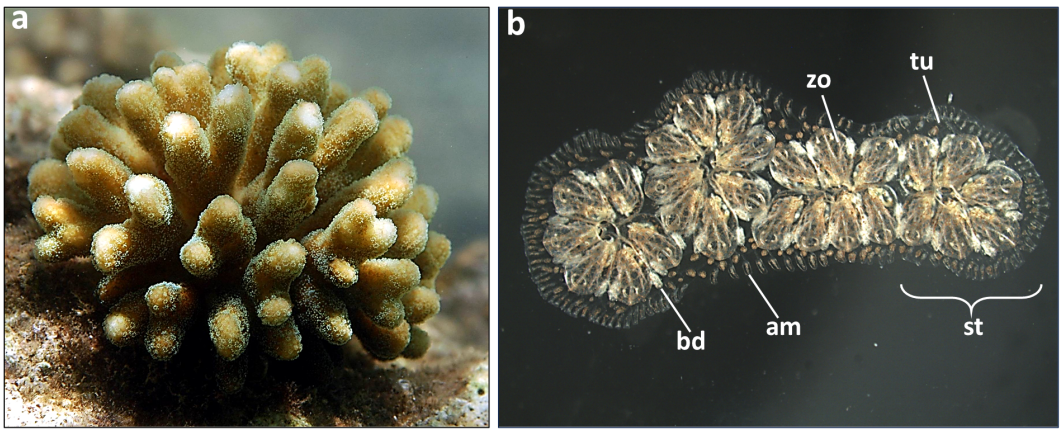

FIGURE 2
The two representative marine invertebrates: **(a)** a colony of the branching coral *Stylophora pistillata* growing in the field; **(b)** a colony of the tunicate *Botryllus schlosseri* growing in the laboratory on a glass slide. Zooids (zo, each 2 mm long) form star-shaped clusters (system, st), each with a centered shared atrial siphon. The zooids are embedded in a transparent tunic(tu) containing vessels and terminal ampullae (am) of the colonial circulatory system. Buds (bd) are partially covered by adult zooids.

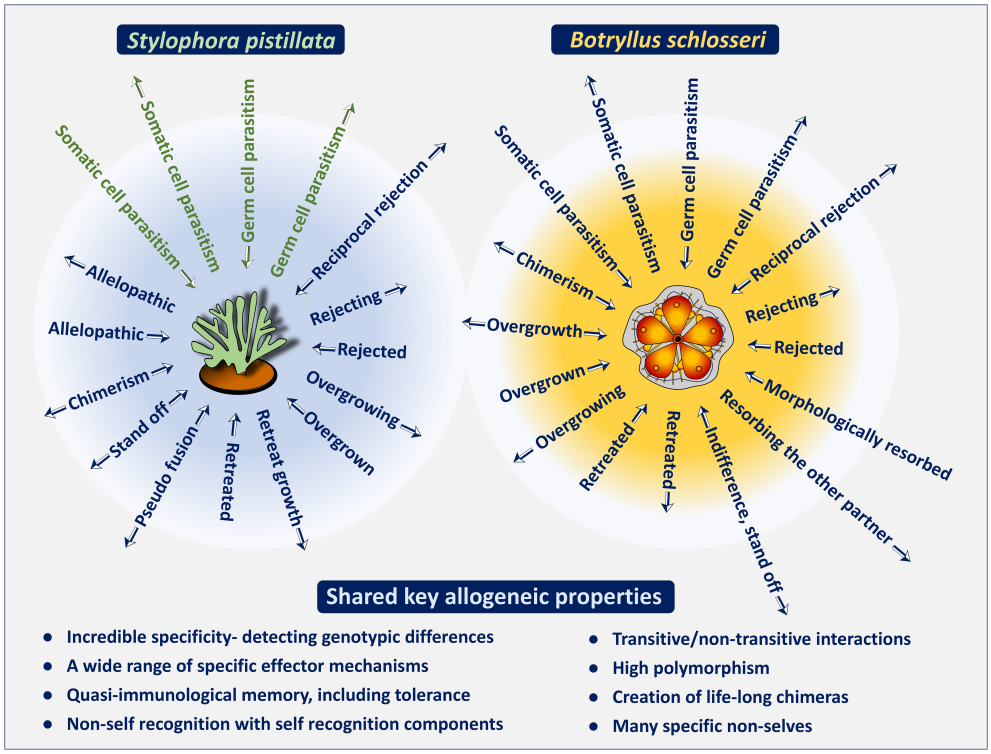

FIGURE 3
A schematic illustration showcasing the remarkable diversity and precise specificity of historecognition in the Cnidaria (represented by *Stylophora pistillata*; left panel) and in the Tunicata (represented by *Botryllus schlosseri*; right panel). Colonies of these marine invertebrates are naturally encountered in various allogeneic responses (arrowheads reveal hierarchies for the effector arms). A single invertebrate genotype is not restricted to a single mode of interaction during allogeneic encounters, thus its extensive repertoire of effector mechanisms allows for precise and specific responses to an unlimited range of 'nonself' attributes. At the bottom: shared key allogeneic properties. The *S. pistillata* green allogeneic interactions- suggested, not yet approved.

colonies that reject each other lack any shared *BHF* allele, even if their genomes are highly similar (9, 63–66).

As proposed by Hildemann et al. (49) the demonstration of specific activity is a key criterion for establishing allorecognition, which is an inherent feature in both representative species. In *S. pistillata* [as well as in other coral species, e.g (53, 60, 67)], studies have shown the nontransitive nature of their effector mechanisms. In these nontransitive hierarchies, a colony that dominates in one interaction may be subordinate or equal in aggression to another colony that underperforms in the previous interaction (Figure 1). Additionally, colonies could specifically distinguish between neighbors and respond differently to allogeneic and xenogeneic challenges (Figure 3) (58–60, 68–70). For xenogeneic interactions, field observations revealed that degraded tissues at contact points between *S. pistillata* and adjacent coral species were marked by aggression hierarchies through highly specific aggressive outcomes, with *S. pistillata* often ranked as an inferior competitor (71). In allogeneic interactions, grafting assays conducted both *in situ* and *ex situ* confirmed that genetic background influences intraspecific interactions and revealed both transitive and non-transitive hierarchies (59–61). Allografts elicited a variety of effector mechanisms, with a single *S. pistillata* genotype reacting differently and specifically to various conspecific genotypes, indicating precise directionality in its effector mechanisms. This intricate pattern of incompatibility in *S. pistillata* reflects a 'non-self recognition' system, as genotypes can detect even subtle differences among closely related kin, exhibiting genotype-specific responses and a wide range of cellular and morphological reactions (Figure 3) (47). In contrast, isogeneic fusions reflect 'self recognition', separate from the 'non-self recognition' seen against conspecifics, indicating discrete recognition alternatives governed by the complex genetic makeup of the interacting partners. Furthermore, the directionalities of allogeneic effector arms in *S. pistillata* were highly consistent and reproducible (60, 61), representing internal, specific outcomes of recognition and not the result of external biological cues such as predation or competition. These organisms, which lack circulatory systems or specific immune cells, demonstrate remarkable precision in distinguishing their isogeneic, allogeneic, and xenogeneic environments.

As in *S. pistillata*, studies on *B. schlosseri* (Figures 3, 4A, B) have shown that colonies can distinguish between neighbors and respond differently to allogeneic and even to xenogeneic challenges (including phenomena such as reciprocal or unilateral rejections, indifference, retreat growths, fusion, colony resorption, somatic/germ cell parasitism, and more), governed by nontransitive and transitive hierarchies of effector mechanisms with highly consistent and reproducible outcomes, as well as genotype-specific effector mechanisms targeting specific conspecifics (9, 63, 72–75). In

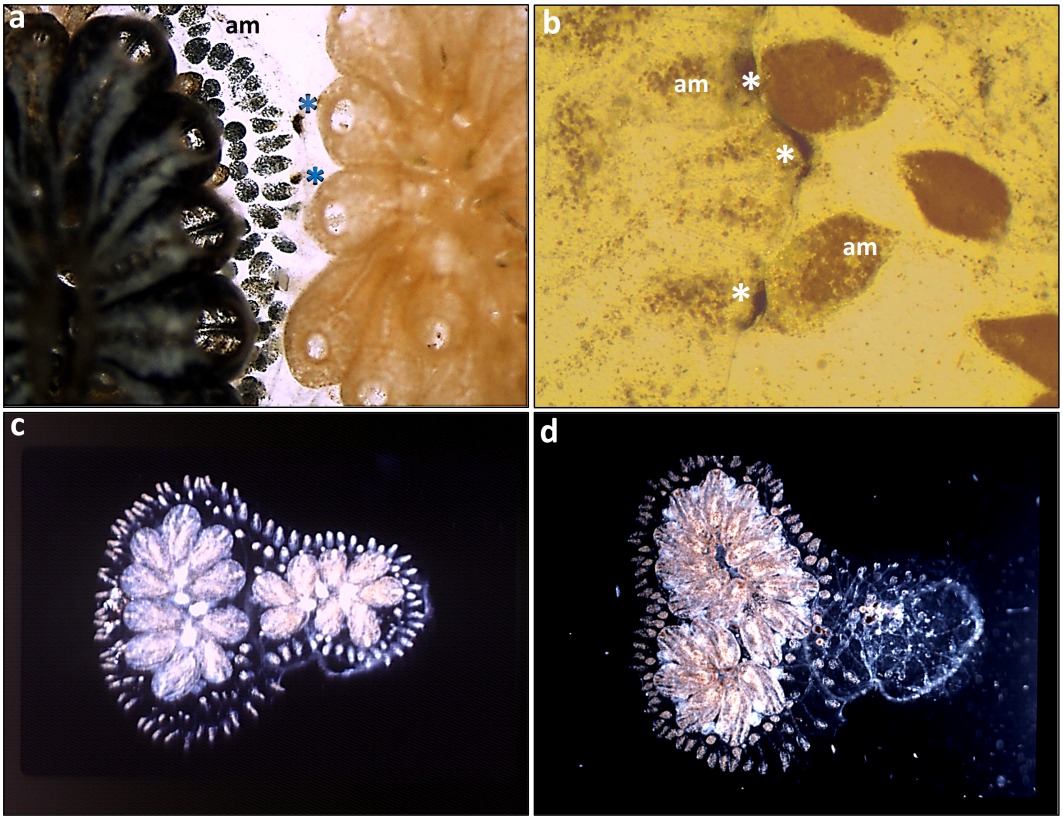

FIGURE 4
Botryllus schlosseri allorecognition. **(a, b)** Non-self recognition: **(a)** two PORs at contacting ampullae in the left colony tunic, marked by blue asterisks. **(b)** a close up of non-self recognition with 3 PORs at contacting ampullae in the left colony tunic, marked by white asterisks. **(c, d)** Resorption of the right partner in a chimera: **(c)** two weeks following chimera formation between two compatible young colonies. The left colony with 10 zooids, the right colony with 8 zooids. **(d)** several months thereafter. The right colony is completely resorbed, the left colony with two systems of functional zooids. am= ampullae.

allogeneic rejection cases, results (72) further revealed that a complete repertoire of points of rejection (PORs; Figures 4A, B) was established within 10 days, yet not all ampulla-ampulla interactions developed PORs. Additionally, cases of indifference, where ampulla-ampulla contacts did not lead to any rejection, were consistently observed in specific pair combinations, with their frequency increasing in repeated testing rounds, suggesting that the rejection phenomenon aligns with the characteristics of a low responder (72). These findings are compared with aspects of tolerance in mammalian systems. Following fusions between allogeneic conspecifics, partners in the chimeras are morphologically eliminated (the resorption phenomenon; Figures 4C, D). Fusions between compatible *BHF* genotypes reflect the ability for 'self recognition', while aggressive phenomena in the chimera elicit components of 'non-self recognition', as demonstrated by the rejection outcomes (Figures 4A, B) developed between non-compatible *BHF* genotypes.

Bypassing the usual interaction site (the extended ampullae) through the transplantation of zooids between *BHF* -incompatible pairs (76), revealed that: (1) instead of the typical tissue rejection (necrosis) observed during natural contacts at peripheral blood vessels, transplanted tissues were eliminated morphologically within a few days, consistent with the normal weekly developmental growth of the colony (76); and (2) donor-recipient chimerism was established after the complete removal of transplanted tissues. These results indicate that *BHF*-based allorecognition in *B. schlosseri* occurs exclusively at the ampullae, and once cells bypass this site, they can survive and proliferate in the host colony (76).

5 What can chimerism in marine invertebrates teach us?

Chimerism, the phenomenon that a single organism possesses cells of more than a single genotype of the same species, stands out as a crucial ecological and evolutionary mechanism, influencing the life history traits of protists, metazoans, and even humans (24, 25, 77–79). Clearly, natural chimerism is directly associated with allorecognition, the self/non-self recognition (21, 25, 48, 64, 77). In numerous instances, including in algae (80), invertebrates (58, 81, 82), and vertebrates, such as human (21, 83), chimerism occurs only briefly during early developmental stages. As in humans, fusion and chimera formation in *S. pistillata* can occur only during early life stages (0–4 months young colonies (57, 58),). In *B. schlosseri*, colonies may fuse upon contacts in any stage of their

life span (47, 65, 73, 74). Chimerism thus reveals limitations or failures in the effectiveness of self/non-self recognition mechanisms. While humans reliably reject allogeneic transplanted tissues in iatrogenic settings, they cannot prevent the lifelong establishment of natural transplantations that result in chimerism (21, 83–85).

Tissue transplantations and chimerism in *S. pistillata* and *B. schlosseri*, while likely underrecognized in nature, have raised important questions about the diverse costs and benefits associated with the chimeric state. The literature highlights chimerism as a highly complex phenomenon with intricate biological and ecological implications, often described as a "double-edged sword" (77, 79), capable of circumventing both innate and adaptive immune responses. For *S. pistillata* chimeras, as with other coral species, chimerism represents a partnership between allogeneic individuals, conferring various advantages (56, 79, 86–89), which may explain why natural fusions among conspecific corals are common. Fusion between colonies offers chimeric organisms an immediate survival advantage by facilitating rapid size growth. Chimerism is believed to be a crucial strategy for enhancing survival during the vulnerable early life stages of corals and promoting growth, especially in these stages (56, 88, 90). Moreover, chimerism affects various biological and ecological traits, including increased reproductive success, earlier reproduction onset, improved competitive abilities during juvenile stages, reduced mortality rates for the entire entity (91), and greater resilience to adverse environmental conditions. This adaptability may act as an evolutionary rescue mechanism to mitigate the impacts of global climate change (87, 89). In turn, chimerism in *S. pistillata* bears impacts on pattern formation and polyp's landscape (92).

In *B. schlosseri* chimeras, one of the partners or more partners (in chimeras made of multi-partners, multichimeras) are morphologically resorbed (73, 79, 93, 94), a process governed by multilevel hierarchical organization of allorecognition elements (95) and stress induced reversals (74). The rate of colony resorption in chimeras depends on the relative sizes of the colonies, with larger colonies requiring up to eight months and smaller ones as little as a week (96). Chimerism in this species can result in somatic and/or germ cell parasitism. Germ cell parasitism often leads to the complete reproductive dominance of one colony's genotype, is asexually heritable, and frequently differs in directionality from somatic cell parasitism (65, 79, 97–99). While germ line parasitism is inherited through a pedigree, the somatic components of chimeric zooids can shift between genotypes in response to environmental changes (65, 100). This dynamic reorganization optimizes the chimeric entity by synergistically presenting the best-suited combination of genetic components under varying conditions (77, 87, 89, 100). Additionally, the deliberate co-settlement of histocompatible conspecific kin larvae (observed in *S. pistillata* and *B. schlosseri* (88, 96, 101);) significantly increases the likelihood of fusion compared to random settlement. This behavior raises important ecological and evolutionary questions regarding the costs and benefits associated with this widespread phenomenon.

Chimerism serves as a crucial ecological and evolutionary mechanism influencing the life history traits of metazoans, presenting in numerous forms and biological statuses (9, 20, 21, 25, 57, 65, 66, 73, 77, 79, 83, 87, 91, 94, 97, 99, 100). This intricate phenomenon functions as a "double-edged sword," as while something provides benefits or advantages, it also has the potential for harmful effects or drawbacks. A recent analysis of chimerism (102) identified six dynamic and inter-changeable somatic forms (purged, sectorial, mosaic, mixed, micro, and multi-chimerism) and three active germline forms (mixed, male/female, and parasitic germline chimerism), based on the proportional contributions and spatial arrangements of chimeric partners within an organism. These variations in chimerism fall along two continua, 'somatic cell chimerism' and 'germline chimerism'. Transitions between these states are fluid, with specific chimeric states capable of shifting into others over time. Thus, the chimeric state of an organism is part of a dynamic spectrum, where different states emerge and are replaced by others as the organism develops and adapts to its environment.

6 Natural transplantations in vertebrates

Allograft rejection is a strong response orchestrated by both the adaptive and innate immune systems (7), particularly through pathways that detect non-self and modified-self entities. While vertebrates consistently reject transplanted tissues from other members of the same species, they paradoxically tolerate various natural cell engraftments throughout their lives. These instances include phenomena such as cytomictical transplantation, fetal-maternal cell exchange, natural germ cell transplantations, transmissible allogeneic tumors, and male-to-female cell transplantation, all of which illustrate the complex interplay between immune tolerance and rejection mechanisms [details in (20, 21, 77, 83, 85, 103)]. Notable, many cases of these natural transplantation events, including those related to pregnancy, are closely linked to disease outcomes (21, 77, 83). Nevertheless, throughout mammalian pregnancy, the mother's immune system not only tolerates the immunologically foreign fetus but actively supports it, facilitating both embryo implantation and development. This phenomenon challenges the traditional self–nonself theory of immune recognition. Remarkably, the concentration of fetal cells in maternal blood steadily increases during pregnancy, reaching over 100 fetal cells per milliliter at parturition (104), highlighting a close relationship between fetal cell dynamics and embryonic development. Furthermore, fetal cells have been shown to persist and fluctuate in the maternal body for decades after childbirth, suggesting a long-lasting biological connection between mother and offspring (21, 83, 85, 105, 106).

From an evolutionary perspective, certain natural engraftments, such as fetal-maternal transplantation in mammals, are thought to be by-products of the functions developed in primitive immune components. These components contribute to developing embryos that are immunologically "educated", by equipping them with effector mechanisms designed to eliminate pervasive somatic and germline variations. This perspective challenges the earlier notion that such processes were merely evolutionary vestiges (21).

Understanding this immunological discrepancy, where alien transplants are supported rather than rejected, is crucial for uncovering the fundamental principles underlying natural transplantation phenomena and their diverse manifestations (107).

7 So, why transplanted organs are rejected?

Iatrogenic transplantation is the standard treatment for end-stage organ diseases, including those affecting the kidney, liver, heart, and lung. Advances in immunosuppressive therapies and medical care have significantly improved 1-year graft survival rates to over 90% for most transplanted organs. However, long-term graft survival remains a challenge, with transplant half-lives ranging from 8–11 years for kidneys to less than 5 years for lungs (1–3, 108).

The rejection of transplanted organs is fundamentally linked to the concept of self versus non-self recognition, a principle that has evolved over time (4, 5, 7, 109). Modern immunology offers various interpretations of the self–nonself theory (15, 22, 23, 26–28, 31, 34, 110), all based on the premise that the immune system originally evolved to protect the body against infections. Traditionally viewed as a defense mechanism against microbial threats, this raises the question of how the immune system recognizes parasitic entities while distinguishing them from the body's own tissues, the core concept of 'self' versus 'non-self' recognition (26–28, 30, 31, 110). Additionally, it underscores the immune system's remarkable ability to differentiate between various forms of "non-self" and adjust its responses accordingly (27, 110).

Natural transplantation in humans and other mammals occurs independently of iatrogenic transplantation and is inherently associated with the development of chimerism (20, 21). Chimerism is also evident in iatrogenic transplantation, where it is intentionally induced through the introduction of immune cells during organ transplantation. This artificial process parallels the natural implantation and development of a genetically 'haploidentical' fetus within the mother's uterus. Yet the process is further more complex. Along pregnancy as an example, fetal microchimeric cells from one pregnancy are replaced by those from subsequent pregnancies, emphasizing the dynamic nature of chimeric status and the importance of microchimeric cell turnover for successful pregnancies (reviewed in (103)). In transplantation, an early major wound is made, where ischemia-reperfusion injury influences both the activation and response phases of alloimmunity. While these early events may obscure non-self recognition, akin to microbial infections, they fail to account for the persistence of alloimmunity long after the injury has resolved (110). It is also true that the process of iatrogenic transplantation is rarely analyzed within the context of natural transplantation in vertebrates or compared to analogous phenomena observed in marine invertebrates (20, 48, 78).

Allorecognition phenomena in marine invertebrates are marked by exceptional precision and specificity, as well as transitivity and a high degree of polymorphism (9–11, 25, 48, 49, 53, 57, 59–61, 66, 68, 73). Allorecognition assays performed on the branching coral *Stylophora pistillata* and the tunicate *Botryllus schlosseri* (as described above), reveal that they recognize 'self' and 'non-self' with remarkable accuracy when exposed to different allogeneic combinations. Unlike the concept of "self-recognition", which categorizes all "non-self" entities as a single uniform alien (47), "non-self" recognition in these invertebrates allows for the individual identification of distinct 'non-self' allogeneic organisms (57, 59–61, 63, 67–69, 71–74). Further, in *Botryllus schlosseri*, 'self' recognition is so precise that fusion between allogeneic partners and chimera formation can occur with just one shared allele at the fusibility locus (9, 47, 48, 73), even when the second allele is identified as 'nonself'. Thus, as noted by Neigel and Avise (53), a single marine invertebrate is not confined to a single mode of interaction during allogeneic encounters but instead responds adaptively based on the "properties of the system."

Self-recognition among allogeneic marine invertebrates results in chimera formation, accompanied by both costs and benefits, as previously discussed (see also (9, 66, 73, 77, 83, 87, 97, 100)). If the immune system's primary function was to maintain individuality by preventing the invasion of conspecific foreign cells into the somatic and germline tissues, or by removing newly formed somatic mutations, then human natural chimerism warrants further examination. In this context, it seems that the immune system's original function has been compromised, leading to the complex and potentially conflicting ("double-edged sword") effects of chimerism (20, 21, 77).

Iatrogenic transplantation bypasses the natural pathways that facilitate immune tolerance, pathways which are not yet fully understood, despite their associated costs, such as autoimmune diseases (84, 103, 105, 107). These natural processes, which enable successful transplantations in humans, involve complex mechanisms including substantial T helper and T regulatory cell activation, B cell involvement, and the innate immune system's recognition of non-self or 'damaged' self through pattern recognition receptors. These receptors typically detect conserved microbial PAMPs, as well as theories like the missing-self theory and the danger hypothesis (reviewed in (5–7)). While the various self-nonself theories offer a useful framework for pre-transplant preparation, they fall short in explaining the diversity of post-transplant phenomena, primarily when compared with human natural transplantation events. In contrast, allorecognition patterns in marine invertebrates, such as *Stylophora pistillata* and *Botryllus schlosseri*, offer a more comprehensive explanation for post-transplant outcomes by accounting for the dynamic, spatiotemporal evolution of the immune self in response to environmental factors.

Our critical evaluation of the mammalian and the marine invertebrates allorecognition processes, provide a unified conceptualization idea that the immune self is continuously changing, alternating between self and non-self statuses, highlighting the philosophical essence of its ongoing transformation (the proposed 'allorecognition landscape' metaphor; Figure 5), as further demonstrated above by discussions on allorecognition in marine invertebrates.

The clinical outcomes of transplant patients are highly variable, even with extensive knowledge of HLA molecules and immune mechanisms, as outcomes range from excellent to poor. Immune performance remains unpredictable, as some patients avoid rejection despite high-risk pre-transplant profiles, while others experience severe, unexpected rejection. Complications also vary widely among patients, both in type and sequence, highlighting our gap knowledge. This complex variability reflects the remarkable complexity, precision, and specificity observed in marine invertebrate allorecognition phenomena, including their intricate transitivity, high polymorphism, and ability to recognize in parallel multiple selves, each reacted distinctly by unalike effector mechanisms, and in different allogeneic combinations (9–11, 25, 48, 49, 53, 57, 59–61, 66, 68, 73). Even pregnancy that is believed to be a tolerant state because the fetus is not being rejected, is not always like that. We usually consider successful pregnancies when making this assessment, yet documentations exist for many unsuccessful fertilizations, implantations, and pregnancies represent in various ways the effects of various intolerant states (111).

The immunological 'self/nonself' is a key principle in immunology that serves as a fundamental framework for understanding how the immune system distinguishes and manages foreign entities, cells of related species and the body's own components. This is illustrated by the metaphor of the 'allorecognition landscape', as illustrated in Figure 5. The interactions between a transplanted organ and the recipient's body operate within two distinct, yet interconnected continuums of 'self' and 'nonself' recognition statuses, resembling an infinite 'Escherian stairwell' of selfhood. Each continuum features a complex array of precise and specific allorecognition elements, allowing the recognition state of the organ to fluctuate in response to environmental cues and the interaction of adaptive and innate immunity. These allogeneic states are dynamic and transient, capable of changing over time, which requires adaptable clinical strategies and considerations. The transition between these states can range from tolerance to complete rejection, potentially persisting throughout the patient's lifespan. Thus, the 'self' and 'nonself' metaphors are not defined by fixed molecular recognition, rather, they embody a dynamic and ever-evolving allorecognition landscape that encompasses a wide range of states, from complete (100% in Figure 5) 'self' or 'nonself' recognition to myriad intermediate combinations where both recognition types coexist and function simultaneously to varying extents at any given moment.

It is important to recognize that the commonly employed anti-rejection therapies target immune effector mechanisms and clinical outcomes, rather than addressing the immune self/nonself metaphors. This current clinical approach reflects the broad suppression of the immune response without accounting for the redefinition of immune selfhood introduced by the transplanted organ. Thus, by providing a robust explanation of real-world chimeric phenomena with shared underlying structures, examining immunological scenarios through ecological and evolutionary perspectives, and exploring the extensive prevalence of natural transplantation (most notably in marine invertebrates), innovative clinical strategies for managing transplanted organ rejection may emerged.

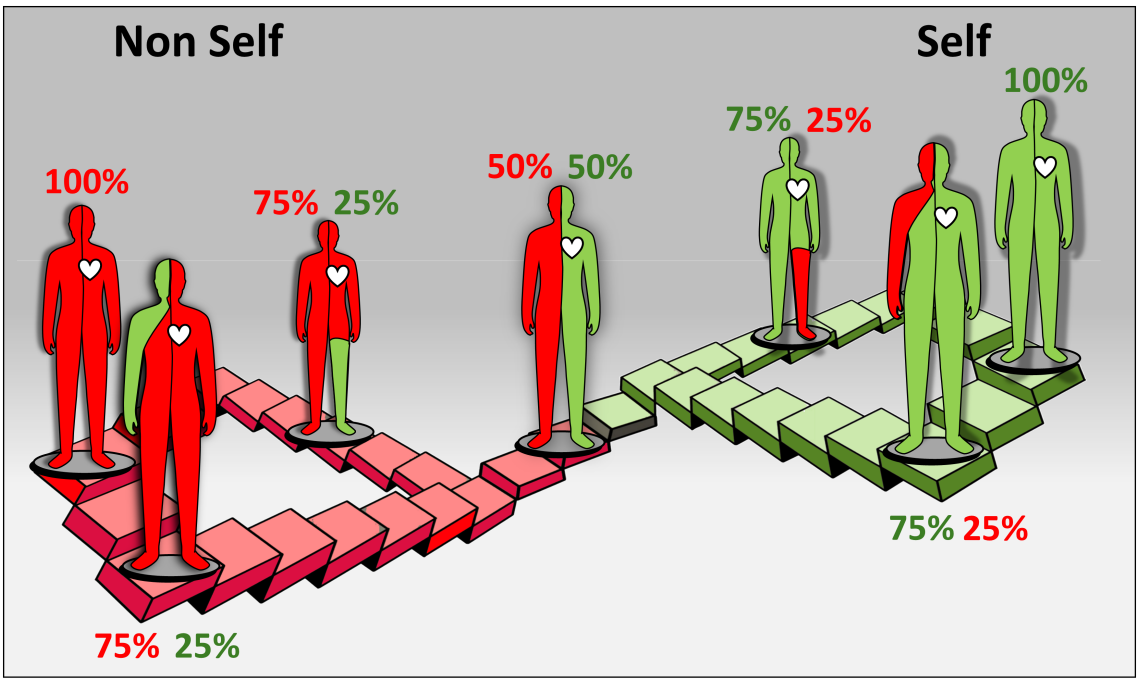

FIGURE 5
A schematic illustration of the evolving 'allorecognition landscape' metaphor and the shifting 'self/nonself'. The figure illustrates the dynamic nature of immunological "self/nonself" recognition (distinct from effector mechanisms) in humans with transplanted organs. This process is represented as a unified allorecognition landscape, shaped by two recognition planes or continuums (depicted in red and green). Throughout an individual's lifespan, these continuums reflect diverse arrays of specific allorecognition states, including reciprocal states of 75:25%, 50:50%, and 25:75%. These recognition states are transient and can shift over time in either direction, transitioning into various states and requiring tailored clinical considerations.

Data availability statement

The original contributions presented in the study are included in the article/supplementary material. Further inquiries can be directed to the corresponding author.

Author contributions

BR: Conceptualization, Writing – original draft, Writing – review & editing.

Funding

The author(s) declare that financial support was received for the research and/or publication of this article. This study was funded by the Israeli Science Foundation, grant no. 1024/23.

Acknowledgments

I thank Guy Paz for drawing the figures.

Conflict of interest

The author declares that the research was conducted in the absence of any commercial or financial relationships that could be construed as a potential conflict of interest.

The author(s) declared that they were an editorial board member of Frontiers, at the time of submission. This had no impact on the peer review process and the final decision.

Generative AI statement

The author(s) declare that no Generative AI was used in the creation of this manuscript.

Publisher's note

References

1. Watson CJE, Dark JH. Organ transplantation: historical perspective and current practice. *Br J Anaesth*. (2012) 108:i29–42. doi: 10.1093/bja/aer384

2. Lai X, Zheng X, Mathew JM, Gallon L, Leventhal JR, Zhang ZJ. Tackling chronic kidney transplant rejection: Challenges and promises. *Front Immunol*. (2021) 12:661643. doi: 10.1093/bja/aer384

3. Hariharan S, Israni AK, Danovitch G. Long-term survival after kidney transplantation. *N Engl J Med*. (2021) 385:729–43. doi: 10.1056/NEJMra20145

4. Callemeyn J, Lamarthée B, Koenig A, Koshy P, Thaunat O, Naesens M. Allorecognition and the spectrum of kidney transplant rejection. *Kidney Int*. (2022) 101:692–710. doi: 10.1016/j.kint.2021.11.029

5. Hamada S, Dubois V, Koenig A, Thaunat O. Allograft recognition by recipient's natural killer cells: Molecular mechanisms and role in transplant rejection. *HLA*. (2021) 98:191–9. doi: 10.1111/tan.14332

6. Zhao D, Abou-Daya KI, Dai H, Oberbarnscheidt MH, Li XC, Lakkis FG. Innate allorecognition and memory in transplantation. *Front Immunol*. (2020) 11:918. doi: 10.3389/fimmu.2020.00918

7. Oberbarnscheidt MH, Zecher D, Lakkis FG. The innate immune system in transplantation. *Semin Immunol*. (2011) 23:264–72. doi: 10.1016/j.smim.2011.06.006

8. Watkins B, Williams KM. Controversies and expectations for the prevention of GVHD: A biological and clinical perspective. *Front Immunol*. (2022) 13:1057694. doi: 10.3389/fimmu.2022.1057694

9. Magor BG, De Tomoso A, Rinkevich B, Weissman IL. Allorecognition in colonial tunicates: protection against predatory cell lineages? *Immunol Rev*. (1999) 167:69–79. doi: 10.1111/j.1600-065X.1999.tb01383.x

10. Rinkevich B. Invertebrates versus vertebrates innate immunity: in the light of evolution. *Scan J Immunol*. (1999) 50:456–60. doi: 10.1046/j.1365-3083.1999.00626.x

11. Cooper EL, Rinkevich B, Uhlenbruck G, Valembois P. Invertebrate immunity: Another viewpoint. *Scan J Immunol*. (1992) 35:247–66. doi: 10.1111/j.1365-3083.1992.tb02857.x

12. De Boer RJ. The evolution of polymorphic compatibility molecules. *Mol Biol Evol*. (1995) 12:494–502.

13. Fearon DT, Locksley RM. The instructive role of innate immunity in the acquired immune response. *Science*. (1996) 272:50–4. doi: 10.1126/science.272.5258.50

14. Buss LW, Green DR. Histoincompatibility in vertebrates: the relict hypothesis. *Dev Comp Immunol*. (1985) 9:191–201. doi: 10.1016/0145-305X(85)90110-7

15. Medzhitov R, Janeway C.OMMAJr. CA. Innate immunity: The virtues of a nonclonal system of recognition. *Cell*. (1997) 91:295–8. doi: 10.1016/S0092-8674(00)80412-2

16. Weissman IL. Was the MHC made for the immune system, or did immunity take advantage of an ancient polymorphic gene family encoding cell surface interaction molecules? A speculative assay. *Int Rev Immunol*. (1988) 3:397–416.

17. Chen M-H, Shen Z-M, Bobin S, Kahn PC, Lipke PN. Structure of *saccharomyces cerevisiae* α-agglutinin. *J Biol Chem*. (1995) 270:26168–77. doi: 10.1074/jbc.270.44.26168

18. Schaecke H, Rinkevich B, Gamulin V, Mueller IM, Mueller WEG. Immunoglobulin-like domain is present in the extracellular part of the receptor tyrosine kinase from the marine sponge *Geodia cydonium*. *J Mol Recognit*. (1994) 7:273–6.

19. Oren M, Paz G, Douek J, Rosner A, Amar KO, Rinkevich B. Marine invertebrates cross phyla comparisons reveal highly conserved immune machinery. *Immunobiol*. (2013) 218:484–95. doi: 10.1016/j.imbio.2012.06.004

20. Rinkevich B. Immunology of human implantation: from the invertebrates' point of view. *Hum Reprod*. (1998) 13:455–9. doi: 10.1093/humrep/13.2.455

21. Rinkevich B. Human natural chimerism: an acquired character or a vestige of evolution? *Hum Immunol*. (2001) 62:651–7. doi: 10.1016/S0198-8859(01)00249-X

22. Burnet FM. *The Clonal Selection Theory of Acquired Immunity*. Nashvill TN, USA: Vanderbilt Univ. Press (1959).

23. Tauber AI. *Immunity: The Evolution of an Idea*. New York, USA: Oxford University Press (2017).

24. Rinkevich B. A critical approach to the definition of Darwinian units of selection. *Biol Bull*. (2000) 199:231–40. doi: 10.2307/1543179

25. Grosberg RK. The evolution of allorecognition specificity in clonal invertebrates. *Q Rev Biol*. (1988) 63:377–412. doi: 10.1086/416026

26. Cohn M. The evolutionary context for a self–nonself discrimination. *Cell Mol Life Sci*. (2010) 67:2851–62. doi: 10.1007/s00018-010-0438-z

27. Janeway CA Jr. The immune system evolved to discriminate infectious nonself from noninfectious self. *Immunol Today*. (1992) 13:11–6. doi: 10.1016/0167-5699(92)90198-G

28. Kourilsky P, Claverie JM. The peptidic self model: a hypothesis on the molecular nature of the immunological self. *Ann Inst Pasteur Immunol*. (1986) 137:3–21.

29. Grignolio A, Mishto M, Faria AM, Garagnani P, Franceschi C, Tieri . Towards a liquid self: How time, Geography, and life experiences reshape the biological identity. *Front Immunol*. (2014) 5. doi: 10.3389/fimmu.2014.00153

30. Bevan MJ. High determinant density may explain the phenomenon of alloreactivity. *Immunol Today*. (1984) 5:128–30. doi: 10.1016/0167-5699(84)90233-0

31. Kärre K. An unexpected petition for pardon. *Curr Biol*. (1992) 2:613–5. doi: 10.1016/0960-9822(92)90179-E

32. Versteeg R. NK cells and T cells: mirror images. *Immunol Today*. (1992) 13:244–7. doi: 10.1016/0167-5699(92)90003-P

33. Daunter B. RISH VI: General evolutionary aspects of the immune system. *Med Hypoth*. (1988) 27:115–26. doi: 10.1016/0306-9877(88)90156-9

34. Matzinger P. The danger model: A renewed sense of self. *Science*. (2002) 296:301–5. doi: 10.1126/science.1071059

35. Sternberg SH, Richter H, Charpentier E, Qimron U. Adaptation in CRISPR-cas systems. *Mol Cell*. (2016) 61:797–808. doi: 10.1016/j.molcel.2016.01.030

36. Amitai G, Sorek R. CRISPR–Cas adaptation: insights into the mechanism of action. *Nat Rev Microbiol*. (2016) 14:67–76. doi: 10.1038/nrmicro.2015.14

37. Garg AD, Agostinis P. Cell death and immunity in cancer: From danger signals to mimicry of pathogen defense responses. *Immunol Rev*. (2017) 280:126–48. doi: 10.1111/imr.2017.280.issue-1

38. Patel SA, Minn AJ. Combination cancer therapy with immune checkpoint blockade: mechanisms and strategies. *Immunity*. (2018) 48:417–33. doi: 10.1016/j.immuni.2018.03.007

39. Fesnak AD, June CH, Levine BL. Engineered T cells: the promise and challenges of cancer immunotherapy. *Nat Rev Cancer*. (2016) 16:566–81. doi: 10.1038/nrc.2016.97

40. Pandya PH, Murray ME, Pollok KE, Renbarger JL. The immune system in cancer pathogenesis: potential therapeutic approaches. *J Immunol Res*. (2016) 2016:1–13. doi: 10.1155/2016/4273943

41. Lee C-H, Yelensky R, Jooss K, Chan TA. Update on tumor neoantigens and their utility: why it is good to be different. *Trends Immunol*. (2018) 39:536–48. doi: 10.1016/j.it.2018.04.005

42. Gebre MS, Brito LA, Tostanoski LH, Edwards DK, Carfi A, Barouch DH. Novel approaches for vaccine development. *Cell*. (2021) 184:1589–603. doi: 10.1016/j.cell.2021.02.030

43. Gong T, Liu L, Jiang W, Zhou R. DAMP-sensing receptors in sterile inflammation and inflammatory diseases. *Nat Rev Immunol*. (2020) 20:95–112. doi: 10.1038/s41577-019-0215-7

44. Bartok E, Hartmann G. Immune sensing mechanisms that discriminate self from altered self and foreign nucleic acids. *Immunity*. (2020) 53:54–77. doi: 10.1016/j.immuni.2020.06.014

45. Roers A, Hiller B, Hornung V. Recognition of endogenous nucleic acids by the innate immune system. *Immunity*. (2016) 44:739–54. doi: 10.1016/j.immuni.2016.04.002

46. Cooper EL. Evolution of immune systems from self/not self to danger to artificial immune systems (AIS). *Phys Life Rev*. (2010) 7:55–78. doi: 10.1016/j.plrev.2009.12.001

47. Rinkevich B. Links between alloresponses and their genetic background in colonial urochordates and cnidarians: Evidence for the recognition of 'nonself' as opposed to 'self'. In: Stolen JS, Fletcher TC, Bayne CJ, Secombes CJ, Zelikoff JT, Twerdok L, et al, editors. *Modulators of immune responses: the evolutionary trail*. SOS Publications, Fair Haven, USA (1996). p. 1–13.

48. Rinkevich B. Immune responsiveness in marine invertebrates revisited: the concourse of puzzles. In: Söderhäll K, Vasta G, Iwanaga S, editors. *New Directions in Invertebrate Immunology*. SOS Publications, Fair Haven, USA (1995). p. 55–90.

49. Hildemann HH, Bigger CH, Johnston IS. Histoincompatibility reactions and allogeneic polymorphism among invertebrates. *Transplat Proc*. (1979) 11:1136–42.

50. Janeway CA Jr. The targeting of effector molecules in the immune system. *BioEssays*. (1986) 5:216–20. doi: 10.1002/bies.950050507

51. Pradeu T. *The Limits of the Self: Immunology and Biological Identity*. New York, USA: Oxford University Press (2011).

52. Koncz B, Balogh GM, Manczinger M. A journey to your self: The vague definition of immune self and its practical implications. *Proc Natl Acad Sci USA*. (2024) 121:e2309674121. doi: 10.1073/pnas.2309674121

53. Neigel JE, AvIse JC. Clonal diversity and population structure in a reef-building coral, *Acropora cervicornis*: self-recognition analysis and demographic interpretation. *Evolution*. (1983) 37:437–53.

54. Shefy D, Rinkevich B. *Stylophora pistillata*—A model colonial species in basic and applied studies. In: *Handbook of Marine Model Organisms in Experimental Biology*. CRC Press, Boca Raton, USA (2021). p. 195–216. doi: 10.1201/9781003217503-11

55. Ben-Hamo O, Rinkevich B. *Botryllus schlosseri*—A model colonial species in basic and applied studies. In: *Handbook of Marine Model Organisms in Experimental Biology*. CRC Press, Boca Raton, USA (2021). p. 385–402. doi: 10.1201/9781003217503-21

56. Amar K-O, Chadwick NE, Rinkevich B. Coral kin aggregations exhibit mixed allogeneic reactions and enhanced fitness during early ontogeny. *BMC Evol Biol*. (2008) 8:126. doi: 10.1186/1471-2148-8-126

57. Amar K-O, Rinkevich B. Mounting of erratic histoincompatible responses in hermatypic corals: a multi-year interval comparison. *J Exp Biol*. (2010) 213:535–40. doi: 10.1242/jeb.039529

58. Frank U, Oren U, Loya Y, Rinkevich B. Alloimmune maturation in the coral *Stylophora pistillata* is achieved through three distinctive stages, 4 months post–metamorphosis. *Proc R Soc Lond B*. (1997) 264:99–104. doi: 10.1098/rspb.1997.0015

59. Müller WE, Müller I, Zahn RK, Maidhof A. Intraspecific recognition system in scleractinian corals: morphological and cytochemical description of the autolysis mechanism. *J Histochem Cytochem*. (1984) 32:285–8. doi: 10.1177/32.3.6141203

60. Chadwick-Furman N, Rinkevich B. A complex allorecognition system in a reef-building coral: delayed responses, reversals and nontransitive hierarchies. *Coral Reefs*. (1994) 13:57–63. doi: 10.1007/BF00426436

61. Rinkevich B, Loya Y. Intraspecific competitive networks in the Red Sea coral. *Stylophora pistillata Coral Reefs*. (1983) 1:161–72. doi: 10.1007/BF00571193

62. Voskoboynik A, Newman AM, Corey DM, Sahoo D, Pushkarev D, Neff NF, et al. Identification of a colonial chordate histocompatibility gene. *Science*. (2013) 341:384–7. doi: 10.1126/science.1238036

63. Rinkevich B, Porat R, Goren M. Allorecognition elements on a urochordate histocompatibility locus indicate unprecedented extensive polymorphism. *Proc R Soc B*. (1995) 259:319–24. doi: 10.1098/rspb.1995.0047

64. Weissman I, Saito Y, Rinkevich B. Allorecognition in colonial tunicates: Parallels with and tangents from vertebrate immunity. In: Melchers F, editor. *Progress in Immunology*. Springer, Berlin, Heidelberg (1989). p. 1256–63. doi: 10.1007/978-3-642-83755-5_167

65. Stoner DS, Rinkevich B, Weissman IL. Heritable germ and somatic cell lineage competitions in chimeric colonial protochordates. *Proc Natl Acad Sci USA*. (1999) 96:9148–53. doi: 10.1073/pnas.96.16.9148

66. Rinkevich B. Primitive immune systems: Are your ways my ways? *Immunol Rev*. (2004) 198:25–35. doi: 10.1111/j.0105-2896.2004.0114.x

67. Rinkevich B, Frank U, Bak RPM, Müller WEG. Alloimmune responses between *Acropora hemprichi* conspecifics: nontransitive patterns of overgrowth and delayed cytotoxicity. *Mar Biol*. (1994) 118:731–7. doi: 10.1007/BF00347522

68. Rinkevich B. Allorecognition and xenorecognition in reef corals: a decade of interactions. *Hydrobiologia*. (2004) 530/531:443–50. doi: 10.1007/s10750-004-2686-0

69. Rinkevich B. Neglected biological features in cnidarians self-nonself recognition. In: López-Larrea C, editor. *Self and Nonself*, vol. 738 . Springer USA, New York, NY (2012). p. 46–59.

70. Frank U, Rinkevich B. Nontransitive patterns of historecognition phenomena in the Red Sea hydrocoral. *Millepora dichotoma Mar Biol*. (1994) 118:723–9. doi: 10.1007/BF00347521

71. Rinkevich B, Shashar N, Liberman T. Nontransitive xenogeneic interactions between four common Red Sea sessile invertebrates. In: *Proceedings of the 7th International Coral Reef Symposium*, vol. 2. Coral Reef Society, Guam, USA (1993). p. 833–9.

72. Rinkevich B, Weissman IL. Incidents of rejection and indifference in Fu/HC incompatible protochordate colonies. *J Exp Zool*. (1992) 263:105–11. doi: 10.1002/jez.1402630111

73. Rinkevich B, Weissman IL. Allogeneic resorption in colonial protochordates: consequences of nonself recognition. *Dev Comp Immun*. (1992) 16:275–86. doi: 10.1016/0145-305X(92)90002-T

74. Rinkevich B, Weissman IL. Alloimmune hierarchies and stress-induced reversals in the resorption of chimeric protochordate colonies. *Proc R Soc Lond B*. (1994) 258:215–20. doi: 10.1098/rspb.1994.0165

75. Rinkevich B. Rejection patterns in botryllid ascidian immunity: the first tier of allorecognition. *Can J Zool*. (2005) 83:101–21. doi: 10.1139/z04-161

76. Rinkevich B, Weissman IL, De Tomaso AW. Transplantation of Fu/HC-incompatible zooids in *Botryllus schlosseri* results in chimerism. *Biol Bull*. (1998) 195:98–106. doi: 10.2307/1542816

77. Rinkevich B. Quo vadis chimerism? *Chimerism*. (2011) 2:1–5. doi: 10.4161/chim.2.1.14725

78. Lakkis FG, Dellaporta SL, Buss LW. Allorecognition and chimerism in an invertebrate model organism. *Organogenesis*. (2008) 4:236–40. doi: 10.4161/org.4.4.7151

79. Rinkevich B, Weissman IL. Chimeras vs genetically homogeneous individuals: potential fitness costs and benefits. *Oikos*. (2012) 63:119–24. doi: 10.2307/3545520

80. González AV, Santelices B. Frequency of chimerism in populations of the kelp *Lessonia spicata* in central Chile. *PloS One*. (2017) 12:e0169182. doi: 10.1371/journal.pone.0169182

81. Maldonado M. Do chimeric sponges have improved chances of survival? *Mar Ecol Prog Ser*. (1998) 164:301–6. doi: 10.3354/meps164301

82. Barki Y, Gateño D, Graur D, Rinkevich B. Soft-coral natural chimerism: a window in ontogeny allows the creation of entities comprised of incongruous parts. *Mar Ecol Prog Ser*. (2002) 231:91–9. doi: 10.3354/meps231091

83. Madan K. Natural human chimeras: A review. *Eur J Med Genet*. (2020) 63:103971. doi: 10.1016/j.ejmg.2020.103971

84. Boddy AM, Fortunato A, Wilson Sayres M, Aktipis A. Fetal microchimerism and maternal health: A review and evolutionary analysis of cooperation and conflict beyond the womb. *BioEssays*. (2015) 37:1106–18. doi: 10.1002/bies.201500059

85. Bianchi DW, Khosrotehrani K, Way SS, MacKenzie TC, Bajema I, O'Donoghue K. Forever connected: The lifelong biological consequences of fetomaternal and maternofetal microchimerism. *Clin Chem*. (2021) 67:351–62. doi: 10.1093/clinchem/hvaa304

86. Rinkevich B, Shaish L, Douek J, Ben-Shlomo R. Venturing in coral larval chimerism: a compact functional domain with fostered genotypic diversity. *Sci Rep*. (2016) 6:19493. doi: 10.1038/srep19493

87. Vidal-Dupiol J, Harscouet E, Shefy D, Toulza E, Rey O, Allienne JF, et al. Frontloading of stress response genes enhances robustness to environmental change in chimeric corals. *BMC Biol*. (2022) 20:167. doi: 10.1186/s12915-022-01371-7

88. Shefy D, Shashar N, Rinkevich B. Exploring traits of engineered coral entities to be employed in reef restoration. *J Mar Sci Eng*. (2020) 8:1038. doi: 10.3390/jmse8121038

89. Rinkevich B. Coral chimerism as an evolutionary rescue mechanism to mitigate global climate change impacts. *Glob Change Biol*. (2019) 25:1198–206. doi: 10.1111/gcb.2019.25.issue-4

90. Mizrahi D, Navarrete SA, Flores AAV. Groups travel further: pelagic metamorphosis and polyp clustering allow higher dispersal potential in sun coral propagules. *Coral Reefs*. (2014) 33:443–8. doi: 10.1007/s00338-014-1135-4

91. Buss LW. Somatic cell parasitism and the evolution of somatic tissue compatibility. *Proc Natl Acad Sci USA*. (1982) 79:5337–41. doi: 10.1073/pnas.79.17.5337

92. Guerrini G, Shefy D, Shashar N, Shafir S, Rinkevich B. Morphometric and allometric rules of polyp's landscape in regular and chimeric coral colonies of the branching species. *Stylophora pistillata Dev Dyn*. (2021) 250:652–68. doi: 10.1002/dvdy.v250.5

93. Rinkevich B. Immunological resorption in *Botryllus schlosseri* (Tunicata) chimeras is characterized by multilevel hierarchial organization of histocompatibility alleles. A speculative endeavor. *Biol Bull*. (1993) 184:342–5. doi: 10.2307/1542453

94. Rinkevich B, Weissman IL. A long-term study on fused subclones in the ascidian *Botryllus schlosseri*: the resorption phenomenon (Protochordata: Tunicata). *J Zool*. (1987) 213:717–33. doi: 10.1111/j.1469-7998.1987.tb03736.x

95. Rinkevich B, Saito Y, Weissman IL. A colonial invertebrate species that displays a hierarchy of allorecognition responses. *Biol Bull*. (1993) 184:79–86. doi: 10.2307/1542381

96. Rinkevich B, Weissman IL. The fate of *Botryllus* (Ascidiacea) larvae cosettled with parental colonies: beneficial or deleterious consequences? *Biol Bull*. (1987) 173:474–88. doi: 10.2307/1541694

97. Rinkevich B. Germ cell parasitism as an ecological and evolutionary puzzle: hitchhiking with positively selected genotypes. *Oikos*. (2002) 96:25–30. doi: 10.1034/j.1600-0706.2002.960102.x

98. Rinkevich B. Natural chimerism in colonial urochordates. *J Exp Mar Biol Ecol*. (2005) 322:93–109. doi: 10.1016/j.jembe.2005.02.020

99. Pancer Z, Gershon H, Rinkevich B. Coexistence and possible parasitism of somatic and germ cell lines in chimeras of the colonial urochordate *Botryllus schlosseri*. *Biol Bull*. (1995) 189:106–12. doi: 10.2307/1542460

100. Rinkevich B, Yankelevich I. Environmental split between germ cell parasitism and somatic cell synergism in chimeras of a colonial urochordate. *J Exp Biol*. (2004) 207:3531–6. doi: 10.1242/jeb.01184

101. Shefy D, Guerrini G, Marom N, Shashar N, Rinkevich B. Settling in aggregation: Spatial planning consideration for brooding coral transplants. *Mar Environ Res*. (2022) 176:105612. doi: 10.1016/j.marenvres.2022.105612

102. Guerrini G, Shefy D, Douek J, Shashar N, Goulet TL, Rinkevich B. Spatial distribution of conspecific genotypes within chimeras of the branching coral *Stylophora pistillata*. *Sci Rep*. (2021) 11:22554. doi: 10.1038/s41598-021-00981-5

103. Kruchen A, Fehse B, Müller I. Clinical relevance of feto-maternal microchimerism in (hematopoietic stem cell) transplantation. *Semin Immunopathol*. (2025) 47:4. doi: 10.1007/s00281-024-01028-3

104. Krabchi K, Gros-Louis F, Yan J, Bronsard M, Masse J, Forest JC, et al. Quantification of all fetal nucleated cells in maternal blood between the 18th and 22nd weeks of pregnancy using molecular cytogenetic techniques. *Clin Genet*. (2001) 60:145–50. doi: 10.1034/j.1399-0004.2001.600209.x

105. Khosrotehrani K, Reyes RR, Johnson KL, Freeman RB, Salomon RN, Peter I, et al. Fetal cells participate over time in the response to specific types of murine maternal hepatic injury. *Hum Reprod*. (2007) 22:654–61. doi: 10.1093/humrep/del426

106. Bianchi DW, Zickwolf GK, Weil GJ, Sylvester S, DeMaria MA. Male fetal progenitor cells persist in maternal blood for as long as 27 years postpartum. *Proc Natl Acad Sci USA*. (1996) 93:705–8. doi: 10.1073/pnas.93.2.705

107. Devanesan A. Pregnancy, a test case for immunology. *Synthese*. (2024) 203:22. doi: 10.1007/s11229-023-04444-4

108. Lodhi SA, Lamb KE, Meier-Kriesche HU. Solid organ allograft survival improvement in the United States: The long-term does not mirror the dramatic short-term success. *Am J Transplant*. (2011) 11:1226–35. doi: 10.1111/j.1600-6143.2011.03539.x

109. Li Q, Lan P. Activation of immune signals during organ transplantation. *Sig Transduction Targeting Ther*. (2023) 8:110. doi: 10.1038/s41392-023-01377-9

110. Janeway C. Immunogenecity signals 1, 2, 3… and 0. *Immunol Today*. (1989) 10:283–6. doi: 10.1016/0167-5699(89)90081-9

111. Ghaebi M, Nouri M, Ghasemzadeh A, Farzadi L, Jadidi-Niaragh F, Ahmadi M, et al. Immune regulatory network in successful pregnancy and reproductive failures. *Biomed Pharmacother*. (2017) 88:61–73. doi: 10.1016/j.biopha.2017.01.016

frontiers | Frontiers in Immunology

TYPE Original Research
PUBLISHED 16 April 2025
DOI 10.3389/fimmu.2025.1538795

OPEN ACCESS

EDITED BY
Mohammad Hossein Karimi,
Shiraz University of Medical Sciences, Iran

REVIEWED BY
Ramin Yaghobi,
Shiraz University of Medical Sciences, Iran
Roberto Crocchiolo,
Niguarda Ca' Granda Hospital, Italy
Luigi Nespoli,
University of Insubria, Italy

*CORRESPONDENCE
Cassaniti Irene
i.cassaniti@smatteo.pv.it;
irene.cassaniti@unipv.it

RECEIVED 03 December 2024
ACCEPTED 28 March 2025
PUBLISHED 16 April 2025

CITATION
Zavaglio F, Cassanti I, Gregorini M, Grignano MA, Rampino T, Lilleri D and Baldanti F (2025) Pre-transplant IE1-specific T-cell response and CD8$^+$ T-cell count as predictive markers of treated HCMV reactivation in kidney transplant recipients. *Front. Immunol.* 16:1538795. doi: 10.3389/fimmu.2025.1538795

Pre-transplant IE1-specific T-cell response and CD8$^+$ T-cell count as predictive markers of treated HCMV reactivation in kidney transplant recipients

Federica Zavaglio[1], Irene Cassanti[1,2*], Marilena Gregorini[3,4], Maria Antonietta Grignano[4], Teresa Rampino[4], Daniele Lilleri[2] and Fausto Baldanti[1,2]

[1]Microbiology and Virology Department, Fondazione IRCCS Policlinico San Matteo, Pavia, Italy, [2]Department of Clinical, Surgical, Diagnostic and Pediatric Sciences, University of Pavia, Pavia, Italy, [3]Department of Internal Medicine and Therapeutics, University of Pavia, Pavia, Italy, [4]Unit of Nephrology and Dialysis and Transplantation, Fondazione IRCCS Policlinico San Matteo, Pavia, Italy

Background: Human cytomegalovirus (HCMV) infection represents a significant complication for kidney transplant recipients (KTRs). The goal of this study was to evaluate potential immunological markers at pre-transplant in HCMV-seropositive KTRs for predicting HCMV severe reactivation (e.g treated HCMV reactivation) during the first year after transplant.

Methods: Before transplant, lymphocyte count was measured in whole blood and HCMV-specific T-cell response was determined using ELISpot assay after stimulation with pp65, IE-1 and IE-2 peptides pool. HCMV DNA was monitored during the first year after transplant. Among the 65 KTRs enrolled, 44 (68%) patients had HCMV self-resolving reactivation (Controllers) while 21 (32%) required antiviral treatment for HCMV reactivation (Non-Controllers).

Results: No significant difference in CD4 T-cell count was observed, but Controllers had higher CD8$^+$ T-cell counts compared to Non-Controllers. Based on ROC analysis, a CD8$^+$ T-cell count ≥215 cells/µl was associated with a lower incidence of HCMV reactivation after transplant. Additionally, a higher IE-1-specific T-cell response was observed in Controllers and patients with IE1-specific T-cell response ≥60 spots showed a reduced incidence of HCMV reactivation and lower DNAemia peak.

Discussion: Lymphocyte counts and HCMV-specific T-cell response can be measured at pre-transplant in KTRs in order to efficiently predict the risk of treated HCMV reactivation during the first year after transplant. Potential cut-off and diagnostics algorithm should be better investigated in a large patients setting.

KEYWORDS

pre-transplant immunity, human cytomegalovirus, kidney transplant, immunological markers, T-cell response

1 Introduction

Human Cytomegalovirus (HCMV) infection still represents one of the most important opportunistic infection in solid organ transplant recipients (SOTRs) (1). Two approaches have been proposed for control of HCMV prevention, pre-emptive therapy (PET), which involves a PCR-guided administration of anti-HCMV treatment to patients at risk for HCMV disease (i.e., monitoring the blood viral load and giving antiviral drugs to patients at predetermined levels of viral load), and universal prophylaxis (i.e., administration of antiviral drugs to all transplanted patients for 6-12 months) (2, 3). Although it is widely known that patients who are HCMV-seronegative at transplant and receive the organ from a HCMV-seropositive donor (D+/R-) are at higher risk of HCMV infection, HCMV-seropositive recipients (R+) may be at risk of reactivation in the post-transplant period, especially in relation to the type of transplanted organ and immunosuppressive therapies (4–6).

To date, the assessment of immunological tools able to predict the spontaneous clearance of HCMV infection in HCMV-seropositive SOTRs represents a crucial milestone for the success of transplant. In this setting, monitoring of lymphocytes subsets in SOTRs could be used as simple approach for stratification of the risk of HCMV infection, reactivation or relapse after treatment (7–12). Moreover, HCMV-specific T cells are crucial for the prevention of HCMV disease, observing that both $CD4^+$ and $CD8^+$ HCMV-specific T cells are involved in the first line of specific cellular immune response in HCMV-seropositive transplanted recipients, as well as in a long term control of reactivation (13–18). Furthermore, the risk of high-level DNAemia and consequently early treatment is reduced in those patients with higher T-cell response between 2 and 4 week post-transplant (16, 19).

On the other side, the evaluation of pre-transplant HCMV-specific immune response seems to be useful for a preliminary patients' stratification of the risk of HCMV reactivation in HCMV-seropositive recipients (20–25). However, the role of pre-transplant HCMV-specific T-cell response and its potential use in clinical practice should be better elucidated.

In this study, we aimed to evaluate HCMV-specific T-cell response at pre-transplant in HCMV-seropositive kidney transplant recipients in order to investigate the predictive role in the stratification of HCMV DNAemia and requirement of antiviral treatment.

2 Materials and methods

2.1 Patients enrolment and HCMV monitoring

HCMV-seropositive kidney transplant recipients were consecutively enrolled at Nephrology and Dialysis Department of IRCCS Policlinico San Matteo in Pavia (Northern Italy). At baseline (day of transplant), heparinized whole blood samples were collected for peripheral blood mononuclear cells (PBMC) isolation and lymphocyte T cell count. Detailed flow-chart representing patients' enrollment, follow-up and stratification is included in Supplementary Figure 1 (Supplementary Figure S1).

All the patients were treated with induction therapy with anti-thymocyte globulin (ATG; 1 mg/kg/die for three days) or anti-CD25 monoclonal antibody (basiliximab; 20 mg at time of transplant and 20 mg at the fourth day post-transplant). Methylprednisolone was added in both cases. Triple immunosuppressive standard regimens was also administered after transplant (cyclosporin or tacrolimus/micophenolic acid or mycophenolatemofetil/methylprednisolone), according to therapeutic protocols. All the analysis were performed according to our Institutional Review Board and written informed consent was obtained by all enrolled patients (Protocol number 20180004199).

2.2 HCMV management and infection definitions

After transplant, HCMV DNAemia was monitored according to diagnostic protocols. In detail, HCMV DNAemia was monitored in whole blood weekly for the first 8 weeks and subsequently every 15 days until the 4^{th} month, then monthly until first year after transplant.

HCMV DNA was quantified using in-house real-time PCR performed on blood samples (26) with some modification. In detail, extraction QIAsymphony® DSP DNA Mini kit (Qiagen; Hilden, Germany) (200 µl of extraction volume) and QuantiFast Pathogen PCR kit (Qiagen) were used for DNA extraction and DNA amplification, respectively.

In case of suspected tissue invasive disease (TID), a tissue biopsy (gastrointestinal disease) or a bronco-alveolar lavage (BAL) fluid sample (pneumonia) was collected for HCMV DNA quantification and histopathological analysis. HCMV disease was defined as possible, probable, or proven according to Ljungman et al. (27).

Self-resolving HCMV DNAemia was defined as the detection of HCMV DNA in blood at any level with subsequent spontaneous clearance without antiviral treatment. Clinically significant HCMV infection was defined as HCMV infection requiring antiviral treatment (either as pre-emptive therapy or for treatment of HCMV disease).

2.3 Peripheral blood mononuclear cells isolation

Peripheral blood mononuclear cells (PBMC) were isolated from heparinized whole blood samples by density gradient centrifugation (Lymphoprep, Axis-Shield, Norway) and resuspended in culture

medium (RPMI 1640 supplemented with 2mM L-glutamine, 100U/mL penicillin and 100 µg/mL streptomycin and 10% of heat inactivated fetal bovine serum (Euroclone, Italy). Isolated PBMC were stored in nitrogen liquid using freezing medium (65% RPMI 1640 supplemented with 2mM L-glutamine, 100U/mL penicillin and 100 µg/mL streptomycin, 25% human albumin (Grifolds Biologicals, CA, USA) and 10% DMSO (Sigma-Aldrich, MO, USA). Before the use, PBMC were thawed, washed, resuspended in cultured medium and rested overnight at 37°C in a 5% CO_2 humidified atmosphere (28).

2.4 Synthetic peptides

For the evaluation of HCMV-specific T-cell response three peptide pools representative of the whole proteins pp65, IE1 and IE2 were used (JPT Peptide Technologies, Germany). All peptides were 15 aminoacids in length with an overlap of 11 aminoacids, representing a good compromise for stimulation of both $CD4^+$ and $CD8^+$ T cells (29). Pp65 peptide pool was composed by 138 peptides, IE1 by 120 peptides and IE2 by 143 peptides. Peptides were dissolved in DMSO (Sigma-Aldrich) and diluted in RPMI 1640 medium supplemented with 2mM L-glutamine, 100U/mL penicillin and 100 µg/mL streptomycin. Aliquotes were stored at -20°C until use. All peptide pools were used at the final concentration of 0,25 µg/mL for each peptide.

2.5 HCMV-specific T-cell response detected by ELISpot assay

HCMV-specific T-cell response was determined by ELISpot assay, using ELISpot IFN-γ Basis kits from ELITech (Milan, Italy) according to manufacturer's instructions.

The Multitestplates (MTP) fitted with membranes and coated with anti-human IFN-γ antibody were supplied in the test kit. PBMC ($2x10^5$ cells/100 µl per well) were added in duplicate and stimulated with100 µl of antigen solution or culture medium only (negative control) or phytoheamagglutin (PHA; 5 µg/ml, Sigma-Aldrich). Plates were incubated from 20 to 24 hours at 37°C 5%CO_2 humidified atmosphere. After cells remove, the alkaline phosphatase (AP)-labeled secondary antibody was added. Two hours later a substrate solution (BCIP/NBT) was added. After several washes under running water, plates were dried. Spots per counted using automated AID ELISpot reader system (AutoImmunDiagnostika GmbH, Germany).

2.6 Lymphocyte count

Fresh whole blood was stained with anti-CD3-PC5, anti-CD45-FITC, anti-CD4-RD1 and anti-CD8-ECD monoclonal antibodies (Beckman Coulter, Milan, Italy). After lysis of red blood cells, the absolute number of $CD3^+$, $CD3^+CD4^+$ and $CD3^+CD8^+$ T-cell counts were determined by flow cytometry (Navios, Beckman Coulter) using Flow-Count Fluorospheres (Beckman Coulter).

2.7 Data analysis

The mean number of spots obtained from duplicate wells was adjusted to 10^6 PBMC. The mean number of spots/million PBMC obtained by culture medium only was subtracted by the mean number of spots/million PBMC in response to the corresponding antigen in order to obtain the net spots/million PBMC. Results were then given as net spots/million PBMC (later in the text defined as "spots"). Quantitative variables were shown in terms of median or mean values and interquartile range (IQR) while categorical variables were presented as number or percentage. Mann-Whitney test and Fisher's test were used for data analysis, as well as receiver-operator characteristic (ROC) analysis. Log-rank test was used for the evaluation of cumulative incidence. The best cut-off to predict the spontaneous clearance of HCMV infection at pre-transplant was calculated according to the Youden Index. A multivariate logistic regression was also performed. All the statistical analysis were performed by using GraphPad Prism 8.3.0 (GraphPad Software Inc, CA, USA). All tests were two tailed and p value<0.05 was considered significant.

3 Results

3.1 Patients

Sixty-five HCMV-seropositive KTRs (47 males and 18 females; median age 51 years, [IQR 46-61]) were enrolled at time of transplant. HCMV serological status was positive in 39 (60%) donors, negative in 8 (12.3%) donors and un-known in 18 (27.7%) donors. Clinical characteristics of the patients are shown in Table 1. Overall, 44/65 (68%) patients showed at least one self-resolved HCMV reactivation event or undetectable HCMV DNA during the follow up period and were defined as "Controllers", while 21/65 (32%) were treated for clinically significant HCMV reactivation and were defined as "Non-Controllers".

There were no significant differences in baseline characteristics between the two groups of Controllers and Non-Controllers, except for the age at time of transplant (p=0.046). Additionally, even if the difference is not statistically significant, the rate of HCMV seropositive donors was higher in Non-controllers (p=0.069) (Table 1). The median follow-up after transplantation was 7.2 years (IQR 5.9–8.5 years) for the entire cohort of patients, 7 years (IQR 5.9–8.5 years) for Controllers and 7.3 years (IQR 5.4–8.4 years) for Non-Controllers. Overall, 10/65 (15%) patients died, and 5 of them were Non-Controllers (Figure 1A). Based on our results, the overall

TABLE 1 Clinical and demographic patients' characteristics.

Characteristics	All patients (n=65)	Controllers (n=44)	Non-Controllers (n=21)	*p value*
Age, median [IQR]	51 (46–61)	50 (45–57)	59 (47–64)	**0.046**
Gender, n (%):				
Male	47 (72)	32 (73)	15 (71)	0.999
Female	18 (28)	12 (27)	6 (29)	
Donor Serostatus n (%)				
HCMV positive (D+) HCMV negative (D-) HCMV unknown	39 (60) 8 (12) 18 (28)	27 (62) 8 (18) 9 (20)	12 (57) 0 9 (43)	0.069
Primary Diagnosis, n (%)				
Polycystic kidney	14 (22)	8 (18)	6 (29)	0.352
Nephropathy	13 (20)	11 (25)	1 (5)	0.084
Glomerulonephritis	7 (11)	5 (11)	2 (19)	0.999
Nephroangiosclerosis	5 (7)	3 (7)	2 (9)	0.654
Other	14 (22)	9 (20)	6 (29)	0.535
Unknown	12 (18)	8 (18)	4 (19)	0.999
Induction Therapy, n (%):				
Anti-CD25	51 (78)	35 (79)	16 (76)	0.988
ATG	14 (22)	9 (21)	5 (24)	
Immunosuppressive regimen, n (%):				
Cya, MMF, Steroids	8 (12)	4 (9)	4 (19)	0.420
FK-506, MMF, Steroids	53 (82)	37 (84)	16 (76)	0.502
FK-506, Steroids	1 (2)	0	1 (5)	0.323
Everolimus, FK-506, MMF, Steroids	3 (4)	3 (7)	0	0.545

ATG, anti-human thymocyte globulin; Cya, Cyclosporien A; FK506, tacrolimus; MMF, mycophenolate mofetil.
The value in bold refers to a significant difference.

survival in controllers seems to be higher than that measured in non-controllers. However, this difference is not statistically significant. Regarding the graft survival, 9/65 (14%) patients had graft failure and 3 of them were Non-Controllers (Figure 1B).

3.2 Pre-transplant absolute number of total CD8$^+$ T cell as predictive marker of spontaneously resolving HCMV reactivation during the first year post-transplant

The pre-transplant absolute number of total CD4$^+$ and CD8$^+$ T cells in blood was compared in 44 Controllers and 21 Non-Controllers at pre-transplant. No difference was observed in terms of the median of total CD4$^+$ T cell between Controllers and Non-Controllers (610 [IQR 418-838] vs 528 [IQR 377-788] T-cell/µl, respectively) while the median of total CD8$^+$T cell was found to be higher in Controllers than Non-Controllers (310 [IQR 215-424] vs 212 [IQR 157-338] T-cell/µl, respectively, p=0.025) (Figure 2A). In order to predict the spontaneous clearance of HCMV infection based on the absolute number of CD8$^+$ T cell, the ROC curve analysis was performed. The optimal cut-off value of 215 CD8$^+$ T cell/µl was selected using the Youden index (AUC: 0.67, 95% CI: 0.52-0.82, p=0.025) (Supplementary Table 1).

Interestingly, the cumulative incidence of HCMV reactivations during the first year after transplant in patients with the absolute number of CD8$^+$< 215 T cell/µl was 85%, while in patients with the absolute number of CD8$^+$ ≥215 T cell/µl it was 79% (p=0.005, Figure 2B). HCMV DNAemia at peak was measured and compared

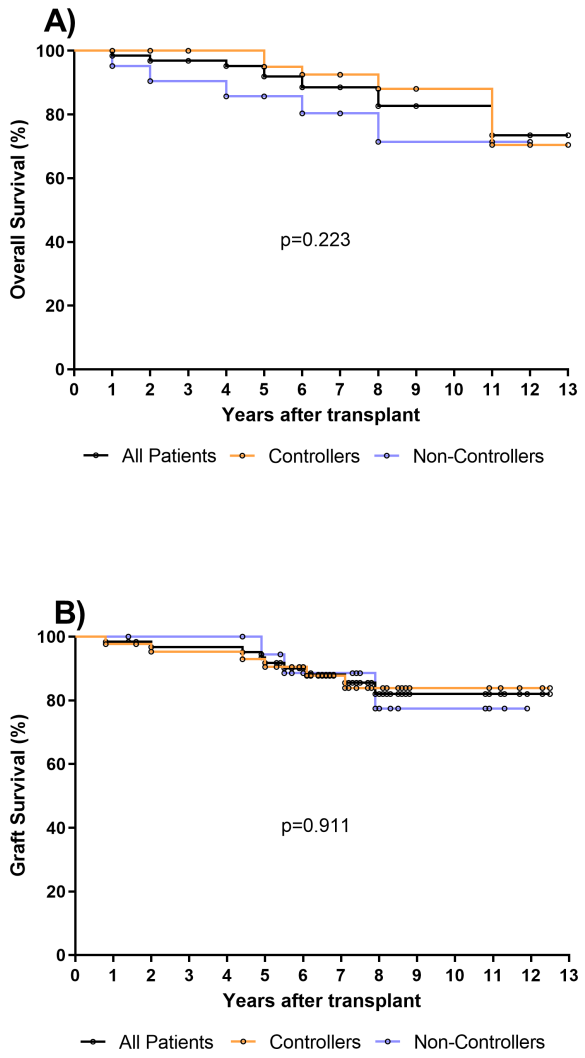

FIGURE 1
(A) Overall survival was evaluated in all kidney transplant recipients (KTR, n=65) (black line), in 44 Controllers (orange line) and in 21 Non-Controllers (purple line). No difference in overall survival was observed between controllers and non-controllers (p=0.223). **(B)** Graft survival was evaluated in all kidney transplant recipients (KTR, n=65) (black line), in 44 Controllers (orange line) and in 21 Non-Controllers (purple line). No difference of graft survival was observed between controllers and non-controllers (p=0.911).

in 22 patients with the absolute number of $CD8^+$< 215 T cell/µl and in 43 patients with $CD8^+$ ≥ 215 T cell/µl in blood. We observed that median of HCMV DNAemia at peak was 47295 [IQR 4455-243863] copies/mL in patients with the absolute number of $CD8^+$< 215 T cell/µl in blood, and 13050 (2250–64150) copies/mL in patients with the absolute number of $CD8^+$ ≥ 215 T cell/µl in blood (Figure 2C), even if this difference was not statistically significant (p=0.169). Regarding patients with the absolute number of $CD8^+$< 215 T cell/µl, 12 out of 22 (55%) were Non-Controllers, while 10 out of 22 (45%) patients were Controllers. On the other hand, patients with the absolute number of $CD8^+$ ≥ 215 T cell/µl, 9 out of 43 (21%) were Non-Controllers, while 34 out of 43 (79%) were Controllers (p=0.018, Figure 2D).

3.3 Pre-transplant IE1-specific T-cell response as a second predictive marker of spontaneously resolving HCMV reactivation during the first year post-transplant

HCMV-specific T-cell response was evaluated in 62 patients (41 Controllers and 21 Non-Controllers). Both pp65 and IE2-specific T-cell response did not significantly differ between Controllers and Non-Controllers (p=0.193 and p=0.869, respectively). On the contrary, a significantly higher median IE1-specific T-cell response was observed in Controllers compared to Non-Controllers (330 [IQR 69-1744] vs 28 [IQR 7-292] spots, respectively; p=0.015) (Figure 3A). Additionally, a negative correlation between DNAemia peak and IE1-specific T-cell responses was observed (p=0.0092, r= -0.33 IC 95% between -0.54 and -0.07). Based on these results, a ROC curve analysis was used to predict the spontaneous clearance of HCMV infection and cut-off of 60 spots of IE1-specific T-cell response was calculated using Youden index (Supplementary Table 1).

In patients with IE1-specific T-cell response< 60 spots the cumulative incidence of HCMV reactivation events was 90%, while in patients with IE1-specific T-cell response ≥ 60 spots a cumulative incidence of HCMV reactivation events of 77% was observed (p=0.0019, Figure 3B). HCMV DNAemia at peak was measured and compared in the two groups of patients, showing that median of HCMV DNAemia at peak was 81325 [IQR 5378-404325] copies/mL in patients with IE1-specific T-cell response< 60 spots and 8390 (337–50085) copies/mL in patients with IE1-specific T-cell response ≥ 60 spots (p<0.001, Figure 3C). Among patients with an IE1-specific T-cell response at pre-transplant<60 spots, 13 out of 22 (59%) were Non-Controllers, while 9 out of 22 (41%) were Controllers. Otherwise, looking at patients with an IE1-specific T-cell response ≥ 60 spots, 8 out of 40 (20%) were Non-Controllers, while 32 out of 40 (80%) were Controllers (p=0.004, Figure 3D). In other words, since a higher proportion of Controllers patients showed an IE1-specific T-cell response ≥ 60 spots, measuring HCMV-specific T-cell response at baseline might be used for identifying patients with high rate of self-resolving HCMV reactivation in the post-transplant period.

3.4 The use of combined immunological markers might be used for optimizing the HCMV management of transplanted patients

Based on these findings, age at time of transplant, $CD8^+$ T-cell count and IE1-specific T-cell response can be independently used for predicting the risk of treatment for severe HCMV reactivation in HCMV seropositive KTRs. Then, we combined the parameters for identifying the percentage of non-controllers in each group as shown in Figure 4. Groups were classified according to age lower than 60 years, high $CD8^+$ T cell count (≥215 cells/µl), and high level of IE1-specific T-cell response (≥60 spots). In detail, group 1

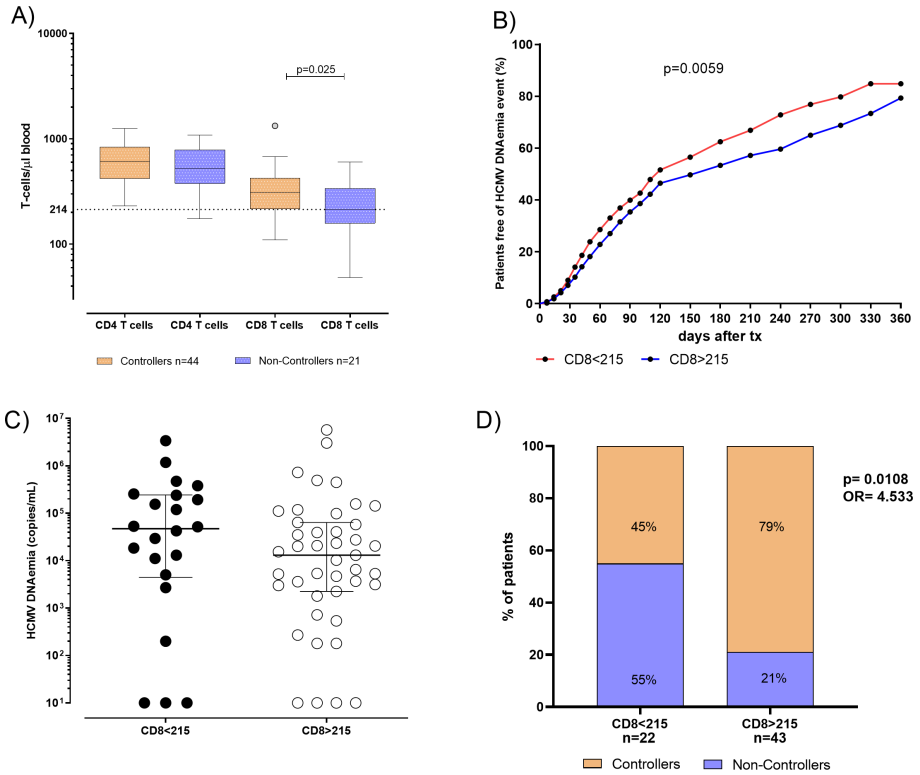

FIGURE 2
(A) Absolute number of total CD4 and CD8 T cells were evaluated and compared in 44 patients Controllers (orange bars) for and 21 Non-Controllers (purple bars). Median of total CD4 and CD8 T cells were shown in the graph as well as significant *p* value. **(B)** Cumulative incidence of HCMV reactivation events in patients absolute number of total CD8 T-cell response<215 CD8 T cells/µl (red line) and in patients with absolute number of total CD8 T-cell response ≥ 215 CD8 T cells/µl (blue line). **(C)** HCMV DNAemia peak in kidney transplant recipients (KTR) was measured in 22 patients with total CD8 T. **(D)** Percentage of Controllers (orange bars) and Non-Controllers patients (purple bars) according to absolute number of total CD8 T-cell response<215 CD8 T cells/µl and in patients with absolute number of CD8 T-cell response ≥ 215 CD8 T cells/µl. P value and Odd ratio (OR) were also given.

included patients with all the three markers (n=21), group 2 included patients at two of the three markers (n=26) while group 3 included patients with only one of the markers described (n=12). Group 4 included patients with none of the markers (n=3). The number and percentage of controllers and non-controllers were given for each group. Interestingly, among group 1, only one of the 21 patients was treated for uncontrolled HCMV infection. On the other hand, all the three patients of group 4 were treated for uncontrolled HCMV infection.

Multivariate logistic analysis for predicting the risk of HCMV Non-Controllers (treated) infection was performed including IE1-specific T-cell response (higher or lower than 60 spots), $CD8^+$ T-cell count (higher or lower than 215 cells/µl) and age (higher or lower than 60 years) as variables. Results were given in Table 2 and Figure 5. Mathematical function is the following:

$$\begin{aligned} \text{Logit}[P(Y=1)] &= \text{Ln}[(P(Y=1)/P(Y=0)] \\ &= \beta 0 + \beta 1 * B + \beta 2 * C + \beta 3 * D \end{aligned}$$

Based on the proposed model, the combination of the three variables are able to predict with high probability the rate of controller patients. In detail, percentages of negative and positive predictive power were 80% and 80.85%, respectively. The percentage of correctly classified "Controllers" was 92.7% while the percentage of correctly classified "Non-Controllers" was 57.2%.

4 Discussion

The evaluation of HCMV serostatus in both donor and recipient at time of transplant is considered the most informative approach for the stratification of the risk for HCMV infection after transplant. However, even if HCMV-seropositive recipients are considered to have HCMV-specific immune response, HCMV can reactivate in some patients leading to the risk of HCMV-related complications (30). For this reason, a tool for a better stratification should be introduced, especially for the risk definition among HCMV-seropositive recipients (31).

In this study, we examined the role of lymphocyte count and HCMV-specific T-cell response measured at pre-transplant as potential predictive markers of spontaneous control of HCMV reactivations following kidney transplant. High absolute number of $CD8^+$ T cells and sustained IE1-specific T-cell response were

10.3389/fimmu.2025.1538795

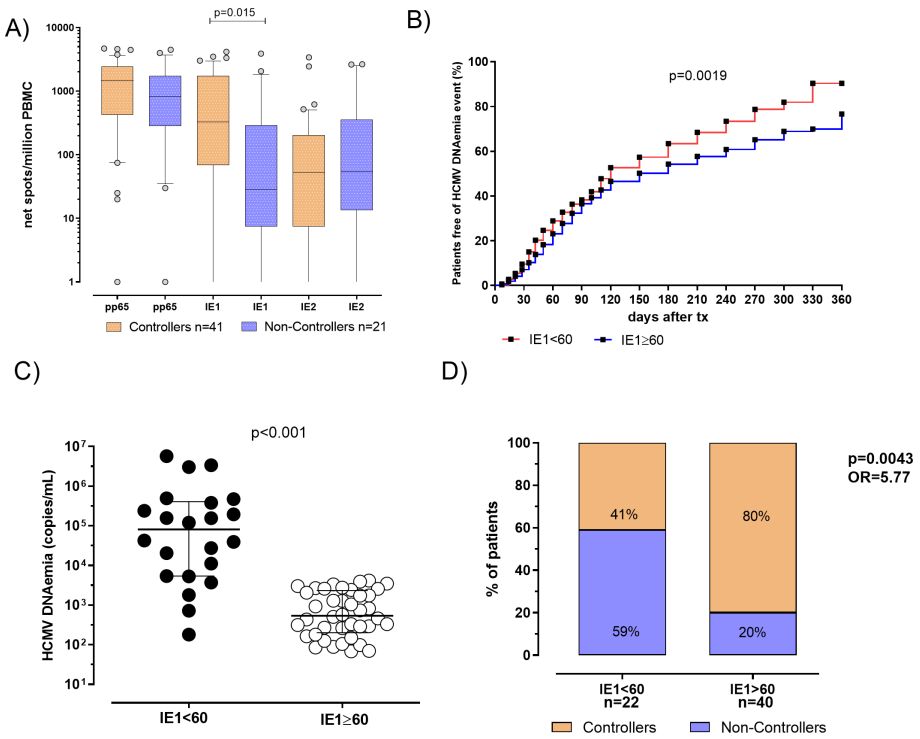

FIGURE 3
(A) Pp65, IE1 and IE2 specific T-cell responses were evaluated and compared in 41 patients Controllers (orange bars) for and 21 Non-Controllers (purple bars). Median antigen-specific T-cell responses were shown in the graph as well as each *p* value. **(B)** Cumulative incidence of HCMV reactivation events in patients with IE1-specific T-cell response<60 spots (red line) patients with IE1-specific T-cell response ≥ 60 spots (blue line). **(C)** HCMV DNAemia peak in patients classified according to pre transplant IE1-specific T-cell response. **(D)** Percentage of Controllers (orange bars) and Non-Controllers patients (purple bars) according to pre-defined IE1-specific T-cell response cut-off of 60 spots. P value and Odd ratio (OR) were also given.

TABLE 2 Multivariate logistic regression.

Odds ratios	Variable	Estimate	95% CI (profile likelihood)	"p value"
β0	Intercept	0,036	0,003082 to 0,2390	0,0022
β1	B: IE1	8,614	2,194 to 42,92	0,0038
β2	C: CD8	7,254	1,841 to 34,98	0,0071
β3	D: age	8,341	1,916 to 46,74	0,0079

independently associated with highest rate of patients with spontaneous resolution of HCMV reactivation (defined as controllers) during the first year after transplant. Moreover, the rate of Controllers was higher in younger subjects. Additionally, even if the difference is not statistically significant, it seems that donor serostatus could have an impact on the occurrence of clinically relevant HCMV reactivations. However, as major limitation of the study, HCMV donor serostatus is unknown for about 30% of the subjects.

Many studies investigated the role of absolute lymphocyte count measured after transplant or at time of treatment in predicting the rate of HCMV infection or recurrent HCMV infection after treatment (10, 32–34). However, the potential role of baseline pre-transplant measurement has been less extensively investigated. In our study, a threshold of IE1-specific T-cell response of 60 net spots/million PBMC was the best cut off for the identification of patients with high probability to control HCMV reactivation spontaneously. Previous studies suggested a possible role of lower IE1-specific T-cell response as risk factor for HCMV reactivation (20, 23, 25, 35). In our study, higher pre-transplant pp65-specific T-cell response was observed in patients with self-resolving HCMV reactivation than in patients with clinically relevant HCMV reactivation, although the difference was not statistically significant. On the contrary, Kim and colleagues reported that pp65-specific T-cell response measured at pre-transplant, but not IE1-specific T-cell response seems to predict

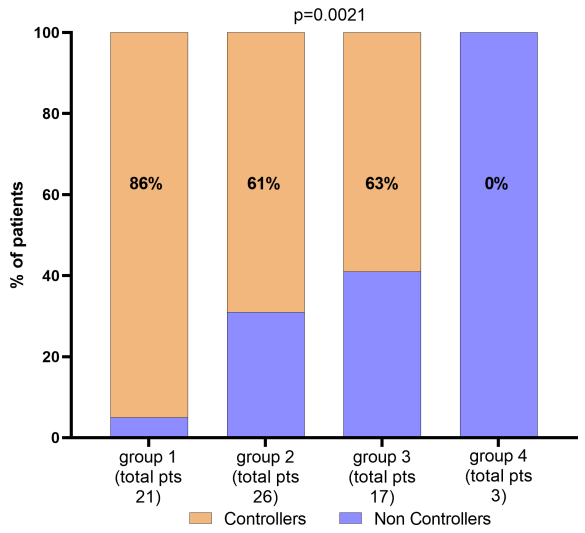

FIGURE 4
Percentage of patients according with CD8 T-cells, IE1 spots levels and age. Total number of patients and percentage of Controllers have been given for each group. Parameters for the classification of each group have been described in the text.

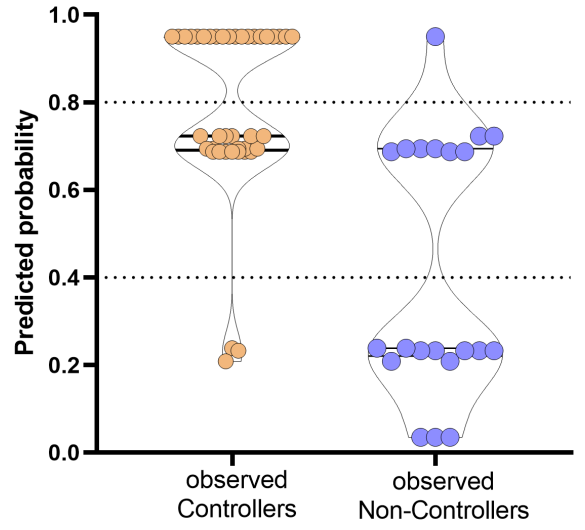

FIGURE 5
Prediction of probability of the event occurrence in observed Controllers (orange dots) and Non-Controllers (purple dots). The y-axis ranges from 0 (highest probability to be HCMV uncontroller) to 1 (highest probability to be HCMV controller). Dotted horizontal lines have been included for indicating grey zone.

the development of HCMV reactivation in HCMV-seropositive patients (36). The reasons for these differences might be related to the type of stimuli used or outcome definition. Further evaluation on this field are necessary. So far, the lack of standardized assays represents a crucial issue for the comparison of results between different clinical settings.

Based on our results, patients with pre-transplant IE1-specific T-cell response above this cut off showed higher probability to develop self-resolving HCMV reactivations. Furthermore, the cumulative incidence of HCMV reactivation events in patients with impaired pre-transplant IE1-specific T-cell response was higher. This means that higher pre-transplant IE1-specific T-cell response could be predictive of sustained immunity in the post-transplant period (15). According to this hypothesis, it was previously observed that patients with positive pre-transplant HCMV-specific T-cell response showed higher HCMV-specific immune response in the post-transplant period. On the contrary, in patients with no pre-transplant HCMV-specific immune response, post-transplant T-cell response specific for HCMV was detectable 3 months after transplant in less than 50% of patients, suggesting a long-term impairment in the control of HCMV infection (21). To date, no universal cut-off of DNAemia have been chosen for starting pre-emptive therapy; for this reason pre-transplant HCMV-specific T-cell response should be evaluated in different transplant setting, in relation to diagnostic and therapeutic protocols. To conclude, in addition to the assessment of HCMV serostatus in patients attending for transplant, pre-transplant IE1-specific T-cell response and $CD8^+$ T cell count evaluation should be further investigated for definition of potential algorithm for a better stratification of the risk in HCMV-seropositive recipients and "*ad hoc*" therapeutic strategies, including modulation of immunosuppression therapy.

Data availability statement

The raw data supporting the conclusions of this article will be made available by the authors, without undue reservation.

Ethics statement

The studies involving humans were approved by The study was approved by the Ethics Committee and Fondazione IRCCS Policlinico San Matteo Institutional Review Board (Protocol number 20180004199) and patients gave written informed consent. The studies were conducted in accordance with the local legislation and institutional requirements. The participants provided their written informed consent to participate in this study.

Author contributions

FZ: Data curation, Formal Analysis, Writing – review & editing, Investigation, Methodology. IC: Data curation, Formal Analysis, Writing – review & editing, Conceptualization, Funding acquisition, Supervision, Writing – original draft. MGre: Data

curation, Writing – review & editing. MGri: Data curation, Writing – review & editing. TR: Data curation, Supervision, Writing – review & editing. DL: Supervision, Writing – review & editing. FB: Funding acquisition, Supervision, Writing – review & editing.

Funding

The author(s) declare that financial support was received for the research and/or publication of this article. This study was supported by grants from the Ministero della Salute, Fondazione IRCCS Policlinico San Matteo, Ricerca Corrente grant no. 08075023 (to I.C) and Ricerca Finalizzata (Grant RF-2019-12370797 to F.B.).

Acknowledgments

We thank Daniela Sartori for manuscript editing.

Conflict of interest

The authors declare that the research was conducted in the absence of any commercial or financial relationships that could be construed as a potential conflict of interest

Generative AI statement

The author(s) declare that no Generative AI was used in the creation of this manuscript.

Publisher's note

Supplementary material

The Supplementary Material for this article can be found online at: https://www.frontiersin.org/articles/10.3389/fimmu.2025.1538795/full#supplementary-material

SUPPLEMENTARY FIGURE 1
Flow-chart representing the enrollment and monitoring of kidney transplant recipients. KTR: kidney transplant recipients; PBMC: peripheral blood mononuclear cells; (*) patients with self-resolving HCMV reactivations or undetectable HCMV DNAemia; (**) patients treated for clinically significant HCMV reactivation

References

1. Fishman JA. Infection in organ transplantation. *Am J Transplant*. (2017) 17:856–79. doi: 10.1111/ajt.14208

2. Fishman JA, Emery V, Freeman R, Pascual M, Rostaing L, Schlitt HJ, et al. Cytomegalovirus in transplantation - challenging the status quo. *Clin Transplant*. (2007) 21:149–58. doi: 10.1111/j.1399-0012.2006.00618.x

3. Bruminhent J, Razonable RR. Management of cytomegalovirus infection and disease in liver transplant recipients. *World J Hepatol*. (2014) 6:370–83. doi: 10.4254/wjh.v6.i6.370

4. Kotton CN, Kumar D, Caliendo AM, Asberg A, Chou S, Danziger-Isakov L, et al. Updated international consensus guidelines on the management of cytomegalovirus in solid-organ transplantation. *Transplantation*. (2013) 96:333–60. doi: 10.1097/TP.0b013e31829df29d

5. Grossi PA, Peghin M. Recent advances in cytomegalovirus infection management in solid organ transplant recipients. *Curr Opin Organ Transplant*. (2024) 29:131–7. doi: 10.1097/MOT.0000000000001139

6. Razonable RR, Humar A. AST Infectious Diseases Community of Practice. Cytomegalovirus in solid organ transplantation. *Am J Transplant*. (2013) 13 Suppl 4:93–106. doi: 10.1111/ajt.12103

7. Calarota SA, Zelini P, De Silvestri A, Chiesa A, Comolli G, Sarchi E, et al. Kinetics of T-lymphocyte subsets and posttransplant opportunistic infections in heart and kidney transplant recipients. *Transplantation*. (2012) 93:112–9. doi: 10.1097/TP.0b013e318239e90c

8. Calarota SA, Chiesa A, De Silvestri A, Morosini M, Oggionni T, Marone P, et al. T-lymphocyte subsets in lung transplant recipients: association between nadir CD4 T-cell count and viral infections after transplantation. *J Clin Virol*. (2015) 69:110–6. doi: 10.1016/j.jcv.2015.06.078

9. Hall VG, Humar A, Kumar D. Utility of cytomegalovirus cell-mediated immunity assays in solid organ transplantation. *J Clin Microbiol*. (2022) 60:e0171621. doi: 10.1128/jcm.01716-21

10. Gardiner BJ, Nierenberg NE, Chow JK, Ruthazer R, Kent DM, Snydman DR. Absolute lymphocyte count: A predictor of recurrent cytomegalovirus disease in solid organ transplant recipients. *Clin Infect Dis*. (2018) 67:1395–402. doi: 10.1093/cid/ciy295

11. Zavaglio F, Rivela F, Cassaniti I, Arena F, Gabanti E, Asti AL, et al. ELISPOT assays with pp65 peptides or whole HCMV antigen are reliable predictors of immune control of HCMV infection in seropositive kidney transplant recipients. *J Med Virol*. (2023) 95:e28507. doi: 10.1002/jmv.28507

12. Zavaglio F, Cassaniti I, d'Angelo P, Zelini P, Comolli G, Gregorini M, et al. Immune control of human cytomegalovirus (HCMV) infection in HCMV-seropositive solid organ transplant recipients: the predictive role of different immunological assays. *Cells*. (2024) 13:1325. doi: 10.3390/cells13161325

13. Gabanti E, Bruno F, Lilleri D, Fornara C, Zelini P, Cane I, et al. Human cytomegalovirus (HCMV)-specific CD4+ and CD8+ T cells are both required for prevention of HCMV disease in seropositive solid-organ transplant recipients. *PloS One*. (2014) 9:e106044. doi: 10.1371/journal.pone.0106044

14. Meesing A, Razonable RR. New developments in the management of cytomegalovirus infection after transplantation. *Drugs*. (2018) 78:1085–103. doi: 10.1007/s40265-018-0943-1

15. Gerna G, Lilleri D, Fornara C, Comolli G, Lozza L, Campana C, et al. Monitoring of human cytomegalovirus-specific CD4 and CD8 T-cell immunity in patients receiving solid organ transplantation. *Am J Transplant*. (2006) 6:2356–64. doi: 10.1111/j.1600-6143.2006.01488.x

16. Gerna G, Lilleri D, Chiesa A, Zelini P, Furione M, Comolli G, et al. Virologic and immunologic monitoring of cytomegalovirus to guide preemptive therapy in solid-organ transplantation. *Am J Transplant*. (2011) 11:2463–71. doi: 10.1111/j.1600-6143.2011.03636.x

17. Rogers R, Saharia K, Chandorkar A, Weiss ZF, Vieira K, Koo S, et al. Clinical experience with a novel assay measuring cytomegalovirus (CMV)-specific CD4+ and CD8+ T-cell immunity by flow cytometry and intracellular cytokine staining to predict clinically significant CMV events. *BMC Infect Dis*. (2020) 20:58. doi: 10.1186/s12879-020-4787-4

18. Fernández-Ruiz M, Giménez E, Vinuesa V, Ruiz-Merlo T, Parra P, Amat P, et al. Regular monitoring of cytomegalovirus-specific cell-mediated immunity in intermediate-risk kidney transplant recipients: predictive value of the immediate post-transplant assessment. *Clin Microbiol Infect*. (2019) 25:381. doi: 10.1016/j.cmi.2018.05.010

19. Mena-Romo JD, Pérez Romero P, Martín-Gandul C, Gentil M.Á., Suárez-Artacho G, Lage E, et al. CMV-specific T-cell immunity in solid organ transplant recipients at low risk of CMV infection. Chronology and applicability in preemptive therapy. *J Infect*. (2017) 75:336–45. doi: 10.1016/j.jinf.2017.05.020

20. Rittà M, Costa C, Sidoti F, Ballocco C, Ranghino A, Messina M, et al. Pre-transplant assessment of CMV-specific immune response by Elispot assay in kidney transplant recipients. *New Microbiol*. (2015) 38:329–35.

21. Molina-Ortega A, Martín-Gandul C, Mena-Romo JD, Rodríguez-Hernández MJ, Suñer M, Bernal C, et al. Impact of pretransplant CMV-specific T-cell immune response in the control of CMV infection after solid organ transplantation: a prospective cohort study. *Clin Microbiol Infect*. (2019) 25:753–8. doi: 10.1016/j.cmi.2018.09.019

22. Cantisán S, Lara R, Montejo M, Redel J, Rodríguez-Benot A, Gutiérrez-Aroca J, et al. Pretransplant interferon-γ secretion by CMV-specific CD8+ T cells informs the risk of CMV replication after transplantation. *Am J Transplant*. (2013) 13:738–45. doi: 10.1111/ajt.12049

23. López-Oliva MO, Martinez V, Buitrago A, Jiménez C, Rivas B, Escuin F, et al. Pretransplant CD8 T-cell response to IE-1 discriminates seropositive kidney recipients at risk of developing CMV infection posttransplant. *Transplantation*. (2014) 97:839–45. doi: 10.1097/01.TP.0000438025.96334.eb

24. López-Oliva MO, Martínez V, Rodríguez-Sanz A, Álvarez L, Santana MJ, Selgas R, et al. Pre-transplant assessment of pp65-specific CD4 T cell responses identifies CMV-seropositive patients treated with rATG at risk of late onset infection. *Clin Immunol*. (2020) 211:108329. doi: 10.1016/j.clim.2019.108329

25. Bestard O, Lucia M, Crespo E, Van Liempt B, Palacio D, Melilli E, et al. Pretransplant immediately early-1-specific T cell responses provide protection for CMV infection after kidney transplantation. *Am J Transplant*. (2013) 13:1793–805. doi: 10.1111/ajt.12256

26. Furione M, Rognoni V, Cabano E, Baldanti F. Kinetics of human cytomegalovirus (HCMV) DNAemia in transplanted patients expressed in international units as determined with the Abbott RealTime CMV assay and an in-house assay. *J ClinVirol*. (2012) 55:317–22. doi: 10.1016/j.jcv.2012.08.017

27. Ljungman P, Boeckh M, Hirsch HH, Josephson F, Lundgren J, Nichols G, et al. Disease definitions working group of the cytomegalovirus drug development forum. Definitions of cytomegalovirus infection and disease in transplant patients for use in clinical trials. *Clin Infect Dis*. (2017) 64:87–91. doi: 10.1093/cid/ciw668

28. Cassaniti I, Calarota SA, Adzasehoun KM, Chiesa A, Comolli G, Parea M, et al. Memory T cells specific for HBV enumerated by a peptide-based cultured enzyme-linked immunospot assay in healthy HBV-vaccinated subjects. *Hum VaccinImmunother*. (2016) 12:2927–33. doi: 10.1080/21645515.2016.1204500

29. Kiecker F, Streitz M, Ay B, Cherepnev G, Volk HD, Volkmer-Engert R, et al. Analysis of antigen-specific T-cell responses with synthetic peptides–what kind of peptide for which purpose? *Hum Immunol*. (2004) 65:523–36. doi: 10.1016/j.humimm.2004.02.017

30. Westall GP, Mifsud NA, Kotsimbos T. Linking CMV serostatus to episodes of CMV reactivation following lung transplantation by measuring CMV-specific CD8+ T-cell immunity. *Am J Transplant*. (2008) 8:1749–54. doi: 10.1111/j.1600-6143.2008.02294.x

31. Yong MK, Lewin SR, Manuel O. Immune monitoring for CMV in transplantation. *Curr Infect Dis Rep*. (2018) 20:4. doi: 10.1007/s11908-018-0610-4

32. Meesing A, Abraham RS, Razonable RR. Clinical correlation of cytomegalovirus infection with CMV-specific CD8+ T-cell immune competence score and lymphocyte subsets in solid organ transplant recipients. *Transplantation*. (2019) 103:832–8. doi: 10.1097/TP.0000000000002396

33. Schoeberl AK, Zuckermann A, Kaider A, Aliabadi-Zuckermann A, Uyanik-Uenal K, Laufer G, et al. Absolute lymphocyte count as a marker for cytomegalovirus infection after heart transplantation. *Transplantation*. (2023) 107:748–52. doi: 10.1097/TP.0000000000004360

34. Yoon M, Oh J, Chun KH, Lee CJ, Kang SM. Post-transplant absolute lymphocyte count predicts early cytomegalovirus infection after heart transplantation. *Sci Rep*. (2021) 11:1426. doi: 10.1038/s41598-020-80790-4

35. Bunde T, Kirchner A, Hoffmeister B, Habedank D, Hetzer R, Cherepnev G, et al. Protection from cytomegalovirus after transplantation is correlated with immediate early 1-specific CD8 T cells. *J Exp Med*. (2005) 201:1031–6. doi: 10.1084/jem.20042384

36. Kim SH, Lee HJ, Kim SM, Jung JH, Shin S, Kim YH, et al. Diagnostic usefulness of cytomegalovirus (CMV)-specific T cell immunity in predicting CMV infection after kidney transplantation: A pilot proof-of-concept study. *Infect Chemother*. (2015) 47:105–10. doi: 10.3947/ic.2015.47.2.105

frontiers | Frontiers in Immunology

TYPE Original Research
PUBLISHED 28 April 2025
DOI 10.3389/fimmu.2025.1562951

OPEN ACCESS

EDITED BY
Rita Maccario,
San Matteo Hospital Foundation (IRCCS), Italy

REVIEWED BY
Roberto Crocchiolo,
Niguarda Ca' Granda Hospital, Italy
Daniele Lilleri,
San Matteo Hospital Foundation (IRCCS), Italy

*CORRESPONDENCE
Yifu Hou
houyifu0726@foxmail.com
Hongji Yang
hongji_yang65@126.com

†These authors have contributed equally to this work and share first authorship

RECEIVED 18 January 2025
ACCEPTED 07 April 2025
PUBLISHED 28 April 2025

CITATION
Zhong L, Tang S, Pu Z, Chen K, Di W, Hou Y and Yang H (2025) Impact of prophylactic cytomegalovirus immunoglobulin on cytomegalovirus viremia and graft function in ABO-incompatible living donor kidney transplantation: a retrospective analysis. *Front. Immunol.* 16:1562951. doi: 10.3389/fimmu.2025.1562951

Impact of prophylactic cytomegalovirus immunoglobulin on cytomegalovirus viremia and graft function in ABO-incompatible living donor kidney transplantation: a retrospective analysis

Linhong Zhong[1†], Shijie Tang[1†], Zhongping Pu[1†], Kai Chen[2], Wenjia Di[2], Yifu Hou[2*] and Hongji Yang[1,2*]

[1]Department of Hepatobiliary Surgery, The Affiliated Hospital, Southwest Medical University, Luzhou, Sichuan, China, [2]Department of Organ Transplantation, Sichuan Provincial Peoples Hospital, University of Electronic Science and Technology of China, Chengdu, China

Background: Cytomegalovirus (CMV) infection poses a significant risk to kidney transplant recipients. CMV immunoglobulin shows promising prophylactic effect, particularly in the context of ABO-incompatible transplants. However, its efficacy in preventing CMV viremia remains underexplored.

Methods: In this retrospective study, we enrolled patients who underwent ABO-incompatible living donor kidney transplantation between May 2021 and September 2023. Prophylactic CMV immunoglobulin was administered at 100 mg/kg weekly for one month in the combined prophylaxis group, while no prophylactic medication was applied in the preemptive therapy group. The primary outcome was measured as the incidence of clinically relevant CMV viremia (CMV DNA >10,000 copies/mL) within one year after transplantation. Both groups received standard preemptive therapy with ganciclovir or valganciclovir after diagnosed with clinically relevant CMV viremia.

Results: Prophylactic CMV immunoglobulin significantly reduced clinically relevant viremia incidence compared to preemptive therapy group (16.0% vs. 34.0%, P = 0.04). At the end of the follow-up, the combined prophylaxis group showed higher eGFR (56.40 ± 14.19 vs. 47.30 ± 13.01 mL/min/1.73m^2, P = 0.0014) and lower serum creatinine (146.5 ± 57.07 vs. 171.2 ± 51.48 μmol/L, P = 0.0274). However, no significant differences in renal function were observed between the groups at1,3, or 6 months post-transplantation.

Conclusion: CMV immunoglobulin represents a promising prophylactic option for reducing clinically relevant CMV viremia incidence and delaying infection onset in ABO-incompatible kidney transplant recipients.

KEYWORDS

ABO-incompatible kidney transplantation, CMV immunoglobulin, desensitization, graft function, immune deficiency

1 Introduction

Cytomegalovirus (CMV) infection is a major complication in kidney transplantation, significantly impacting patient survival, prognosis, and graft function (1, 2).With the increasing demand for donor organs among patients with end-stage renal disease, ABO-incompatible (ABOi) kidney transplantation has become widely adopted as a strategy to address donor shortages (3).To successfully perform ABOi transplantation, pretransplant desensitization protocols, which include intensified immunosuppression and antibody removal treatments, are necessary to lower anti-ABO antibody titers and reduce the risk of rejection (4, 5). However, these strategies may increase the risk of CMV infection in ABOi kidney transplant recipients.

Currently, ganciclovir or valganciclovir is widely recommended for the universal prophylaxis and preemptive therapy of CMV infection (5). However, these antiviral medications face significant challenges in the context of prophylaxis, particularly in ABOi transplantation. To begin with, the adverse effects of universal prophylaxis ganciclovir or valganciclovir, particularly the bone marrow suppression and nephrotoxicity, often lead to treatment discontinuation in ABOi transplant recipients (6, 7). Secondly, prolonged use of antiviral drugs may induce resistance, increasing the risk of CMV recurrence and indirectly threatening graft survival (8). Moreover, High economic costs, poor adherence to therapy, and limited drug availability further exacerbate the difficulties of CMV management in ABOi kidney transplant recipients (7, 9). In light of these challenges, the potential role of CMV immunoglobulin (CMVig) as a prophylactic agent in ABOi kidney transplantation remains underexplored, with limited data available to support its efficacy and application in this specific setting.

Notably, before the advent of antiviral drugs, CMVig had already been used to some extent for preventing CMV infection in kidney transplant recipients (10, 11). Recent studies and supplementary preclinical data have provided supportive evidence, reigniting interest in the potential of CMVig among ABOi transplant populations (12, 13). Given the unique immunological status and therapeutic needs of ABOi kidney transplant recipients, more personalized and intensive prophylactic measures are warranted (14, 15). If short-term CMVig administration can significantly reduce CMV infection rates or delay infection events, this could effectively alleviate the burden of ganciclovir/valganciclovir treatment. This would further address long-standing concerns of immunosuppressive load and drug-related adverse effects in ABOi kidney transplant recipients.

While CMVig demonstrates promising potential, its precise application protocols and long-term efficacy in ABOi kidney transplantation remain to be fully elucidated. This study aims to explore the role of CMVig in preventing CMV infections post-ABOi kidney transplantation, evaluate its effectiveness and safety under unique immune conditions, and provide a theoretical and clinical basis for optimizing infection management strategies in ABOi kidney transplantation.

Abbreviations: CMV, Cytomegalovirus; ABOi, ABO incompatible; CMVig, Cytomegalovirus immunoglobulin; HSV, herpes simplex virus; VZV, varicella-zoster virus; HHV, human herpesvirus.

2 Materials and methods

2.1 Patients and study design

This retrospective, single-center study analyzed patients who underwent ABOi kidney transplantation at our hospital between May 2021 and September 2023. The study design and workflow are illustrated in Figure 1. Inclusion criteria included: (a) ABOi kidney transplantation, (b) age 18–60 years, (c) no gender restrictions, (d) first or multiple kidney transplants, and (e) with or without other organ transplants. Patients with follow-up periods of less than one year or those who declined informed consent were excluded. The study adhered to the Declaration of Helsinki and was approved by the hospital's Ethics Committee and was approved by the Ethics Committee of the Sichuan Provincial Peoples Hospital (No. 20244631).

Patients were divided into two groups based on their postoperative CMV infection prevention protocol through patient-physician shared decision-making. The preemptive therapy group(PET group) received standard preemptive therapy with ganciclovir or valganciclovir initiated upon the detection of clinically relevant CMV viremia (CMV DNA >10,000 copies/mL). The combined prophylaxis group (CMVig group), defined as patients receiving CMV immunoglobulin (CMVig) in addition to preemptive therapy, was administered an additional prophylactic

regimen of CMV immunoglobulin (CMVig) administered at a dose of 100 mg/kg weekly for one month, starting on the first postoperative day. Outcomes assessed during a one-year follow-up included the incidence of clinically relevant CMV viremia, renal function (eGFR and serum creatinine), and postoperative complications (Figure 1).

2.2 ABO desensitization protocol and immunosuppressive regimen

Desensitization was achieved using plasmapheresis and monoclonal antibody therapy. Plasmapheresis was initiated seven days before transplantation (Day -7) with the goal of reducing anti-ABO antibody titers (IgM and IgG) to ≤1:16 prior to surgery. Monoclonal antibody therapy is carried out in two regimens. the first regimen consists of a single 200 mg dose of CD20 monoclonal antibody (administered two weeks preoperatively). The second regimen combines a reduced 100 mg dose of CD20 monoclonal antibody (administered two weeks preoperatively), with a complement C5 inhibitor, eculizumab (600 mg for patients <60 kg and 900 mg for patients ≥60 kg, administered one day before surgery) (Figure 2). Two weeks prior to transplantation, patients began a triple immunosuppressive regimen consisting of a calcineurin inhibitor, an antimetabolite (mycophenolate mofetil), and oral prednisone. Induction therapy involved rabbit anti-thymocyte globulin or basiliximab.

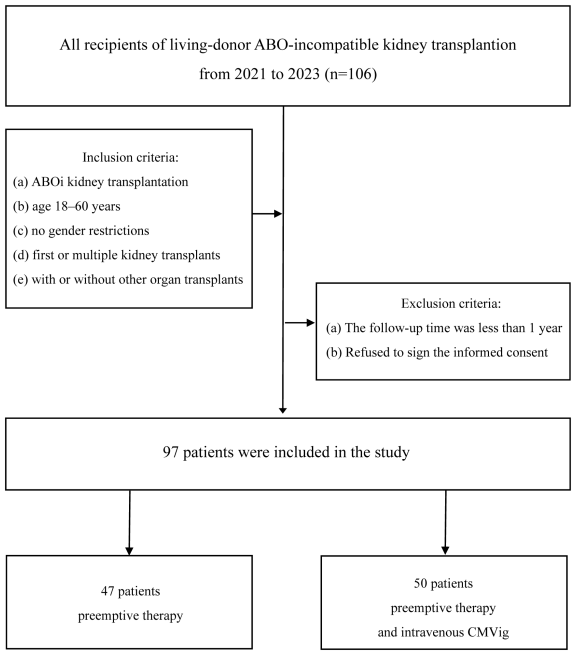

FIGURE 1
Study cohort and workflow. Patients were divided into two groups: preemptive therapy group (n=47) and combined prophylaxis group (preemptive therapy+CMVig, n=50). ABOi, ABO-incompatible; CMVig, Cytomegalovirus immunoglobulin.

2.3 Surgical procedure

Living donor organ procurement followed strict legal and ethical protocols, including approval from the hospital Ethics Committee and provincial health authorities. Donors were categorized as genetically related (e.g., parents, siblings, nephews/nieces) or non-genetically related (spouses). The methods for living donor nephrectomy are primarily classified into two types: open donor nephrectomy and laparoscopic donor nephrectomy via the retroperitoneal approach (Supplementary Table S1).

2.4 CMV infection monitoring and prevention

Clinically relevant CMV viremia was defined as CMV DNA levels exceeding 10,000 copies/mL. CMV DNA quantification was performed using quantitative nucleic acid testing with the Human Cytomegalovirus Nucleic Acid Quantitative Detection Kit (PCR-fluorescence probing; DAAN Gene Co., Ltd., China). Whole blood samples were analyzed. Postoperative CMV DNA levels were monitored weekly for the first three months, then monthly until one year. Prevention strategies included either standard preemptive therapy alone or combined with prophylactic CMVig. In the PET group, antiviral treatment was initiated upon detecting a viral load exceeding the threshold(CMV DNA >10,000 copies/mL). Patients received either valganciclovir (900 mg, twice daily, with dosage adjusted based on renal function) or ganciclovir (5 mg/kg, every 12 hours, with dosage adjusted based on renal function). The treatment duration was at least two weeks and continued until viral replication was completely eradicated. To evaluate response to preemptive therapy, weekly quantitative CMV DNA monitoring was performed. In the CMVig group, in addition to the preemptive therapy protocol, prophylactic CMVig (Human Immunoglobulin for Intravenous Injection, Shandong Taibang Biological Products Co., Ltd., China; potency: 721 IU/mL) was administered at 100 mg/kg (1442 IU/kg) weekly for one month, starting on the first postoperative day.

2.5 B cells monitoring and other outcomes

Peripheral blood B-cell counts were analyzed by flow cytometry (Beckman Coulter CytoFLEX) using whole blood staining with PE-Cy7-conjugated anti-CD19 (clone J3-119; Beckman Coulter).Results were expressed as absolute cell counts (cells/μL) and relative percentages of total lymphocytes. Data were retrospectively collected from the following time points: 14 days pre-transplant(day of rituximab administration), day of transplantation, and postoperative follow-ups. We also followed the rejection and infection-related events. Rejection (TCMR or ABMR) was diagnosed via Banff 2019 criteria. Infections were defined as: pulmonary infections (clinical symptoms and radiological/microbiological confirmation), BK virus infections (viruria/viremia via PCR, viruria $\geq 1\times10_7$ copies/mL, viremia $\geq 1\times10_4$ copies/mL), and herpesvirus infections (PCR/serology).

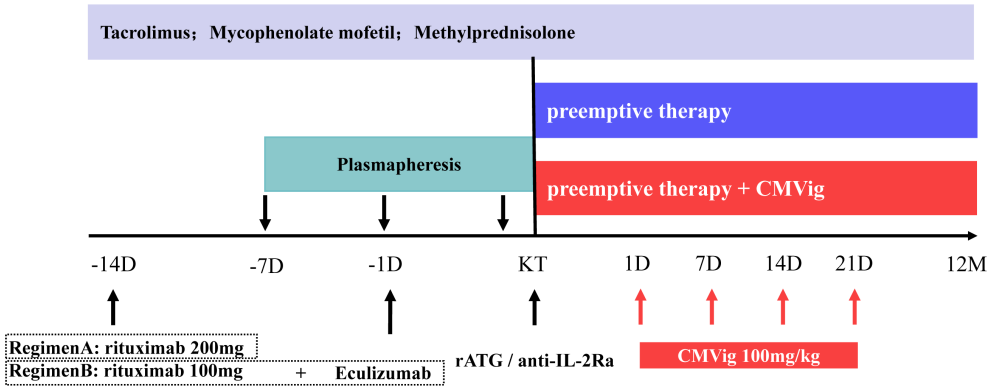

FIGURE 2
ABO desensitization protocols and immunosuppressive regimen. CMVig, Cytomegalovirus immunoglobulin; KT, kidney transplantation; rATG, rabbit anti-thymocyte globulin; anti-IL-2Ra, basiliximab; D, day; M, month.

2.6 Statistical analysis

All statistical analyses were performed using SPSS version 26.0 and R version 4.0. Continuous variables are presented as mean ± standard deviation (SD) or median (interquartile range, IQR), and were compared using either t-tests or Mann-Whitney U tests, as appropriate. Categorical variables were analyzed using chi-square or Fisher's exact tests. Kaplan-Meier survival analysis with log-rank tests was used to compare the incidence of clinically relevant CMV viremia between the groups. To identify factors influencing CMV viremia, both univariate and multivariate logistic regression analyses were conducted. Univariate analysis was first performed to assess the relationship between each individual factor and CMV viremia, including the following variables: group, gender, induction therapy type, body mass index, dialysis duration, pretransplant anti-A/B antibody titer, renal glomerular filtration rate, warm ischemia time, cold ischemia time, and HLA mismatch. Subsequently, multivariate analysis was used to identify independent factors significantly associated with CMV viremia, adjusting for potential confounders. Given its potential clinical significance, induction therapy type was forced into the multivariate regression model regardless of its univariate statistical results. A backward stepwise regression approach was employed to select the most relevant variables for the multivariate model. Changes in renal function over time were assessed using repeated measures ANOVA. A two-tailed P-value of < 0.05 was considered statistically significant.

3 Results

3.1 Patient characteristics

A total of 106 patients underwent ABOi kidney transplantation, with 50 patients in the CMVig group and 47 in the PET group. Nine patients were excluded due to insufficient follow-up (n = 4) or refusal to participate (n = 5). Baseline characteristics, as summarized in Table 1, were comparable between the two groups. The mean recipient age was 37.8 ± 9.0 years in the CMVig group and 35.5 ± 10.0 years in the PET group (P = 0.234). The median dialysis duration was 12.0 months (IQR: 3.0–24.0) in the CMVig group and 8.0 months (IQR: 5.0–12.0) in the PET group (P = 0.594). The mean donor kidney glomerular filtration rate (GFR) was 41.7 ± 5.4 mL/min in the CMVig group and 42.9 ± 5.6 mL/min in the PET group (P = 0.280). Both groups had a median of two HLA mismatches (IQR: 2–3 in the CMVig group vs. 1–3 in the PET group, P = 0.100). Pre-transplant anti-A/B antibody titers were similar, with a median titer of 1:4 (IQR: 1:4–1:8) in both groups (P = 0.836). All donor-recipient pairs were CMV seropositive (D+/R+). Additionally, there were no significant differences in other parameters, including gender distribution, warm ischemia time, or cold ischemia time (all P > 0.05).

3.2 CMV infection outcomes

During the one-year follow-up, the clinically relevant CMV viremia occurred in 24.7% (24/97) of patients. The incidence was significantly lower in the CMVig group (16.0%, 8/50) compared to the PET group (34.0%, 16/47; P = 0.04). Notably, no cases of CMV end-organ disease were observed in either group. Furthermore, the median time to post-transplant infection was 8 weeks (IQR: 4-15.75) in the PET group versus 22 weeks (IQR: 13-24) in the CMVig group (P = 0.032). Kaplan-Meier analysis demonstrated clear divergence in cumulative CMV progression between groups (Figure 3). The log-rank test confirmed statistical significance (P = 0.027) (Figure 3). Regarding treatment duration, the median course of preemptive antiviral therapy was shorter in the CMVig group (2 weeks, IQR: 2-4) compared to the PET group (3.5 weeks, IQR: 2-4), although this difference did not reach statistical significance (P = 0.383).

To explore factors associated with CMV viremia, univariate logistic regression analysis was conducted. The results indicated that patients in the CMVig group (i.e., CMVig intervention) had a significantly lower risk of clinically relevant CMV viremia compared to the PET group (OR = 0.37, 95% CI: 0.13–0.95, P = 0.043). Univariate logistic regression analysis also identified three

10.3389/fimmu.2025.1562951

TABLE 1 Patient Characteristics.

	preemptive therapy(n=47)	preemptive therapy+CMVig(n=50)	p-value
Recipient's characteristics			
Age (years, mean ± SD)	37.8 (± 9.0)	35.5 (± 10.0)	P=0.234
Male/female (n)	30/17	31/19	P=0.852
BMI (kg/m^2, median, IQR)	22.1 (19.8-24.2)	21.2 (18.7-23.4)	P=0.175
Time on dialysis (months, median, IQR)	8.0 (5.0-12.0)	12.0 (3.0-24.0)	P=0.594
Comorbidity (n)			
hypertension	28 (59.6%)	30 (60.0%)	P=0.966
diabetes	7 (14.9%)	15 (30.0%)	P=0.076
cardiovascular disease	4 (8.5%)	5 (10.0%)	P=0.801
hepatitis B	6 (12.8%)	8 (16.0%)	P=0.651
Diagnosis of end stage renal disease (n)			P=0.327
diabetic nephropathy	6 (12.8%)	13 (26.0%)	
hypertensive nephropathy	22 (20.4%)	20 (40.0%)	
glomerulonephritis	8 (17.0%)	4 (8.0%)	
others and undetermined	11 (23.4%)	13 (26.0%)	
Blood group (n)			P=0.549
A→B	7 (14.9%)	6 (12.0%)	
A→O	9 (19.1%)	9 (18.0%)	
B→A	12 (25.5%)	11 (22.0%)	
B→O	7 (14.9%)	11 (22.0%)	
AB→A	9 (19.1%)	8 (16.0%)	
AB→B	3 (6.4%)	5 (10.0%)	
Donor specific antibodies (n)	2	1	
Donor characteristics			
Age (years, mean ± SD)	53.7 (± 7.1)	52.0 (± 9.1)	P=0.304
Male/female (n)	21/26	25/25	P=0.600
Renal GFR (ml/min, mean ± SD)	42.9 (± 5.6)	41.7 (± 5.4)	P=0.280
Desensitization Protocol and Immunosuppressive regimen (n)			
Desensitization regimen A/B	47/0	46/4	P=0.118
Basiliximab/anti-thymocyte globulin	7/40	3/47	P=0.320
Surgery-related statistics			
Donor/recipient serostatus (D/R)			
D+/R+ (n)	47 (100%)	50 (100%)	
Peak baseline anti-A/B antibody titer (median, IQR)	1:32 (1:16-1:128)	1:32 (1:16-1:80)	P=0.698
Pretransplant anti-A/B antibody titer (median, IQR)	1:4 (1:4-1:8)	1:4 (1:4-1:8)	P=0.836
HLA mismatch (n, median, IQR)	2 (1-3)	2 (2-3)	P=0.100
Warm ischemia time (min, median, IQR)	3 (2-3)	2 (2-3)	P=0.114
Cold ischemia time (min, median, IQR)	168.0 (± 50.4)	157.4 (± 44.1)	P=0.269

CMVig = Cytomegalovirus immunoglobulin, SD = Standard deviation, BMI = Body mass index, IQR = Interquartile range, GFR = Glomerular filtration rate, HLA = human leukocyte antigen.

10.3389/fimmu.2025.1562951

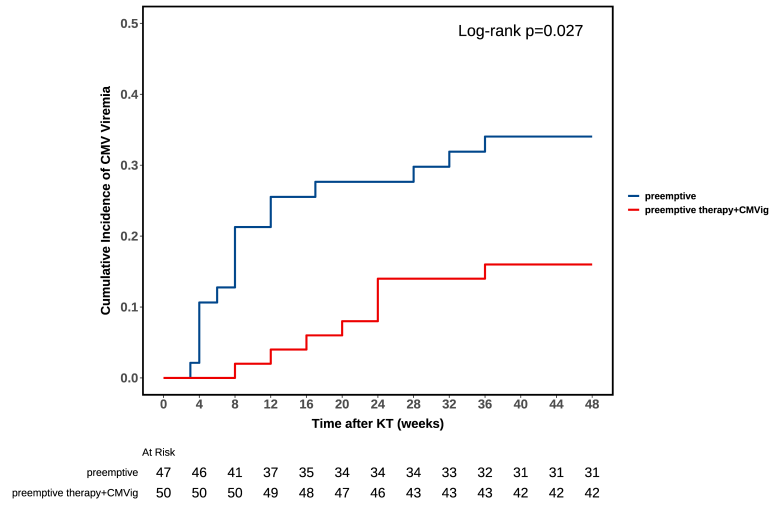

FIGURE 3
Kaplan-Meier analysis of CMV viremia-free survival. The curve compares clinically relevant CMV viremia-free survival rates between the combined group (preemptive therapy + CMVig) and the preemptive therapy group. A significant difference was observed (log-rank test, P = 0.027).

independent risk factors: higher pre-transplant anti-A/B antibody titers (OR = 1.13, 95% CI: 1.02–1.25, P = 0.014), prolonged warm ischemia time (OR = 2.06, 95% CI: 1.18–3.69, P = 0.012), and a greater number of HLA mismatches (OR = 2.25, 95% CI: 1.45–3.77, P < 0.001). Different induction therapy, Gender, Body mass index, dialysis duration, renal GFR, and cold ischemia time did not show significant associations with CMV viremia (all P > 0.05) (Table 2). Multivariate logistic regression analysis further confirmed the independent impact of these factors. CMVig intervention was a strong protective factor, significantly reducing the risk of CMV viremia (adjusted OR = 0.19, 95% CI: 0.04–0.68, P = 0.016). Conversely, higher pre-transplant anti-A/B antibody titers

TABLE 2 Univariate and Multivariate Analyses of Factors Influencing cytomegalovirus viremia.

Characteristic	Univariable			Multivariable		
	OR	95% CI	p-value	OR	95% CI	p-value
Group						
preemptive therapy	Referent	—		—	—	
preemptive therapy+CMVig	0.37	0.13, 0.95	0.043	0.19	0.04, 0.68	0.016
Gender						
male	Referent	—		—	—	
female	0.36	0.11, 1.00	0.063	0.28	0.06, 1.05	0.075
Induction therapy						
basiliximab	Referent	—		—	—	
rabbit anti-thymocyte globulin	0.74	0.19, 3.68	0.685	0.95	0.12, 10.76	0.962
Body mass index (kg/m²)	1.06	0.94, 1.21	0.335			
Time on dialysis (months)	0.99	0.95, 1.03	0.645			
Pretransplant anti-A/B antibody titer	1.13	1.02, 1.25	0.014	1.19	1.04, 1.38	0.016
Renal glomerular filtration rate	1.04	0.95, 1.13	0.386			
Warm ischemia time (min)	2.06	1.18, 3.69	0.012	2.67	1.24, 6.46	0.018
Cold ischemia time (min)	1.00	0.99, 1.01	0.683			
HLA mismatch (n)	2.25	1.45, 3.77	<0.001	2.79	1.63, 5.47	<0.001

OR, Odds ratio; CI, Confidence interval; CMVig, Cytomegalovirus immunoglobulin; HLA, human leukocyte antigen.

(adjusted OR = 1.19 per unit increase, 95% CI: 1.04–1.38, P = 0.016), prolonged warm ischemia time (adjusted OR = 2.67, 95% CI: 1.24–6.46, P = 0.018), and increased HLA mismatches (adjusted OR = 2.78, 95% CI: 1.63–5.47, P < 0.001) were identified as independent risk factors for CMV viremia (Table 2).

3.3 Renal allograft function

CMV infection impacts kidney function in transplant patients. In this study, renal allograft function was consistently poorer in clinically relevant CMV viremia-positive patients compared to viremia-negative patients at multiple time points during the follow-up period. Specifically, the mean estimated glomerular filtration rate (eGFR) in CMV viremia-positive patients was significantly lower than in viremia-negative patients at 1, 3, 6, and 12 months post-transplant: 56.68 ± 14.59 vs. 66.84 ± 14.54ml/min/1.73m^2 (P = 0.0051) at 1 month, 48.82 ± 16.16 vs. 63.49 ± 15.70 ml/min/1.73m^2 (P = 0.0004) at 3 months, 44.06 ± 9.09 vs. 59.23 ± 12.85 ml/min/1.73m^2 (P < 0.0001) at 6 months, and 44.36 ± 10.59 vs. 54.50 ± 14.54ml/min/1.73m^2 (P = 0.0005) at 12 months. Similarly, serum creatinine levels also differed significantly between the two groups, being higher in clinically relevant CMV viremia-positive patients at 3, 6, and 12 months: 185.95 ± 122.98 vs. 131.58 ± 46.26 μmol/L (P = 0.0443) at 3 months, 181.38 ± 73.79 vs. 129.54 ± 48.94 μmol/L (P = 0.0031) at 6 months, and 200.76 ± 79.45 vs. 144.60 ± 36.15 μmol/L (P = 0.0025) at 12 months (Figures 4A, C). A comparison of renal allograft function between the two groups over the one-year follow-up period demonstrated significant differences (Figures 4B, D). At 12 months post-transplant, the eGFR in CMVig group was significantly higher than in the PET group (56.40 ± 14.19 vs. 47.30 ± 13.01 ml/min/1.73m^2, P = 0.0014). Additionally, serum creatinine levels in the CMVig group were significantly lower than those in PET group at the same time point (146.52 ± 57.07 vs. 171.22 ± 51.48 μmol/L, P = 0.0274) (Figure 4). Although urinary protein positivity rates increased over time in both groups, the PET group consistently exhibited higher positivity rates at 1,3,6 and 12 months post-transplant. However, these differences were not statistically significant (Supplementary Figure S1).

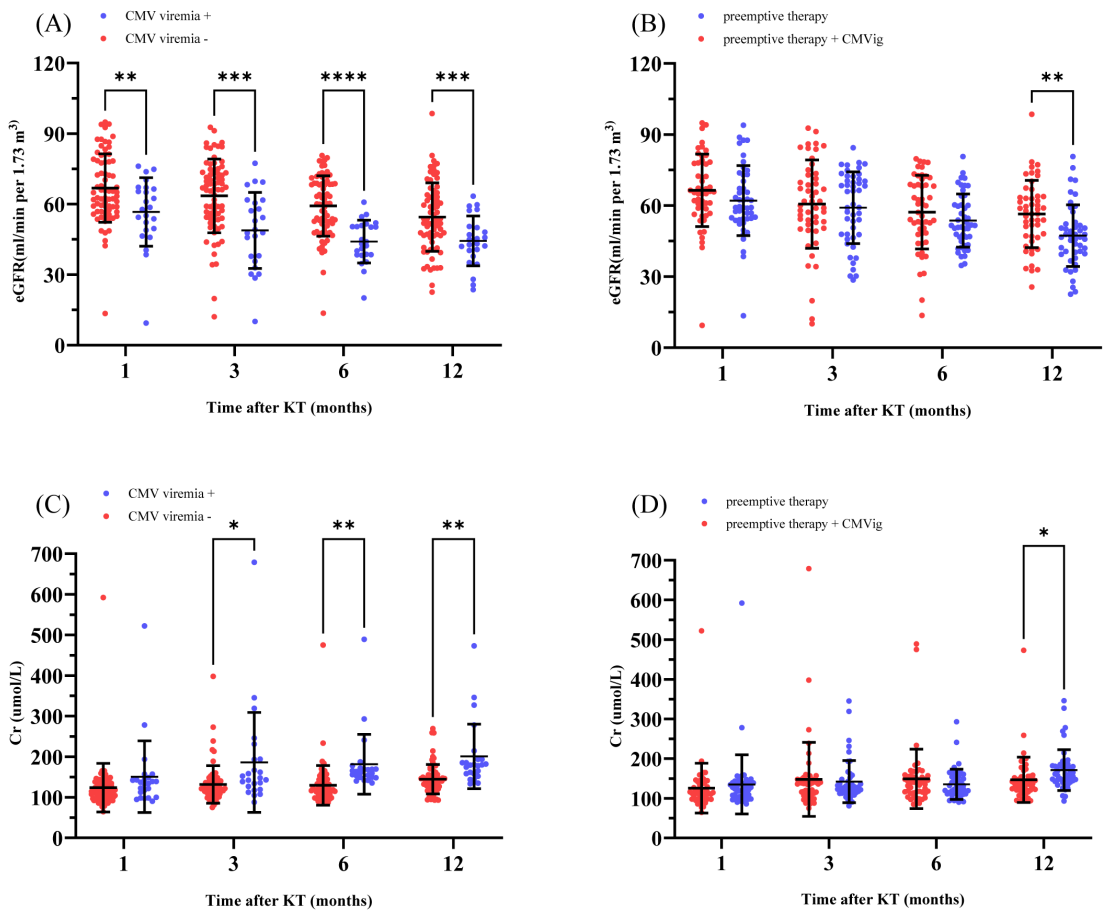

FIGURE 4
Renal allograft function over time. **(A)** eGFR comparison between patients with and without clinically relevant CMV viremia post-transplant. **(B)** eGFR comparison between the two groups. **(C)** Cr levels in patients with and without clinically relevant CMV viremia. **(D)** Cr levels in the two groups. eGFR, estimated Glomerular Filtration Rate; Cr, Serum creatinine; CMVig, Cytomegalovirus immunoglobulin; KT, kidney transplantation. *P<0.05; **P<0.01; ***P<0.001; ****P<0.0001.

3.4 B cells reconstitution

The dynamics of B cells recovery following rituximab treatment were assessed. Before treatment, the median B cell count was 117 cells/μL (IQR: 84–154) in the PET group and 125 cells/μL(IQR: 78–173) in the CMVig group. By 14 days post-treatment, the median B cell count in both groups had dropped to undetectable levels. At the 12-month follow-up, repopulation remained limited, with median B cell counts of 10 cells/μL (IQR: 7–14) in the PET group and 8.5 cells/μL (IQR: 3–15) in the CMVig group, both of which remained below the normal lower limit (Figure 5). These findings demonstrate that rituximab-induced B cell depletion persists over an extended period in both groups.

3.5 Other secondary outcomes

The overall incidence of infection and rejection complications following kidney transplantation showed no significant differences between the two groups. T cell-mediated rejection (TCMR) occurred in 2.00% (1/50) of patients in the CMVig group and 2.12% (1/47) of patients in the PET group. No cases of antibody-mediated rejection (ABMR) were reported in either group. The incidence of pulmonary infections was 10.00% (5/50) in the CMVig group and 8.51% (4/47) in the PET group. BK virus-associated complications, including viruria and viremia, were comparable between the two groups. Additionally, no cases of herpes simplex virus (HSV-1, HSV-2) or varicella-zoster virus (VZV) infections were observed in either group (Table 3).

TABLE 3 Other secondary outcomes.

	preemptive therapy(n=47)	preemptive therapy +CMVig(n=50)
T cell-mediated rejection, TCMR (n)	1 (2.12%)	1 (2.00%)
Antibody-mediated rejection, ABMR (n)	0	0
Pulmonary infection (n)	4 (8.51%)	5 (10.00%)
BK virus viruria (n)	15 (31.9%)	18 (36.0%)
BK virus viremia (n)	5 (10.6%)	4 (8.0%)
BK virus-associated nephropathy (n)	0	1 (2%)
Varicella zoster virus infection (n)	0	0
Herpes simplex virus, HSV-1 HSV-2 (n)	0	0

4 Discussion

Cytomegalovirus (CMV), or human herpesvirus 5 (HHV-5), is a member of the Herpesviridae family that establishes lifelong latency following primary infection, with reactivation occurring under conditions of immunosuppression (16, 17). CMV infection represents a major challenge in post-transplant management, with infection rates reported as high as 30–67% in solid organ transplant recipients, depending on the transplanted organ and the intensity of the immunosuppressive regimen (5, 18, 19). In ABOi kidney transplantation, the need for enhanced immunosuppressive protocols and preconditioning regimens poses additional challenges in CMV management (20, 21). These desensitization protocols are designed to lower anti-A/B antibody (isoagglutinin) levels to a safe threshold to prevent rejection but inadvertently weaken immune defenses, significantly increasing susceptibility to opportunistic infections such as CMV (2, 22). These considerations underscore the critical need for tailored infection prevention strategies specifically for ABOi transplant recipients.

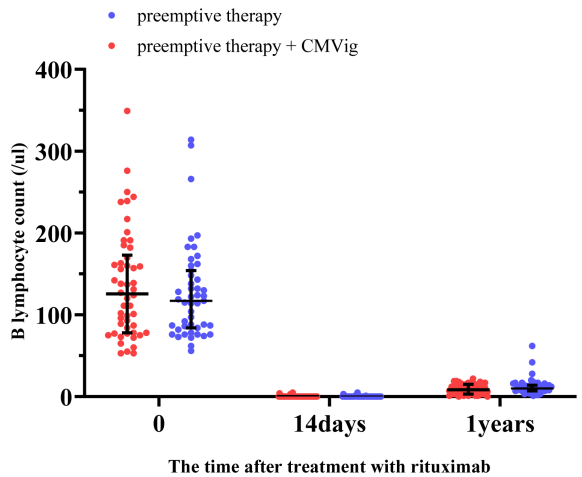

FIGURE 5
B lymphocyte depletion and reconstitution after rituximab treatment. This figure demonstrates the changes in peripheral blood B lymphocyte counts (cells/μL) in the two groups over time.

In some cases, CMVig has demonstrated efficacy and potential in preventing and treating CMV infections following ABOi kidney transplantation (23, 24).Mechanistic studies also suggest that CMVig could be a promising therapeutic candidate. In previous studies on CMVig, its multifaceted protective mechanisms have been documented. CMVig provides passive immunity by neutralizing circulating CMV particles (25). Additionally, CMVig enhances the body's antiviral immune response while suppressing excessive immune activation, thereby balancing immune responses (5, 26). This dual modulation, involving both innate and adaptive immunity, facilitates viral clearance in high-risk populations, making it particularly crucial for ABO-incompatible kidney transplant recipients (25, 26). However, its specific clinical efficacy in ABOi kidney transplant recipients remains to be comprehensively observed and reported.

Our study demonstrates that prophylactic use of CMVig significantly reduces the incidence of CMV infection within 12 months. Patients receiving CMVig treatment showed a significantly lower incidence of clinically relevant CMV viremia compared to the preemptive therapy group. This finding is consistent with prior

studies on solid organ transplantation. For instance, a systematic review and meta-analysis conducted by Barten et al. found that CMVig prophylaxis significantly reduced CMV infection rates in solid organ transplant recipients, reporting an infection rate of 35.8% in the CMVig group compared to 41.4% in the PET group (27).However, conflicting evidence exists. For instance, a randomized double-blind trial conducted by Ishida JH indicated that although CMVig delayed the onset of CMV viremia in some kidney transplant recipients, the difference compared to the placebo group was not statistically significant (28). The authors attributed these findings to factors such as insufficient sample size, selection bias in the study population, and inadequate follow-up duration.

Beyond reducing infection rates, CMVig delayed the onset of CMV viremia in our cohort, highlighting its potential for controlling CMV infection during the critical early post-transplant period. This extended protection may reduce reliance on antiviral drugs, thereby minimizing associated adverse effects such as nephrotoxicity and bone marrow suppression. Our clinical findings align with the mechanistic evidence supporting the therapeutic potential of CMVig, further reinforcing its role as a promising preventive strategy in ABOi kidney recipients.

CMV infection is a well-documented contributor to graft dysfunction and loss. Prior studies by Hellemans et al. and Ishikawa et al. have established a significant correlation between CMV infection and progressive declines in graft function (29, 30). Consistent with these findings, our one-year follow-up revealed that patients with clinically relevant CMV viremia exhibited significantly lower eGFR at multiple time points compared to those without, indicating sustained graft dysfunction attributable to CMV. These findings further underscore the critical importance of early CMV detection and intervention to prevent sustained graft damage and optimize transplantation outcomes.

Thus, we also investigated whether prophylactic CMVig directly enhances graft function. During the early follow-up period (1, 3, and 6 months), no significant differences in eGFR or serum creatinine levels were observed between the CMVig-treated and the preemptive group, suggesting limited direct protective effects of CMVig on graft function. However, by the 12-month follow-up, patients receiving CMVig demonstrated significantly improved eGFR and serum creatinine levels compared to patients in preemptive group. These improvements are likely attributable to the reduced incidence of CMV infection in the CMVig-treated group, which indirectly mitigated CMV-induced graft damage rather than reflecting a direct protective effect of CMVig itself.

Finally, our study evaluated the reconstitution of immune function and explored alternative desensitization strategies in ABOi kidney recipients. Previous studies, including those by Thiel and Colucci, have shown that peripheral B cell counts typically recover within 6 to 12 months following rituximab treatment (31, 32). However, persistently low B cell counts were observed throughout the entire observation period in our cohort. This prolonged immunosuppression likely accounts for the increased susceptibility to CMV infection observed in ABOi recipients (33). To address this, we explored a modified desensitization strategy in four patients, reducing rituximab doses from 200mg to 100 mg and administering a single preoperative dose of eculizumab. This C5 complement inhibitor supports desensitization by suppressing complement-mediated humoral immunity (34). While its efficacy is well-documented in atypical hemolytic uremic syndrome (aHUS), its role in preventing ABOi-associated antibody-mediated rejection (ABMR) remains uncertain (35, 36). Given that ABOi desensitization involves multiple immune pathways, including complement-dependent mechanisms and antibody-dependent cellular cytotoxicity (ADCC), relying solely on complement inhibitors may not be sufficient (37). Notably, none of the four patients experienced CMV infections or ABMR. These findings suggest that personalized desensitization protocols incorporating alternative strategies may help balance infection risk and immunosuppression in ABOi kidney transplantation.

Of course, this study has certain limitations. First, as a single-center study, the generalizability of the findings to other populations or different clinical settings may be limited. Second, the relatively short follow-up period restricts observations of long-term outcomes, such as graft survival and CMV-related mortality.

5 Conclusions

In conclusion, CMVig represents a promising prophylactic option for reducing CMV viremia incidence and delaying infection onset in ABOi kidney transplant recipients. Additionally, personalized desensitization protocols may further enhance CMV management and improve long-term outcomes for this high-risk population. However, further multi-center studies with extended follow-up periods are needed to validate these findings and establish optimized protocols for integrating CMVig into clinical practice.

Data availability statement

The original contributions presented in the study are included in the article/Supplementary Material. Further inquiries can be directed to the corresponding authors.

Ethics statement

The studies involving humans were approved by Ethics Committee of Sichuan Provincial People's Hospital. The studies were conducted in accordance with the local legislation and institutional requirements. The participants provided their written informed consent to participate in this study.

Author contributions

LZ: Data curation, Formal analysis, Methodology, Software, Visualization, Writing – original draft. ST: Conceptualization, Data curation, Formal analysis, Investigation, Writing – original draft.

ZP: Investigation, Formal analysis, Validation, Writing – review & editing. KC: Data curation, Investigation, Writing – original draft. WD: Data curation, Investigation, Writing – original draft. YH: Project administration, Resources, Supervision, Validation, Writing – review & editing. HY: Project administration, Resources, Supervision, Validation, Writing – review & editing.

Funding

The author(s) declare that no financial support was received for the research and/or publication of this article.

Acknowledgments

We sincerely thank Sichuan Provincial People's Hospital for providing patient data and follow-up information. We also extend our heartfelt gratitude to the volunteer patients who generously participated in this research and supported its completion.

Conflict of interest

The authors declare that the research was conducted in the absence of any commercial or financial relationships that could be construed as a potential conflict of interest.

Generative AI statement

The author(s) declare that no Generative AI was used in the creation of this manuscript.

Publisher's note

Supplementary material

The Supplementary Material for this article can be found online at: https://www.frontiersin.org/articles/10.3389/fimmu.2025.1562951/full#supplementary-material

SUPPLEMENTARY FIGURE 1
Urinary proteins positive percentage over time. The bar chart shows the percentage of patients with urinary protein positivity at 1,3,6 and 12 months post-kidney transplantation (KT).

SUPPLEMENTARY TABLE 1
Donor-recipient relationships and surgical methods.

References

1. Limaye AP, Budde K, Humar A, Vincenti F, Kuypers DRJ, Carroll RP, et al. Letermovir vs valganciclovir for prophylaxis of cytomegalovirus in high-risk kidney transplant recipients: A randomized clinical trial. *Jama*. (2023) 330:33–42. doi: 10.1001/jama.2023.9106

2. Razonable RR, Humar A. Cytomegalovirus in solid organ transplant recipients-Guidelines of the American Society of Transplantation Infectious Diseases Community of Practice. *Clin Transplant*. (2019) 33:e13512. doi: 10.1111/ctr.13512

3. Lewis A, Koukoura A, Tsianos GI, Gargavanis AA, Nielsen AA, Vassiliadis E. Organ donation in the US and Europe: The supply vs demand imbalance. *Transplant Rev (Orlando)*. (2021) 35:100585. doi: 10.1016/j.trre.2020.100585

4. Morath C, Zeier M, Döhler B, Opelz G, Süsal C. ABO-incompatible kidney transplantation. *Front In Immunol*. (2017) 8:234. doi: 10.3389/fimmu.2017.00234

5. Kotton CN, Kumar D, Caliendo AM, Huprikar S, Chou S, Danziger-Isakov L, et al. The third international consensus guidelines on the management of cytomegalovirus in solid-organ transplantation. *Transplantation*. (2018) 102:900–31. doi: 10.1097/TP.0000000000002191

6. Cowley NJ, Owen A, Shiels SC, Millar J, Woolley R, Ives N, et al. Safety and efficacy of antiviral therapy for prevention of cytomegalovirus reactivation in immunocompetent critically ill patients: A randomized clinical trial. *JAMA Intern Med*. (2017) 177:774–83. doi: 10.1001/jamainternmed.2017.0895

7. Kotton CN, Kamar N. New insights on CMV management in solid organ transplant patients: prevention, treatment, and management of resistant/refractory disease. *Infect Dis Ther*. (2023) 12:333–42. doi: 10.1007/s40121-022-00746-1

8. Yong MK, Shigle TL, Kim YJ, Carpenter PA, Chemaly RF, Papanicolaou GA. American Society for Transplantation and Cellular Therapy Series: 4 - Cytomegalovirus treatment and management of resistant or refractory infections after hematopoietic cell transplantation. *Transplant Cell Ther*. (2021) 27:957–67. doi: 10.1016/j.jtct.2021.09.010

9. Axelrod D, Segev DL, Xiao H, Schnitzler MA, Brennan DC, Dharnidharka VR, et al. Economic impacts of ABO-incompatible live donor kidney transplantation: A national study of medicare-insured recipients. *Am J Transplant*. (2016) 16:1465–73. doi: 10.1111/ajt.13616

10. Limaye AP, Babu TM, Boeckh M. Progress and challenges in the prevention, diagnosis, and management of cytomegalovirus infection in transplantation. *Clin Microbiol Rev*. (2020) 34(1):e00043-19. doi: 10.1128/CMR.00043-19

11. Snydman DR, Werner BG, Heinze-Lacey B, Berardi VP, Tilney NL, Kirkman RL, et al. Use of cytomegalovirus immune globulin to prevent cytomegalovirus disease in renal-transplant recipients. *N Engl J Med*. (1987) 317:1049–54. doi: 10.1056/NEJM198710223171703

12. Martins JP, Andoniou CE, Fleming P, Kuns RD, Schuster IS, Voigt V, et al. Strain-specific antibody therapy prevents cytomegalovirus reactivation after transplantation. *Science*. (2019) 363:288–93. doi: 10.1126/science.aat0066

13. Zamora D, Krantz EM, Green ML, Joncas-Schronce L, Blazevic R, Edmison BC, et al. Cytomegalovirus humoral response against epithelial cell entry-mediated infection in the primary infection setting after hematopoietic cell transplantation. *J Infect Dis*. (2020) 221:1470–9. doi: 10.1093/infdis/jiz596

14. Ko Y, Kim JY, Kim SH, Kim DH, Lim SJ, Shin S, et al. Acute rejection and infectious complications in ABO- and HLA-incompatible kidney transplantations. *Ann Transplant*. (2020) 25:e927420. doi: 10.12659/AOT.927420

15. Orandi BJ, Garonzik-Wang JM, Massie AB, Zachary AA, Montgomery JR, Van Arendonk KJ, et al. Quantifying the risk of incompatible kidney transplantation: a multicenter study. *Am J Transplant*. (2014) 14:1573–80. doi: 10.1111/ajt.12786

16. Wills MR, Poole E, Lau B, Krishna B, Sinclair JH. The immunology of human cytomegalovirus latency: could latent infection be cleared by novel immunotherapeutic strategies? *Cell Mol Immunol*. (2015) 12:128–38. doi: 10.1038/cmi.2014.75

17. Griffiths P, Reeves M. Pathogenesis of human cytomegalovirus in the immunocompromised host. *Nat Rev Microbiol*. (2021) 19:759–73. doi: 10.1038/s41579-021-00582-z

18. Silva Junior HT, Tokat Y, Cai J, Singh I, Sandhu A, Demuth D, et al. Epidemiology, management, and burden of cytomegalovirus in solid organ transplant recipients in selected countries outside of Europe and North America: A systematic review. *Transpl Infect Dis*. (2023) 25:e14070. doi: 10.1111/tid.14070

19. Khawaja F, Spallone A, Kotton CN, Chemaly RF. Cytomegalovirus infection in transplant recipients: newly approved additions to our armamentarium. *Clin Microbiol Infect*. (2023) 29:44–50. doi: 10.1016/j.cmi.2022.07.001

20. Roberts MB, Fishman JA. Immunosuppressive agents and infectious risk in transplantation: managing the "Net state of immunosuppression. *Clin Infect Dis*. (2021) 73:e1302–e17. doi: 10.1093/cid/ciaa1189

21. Kumar R, Ison MG. Opportunistic infections in transplant patients. *Infect Dis Clin North Am*. (2019) 33:1143–57. doi: 10.1016/j.idc.2019.05.008

22. Lee J, Lee JG, Kim S, Song SH, Kim BS, Kim HO, et al. The effect of rituximab dose on infectious complications in ABO-incompatible kidney transplantation. *Nephrol Dial Transplant*. (2016) 31:1013–21. doi: 10.1093/ndt/gfw017

23. Wiening V, Schmidt T, Dahmen M, Siam S, Reuter S, Pavenstädt HJ, et al. Case report: management of a multidrug-resistant CMV-strain in a renal transplant recipient by high-dose CMV-specific immunoglobulins, modulation in immunosuppression, and induction of CMV-specific cellular immunity. *Front Immunol*. (2020) 11:623178. doi: 10.3389/fimmu.2020.623178

24. Kodama H, Hatakeyama S, Matsuura T, Saito M, Nishida H, Hamaya T, et al. Incidence of postoperative cytomegalovirus and BK-polyoma virus infections and graft loss in ABO-incompatible renal transplant recipients: a multicenter retrospective study. *Int Urol Nephrol*. (2024) 56:2187–93. doi: 10.1007/s11255-023-03934-1

25. Carbone J. The immunology of posttransplant CMV infection: potential effect of CMV immunoglobulins on distinct components of the immune response to CMV. *Transplantation*. (2016) 100 Suppl 3:S11–8. doi: 10.1097/TP.0000000000001095

26. Deml L, Hüber CM, Barabas S, Spindler T, Cozzi E, Grossi P. Stimulatory effect of CMV immunoglobulin on innate immunity and on the immunogenicity of CMV antigens. *Transplant Direct*. (2021) 7:e781. doi: 10.1097/TXD.0000000000001236

27. Barten MJ, Baldanti F, Staus A, Hüber CM, Glynou K, Zuckermann A. Effectiveness of prophylactic human cytomegalovirus hyperimmunoglobulin in preventing cytomegalovirus infection following transplantation: A systematic review and meta-analysis. *Life (Basel)*. (2022) 12(3):361. doi: 10.3390/life12030361

28. Ishida JH, Patel A, Mehta AK, Gatault P, McBride JM, Burgess T, et al. Phase 2 randomized, double-blind, placebo-controlled trial of RG7667, a combination monoclonal antibody, for prevention of cytomegalovirus infection in high-risk kidney transplant recipients. *Antimicrob Agents Chemother*. (2017) 61(2):e01794-16. doi: 10.1128/AAC.01794-16

29. Hellemans R, Abramowicz D. Cytomegalovirus after kidney transplantation in 2020: moving towards personalized prevention. *Nephrol Dial Transplant*. (2022) 37:810–6. doi: 10.1093/ndt/gfaa249

30. Ishikawa S, Tasaki M, Saito K, Nakagawa Y, Ikeda M, Takahashi K, et al. Long-term CMV monitoring and chronic rejection in renal transplant recipients. *Front Cell Infect Microbiol*. (2023) 13:1190794. doi: 10.3389/fcimb.2023.1190794

31. Colucci M, Carsetti R, Cascioli S, Casiraghi F, Perna A, Ravà L, et al. B cell reconstitution after rituximab treatment in idiopathic nephrotic syndrome. *J Am Soc Nephrol*. (2016) 27:1811–22. doi: 10.1681/ASN.2015050523

32. Thiel J, Rizzi M, Engesser M, Dufner AK, Troilo A, Lorenzetti R, et al. B cell repopulation kinetics after rituximab treatment in ANCA-associated vasculitides compared to rheumatoid arthritis, and connective tissue diseases: a longitudinal observational study on 120 patients. *Arthritis Res Ther*. (2017) 19:101. doi: 10.1186/s13075-017-1306-0

33. Nixon A, Ogden L, Woywodt A, Dhaygude A. Infectious complications of rituximab therapy in renal disease. *Clin Kidney J*. (2017) 10:455–60. doi: 10.1093/ckj/sfx038

34. Schinstock C, Tambur A, Stegall M. Current approaches to desensitization in solid organ transplantation. *Front Immunol*. (2021) 12:686271. doi: 10.3389/fimmu.2021.686271

35. Legendre CM, Licht C, Muus P, Greenbaum LA, Babu S, Bedrosian C, et al. Terminal complement inhibitor eculizumab in atypical hemolytic-uremic syndrome. *N Engl J Med*. (2013) 368:2169–81. doi: 10.1056/NEJMoa1208981

36. Tan EK, Bentall A, Dean PG, Shaheen MF, Stegall MD, Schinstock CA. Use of eculizumab for active antibody-mediated rejection that occurs early post-kidney transplantation: A consecutive series of 15 cases. *Transplantation*. (2019) 103:2397–404. doi: 10.1097/TP.0000000000002639

37. Bhalla A, Alachkar N, Alasfar S. Complement-based therapy in the management of antibody-mediated rejection. *Adv Chronic Kidney Dis*. (2020) 27:138–48. doi: 10.1053/j.ackd.2019.12.002

frontiers | Frontiers in Immunology

TYPE Brief Research Report
PUBLISHED 15 May 2025
DOI 10.3389/fimmu.2025.1553305

OPEN ACCESS

EDITED BY
Cynthia Giver,
Emory University, United States

REVIEWED BY
Luigi Nespoli,
University of Insubria, Italy
Jorge Valle Arroyo,
Fundación para la Investigación Biosanitaria de Andalucía Oriental (FIBAO), Spain

*CORRESPONDENCE
Daniele Lilleri
d.lilleri@smatteo.pv.it

RECEIVED 30 December 2024
ACCEPTED 15 April 2025
PUBLISHED 15 May 2025

CITATION
Mele D, Zavaglio F, Bergami F, Gregorini M, Briganti DF, Pellegrini C, Comolli G, Cassaniti I, Lilleri D and Baldanti F (2025) Performance of new pp65-IGRA for the quantification of HCMV-specific CD4$^+$ T-cell response in healthy subjects and in solid organ transplant recipients.
Front. Immunol. 16:1553305.
doi: 10.3389/fimmu.2025.1553305

Performance of new pp65-IGRA for the quantification of HCMV-specific CD4$^+$ T-cell response in healthy subjects and in solid organ transplant recipients

Dalila Mele[1], Federica Zavaglio[1], Federica Bergami[1], Marilena Gregorini[2,3], Domenica Federica Briganti[3,4], Carlo Pellegrini[4,5], Giuditta Comolli[1], Irene Cassaniti[1,4], Daniele Lilleri[1]* and Fausto Baldanti[1,4]

[1]Molecular Virology Unit, Department of Microbiology and Virology, Fondazione IRCCS Policlinico San Matteo, Pavia, Italy, [2]Unit of Nephrology, Dialysis and Transplantation, Fondazione IRCCS Policlinico San Matteo, Pavia, Italy, [3]UOS Transplant Center, Fondazione IRCCS Policlinico San Matteo, Pavia, Italy, [4]Department of Clinical, Surgical, Diagnostic and Pediatric Sciences, University of Pavia, Pavia, Italy, [5]Department of Cardiothoracic Surgery, Fondazione IRCCS Policlinico San Matteo, Pavia, Italy

Immune control of human cytomegalovirus (HCMV) replication is critical in bone marrow and solid organ transplant recipients, where uncontrolled replication can lead to high mortality. Current commercial immune monitoring tools have several limitations, such as a lack of appropriate test cutoff values and the inability to characterise antigen-specific T cells. The main aim of our study was to develop a new interferon-γ (IFN-γ) release assay (IGRA), easy to use, to quantify and characterise the HCMV-specific T-cell response (pp65-IGRA). Secondary analyses included an evaluation of the performance of pp65-IGRA to assess whether its specificity and sensitivity were equal to or greater than those of the intracellular cytokine staining (ICS) and enzyme-linked immunospot (ELISpot) assays. In the study, 76 immunocompetent donors and nine solid organ transplant recipients were enrolled. Blood samples or peripheral blood mononuclear cells were stimulated with HCMV pp65-recombinant protein or with a complete pool of overlapping pp65 peptides. IFN-γ production was analysed by enzyme-linked immunoassay, ELISpot assays, and flow cytometry. For each assay, appropriate cutoff values were calculated. Our data demonstrate the suitability of pp65-IGRA for the quantification of HCMV-specific CD4$^+$ T-cell responses and may support its use in routine clinical practice to improve the management of immunocompromised patients.

KEYWORDS

HCMV, IFN-γ, IGRA, pp65, HCMV-specific T cell response

1 Introduction

Human cytomegalovirus (HCMV) is a ubiquitous DNA virus capable of establishing lifelong latency in bone marrow hematopoietic progenitor cells after primary infection (1). Periodically, a latently infected virus can restart replication, causing reactivation episodes.

Upon primary HCMV infection, the virus can trigger an overwhelming response involving many arms of the immune system (2). Several studies have documented that cell-mediated adaptive immunity (CMI) plays a key role in the control of the replication of HCMV (3, 4). Particularly, HCMV-specific $CD8^+$ T lymphocytes are essential for limiting HCMV viremia during the acute phase of primary infection, whereas long-term immune control of infection is established by the $CD4^+$ T lymphocyte subset. Indeed, several works, including ours, give direct evidence that the presence of an HCMV-specific $CD4^+$ T-cell response is associated with a lower risk of HCMV disease (5–8). HCMV infection or reactivation in the immunocompetent individual is rarely a cause of morbidity. Conversely, the reduced immune response in bone marrow or solid organ transplant recipients, due to immunosuppressive therapies, makes them susceptible to viral reactivation with serious life-threatening risks (3).

Current guidelines suggest two main strategies to prevent HCMV disease in transplant recipients: the universal prophylaxis (based on administration of antiviral drugs to all patients for up to 12 months) and preemptive therapy (based on monitoring the viral burden in the blood and treatment when transplant recipients are deemed to be at high risk (9, 10). Both approaches have limitations, such as cost, toxicity, and risk for emergence of resistance. However, patients without significant HCMV-specific T-cell dysfunction could avoid both prophylactic and preventive therapies. In fact, HCMV reactivation episodes and the risk of disease are associated with each patient's immune status, and transplant recipients who maintain a sufficient HCMV-specific T-cell response can control HCMV infection despite immune suppression (5, 8, 11–15). Therefore, it is important in the clinical practice the employment of HCMV–CMI assays, particularly those that track the specific CD4 T-cell response, to guide personalized strategies aimed at preventing HCMV in immunocompromised individuals (11–15).

Different clinical tools have been evaluated for *ex-vivo* quantitation and functional characterization of antigen-specific T-cell responses, including enzyme-linked immunospot (ELISPOT), enzyme-linked immunoassay (ELISA), and flow cytometry. Of these, ELISA and ELISpot are highly specific and sensitive but do not provide the phenotypic characterization of antigen-stimulated T cells (16–18). On the other hand, the flow cytometry approach allows the analysis of cell function and phenotype in parallel (5, 8, 14, 15), but it is labor intensive, expensive, and poorly standardized. Moreover, flow cytometry or ELISpot requires trained operators to perform the tests accurately and interpret the results. The preparation of peripheral blood mononuclear cells (PBMCs) requires considerable expertise. Specifically, PBMCs should be used or cryopreserved within hours of blood collection to ensure data quality. Therefore, whole blood assays could be more advantageous than PBMC-based methods by significantly reducing blood volume, being rapid and automated, and not requiring skilled personnel. The QuantiFERON-CMV assay is the only commercially available method for measuring CMI response in whole blood samples. It is an *in-vitro* assay using HCMV peptides that are designed to specifically target CD8+ T cells and are restricted by HLA class I haplotypes, which cover > 98% of the human population. Therefore, this test is not suitable for subjects with HLA class I haplotypes that are not covered (18, 19). Additionally, it does not analyze HCMV-specific CD4+ T-cell responses. Several studies have reported that 15- to 20-mer overlapping peptides are able to stimulate both $CD4^+$ and $CD8^+$ T cell immunity, whereas whole proteins mainly stimulate $CD4^+$ T cells (20, 21). The aim of our study was to develop a novel, easy-to-perform, whole-blood Interferon-Gamma-Release Assay (IGRA) that requires minimal blood volume and is suitable for accurate quantification of HCMV-specific $CD4^+$ T-cell response and to compare its performance with that of the currently available assays. For this reason, whole blood samples were stimulated with HCMV pp65-recombinant protein or a complete pool of overlapping pp65 peptides (pp65-IGRA). Additionally, three different HCMV-specific IGRAs were evaluated and compared with the novel pp65-IGRA: intracellular cytokine staining (ICS) by flow cytometry, ELISpot assay developed in our institute, and HCMV–IFN-γ ELISA (QuantiFERON-CMV, Germany, Qiagen). Of note, the ELISpot assay detects overall specific T-cell response, whereas the QuantiFERON-CMV assay measures HCMV-CMI by quantifying IFNγ released by $CD8^+$ T cells.

2 Materials and methods

2.1 Study setting

For the setup and the comparative evaluation of pp65-IGRA, peripheral blood samples were collected from 76 immunocompetent donors. In addition, blood samples were collected from 9 HCMV-seropositive solid organ transplant recipients (SOTR) before and 3 months after transplantation to test preliminarily pp65-IGRA in this population. PBMCs were obtained from heparin-treated blood by density gradient centrifugation (Lymphoprep, Sentinel Diagnostics, Milan, Italy) and were used to measure antigen-specific T-cell responses by ICS and ELISpot assay. Serum samples were used for HCMV IgG serology. All subjects signed an informed consent form. The study was approved by the local Ethics Committee (Comitato Etico Area Pavia) and institutional review board (Prot. 0003690/2024).

2.2 HCMV serology

For quantifications of anti-HCMV IgG antibody titre in serum, the automated chemiluminescence analyser technology was used (LIASON XL, Italy, DiaSorin). Values lower than 12 mUI/ml were considered negative.

2.3 Media and antigens

To evaluate the HCMV-specific T-cell response, recombinant pp65 protein (Abcam, Cambridge, UK) and pp65 peptide pool (15 mers, overlapping by 10 amino acids, A&A Labs LLC, San Diego, CA) were used at a final concentration of 1 µg/ml. Commercial phytohaemagglutinin (PHA, 5 µg/ml; MO, USA) or SEB (Staphylococcus aureus, Enterotoxin Type B, 10 µg/ml) was used as a positive control in the ELISpot assay and pp65-IGRA whole blood assay. A peptide pool of human actin (15 mers, overlapping by 10 amino acids, Pepscan, Lelystad, the Netherlands) was used as a negative control in the ICS assay at a final concentration of 1 µg/ml. Culture medium was RPMI 1640 (Euroclone, Milano, Italy) supplemented with 2 mM L-glutamine (Euroclone), 100 U/ml penicillin and 100 µg/ml streptomycin solution (Euroclone), and 10% of heat-inactivated fetal bovine serum.

2.4 Intracellular cytokine staining assay

In a round-bottom 96-well plate, peripheral blood mononuclear cells (PBMCs) were stimulated for 16h–18h (22, 23) with recombinant pp65 protein, pp65 peptide pool, and peptide pool of human actin in the presence of 0.5 µg/ml co-stimulator molecules, CD28 and CD49d (BD Bioscience, New Jersey, USA), and brefeldin A (Sigma-Aldrich-Merck, Darmstadt, Germany) at a final concentration of 10 µg/ml. Cells were seeded at a density of 0.5–1 × 10^6 cells/200 µl culture medium per well. Cells were then incubated overnight at 37°C (5% CO_2). Subsequently, PBMCs were harvested, washed, and stained using CD8 V500, CD3 PerCP-Cy 5.5, and CD4 APC Cy7 (BD Biosciences). After fixation and permeabilization (Fixation/Permeabilization Solution Kit, BD Biosciences), cells were stained with anti–IFN-γ PECy7 (BD Biosciences). Nonviable cells were identified by staining with Live/Dead Fixable Violet Dye Pacific Blue (Invitrogen, MA, USA). Data acquisition was performed with a FACS Lyric flow cytometer using BD FACSuite software (BD Biosciences) (23–25). The frequency of IFN-γ–producing $CD4^+$ and $CD8^+$ T cells is determined by subtracting the frequency of $IFN\gamma^+$ $CD4^+$ or $CD8^+$ T cells incubated with human actin peptides from the $IFN\gamma^+$ $CD4^+$ or $CD8^+$ T cells incubated with recombinant pp65 protein and pp65 peptide pool.

2.5 *Ex-vivo* enzyme-linked immunospot assay

Antigen-specific T-cell responses were evaluated by IFN-γ detection following recombinant pp65 protein and pp65 peptide pool stimulation in an ELISpot assay as previously described (26). Negative control wells lacked peptides, and positive control wells contained PHA. Spots were counted using an automated ELISpot Reader System (Autoimmun Diagnostika GmbH, Strasburg, Germany). Results were expressed as IFN-γ spot-forming units (SFUs)/10^6 PBMCs, after subtracting spots from the negative control.

2.6 HCMV-specific interferon-gamma-release assays (pp65-IGRA)

In a 48-well plate, 400 µl of heparinized whole blood were stimulated with the same stimuli used for the ICS assay and maintained overnight at 37°C (5% CO_2). Unstimulated whole blood was used as a negative control. Subsequently, plasma was harvested and analyzed for IFN-γ [µg/ml ELISA assay, according to manufacturer's instructions (Quantikine ELISA, R&D Systems, MN, USA)]. The IFN-γ levels of the negative control were subtracted from the unstimulated one.

2.7 QuantiFERON-CMV assay

The CE-IVD QuantiFERON-CMV assay had been performed according to the manufacturer's instructions (Qiagen, Germany). Plasma was harvested and analyzed for IFN-γ (IU/ml) using the QuantiFERON-CMV ELISA kit (Qiagen).

2.8 Statistical analysis

GraphPad Prism 9.1.0 (GraphPad Software, La Jolla, CA, USA) was used for statistical analyses. A two-sided p-value < 0.05 was considered statistically significant. Receiver operating characteristic (ROC) curve analysis was done to evaluate the optimum cutoffs to discriminate HCMV seropositive and seronegative subjects. The cutoffs were established according to the Youden's index (or Youden's J statistic) (27), defined as:

$$J = \text{sensitivity} + \text{specificity} - 1$$

The maximum value of the index was used as a criterion for selecting the optimum cutoff value, in order to obtain the best compromise between sensitivity and specificity. The area under the curve (AUC) and its 95% confidence interval (CI) were calculated. Correlations between variables were analysed by Pearson's rank correlation coefficient.

3 Results

3.1 Demographic characteristics of subjects included in the study

For the evaluation of the efficacy of pp65-IGRA in detecting HCMV-specific T-cell response in immunocompetent subjects and for the comparison of its diagnostic efficacy with that of other

assays, we tested 76 immunocompetent donors (48 females and 28 males) whose median age was 50 years (range: 25–89 years).

Detection of HCMV-specific T-cell response by pp65 IGRA was subsequently evaluated in nine SOTR (four females and five males) whose median age was 58 years (range: 19–69 years).

3.2 T-cell response to pp65 after incubation of whole blood and PBMCs with a peptide pool or the recombinant protein

Whole blood (WB) from 54 seropositive and 22 seronegative immunocompetent donors was incubated with a peptide pool of pp65 or the recombinant protein, and the concentration of IFN-γ released was measured (pp65-IGRA; Figure 1A). As expected, both antigen formulations were able to induce IFN-γ release from most seropositive subjects. On the contrary, WB from HCMV-seronegative subjects stimulated with the peptide pool gave a negligible response, while a certain amount of IFN-γ release was observed in a minor portion of recombinant pp65-stimulated WB samples. By ROC analysis, and according to Youden's index, a cutoff of 3 pg/ml for the peptide pool and a cutoff of 50 pg/ml for the recombinant protein were selected for discrimination of seropositive and seronegative subjects. An ELISpot assay was performed with PBMCs using the same pp65 formulations (Figure 1B). Again, IFN-γ–positive spots were produced by the great majority of seropositive subjects, while a small number of spots were produced by few seronegative subjects (the great majority gave negative results). Cutoffs of 40 and 25 SFU/10^6 cells were chosen for the peptide pool or the recombinant protein. According to the selected cutoffs, after stimulation with the peptide pool, no seronegative subjects gave non-specific results with pp65-IGRA and ELISpot, while using recombinant protein 3 and 2 seronegative subjects gave false-positive results with pp65-IGRA and ELISpot.

IFN-γ production was also determined on $CD4^+$ (Figure 1C) and $CD8^+$ (Figure 1D) T cells by ICS. Flow cytometry gate strategies were shown in Supplementary Figure S1. As expected, the peptide pool stimulated both T-cell subpopulations, while the recombinant protein provided an excellent stimulation for $CD4^+$ and a poor stimulation for $CD8^+$ T cells. No seronegative subject gave false-positive results with either peptide pool or recombinant protein in $CD4^+$ T-cell response, and one subject gave a false positive result in $CD8^+$ T-cell response to peptide pool.

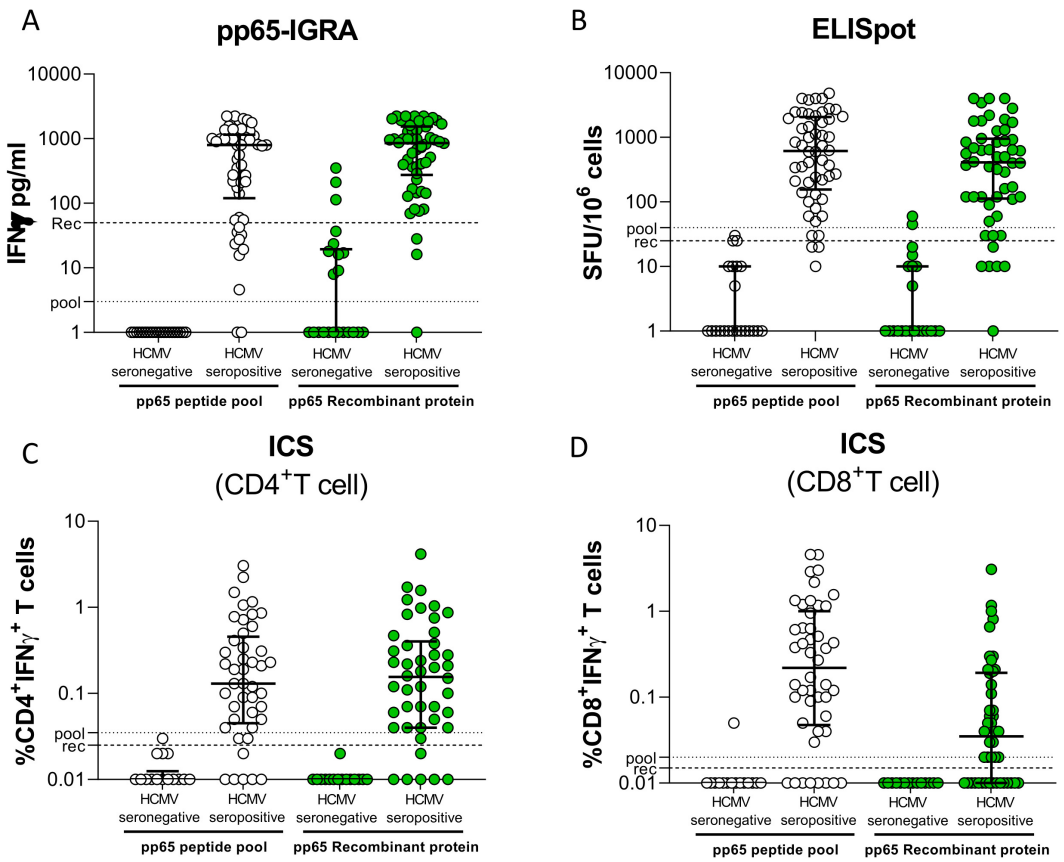

FIGURE 1
Whole blood IFN-γ release was measured in 22 HCMV-seronegative and 54 HCV-seropositive donors following stimulation with pp65 peptide pool (white dot) or recombinant protein (green dot) **(A)**. Number of spot-forming cells in response to stimulation with pp65 peptide pool or recombinant in stratified HD **(B)**. Frequency of $CD4^+$ and $CD8^+$ T cells producing IFN-γ in PBMCs of donors stimulated with pp65 peptide pool or recombinant protein (**C**, **D**, respectively). The horizontal dotted line indicated the cutoff.

The diagnostic performance of pp65-IGRA, ELISpot, and ICS in discriminating seropositive and seronegative subjects is shown in Table 1. A slightly better sensitivity was observed for the pp65-IGRA than the ELISpot. For these two assays, 100% specificity was observed with the peptide pool as stimulus, whereas specificity was close to 100% with the recombinant protein. The ICS assay for $CD4^+$ T cells was highly specific with both antigen formulations, while sensitivity was lower than that of pp65-IGRA and ELISpot. The sensitivity was very poor with ICS for $CD8^+$ T cells using recombinant protein as stimulus.

3.3 Correlation of pp65-IGRA with ELISpot and ICS

7Using a peptide pool for T-cell stimulation, among the 54 HCMV-seropositive subjects, there was a significant and high correlation (Figure 2A) between pp65-IGRA and ELISpot ($p < 0.001$, $R = 0.80$). A lower correlation (Figure 2B) was found between pp65-IGRA and ICS for $CD4^+$ T cells ($R = 0.58$), while the lowest correlation (Figure 2C) was found between pp65-IGRA and ICS for $CD8^+$ T cells ($R = 0.43$). Using the recombinant protein, a significant correlation, albeit low, was found between pp65-IGRA and ELISpot or ICS for $CD4^+$ T cells ($R = 0.53$ and 0.51, respectively; Figures 2D, E); no significant correlation was observed between pp65-IGRA and ICS for $CD8^+$ T cells (Figure 2F).

A more complete characterisation of antigen-specific T-cell response can be achieved by using both pp65 formulations. According to the chosen cutoffs, a positive response against both the pp65 peptide pool and the pp65 recombinant protein likely indicates the presence of HCMV-specific $CD4^+$ and $CD8^+$ T cells. Alternatively, a positive response against the pp65 peptide pool only indicates a response that is primarily associated with $CD8^+$ T cells (Supplementary Figure S2).

3.4 Correlation of QuantiFERON-CMV with pp65-IGRA

In a subgroup of HCMV-seropositive subjects, we analysed the correlation between the commercially available QuantiFERON-CMV, which exploits the incubation of whole blood with $CD8^+$ epitopic peptides of known HLA-restriction derived from different HCMV proteins and pp65-specific pp65-IGRA. There was a good correlation between the two assays when the peptide pool of pp65 was used in the pp65-IGRA ($R = 0.72$; Figure 3A), while the correlation was lower when the recombinant protein was used ($R = 0.50$; Figure 3B).

3.5 T-cell response measured by pp65-IGRA in transplant recipients

Finally, the novel pp65-IGRA assay was used to investigate the antigen-specific T-cell response in nine HCMV-seropositive solid organ recipients before (T0) and 3 months (T3) after transplantation. Overall, 4 of 10 patients were defined as "controllers" due to self-resolving HCMV infection and 5 of 10 patients were defined as "non-controllers" due to needing preemptive therapy. Supplementary Table S1 shows the clinical and demographic characteristics of two groups of patients. At T0, all SOT recipients except one (eight of nine) were able to induce IFN-γ release after stimulation with a peptide pool of pp65, while seven of nine patients showed a positive pp65-specific T-cell response using the recombinant protein. Comparison of the T-cell response before and after 3 months of transplantation in the two groups of patients showed that "non-controllers" had a reduction in T-cell response as measured by pp65-IGRA, whereas "controllers" maintained higher levels of T-cell response despite immunosuppression. This reduction was more clearly observed, although not statistically significant, when using the pp65

TABLE 1 Performance characteristics of all IGRA quantitative assays.

ASSAY	AUC [95% CI]	CUTOFF	Specificity (%)	Sensitivity (%)
pp65-IGRA pp65 pool	0.982 [0.974–1]	3 (pg/ml)	100	96.3
pp65-IGRA pp65 recombinant	0.957 [0.918–0.99]	50 (pg/ml)	94.44	86.36
ELISpot pp65 pool	0.989 [0.954–1]	40 (SFU/10^6 cells)	100	90.38
ELISpot pp65 recombinant	0.959 [0.914–0.99]	25 (SFU/10^6 cells)	90.91	88.46
ICS-CD4 pp65 pool	0.917 [0.848–0.985]	0.035 (%)	100	80
ICS-CD4 pp65 recombinant	0.931 [0.869–0.993]	0.025 (%)	100	84.78
ICS-CD8 pp65 pool	0.918 [0.854–0.983]	0.02 (%)	94.44	82.61
ICS-CD8 pp65 recombinant	0.864 [0.779–0.95]	0.02 (%)	100	65.22

AUC, area under curve; 95% CI, confidence interval; SFU, spot forming cells.

10.3389/fimmu.2025.1553305

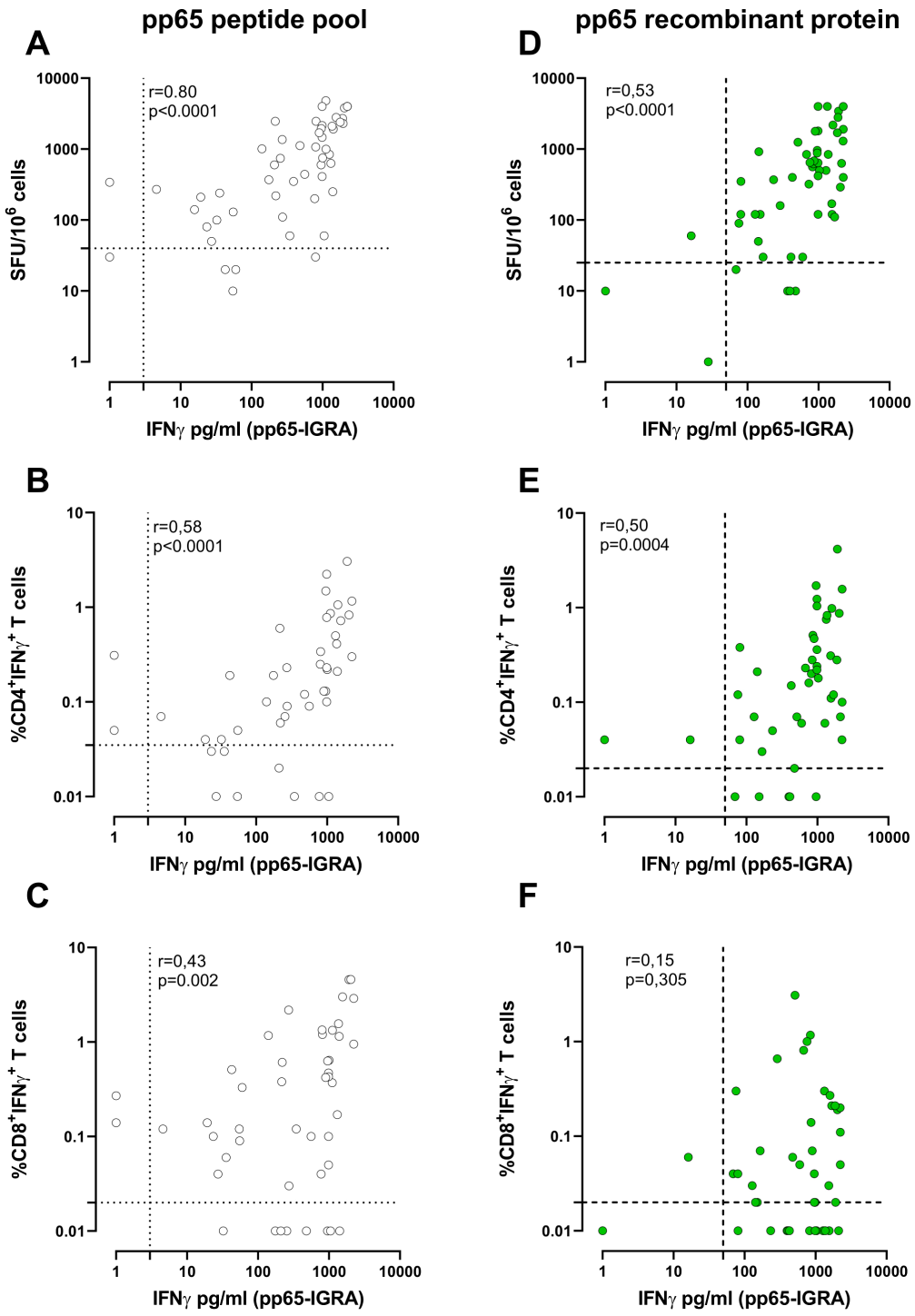

FIGURE 2
Correlation between whole blood IFN-γ production (pg/ml) and the number of spots on ELISpot following stimulation with pp65 pool (white dots, **A**) or pp65 recombinant (green dots, **D**). Correlation between the IFN-γ production (pg/ml) and the frequency of IFN-γ$^+$CD4$^+$ **(B, E)** and CD8$^+$ T cells **(C, F)** measured by ICS assay following pp65 stimulation. Each dot represents a single sample; Correlation was determined using Spearman, r, and *p*-value are given in the graph. The cutoff line of each analysis was shown.

recombinant protein rather than stimulating with the peptide pool (Figure 4). Indeed, five of five non-controllers showed a response below the "recombinant protein" cutoff at 3 months after transplantation.

4 Discussion

This study reports the evaluation of a new whole blood IGRA for HCMV using pp65 as stimulus. Two different antigenic

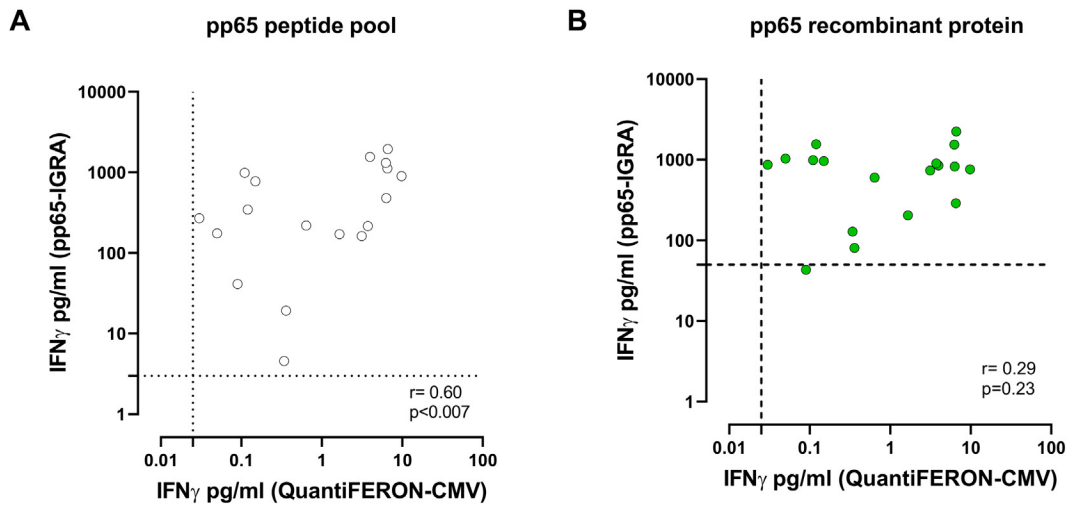

FIGURE 3
Correlation between IFN-γ level (pg/ml) measured by pp65-IGRA, following stimulation with pp65 pool (white dots, **A**) or pp65 recombinant (green dots, **B**), and IFN-γ level measured by QuantiFERON®-CMV. Each dot represents a single sample; correlation was determined using Spearman, r and *p* value are shown in the graph. Cutoff line of each analysis are shown.

formulations were used: a pool of overlapping peptides of 15 aa spanning the entire protein and the recombinant whole protein. Data provided by the pp65-IGRA were compared with those provided by an ELISpot assay using the same antigenic formulations, while ICS was also performed to analyze the relevant contribution of $CD4^+$ or $CD8^+$ T cells in IFN-γ production. Results of the study show that pp65-IGRA is able to detect a T-cell response in the majority of seropositive subjects tested (96%) with either peptide pool or recombinant protein, whereas few seronegative subjects gave non-specific results with the recombinant protein, and no subject gave non-specific results with the peptide pool.

Over the past 2 decades, there has been a push to develop HCMV-specific CMI assays that can accurately measure the HCMV-specific T-cell response, an important predictor of HCMV disease in transplant recipients. Current guidelines endorse the use of HCMV-specific T-cell response monitoring to inform on the risk of HCMV infection (28, 29). ELISpot or QuantiFERON-CMV assays have been widely used for monitoring the reconstitution or

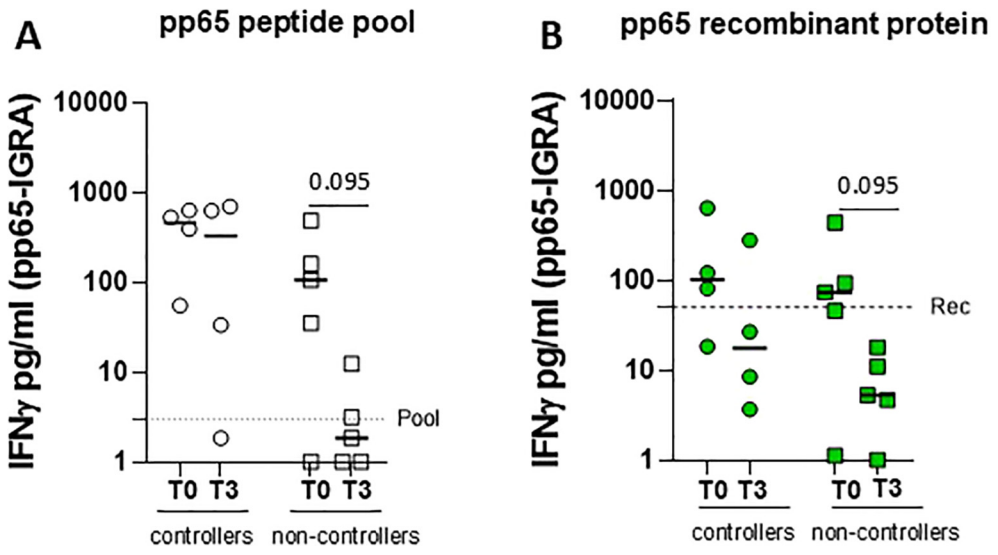

FIGURE 4
Whole blood IFN-γ release was measured in four controllers (circle dots) and five non-controllers (square dots), solid organ recipients (SOTR) **(A)** before (T0) and 3 months after transplantation. Graphs show levels of IFN-γ released following stimulation with pp65 peptide pool (**A**, white) and recombinant protein (**B**, green) in two groups of SOTR. The horizontal dotted line indicated the cutoff. Statistical analysis was performed by the Mann–Whitney test. *p*-values < 0.1 were shown in the graphs.

ex-novo development of HCMV-specific T-cell response in the post-transplant period (30, 31) and to individualize the duration of antiviral prophylaxis (11, 12, 32).

Direct comparison of ELISpot and QuantiFERON (33–35) reported a better performance of ELISPOT in transplant recipients. The commercially available ELISpot and QuantiFERON-CMV assays, although standardised and CE-marked, exhibit drawbacks that hinder their routine use in clinical practice. The former is highly specific and sensitive but does not provide phenotypic characterization of antigen-stimulated T cells. The latter, QuantiFERON-CMV (Qiagen Inc.), is a standardised and easy-to-perform assay based on a stimulation with HLA class 1–restricted HCMV epitopes; therefore detects mainly CD8+ T-cell response and cannot discriminate CD4+ T cells producing IFN-γ.

It is interesting to note that our new assay, pp65-IGRA, showed a slightly better sensitivity than that observed for the ELISpot. We cannot exclude a potential impact of the sample preparation (whole blood vs. PBMCs) on the different performance of the assays.

In addition, the pp65 overlapping peptide pool was shown to stimulate both $CD4^+$ and $CD8^+$ T-cell responses simultaneously, whereas the whole protein was observed to elicit predominantly HCMV-specific CD4+ T-cell responses, which have been reported to be crucial for immune control of CMV viremia after transplantation (5–8). This is further supported by the weak correlation observed between the pp65-IGRA and QuantiFERON-CMV when recombinant protein was used in the pp65-IGRA. Moreover, the QuantiFERON-CMV assay is limited by the HLA type of the patient; the assay is based on the stimulation of CD8+ T cells with a pool of 22 short peptides from 6 HCMV proteins presented by several HLA class I haplotypes, but we showed that mismatching between patient HLA alleles and those cognate to peptides present in the QuantiFERON-CMV pool may impact on the results obtained (19, 25). Conversely, the pp65-IGRA involves overlapping peptides of the pp65 antigen, therefore being able to detect a T-cell response to pp65 independently from specific patient HLA type.

The production of IFN-γ in response to recombinant pp65 found in certain HCMV-seronegative subjects may depend on protein formulation (e.g., purity level, endotoxin presence). It is also possible that the recombinant protein activates the innate immune response in a non-specific manner, inducing IFN-γ production. In addition to T and NK cells, monocytes and macrophages have also been reported to produce IFN-γ (36, 37). We could speculate that in some subjects the recombinant protein may induce IFN-γ production by monocytes or macrophages through the activation of the TLR2, TLR3, or TLR4 pathway, as usually occurs with other microbial products. These facts may be at the basis of a specificity slightly below 100% for the recombinant protein. On the other hand, we cannot completely exclude a humoral/cellular mismatch in these donors, since subgroups of healthy donors who, despite being HCMV-seronegative, show $CD4^+$ and $CD8^+$ T-cell responses have been described (38).

Our study is limited to the evaluation of the efficacy of pp65-IGRA mainly in a cohort of immunocompetent individuals stratified by HCMV-serostatus and analyses only a small number of immunocompromised transplanted subjects. Another limitation is the imbalance between male and female donors, which may have influenced the analysis. However, our data demonstrate the suitability of pp65-IGRA for the quantification of HCMV-specific $CD4^+$ T-cell responses and its potentiality in identifying patients at risk for, or protected from, HCMV infection after transplantation. As a next step, performance of pp65-IGRA and the cutoff values here determined in immunocompetent subjects should be evaluated on larger cohorts of patients in different transplantation settings (organ or hematopoietic stem cell transplantation, adult or pediatric patients) and receiving different immunosuppressive regimens. Results of these future studies, if confirming the preliminary data presented here, will support the use of the assay in routine clinical practice to improve the management of immunocompromised patients. In particular, results of the assay could be used to identify patients requiring strict HCMV surveillance or antiviral prophylaxis and those who can safely avoid or interrupt anti-HCMV treatment or prophylaxis, therefore improving patient management with a personalized approach to HCMV control, able also to spare costs of unnecessary antiviral drug administration.

Data availability statement

The original contributions presented in the study are included in the article/Supplementary Material. Further inquiries can be directed to the corresponding author.

Ethics statement

The studies involving humans were approved by Comitato Etico Area Pavia and Institutional Review Board (Prot. 0003690/2024). The studies were conducted in accordance with the local legislation and institutional requirements. The participants provided their written informed consent to participate in this study.

Author contributions

DM: Data curation, Formal analysis, Investigation, Project administration, Validation, Visualization, Writing – original draft, Writing – review & editing. FZ: Data curation, Formal analysis, Investigation, Validation, Writing – review & editing. FeB: Formal analysis, Investigation, Validation, Writing – review & editing. GC: Formal analysis, Investigation, Validation, Writing – review & editing. IC: Data curation, Formal analysis, Investigation, Validation, Writing – review & editing, Funding acquisition. DL: Conceptualization, Data curation, Formal analysis, Funding acquisition, Investigation, Methodology, Project administration, Supervision, Validation, Visualization, Writing – review & editing,

Writing – original draft. FaB: Conceptualization, Data curation, Funding acquisition, Supervision, Writing – review & editing, Project administration. MG: Formal analysis, Resources, Writing – review & editing. DB: Formal analysis, Resources, Visualization, Writing – review & editing. CP: Formal analysis, Resources, Visualization, Writing – review & editing.

Funding

The author(s) declare that financial support was received for the research and/or publication of this article. This research was funded by Ministero della Salute, Ricerca Corrente grant number 08075023.

Conflict of interest

The authors declare that the research was conducted in the absence of any commercial or financial relationships that could be construed as a potential conflict of interest

Generative AI statement

The author(s) declare that no Generative AI was used in the creation of this manuscript.

Publisher's note

Supplementary material

The Supplementary Material for this article can be found online at: https://www.frontiersin.org/articles/10.3389/fimmu.2025.1553305/full#supplementary-material

References

1. Dupont L, Reeves MB. Cytomegalovirus latency and reactivation: recent insights into an age old problem. *Rev Med Virol.* (2016) 26:75–89. doi: 10.1002/rmv.v26.2

2. Crough T, Khanna R. Immunobiology of human cytomegalovirus: from bench to bedside. *Clin Microbiol Rev.* (2009) 22:76–98. doi: 10.1128/CMR.00034-08

3. Griffiths P, Reeves M.). Pathogenesis of human cytomegalovirus in the immunocompromised host. *Nat Rev Microbiol.* (2021) 19:759–73. doi: 10.1038/s41579-021-00582-z

4. Zangger N, Oxenius A. T cell immunity to cytomegalovirus infection. Curr. *Opin Immunol.* (2022) 77:102185. doi: 10.1016/j.coi.2022.102185

5. Gabanti E, Lilleri D, Ripamonti F, Bruno F, Zelini P, Furione M, et al. Reconstitution of human cytomegalovirus-specific CD4+ T cells is critical for control of virus reactivation in hematopoietic stem cell transplant recipients but does not prevent organ infection. *Biol Blood Marrow. Transplant.* (2015) 21:2192–202. doi: 10.1016/j.bbmt.2015.08.002

6. Ciáurriz M, Zabalza A, Beloki L, Mansilla C, Pérez-Valderrama E, Lachén M, et al. The immune response to cytomegalovirus in allogeneic hematopoietic stem cell transplant recipients. *Cell Mol Life Sci.* (2015) 72:4049–62. doi: 10.1007/s00018-015-1986-z

7. Jackson SE, Sedikides GX, Mason GM, Okecha G, Wills MR. Human cytomegalovirus (HCMV)-specific $CD4^+$ T cells are polyfunctional and can respond to HCMV-infected dendritic cells *in vitro*. *J Virol.* (2017) 91:e02128–16. doi: 10.1128/JVI.02128-16

8. Lauruschkat CD, Muchsin I, Rein A, Erhard F, Grathwohl D, Dölken L, et al. CD4 + T cells are the major predictor of HCMV control in allogeneic stem cell transplant recipients on letermovir prophylaxis. *Front Immunol.* (2023) 14:1148841. doi: 10.3389/fimmu.2023.1148841

9. Ljungman P, de la Camara R, Robin C, Crocchiolo R, Einsele H, Hill JA, et al. Guidelines for the management of cytomegalovirus infection in patients with haematological Malignancies and after stem cell transplantation from the 2017 European Conference on Infections in Leukaemia (ECIL 7). *Lancet Infect Dis.* (2019) 19:e260–72. doi: 10.1016/S1473-3099(19)30107-0

10. Razonable RR, Humar A. Cytomegalovirus in solid organ transplant recipients-Guidelines of the American Society of Transplantation Infectious Diseases Community of Practice. *Clin Transplant.* (2019) 33:e13512. doi: 10.1111/ctr.13512

11. Avetisyan G, Aschan J, Hägglund H, Ringdén O, Ljungman P. Evaluation of intervention strategy based on CMV-specific immune responses after allogeneic SCT. *Bone Marrow Transpl.* (2007) 40:865–9. doi: 10.1038/sj.bmt.1705825

12. Navarro D, Amat P, de la Cámara R, López J, Vázquez L, Serrano D, et al. Efficacy and safety of a preemptive antiviral therapy strategy based on combined virological and immunological monitoring for active cytomegalovirus infection in allogeneic stem cell transplant recipients. *Open Forum Infect Dis.* (2016) 3:ofw107. doi: 10.1093/ofid/ofw107

13. Camargo JF, Wieder ED, Kimble E, Benjamin CL, Kolonias DS, Kwon D, et al. Deep functional immunophenotyping predicts risk of cytomegalovirus reactivation after hematopoietic cell transplantation. *Blood.* (2019) 133:867–77. doi: 10.1182/blood-2018-10-878918

14. Gabanti E, Borsani O, Caldera D, Colombo AA, Ferretti VV, Alessandrino EP, et al. Early T cell reconstitution and cytokine profile may help to guide a personalized management of human cytomegalovirus infection after allogeneic hematopoietic stem cell transplantation. *J Clin Virol.* (2021) 135:104734. doi: 10.1016/j.jcv.2021.104734

15. Lilleri D, Gerna G, Zelini P, Chiesa A, Rognoni V, Mastronuzzi A, et al. Monitoring of human cytomegalovirus and virus-specific T-cell response in young patients receiving allogeneic hematopoietic stem cell transplantation. *PloS One.* (2012) 7:e41648. doi: 10.1371/journal.pone.0041648

16. Walker S, Fazou C, Crough T, Holdsworth R, Kiely P, Veale M, et al. Ex vivo monitoring of human cytomegalovirus-specific CD8+ T-cell responses using QuantiFERON-CMV. *Transplant Infect Dis.* (2007) 9:165–70. doi: 10.1111/j.1399-3062.2006.00199.x

17. Tey SK, Kennedy GA, Cromer D, Davenport MP, Walker S, Jones LI, et al. Clinical assessment of anti-viral CD8+ T cell immune monitoring using QuantiFERON-CMV® assay to identify high risk allogeneic hematopoietic stem cell transplant patients with CMV infection complications. *PloS One.* (2013) 8:e74744. doi: 10.1371/journal.pone.0074744

18. El Haddad L, Ariza-Heredia E, Shah DP, Jiang Y, Blanchard T, Ghantoji SS, et al. The ability of a cytomegalovirus ELISPOT assay to predict outcome of low-level CMV reactivation in hematopoietic cell transplant recipients. *J Infect Dis.* (2019) 219:898–907. doi: 10.1093/infdis/jiy592

19. Valle-Arroyo J, Aguado R, Páez-Vega A, Pérez AB, González R, Fornés G, et al. Lack of cytomegalovirus (CMV)-specific cell-mediated immune response using QuantiFERON-CMV assay in CMV-seropositive healthy volunteers: fact not artifact. *Sci Rep.* (2020) 10:7194. doi: 10.1038/s41598-020-64133-x

20. Zhang H, Hong H, Li D, Ma S, Di Y, Stoten A, et al. Comparing pooled peptides with intact protein for accessing cross-presentation pathways for protective CD8+ and CD4+ T cells. *J Biol Chem.* (2009) 284:9184–91. doi: 10.1074/jbc.M809456200

21. Lauruschkat CD, Page L, Etter S, Weis P, Gamon F, Kraus S, et al. T-cell immune surveillance in allogenic stem cell transplant recipients: are whole blood-based assays ready to challenge ELISPOT? *Open Forum Infect Dis.* (2020) 8:ofaa547. doi: 10.1093/ofid/ofaa547

22. Zelini P, Lilleri D, Comolli G, Rognoni V, Chiesa A, Fornara C, et al. Human cytomegalovirus-specific CD4(+) and CD8(+) T-cell response determination: comparison of short-term (24h) assays vs long-term (7-day) infected dendritic cell assay in the immunocompetent and the immunocompromised host. *Clin Immunol.* (2010) 136:269–81. doi: 10.1016/j.clim.2010.04.008

23. Zavaglio F, Cassaniti I, d'Angelo P, Zelini P, Comolli G, Gregorini M, et al. Immune control of human cytomegalovirus (HCMV) infection in HCMV-seropositive

solid organ transplant recipients: the predictive role of different immunological assays. *Cells*. (2024) 13:1325. doi: 10.3390/cells13161325

24. Lilleri D, Gerna G, Bruno F, Draghi P, Gabanti E, Fornara C, et al. Systemic and local human cytomegalovirus-specific T-cell response in lung transplant recipients. *New Microbiol*. (2013) 36:267–77.

25. Gabanti E, Bruno F, Scaramuzzi L, Mangione F, Zelini P, Gerna G, et al. Predictive value of human cytomegalovirus (HCMV) T-cell response in the control of HCMV infection by seropositive solid-organ transplant recipients according to different assays and stimuli. *New Microbiol*. (2016) 4):247–58.

26. Cassaniti I, Cavagna L, Calarota SA, Adzasehoun KMG, Comolli G, Montecucco C, et al. Evaluation of EBV- and HCMV-specific T cell responses in systemic lupus erythematosus (SLE) patients using a normalized enzyme-linked immunospot (ELISPOT) assay. *J Immunol Res*. (2019), 4236503. doi: 10.1155/2019/4236503

27. Schisterman EF, Perkins NJ, Liu A, Bondell H. Optimal cut-point and its corresponding Youden Index to discriminate individuals using pooled blood samples. *Epidemiology*. (2005) 16:73–81. doi: 10.1097/01.ede.0000147512.81966.ba

28. Kotton CN, Kumar D, Caliendo AM, Huprikar S, Chou S, Danziger-Isakov L, et al. The third international consensus guidelines on the management of cytomegalovirus in solid-organ transplantation. *Transplantation*. (2018) 102:900–31. doi: 10.1097/TP.0000000000002191

29. Girmenia C, Lazzarotto T, Bonifazi F, Patriarca F, Irrera G, Ciceri F, et al. Assessment and prevention of cytomegalovirus infection in allogeneic hematopoietic stem cell transplant and in solid organ transplant: A multidisciplinary consensus conference by the Italian GITMO, SITO, and AMCLI societies. *Clin Transplant*. (2019) 33:e13666. doi: 10.1111/ctr.v33.10

30. Thompson G, Boan P, Purtill D, Cooney J, Cannell P, Wright M, et al. QuantiFERON-cytomegalovirus to predict clinically significant cytomegalovirus infection after allogeneic hematopoietic stem cell transplantation. *Transplant Infect Dis*. (2022) 24:e13786. doi: 10.1111/tid.13786

31. Chemaly RF, El Haddad L, Winston DJ, Rowley SD, Mulane KM, Chandrasekar P, et al. Cytomegalovirus (CMV) cell-mediated immunity and CMV infection after allogeneic hematopoietic cell transplantation: the REACT study. *Clin Infect Dis*. (2020) 71:2365–74. doi: 10.1093/cid/ciz1210

32. Kumar D, Mian M, Singer L, Humar A. An interventional study using cell-mediated immunity to personalize therapy for cytomegalovirus infection after transplantation. *Am J Transplant*. (2017) 17:2468–73. doi: 10.1111/ajt.14347

33. Gliga S, Fiedler M, Dornieden T, Achterfeld A, Paul A, Horn PA, et al. Comparison of three cellular assays to predict the course of CMV infection in liver transplant recipients. *Vaccines*. (2021) 9:88. doi: 10.3390/vaccines9020088

34. Gliga S, Korth J, Krawczyk A, Wilde B, Horn PA, Witzke O, et al. T-Track-CMV and QuantiFERON-CMV assays for prediction of protection from CMV reactivation in kidney transplant recipients. *J Clin Virol*. (2018) 105:91–6. doi: 10.1016/j.jcv.2018.06.009

35. Gajanayaka N, Dong SXM, Ali H, Iqbal S, Mookerjee A, Lawton DA, et al. TLR-4 Agonist Induces IFN-γ Production Selectively in Proinflammatory Human M1 Macrophages through the PI3K-mTOR- and JNK-MAPK-Activated p70S6K Pathway. *J Immunol (Baltimore Md.: 1950)*. (2021) 207:2310–24. doi: 10.4049/jimmunol.2001191

36. Kraaij MD, Vereyken EJ, Leenen PJ, van den Bosch TP, Rezaee F, Betjes MG, et al. Human monocytes produce interferon-gamma upon stimulation with LPS. *Cytokine*. (2014) 67:7–12. doi: 10.1016/j.cyto.2014.02.001

37. Zhu J, Shearer GM, Marincola FM, Norman JE, Rott D, Zou JP, et al. Discordant cellular and humoral immune responses to cytomegalovirus infection in healthy blood donors: existence of a Th1-type dominant response. *Int Immunol*. (2001) 13:785–90. doi: 10.1093/intimm/13.6.785

38. Lee H, Park KH, Ryu JH, Choi AR, Yu JH, Lim J, et al. Cytomegalovirus (CMV) immune monitoring with ELISPOT and QuantiFERON-CMV assay in seropositive kidney transplant recipients. *PloS One*. (2017) 12:e0189488. doi: 10.1371/journal.pone.0189488

frontiers | Frontiers in Immunology

TYPE Original Research
PUBLISHED 19 May 2025
DOI 10.3389/fimmu.2025.1563872

OPEN ACCESS

EDITED BY
Rita Maccario,
San Matteo Hospital Foundation (IRCCS), Italy

REVIEWED BY
Massimo Vitale,
Azienda Ospedaliera Universitaria San Martino (IRCCS), Italy
Jagoda Siemaszko,
Hirszfeld Institute of Immunology and Experimental Therapy (PAS), Poland

*CORRESPONDENCE
Yizhou Zou
211206@csu.edu.cn

†These authors have contributed equally to this work and share first authorship

RECEIVED 20 January 2025
ACCEPTED 14 April 2025
PUBLISHED 19 May 2025

CITATION
Luo Q, Yin X, Zhu Q, Luo W, Liu R, Wei L and Zou Y (2025) Two major human phenotypes of MICA molecules and their differential activation to NK cells via NKG2D receptor. *Front. Immunol.* 16:1563872. doi: 10.3389/fimmu.2025.1563872

Two major human phenotypes of MICA molecules and their differential activation to NK cells via NKG2D receptor

Qizhi Luo†, Xiangli Yin†, Quan Zhu, Weiguang Luo, Rongjiao Liu, Leiyan Wei and Yizhou Zou*

Department of Immunology, School of Xiangya Basic Medical Sciences, Central South University, Changsha, China

Introduction: The major histocompatibility complex class I-related gene A (*MICA*), is a highly polymorphic gene, serve as a crucial role in immune regulator through its interaction with the NKG2D receptor on natural killer (NK) cells. These polymorphisms may influence immune responses, disease susceptibility, and transplant outcomes. However, the precise mechanisms by which *MICA* polymorphisms modulate NKG2D receptor activation remain poorly understood.

Methods: We analyzed 29 representative MICA polymorphic molecules that cover the most prevalent alleles in the population. These variants were systematically examined through Luminex bead assays, monoclonal antibody binding studies, and NKG2D-Ig fusion protein assays. NKG2D receptor activation was assessed *in vitro* using NKG2D reporter cells, while NK cell-mediated cytotoxicity was evaluated through NKL cell killing assays against target cells expressing either Type-I or Type-II MICA molecules.

Results: Our analysis identified two major types of *MICA* polymorphisms based on antigenic epitopes and NKG2D binding characteristics. Type-I MICA characterized by six specific polymorphic site and their associated amino acid variants. exhibited significantly stronger NKG2D receptor binding affinity and more robust receptor activation compared to Type-II polymorphisms. This functional distinction was further corroborated by enhanced NK cells cytotoxicity against target cells expressing Type-I MICA molecules. Importantly, these differences in receptor activation and NK cell killing efficiency were attributable to six critical polymorphic amino acid sites.

Conclusion: This study demonstrates the existence of two distinct types of *MICA* polymorphisms that differentially regulate NKG2D receptor activation and NK cell cytotoxicity. These findings offer new insights into that how genetic variation in MICA may contribute to individual differences in disease susceptibility through immune regulation mechanisms.

KEYWORDS

MICA polymorphisms, NKG2D receptor, NK cell, binding affinity, immune regulation

1 Introduction

The major histocompatibility complex class I-related gene A (*MICA*) is located on the short arm of human chromosome 6 within the major histocompatibility complex (MHC) class I gene region, adjacent to the *HLA-B* locus (1). This highly polymorphic gene exhibits its genetic variation primarily in the α1, α2, and α3 immunoglobulin-like extracellular structural domains, which are encoded by exons 2-4 (2). Current data from the IMGT/HLA database (https://www.ebi.ac.uk/ipd/imgt/hla/; version 3.57, 07-2024) document 576 human *MICA* alleles encoding 280 distinct protein variants. Under normal physiological conditions, MICA molecules exhibits low expression levels on the membranes of human epithelial cells (3), fibroblasts (4), and endothelial cells (5), with minimal to undetectable expression in other cell types. However, the expression of MICA is significantly upregulated in response to tumor transformation or viral infection (6, 7).

The main biological function of MICA is to serve as a ligand for the NKG2D (natural killer group 2 member D) receptor on the surface of natural killer (NK) cells, thereby activating NKG2D-mediated signaling pathway (8). Notably, amino acid polymorphisms in MICA have implicated in the pathogenesis of various diseases. For example, the single nucleotide polymorphism (SNP) rs2596542 is associated with an increased risk of hepatocellular carcinoma in hepatitis C virus (HCV) patients (9, 10) In patients with acute leukemia receiving hematopoietic stem cell transplantation, glycine (G) at position 14 of the MICA protein correlates with significantly decreased overall survival (11). Furthermore, a methionine-to-valine substitution at position 129 (M/V) substantially diminishes binding affinity to the NKG2D receptor (12), and this genotype significantly increases susceptibility to renal transplant rejection (13).

NK cell surface receptors consist of both activating and inhibitory types. Among these, the activating receptor NKG2D plays a pivotal role in immune surveillance: upon ligand engagement, it triggers NK cell activation, enhances cytokine secretion, and mediates cytotoxicity against target cells (14). The ligands for NKG2D, referred to as natural killer group 2 member D ligands (NKG2DL), include MICA, MICB (major histocompatibility complex class I chain-related protein B), and the UL-16 binding protein (ULBP) family. These ligands activate NK cells by binding to the NKG2D receptor on their surface (15). MICA exhibits remarkable polymorphism, with MICA variants displaying distinct binding affinities for NKG2D receptor (16). This polymorphism could modulate the activation potential of the NKG2D receptor, thereby regulating the cytotoxic activity of NK cells (17).

The NKG2D-NKG2DL pathway plays a critical role in immune regulation, with growing recognition of its therapeutic potential in cancer (18). Among NKG2DLs, MICA stands out as the most polymorphic member, exhibiting different binding affinities for the NKG2D receptor, which may result in divergent immune responses. This variability positions MICA as both a key immunoregulatory target and a significant contributor to autoimmune pathogenesis (15). Furthermore, as members of the MHC gene family, *MICA* alleles have been implicated in immune responses against allografts in organ transplant recipients, where the development of specific antibodies contributes to graft rejection (11). These findings suggest that MICA may represent an important target for immunoregulation strategies. However, the precise effects of MICA polymorphisms on the NKG2D receptor signaling pathway remains incompletely understood.

In this study, we identified 29 of the most common and representative MICA polymorphic molecules in the population which had two different response patterns. Multifactorial analysis of these response patterns and the amino acid sequence alignment of revealed the existence of two major types of MICA polymorphic molecules in the population, distinguished by six linked polymorphic amino acid sites and their corresponding residue types. Our findings provide mechanistic insights into how structural variations in MICA influence the activation ability of the NKG2D receptor, offering a new perspective for predicting susceptibility to individual disease.

2 Methods

2.1 Cell culture

NKG2D receptor reporter cells (NKG2D-2B4) were generated by our research team in collaboration with Prof. Chengcheng Zhang's team at The University of Texas Southwestern Medical Center and are maintained in our laboratory (19). Hmy2.CIR cells were purchased from ATCC (USA), and MICA^{+}Hmy2.CIR overexpressing cells were constructed by our team and are also maintained in our laboratory (19, 20). The NKL cell line was generously provided by M. J. Robertson's team at the Indiana University School of Medicine, Indianapolis, IN (19). HEK 293F cells were purchased from Sino Biological.

All cell lines were cultured in RPMI 1640 medium (#11875500BT, Gibco, USA) supplemented with 10% fetal bovine serum (FBS, #10099141, Gibco, USA) and 1% penicillin/streptomycin (P/S, #P1400, Solarbio, China). NKL cells were additionally supplemented with 10 ng/mL interleukin-2 (IL-2, #200-02, PeproTech, USA). HEK 293F cells were cultured in serum-free 293-TII medium (#M293TII, Sino Biological, China) with shaking at 170 rpm. All cells were maintained at 37°C in a 5% CO_2 incubator.

2.2 Soluble recombinant proteins

A total of 12 recombinant proteins, including MICA*045 (coated on Luminex beads), MICA*001, MICA*002, MICA*007, MICA*012, MICA*017, MICA*018, MICA*004, MICA*006, MICA*008, MICA*009, and MICA*019, were constructed in mammalian expression vectors in our laboratory. These proteins were then transfected into 293F cells, expressed, purified, and collected, respectively. Specifically, the signal peptide, extracellular protein sequence, and 6 × His tag sequences of the above 12 MICA proteins were ligated into the pcDNA 3.1(+) eukaryotic expression vector by double digestion Hind III (Cat#: R3104V, NEB, USA) and BamH I (Cat#: R3136V, NEB, USA). The expressing plasmid was

transformed into Trans5α chemically competent cells (#CD201-01, Transgen, China), the recombinant cell colony was amplified, and the plasmids were extracted for sequencing verification. The plasmid was mixed with polyethyleneimine (25 kDa linear PEI, #23966, Polysciences, USA) at a 1:3 ratio (molecular weight) and transferred into 293F cells. After 3 days of expression, cell supernatants were collected, and the proteins were purified using affinity chromatography on nickel columns (Bestchrom, China).

About the NKG2D-Ig soluble recombinant protein, the extracellular nucleotide sequence of NKG2D and the human IgG Fc fragment were synthesized by the Beijing Genomics Institution. And the NKG2D-Ig fragment was ligated into the eukaryotic expression vector pFlag-CMV5.1 using T4 ligase (Cat#: EL0011, Invitrogen, USA) by double digestion. After transfecting the ligase product into Trans5α chemically competent cells, the recombinant cell colony was amplified, and the plasmids were extracted for sequencing verification. The protein was expressed and purified as above mentioned.

2.3 Monoclonal antibodies

The 11 recombinant MICA proteins (20 μg each) were mixed to form solutions of equal concentration and volume, which were then emulsified with Freund's adjuvant as an antigen for immunizing BALB/c mice. Mice were immunized once a week for four consecutive weeks, after which they were sacrificed. Spleen cells were isolated from the mice and fused with mouse myeloma cells (SP2/0) to generate hybridoma cells. Monoclonal hybridomas were selected by limited dilution, expanded in culture, and the monoclonal antibodies were purified and collected. The specific methodology for producing monoclonal antibodies is described in the Zou et al. paper (21). One monoclonal antibody, named 5.2G1, was identified based on its dual response patterns to the MICA polymorphic molecules. The monoclonal antibody 6B3, which was kindly provided by the Southwestern Medical Center, USA, is maintained in our laboratory (21).

2.4 Serum samples

Human serum samples, S001 and S002, were obtained by our research team from the 16th International HLA and Immunogenetics Workshop (IHIW) and are stored in our laboratory (22). These serum samples were extracted from the peripheral blood of renal transplant recipients who had experienced postoperative humoral rejection.

2.5 MICA luminex array

Luminex beads containing 28 types of MICA polymorphic molecules were coated into Luminex Beads separately and assembled with a commission kits (Immunocore, USA). MICA*045 soluble protein was coated onto the beads following the manufacturer's instructions, resulting in Luminex beads containing 29 different MICA polymorphic molecules. The MICA Luminex beads were diluted to 1×10^5 beads/mL in 10% BSA solution, and 50 μL of this mixture was added to each well of a 96-well plate, with three replicate wells per group. Subsequently, 1 μg/mL of S001 serum, S002 serum, 5.2G1 monoclonal antibody (mAb), 6B3 mAb, mouse IgG, NKG2D-Ig fusion protein, and 10% BSA were added to the wells. The plate was incubated at room temperature for 40 minutes on a shaker set to 850 rpm, followed by centrifugation at 1500 rpm and washing with 100 μL of washing buffer. This washing step was repeated three times. Then, 50 μL of PE-conjugated goat anti-human/mouse IgG (#115-115-164, Jackson ImmunoResearch, USA) was added, and the plate was incubated for 30 minutes at room temperature on the shaker at 850 rpm. The beads were washed three times, resuspended in 50 μL PBS, and analyzed using a Luminex 200 instrument (Bio-Rad, USA).

2.6 SDS-PAGE, gel staining, and western blot

The NKG2D-Ig fusion protein was mixed with 6× loading buffer containing β-Mercaptoethanol and incubated in a water bath at 100°C for 5 minutes. A 20 μL sample was then loaded, along with a protein marker (#26619, ThermoFisher, USA), and separated by electrophoresis on a 10% SDS-PAGE gel at 100 V for 80 minutes.

For gel staining, the gel was stained with a 50% Coomassie Brilliant Blue solution (#R-250, Sigma, USA) for 30 minutes at room temperature, followed by destaining in Coomassie Brilliant Blue decolorizing solution, with shaking at 70 rpm at room temperature for 24 hours. The gel was then recorded.

For the western blot, the other piece of gel was transferred to a PVDF membrane. After electrophoretic transfer at 200 mA for 90 minutes, the membrane was blocked with 5% skimmed milk at 37°C for 1 hour. The membrane was subsequently incubated with 1:5000 HRP-conjugated goat anti-human IgG (#109-035-008, Jackson ImmunoResearch, USA) at 37°C for 30 minutes. After three washes with 0.05% PBST, chemiluminescent imaging was performed.

2.7 Amino acid sequence analysis of MICA polymorphic molecules

The amino acid sequences of 280 MICA polymorphic molecules from the IPD-IMGT/HLA database (https://www.ebi.ac.uk/ipd/imgt/hla/) (version 3.57, released July 2024) were analyzed using comparative clustering, with the *MICA*001* sequence serving as the reference.

2.8 Flow cytometry

The cells were adjusted to a concentration of 1×10^6 cells/mL in 2% FBS-PBS buffer, and the corresponding antibody was added at a

1:100 dilution. The cells were incubated for 30 minutes at 4°C, protected from light. After incubation, the cells were washed three times with buffer and then analyzed using a flow cytometer. For secondary antibody staining, the secondary antibody was added at a 1:500 dilution, incubated for 30 minutes at 4°C, protected from light, and washed three times with buffer before flow cytometry analysis.

To detect NKG2D molecules on NKG2D-2B4 and 2B4-mock cells, PE-conjugated anti-NKG2D antibody (#320806, Biolegend, USA) was used. Detection of NKG2D on NKL cells was performed with PE-conjugated anti-NKG2D antibody (#320806, Biolegend, USA), PE-conjugated Mouse IgG1, κ (#400111, Biolegend, USA), and PE-conjugated anti-mouse H-2 antibody (#125505, Biolegend, USA). For detecting MICA molecules on $MICA^+$Hmy2.CIR and Hmy2.CIR cells, anti-MICA antibody (6B3) was used, followed by PE-conjugated anti-mouse IgG (H+L) antibody (#1034-09, SouthernBiotech, USA) and PE-conjugated anti-mouse H-2 antibody (#125505, Biolegend, USA).

2.9 NKG2D receptor reporter cell signaling pathway activation flow cytometry assay

The MICA recombinant protein solution was diluted to 80 μg/mL, and 50 μL of the solution was added to each well of a 96-well plate. The plate was incubated for 4 hours at 37°C, followed by two washes with PBS. NKG2D-2B4 and 2B4 cells were then added to the wells at a density of 8×10^4 cells/well, with three replicate wells per group. In the soluble group, NKG2D-2B4 and 2B4 cells were seeded into uncoated 96-well plates at 8×10^4 cells/well, and 50 μL of the MICA recombinant protein solution was added. The cells were cultured in a 37°C, 5% CO_2 incubator for 16 hours. After incubation, the cells were collected by centrifugation, resuspended in 5% FBS-PBS buffer, and the proportion of GFP-positive cells was determined by flow cytometry. A dose-response curve was constructed with the dose on the horizontal axis and the percentage of GFP-positive reporter cells on the vertical axis.

2.10 NKG2D receptor-activated confocal immunofluorescence

50 μL of the MICA recombinant protein solution was added to each well of a 96-well plate and incubated at 37°C for 4 hours, followed by two washes with PBS. NKG2D-2B4 and 2B4 cells were seeded at a density of 8×10^4 cells per well. The cells were pre-stained with anti-human NKG2D monoclonal antibody (eBioscience, USA) and incubated at 4°C for 30 minutes. After incubation, the cells were washed three times with PBS and then incubated with goat anti-mouse Fluor 594 (Invitrogen, USA) at 4°C for 30 minutes. In parallel, for the soluble group, 50 μL of the MICA recombinant protein solution was added to the uncoated wells, and the plate was incubated in a 5% CO_2 incubator at 37°C for 16 hours. Finally, cells were observed under a confocal fluorescence microscope (Zeiss LSM 710).

2.11 NKL cell blocking and killing assay

$MICA^+$Hmy2.CIR and Hmy2.CIR cells were stained with CFSE (CellTrace CFSE Cell Proliferation Kit, #C34554, ThermoFisher, USA) and then seeded into 96-well plates at a density of 5×10^4 cells per well, followed by the addition of recombinant MICA soluble protein and NKG2D-Ig soluble protein at concentrations of 10 μg/mL for blocking and killing assays. NKL cells were added at E:T ratios of 1:1, 3:1, 5:1, and 10:1. After incubation at 37°C for 4 hours, the cells were stained with 7-AAD (#51-68981E, BD Pharmingen, USA) at a 1:500 dilution and analyzed by flow cytometry. Killing efficiency was calculated as the ratio of $CFSE^+$ $7\text{-}AAD^+$ target cells, with CFSE-stained target cells serving as the 100% reference.

2.12 NKG2D allele sequencing

We collected 89 Chinese south Han healthy individuals to detected NKG2D allele frequency. 89 healthy individuals recruited from the Health Management Center of Xiangya Hospital, Central South University. All participants provided signed informed consent forms, and the study protocol was approved by the Ethics Committee of Xiangya Hospital, Central South University (approval number 201611608). Peripheral blood mononuclear cells (PBMCs) were isolated from 178 healthy donor blood samples using Ficoll (stemcell, Canada) density gradient centrifugation. Total RNA was extracted from PBMCs with a RNA extraction kit (Qiagen, China) following the manufacturer's protocol. First-strand cDNA synthesis was performed using 1 μg total RNA with a reverse transcription kit (Biosharp, China) under recommended conditions: 37°C for 15 min followed by 85°C for 5 sec for enzyme inactivation.

NKG2D gene cDNA was amplified using 100 ng cDNA template with specific primers via PCR. The resulting products were purified and quantified to 20 ng/μL using nuclease-free DEPC-treated water. Sequencing libraries were prepared by mixing 40 μL DEPC water, 252 μL PCR Master Mix, and 8 μL high-fidelity Taq polymerase, followed by incubation at room temperature for 30 min. Amplification was performed under the following thermal procedure: 96°C, 2 min, then 96°C, 30 s, 20 cycles, 69°C for 50 s, 72°C for 90 s, then 72°C for 10 min to extension.

PCR products were electrophoresed (130 V, 30 min) in 1% agarose gel. Sequencing reactions utilized BigDye Terminator v3.1 Cycle Sequencing Kit with 4 μL template DNA and 2 μL primer per well, processed through: 25 cycles: 96°C for 10 s → 50°C for 5 s → 60°C for 2 min.

Post-sequencing cleanup involved SDS treatment (1.5 μL 2% SDS/well) and Sephadex G-50 column purification. Samples were analyzed on an ABI 3730xl Genetic Analyzer, with sequences

aligned to reference NKG2D alleles (GenBank: NM_001349433.1) using CodonCode Aligner v10.0.

2.13 Statistical analysis

The experimental data were statistically analyzed using SPSS 22.0 software. Measurement data are presented as mean ± SD, and comparisons between two groups were made using an independent sample *t*-test (non-parametric and unpaired tests). The allele frequencies of *MICA* were estimated based on the principles of the Poisson distribution. Graphs were generated using GraphPad Prism 9.0. A *P*-value of < 0.05 was considered statistically significant. $^{*}P < 0.05$, $^{**}P < 0.01$, $^{***}P < 0.001$.

3 Result

3.1 More than 90% of the population carries one or two of the 29 common *MICA* polymorphic alleles

A total of 280 MICA polymorphic molecules have been identified in the population. Since the distribution of *MICA* alleles is not evenly distributed across the population, the numbers of the common *MICA* alleles (frequency > 1%) are limited among the populations. In this study, we selected a Luminex bead array kit containing 28 MICA polymorphic proteins, along with the MICA*045 allele protein, which is prevalent in the Chinese population. These 29 proteins were conjugated into a Luminex beads respectively as MICA antigens array, forming a liquid microarray detection platform for testing. A search of the PubMed database was conducted for MICA allele frequency studies across various populations, and statistical analysis was performed. Based on the combined allele frequencies of the 29 MICA polymorphisms and the frequency of prevalent *MICA*010* allele, which encodes a non-expressing protein, it was concluded that the proportion of populations carrying one or two of the 29 MICA polymorphic molecules ranged from 91.6% to 99.4% in different regional populations (Table 1). The 29 MICA polymorphic proteins selected can cover for more than 90% population (Supplementary Material 1).

3.2 Presence of two broadly specific antigenic epitopes in the human polymorphic MICA molecule

The two serum samples (S001 and S002) obtained from the renal transplant recipients had been characterized to contain allo-antibodies with different specificities (23). Using a 29 MICA polymorphic molecules Luminex array, the results revealed that serum S001 showed a strong positive reaction with 18 MICA polymorphic proteins, including MICA*001, MICA*002, MICA*007, MICA*011, MICA*012, MICA*015, MICA*017, MICA*018, MICA*029, MICA*030, MICA*036, MICA*037, MICA*041, MICA*043, MICA*045, MICA*046, MICA*050, and MICA*051, with an average mean fluorescence intensity (MFI) value of 8380.48 ± 351.01. While S001 serum showed a low positive reaction with 11 other MICA polymorphic proteins, including MICA*004, MICA*005, MICA*006, MICA*008, MICA*009, MICA*016, MICA*019, MICA*024, MICA*028, MICA*033, and MICA*042, with an average MFI value of 680.64 ± 93.54 ($P < 0.001$) (Figures 1A, C, Table 2). Conversely, S002 serum exhibited a completely opposite reactivity pattern to S001 serum, showing high reactivity with the MICA polymorphic molecules that had lower MFI values in S001, and low reactivity with the group of MICA polymorphic molecules that had higher MFI values in S001. The MFI values tested by these two groups of MICA molecules with S002 were 307.89 ± 55.45 and 7806.39 ± 498.21, respectively ($P < 0.001$) (Figures 1B, C, Table 2). These results suggest that, despite the high polymorphism of MICA molecules within the population, the antigen-antibody reactions indicate the presence of two major reciprocal antigenic epitopes.

In addition, during the identification of 11 mouse anti-human MICA monoclonal hybridoma cell strains, we observed that the monoclonal antibody produced by one of the hybridoma strains (designated 5.2G1) exhibited a reactive pattern against the 29 MICA polymorphic molecules that closely resembled the reactivity observed in the human allo-antibodies of serum S001. The MFI value for 5.2G1 with the two groups of MICA polymorphic molecules was 1405.06 ± 223.11 vs. 597.55 ± 73.54 ($P < 0.001$) (Figures 1D, F, Table 2). While the general monoclonal antibody 6B3 showed a strong, uniform positive response across all MICA polymorphic molecules in the Luminex beads array, yielding a consistent and broad reactivity pattern (Figures 1E, F). These results confirm the presence of broadly specific antigenic epitopes among human MICA polymorphic molecules.

TABLE 1 The Frequency of Three Groups of *MICA* Alleles in Different Populations.

MICA allele	Chinese (25) (N=144)	American (26) (N=103)	Japanese (27) (N=130)	European (28) (N=154)	African (29) (N=201)
The 29 *MICA*[a]	73.27	84.60	88.10	90.59	98.70
*MICA*010*[b]	22.22	7.00	10.80	4.55	0.70
other	4.51	8.40	1.20	4.86	0.60
Total	100	100	100	100	100

a. The combined frequency of 29 common *MICA* alleles. b. The *MICA*010* allele is not expressed on the cell membrane but is common in population.

10.3389/fimmu.2025.1563872

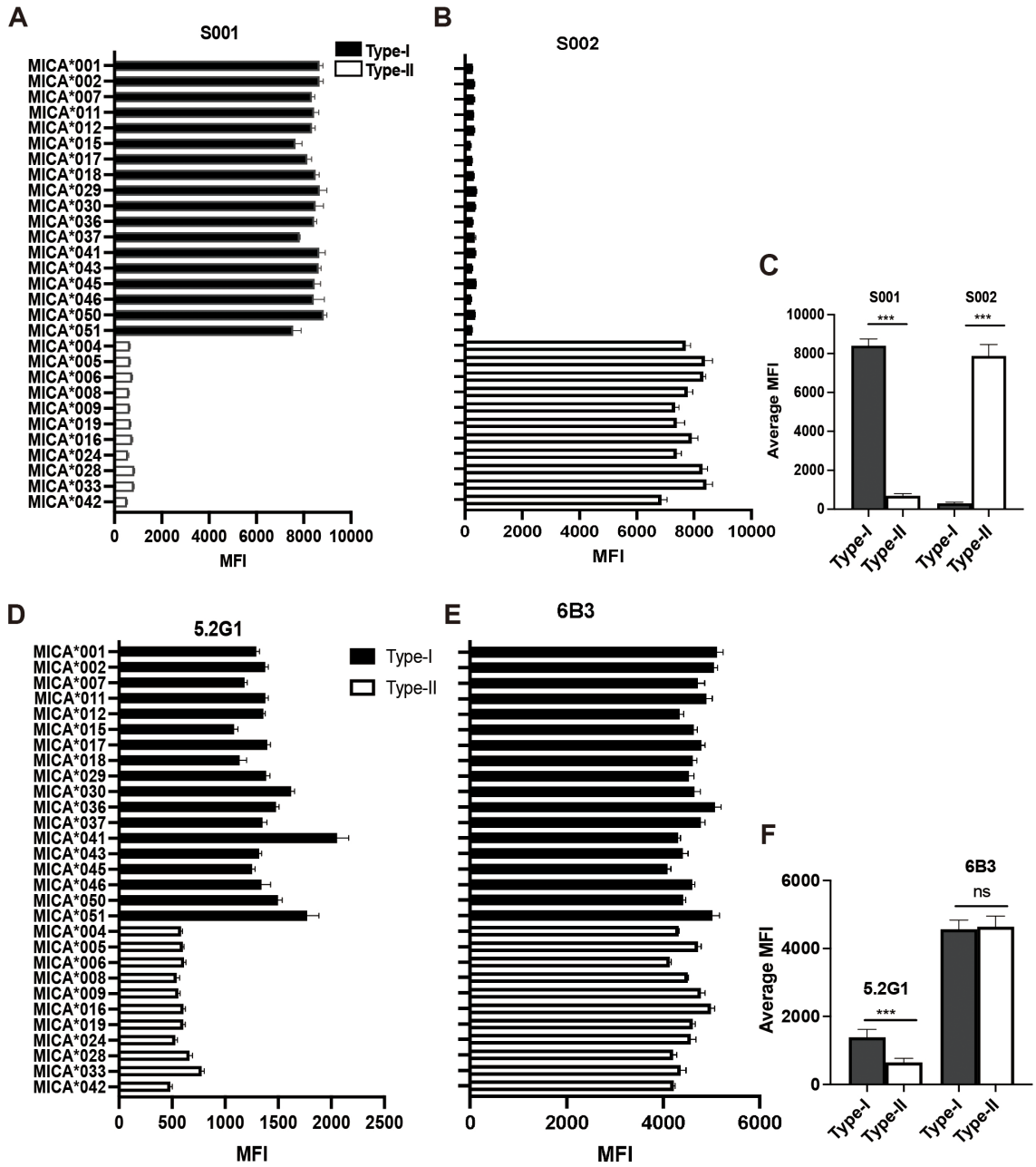

FIGURE 1
Human MICA polymorphic proteins exhibit two major opposing antigenic epitopes. **(A)** Reactivity characteristics of 29 MICA polymorphic molecules with S001 serum. **(B)** Reactivity characteristics of 29 MICA polymorphic molecules with S002 serum. **(C)** Comparison of the average binding ability of S001 and S002 serum to Type-I and Type II MICA proteins of 29 MICA polymorphic proteins, with statistical analysis performed using independent sample *t*-test. **(D)** Reactivity characteristics of 29 MICA polymorphic molecules with monoclonal antibody 5.2G1. **(E)** Reactivity characteristics of 29 MICA polymorphic molecules with monoclonal antibody 6B3. **(F)** Comparison of the average binding ability of 5.2G1 and 6B3 monoclonal antibody to Type-I and Type II MICA proteins of 29 MICA polymorphic proteins, with statistical analysis performed using independent sample *t*-test. ***$P<0.001$; ns, not significant.

The primary biological function of MICA molecules is to activate the NKG2D receptor. Based on this, we hypothesized that the broad-specific antigenic epitopes present in MICA polymorphic molecules may exhibit differential binding affinities for the NKG2D receptor, thereby influencing NK cell activation. To test this hypothesis, we prepared soluble NKG2D receptor fusion proteins (NKG2D-Ig) (Figure 2A). The purified soluble NKG2D fusion proteins displayed a band at the molecular weight of 46 kDa with SDS-PAGE, and Coomassie brilliant blue staining. Meanwhile, the hIgG antibody displayed a band of heavy chain at the molecular weight of 55 kDa and a band of light chain at the molecular weight of 25 kDa. The BSA protein displayed a band at the molecular

TABLE 2 MFI values of the two major types of MICA in response to anti-MICA antibodies and the NKG2D receptor.

Tested	Type I(N=18)	Type II(N=11)	*P*
	Mean ± SD	Mean ± SD	
human Ab S001	8380.48 ± 351.01	680.64 ± 93.54	<0.0001
human Ab S002	307.89 ± 55.45	7806.39 ± 498.21	<0.0001
mAb 5.2G1	1405.06 ± 223.11	597.55 ± 73.54	<0.0001
NKG2D-Ig	1977.52 ± 446.00	655.70 ± 175.68	<0.0001

weight of 66 kDa (Figure 2B). Additionally, the soluble NKG2D receptor fusion protein with a flag of Fc fragment of human IgG was confirmed as the same molecular weight of 46 kDa (Figure 2C).

Subsequently, the NKG2D-Ig protein was incubated with the 29 MICA Luminex beads array, and the MFI value was used as an index to assess the binding affinity between the NKG2D receptor and the MICA polymorphic molecules. The results revealed two distinct reactivity patterns for the NKG2D-Ig protein against the two major groups of MICA polymorphic molecules (1977.52 ± 446.00 vs. 655.70 ± 175.68, $P < 0.0001$) (Figures 2D, E, Table 2). This reactivity pattern closely consistent with the reactivity observed with human serum S001 and monoclonal antibody 5.2G1, further confirming the different binding affinity among the two major groups of the 29 MICA polymorphic molecules.

3.3 Response pattern of NKG2D receptor against two major groups of MICA is dependent on key polymorphic sites and its amino acid types in MICA molecules

We analyzed the binding affinities of allo-antibodies and the NKG2D-Ig protein to the 29 MICA polymorphic molecules, suggesting the presence of two major types of specific epitopes. Then that was confirmed by mAb 5.2G1. To further investigate this, we compared the amino acid polymorphic sites and their corresponding amino acid variants in these two groups of MICA polymorphic molecules by using data from the HLA/IMGT database. There have 27 amino acid polymorphic sites that were located in the extracellular membrane region of these MICA molecules in the MICA polymorphic amino acid alignment (Table 3). The MICA polymorphic molecules with high binding affinity for the NKG2D receptor were strongly correlated with six polymorphic sites and linked with six amino acid types: C_{36}+M_{129} +K_{173}+G_{206}+W_{210}+S_{215}, we call it as Type I MICA. While the six linked amino acid species is Y_{36}+V_{129}+E_{173}+S_{206}+R_{210}+T_{215}, is classified as Type II MICA. Type II MICA polymorphic molecules exhibited a lower binding affinity for NKG2D than Type I MICA molecules (Table 2). Interestingly, human MICA polymorphic molecules are classified into either Type I or Type II. Other polymorphisms sites in the MICA molecules, and their corresponding amino acid variants, did not influence the classification of these two major MICA types.

3.4 Type-I MICA polymorphic molecules activated the signaling pathway of the NKG2D receptor at a significantly lower dose than type-II MICA polymorphic molecules

The above experiments confirmed the existence of differential affinities between the two major types of MICA polymorphic molecules binding with the NKG2D receptor. To test whether this variation in ligand-receptor binding may relate to NKG2D receptor activation, we utilized an NKG2D receptor reporter cell line (NKG2D-2B4), which was previously constructed in our laboratory. The NKG2D receptor reporter cells were constructed by using a human-mouse chimeric receptor structure, with the extracellular domain of human NKG2D receptor and the intracellular domains of the murine NKG2D receptor, enabling interaction with the DAP-12 adapter protein of the murine-derived 2B4 T hybridoma cells, which forward to activate the downstream signaling pathways. Upon binding of its ligand, the NKG2D receptor triggers the activation of downstream signaling pathways, resulting in the expression of GFP and the emission of green biofluorescence (Figures 3A, B). We selected the most common MICA polymorphic proteins in humans (MICA*002 belonging to Type I and MICA*008 to Type II) for dose-response experiments to evaluate the activation of the NKG2D signaling pathway. Our prior studies have shown that soluble MICA proteins can bind to the NKG2D receptor but do not activate the NKG2D signaling pathway (19). To address this, soluble MICA proteins were pre-coated onto a 96-well plate, followed by the addition of NKG2D receptor reporter cells to assess activation with biofluorescence (Figure 3C). The dose of immobilized MICA was positively correlated with the proportion of GFP^+ cells, which was detected by flow cytometry (Figure 3D). Dose-response curves were generated to represent the proportion of activated reporter cells (GFP^+ cells) induced by different concentrations of Type I and Type II proteins. The concentration of MICA protein at the point of 50% of NKG2D reporter cells (GFP^+) reported biofluorescence was defined as the EC 50 value. The results indicated that the EC 50 value for Type I molecules was 24.97 μg/mL, while for Type II molecules, it was 37.34 μg/mL, which means that the lower the EC 50 value was, the stronger the activate ability of the MICA molecules was (Figure 3E).

Using the dose-response curves described earlier, we applied the 11 MICA polymorphic molecules to react with NKG2D receptor reporter cells at six concentrations and determined the EC 50 values for each, as derived from the curves. Among them, Type I MICA molecules (n=6) include MICA*001, MICA*002, MICA*007, MICA*012, MICA*017, and MICA*018, with an average EC 50 value of 24.95 ± 3.14 μg/mL. Type II MICA molecules (n=5) include MICA*004, MICA*006, MICA*008, MICA*009, and MICA*019,

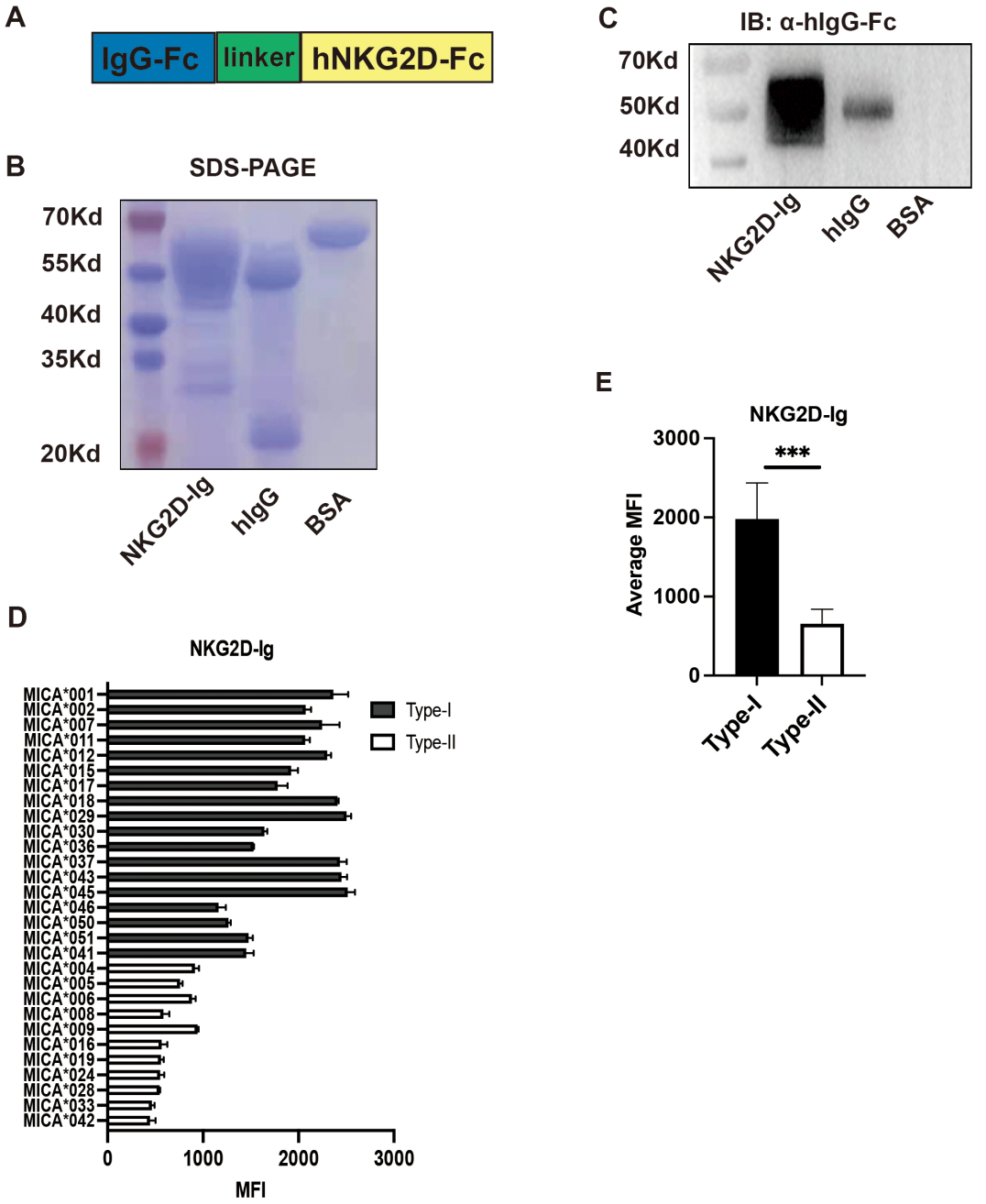

FIGURE 2
Preparation and Functional Detection of NKG2D-Ig Fusion Protein. **(A)** Schematic diagram of the structure of NKG2D-Ig fusion protein, with the N-terminal on the left and C-terminal on the right. **(B)** Coomassie brilliant blue staining showing the molecular size of the NKG2D-Ig fusion protein, with a molecular weight of 46 kDa, using human IgG and bovine serum albumin (BSA) as controls. **(C)** Detection of NKG2D-Ig fusion protein using anti-human IgG Fc antibody by Western blot, with a protein size of approximately 46 kDa, using human IgG and BSA as controls. **(D)** Reactivity characteristics of 29 MICA polymorphic molecules with NKG2D-Ig fusion protein. **(E)** Comparison of the binding ability of Type-I and Type-II proteins of 29 MICA polymorphic proteins, with statistical analysis performed using independent sample *t*-test.***$P<0.001$.

with a mean EC 50 value of 39.68 ± 4.46 μg/mL. The EC 50 value for Type I MICA molecules was significantly lower than that of Type II MICA molecules ($P < 0.001$, Table 4), indicating that a lower dose (24.95 μg/mL) of Type I MICA polymorphic molecules was sufficient to activate 50% of the NKG2D receptor reporter cells (50% GFP^+), while a higher dose (39.68 μg/mL) of Type II MICA polymorphic molecules was required to achieve the same level of activation (50% GFP^+).

10.3389/fimmu.2025.1563872

TABLE 3 Amino acid sequence alignment of 29 MICA polymorphic molecules.

		polymorphic site																										
MICA-		0	0	0	0	0	0	1	1	1	1	1	1	1	1	1	1	1	1	2	2	2	2	2	2	2	2	2
		1	2	2	3	9	9	0	1	2	2	2	4	5	5	7	7	7	8	0	0	1	1	1	2	5	5	7
		4	4	6	6	0	1	5	4	2	5	9	2	1	6	3	5	6	1	6	8	0	3	5	1	1	6	1
	001	W	T	V	C	L	Q	R	G	L	K	M	V	M	H	K	G	V	T	G	Y	W	T	S	V	Q	R	P
Type – I	002	G	A	–	-	–	–	–	–	–	E	-	–	–	–	-	–	–	–	-	–	-	–	-	–	–	–	–
	007	–	A	–	-	–	–	–	–	–	E	-	–	–	–	-	–	–	–	-	–	-	–	-	–	–	–	–
	011	G	A	–	-	–	–	–	–	–	E	-	–	V	–	-	–	–	–	-	–	-	–	-	–	–	–	A
	012	–	–	–	-	–	–	–	–	–	E	-	–	–	L	-	–	–	–	-	–	-	–	-	–	–	–	–
	015	G	A	–	-	–	–	–	R	–	E	-	–	–	–	-	–	–	–	-	–	-	–	-	–	–	–	–
	017	G	A	–	-	–	R	–	–	–	E	-	–	–	–	-	–	–	–	-	–	-	–	-	–	–	–	–
	018	–	–	–	-	–	–	–	–	–	E	-	–	–	–	-	–	–	–	-	–	-	–	-	–	–	–	–
	029	–	A	–	-	–	–	–	–	–	E	-	I	–	–	-	–	–	–	-	–	-	–	-	–	–	–	–
	030	G	A	–	-	–	–	–	–	–	E	-	–	–	–	-	–	–	–	-	–	-	–	-	–	–	–	A
	036	G	A	–	-	–	–	K	–	–	E	-	–	–	–	E	S	–	–	-	–	-	–	-	–	–	–	–
	037	–	A	–	-	–	–	–	–	–	E	-	–	–	–	-	–	–	–	S	–	R	I	T	–	R	–	–
	041	G	A	G	-	–	–	–	–	–	E	-	–	–	–	-	–	–	–	-	–	-	–	-	–	–	–	–
	043	–	A	–	-	–	–	–	–	–	E	-	–	–	R	-	–	–	–	-	–	-	–	-	–	–	S	–
	045	–	A	–	-	–	–	–	–	–	E	-	–	–	–	-	–	–	–	-	–	-	–	-	–	E	–	–
	046	G	A	–	-	–	–	–	–	–	E	-	–	–	–	-	–	–	–	-	C	-	–	-	–	–	–	–
	050	G	A	–	-	F	–	–	–	–	E	-	–	–	–	-	–	–	–	-	–	-	–	-	–	–	–	–
	051	–	A	–	Y	–	–	–	–	–	E	-	–	–	–	-	–	–	–	-	–	-	–	-	–	–	–	–
Type – II	004	–	A	–	Y	–	–	–	–	V	E	V	–	–	–	E	S	–	R	S	–	R	–	T	–	–	–	–
	005	–	A	–	Y	–	–	–	–	–	E	V	–	–	–	-	–	–	–	S	–	R	–	T	–	R	–	–
	006	–	A	–	Y	–	–	–	–	V	E	V	–	–	–	E	S	I	–	S	–	R	–	T	–	–	–	–
	008	–	A	–	Y	–	–	–	–	–	E	V	–	–	–	E	–	–	–	S	–	R	I	T	–	R	–	–
	009	–	A	–	Y	–	–	–	–	V	E	V	–	–	–	E	S	–	–	S	–	R	–	T	–	–	–	–
	016	–	A	–	Y	–	–	–	–	–	E	V	–	–	–	E	–	–	–	S	–	R	–	T	L	–	–	–
	019	–	A	–	Y	–	–	–	–	–	E	V	–	–	–	E	S	–	–	S	–	R	I	T	–	R	–	–
	024	–	A	–	Y	–	–	–	–	–	E	V	–	–	–	E	–	–	–	S	–	R	–	T	–	–	–	–
	028	–	A	–	Y	–	–	–	–	–	E	V	–	–	–	E	–	–	–	-	–	-	–	-	–	–	–	–
	033	–	A	–	Y	–	–	–	–	–	E	V	–	–	–	E	S	–	–	S	–	R	I	T	–	R	–	–
	042	–	A	–	Y	–	–	–	–	–	E	-	–	–	–	-	–	–	–	S	–	R	I	T	–	R	–	–

Polymorphic sites of amino acid residues in MICA protein molecules, with non-polymorphic sites in the sequence not included. *MICA*001* was used as the reference sequence. "-" indicates that the amino acid residue at this position is identical to that in *MICA*001*.

The orange color in the headline means the six-linked polymorphic sites. The blue color of amino acid type means Type-I MICA molecules. The green color of amino acid type means Type-II MICA molecules.

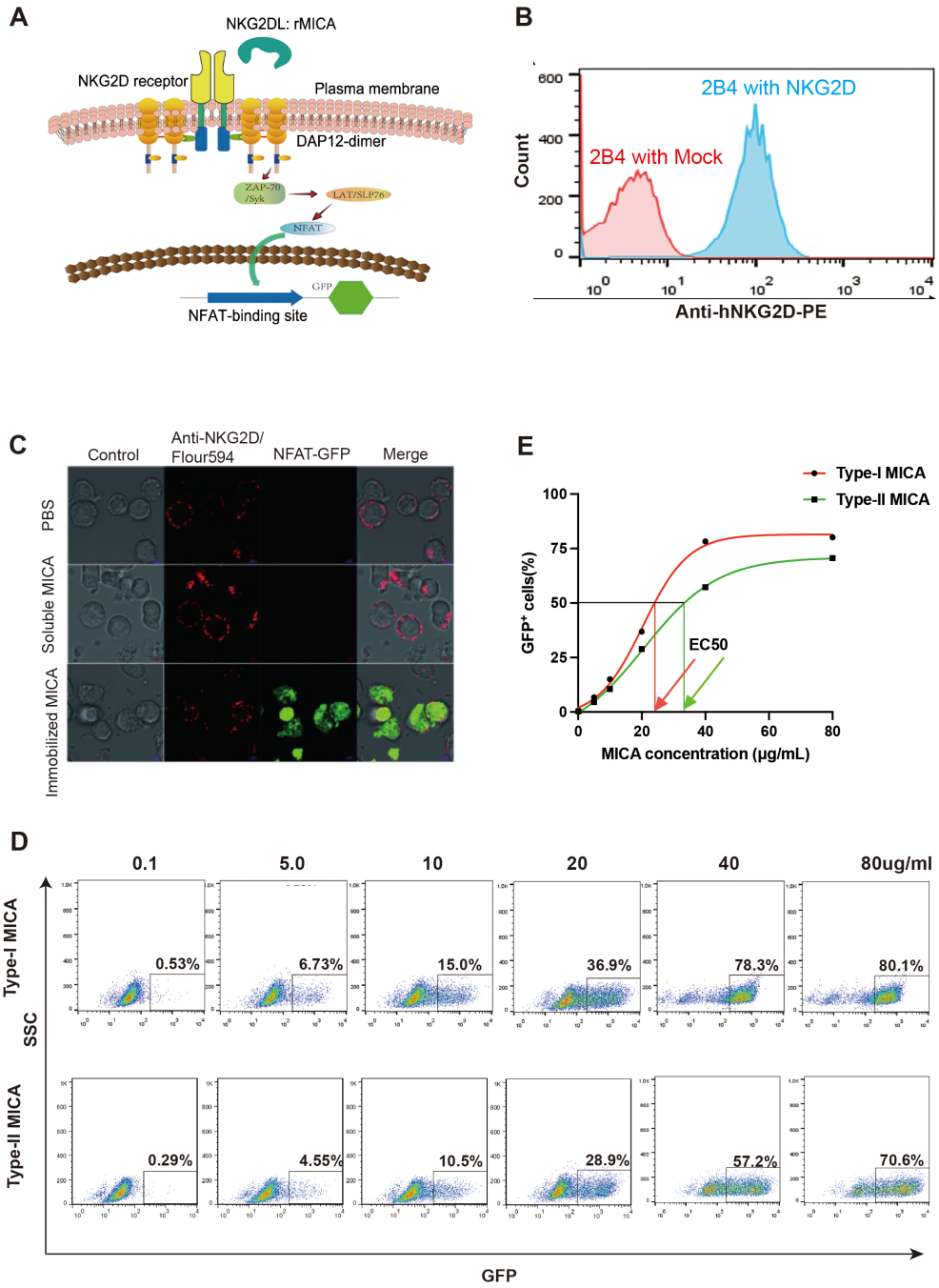

FIGURE 3
There are differences in the ability of the two major types of MICA polymorphic molecules to activate the NKG2D receptor. **(A)** Schematic diagram of the structure of NKG2D receptor reporter cell. **(B)** The NKG2D receptor reporter cells stably express the NKG2D molecule on the surface. **(C)** Immobilized MICA protein could activate NKG2D reporter cell to produce GFP. **(D)** The percentage of GFP^+ reporter cells activated by different concentration of MICA polymorphic molecules. **(E)** The dose-response curves to evaluate the activation of the NKG2D receptor.

3.5 The killing efficiency of NKL cells against MICA stably expressing cells with type-I MICA was significantly higher than that with type-II MICA

The NKG2D receptor on the NKL cell membrane was detected using an anti-NKG2D monoclonal antibody, demonstrating high expression of the NKG2D receptor (Figure 4A). Our previous studies have shown that NKL cells function as effector cells with a specific killing effect on human B lymphoblastoid cells that overexpress MICA. This cytotoxic effect can be inhibited by NKG2D-Ig fusion proteins or soluble recombinant MICA proteins, resulting in a significant reduction in killing efficiency (20). We also genotyped the *NKG2D* gene in a healthy population (Supplementary Material 2) and identified four distinct alleles; however, no amino acid sequence changes were found, indicating

TABLE 4 The dose of 11 MICA polymorphic molecules that activates 50% of the NKG2D receptor response (EC50).

MICA polymorphic molecules		Average EC 50 (μg/mL)	$\bar{X}$ (μg/mL)	*P* value
Type-I (N=6)	001	26.35	24.95	<0.001
	002	21.96		
	007	25.16		
	012	28.61		
	017	21.55		
	018	26.04		
Type-II (N=5)	004	39.54	39.68	
	006	38.67		
	008	41.84		
	009	34.84		
	019	43.49		

that the NKG2D receptor protein is conserved across human individuals. Thus, it can be inferred that the NKG2D receptor expressed on the NKL cell line serves as a reliable model for assessing the killing efficiency of MICA-expressing target cells in the populations.

To evaluate the cytotoxic efficiency of NKL cells, we constructed human B-lymphoblastoid cells (Hmy2.CIR) overexpressing Type-I MICA (MICA*002) and Type-II MICA (MICA*008) molecules. These overexpressing cells were stained with an anti-MICA monoclonal antibody, and two cell strains with comparable membrane expression levels of Type-I and Type-II MICA molecules were selected and expanded as target cells (Figure 4B). Flow cytometry was then used to assess the killing efficiency of NKL cells against these target cells. The proportion of killed target cells (7-AAD^+) was calculated at different effector-to-target (E: T) ratios (1:1, 3:1, 5:1, and 10:1), and killing curves were plotted for NKL cells targeting cells stably expressing either Type-I or Type-II MICA. The results showed that NKL cells exhibited a significantly higher killing efficiency against Type-I MICA target cells compared to Type-II MICA target cells ($P < 0.05$, Figures 4C, D).

4 Discussion

To investigate the functional differences among various MICA polymorphic molecules, we selected 29 representative variants based on their reactivity to anti-MICA antibodies and NKG2D receptor. These polymorphisms correspond to alleles found in more than 90% of the population. Although *MICA*010* is present in the population, it was excluded from this study due to its lack of protein expression (24). The 29 MICA polymorphic molecules selected for structural and functional analysis in this study are considered broadly representative of the population's diversity (25–29).

Variations in the activation of NKG2D receptor by MICA polymorphic molecules may be attributed to specific amino acid polymorphisms. In our previous study, we identified two opposing antigen-antibody reaction profiles in the serum samples from renal transplant patients obtained from ASHI (23). Building on this, our current study further confirmed that the 29 MICA polymorphic molecules exhibited two opposing antigen-antibody response profiles when exposed to allo-antibodies from two renal transplant recipients. Similar dichotomous patterns were also observed in reaction with anti-MICA monoclonal antibodies. These findings suggest the existence of two major types of MICA polymorphic molecules. Notably, these two MICA phenotypes displayed distinct binding affinities to soluble NKG2D receptor proteins.

Most previous studies primarily focused on single amino acid polymorphisms in MICA molecules, particularly the well-characterized M/V dimorphism at position 129. This variant has been linked to differential binding affinity to the NKG2D receptor, with the M variant conferring significantly higher affinity compared to the V variant (13, 30). However, subsequent studies have indicated that the NKG2D binding affinity is not solely determined by the MICA-129 allele (23, 31). In our study, cluster analysis of the amino acid polymorphisms across all 280 MICA variants revealed two major groups characterized by six linked polymorphic residues: position 36, 129, 173, 206, 210, and 215. Notably, the residue at position 129 was found to be tightly linked to these sites. When position 129 is M, the six linked amino acids at the six sites typically form the sequence $C_{36}+M_{129}+K_{173}+G_{206}+W_{210}+S_{215}$. MICA polymorphic molecules with this combination exhibit higher binding affinity to both antibodies and the NKG2D receptor. In contrast, when position 129 is V, the linked amino acids at these six sites are usually $Y_{36}+V_{129}+E_{173}+S_{206}+R_{210}+T_{215}$, resulting in a lower binding affinity to the NKG2D receptor. Consequently, MICA polymorphic molecules with high binding affinity and these six linked amino acids were classified as Type-I MICA, while those with lower affinity were classified as Type-II MICA. The extracellular domains of MICA consist of the α1, α2, and α3 immunoglobulin-like structural domains, with the α1 and α2 domains being primary responsible for NKG2D receptor binding. The amino acids at positions 36, 129, and 173, located within the α1 and α2 domains, are key components of antigenic epitopes, forming the molecular structural basis for distinguishing the two major types of MICA (31, 32).

To investigate whether there is a significant difference in the ability of the two of MICA polymorphic phenotypes to activate the NKG2D receptor signaling pathway, we stimulated NKG2D receptor reporter cells with recombinant MICA proteins at varying concentrations. The EC50 value, defined as the concentration at which 50% of the reporter cells exhibited biofluorescence (GFP^+), was determined.

As a key effector cell type in innate immunity, NK cells play a crucial role in the early-stage elimination of tumor cells and virus-infected cells. The NKG2D receptor is essential for NK cell activation and transduces signals through the DAP10 adaptor via multiple signaling pathways. NKG2D can initiate various forms of signal transduction via phosphorylation, activating mitogen-

10.3389/fimmu.2025.1563872

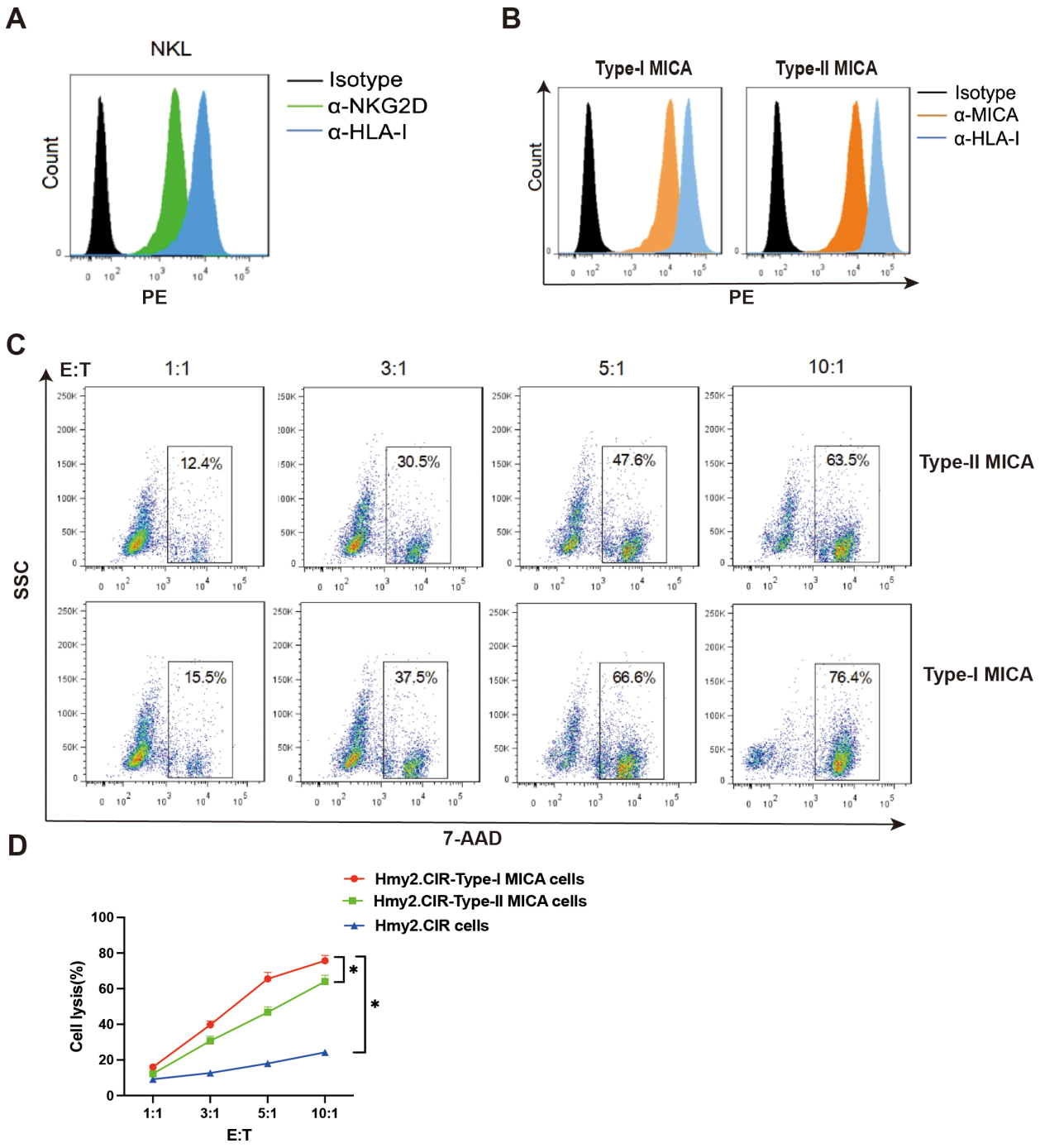

FIGURE 4
The killing efficiency of NKL cells against Type-I MICA cells is higher than that against Type-II MICA cells. **(A)** The NKL cells stably express the NKG2D molecule on the surface. **(B)** The two types of MICA overexpressing Hmy2.CIR cells stably and evenly express the MICA molecule on the surface. **(C, D)** The killing efficiency of NKL cells against the two types of MICA^{+} Hmy2.CIR cells. *P<0.05.

activated protein kinase (MAPK) and Janus kinase (Jak)/signal transducer and activator of transcription (STAT) signaling pathways (33). NKG2D ligands, such as MICA, regulate the receptor function, with upregulation of MICA expression leading to increased NKG2D receptor expression (34). The variable affinity of NKG2D for MICA may influence receptor activation in predisposed individuals, which has been observed in various autoimmune diseases (34). The affinity of the NKG2D receptor for MICA is higher than that for other ligands. However, mutations in certain MICA sites can reduce the formation of hydrogen bonds, thereby suppressing NKG2D receptor-mediated NK cell activation (35). In this study, we found that Type-I and Type-II MICA molecules differed in their ability to activate the NKG2D receptor signaling pathway. These findings indicate that the two major

MICA polymorphic types not only vary in their binding affinity to the NKG2D receptor but also in their capacity to activate the NKG2D signaling pathway. Furthermore, our results demonstrate that these two MICA phenotypes also differ in the efficiency of NKL cell-mediated cytotoxicity, highlighting distinct molecular mechanisms that regulate NK cell activation and target cell killing.

The NKG2D receptor is encoded by the highly conserved *KLRK1* gene, which exhibits limited polymorphisms (36). While certain variants have been implicated in diseases such as rheumatoid arthritis (RA) and HPV-induced cancers, their causal relationships and underlying mechanisms remain unclear (37, 38). Our SBT sequencing analysis of *KLRK1* transcripts across study populations detected no amino acid-altering polymorphisms suggesting that the structural variation in NKG2D receptor itself does not account for observed differences in receptor activation. Rather these functional variations appear to stem primarily from polymorphisms in the MICA molecules. Although, the NKG2D receptor interacts with multiple ligands-including the MICB and ULBP families- MICA is considered the most important due to its highest degree of polymorphism and its dominant role in receptor activation (15). The differential effects of the NKG2D-MICA axis in innate immune responses are primarily determined by MICA polymorphisms.

In summary, our results are the first to identify two major types of MICA polymorphic molecules distinguished by six linked amino acid sites, offering insight into how MICA polymorphism regulates the NKG2D signaling pathway. Based on these findings, individuals can be classified into three MICA phenotypic groups: Type-I homozygote, Type-II homozygote, and Type-I/Type-II heterozygote. Since Type-I MICA ligands more efficiently activate the NKG2D receptor on NK cells compared to Type-II ligands, individuals with the Type-I homozygous phenotype may exhibit heightened NK cell responsiveness. This could enhance protection against infections and tumors but may also increase susceptibility to autoimmune diseases (39). Conversely, individuals with the Type-II homozygous phenotype may show reduced NK cell activation and potentially exhibit the opposite disease susceptibility. The relationship between *MICA* phenotypes and disease outcomes across these three groups remains unclear, and further clinical data are necessary to explore these correlations. Our findings provide valuable insights into the molecular and functional regulation of the NKG2D-MICA axis, which demand further in-depth investigation.

Data availability statement

The original contributions presented in the study are publicly available. This data can be found here: https://www.ncbi.nlm.nih.gov/sra/PRJNA1260497.

Ethics statement

The genotype of healthy people in which all participants provided signed informed consent forms, and the study protocol was approved by the Ethics Committee of Xiangya Hospital, Central South University (approval number 201611608).

Author contributions

QL: Conceptualization, Investigation, Project administration, Supervision, Writing – review & editing. XY: Conceptualization, Investigation, Data curation, Formal analysis, Methodology, Writing – original draft. QZ: Data curation, Formal analysis, Investigation, Methodology, Writing – original draft. WL: Resources, Writing - review & editing. RL: Investigation, Methodology, Writing – review & editing. LW: Investigation, Methodology, Writing – review & editing. YZ: Conceptualization, Funding acquisition, Project administration, Supervision, Validation, Writing – review & editing.

Funding

The author(s) declare that financial support was received for the research and/or publication of this article. This study was funded by the National Natural Science Foundation of China (82171763) and the Hunan Provincial Natural Science Foundation (2020JJ4768).

Conflict of interest

The authors declare that the research was conducted in the absence of any commercial or financial relationships that could be construed as a potential conflict of interest.

Generative AI statement

The author(s) declare that no Generative AI was used in the creation of this manuscript.

Publisher's note

Supplementary material

The Supplementary Material for this article can be found online at: https://www.frontiersin.org/articles/10.3389/fimmu.2025.1563872/full#supplementary-material

References

1. Kasahara M, Sutoh Y. Comparative genomics of the NKG2D ligand gene family. *Immunol Rev*. (2015) 267:72–87. doi: 10.1111/imr.12320

2. Stephens HAF. MICA and MICB genes: Can the enigma of their polymorphism be resolved? *Trends Immunol*. (2001) 22:378–85. doi: 10.1016/S1471-4906(01)01960-3

3. Groh V, Bahram S, Bauer S, Herman A, Beauchamp M, Spies T. Cell stress-regulated human major histocompatibility complex class I gene expressed in gastrointestinal epithelium. *Proc Natl Acad Sci U S A*. (1996) 93:12445–50. doi: 10.1073/pnas.93.22.12445

4. Wang DR, Dou LY, Sui LH, Xue Y, Xu S. Natural killer cells in cancer immunotherapy. *MedComm*. (2024) 5. doi: 10.1002/MCO2.626

5. Zhang X, Zhang Y, Liu H, Tang K, Zhang C, Wang M, et al. IL-15 induced bystander activation of CD8+ T cells may mediate endothelium injury through NKG2D in Hantaan virus infection. *Front Cell Infect Microbiol*. (2022) 12:1084841. doi: 10.3389/fcimb.2022.1084841

6. Vulpis E, Loconte L, Peri A, Molfetta R, Caracciolo G, Masuelli L, et al. Impact on NK cell functions of acute versus chronic exposure to extracellular vesicle-associated MICA: Dual role in cancer immunosurveillance. *J Extracell Vesicles*. (2022) 11:e12176. doi: 10.1002/jev2.12176

7. Groh V, Rhinehart R, Randolph-Habecker J, Topp MS, Riddell SR, Spies T. Costimulation of CD8αβ T cell by NKG2D *via* engagement by MIC induced on virus-infected cells. *Nat Immunol*. (2001) 2:255–60. doi: 10.1038/85321

8. de Andrade LF, En Tay R, Pan D, Luoma AM, Ito Y, Badrinath S, et al. Antibody-mediated inhibition of MICA and MICB shedding promotes NK cell-driven tumor immunity. *Sci (80-)*. (2018) 359:1537–42. doi: 10.1126/SCIENCE.AAO0505

9. Marangon CG, de Bitencorte JT, Michita RT, Lunge VR, dos Santos DC, Álvares-da-Silva MR, et al. Association between MICA rs2596542 polymorphism with the risk of hepatocellular carcinoma in chronic hepatitis C patients. *Pathol Oncol Res*. (2020) 26:1519–25. doi: 10.1007/s12253-019-00738-6

10. Wang H, Cao H, Xu Z, Wang D, Zeng Y. SNP rs2596542G>A in MICA is associated with risk of hepatocellular carcinoma: A meta-analysis. *Biosci Rep*. (2019) 39. doi: 10.1042/BSR20181400

11. Machuldova A, Houdova L, Kratochvilova K, Leba M, Jindra P, Ostasov P, et al. Single-nucleotide polymorphisms in MICA and MICB genes could play a role in the outcome in AML patients after HSCT. *J Clin Med*. (2021) 10. doi: 10.3390/jcm10204636

12. Isernhagen A, Malzahn D, Bickeböller H, Dressel R. Impact of the MICA-129Met/val dimorphism on NKG2D-mediated biological functions and disease risks. *Front Immunol*. (2016) 7:588. doi: 10.3389/fimmu.2016.00588

13. Littera R, Mocci S, Argiolas D, Littarru L, Lai S, Melis M, et al. MICA and NKG2D gene polymorphisms influence graft survival, and response to therapy in kidney transplantation. *Front Immunol*. (2024) 15:1440887. doi: 10.3389/FIMMU.2024.1440887

14. Khan M, Arooj S, Wang H. NK cell-based immune checkpoint inhibition. *Front Immunol*. (2020) 11:167. doi: 10.3389/fimmu.2020.00167

15. Fuertes MB, Domaica CI, Zwirner NW. Leveraging NKG2D ligands in immuno-oncology. *Front Immunol*. (2021) 12:713158. doi: 10.3389/fimmu.2021.713158

16. Apithy MJ, Charbonnier A, Desoutter J, Diouf M, Morel P, Garçon L, et al. Impact of MICA and NKG2D polymorphisms in HLA-fully matched related and unrelated hematopoietic stem cell transplantation. *Bone Marrow Transplant*. (2018) 53:918–22. doi: 10.1038/s41409-017-0083-3

17. Duan S, Guo W, Xu Z, He Y, Liang C, Mo Y, et al. Natural killer group 2D receptor and its ligands in cancer immune escape. *Mol Cancer*. (2019) 18. doi: 10.1186/s12943-019-0956-8

18. Liu Z, Wang H, Liu H, Ding K, Shen H, Zhao X, et al. Targeting NKG2D/NKG2DL axis in multiple myeloma therapy. *Cytokine Growth Factor Rev*. (2024) 76:1–11. doi: 10.1016/J.CYTOGFR.2024.02.001

19. Zou Y, Luo W, Guo J, Luo Q, Deng M, Lu Z, et al. NK cell-mediated anti-leukemia cytotoxicity is enhanced using a NKG2D ligand MICA and anti-CD20 scfv chimeric protein. *Eur J Immunol*. (2018) 48:1750–63. doi: 10.1002/eji.201847550

20. Liu R, Luo Q, Luo W, Wan L, Zhu Q, Yin X, et al. A soluble NK-CAR mediates the specific cytotoxicity of NK cells toward the target CD20+ Lymphoma cells. *Aging Dis*. (2022) 13:1576–88. doi: 10.14336/AD.2022.0415

21. Zou Y, Mirbaha F, Stastny P. Contact inhibition causes strong downregulation of expression of MICA in human fibroblasts and decreased NK cell killing. *Hum Immunol*. (2006) 67:183–7. doi: 10.1016/J.HUMIMM.2006.02.018

22. Stastny P, Zou Y. 16 th IHIW: Report of the MICA P roject. *Int J Immunogenet*. (2013) 40:11–6. doi: 10.1111/iji.12016

23. Zou Y, Qin Z, Silveus A, Fan Y, Stastny P. Polymorphisms of MICA recognized by human alloantibodies. *Immunogenetics*. (2009) 61:91–100. doi: 10.1007/s00251-008-0344-9

24. Phanabamrung S, Jumnainsong A, Anuwongcharoen N, Phanus-umporn C, Rareongjai S, Leelayuwat C. Expression and function of the major histocompatibility complex (MHC) class I chain-related A (MICA)*010 in NK cell killing activity. *Hum Immunol*. (2024) 85. doi: 10.1016/J.HUMIMM.2024.111085

25. Xu X, Xia W, Tian L, Chen Y, Ding H, Shao Y, et al. Distribution of MICA haplotypes in a Chinese Han population. *Hum Immunol*. (2012) 73:75–9. doi: 10.1016/j.humimm.2011.08.021

26. Oliveira LA, Ribas F, Bicalho MG, Tsuneto LT, Petzl-Erler ML. High frequencies of alleles MICA*020 and MICA*027 in AmerIndians and evidence of positive selection on exon 3. *Genes Immun*. (2008) 9:697–705. doi: 10.1038/GENE.2008.65

27. Ahmad T, Marshall SE, Mulcahy-Hawes K, Orchard T, Crawshaw J, Armuzzi A, et al. High resolution MIC genotyping: Design and application to the investigation of inflammatory bowel disease susceptibility. *Tissue Antigens*. (2002) 60:164–79. doi: 10.1034/j.1399-0039.2002.600207.x

28. Lucas D, Campillo JA, López-Hernández R, Martínez-García P, López-Sánchez M, Botella C, et al. Allelic diversity of MICA gene and MICA/HLA-B haplotypic variation in a population of the Murcia region in southeastern Spain. *Hum Immunol*. (2008) 69:655–60. doi: 10.1016/J.HUMIMM.2008.07.011

29. Zhang Y, Han M, Vorhaben R, Giang C, Lavingia B, Stastny P. Study of MICA alleles in 201 African Americans by multiplexed single nucleotide extension (MSNE) typing. *Hum Immunol*. (2003) 64:130–6. doi: 10.1016/S0198-8859(02)00743-7

30. Fuerst D, Neuchel C, Niederwieser D, Bunjes D, Gramatzki M, Wagner E, et al. Matching for the MICA-129 polymorphism is beneficial in unrelated hematopoietic stem cell transplantation. *Blood*. (2016) 128:3169–76. doi: 10.1182/blood-2016-05-716357

31. Xing S, Ferrari de Andrade L. NKG2D and MICA/B shedding: a 'tag game' between NK cells and Malignant cells. *Clin Transl Immunol*. (2020) 9:1–10. doi: 10.1002/cti2.1230

32. Verhaar ER, Knoflook A, Pishesha N, Liu X, van Keizerswaard WJC, Wucherpfennig KW, et al. MICA-specific nanobodies for diagnosis and immunotherapy of MICA+ tumors. *Front Immunol*. (2024) 15:1368586. doi: 10.3389/fimmu.2024.1368586

33. Chen Y, Lu D, Churov A, Fu R. Research progress on NK cell receptors and their signaling pathways. *Mediators Inflammation*. (2020) 2020. doi: 10.1155/2020/6437057

34. Kucuksezer UC, Aktas Cetin E, Esen F, Tahrali I, Akdeniz N, Gelmez MY, et al. The role of natural killer cells in autoimmune diseases. *Front Immunol*. (2021) 12:622306. doi: 10.3389/fimmu.2021.622306

35. Fan J, Shi J, Zhang Y, Liu J, An C, Zhu H, et al. NKG2D discriminates diverse ligands through selectively mechano-regulated ligand conformational changes. *EMBO J*. (2022) 41:1–18. doi: 10.15252/embj.2021107739

36. Lanier LL. NKG2D receptor and its ligands in host defense. *Cancer Immunol Res*. (2015) 3:575–82. doi: 10.1158/2326-6066.CIR-15-0098

37. Mariaselvam CM, Tamouza R, Krishnamoorthy R, Charron D, Misra DP, Jain VK, et al. Association of NKG2D gene variants with susceptibility and severity of rheumatoid arthritis. *Clin Exp Immunol*. (2017) 187:369–75. doi: 10.1111/cei.12891

38. Luis Espinoza J, Nguyen VH, Ichimura H, Pham TTT, Nguyen CH, Pham TV, et al. A functional polymorphism in the NKG2D gene modulates NK-cell cytotoxicity and is associated with susceptibility to Human Papilloma Virus-related cancers. *Sci Rep*. (2016) 6:1–12. doi: 10.1038/srep39231

39. Yin X, Zhu Q, Li Ji, Zou Y. The relationship between six linked single nucleotide polymorphisms (SNPs) in the MICA gene and susceptibility to rosacea. *J Cent South Univ Med Sci*. (2025). doi: 10.11817/j.issn.1672-7347.2024.240531

frontiers | Frontiers in Immunology

TYPE Case Report
PUBLISHED 19 May 2025
DOI 10.3389/fimmu.2025.1586349

OPEN ACCESS

EDITED BY
Rita Maccario,
San Matteo Hospital Foundation (IRCCS), Italy

REVIEWED BY
Franca Fagioli,
Regina Margherita Hospital, Italy
John Marra,
Università Cattolica del Sacro Cuore, Italy

*CORRESPONDENCE
Nainong Li
nainong.li@aliyun.com

RECEIVED 02 March 2025
ACCEPTED 10 April 2025
PUBLISHED 19 May 2025

CITATION
Li H, Li X, Xian N, Huang G and Li N (2025) Case Report: CD19 CAR-T cells derived from recipient of umbilical cord blood transplantation effectively treated relapsed acute lymphoblastic leukemia after UCBT. *Front. Immunol.* 16:1586349. doi: 10.3389/fimmu.2025.1586349

Case Report: CD19 CAR-T cells derived from recipient of umbilical cord blood transplantation effectively treated relapsed acute lymphoblastic leukemia after UCBT

Hua Li[1,2], Xiaofan Li[2], Na Xian[3], Gangxiong Huang[3,4] and Nainong Li[2*]

[1]Department of Hematology, Xiamen Medical College Affiliated Second Hospital, Xiamen, China, [2]Hematopoietic Stem Cell Transplantation Center, Fujian Institute of Hematology, Fujian Provincial Key Laboratory on Hematology, Department of Hematology, Fujian Medical University Union Hospital, Fuzhou, China, [3]Institute of Immunotherapy, Fujian Medical University, Fuzhou, China, [4]Tcelltech Biological Science and Technology Inc., Fuzhou, China

Recent advances in chimeric antigen receptors have provided an alternative approach for treating relapsed acute lymphocyte leukemia after allogeneic hematopoietic stem cell transplantation (allo-HSCT). However, relapsed patients who had undergone allogeneic umbilical cord blood transplantation (UCBT) have no chance of having CAR-T cells derived from donors due to lacking UCB. We present a case of a patient with Ph+ ALL who relapsed after UCBT and achieved complete morphological and molecular remission following treatment with CD19 CAR-T cells derived from the recipient post-UCBT. The patient had only grade I CRS. GVHD or neurotoxicity was not observed. More than 6 years after CAR-T cell infusion, the patient was still in hematologic and molecular complete remission with negative minimal residual disease (MRD). This case is the first to show a new strategy of practicality, efficacy, and safety of CD19 CAR-T cells derived from UCBT recipients for treating relapsed ALL after UCBT.

KEYWORDS

chimeric antigen receptor T (CAR-T), relapsed acute lymphoblastic leukemia, allogeneic umbilical cord blood transplantation (UCBT), Ph+ acute lymphoblastic leukemia, umbilical cord derived CART

Background

Adult patients with acute B-cell lymphoblastic leukemia (B-ALL) often relapse after chemotherapy alone, with a long-term survival rate of approximately 30% (1, 2). Although hematopoietic stem cell transplantation (HSCT) has improved the survival of patients with hematologic malignancies, relapse after HSCT remains a challenge. Progressive malignancy is the leading cause of death following allo-HSCT (3). Patients with relapsed acute lymphoblastic leukemia after allo-HSCT have a median survival of 5.5 months (4). Donor leukocyte infusion (DLI) is commonly used for patients with high-risk relapse post-HSCT, but its efficacy is 15%–40% and induces severe graft-versus-host disease (GVHD), which increases transplantation-related mortality (5, 6). Recent advances in chimeric antigen receptor (CAR) T-cell therapy have shown significant progress and have changed the landscape of treatment for hematologic malignancies (7). Multiple clinical trials have demonstrated that infusion of CD19 CAR-T cells resulted in overall remission rates of 70%–90% in patients with relapsed B-cell ALL after autologous and allogeneic donors (8–11). However, relapsed patients who received UCBT do not have a chance for DLI or CAR-T cells from donors owing to the limitation of the source. To solve this problem, we attempted a new strategy of CAR-T cell therapy in UCBT recipients. We report that a patient with B-ALL who relapsed after UCBT achieved a second complete remission after treatment with CD19 CAR-T cells derived from the recipient (Figure 1).

Case representation

A 27-year-old man presented to our hospital with cough and fever in May 2017. Peripheral blood examination revealed a white blood cell count of 183.5 × 10^9/L, hemoglobin level of 110 g/L, and platelet count of 119 × 10^9/L. Bone marrow examination revealed 88% blast cells with negative myeloperoxidase staining. Flow cytometry analysis revealed an abnormal blast population (48%) expressing HLA-DR, CD10, CD19, CD22, CD33, CD34, CD38, CD58, CD123, cCD79a, and TdT. Cytogenetic and molecular biology analyses revealed t (9, 22)(q34;q11) and BCR-ABL1(p210) fusion gene transcripts. No other gene mutations were detected by next-generation DNA sequencing. The patient was diagnosed with Philadelphia chromosome-positive B-cell acute lymphoblastic leukemia (Ph^+ B-ALL).

Treatment

Reducing tumor load with cyclophosphamide and prednisone was given to, following induction chemotherapy with Vindesine, Idarubicin, Cyclophosphamide, Prednisone, and L-asparaginase (VICLP). He received one more cycle of VICLP and started a tyrosine-kinase inhibitor (imatinib) for consolidation. Complete hematologic remission (CHR) was achieved for two months. Subsequently, on 2 October 2017, the patient received a single allogeneic unit of UCBT with a myeloablative regimen of busulfan/cyclophosphamide. Peripheral myeloid engraftment (absolute neutrophil count, >0.5 ×10 ^{9}/L) was evident on day 22, and he was platelet transfusion-dependent (platelet count, >20 × 10^9/L) until day 50 post-transplantation. Donor HLA-matched complete chimerism (100%) was achieved within the initial 14 days. The patient achieved a complete molecular remission (CMR) 3 months after transplantation. At molecular relapse, the patient was treated with interferon-γ for its antitumor effects and received BCR-ABL-targeted therapy using the TKI Dasatinib.

After treatment, the patient achieved complete CHR with sustained MRD negativity, as confirmed using flow cytometry. However, molecular monitoring revealed persistent detection of the BCR-ABL1 fusion gene by reverse transcription-polymerase chain reaction (RT-PCR) for 2 months. But the disease was going to progress over the next 3 months. CAR-T cell therapy was performed after obtaining informed consent from the patient. When the patient relapsed with 7% blast cells in the bone marrow and BCR-ABL1 30.88% (IS), analysis of short tandem

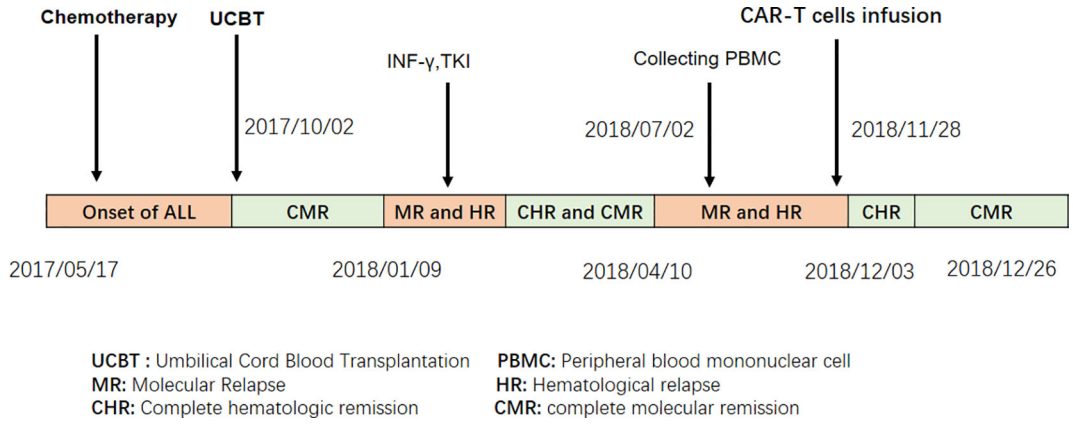

FIGURE 1
Treatment procedures for the ALL patient who, after UCBT, received autologous CAR T cell therapy due to relapse.

10.3389/fimmu.2025.1586349

repeats (STRs) showed 100% chimerism with umbilical cord donor cells. Peripheral blood mononuclear cells (PBMC) from the patients were collected for preparation of CAR-T cells. Following isolation and procurement, T-cells were *ex vivo* activated and transduced using a lentiviral vector encoding the CAR gene. CD19-targeting CAR-T cells were generated using a murine single-chain antibody with a 4-1BB co-stimulatory domain carrying IL-6shRNA. After continuous *in vitro* culture for 7 days–10 days, testing was conducted in accordance with the relevant standards to ensure the function and safety of the final product, including the quantification of target CD19 CAR-T cells, bacteria, mycoplasma, endotoxins, and other potential contaminants. The patient then received a conditioning regimen of fludarabine (30 mg/m^2) and cyclophosphamide (300 mg/m^2) from Days-4 to -2 before CAR-T cell therapy. Before CAR-T cell infusion, the patient had 9.5% leukemia blast cells in the bone marrow. STR analysis decreased to 93.66%. On 8 November 2018, 7.8 × 10^6/kg of CD19 CAR-T cells were transfused on day 0. The number of CAR-T cells reached a peak on the 7th day after infusion, which expanded to 110 folds *in vivo* (Figure 2A; Table 1).

Outcome and follow-up

The patient developed high fever for 1 week and diarrhea for 5 days after CAR-T cell infusion (Figure 2B). The patient's temperature tended to be normal, and diarrhea was relieved after treatment with nonsteroidal drugs (indomethacin) and supportive care. The levels of cytokines, including plasma interleukin IL-6, IL-2, IL-10, interferon-γ, C-reactive protein (CRP), and ferritin, significantly increased with CAR-T cell expansion (Figures 2C, D). IL-6 levels peaked at 229 pg/ml (200-fold higher than the baseline) on day 7. Grade I cytokine release syndrome (CRS) was diagnosed. No hypotension, tachycardia, hypoxia, coagulopathy, or multiple organ failure was observed. GVHD did not occur. On day 30 after CAR-T cell infusion, the patient regained CHR and CMR with negative BCR-ABL. After 6 years, the patient underwent annual tests, including routine blood tests, bone marrow cytology, MRD, and quantitative detection of the BCR::ABL1 P210 fusion gene and STR. The patient remained in hematological and molecular complete remission.

Discussion

Relapse after chemotherapy is the main cause of death in patients with ALL, as well as in patients after allo-HSCT. Donor lymphocyte infusions (DLIs) and allogeneic anti-CD19 CAR-T cells from HLA-matched donors can effectively treat progressive B-cell malignancies. However, DLI and allogeneic donor-derived CAR-T cells are not available for UCBT recipients. Autologous and allogeneic CD19 CAR-T cells have achieved complete remission in previously treated relapsed/refractory B cell malignancies (10, 12–14). In our case, therapy with CAR-T cells derived from UCBT recipient-self was the only strategy for treating relapse after UCBT. When T cells were collected to generate CAR-T cells,

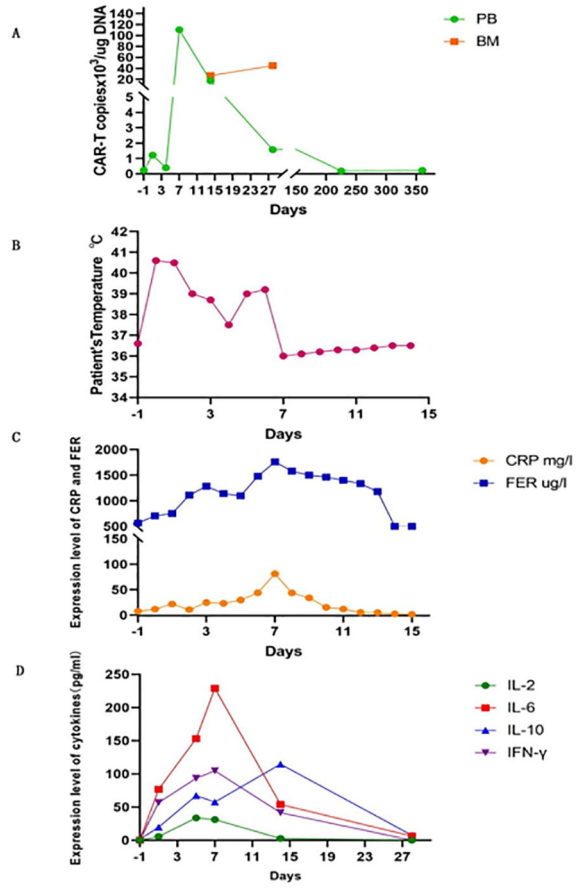

FIGURE 2
CAR-T expansion *in vivo*, patient's temperature, CRP and ferritin, serum levels of cytokines after CAR-T cell infusion. **(A)** The number of CAR-T cells expansion in PB and BM. **(B)** Patient's temperature. **(C)** Changes in CRP and ferritin. **(D)** Serum levels of cytokines. PB, peripheral blood; BM, bone marrow.

chimerism in the UCBT patient was 100%. The patient experienced CR again, with a negative MRD after CAR-T cell therapy. Our case is the first to show the feasibility, safety, and efficacy of CD19 CAR-T cells derived from a recipient of UCBT for treating relapsed Ph$^+$-ALL. This strategy is important for patients

TABLE 1 The number of CAR-T cells expansion in PB and BM.

Days post CAR-T cells infusion	Peripheral blood (copies x10^3/ug)	Bone marrow (copies/ug)
D1	1.22	/
D4	0.39	/
D7	110.63	/
D14	17.09	26.73
D28	1.58	44.87
D120	2.15	/
D225	0.19	/
D360	0.23	/

who have no DLI treatment after UCBT. This provides an alternative approach to overcome the barriers of UCBT recipients who have no better treatment choices for relapsed ALL.

The current duration of complete remission in our patient was more than 6 years after CAR-T cell infusion. CAR-T cells were still detected 12 months after infusion. Park et al. (15) found that a higher ratio of peak CAR T-cell expansion to tumor burden significantly correlated with the event-free survival and overall survival, which was a better predictor of long-term survival. In terms of the efficacy of CAR-T cell therapy, the ratio of infused CAR-T cell expansion fold to tumor load was superior to the absolute magnitude of T-cell expansion in patients receiving CAR-T cell treatment. Clinical trials have demonstrated that persistence of CAR-T cells is a key factor in the success of CD-19 CAR-T cell therapy (16). The 4-1BB co-stimulator plays the role prolonged CAR-T cell persistence. It was reported that 4-1BB based CAR-T cells in the blood can persist for a median duration of 168 days (range, 20 days–617 days) (17). In our case, the number of infused CAR-T cells was expanded to 110 folds and sustained for 12 months in the recipient. Therefore, we believe that CAR-T cell expansion folds and CAR-T cell persistence of 4-1BB co-stimulation contributed to the efficacy of CAR-T cell therapy in our case. Additionally, some studies have indicated that umbilical cord-derived CAR-T therapy exhibits favorable clinical outcomes. Xu et al. reported that 11 patients with R/R B-ALL after UCBT following CD19-targeted CAR-T therapy achieved a high remission rate and experienced mild adverse events (18). Marra et al. report that a patient with multiple relapsing Ph+ B-ALL achieved good clinical outcomes after CAR-T therapy after UCBT. The case report also confirmed the positive therapeutic effects of umbilical cord-derived CAR-T therapy (19). Notably, in our case, the patient received CAR-T therapy after UCBT and achieved long-term survival for more than 6 years, which may have contributed to the patient's sustained remission. First, at the time of peripheral blood T-cell collection, the patient's bone marrow blasts were only 7%, indicating a low tumor burden at relapse. Second, short tandem repeat (STR) analysis confirmed 100% cord blood chimerism. CD19 CAR-T cells derived from recipient T-cells after UCBT. This represents CAR-T cells derived from cord blood (20–22), which exhibit characteristics of cord blood-derived T cells. This contributes to a robust graft-versus-leukemia (GVL) effect, similar to that of fresh cord blood-derived T cells, thereby potentially enhancing the therapeutic efficacy in this clinical setting.

CRS is a common side effect of immune-mediated response to CAR-T cell therapy. In our case, the patient developed grade I CRS with fever and diarrhea according to the revised grading system (23). The cytokines detected included IL-6, IL-2, IL-10, and IFN-γ, which increased dramatically on the 7th day after CAR-T cell infusion. They coincided with CD19 CAR-T cell expansion *in vivo* and then decreased rapidly to the normal range within one month. The peaks of CRP and ferritin lagged behind the tested cytokine levels by 1 to 2 days. CRS is caused by the release of numerous cytokines from CAR-T cells and other cells including monocytes, macrophages, and dendritic cells, which generally occurs 1 to 14 days after CAR-T cell infusion and is sustainable for 1–10 days (24–27). Risk factors for CRS include tumor load, the time of CAR-T cell infusion, infection status, the amount of CAR-T cells for infusion, and the preparative regimen of CAR-T cell therapy (15, 28, 29). Patients with a low tumor burden have a markedly lower incidence of CRS and neurotoxic events (15). The patient's CRS with fever and diarrhea was grade I and was managed well. We believe that the efficacy of CAR-T cell therapy in this case might be due to the lower tumor load before CAR-T cell therapy and the infusion of an appropriate number of CAR-T cells. Furthermore, upon observing the clinical and laboratory findings in the patient, we promptly initiated supportive measures and nonsteroidal drug (indomethacin) intervention to prevent subsequent severe CRS events. Finally, compared to CD28 as a costimulatory domain, CAR-T cells with a 4-1BB costimulatory domain induce less severe CRS events (30). Based on the data presented, it is evident that the incidence of severe cytokine release syndrome (CRS) associated with CAR-T cell treatment is remarkably low.

In the present case, GVHD and neurotoxicity were not observed. Our patient exhibited 100% chimerism after undergoing UCBT. Although the infusion of CAR-T cells derived from patients post-UCBT was alloidentical transplantation (31), we believe that the CD19 CAR-T cells made from the recipient of UCBT would cause no GVHD or less GVHD, and that the transplanted grafts in UCBT recipients would not be attacked by their own CAR-T cells. The levels of acute and chronic GVHD after infusion of recipient-derived CAR-T cells were lower than those of allo-derived CAR-T cells. In this case, it is hypothesized that the recipient's tolerance to the cells facilitates avoidance of allo-rejection (32). We believe that the lack of GVHD in this patient may be due to the following reasons: First, the lower dose of CAR-T cells reduced the possibility of GVHD compared with DLI. Second, T cells from a patient after UCBT may have been tolerated by the recipient's immune system. CAR-T cell therapy has shown better clinical efficacy in patients with R/R B-ALL after UCBT. CAR-T cells of umbilical origin may facilitate rapid expansion and enhance the therapeutic effect of the treatment. Therefore, further confirmation with a larger sample size is needed to validate these findings.

Data availability statement

The original contributions presented in the study are included in the article, further inquiries can be directed to the corresponding authors.

Ethics statement

The study protocol was approved by the Ethics Committee of Union Hospital, Fujian Medical University. The studies were conducted in accordance with the local legislation and institutional requirements. The participants provided their written informed consent to participate in this study. Written informed consent was obtained from the individual(s) for the publication of any potentially identifiable images or data included in this article.

Author contributions

HL: Writing – original draft, Validation. XL: Supervision, Writing – review & editing, Formal analysis. NX: Methodology, Writing – review & editing. GH: Writing – review & editing, Methodology, Resources. NL: Writing – review & editing, Funding acquisition, Project administration, Supervision.

Funding

The author(s) declare that financial support was received for the research and/or publication of this article. This work was supported by the National Natural Science Foundation of China (82470211 to NL).

Acknowledgments

We would like to thank Dr. Na Xian for conducting experiments and making CAR-T cells. We would also like to thank Prof. Tao Chen for polishing the manuscript.

Conflict of interest

Author GH was employed by the company Fuzhou Tcelltech Biological Science and Technology Inc.

The remaining authors declare that the research was conducted in the absence of any commercial or financial relationships that could be construed as a potential conflict of interest.

Generative AI statement

The author(s) declare that no Generative AI was used in the creation of this manuscript.

Publisher's note

References

1. Iacobucci I, Mullighan CG. Genetic basis of acute lymphoblastic leukemia. *J Clin Oncol*. (2017) 35:975–83. doi: 10.1200/JCO.2016.70.7836

2. Terwilliger T, Abdul-Hay M. Acute lymphoblastic leukemia: a comprehensive review and 2017 update. *Blood Cancer J*. (2017) 7:e577. doi: 10.1038/bcj.2017.53

3. Pavletic SZ, Kumar S, Mohty M, de Lima M, Foran JM, Pasquini M, et al. NCI First International Workshop on the Biology, Prevention, and Treatment of Relapse after Allogeneic Hematopoietic Stem Cell Transplantation: report from the Committee on the Epidemiology and Natural History of Relapse following Allogeneic Cell Transplantation. *Biol Blood Marrow Transpl*. (2010) 16(7):871–90. doi: 10.1016/j.bbmt.2010.04.004

4. Spyridonidis A, Labopin M, Schmid C, Volin L, Yakoub-Agha I, Stadler M, et al. Outcomes and prognostic factors of adults with acute lymphoblastic leukemia who relapse after allogeneic hematopoietic cell transplantation. An analysis on behalf of the Acute Leukemia Working Party of EBMT. *Leukemia*. (2012) 26(6):1211–7. doi: 10.1038/leu.2011.351

5. Castagna L, Sarina B, Bramanti S, Perseghin P, Mariotti J, Morabito L. Donor lymphocyte infusion after allogeneic stem cell transplantation. *Transfus Apher Sci*. (2016) 54:345–55. doi: 10.1016/j.transci.2016.05.011

6. Yan CH, Wang Y, Wang JZ, Chen YH, Chen Y, Wang FR, et al. Minimal residual disease- and graft-vs.-host disease-guided multiple consolidation chemotherapy and donor lymphocyte infusion prevent second acute leukemia relapse after allotransplant. *J Hematol Oncol*. (2016) 9(1):87. doi: 10.1186/s13045-016-0319-5

7. Testa U, Sica S, Pelosi E, Castelli G, Leone G. CAR-T cell therapy in B-cell acute lymphoblastic leukemia. *Mediterr J Hematol Infect Dis*. (2024) 16:e2024010. doi: 10.4084/MJHID.2024.010

8. Maude SL, Frey N, Shaw PA, Aplenc R, Barrett DM, Bunin NJ, et al. Chimeric antigen receptor T cells for sustained remissions in leukemia. *N Engl J Med*. (2014) 371 (16):1507–17. doi: 10.1056/NEJMoa1407222

9. Ding ZC. The promise and challenges of chimeric antigen receptor T cells in relapsed B-cell acute lymphoblastic leukemia. *Ann Transl Med*. (2018) 6:235. doi: 10.21037/atm.2018.05.35

10. Lee DW, Kochenderfer JN, Stetler-Stevenson M, Cui YK, Delbrook C, Feldman SA, et al. T cells expressing CD19 chimeric antigen receptors for acute lymphoblastic leukaemia in children and young adults: a phase 1 dose-escalation trial. *Lancet*. (2015) 385(9967):517–28. doi: 10.1016/S0140-6736(14)61403-3

11. Luo Y, Gao L, Liu J, Yang L, Wang L, Lai X, et al. Donor-derived Anti-CD19 CAR T cells GC007g for relapsed or refractory B-cell acute lymphoblastic leukemia after allogeneic HSCT: a phase 1 trial. *EClinicalMedicine*. (2024) 67:102377. doi: 10.1016/j.eclinm.2023.102377

12. Porter DL, Levine BL, Kalos M, Bagg A, June CH. Chimeric antigen receptor-modified T cells in chronic lymphoid leukemia. *N Engl J Med*. (2011) 365:725–33. doi: 10.1056/NEJMoa1103849

13. Kochenderfer JN, Dudley ME, Carpenter RO, Kassim SH, Rose JJ, Telford WG, et al. Donor-derived CD19-targeted T cells cause regression of Malignancy persisting after allogeneic hematopoietic stem cell transplantation. *Blood*. (2013) 122(25):4129–39. doi: 10.1182/blood-2013-08-519413

14. Liu S, Deng B, Yin Z, Lin Y, An L, Liu D, et al. Combination of CD19 and CD22 CAR-T cell therapy in relapsed B-cell acute lymphoblastic leukemia after allogeneic transplantation. *Am J Hematol*. (2021) 96(6):671–9. doi: 10.1002/ajh.26160

15. Park JH, Riviere I, Gonen M, Wang X, Senechal B, Curran KJ, et al. Long-term follow-up of CD19 CAR therapy in acute lymphoblastic leukemia. *N Engl J Med*. (2018) 378(5):449–59. doi: 10.1056/NEJMoa1709919

16. Davila ML, Riviere I, Wang X, Bartido S, Park J, Curran K, et al. Efficacy and toxicity management of 19-28z CAR T cell therapy in B cell acute lymphoblastic leukemia. *Sci Transl Med*. (2014) 6(224):224ra225. doi: 10.1126/scitranslmed.3008226

17. Shah NN, Fry TJ. Mechanisms of resistance to CAR T cell therapy. *Nat Rev Clin Oncol*. (2019) 16:372–85. doi: 10.1038/s41571-019-0184-6

18. Xu Q, Xu H, Xue L, Wang M, Pan G, Zhang X, et al. CD19-targeted chimeric antigen receptor-modified T cells induce remission in patients with relapsed acute B lymphoblastic leukemia after umbilical cord blood transplantation. *Chin Med J (Engl)*. (2022) 135(1):98–100. doi: 10.1097/CM9.0000000000001491

19. Marra JD, Galli E, Giammarco S, Metafuni E, Minnella G, Fosso F, et al. CAR-T from cord blood in a patient with Ph+ acute lymphoblastic leukemia relapsing after hematopoietic stem cell transplantation. *Eur J Haematol*. (2024) 113(1):127–9. doi: 10.1111/ejh.v113.1

20. Cael B, Galaine J, Bardey I, Marton C, Fredon M, Biichle S, et al. Umbilical cord blood as a source of less differentiated T cells to produce CD123 CAR-T cells. *Cancers (Basel)*. (2022) 14(13). doi: 10.3390/cancers14133168

21. Liu DD, Hong WC, Qiu KY, Li XY, Liu Y, Zhu LW, et al. Umbilical cord blood: A promising source for allogeneic CAR-T cells. *Front Oncol*. (2022) 12:944248. doi: 10.3389/fonc.2022.944248

22. Lo Presti V, Nierkens S, Boelens JJ, van Til NP. Use of cord blood derived T-cells in cancer immunotherapy: milestones achieved and future perspectives. *Expert Rev Hematol*. (2018) 11:209–18. doi: 10.1080/17474086.2018.1431119

23. Lee DW, Gardner R, Porter DL, Louis CU, Ahmed N, Jensen M, et al. Current concepts in the diagnosis and management of cytokine release syndrome. *Blood*. (2014) 124(2):188–95. doi: 10.1182/blood-2014-05-552729

24. Yakoub-Agha I, Chabannon C, Bader P, Basak GW, Bonig H, Ciceri F, et al. Management of adults and children undergoing chimeric antigen receptor T-cell therapy: best practice recommendations of the European Society for Blood and Marrow Transplantation (EBMT) and the Joint Accreditation Committee of ISCT and EBMT (JACIE). *Haematologica*. (2020) 105(2):297–316. doi: 10.3324/haematol.2019.229781

25. Porter D, Frey N, Wood PA, Weng Y, Grupp SA. Grading of cytokine release syndrome associated with the CAR T cell therapy tisagenlecleucel. *J Hematol Oncol*. (2018) 11:35. doi: 10.1186/s13045-018-0571-y

26. Lee DW, Santomasso BD, Locke FL, Ghobadi A, Turtle CJ, Brudno JN, et al. ASTCT consensus grading for cytokine release syndrome and neurologic toxicity associated with immune effector cells. *Biol Blood Marrow Transpl*. (2019) 25(4):625–38. doi: 10.1016/j.bbmt.2018.12.758

27. Frey NV. Chimeric antigen receptor T cells for acute lymphoblastic leukemia. *Am J Hematol*. (2019) 94:S24–7. doi: 10.1002/ajh.v94.S1

28. Majzner RG, Mackall CL. Clinical lessons learned from the first leg of the CAR T cell journey. *Nat Med*. (2019) 25:1341–55. doi: 10.1038/s41591-019-0564-6

29. Hay KA, Hanafi LA, Li D, Gust J, Liles WC, Wurfel MM, et al. Kinetics and biomarkers of severe cytokine release syndrome after CD19 chimeric antigen receptor-modified T-cell therapy. *Blood*. (2017) 130(21):2295–306. doi: 10.1182/blood-2017-06-793141

30. Zhao X, Yang J, Zhang X, Lu XA, Xiong M, Zhang J, et al. Efficacy and safety of CD28- or 4-1BB-based CD19 CAR-T cells in B cell acute lymphoblastic leukemia. *Mol Ther Oncolytics*. (2020) 18:272–81. doi: 10.1016/j.omto.2020.06.016

31. Hu Y, Wang J, Wei G, Yu J, Luo Y, Shi J, et al. A retrospective comparison of allogenic and autologous chimeric antigen receptor T cell therapy targeting CD19 in patients with relapsed/refractory acute lymphoblastic leukemia. *Bone Marrow Transpl*. (2019) 54(8):1208–17. doi: 10.1038/s41409-018-0403-2

32. Smith M, Zakrzewski J, James S, Sadelain M. Posttransplant chimeric antigen receptor therapy. *Blood*. (2018) 131:1045–52. doi: 10.1182/blood-2017-08-752121

frontiers | Frontiers in Immunology

TYPE Clinical Trial
PUBLISHED 06 June 2025
DOI 10.3389/fimmu.2025.1601961

OPEN ACCESS

EDITED BY
Luigi Nespoli,
University of Insubria, Italy

REVIEWED BY
Irma Airoldi,
Department of Giannina Gaslini Institute (IRCCS), Italy
Liane Daudt,
Liane Esteves Daudt, Esteves Daudt, Liane, Federal University of Rio Grande do Sul, Brazil

*CORRESPONDENCE
Daniela Montagna
d.montagna@smatteo.pv.it;
daniela.montagna@unipv.it

†These authors contributed equally to this work and share first authorship

RECEIVED 28 March 2025
ACCEPTED 02 May 2025
PUBLISHED 06 June 2025

CITATION
Montagna D, Comoli P, Tanzi M, Montini E, Moretta A, Taurino G, Boghen S, Panigari A, Mina T, Giorgiani G, Del Fante C, Perotti C and Zecca M (2025) Phase I/II clinical trial on the safety and preliminary efficacy of donor-derived anti-leukemia cytotoxic T lymphocytes for the prevention of leukemia relapse in children given haploidentical hematopoietic stem cell transplantation: study rational and design.
Front. Immunol. 16:1601961.
doi: 10.3389/fimmu.2025.1601961

Phase I/II clinical trial on the safety and preliminary efficacy of donor-derived anti-leukemia cytotoxic T lymphocytes for the prevention of leukemia relapse in children given haploidentical hematopoietic stem cell transplantation: study rational and design

Daniela Montagna[1,2,3*†], Patrizia Comoli[1†], Matteo Tanzi[1,4], Enrica Montini[1,4], Antonia Moretta[1,4], Gloria Taurino[1,2], Stella Boghen[4], Arianna Panigari[4], Tommaso Mina[4], Giovanna Giorgiani[4], Claudia Del Fante[5], Cesare Perotti[5] and Marco Zecca[4]

[1]Cell Factory, Fondazione IRCCS Policlinico San Matteo, Pavia, Italy, [2]Pediatric Clinic, Fondazione IRCCS Policlinico San Matteo, Pavia, Italy, [3]Department of Sciences Clinic-Surgical, Diagnostic and Pediatric, University of Pavia, Pavia, Italy, [4]Pediatric Hematology/Oncology, Fondazione IRCCS Policlinico San Matteo, Pavia, Italy, [5]Immunohaematology and Transfusion Medicine Service (SIMT), Fondazione IRCCS Policlinico San Matteo, Pavia, Italy

Leuk-CTL-001 (EudraCT n. 2019-003362-41) is a Phase I/II clinical trial on the safety and preliminary efficacy of donor-derived anti-leukemia cytotoxic T lymphocytes (CTLs) for the prevention of leukemia relapse in children given haploidentical hematopoietic stem cell transplantation (HCT). The prognosis for children affected by acute leukemia and transplanted in an advanced disease stage, in the presence of measurable minimal residual disease (MRD) or with unfavorable cytogenetic abnormalities, is still poor and often less than 50%. Adoptive cell therapy based on the infusion of donor-derived CTLs able to recognize patients' leukemia blasts (LB) is a promising approach to control leukemia relapse after allogeneic HCT. We previously described a procedure for *ex vivo* generating and expanding large numbers of donor-derived anti-leukemia CTL in compliance with Good Manufacturing Practice (GMP). The analysis of all batches of anti-leukemia CTLs produced so far documented that the majority of effector cells were CD3+/CD8+ cells, with a memory/terminal activated phenotype displaying efficient capacity to lyse patients' LB and to secrete IFNγ and TNFα in response to leukemia cells. The Leuk-001 trial explores the safety of infusion of escalating doses of anti-leukemia CTLs in a cohort of high-risk relapse pediatric patients given haploidentical HCT for acute leukemia, starting within 60 days after transplantation. The safety is evaluated in terms of incidence of acute and

chronic graft versus host disease (GVHD). The secondary objective is the evaluation of efficacy defined as cumulative incidence of relapse.

Clinical Trial Registration: https://www.isrctn.com/, identifier ISRCTN13301166; https://clinicaltrials.gov/, NCT06865352.

KEYWORDS

cytotoxic T lymphocytes, haploidentical hematopoietic stem cell transplantation, adoptive cell therapy, pediatric acute leukemia, graft-versus-host-disease

Introduction

The Italian age standardized incidence rate for acute lymphoblastic leukemia (ALL) in the 0–19 age population is 36.7 cases per million (95% CI 34.2-39.3) while, for acute myeloid leukemia (AML) it is 6.8 cases per million (95% CI 5.6-8.1). These incidence rates correspond to about 400 new diagnoses of pediatric ALL and 100 new diagnoses of pediatric AML per year in Italy. Even though, currently, more than 80% of children with ALL can be cured with conventional first line chemotherapy, 15-20% of children with ALL still present with disease relapse. The majority of relapsing patients are given an HCT after second-line chemotherapy, but only 30-70% can be cured by HCT (1). A subsequent relapse is the most frequent cause of treatment failure. Considering AML, the event-free survival probability for children treated with the AIEOP-AML 2002/01 protocol was 55% for the whole study population and 53% for high-risk patients (2) and leukemia relapse represented the most common cause of treatment failure. The probability of long-term survival for children relapsing after an allogeneic HCT is low: the vast majority die due to disease progression or for the complications of therapies.

Over the last four decades, allogeneic HCT from an HLA-matched donor, either related or unrelated, has been increasingly used to treat patients affected by various malignant or non-malignant disorders, including acute leukemia. However, only 25% of patients have an HLA-identical sibling and fewer than 60% of the remaining patients can be matched with suitable HLA-compatible, unrelated donors. In the absence of an HLA-matched donor, alternative donors, such as HLA-haploidentical relatives, are being increasingly used (3).

A study by The Acute Leukemia and Pediatric Working Parties of the European Society for Blood and Marrow Transplantation (EBMT) showed that the 5-year leukemia-free survival (LFS) for children with ALL, transplanted in complete remission was about 30%, indicating that haploHCT is a useful treatment for patients in morphological remission of disease (4). In particular, in the last years, T-cell receptor (TCR)αβ/CD19 cell depletion has emerged as an effective graft manipulation strategy for preventing GVHD in patients lacking HLA–matched donor and in need of an urgent transplant (5). Despite great improvements, leukemia relapse remains the most frequent cause of transplant failure, especially in high-risk patients, and the prognosis for children affected by acute leukemia and transplanted in an advanced disease stage, in the presence of measurable MRD or with unfavorable cytogenetic abnormalities is still poor, and often less that 50%. Further intensification of pre-transplant chemotherapy and conditioning regimen would increase the incidence of treatment-related toxicity and non-relapse mortality. Thus, in the last few years, clinical research has been directed towards the early identification of patients who cannot be cured by conventional treatment and who could benefit from the use of targeted therapy therapies (6–8).

Harnessing the cytotoxicity and targeting the ability of the cellular immune system could improve the efficacy of anticancer therapy. While the use of monoclonal antibodies is now well established in clinical practice, the development of cellular therapies against cancer has been slower, largely because of the complexity of this approach. Among the different forms of cellular immunotherapy, the adoptive transfer of T lymphocytes is the most promising to overcome leukemia resistance to chemotherapy. T cell therapy for solid and hematological tumors has proved to be effective in preventing or treating cancer growth in patients with different diseases such as melanoma, lymphoma, nasopharyngeal carcinoma (9, 10). Despite these results, cancer immunotherapy still has many limitations and obstacles. Most neoplasms can develop a range of immune escape strategies resulting in failure to appropriately present tumor antigens to immunocompetent cells. Other limitations of immunotherapy based on the infusion of T cells are the suboptimal persistence of transferred cells in the patient and the necessity to define the best tumor associated antigens (TAA) for cellular therapy.

In recent years, excellent results have been achieved in the control of relapsed/refractory ALL with the infusion of T lymphocytes genetically modified to express chimeric antigen receptors (CAR) targeting B cell-associated antigens (11–13). The increase in CAR-T cell efficacy, however, has been paralleled by the potential to induce severe adverse events, including cytokine release syndrome, B cell aplasia, and other severe on-target off-tumor toxicities (14). In addition, despite encouraging data on the treatment of B cell precursor ALL, major challenges remain to be overcome to safely apply CAR-T cell therapy to patients with other leukemia subtypes (T cell precursor ALL or AML) (15–17).

The use of autologous T cells may result in disparities in efficiency or yield of the final product, due to the patient's prior treatment leading also to a manufacturing failure rate (18). This has led over the years to the development of allogeneic and/or 'off-the-shelf' CAR-Ts from healthy donors with the aim of providing a readily available therapeutic solution for patients who needed this therapy. CAR-T production using genome-editing as well as non-gene-editing technologies were evaluated. While these technologies have many advantages, they also have limitations due to associated safety risks, including inducing GVHD and rejection. At present, more extensive researches are required for the development of technologies that allow safe administration of allogeneic CAR-Ts while improving their persistence and their efficacy and maintaining a favorable safety profile (19).

The pivotal therapeutic role of immunity against acute leukemia has been revealed by the graft-versus-leukemia (GVL) effect observed following allogeneic HCT. Moreover, circulating leukemia-specific CTLs have been detected in patients with different forms of acute leukemia, and the presence of these specific T-cell responses in peripheral blood and bone marrow samples of leukemia patients has been associated with improved disease control and longer survival (20–23). This body of data suggests that allogeneic or naturally elicited leukemia reactive T cells could have an effect in preventing relapse and improving transplant outcome.

Unmanipulated donor lymphocyte infusion (DLI) is used after stem cell transplantation to treat and prevent relapse, to prevent infections and to establish full donor chimerism. However, an expected side effect of the presence of mature T cells is the potential occurrence of acute GVHD (24). Evidence has emerged that escalating DLI has achieved higher clinical response rates with lower GVHD occurrence (25). Optimization of DLI dose and schedule as well as strategies of donor T-cell manipulation may lead to the consistent ability to separate GVHD from GVL activity and improve the safety of DLI treatment. One way to manipulate donor lymphocytes to reduce GVHD is leukemia antigen stimulation, in order to increase antileukemia activity while reducing the number of alloreactive T cells by specific culture.

Somatic cell therapy with anti-leukemia CTLs may offer a new tool to prevent or treat relapse. The major advantage of immune-based therapies is the possibility to use highly selective immune effector cells directed against malignant cells, thus limiting treatment related toxicities.

Pre-clinical background

Allogeneic or autologous anti-leukemia CTL directed against minor histocompatibility antigens or the BCR/ABL neoantigen (26–29), have been successfully employed to treat relapsed leukemia in adult patients representing proof of principle for the potential efficacy of this form of T cell therapy.

During the last decade, the proponent's research unit has developed and optimized a procedure to generate donor-derived CTLs directed against pediatric acute LB, through the stimulation of peripheral blood mononuclear cells (PBMC) with IFN-dendritic cells (IFN-DC) pulsed with apoptotic LB as source of tumor antigens. CTLs generated *ex vivo* with this approach are likely to recognize a broader range of TAA, potentially reducing the risk of selecting variant leukemic subclones (30–32). Anti-leukemia CTLs include both effector and memory T-cells, suggesting the presence of lymphocytes able to exert, not only an immediate cytotoxic effector activity, but also to maintain long-term immune surveillance (33).

A major risk with the use of donor-derived anti-leukemia CTL is the subsequent development of GVHD. This risk is particularly relevant in the setting of haplo-HCT, where the donor and recipient are HLA partially-matched. In this regard it has been documented that although some anti-leukemia CTL lines showed sizeable cytotoxicity against patients' derived PHA-blasts, the vast majority displayed lower levels of alloreactivity compared with that observed against LB, especially at the lowest E:T (31, 32).

Any successful cell therapy approach strongly depends on the possibility to *in vitro* generate a product with a high level of standardization in compliance with GMP. Anti-leukemia CTL are Advanced Therapy Medical products (ATMP) and GMP guidelines ensure their quality and safety in terms of sterility, purity and potency for *in vivo* use. Since 2016, after optimizing protocols for obtaining highly specific anti-leukemia CTL, ATMP have been prepared in the Fondazione IRCCS Policlinico San Matteo's GMP facility "Cell Factory".

In a recent paper (34), we reported data obtained in 51 batches of ATMP documenting that biological QC, including cell viability, identity, phenotype and potency were in compliance with the defined cut offs. We also deeply evaluated the phenotypic and functional features of ATMP batches using biological assays, other than those necessary for batch release. By comparing the ability of each ATMP to lyse LB in the cytotoxicity assay and to secrete IFN-γ and TNF-α in response to LB, we documented that the majority of ATMPs displayed sizeable levels of cytotoxic activity against LB and high percentages of cytokine-secreting cells. No significant differences were documented in the potency of ATMP obtained after 1st and the 2nd round of rapid expansion. In few ATMP derived from different donors, unable to mount sizable levels of cytotoxic activity against patients LB, high percentages of IFN-γ and/or TNF-α-secreting cells were documented. These data suggested that anti-leukemia CTL are able to mediate anti-leukemia activity by different mechanisms and that the secretion of cytokines with anti-tumor activity can make up for low levels of direct lytic activity (34).

ATMP were also characterized for surface antigens of terminal differentiation and exhaustion, which can be an indirect sign of impaired function or persistence. The analysis of all batches of ATMP produced so far documented that the majority of cells were CD3+/CD8+ cells, with a memory/terminal activated phenotype including also measurable percentages of T central memory (TCM). Anti-leukemia CTL appear more highly differentiated than exhausted in that we also documented a low percentages of the PD1+/TIM3 population, usually associated with an exhausted phenotype. In donor/recipient pairs in which more than one batch of ATMP was produced, biological QC and additional biological assays documented that they were homogeneous in terms of surface antigens and potency (34).

Altogether these results demonstrated that the methodological approach we have optimized protocol is highly reproducible and allows the generation of large numbers of immunologically safe and functional anti-leukemia CTL with a high level of standardization. Based on their features, anti-leukemia CTLs could be a safe and efficient somatic cell therapy to prevent/treat leukemia relapse in children given haplo-HCT for high-risk acute leukemia.

Methods and analysis

Trial design

Leuk-001 is a Phase I/II, monocentric, open label, non-randomized, prospective clinical trial of donor-derived anti-leukemia CTLs in pediatric haplo-HCT recipients transplanted for ALL or AML and with a risk of leukemia relapse after haplo-HCT ≥ 50%. The outcome of treated patients will be compared with that of pediatric recipients of haplo-HCT with the same disease characteristics and prognosis, who received infusions of unmanipulated DLI. Patients will be assigned to the treatment with anti-leukemia CTLs (experimental arm) or to standard treatment with DLI (control arm) based on the availability of cryopreserved viable LB collected at the diagnosis or at relapse, necessary for the production of anti-leukemia CTLs (Figure 1). Therefore, this will be the only difference between the study population and the control population.

Study objectives

The primary objective will be safety, measured as the incidence of acute GVHD after treatment. Acute GVHD will be diagnosed and graded according to the NIH criteria. Grade II-IV acute GVHD will be expressed as cumulative incidence considering disease relapse and death in remission without GVHD as competing events. The key secondary objective will be preliminary efficacy, measured as the incidence of relapse, (REL) defined as the time from HCT to the date of disease relapse, will be calculated at 3, 6, 9, 12–18 and 24 months after HCT and expressed as cumulative incidence considering death in remission as competing event.

Patients' selection

Fifteen pediatric subjects will be enrolled in this study after obtaining informed consent. The study population will comprise any infant (1 month- 24 months), child (2–11 years) and teenager (12–18 years) affected by high-risk ALL or AML, candidate to an haplo-HCT and with an expected risk of leukemia relapse after transplantation ≥ 50% according to the available literature data. In Tables 1, 2 patients' inclusion and exclusion criteria are reported, respectively. Eligible donors are HLA haploidentical relatives, including but not limited to biological parents, siblings, or half-siblings. Matching will be determined by class I and class II DNA typing. In Table 3, donor inclusion and exclusion criteria are reported.

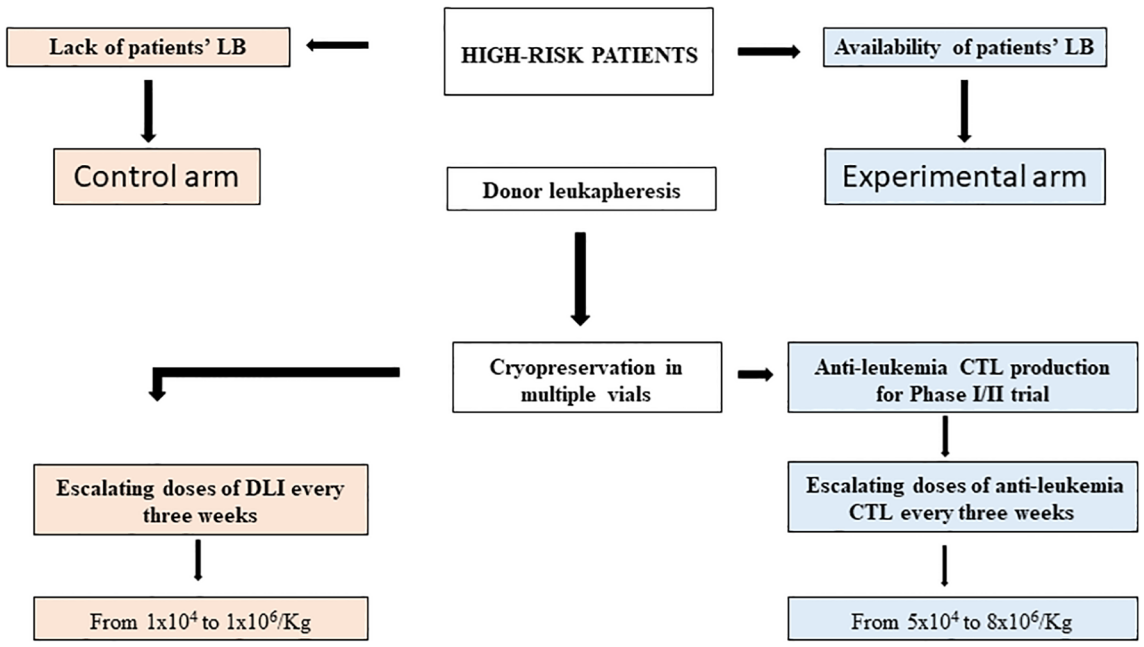

FIGURE 1
Trial design flow chart. The study population includes high-risk ALL or AML pediatric patients candidate to haplo-HCT and with an expected risk of leukemia relapse after transplantation ≥ 50%. The donor, once screened and deemed eligible, will undergo leukapheresis to obtain PBMC cryopreserved in multiple vials. Depending on the availability of cryopreserved LB patients will be assigned to the treatment with anti-leukemia CTLs (experimental arm), otherwise they will proceed to standard treatment with DLI (control arm).

10.3389/fimmu.2025.1601961

TABLE 1 Inclusion criteria for ALL and AML patients' enrolment.

ALL patients' inclusion criteria	AML patients' inclusion criteria
Age ≥ 1 month and ≤ 18 years	Age ≥ 1 month and≤ 18 years
Life expectancy > 12 weeks	Life expectancy > 12 weeks
ALL in first morphological remission but with a positive MRD≥ 1 x 10^{-3} before HCT	AML in first morphological remission and with a flow cytometry MRD at the end of induction therapy ≥ 0.1%;
ALL in second morphological remission after a high-risk relapse (patients belonging to the S3-S4 BFM risk group), independently of the level of MRD	AML in first morphological remission and with high-risk disease according to the presence of unfavorable cytogenetic or molecular aberrations
ALL in second morphological remission with any MRD positivity before HCT	AML in first morphological remission after a primary induction failure
ALL in third or subsequent morphological remission, independently of the level of MRD	AML in second morphological remission
ALL patients not in morphological remission at time of HSCT	AML in third or subsequent morphological remission
Pre-HSCT Lansky/Karnofsky score ≥ 40%.	Pre-HSCT Lansky/Karnofsky score ≥ 40%.
HIV negativity	HIV negativity

Anti-leukemia CTLs production

The production of anti-leukemia CTLs is carried out in compliance with current European GMP regulations. The active substance consists of donor T lymphocytes with cytotoxic capacity directed against LB of the patient for whom the cell therapy medicinal product is intended. Starting material consists of mononuclear cells obtained by HCT donor. The donor once screened and deemed eligible, before mobilization for hematopoietic stem cell collection, will undergo leukapheresis, following the established regulatory guidelines for monitoring and institutional standard procedures for collection. PBMC will be isolated by density gradient centrifugation and cryopreserved. Patients' LB are collected and cryopreserved at the time of leukemia diagnosis/recurrence. The methodological approach for the production of anti-leukemia CTL was optimized over time and consists in three different phases: priming, leukemia-specific stimulation and rapid antigen independent expansion. Priming is based on the use of donor DC, derived from CD14+ cells cultured four days in the presence of rGM-CSF and IFN-α2b, pulsed with irradiated (200Gy) apoptotic patients' LB as the source of leukemia associated antigens, as previously described (31) in medium supplemented with appropriate concentration of IL-7, IL-12, IL-15 and IFNα 2b (34).

As shown in Figure 2, after priming and leukemia-specific stimulation, CTLs undergo the 1st round of antigen independent expansion. After leukemia-specific stimulation, CTLs are recovered and can be cryopreserved or undergo the first round of rapid expansion. Anti-leukemia CTLs recovered after the 1st round of rapid expansion are cryopreserved in vials. Batch 1 of the ATMP can be administered to patients or, if necessary, undergo a subsequent round of rapid expansion for the production of further batches of ATMP. Following this protocol, virtually billions of CTLs can be obtained for each patient. The time necessary to expand CTL batch 1 is just over a month, while subsequent batches are produced in about two weeks. At the end of the culture, CTLs mostly contain CD3+/CD8+ T lymphocytes, and a low percentage of CD3+/CD4+ T lymphocytes. ATMP batches are subjected to microbiological and biological quality controls (QC) before product release. Microbiological QC include testing for sterility, endotoxin by LAL assay and Mycoplasma by

TABLE 2 Exclusion criteria for patients' enrolment.

Patients' exclusion criteria
Ongoing active acute GVHD or chronic GVHD due to a previous allograft
Presence of clinically active infectious disease (including positive HIV serology or viral RNA)
Severe cardiovascular disease (arrhythmias requiring chronic treatment, congestive heart failure or left ventricular ejection fraction <40%)
Liver dysfunction (AST/ALT ≥ 3 times institutional upper limit normal value – ULN- or bilirubin > 3 times ULN)
Renal dysfunction: serum creatinine > 1.5 times ULN or calculated creatinine clearance < 60 ml/min/1.73 m^2
End stage irreversible multi-system organ failure.
Other active malignancy.
Pregnant or breast feeding female patient
Lack of parents'/guardian's written informed consent for children who are minors or lack of written informed consent for patients aged 18 y

TABLE 3 Parameters for batch release.

Parameter	Methodology	Cutoff value
Sterility	Automated culture method	negative
Bacterial endotoxin content	LAL test	<0.5 EU/ml
Mycoplasma content	RT-PCR	absent
Viability	Trypan blue staining	>80%
Genotype identity	Molecular analysis	- molecular identity between ATMP, starting material and donor - absence of foreign genetic material
Phenotype	Flow cytometry analysis	T-CD3+ ≥ 75%, CD3-neg/CD56 + 0-25%, CD19+/CD20+ CD14+ ≤ 5%
Potency	Cytotoxicity by ^{51}Cr assay ¶	% specific lysis >45%

Microbiologic controls of ATMP were performed under aseptic conditions, according to European Pharmacopoeia (Eu.Ph.) guidelines. ¶ Potency was evaluated by CD3-redirected assay against P815 cell line.

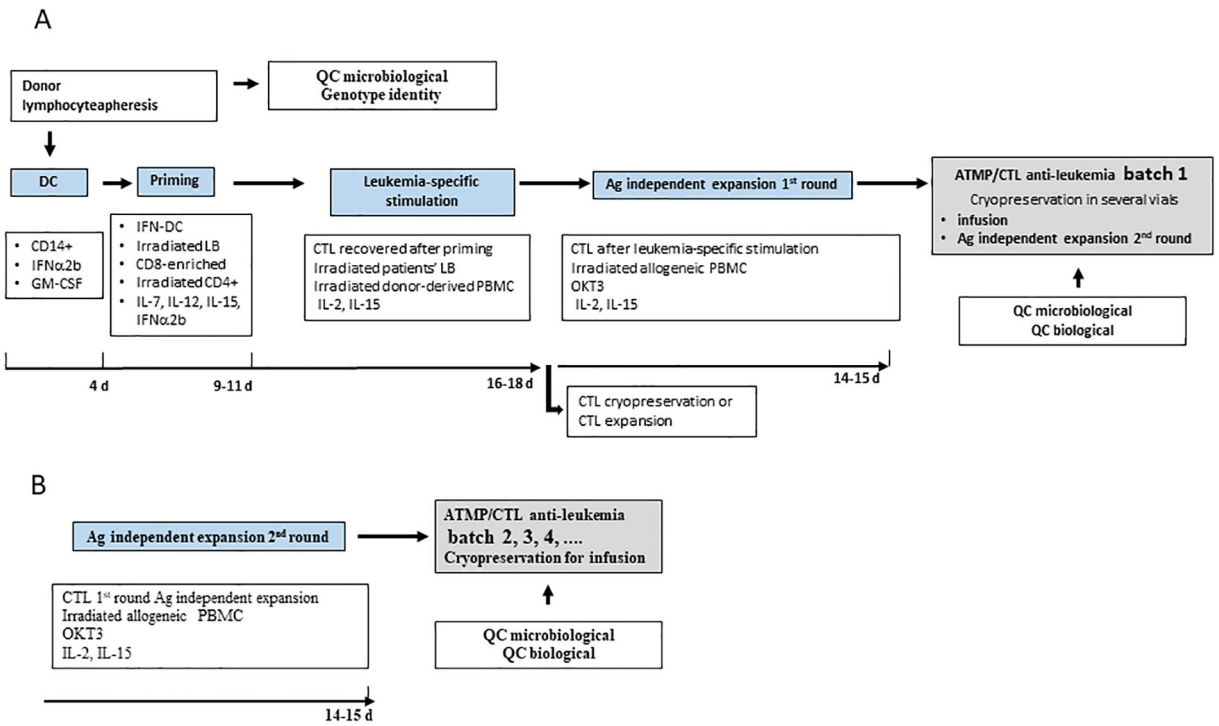

FIGURE 2
Protocol of production of anti-leukemia CTL. **(A)** After priming and leukemia-specific stimulation, CTL underwent the 1st round of antigen independent expansion. Anti-leukemia CTL recovered after the 1st round of rapid expansion were cryopreserved in several vials. Some vials represent the batch 1 of ATMP and can be infused to patients or alternately undergo a 2nd round of rapid expansion **(B)**, to produce the next batches of ATMP. Batch 1 and subsequent ones were subjected to microbiological and biological quality controls for the release of ATMP.

RT-PCR. Biological QC include: i) count of viable cells before and after cryopreservation; ii) immune phenotype characterization; iii) genotypic identity; iv) potency by means of CD3-redirected cytotoxicity test (Table 3). After confirming the stability of ATMP up to eight years after cryopreservation, biological CQ that included evaluation of phenotype and potency are performed on cryopreserved ATMPs as they represent the product that will be infused.

Study procedures

Anti-leukemia CTLs will be administered at progressively increasing doses every 3 weeks according to the following schedule: $5x10^4$/kg; $1x10^5$/kg; $5x10^5$/kg; $1x10^6$/kg; $2x10^6$/kg; $4x10^6$/kg; $8x10^6$/kg and $8x10^6$/kg. Treatment will start within 60 days after transplantation, and it will continue for the next 6–8 months, depending on the frequency of CTL infusions. In the absence of complications, the minimum number of infusions is eight. Considering the high risk of recurrence, based on the clinician's judgement, it will be possible to administer subsequent monthly CTL infusions, at the same dose used for the last administration, until month +12 from HCT.

Anti-viral prophylaxis will be administered per standard site procedures. During the treatment, the administration of corticosteroids should be avoided, unless necessary, and in this case it will be recorded.

In case of development of grade I acute GVHD, subsequent CTL administrations will be delayed by 1 week and CTLs will be given at the immediately lower dose than that which preceded the occurrence of GVHD. Subsequently, the treatment will continue with the same schedule. In case of development of acute GVHD of grade ≥ II, treatment will be stopped until complete resolution of GVHD. Subsequently, based on the clinician's judgement, anti-leukemia CTLs may be resumed, starting from the immediately lower dose than that which preceded the occurrence of GVHD, every 3 weeks with the same schedule. Subjects who develop grade I or II skin GVHD (up to Stage 3 skin GVHD without any gut or liver involvement) will be treated with topical steroids and/or other standard of care (SOC) therapies. Subjects who experience Grade III skin and/or Grade II- III non-cutaneous GVHD will be treated with standard therapy. Chronic GVHD will be treated according to SOC. In Table 4 the stopping rules are reported.

A screening evaluation that includes clinical and laboratory assessment will be performed at enrollment, prior to each CTL infusion, and at day 30, 90, 180, 360, 540 and 720 from HCT (if they do not coincide with CTL infusions). Prior to each CTL infusion, chimerism analysis and immunological follow up on peripheral blood will be performed. The immunological follow up will include evaluation of the percentages of circulating T, Treg, B and NK

10.3389/fimmu.2025.1601961

TABLE 4 Stopping rules.

Stopping rules
Development of grade III-IV acute GVHD in 2 out of the first 4 patients treated.
Development of any severe adverse event (AE) in 2 out of the first 4 patients treated.
Development of any serious adverse event (SAE) in 2 of the 4 patients of each subsequent group of 4 patients.
Incidence of grade II-IV acute GVHD ≥ 40% in the enrolled patient population.
Incidence of chronic GVHD (mild, moderate or severe) ≥ 40 in the enrolled patient population.

subsets, interferon-gamma secreting cells in response to LB stimulation *in vitro* on peripheral blood. MRD evaluation on bone marrow will be performed at baseline, at +90, +180 and +360 days after Haplo-HCT.

Toxicity evaluation

Safety assessments will consist of monitoring protocol-defined endpoints, such as acute GVHD, measurement of protocol-specified hematology, clinical chemistry variables, vital signs and other protocol-specified tests that are deemed critical to the safety evaluation of the ATMP. All adverse events (AEs) and serious adverse events (SAEs) will be recorded. AEs will be collected for 30 days following the final infusion of anti-leukemia CTLs. All SAEs will be collected until 90 days following the last anti-leukemia CTL infusion. After this period, investigators will report SAEs considered related to the study treatment.

Sample size and data analysis

The sample size is calculated based on the primary safety endpoint, using the single stage method for phase II studies proposed by Fleming (35). This method has been primarily designed to provide sufficient clinical experience to support the design of later-stage clinical development such as phase III studies. We assumed a maximum proportion P0 of patients developing GVHD, for patients receiving the standard treatment (DLI), of 40% based on our previous experience, and on data reported in the literature (H0). We consider 10% as the maximum proportion P1 of patients developing GVHD for the study treatment (CTLs) to consider the study treatment for preliminary success (H1). A sample size of 15 patients (including a dropout of 1 patient) will be able to reject H0 with a power of 80% and a type I error of 5%. If the number of responses at the end of the study is ≤ 2, H0 will be rejected; if the number of responses is > 2, H1 will be rejected. Quantitative variables will be reported as the median value and range, while categorical variables will be expressed as absolute numbers and percentage. The demographic and clinical characteristics of patients and controls will be compared using the Chi-square test or Fisher's exact test for categorical variables, while the Mann-Whitney rank sum test or the Student's t-test will be used for continuous variables as appropriate. Overall survival (OS) and event-free survival (EFS) will be calculated according to the Kaplan-Meier method, while the risk of acute and chronic GVHD, relapse and death in remission, defined as non-relapse mortality (NRM) will be calculated as cumulative incidences (CI) in order to adjust the analysis for competing risks. Comparisons between different OS and EFS probabilities will be performed using the Log-Rank test, while the Gray's test will be used to assess, in univariable analyses, differences between cumulative incidences. All results will be expressed as probabilities (%) or cumulative incidences (%) and 95% confidence interval (95% CI), at 3, 6, 9, 12, 18 and 24 months from HCT. P values < 0.05 will be considered statistically significant. Statistical analysis will be performed using NCSS [NCSS 10 Statistical Software (2015). NCSS, LLC. Kaysville, Utah, ncss.com/software/ncss.] and MP/15 (StataCorp LP, 4905 Lakeway Drive, College Station, TX 77845 USA (http://www.stata.com).

Discussion

This study explores the use of escalating doses of donor-derived anti-leukemia CTL to prevent leukemia relapse in high-risk pediatric patients affected by acute leukemia and given haplo-HCT. The primary objective is the incidence of acute GVHD compared with that observed in a control cohort of patients with identical characteristics, treated with infusion of unmanipulated DLI. Haplo-HCT based on selective depletion of TCRα/β+ and CD19+ cells has been increasingly used in pediatric patients affected by high-risk acute leukemia. By this kind of graft manipulation, T cells expressing the αβ chains of the T cell receptor, which are responsible for the development of GVHD, are removed with a high depletion efficiency (36). However, the almost complete elimination of T cells on the graft increases the risk of infections and relapse. Infusion of donor-derived mature T cells represents a way to overcome these complications. Over the years, several strategies of donor-T cell manipulation prior transfer in patients have been proposed to improve the outcome of patients without the emergence of acute and chronic GVHD that represent the most common complications after DLI. Results of clinical trials documented that the transfer of selective populations of mature T cells may improve the recovery of pathogen-specific immunity but there are no significant data regarding the incidence of relapse (37, 38).

Anti-leukemia CTLs obtained by stimulation with patients' LB are specific for each individual blast signature, and, due to their physiological recognition and effector mechanism through their natural T cell receptor, exert leukemia-specific killing with less severe adverse reactions than CAR-T cells. In addition, their potential to recognize multiple leukemia-associated antigens present on the blast surface should make them less susceptible to immune evasion strategies developed by leukemic cells. Additionally, the risk of GVHD should be reduced by the culture procedure, which decreases the number of alloreactive T cells. For these reasons, the use of these T cells after HCT in a highly

personalized approach may be a safer and more effective option than unmanipulated DLI to prevent leukemia relapse after HCT. To support this hypothesis, in a pioneer study performed in patients treated on a compassionate basis, we documented that the infusion of large numbers of anti-leukemia CTL is safe, as no patient experienced acute or chronic GVHD or severe immune adverse reactions, and may contribute to the restoration of CR in a proportion of patients relapsing after the allograft. In case of overt clinical relapse, prior reduction of the tumor burden may facilitate the anti-leukemia effect displayed by CTLs (39).

Overall, the results of this clinical study may open the way to a new approach, different from CAR-T cell therapy, for the management of high-risk patients given haplo-HCT. Overall, analysis of the features of ATMP produced so far documented that there is a certain degree of homogeneity in terms of potency and surface markers among ATMP batches in different donors and among batches produced from the same donor. Batches from different donors could show variability in lytic capacity always within the acceptable release criteria range. The evaluation of immunological properties of the infused anti-leukemia CTL and clinical follow up of treated patients could allow a better understanding of how the functional and phenotypical CTL characteristics may affect patients' outcome.

Data availability statement

The original contributions presented in the study are included in the article/supplementary material. Further inquiries can be directed to the corresponding author.

Ethics statement

The studies involving humans were approved by Comitato Etico Pavia/Fondazione IRCCS Pol san Matteo, Pavia. The studies were conducted in accordance with the local legislation and institutional requirements. Written informed consent for participation in this study was provided by the participants' legal guardians/next of kin.

Author contributions

DM: Data curation, Formal Analysis, Funding acquisition, Conceptualization, Writing – review & editing, Writing – original draft. PC: Funding acquisition, Writing – review & editing, Writing – original draft, Formal Analysis, Conceptualization, Data curation. MT: Methodology, Writing – original draft, Data curation, Funding acquisition. EM: Methodology, Writing – original draft, Data curation. AM: Data curation, Writing – original draft. GT: Writing – original draft, Methodology. SB: Writing – original draft, Data curation. AP: Data curation, Writing – original draft. TM: Data curation, Writing – original draft. GG: Investigation, Supervision, Writing – original draft. CD: Methodology, Writing – original draft. CP: Data curation, Methodology, Supervision, Writing – original draft. MZ: Investigation, Writing – review & editing, Funding acquisition, Supervision, Writing – original draft, Conceptualization, Data curation, Formal Analysis.

Funding

The author(s) declare that financial support was received for the research and/or publication of this article. This work was partly supported by the Italian Ministry of Health, PNRR-POC-2023-12377847 to PC, Ricerca Corrente Fondazione IRCCS Policlinico San Matteo, (08059819 to DM, 08072621 to MT, 08045823 to MZ, 08069119 to PC).

Conflict of interest

The authors declare that the research was conducted in the absence of any commercial or financial relationships that could be construed as a potential conflict of interest.

Generative AI statement

The author(s) declare that no Generative AI was used in the creation of this manuscript.

Publisher's note

References

1. Locatelli F, Schrappe M, Bernardo ME, Rutella S. How I treat relapsed childhood acute lymphoblastic leukemia. *Blood*. (2012) 120:2807–16. doi: 10.1182/blood-2012-02-265884

2. Pession A, Masetti R, Rizzari C, Putti MC, Casale F, Fagioli F, et al. Results of the AIEOP AML 2002/01 multicenter prospective trial for the treatment of children with acute myeloid leukemia. *Blood*. (2013) 122:170–8. doi: 10.1182/blood-2013-03-491621

3. Passweg JR, Baldomero H, Bader P, Basak GW, Bonini C, Duarte R, et al. Is the use of unrelated donor transplantation leveling off in Europe? The 2016 European Society for Blood and Marrow Transplant activity survey report. *Bone Marrow Transplant*. (2018) 53:1139–48. doi: 10.1038/s41409-018-0153-1

4. Klingebiel T, Cornish J, Labopin M, Locatelli F, Darbyshire P, Handgretinger R, et al. Results and factors influencing outcome after fully haploidentical hematopoietic

stem cell transplantation in children with very high-risk acute lymphoblastic leukemia: impact of center size: an analysis on behalf of the Acute Leukemia and Pediatric Disease Working Parties of the European Blood and Marrow Transplant group. *Blood*. (2010) 115:3437–46. doi: 10.1182/blood-2009-03-207001

5. Bertaina A, Zecca M, Buldini B, Sacchi N, Algeri M, Saglio F, et al. Unrelated donor vs HLA-haploidentical α/β T-cell– and B-cell–depleted HSCT in children with acute leukemia. *Blood*. (2018) 132:2594–607. doi: 10.1182/blood-2018-07-861575

6. Pre- and post-transplant minimal residual disease predicts relapse occurrence in children with acute lymphoblastic leukaemia. Available online at: https://onlinelibrary.wiley.com/doi/epdf/10.1111/bjh.15086 (Accessed March 10, 2025).

7. Locatelli F, Masetti R, Rondelli R, Zecca M, Fagioli F, Rovelli A, et al. Outcome of children with high-risk acute myeloid leukemia given autologous or allogeneic hematopoietic cell transplantation in the aieop AML-2002/01 study. *Bone Marrow Transplant*. (2015) 50:181–8. doi: 10.1038/bmt.2014.246

8. Buldini B, Rizzati F, Masetti R, Fagioli F, Menna G, Micalizzi C, et al. Prognostic significance of flow-cytometry evaluation of minimal residual disease in children with acute myeloid leukaemia treated according to the AIEOP-AML 2002/01 study protocol. *Br J Haematology*. (2017) 177:116–26. doi: 10.1111/bjh.14523

9. Comoli P, Pedrazzoli P, Maccario R, Basso S, Carminati O, Labirio M, et al. Cell therapy of stage IV nasopharyngeal carcinoma with autologous Epstein-Barr virus–targeted cytotoxic T lymphocytes. *JCO*. (2005) 23:8942–9. doi: 10.1200/JCO.2005.02.6195

10. Restifo NP, Dudley ME, Rosenberg SA. Adoptive immunotherapy for cancer: harnessing the T cell response. *Nat Rev Immunol*. (2012) 12:269–81. doi: 10.1038/nri3191

11. Maude SL, Laetsch TW, Buechner J, Rives S, Boyer M, Bittencourt H, et al. Tisagenlecleucel in children and young adults with B-cell lymphoblastic leukemia. *N Engl J Med*. (2018) 378:439–48. doi: 10.1056/NEJMoa1709866

12. Maude S, Barrett DM. Current status of chimeric antigen receptor therapy for haematological Malignancies. *Br J Haematology*. (2016) 172:11–22. doi: 10.1111/bjh.13792

13. Martino M, Alati C, Canale FA, Musuraca G, Martinelli G, Cerchione C. A review of clinical outcomes of CAR T-cell therapies for B-acute lymphoblastic leukemia. *Int J Mol Sci*. (2021) 22:2150. doi: 10.3390/ijms22042150

14. Heslop HE. Safer CARS. *Mol Ther*. (2010) 18:661–2. doi: 10.1038/mt.2010.42

15. Fan M, Li M, Gao L, Geng S, Wang J, Wang Y, et al. Chimeric antigen receptors for adoptive T cell therapy in acute myeloid leukemia. *J Hematol Oncol*. (2017) 10:151. doi: 10.1186/s13045-017-0519-7

16. Kenderian S, Ruella M, Shestova O, Klichinsky M, Aikawa V, Morrissette J, et al. CD33-specific chimeric antigen receptor T cells exhibit potent preclinical activity against human acute myeloid leukemia. *Leukemia*. (2015) 29:1637–47. doi: 10.1038/leu.2015.52

17. Casucci M, Nicolis di Robilant B, Falcone L, Camisa B, Norelli M, Genovese P, et al. CD44v6-targeted T cells mediate potent antitumor effects against acute myeloid leukemia and multiple myeloma. *Blood*. (2013) 122:3461–72. doi: 10.1182/blood-2013-04-493361

18. Martinez-Cibrian N, Español-Rego M, Pascal M, Delgado J, Ortiz-Maldonado V. Practical aspects of chimeric antigen receptor T-cell administration: From commercial to point-of-care manufacturing. *Front Immunol*. (2022) 13:1005457. doi: 10.3389/fimmu.2022.1005457

19. Lonez C, Breman E. Allogeneic CAR-T therapy technologies: has the promise been met? *Cells*. (2024) 13:146. doi: 10.3390/cells13020146

20. Rezvani K, Yong ASM, Savani BN, Mielke S, Keyvanfar K, Gostick E, et al. Graft-versus-leukemia effects associated with detectable Wilms tumor-1–specific T lymphocytes after allogeneic stem-cell transplantation for acute lymphoblastic leukemia. *Blood*. (2007) 110:1924–32. doi: 10.1182/blood-2007-03-076844

21. Greiner J, Ono Y, Hofmann S, Schmitt A, Mehring E, Götz M, et al. Mutated regions of nucleophosmin 1 elicit both CD4+ and CD8+ T-cell responses in patients with acute myeloid leukemia. *Blood*. (2012) 120:1282–9. doi: 10.1182/blood-2011-11-394395

22. Hofmann S, Götz M, Schneider V, Guillaume P, Bunjes D, Döhner H, et al. Donor lymphocyte infusion induces polyspecific CD8(+) T-cell responses with concurrent molecular remission in acute myeloid leukemia with NPM1 mutation. *J Clin Oncol*. (2013) 31:e44–47. doi: 10.1200/JCO.2011.41.1116

23. Riva G, Luppi M, Barozzi P, Quadrelli C, Basso S, Vallerini D, et al. Emergence of BCR-ABL–specific cytotoxic T cells in the bone marrow of patients with Ph+ acute lymphoblastic leukemia during long-term imatinib mesylate treatment. *Blood*. (2010) 115:1512–8. doi: 10.1182/blood-2009-06-230391

24. Klingebiel T, Handgretinger R, Lang P, Bader P, Niethammer D. Haploidentical transplantation for acute lymphoblastic leukemia in childhood. *Blood Rev*. (2004) 18:181–92. doi: 10.1016/S0268-960X(03)00063-8

25. Dazzi F, Szydlo RM, Craddock C, Cross NCP, Kaeda J, Chase A, et al. Comparison of single-dose and escalating-dose regimens of donor lymphocyte infusion for relapse after allografting for chronic myeloid leukemia. *Blood*. (2000) 95:67–71. doi: 10.1182/blood.V95.1.67

26. Warren EH, Fujii N, Akatsuka Y, Chaney CN, Mito JK, Loeb KR, et al. Therapy of relapsed leukemia after allogeneic hematopoietic cell transplantation with T cells specific for minor histocompatibility antigens. *Blood*. (2010) 115:3869–78. doi: 10.1182/blood-2009-10-248997

27. Comoli P, Basso S, Riva G, Barozzi P, Guido I, Gurrado A, et al. BCR-ABL–specific T-cell therapy in Ph+ ALL patients on tyrosine-kinase inhibitors. *Blood*. (2017) 129:582–6. doi: 10.1182/blood-2016-07-731091

28. Falkenburg JH, Wafelman AR, Joosten P, Smit WM, van Bergen CA, Bongaerts R, et al. Complete remission of accelerated phase chronic myeloid leukemia by treatment with leukemia-reactive cytotoxic T lymphocytes. *Blood*. (1999) 94:1201–8. doi: 10.1182/blood.V94.4.1201

29. Marijt WAE, Heemskerk MHM, Kloosterboer FM, Goulmy E, Kester MGD, van der Hoorn MAWG, et al. Hematopoiesis-restricted minor histocompatibility antigens HA-1- or HA-2-specific T cells can induce complete remissions of relapsed leukemia. *Proc Natl Acad Sci U S A*. (2003) 100:2742–7. doi: 10.1073/pnas.0530192100

30. Montagna D, Daudt L, Locatelli F, Montini E, Turin I, Lisini D, et al. Single-cell cloning of human, donor-derived antileukemia T-cell lines for *in vitro* separation of graft-versus-leukemia effect from graft-versus-host reaction. *Cancer Res*. (2006) 66:7310–6. doi: 10.1158/0008-5472.CAN-06-0591

31. Montagna D, Maccario R, Locatelli F, Rosti V, Yang Y, Farness P, et al. Ex vivo priming for long-term maintenance of antileukemia human cytotoxic T cells suggests a general procedure for adoptive immunotherapy. *Blood*. (2001) 98:3359–66. doi: 10.1182/blood.V98.12.3359

32. Montagna D, Maccario R, Montini E, Tonelli R, Lisini D, Pagani S, et al. Generation and ex vivo expansion of cytotoxic T lymphocytes directed toward different types of leukemia or myelodysplastic cells using both HLA-matched and partially matched donors. *Exp Hematol*. (2003) 31:1031–8. doi: 10.1016/S0301-472X(03)00230-3

33. Daudt L, Maccario R, Locatelli F, Turin I, Silla L, Montini E, et al. Interleukin-15 favors the expansion of central memory CD8+ T cells in ex vivo generated, antileukemia human cytotoxic T lymphocyte lines. *J Immunotherapy*. (2008) 31:385. doi: 10.1097/CJI.0b013e31816b1092

34. Tanzi M, Montini E, Rumolo A, Moretta A, Comoli P, Acquafredda G, et al. Production of donor-derived cytotoxic T lymphocytes with potent anti-leukemia activity for adoptive immunotherapy in high-risk pediatric patients given haploidentical hematopoietic stem cell transplantation. *Cytotherapy*. (2024) 26:878–89. doi: 10.1016/j.jcyt.2024.04.005

35. Fleming TR. One-sample multiple testing procedure for phase II clinical trials. *Biometrics*. (1982) 38:143–51. doi: 10.2307/2530297

36. Merli P, Algeri M, Galaverna F, Bertaina V, Lucarelli B, Boccieri E, et al. TCRαβ/CD19 cell–depleted HLA-haploidentical transplantation to treat pediatric acute leukemia: updated final analysis. *Blood*. (2024) 143:279–89. doi: 10.1182/blood.2023021336

37. Dunaikina M, Zhekhovtsova Z, Shelikhova L, Glushkova S, Nikolaev R, Blagov S, et al. Safety and efficacy of the low-dose memory (CD45RA-depleted) donor lymphocyte infusion in recipients of αβ T cell-depleted haploidentical grafts: results of a prospective randomized trial in high-risk childhood leukemia. *Bone Marrow Transplant*. (2021) 56:1614–24. doi: 10.1038/s41409-021-01232-x

38. Cheuk DKL, Lee PPW, Chan WYK, Chan GCF, So CC, Leung WH. Novel CD62L depleted donor lymphocyte infusion with T-cell receptor alpha-beta depleted haploidentical hematopoietic stem cell transplantation in children. *Transplant Immunol*. (2025) 89:102176. doi: 10.1016/j.trim.2025.102176

39. Montagna D, Maccario R, Montini E, Turin I, Lisini D, Caliogna L, et al. Anti-leukaemia CTL infusion for treatment of leukaemia relapse in children given allogeneic haematopoietic stem cell transplantation. *Bone Marrow Transplant*. (2007) 39:S54–5.

frontiers | Frontiers in Immunology

TYPE Original Research
PUBLISHED 12 June 2025
DOI 10.3389/fimmu.2025.1605716

OPEN ACCESS

EDITED BY
Rita Maccario,
San Matteo Hospital Foundation (IRCCS), Italy

REVIEWED BY
Javier Carbone,
Gregorio Marañón Hospital, Spain
Daniele Lilleri,
San Matteo Hospital Foundation (IRCCS), Italy

*CORRESPONDENCE
Ricardo Cuesta-Martín de la Cámara
ricardocuestamartin@gmail.com

†These authors have contributed equally to this work and share last authorship

RECEIVED 03 April 2025
ACCEPTED 22 May 2025
PUBLISHED 12 June 2025

CITATION
Cuesta-Martín de la Cámara R, Miguel-Berenguel L, Cámara C, Losantos-García I, Frauca-Remacha E, Hierro-Llanillo L, Muñoz-Bartolo G, Lledín-Barbacho MD, Martínez-Feito A, López-Granados E and Sánchez-Zapardiel E (2025) Immune monitoring and risk of infection in pediatric liver transplantation: a prospective study.
Front. Immunol. 16:1605716.
doi: 10.3389/fimmu.2025.1605716

Immune monitoring and risk of infection in pediatric liver transplantation: a prospective study

Ricardo Cuesta-Martín de la Cámara[1,2,3]*, Laura Miguel-Berenguel[1,3], Carmen Cámara[1,2], Itsaso Losantos-García[4], Esteban Frauca-Remacha[5,6,7], Loreto Hierro-Llanillo[5,6,7], Gema Muñoz-Bartolo[5,6,7], María Dolores Lledín-Barbacho[5,6,7], Ana Martínez-Feito[1], Eduardo López-Granados[1,2,7,8†] and Elena Sánchez-Zapardiel[1,2,7†]

[1]Clinical Immunology Department, University Hospital La Paz, Madrid, Spain, [2]Lymphocyte Pathophysiology in Immunodeficiencies Group, La Paz Institute for Health Research (IdiPAZ), Madrid, Spain, [3]Medicine and Surgery Department, PhD School, Autonomous University of Madrid, Madrid, Spain, [4]Biostatistics Platform, La Paz Institute for Health Research (IdiPAZ), Madrid, Spain, [5]Paediatric Hepatology Department, University Hospital La Paz, Madrid, Spain, [6]European Reference Network (ERN) RARE LIVER, Madrid, Spain, [7]European Reference Network (ERN) TransplantChild, Madrid, Spain, [8]Centre for Biomedical Network Research on Rare Diseases (CIBERER U767), Madrid, Spain

Background: Immune monitoring has been proposed to optimize immunosuppressive therapy in liver recipients. This study aims to describe immunological changes following liver transplantation in pediatric recipients and to identify immune markers associated with post-transplant complications.

Methods: The immunological status of 95 pediatric liver recipients was prospectively assessed before transplantation and at 1, 3, 6, 9 and 12 months post-transplantation. Serum immunoglobulins (Ig) were measured by nephelometry and immunophenotype was evaluated by flow cytometry. T, B and NK lymphocyte counts were adjusted for age using standard reference ranges.

Results: Graft rejection, post-transplant lymphoproliferative disorder and autoimmune hepatitis was diagnosed in 6%, 2% and 0% patients, respectively. Early infections affected 43% patients, while late infections occurred in 17%, 24%, 10% and 9% recipients at each follow-up interval. Baseline immune dysregulation primarily involved the cellular compartment, with 78% recipients showing lymphopenia. Lymphocyte subpopulation scores improved following liver transplantation, with $CD4^+$ score normalizing by month 1 and $CD8^+$, $CD19^+$ and NK scores by month 6. First-month IgG hypogammaglobulinemia, observed in 20% recipients, resolved completely at month 12. First-month T-cell lymphopenia ($CD3^+$ hazard ratio [HR] 2.48, p=0.005; $CD8^+$ HR 2.38, p=0.008) and hypogammaglobulinemia (IgG HR 2.18, p=0.036; IgA HR 2.40, p=0.011; IgM HR 2.61, p=0.006) were associated with higher risk of late infections. In multivariate analysis, only $CD3^+$ T-cell lymphopenia remained a significant predictor (HR 2.13, p=0.030).

Conclusions: Baseline immune dysregulation resolved within the first months post-transplantation. Early infections were unrelated to immune markers, while late infections were associated with $CD3^+$ T-cell lymphopenia and hypogammaglobulinemia.

KEYWORDS

liver transplantation, humoral immunity, cellular immunity, immune monitoring, flow cytometry

1 Introduction

Liver transplantation (LT) remains the most effective treatment for end-stage liver disease (1). Advances in immunosuppressive therapies and surgical techniques have improved survival rates, both in adults (72-73%) (2, 3) and children (73-94%) (4, 5). However, the precise tailoring of immunosuppressive treatments for each recipient remains challenging. Striking the optimal balance between minimizing the risk of rejection and avoiding complications related to immunosuppressive drugs remains crucial (6). Among these complications, infections are the leading cause of mortality in pediatric LT recipients (4.1%) (7).

Currently, clinical practice relies primarily on pharmacokinetics to estimate immunosuppression, but this approach is often insufficient in pediatric LT (8). New strategies, including pharmacogenomics, immune biomarkers, cellular therapy, tolerance induction and alternative immunosuppressants, show promise for managing narrow therapeutic range drugs (9). Hence, immune monitoring has been proposed as a valuable tool to predict immunological and infectious complications after LT (10).

In LT humoral immune responses are monitored by the presence of donor-specific antibodies, which are often a contraindication for immunosuppression weaning (11). However, there are no standardized techniques to measure cellular responses against infections and/or malignancies. Specific T-cell responses have been proposed as biomarkers for predicting post-transplant lymphoproliferative disorder (PTLD) (12). Our previous study evaluated this approach in the pediatric LT setting, to identify patients with inadequate control of Epstein-Barr virus (EBV) infection (13).

In recent years, new follow-up strategies combining both humoral and cellular immunity in LT have been explored (14–16). Fukui et al. studied 82 adult liver recipients, finding that low serum complement 3 (C3) levels before and one month after transplantation predicted 90-day mortality (14). Previously, Iovino et al. found that liver recipients who develop infections had lower immunoglobulin G (IgG) levels at day 3 post-transplantation and higher CD64 monocyte counts at day 7 (15). Similarly, Carbone et al. had observed that liver recipients at higher infection risk had baseline hypocomplementemia C3 and hipergammablobulinemia IgG, but showed reduced IgG levels by day 7 post-transplantation (16).

While those studies focused on adults, research on immune changes in pediatric LT is limited (8), as studying immunity in children is challenging due to age-related effects on T- and B-cell number and function, influencing their susceptibility to infections and other complications (17). However, epidemiological observations (18) suggest that children exhibit more favorable outcomes than adults when confronted with viruses like EBV and Severe Acute Respiratory Syndrome Coronavirus 2, likely due to their robust innate immune responses, characterized by more active natural killer (NK) and NKT cells, as well as increased regulatory T cells (Tregs).

Given these differences, it is crucial to translate this understanding into the context of immunosuppression in pediatric LT. This prospective study aims to define humoral and cellular immunity changes before LT and up to one year after the procedure in a cohort of pediatric recipients, considering age-related variations. Additionally, we seek to identify immune markers associated with the risk of clinically relevant infections, autoimmunity, PTLD and rejection events.

2 Methods

2.1 Patients and study design

Our prospective study included 106 pediatric patients from University Hospital La Paz, who received a liver graft between January 2019 and December 2023. All patients gave informed consent, approved by the ethics committee of our institution (reference PI-4000). Eleven patients were withdrawn from the study (Figure 1), resulting in a final cohort of 95 patients. Transplant indication was categorized in five groups (Table 1), according to Díaz Fernandez et al. (19).

Patients were monitored for 1 year. Follow-up periods included a baseline study just before transplantation (PreTx) and five studies post-transplantation at 1, 3, 6, 9 and 12 months after the procedure (1M, 3M, 6M, 9M and 12M). Demographic and clinically relevant information was collected (Table 1). Immune status was assessed at

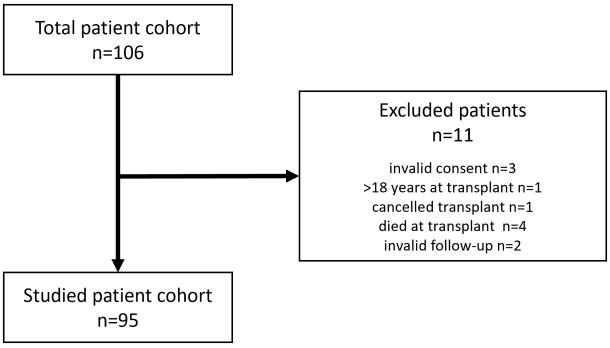

FIGURE 1
Flowchart for the inclusion of the pediatric liver transplanted patient cohort (n=95).

each timepoint. We considered clinically relevant infections, rejection, liver autoimmunity and PTLD as primary outcomes.

The standard induction regimen consisted of basiliximab administered on days 0 and 4 post-transplantation, combined with tacrolimus and corticosteroids. Maintenance immunosuppression mainly consisted of tacrolimus and corticosteroids. In selected cases experiencing rejection episodes, mycophenolate mofetil was added to the regimen.

Antimicrobial prophylaxis included trimethoprim-sulfamethoxazole for Pneumocystis jirovecii, administered for two years post-transplantation, and either ganciclovir or valganciclovir for Cytomegalovirus, prescribed for six months post-transplantation regardless of donor/recipient serostatus.

Infectious events were categorized according to Van Delden et al. (20), and their relevance was defined as proven bacterial, probable/proven fungal and probable/proven viral infections, as well as viral syndromes. Early infections were defined as those

TABLE 1 Epidemiologic and clinical features in a cohort of pediatric liver recipients, further categorized as early/late infected and non-infected patients.

Characteristics	Total (n=95)	Early infection		p-value	Late infection		p-value
		No (n=54)	Yes (n=41)		No (n=56)	Yes (n=39)	
Sex, n (%)				0.540			1.000
Male	50 (53)	30 (59)	20 (49)		29 (52)	21 (54)	
Female	45 (47)	24 (41)	21 (51)		27 (48)	18 (46)	
Age at transplantation, months (IQR)	16 (7-88)	60 (13-151)	13 (8-36)	0.001	60 (17-120)	14 (10-24)	<0.001
Type of donor, n (%)				0.001			0.004
Deceased donor - split graft	39 (41)	14 (24)	25 (61)		17 (30)	22 (56)	
Deceased donor - reduced graft	23 (24)	13 (24)	10 (24)		17 (30)	6 (15)	
Deceased donor - whole graft	22 (23)	19 (17)	3 (7)		18 (32)	4 (10)	
Living donor	11 (12)	8 (15)	3 (7)		4 (7)	7 (18)	
ABO compatibility, n (%)				0.233			0.696
Compatible	88 (93)	52 (96)	36 (88)		51 (91)	37 (95)	
Incompatible	7 (7)	2 (4)	5 (12)		5 (9)	2 (5)	
Indication for transplantation, n (%)				0.489			0.179
Cholestasis/biliary atresia	60 (63)	33 (61)	27 (66)		32 (57)	28 (71)	
Metabolic diseases	12 (13)	6 (11)	6 (15)		9 (16)	3 (8)	
Liver tumours	11 (12)	9 (17)	2 (5)		9 (16)	2 (5)	
Cirrhosis (other)	8 (8)	4 (7)	4 (10)		5 (9)	3 (8)	
Severe acute liver failure	4 (4)	2 (4)	2 (5)		1 (2)	3 (8)	
Type of transplantation, n (%)				0.231			1.000
Hepatic	89 (94)	49 (81)	40 (98)		52 (93)	37 (95)	
Combined	6 (6)	5 (9)	1 (2)		4 (7)	2 (5)	
Transplant number, n (%)				0.727			0.733
First	86 (91)	48 (89)	38 (93)		50 (89)	36 (92)	

(Continued)

10.3389/fimmu.2025.1605716

TABLE 1 Continued

Characteristics	Total (n=95)	Early infection		p-value	Late infection		p-value
		No (n=54)	Yes (n=41)		No (n=56)	Yes (n=39)	
Second	9 (9)	6 (11)	3 (7)		6 (11)	3 (8)	
Induction treatment, n (%)				0.504			0.066
TAC+CE+BSX	92 (97)	51 (94)	41 (100)		56 (100)	36 (92)	
TAC+CE+BSX+MMF	2 (2)	2 (4)	0 (0)		0 (0)	2 (5)	
TAC+CE+BSX+QT	1 (1)	1 (2)	0 (0)		0 (0)	1 (3)	
Maintenance treatment at 1M, n (%)				N/A			0.938
TAC+CE	76 (80)	N/A	N/A		44 (78)	32 (82)	
TAC+CE+BSX+MMF	16 (17)				10 (18)	6 (15)	
TAC+CE+BSX+CTX	2 (2)				1 (2)	1 (3)	
No immunosuppression	1 (1)				1 (2)	0 (0)	
Tacrolimus blood levels at 1M, ng/mL (IQR)	10 (8 - 11)	N/A	N/A	N/A	9 (7-11)	10 (8-12)	0.264
Prophylaxis treatment at 1M, n (%)				N/A			0.890
TMP-SMX+VGCV	85 (90)	N/A	N/A		50 (89)	35 (90)	
TMP-SMX+VGCV+Others	7 (7)				4 (7)	3 (8)	
TMP-SMX+ACV+Others	1 (1)				1 (2)	0 (0)	
TMP+VGCV	1 (1)				0 (0)	1 (2)	
No prophylaxis	1 (1)				1 (2)	0 (0)	
EBV-serology pre-transplantation, n (%)				0.559			0.309
Positive	48 (51)	25 (46)	23 (56)		26 (46)	22 (56)	
Negative	40 (42)	24 (44)	16 (39)		27 (48)	13 (33)	
Unknown	7 (7)	5 (9)	2 (5)		3 (5)	4 (10)	
CMV-serology pre-transplantation, n (%)				0.300			0.980
Positive	55 (58)	35 (65)	20 (49)		31 (55)	24 (62)	
Negative	35 (37)	17 (31)	18 (44)		22 (39)	13 (33)	
Unknown	5 (5)	2 (4)	3 (7)		3 (5)	2 (5)	

1M, 1 month post-transplantation; ACV, acyclovir; BSX, Basiliximab, CE, corticosteroids; CMV, Cytomegalovirus; EBV, Epstein-Barr virus; IQR, interquartile range; MMF, mycophenolate mofetil; N/A, not applicable; CTX, chemotherapy, SMX, sulfamethoxazole; TAC, tacrolimus; TMP, trimethoprim; VGCV, valganciclovir.

occurring within the first month post-transplantation, while infections occurring thereafter were classified as late infections. Autoimmune hepatitis (AIH) was defined by a positive test result for any of the following antibodies: anti-mitochondrial M2, anti-filamentous-actin (F-actin), anti-Liver Cytosol Antigen Type 1 or anti-Liver-Kidney Microsomal antibodies, along with meeting clinical criteria. PTLD diagnosis was based on histopathologic criteria. The histopathological diagnosis of acute allograft rejection was determined based on the Banff criteria (21).

2.2 Immune status assessment

Cellular immune status was evaluated by multiparametric flow cytometry. Briefly, 75µL of whole blood was stained with various monoclonal antibody combinations, using different panels over time due to supplier changes (Supplementary Table S1). Comparative analyses were conducted to ensure that the percentages remained consistent across all panels (data not shown). Cell acquisition was made on a BD FACSCanto™ or a DxFLEX flow cytometer. The resulting data were analyzed by FACSDiva™ (BD, USA) or Kaluza (Beckman Coulter, USA) software.

Immunophenotype of T lymphocytes ($CD3^+$, further classified as $CD4^+$ and $CD8^+$), B lymphocytes ($CD19^+$), NK lymphocytes ($CD3^-CD16^+CD56^+$) and NKT cells ($CD3^+CD16^+CD56^+$) was performed. $CD4^+$ and $CD8^+$ T lymphocytes were further distributed in naïve (Tn, $CD27^+CD45RO^-$), effector (Teff, $CD27^-CD45RO^-$), central memory (Tcm, $CD27^+CD45RO^{+-}$) and effector memory (Tefm, $CD27^-CD45RO^{+-}$) subsets. Additional quantified subpopulations included recent thymic emigrants (RTE,

$CD4^+CD45RA^+CD31^+$), Treg ($CD3^+CD4^+CD25^+CD127^{low}$), gamma-delta T lymphocytes (Tγδ, $CD3^+TCR\gamma\delta^+$), activated T cells ($CD3^+HLA\text{-}DR^+$) and memory B cells (Bm, $CD19^+CD27^+$).

Absolut numbers of T, B and NK lymphocytes were normalized to a patient-specific age range (22), creating a variable called "score". To calculate the score, the median of the age-specific normal range was subtracted from the absolute number of lymphocytes in the subpopulation. The result was then divided by the difference between the 90^{th} percentile and the 10^{th} percentile of the normal range for that age group. Lymphopenia was defined as a score under -0.5 and lymphocytosis as a score over 0.5.

Regarding humoral immunity, levels of immunoglobulins G, A and M (IgG, IgA and IgM) were quantified on serum by nephelometry following manufacturer's instructions (Siemens, Altona). Hypogammaglobulinemia was defined as values of IgG, IgA or IgM below the lower 95% confidence interval for each age group (23).

2.3 Statistical analysis

Quantitative variables were compared between two groups using the Mann–Whitney U test, except for the Δscore, for which the Student's t-test was applied after confirming normal distribution with the Shapiro–Wilk test. When comparing quantitative variables across more than two groups, the Kruskal-Wallis test was used, followed by Dunn's *post hoc* test for pairwise comparisons. Survival analysis was performed using the Cox proportional hazards model. The optimal multivariate model was selected using the Akaike Information Criterion, starting with variables with a p-value <0.100 from univariate analysis. The final model retained variables with the best fit. Statistical significance was set at $p < 0.05$. All analyses were conducted with RStudio (version 4.3.3, R Core Team, 2024).

3 Results

3.1 Baseline clinical features

Ninety-five patients were ultimately included in our prospective study (Figure 1), with a median age of 16 (7–88) months. The baseline characteristics of the cohort are detailed in Table 1. Split graft from a deceased donor was the most common type of donation (41%), with biliary atresia being the predominant indication for LT (63%). Only 6 patients (6%) underwent combined liver-kidney transplantation, while 9 others (9%) required a second transplant due to primary graft failure (n=7), acute rejection (n=1) or tumor recurrence (n=1).

Ninety-seven percent of the patients received the standard induction regimen. Two patients (2%) also received mycophenolate as part of their induction therapy due to a combined transplant with a kidney graft, whereas one patient (1%) with a liver tumor was on chemotherapy at the time of transplantation.

Seven patients (7%) received intravenous immunoglobulin (IVIG). Two (2%) were prescribed IVIG prior to transplantation: one as part of the treatment for Gestational Alloimmune Liver Disease and another in the context of Evans syndrome associated with Autoimmune Lymphoproliferative Syndrome. Two patients (2%) received IVIG post-transplantation for the management of either adenovirus or Epstein–Barr virus infections. Three additional patients (3%) were treated with IVIG due to severe post-transplant hypogammaglobulinemia. Only two of these seven patients (29%) remained free of infections.

3.2 Events of rejection, AIH, PTLD and infection post-transplantation

Regarding post-transplant outcomes, 6 episodes of acute cellular rejection were diagnosed (6%) along the follow-up (median time 233 [50 – 349] days). Three patients had a diagnosis of AIH before transplantation: one with type 1 AIH, one with seronegative AIH and one with suspected AIH. One patient tested positive for anti-F-actin antibodies at a titer of 1:80 at 6M, though the antibody was undetectable in subsequent tests. Other autoimmune complications included one case of autoimmune neutropenia and one of autoimmune hemolytic anemia. PTLD was diagnosed in 2 patients (2%) at 6M and 9M, respectively. The low number of rejection, AIH or PTLD events reported prevented us from doing statistical analysis.

Regarding infections, most of them occurred within the first month post-transplantation (early infections) (median time 4 [1-12] days), affecting 41 patients (43%) (Figure 2A). In subsequent months, the proportion decreased to 17%, 24%, 10% and 9% during their respective follow-up periods (Figure 2A). Early infections were predominantly bacterial, accounting for 51% of cases (Figure 2B). In contrast, late infections (median time 100 [30-150] days) were primarily viral, comprising 68%, 67%, 47% and 75% of infections during the corresponding follow-up periods (Figure 2B). Pathogens causing early and late infections are detailed in Supplementary Table S2.

3.3 Evolution of immunoglobulins and lymphocyte populations during the first year post-transplantation

IgA hypogammaglobulinemia was detected in 2 (3%) recipients before the procedure, while the rest of patients maintained normal levels of both IgG and IgM (Supplementary Table S3). Transplantation had a negative impact on immunoglobulin levels during the first month post-transplantation, with 18 (20%), 19 (21%) and 17 (19%) recipients developing hypogammaglobulinemia for IgG, IgA, and IgM, respectively. During the subsequent months, immunoglobulin levels gradually increased (Figures 3A-C) and, by the end of the follow-up period, most patients had returned to normal levels. However, 7 (11%) patients still had IgM hypogammaglobulinemia, and 2 (3%) patients had hypogammaglobulinemia of either IgG or IgA (Supplementary Table S3).

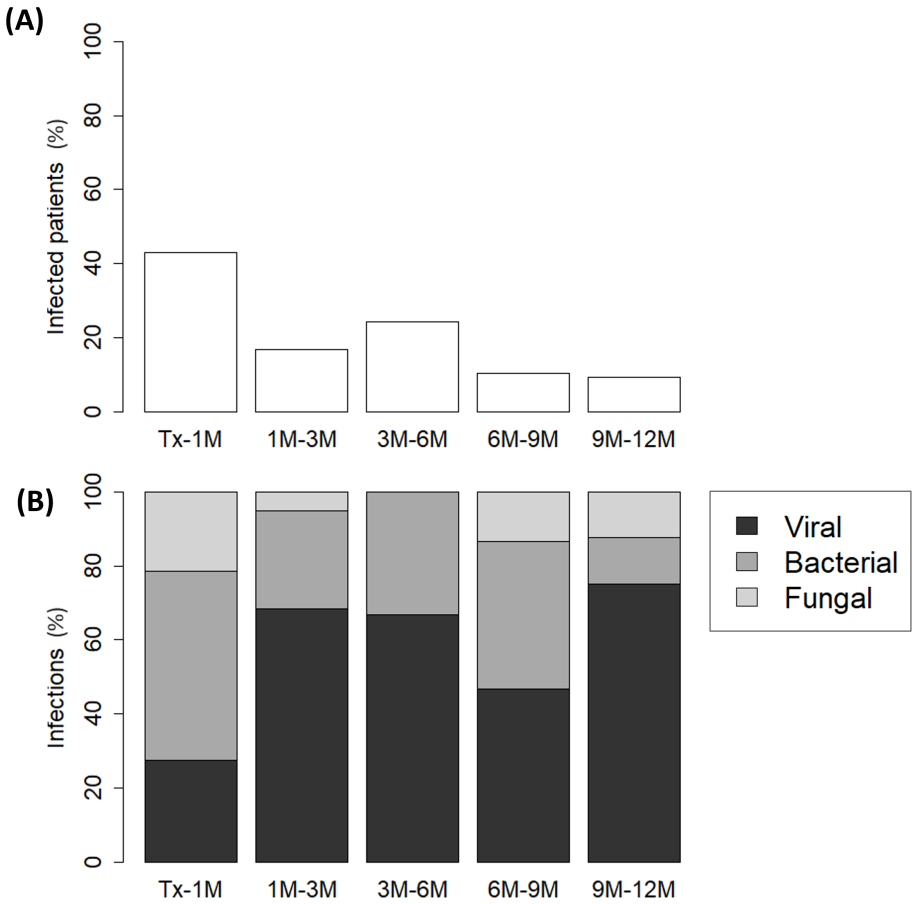

FIGURE 2
Percentage of **(A)** infected pediatric liver recipients and **(B)** distribution of infection types (viral, bacterial, or fungal) across each follow-up period: from transplantation (Tx) to 1 month post-transplantation (1M), 1M to 3M, 3M to 6M, 6M to 9M and 9M to 12M.

Lymphopenia was frequent among recipients prior to transplantation (78%) (Supplementary Table S3), and mainly attributable to baseline $CD3^+$ T lymphopenia (81%). In contrast, pre-transplant B and NK lymphopenia was observed in lower percentages (42% and 6%, respectively) (Supplementary Table S3). Accordingly, the baseline median score of total lymphocytes (Figure 4A) and T lymphocytes (Figure 4B) mirrored each other, both being below -0.5 prior to transplantation, including $CD4^+$ (Figure 4C) and $CD8^+$ (Figure 4D) T subsets. Upon transplantation, T lymphocytes already increased above -0.5 at 1M (Figure 4B), rising from -0.77 (-0.94 to -0.60) to -0.30 (-0.60 to 0.07) ($p<0.001$). Concomitantly, both $CD4^+$ (PreTx -0.76 [-0.89 to -0.57] vs 1M -0.30 [-0.53 to 0.13], $p<0.001$) and $CD8^+$ (PreTx -0.71 [-0.80 to -0.51] vs 1M -0.34 [-0.58 to 0.02], $p<0.001$) T-cell scores also exceeded -0.5 at 1M (Figures 4C, D, respectively).

$CD3^+$ T lymphocytes at 1M and 3M were significantly lower compared to 12M values (1M -0.30 [-0.60 to 0.07] and 3M -0.30 [-0.54 to 0.04] vs 12M -0.01 [-0.24 to 0.20], $p=0.005$ and $p=0.008$, respectively), with the $CD3^+$ T-cell score remaining comparable from 6M onwards. Regarding $CD4^+$ T-cell score, it normalized at 1M and remained stable throughout the follow-up (Figure 4C), with no significant differences observed. Kinetics of the $CD8^+$ T-cell score paralleled those described for $CD3^+$ T lymphocytes (Figure 4D). $CD8^+$ T lymphocytes at 1M and 3M were significantly lower compared to 12M values (1M -0.34 [-0.58 to 0.02] and 3M -0.24 [-0.49 to 0.05] vs 12M 0.11 [-0.18 to 0.30], $p<0.001$ and $p=0.003$, respectively). Normalization was observed at 6M, after which the $CD8^+$ T-cell score remained stable.

Regarding B lymphocytes, a significant expansion at 1M was observed (PreTx -0.46 [-0.59 to -0.21] vs 1M -0.04 [-0.36 to 0.57], $p<0.001$) (Figure 4E), showing values over 0.5 score (lymphocytosis) in 27 (30%) patients at that timepoint. B-cell expansion observed at 1M significantly decreased by 6M (-0.25 [-0.49 to -0.14], $p<0.001$), when normalization was achieved. From that time onwards, B-cell score remained stable, with no significant differences observed.

The impact of transplantation on NK-cell score appeared less pronounced initially (Figure 4F). Compared to pre-transplant study, a significant increase was detected at 3M (PreTx -0.33 [-0.43 to -0.21] vs 3M -0.17 [-0.34 to -0.02], $p<0.001$). After 6M, NK-cell scores normalized and remained stable in the following months.

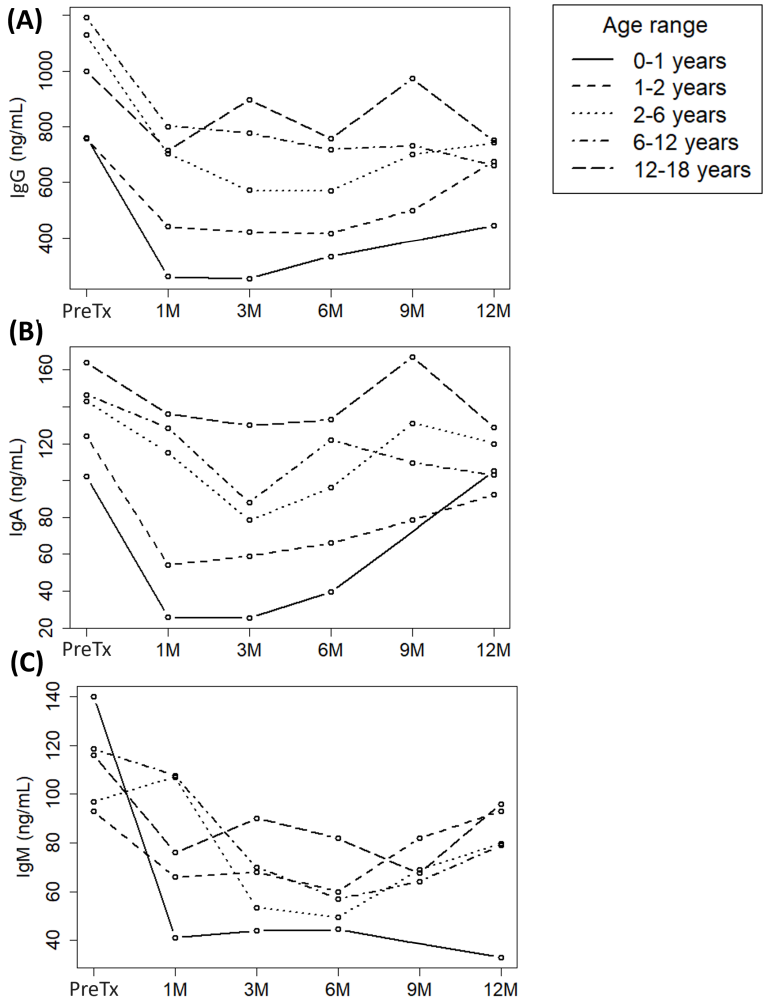

FIGURE 3
Evolution of **(A)** immunoglobulin G (IgG), **(B)** IgA and **(C)** IgM serum levels in a cohort of pediatric liver recipients grouped by age ranges across each follow-up period: pre-transplantation (Pre-Tx) and 1, 3, 6, 9 and 12 months post-transplantation (1M, 3M, 6M, 9M and 12M, respectively).

3.4 Evolution of expanded-phenotype cell populations during the first year post-transplantation

Firstly, the decrease in Treg subpopulation at 1M (Table 2) was likely an artifact of the technique, as basiliximab (anti-CD25) used in induction therapy interfered with CD25 detection by flow cytometry. Therefore, 1-month Treg frequencies were excluded from our analysis.

Infant patients aged 0–1 year (Table 2) showed a significant increase in Tγδ lymphocyte frequency, rising from 2.63% pre-transplantation and 3.22% at 1M to 5.10% at 3M ($p= 0.008$ and $p =0.001$, respectively) and 9.01% at 6M ($p=0.015$ and $p=0.002$, respectively). In recipients aged 1–2 years, Tγδ lymphocyte frequency significantly increased from 5.40% pre-transplantation to 9.72% at 9M and 10.62% at 12M ($p=0.005$ and $p=0.003$, respectively). This rise was also significant when comparing 1M (3.48%) to 6M (6.37%), 9M and 12M ($p=0.008$, $p<0.001$ and $p<0.001$, respectively), and when comparing 3M (4.60%) to 9M and 12M ($p<0.001$ for both comparisons).

Regarding NKT lymphocytes in patients aged 1–2 years (Table 2), their frequency increased from 0.25% at 1M to 0.61% at 9M ($p= 0.003$) and 0.62% at 12M ($p=0.006$). Conversely, Treg frequency decreased from 8.49% at 3M to 5.10% at 9M ($p<0.001$) and 5.17% at 12M ($p<0.001$), while the frequency of RTE declined from 67.20% at 1M to 52.07% at 6M and 52.79% at 9M ($p= 0.015$ and $p= 0.012$, respectively). In contrast, activated $CD3^+HLA\text{-}DR^+$ T lymphocytes showed an increase from 7.51% at 1M to 17.79% at 9M ($p=0.023$).

Similarly, patients aged 2–6 years increased their Tγδ and $CD3^+HLA\text{-}DR^+$ subsets throughout the follow-up period (Table 2). Interestingly, frequencies of Bm only showed an increase in that age group, rising from baseline 10.67% and 11.74% at 1M to 20.33% at 12M ($p=0.007$ and $p=0.016$, respectively). On the other hand, in older patients aged 6–12 years, only an increase in Tγδ lymphocytes from 6.66% at 1M

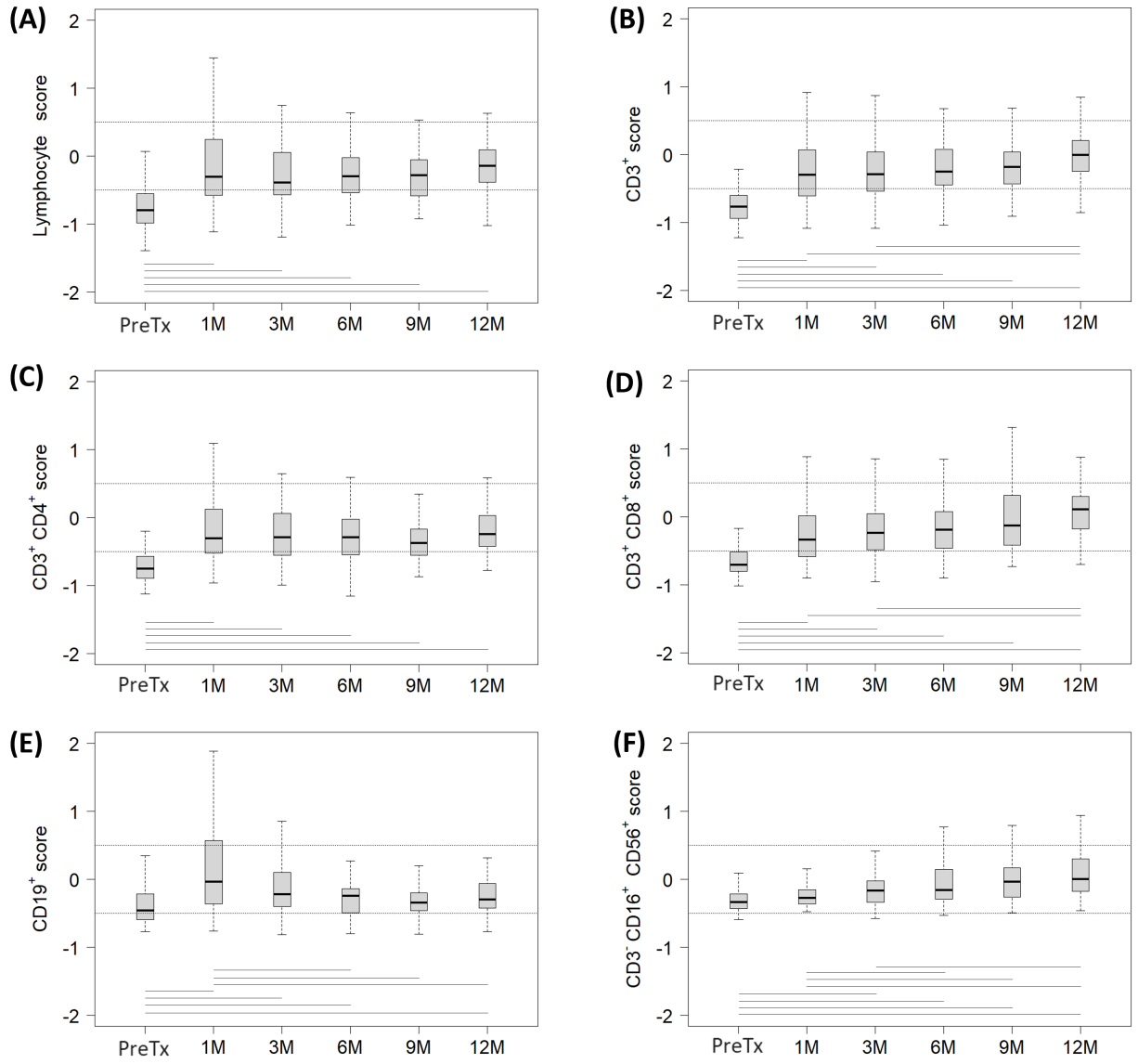

FIGURE 4
Evolution of each lymphocyte subpopulation score in a cohort of pediatric liver recipients across each follow-up period: pre-transplantation (Pre-Tx) and 1, 3, 6, 9 and 12 months post-transplantation (1M, 3M, 6M, 9M and 12M, respectively). Studied subsets included **(A)** total lymphocytes, **(B)** $CD3^+$ T lymphocytes, **(C)** $CD3^+CD4^+$ T lymphocytes, **(D)** $CD3^+CD8^+$ T lymphocytes, **(E)** $CD19^+$ B lymphocytes and **(F)** $CD3^-CD16^+CD56^+$ NK lymphocytes. Scores were calculated by substracting the median of the age-specific normal range from the absolute number of lymphocytes in the subpopulation. Dashed lines mark the normal range, defined as scores between -0.5 and 0.5. Horizontal lines represent statistically significant differences between the median scores of two distinct follow-up periods.

and 6.62% at 3M to 17.56% at 12M (p=0.009 and p=0.008, respectively) was detected. For recipients aged 12–18 years, the frequencies remained stable throughout the entire follow-up period, with multiple comparisons yielding no significant p-values.

The distribution by age of $CD4^+$ and $CD8^+$ Tn, Teff, Tcm, and Tefm lymphocyte subpopulations throughout the follow-up period remained comparable (Supplementary Figures S1, S2). However, in patients aged from 2–6 years, median frequencies of $CD8^+$ Tn significantly decreased from 1M to 12M (75.61% vs 54.20%, p=0.012). Conversely, $CD8^+$ Teff and Tefm subsets in this age group significantly increased in the same period ($CD8^+$ Teff 1.71% vs 11.34%, p=0.005; $CD8^+$ Tefm 3.81% vs 10.00%, p=0.010) (Supplementary Figure S2).

3.5 Association of T-cell lymphopenia and hypogammaglobulinemia with the risk of infection

When segregated according to the time of infection (early/late), statistical analysis showed that infected patients were significantly younger at transplant and primarily received split grafts (Table 1).

TABLE 2 Lymphocyte frequencies along the different follow-up periods in a cohort of pediatric liver recipients segregated by age ranges.

T-lympho-cyte subset	PreTx		1M		3M		6M		9M		12M		p-value
	n	median (IQR)	n	median (IQR)	n	median (IQR)	n	median (IQR)	n	median (IQR)	n	median (IQR)	
Tγδ													
0–1 years	26	2.63 (1.68 - 3.58)[a,b]	28	3.22 (1.61 - 3.85)[c,d]	20	5.10 (3.49 - 8.67)[a,c]	6	9.01 (7.13 - 15.11)[b,d]	0	NA	1	22.29 (22.29 - 22.29)	<0.001
1–2 years	13	5.40 (4.35 - 5.82)[a,b]	19	3.48 (2.31 - 4.85)[c,d,e]	21	4.60 (2.93 - 6.10)[f,g]	33	6.37 (3.83 - 11.75)[c]	28	9.72 (7.56 - 14.21)[a, d,f]	24	10.62 (9.04 - 13.30)[b, e,g]	<0.001
2–6 years	15	6.16 (3.78 - 7.89)	17	3.90 (2.69 - 4.98)[a,b,c]	18	5.21 (3.10 - 8.92)[d]	16	8.09 (5.68 - 10.98)[a]	17	10.05 (7.43 - 13.80)[b]	20	11.81 (7.21 - 14.70)[c,d]	<0.001
6–12 years	12	8.67 (5.60 - 16.50)	12	6.66 (3.48 - 10.96)[a]	13	6.62 (5.67 - 12.52)[b]	13	11.14 (7.72 - 15.12)	12	15.54 (14.00 - 18.48)	11	17.56 (12.08 - 19.63)[a,b]	0.002
12–18 years	13	9.10 (5.64 - 11.40)	13	4.49 (3.60 - 8.12)	13	6.42 (4.53 - 9.58)	14	7.74 (5.11 - 11.97)	10	7.98 (7.44 - 12.69)	8	9.09 (6.97 - 15.10)	0.220
NKT													
0–1 years	26	0.26 (0.10 - 0.55)	28	0.29 (0.16 - 0.60)	20	0.29 (0.16 - 0.52)	6	1.03 (0.29 - 1.45)	0	NA	1	0.95 (0.95 - 0.95)	0.269
1–2 years	13	0.31 (0.21 - 0.99)	19	0.25 (0.19 - 0.36)[a,b]	21	0.49 (0.20 - 0.81)	33	0.46 (0.22 - 0.63)	28	0.61 (0.30 - 1.61)[a]	24	0.62 (0.32 - 1.15)[b]	0.006
2–6 years	15	0.41 (0.29 - 1.21)	17	0.38 (0.24 - 0.80)	18	0.50 (0.23 - 0.77)	16	0.65 (0.36 - 1.48)	17	0.56 (0.46 - 0.80)	20	0.88 (0.53 - 1.39)	0.111
6–12 years	12	1.20 (0.67 - 2.33)	12	0.95 (0.62 - 1.93)	13	0.86 (0.66 - 1.13)	13	1.39 (1.10 - 2.78)	12	1.05 (0.72 - 1.58)	11	1.26 (1.11 - 1.97)	0.388
12–18 years	13	3.40 (1.10 - 4.15)	13	0.87 (0.60 - 2.16)	13	1.14 (0.80 - 3.02)	14	1.68 (1.07 - 4.23)	10	2.63 (1.54 - 4.28)	8	2.49 (1.49 - 4.92)	0.234
Treg													
0–1 years	26	8.95 (5.07 - 11.30)	25	0.70 (0.02 - 7.00)*	20	8.33 (6.82 - 10.39)	5	8.81 (8.06 - 10.24)	0	NA	1	3.49 (3.49 - 3.49)	0.113
1–2 years	13	8.95 (5.07 - 11.30)	18	0.00 (0.00 - 0.30)*	18	8.49 (7.63 - 9.58)[a,b]	29	6.46 (5.62 - 7.53)	26	5.10 (4.04 - 6.76)[a]	24	5.17 (3.96 - 6.11)[b]	<0.001
2–6 years	15	8.62 (4.95 - 11.05)	16	5.82 (1.07 - 11.59)*	18	7.72 (6.38 - 10.66)	15	8.34 (6.04 - 9.01)	17	6.02 (5.01 - 7.02)	20	5.55 (4.98 - 7.31)	0.069

(Continued)

10.3389/fimmu.2025.1605716

TABLE 2 Continued

T-lympho-cyte subset	PreTx		1M		3M		6M		9M		12M		p-value
	n	median (IQR)	n	median (IQR)	n	median (IQR)	n	median (IQR)	n	median (IQR)	n	median (IQR)	
Treg													
6–12 years	12	6.60 (5.46 - 8.57)	11	0.45 (0.00 - 4.92)*	13	7.49 (6.90 - 13.70)	13	5.80 (4.72 - 8.79)	12	5.12 (4.38 - 7.85)	11	6.55 (4.56 - 7.96)	0.198
12–18 years	13	6.66 (4.52 - 8.34)	12	0.02 (0.00 - 1.66)*	13	6.56 (4.96 - 7.73)	11	6.74 (5.39 - 7.14)	10	5.75 (4.59 - 6.68)	8	4.83 (4.58 - 6.31)	0.621
RTE													
0–1 years	26	64.48 (56.75 - 75.83)	27	61.60 (56.61 - 72.32)	19	53.52 (47.34 - 67.34)	6	64.20 (44.83 - 69.66)	0	NA	1	46.51 (46.51 - 46.51)	0.278
1–2 years	13	56.16 (45.15 - 66.04)	19	67.20 (57.24 - 74.30)[a,b]	20	57.36 (45.12 - 71.54)	31	52.07 (39.15 - 60.62)[a]	28	52.79 (42.76 - 59.54)[b]	24	52.23 (46.63 - 58.75)	0.020
2–6 years	14	44.86 (36.89 - 48.80)	17	51.75 (37.17 - 58.72)	18	47.38 (41.94 - 58.76)	16	48.12 (38.49 - 56.53)	17	44.74 (35.30 - 62.22)	20	46.22 (32.38 - 51.52)	0.654
6–12 years	12	46.78 (40.36 - 53.59)	12	46.67 (36.46 - 53.26)	12	52.98 (45.17 - 55.59)	13	48.40 (43.10 - 54.23)	12	47.31 (45.19 - 50.66)	11	38.92 (38.28 - 51.35)	0.693
12–18 years	13	44.08 (37.40 - 48.31)	13	50.20 (36.30 - 54.22)	13	47.46 (34.21 - 52.41)	14	47.74 (32.57 - 49.90)	10	43.67 (29.34 - 45.56)	8	42.41 (30.70 - 52.22)	0.687
Bm													
0–1 years	26	8.98 (5.93 - 14.75)	28	7.29 (4.29 - 11.73)	20	7.08 (5.59 - 8.46)	6	11.73 (8.06 - 13.97)	0	NA	1	8.20 (8.20 - 8.20)	0.386
1–2 years	13	8.60 (6.62 - 15.80)	19	9.33 (6.70 - 11.74)	21	9.24 (7.83 - 12.55)	33	11.04 (7.64 - 15.13)	28	12.15 (9.62 - 16.36)	24	11.92 (8.68 - 15.88)	0.446
2–6 years	15	10.67 (7.43 - 14.02)[a]	17	11.74 (8.01 - 14.50)[b]	18	13.21 (10.81 - 16.74)	16	17.32 (14.10 - 21.13)	17	16.60 (13.15 - 20.96)	20	20.33 (15.68 - 22.53)[a,b]	0.003
6–12 years	12	15.80 (11.82 - 23.05)	11	14.29 (10.79 - 16.34)	13	13.77 (9.80 - 17.93)	13	17.52 (10.28 - 22.57)	12	14.17 (10.36 - 26.72)	10	12.97 (11.46 - 14.31)	0.911
12–18 years	13	20.10 (8.10 - 24.85)	13	18.50 (5.36 - 22.62)	13	16.61 (10.05 - 28.00)	14	11.53 (7.53 - 19.01)	10	14.45 (8.83 - 17.17)	8	15.64 (8.02 - 20.91)	0.961
$CD3^+HLA\text{-}DR^+$													
0–1 years	26	6.45 (3.69 - 17.21)	28	4.92 (3.58 - 11.15)	20	8.80 (4.90 - 11.88)	6	17.57 (9.04 - 18.23)	0	NA	1	8.41 (8.41 - 8.41)	0.246

(Continued)

10.3389/fimmu.2025.1605716

10.3389/fimmu.2025.1605716

TABLE 2 Continued

T-lymphocyte subset	PreTx		1M		3M		6M		9M		12M		p-value
	n	median (IQR)	n	median (IQR)	n	median (IQR)	n	median (IQR)	n	median (IQR)	n	median (IQR)	
$CD3^+HLA\text{-}DR^+$													
1–2 years	13	17.80 (10.94 - 21.32)	19	7.51 (3.72 - 12.79)[a]	21	13.26 (8.60 - 19.61)	33	15.48 (11.16 - 22.08)	28	17.79 (10.39 - 29.34)[a]	24	21.18 (9.59 - 28.73)	0.040
2–6 years	15	14.55 (9.04 - 29.80)	17	10.00 (5.08 - 12.11)[a]	18	7.26 (5.56 - 17.03)[b]	16	8.24 (6.09 - 12.35)[c]	17	16.95 (7.27 - 34.11)	20	26.16 (17.29 - 30.41)[a,b,c]	0.001
6–12 years	12	10.40 (6.68 - 14.67)	12	13.23 (9.31 - 20.36)	13	18.16 (4.69 - 22.10)	13	13.55 (7.37 - 30.90)	12	11.82 (7.04 - 20.43)	11	26.56 (12.44 - 35.21)	0.368
12–18 years	13	15.40 (10.48 - 20.30)	13	14.70 (8.70 - 23.33)	13	13.50 (12.20 - 19.37)	14	22.31 (12.46 - 30.75)	10	32.92 (19.08 - 37.09)	8	21.28 (15.32 - 35.97)	0.248

1M, 1 month post-transplantation; 3M, 3 months post-transplantation; 6M, 6 months post-transplantation; 9M, 9 months post-transplantation; 12M, 12 months post-transplantation; Bm, memory B lymphocytes; CD3+HLA-DR+, activated T lymphocytes; IQR, interquartile range; PreTx, pre-transplantation; NA, not applicable; RTE, recent thymic emigrants lymphocytes; Treg, regulatory T lymphocytes; Tγδ, gamma-delta T lymphocytes.

[a–c]Significant differences ($p<0.05$).

*Frequencies were ommited from the analysis due to the impossibility to detect CD25 by flow cytometry for some patients.

To better assess immunological parameters post-transplantation, we subtracted each subpopulation score from pre-transplant study to the one obtained at 1M (Δscore). The higher the Δscore, the better the normalization of lymphocyte subpopulations. Patients that remained free from late infections had higher Δscore for T $CD3^+$ (0.524 vs 0.263, p=0.018) and T $CD4^+$ (0.452 vs 0.287, p=0.036) than those who developed late infections (Table 3). Interestingly, T $CD8^+$ Δscore was also higher in non-infected patients, although this increase nearly reached statistical significance (0.483 vs 0.178, p=0.054).

Subsequently, a survival analysis was performed to explore the relationship between pre-transplant immunological status and the risk of early infections (Table 4). The univariate analysis identified a significant association between the risk of post-transplant infections and both the age at transplantation and the type of graft. Patients aged 0–1 years (hazard ratio [HR] 5.23, p=0.027) or 1–2 years (HR 5.29, p=0.034) had a significantly higher risk of infection. Transplantation using a split graft was associated with a threefold risk for infection (HR 3.02, p=0.071), although this correlation was not statistically significant in the univariate analysis. None of the immunological variables analyzed were associated with the risk of early infection. Interestingly, in the multivariate analysis, only transplantation with a split graft was independently associated with an increased risk of early infection (HR 3.42, p=0.047).

We next analyzed how immune status at 1M influenced the likelihood of remaining free from late infection (Table 5). The univariate model revealed that infants aged 0–1 years had a significantly higher risk of late infection (HR 3.49, p=0.046). Conversely, patients who received a whole graft from deceased donor had a significantly lower risk (HR 0.28, p=0.044). In terms of immunological status, $CD3^+$ or $CD8^+$ T lymphopenia (HR 2.48, p=0.005 and HR 2.38, p=0.008, respectively) and hypogammaglobulinemia (IgG, IgA or IgM), were associated with a higher risk of late infection (HR 2.18, p=0.036 and HR 2.40, p=0.011 and HR 2.61, p=0.006, respectively). The multivariate model showed that only lymphopenia T $CD3^+$ was independently associated with an increased risk of late infection (HR 2.13, p=0.030). Kaplan-Meier curves for patients with or without T lymphopenia are graphed in Figure 5. Patients with $CD3^+$ T lymphopenia showed significantly higher infection rates after the first month post-transplantation (p=0.005) (Figure 5A). While $CD4^+$ T lymphopenia did not show a statistically significant association with infection rates (Figure 5B), the presence of $CD8^+$ T lymphopenia was significantly associated with higher infection rates, highlighting the differential impact of T-cell subsets on infection risk (Figure 5C).

Furthermore, we stratified patients into four groups based on IgG levels and $CD3^+$ T-cell counts at 1M: normal IgG/normal $CD3^+$ (n=50), normal IgG/$CD3^+$ T lymphopenia (n=22), IgG hypogammaglobulinemia/normal $CD3^+$ (n=6) and IgG hypogammaglobulinemia/$CD3^+$ T lymphopenia (n=11). The risk of late infection was significantly higher in patients with normal IgG/$CD3^+$ T lymphopenia (HR 3.03, 95% CI 1.46–6.30, p=0.003), IgG hypogammaglobulinemia/normal $CD3^+$ (HR 4.16, 95% CI 1.36–12.74, p=0.013) and IgG hypogammaglobulinemia/$CD3^+$ T

TABLE 3 Estimation of cellular immunity recovery following pediatric liver transplantation calculated by differences between pre-transplant score and 1-month post-transplant score (Δscore).

Δscore	Infection (n=35)	No infection (n=41)	p-value
Lymphocytes	0.342 (0.017 to 0.960)	0.532 (0.172 to 0.961)	0.155
T cell $CD3^+$	0.263 (-0.071 to 0.680)	0.524 (0.227 to 0.906)	0.018
T cell $CD3^+CD4^+$	0.287 (0.001 to 0.695)	0.452 (0.244 to 0.882)	0.036
T cell $CD3^+CD8^+$	0.178 (-0.058 to 0.666)	0.483 (0.207 to 0.753)	0.054
B cell $CD19^+$	0.280 (0.070 to 1.065)	0.392 (0.130 to 1.025)	0.679
NK cell $CD3^-CD16^+$ $CD56^+$	0.049 (-0.168 to 0.253)	0.088 (-0.053 to 0.208)	0.767

lymphopenia (HR 2.86, 95% CI 1.10–7.44, p=0.031), compared to the normal IgG/normal $CD3^+$ group.

4 Discussion

This study aimed to define the immune changes in pediatric LT and identify markers related to post-transplant complications. Our findings revealed that baseline T lymphopenia and first-month post-transplant IgG hypogammaglobulinemia mostly recover early in the follow-up. Additionally, patients with T $CD3^+$ lymphopenia at 1M have a twofold increased risk of late infections.

In our cohort, end-stage liver disease negatively impacted the cellular compartment. Although the detrimental effect of biliary atresia on cellular immunity has been previously described (24), we found no association when comparing baseline immune scores of patients grouped by their underlying diagnosis (Supplementary Table S4). However, in line with previous results published by Möhring et al. (25), patients with liver tumors had the highest numbers of lymphocytes when adjusted for age (median score -0.63

TABLE 4 Early infection univariate and multivariate analysis in a cohort of pediatric liver recipients categorized by their immune status of lymphopenia or hypogammaglobulinemia pre-transplantation.

Baseline characteristics	n	UNIVARIATE		MULTIVARIATE	
		HR (95% CI)	p-value	HR (95% CI)	p-value
Age (years)					
0-1	31	5.23 (1.21 - 22.58)	0.027	3.09 (0.58 – 16.30)	0.185
1-2	16	5.29 (1.14 – 24.57)	0.034	3.78 (0.70 – 20.43)	0.122
2-6	18	3.82 (0.82 – 17.84)	0.089	2.15 (0.41 – 11.36)	0.370
6-12	15	2.13 (0.39 – 11.61)	0.384	1.33 (0.23 – 7.61)	0.750
12-18	15	Reference		Reference	
Type of donor					
Deceased donor - reduced graft	23	2.14 (0.60 – 7.60)	0.242	3.75 (0.96 – 14.73)	0.058
Deceased donor - split graft	39	3.02 (0.91 – 10.04)	0.071	3.42 (1.02 – 11.50)	0.047
Deceased donor - whole graft	22	0.48 (0.10 - 2.39)	0.371	1.00 (0.18 – 5.67)	0.997
Living donor	11	Reference		Reference	
Lymphopenia					
Yes	63	2.38 (0.84 – 6.74)	0.102		
No	16	Reference			
Lymphopenia T $CD3^+$					
Yes	64	2.16 (0.77 – 6.13)	0.145		
No	15	Reference			

(Continued)

TABLE 4 Continued

Baseline characteristics	n	UNIVARIATE		MULTIVARIATE	
		HR (95% CI)	p-value	HR (95% CI)	p-value
Lymphopenia T $CD3^+CD4^+$					
Yes	64	1.60 (0.62 – 4.12)	0.330		
No	15	Reference			
Lymphopenia T $CD3^+CD8^+$					
Yes	60	1.93 (0.75 – 4.97)	0.173		
No	19	Reference			
Lymphopenia B $CD19^+$					
Yes	63	1.19 (0.62 – 2.29)	0.603		
No	16	Reference			
Lymphopenia NK $CD3^-CD16^+CD56^+$					
Yes	5	0.82 (0.20 – 3.41)	0.783		
No	74	Reference			
Hypogammaglobulinemia IgG					
Yes	0	NA	NA		
No	76	Reference			
Hypogammaglobulinemia IgA					
Yes	2	1.58 (0.23 – 11.56)	0.652		
No	74	Reference			
Hypogammaglobulinemia IgM					
Yes	0	NA	NA		
No	76	Reference			

CI, confidence interval; Ig, immunoglobulin; NA, not applicable; NK, natural killer; OR, odds ratio.

[-0.89 to -0.37]). In a cohort of 60 adult patients with cirrhosis T $CD4^+$ lymphopenia was observed (26), attributing it to defective lymphocyte production, splenic pooling and apoptosis from bacterial translocation. This may help understanding the variations in immune pre-transplant status within our cohort.

LT differently affected humoral and cellular immunity. Humoral immunity was negatively affected by LT, since patients who did not have hypogammaglobulinemia prior to the transplant developed it after receiving the graft. Our results are consistent with previous findings in pediatric liver recipients (14, 27), and are likely due to the excessive loss of immunoglobulin-rich ascitic serum during surgery. However, the effect of the immunosuppressive treatment should also be considered.

Conversely, cellular immunity immediately benefits from LT, as the frequency of patients with total lymphopenia decreased from 78% PreTx to 36% at 1M. In a cohort of 304 adult kidney recipients, lymphocyte subpopulations were analyzed at PreTx, 1M and 6M. Consistent with our results, those without anti-thymocyte globulin induction showed increased T-cell counts at 1M (28).

Our approach focuses on simultaneously monitoring humoral and cellular immunity after LT, allowing us to determine the timepoint at which normalization occurs for each Ig and lymphocyte subpopulation. The number of patients with hypogammaglobulinemia of any isotype began to decrease immediately after 1M. By 12M, only two patients showed IgG hypogammaglobulinemia, both of whom had received rituximab treatment for either PTLD or autoimmune hemolytic anemia. While $CD3^+$ and $CD8^+$ T-cell score normalization occurred at 6M, $CD4^+$ T-cell score normalized at 1M; on the other hand, B-cell and NK-cell scores normalized at 6M. Interestingly, we noticed a remarkable expansion of B cells at 1M, likely compensating for the hypogammaglobulinemia present at that time.

Regarding expanded-phenotype subpopulations, transplantation had a less pronounced impact, since differences with PreTx values were only found for Tγδ lymphocytes in patients aged 0–2 years and

10.3389/fimmu.2025.1605716

TABLE 5 Late infection univariate and multivariate analysis in a cohort of pediatric liver recipients categorized by their immune status of lymphopenia or hypogammaglobulinemia at one month post-transplantation.

One month post-transplantation characteristics	n	UNIVARIATE		MULTIVARIATE	
		HR (95% CI)	p-value	HR (95% CI)	p-value
Age (years)					
0-1	28	3.49 (1.02 - 11.92)	0.046		
1-2	19	3.28 (0.92 - 11.65)	0.066		
2-6	17	1.47 (0.37 - 5.87)	0.589		
6-12	12	0.32 (0.03 - 3.10)	0.327		
12-18	13	Reference			
Type of donor					
Deceased donor - reduced graft	22	0.39 (0.13 - 1.16)	0.090	0.50 (0.16 - 1.20)	0.220
Deceased donor - split graft	39	1.09 (0.46 - 2.55)	0.852	1.17 (0.48 - 2.82)	0.730
Deceased donor - whole graft	17	0.28 (0.08 - 0.97)	0.044	0.30 (0.09 - 1.05)	0.060
Living donor	11	Reference		Reference	
Lymphopenia					
Yes	32	1.88 (0.99 - 3.55)	0.053		
No	57	Reference			
Lymphopenia T $CD3^+$					
Yes	33	2.48 (1.32 - 4.67)	0.005	2.13 (1.08 - 4.21)	0.030
No	56	Reference		Reference	
Lymphopenia T $CD3^+CD4^+$					
Yes	23	1.64 (0.84 - 3.17)	0.145		
No	66	Reference			
Lymphopenia T $CD3^+CD8^+$					
Yes	28	2.38 (1.26 - 4.50)	0.008		
No	61	Reference			
Lymphopenia B $CD19^+$					
Yes	10	0.77 (0.24 - 2.50)	0.664		
No	79	Reference			
Lymphopenia NK $CD3^-CD16^+CD56^+$					
Yes	0	NA	NA		
No	89	Reference			
Hypogammaglobulinemia IgG					
Yes	17	2.18 (1.05 - 4.51)	0.036		
No	72	Reference			
Hypogammaglobulinemia IgA					
Yes	19	2.40 (1.22 - 4.72)	0.011		
No	70	Reference			

(Continued)

TABLE 5 Continued

One month post-transplantation characteristics	n	UNIVARIATE		MULTIVARIATE	
		HR (95% CI)	p-value	HR (95% CI)	p-value
Hypogammaglobulinemia IgM					
Yes	17	2.61 (1.31 - 5.19)	0.006	1.90 (0.91 – 3.95)	0.087
No	78	Reference		Reference	

CI, confidence interval; HR, hazard ratio; Ig, immunoglobulin; NA, not applicable; NK, natural killer.

Bm lymphocytes in patients 2–6 years old. Further differences appeared at 9M and 12M, likely reflecting age-related changes occurring throughout the follow-up period. This is supported by the absence of significant differences in patients over 12 years, suggesting diminished age-related fluctuations as patients mature. However, stratifying patients by age resulted in a reduced sample size in each subgroup, which may have limited the statistical power to detect additional differences.

Similarly, slight differences appeared in frequencies of Tn, Teff, Tcm and Tefm subsets. As children age, the frequency of Tn cells decreases, while the percentage of Teff, Tefm, and Tcm subpopulations increase, as anticipated (29). However, in patients aged 2–6 years, there was a significant decrease in $CD8^+$ Tn cells and a significant increase in $CD8^+$ Teff and Tefm subsets from 1M onwards, which might be related with cytotoxic immune response to viral late infections at that period.

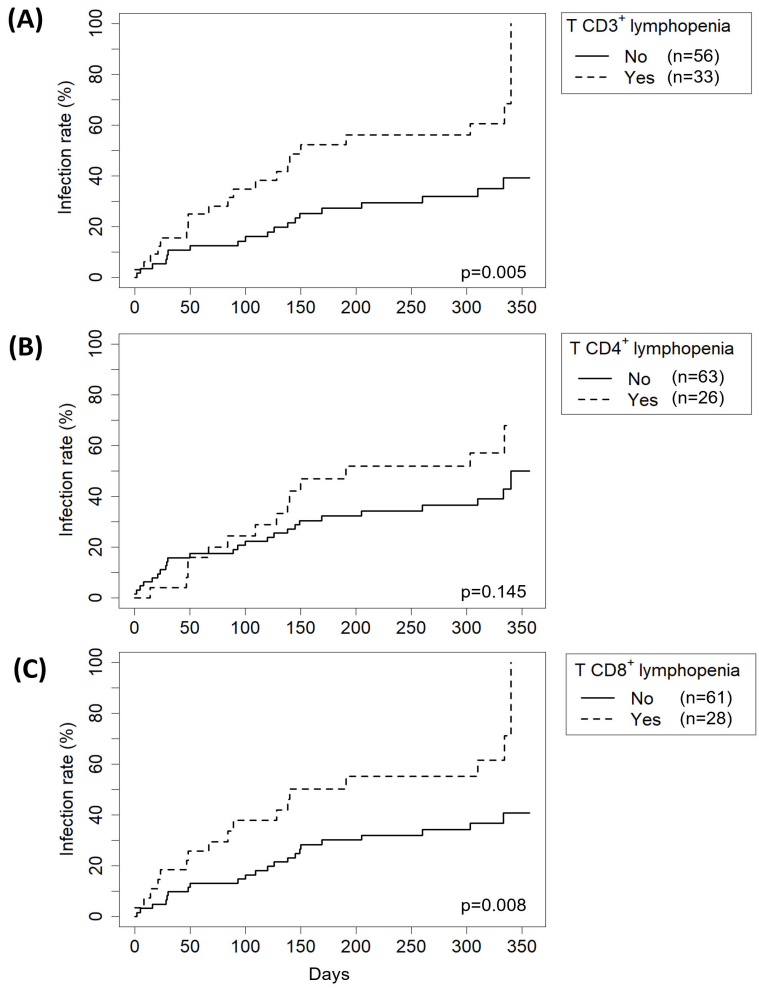

FIGURE 5
Effect of the presence of **(A)** T $CD3^+$ T lymphopenia, **(B)** $CD4^+$ T lymphopenia or **(C)** $CD8^+$ T lymphopenia on late infection risk. Global p-values were obtained at 1 month post-transplantation by Kaplan-Meier analysis.

In our cohort, acute cellular rejection occurred in 6% of patients, lower than previously reported. A 2004 study of 1,092 pediatric LT found a 48.4% incidence, with biopsies confirming 92% of cases (30), while a recent study in 50 pediatric cases reported a 68% incidence, with biopsies conducted at the physician's discretion (31). The absence of serial biopsies in our cohort may have led to an underestimation of the true incidence, as subacute rejections could have been missed.

Autoimmune and PTLD complications were rare in our cohort. None of the recipients developed either *de novo* or recurrent AIH, despite reported incidences in pediatric LT of 1-11% (onset at 2–12 years post-LT) (32) and 38-89% (onset at 11–43 months) (33), respectively. Similarly, PTLD was diagnosed in 2% of our recipients, lower than reported incidences of 7.8-9.7% (4, 12). This may be attributed to our relatively short 1-year follow-up period compared to the 4–12 years of follow-up in other studies (4, 12).

Consistent with previous reports, early infections in our cohort were associated with surgery, while late infections resulted from heightened immunosuppression (34, 35). Thus, bacterial infections dominated the first month, whereas opportunistic viral infections become more frequent thereafter, due to prolonged immunosuppressive therapy (34–37). Since most of the studies have focused on adult liver recipient (14–16, 38–40), we specifically monitored the immune status in pediatric recipients to better assess their risk of infections.

Previous research had established that pre-transplant lymphopenia increases infection risk in adult LT (39, 40). Furthermore, Lei et al. found an association between the number of pre-transplant double-negative $CD3^+CD4^-CD8^-$ T-cells and infection risk in a cohort of 19 adult LT (38). However, we did not identify pre-transplant immunological predictors for early infections in pediatric patients. Instead, split graft recipients were at a higher risk of early infections, likely due to increased biliary leakage leading to severe infections (41).

In contrast, we found that T $CD3^+$ lymphopenia at 1M was associated with increased risk of late infections. This is consistent with Fernandez-Ruiz et al., who observed that adult kidney-transplant recipients with T $CD8^+$ lymphopenia had a threefold increased risk of late infections (28). Interestingly, although in our multivariate analysis we did not find an association with hypogammaglobulinemia, other prospective studies have reported that infected adult liver recipients had lower IgG levels at days 3 (15) or 7 (16) post-transplantation. In line with these findings, our stratified analysis revealed that both isolated and combined alterations in IgG levels and $CD3^+$ T-cell counts at 1M were associated with a significantly increased risk of late infections.

Previous studies have shown that lymphopenia is associated with an increased risk of both opportunistic and community-acquired infections. A large Danish cohort study in the general population demonstrated that individuals with lymphopenia had a significantly higher risk of hospital admission with an infection, as well as infection-related mortality (42). Similarly, in patients with solid tumors, radiation-induced lymphopenia has been linked to an elevated risk of bacterial infections (43). These findings support the relevance of peripheral T-cell counts as general markers of immune competence and infection susceptibility.

Beyond the markers explored in this research, assessing immune function could provide additional insights. A prospective study by Sood et al. (n=75) demonstrated that low interferon-gamma production after non-pathogen specific stimulation at week 1 post-transplant was associated with a higher risk of early infections, whereas elevated levels correlated with an increased risk of rejection (44). Incorporating such functional assays alongside markers like CD64 monocyte counts (15) or PD1 exhaustion marker (38) may enhance our ability to predict infection risk.

To our knowledge, this is the first prospective study monitoring the immune response of pediatric liver recipients. The ChilSFree cohort study proposed a similar approach (8), but results are yet to be reported. Based on our findings, we propose that measuring serum Ig levels, T (including $CD4^+$ and $CD8^+$ subsets), B and NK lymphocytes at PreTx, 1M, 6M and 12M provides a comprehensive assessment of immune recovery and identifies late infections risks. To validate these results, future multicenter studies should adopt a standardized protocol across all participating centers. Sample collection timepoints and technical procedures must be harmonized, and inclusion criteria and clinical endpoints unified. Such collaborative efforts would not only confirm the utility of these biomarkers but also support the development of personalized immunosuppression strategies in pediatric liver transplantation.

A key limitation of our study is the low incidence of autoimmune complications, PTLD and rejection, which restricted our ability to identify additional markers. Moreover, the lack of a more detailed classification of infections based on anatomical site and clinical severity limits our ability to accurately differentiate community-acquired infections from those opportunistic infections. Another limitation is the lack of immune function analysis. Thus, further studies with larger cohorts and immune function assessment are necessary to better understand the immunological landscape of post-transplant complications.

In conclusion, we showed that pediatric liver recipients have baseline immune dysregulation that is resolved during the first months after transplantation. While early infections in our cohort did not show significant immunological predictors, late infections appeared to be influenced by T-cell lymphopenia and hypogammaglobulinemia. Our findings highlight potential factors that could guide strategies for managing post-transplant infections. These insights could contribute to more personalized approaches in immunosuppressive therapy.

Data availability statement

The original contributions presented in the study are included in the article/Supplementary Material. Further inquiries can be directed to the corresponding author.

Ethics statement

The studies involving humans were approved by University Hospital La Paz ethics committee. The studies were conducted in accordance with the local legislation and institutional requirements. Written informed consent for participation in this study was provided by the participants' legal guardians/next of kin.

Author contributions

RC: Methodology, Conceptualization, Data curation, Investigation, Writing – review & editing, Writing – original draft. LM: Writing – review & editing, Investigation, Methodology. CC: Writing – review & editing, Investigation, Conceptualization. IL: Writing – review & editing, Data curation. EF: Writing – review & editing, Conceptualization, Investigation. LH: Writing – review & editing, Investigation, Conceptualization. GM: Investigation, Writing – review & editing. ML: Writing – review & editing, Investigation. AM: Writing – review & editing, Investigation. EL: Conceptualization, Writing – review & editing, Writing – original draft, Supervision, Investigation. ES: Conceptualization, Supervision, Writing – review & editing, Investigation, Writing – original draft.

Funding

The author(s) declare that financial support was received for the research and/or publication of this article. This work was supported by FIS (ISCIII) grant no. PI19-01311. The publication of this study has been funded by "Ayudas Luis Álvarez" promoted by La Paz Institute for Health Research (IdiPAZ).

Acknowledgments

The authors are grateful to all participating patients and their families. They would also like to express their appreciation to Teresa Plaza, Amaya Iturralde, Sergio Ruiz, Natividad Herraiz and Concepción Esteban, for their excellent technical assistance. This study has been funded by Instituto de Salud Carlos III (ISCIII) through the project "PI19-01311" and co-funded by the European Union.

Conflict of interest

The authors declare that the research was conducted in the absence of any commercial or financial relationships that could be construed as a potential conflict of interest.

The author(s) declared that they were an editorial board member of Frontiers, at the time of submission. This had no impact on the peer review process and the final decision.

Generative AI statement

The author(s) declare that no Generative AI was used in the creation of this manuscript.

Publisher's note

Supplementary material

The Supplementary Material for this article can be found online at: https://www.frontiersin.org/articles/10.3389/fimmu.2025.1605716/full#supplementary-material

SUPPLEMENTARY FIGURE 1
Distribution of $CD4^+$ T naïve (Tn), effector (Teff), central memory (Tcm) and effector memory (Tefm) subsets in a cohort of pediatric liver recipients grouped by age ranges across each follow-up period: pre-transplantation (PreTx) and 1, 3, 6, 9 and 12 months post-transplantation (1M, 3M, 6M, 9M and 12M, respectively).

SUPPLEMENTARY FIGURE 2
Distribution of $CD8^+$ T naïve (Tn), effector (Teff), central memory (Tcm) and effector memory (Tefm) subsets in a cohort of pediatric liver recipients grouped by age ranges across each follow-up period: pre-transplantation (PreTx) and 1, 3, 6, 9 and 12 months post-transplantation (1M, 3M, 6M, 9M and 12M, respectively).

References

1. Adams DH, Sanchez-Fueyo A, Samuel D. From immunosuppression to tolerance. *J Hepatol.* (2015) 62:S170–85. doi: 10.1016/j.jhep.2015.02.042

2. Adam R, Karam V, Delvart V, O'Grady J, Mirza D, Klempnauer J, et al. Evolution of indications and results of liver transplantation in Europe. A report from the European Liver Transplant Registry (ELTR). *J Hepatol.* (2012) 57:675–88. doi: 10.1016/j.jhep.2012.04.015

3. Ghelichi-Ghojogh M, Rajabi A, Mohammadizadeh F, Shojaie L, Vali M, Afrashteh S, et al. Survival Rate of Liver Transplantation in Asia: A Systematic Review and Meta-Analysis. *Iran J Public Health.* (2022) 51:2207–20. doi: 10.18502/ijph.v51i10.10979

4. Jain A, Mazariegos G, Kashyap R, Kosmach-Park B, Starzl TE, Fung J, et al. Pediatric liver transplantation: A Single Center Experience Spanning 20 Years1. *Transplantation.* (2002) 73:941–7. doi: 10.1097/00007890-200203270-00020

5. Jara P, Hierro L. Trasplante hepático infantil. Resultados a largo plazo. *Gastroenterología y Hepatología.* (2010) 33:398–410. doi: 10.1016/j.gastrohep.2009.11.004

6. Singer A, Locke JE, Singer A. Evolving concepts in the selection of immunosuppression regimen for liver transplant recipients. *HMER.* (2011) 3(3):53-62. doi: 10.2147/HMER.S13682

7. Baumann U, Karam V, Adam R, Fondevila C, Dhawan A, Sokal E, et al. Prognosis of children undergoing liver transplantation: A 30-year European study. *Pediatrics.* (2022) 150:e2022057424. doi: 10.1542/peds.2022-057424

8. Goldschmidt I, Karch A, Mikolajczyk R, Mutschler F, Junge N, Pfister ED, et al. Immune monitoring after pediatric liver transplantation – the prospective ChilSFree cohort study. *BMC Gastroenterol.* (2018) 18:63. doi: 10.1186/s12876-018-0795-x

9. Zarrinpar A, Busuttil RW. Immunomodulating options for liver transplant patients. *Expert Rev Clin Immunol*. (2012) 8:565–78. doi: 10.1586/eci.12.47

10. Sood S. Immune monitoring post liver transplant. *WJT*. (2014) 4:30. doi: 10.5500/wjt.v4.i1.30

11. Lefaucheur C, Louis K, Morris AB, Taupin JL, Nickerson P, Tambur AR, et al. Clinical recommendations for posttransplant assessment of anti–HLA (Human Leukocyte Antigen) donor-specific antibodies: A Sensitization in Transplantation: Assessment of Risk consensus document. *Am J Transplantation*. (2023) 23:115–32. doi: 10.1016/j.ajt.2022.11.013

12. Baker A, Frauca Remacha E, Torres Canizales J, Bravo-Gallego LY, Fitzpatrick E, Alonso Melgar A, et al. Current practices on diagnosis, prevention and treatment of post-transplant lymphoproliferative disorder in pediatric patients after solid organ transplantation: results of ERN transplantChild healthcare working group survey. *Children*. (2021) 8:661. doi: 10.3390/children8080661

13. Cuesta-Martín de la Cámara R, Torices-Pajares A, Miguel-Berenguel L, Reche-Yebra K, Frauca-Remacha E, Hierro-Llanillo L, et al. Epstein-Barr virus-specific T-cell response in pediatric liver transplant recipients: a cross-sectional study by multiparametric flow cytometry. *Front Immunol*. (2024) 15:1479472. doi: 10.3389/fimmu.2024.1479472

14. Fukui S, Hidaka M, Fukui S, Morimoto S, Hara T, Soyama A, et al. The contribution of serum complement component 3 levels to 90-day mortality in living donor liver transplantation. *Front Immunol*. (2021) 12:652677. doi: 10.3389/fimmu.2021.652677

15. Iovino L, Taddei R, Bindi ML, Morganti R, Ghinolfi D, Petrini M, et al. Clinical use of an immune monitoring panel in liver transplant recipients: A prospective, observational study. *Transplant Immunol*. (2019) 52:45–52. doi: 10.1016/j.trim.2018.11.001

16. Carbone J, Micheloud D, Salcedo M, Rincon D, Bañares R, Clemente G, et al. Humoral and cellular immune monitoring might be useful to identify liver transplant recipients at risk for development of infection. *Transplant Infect Dis*. (2008) 10:396–402. doi: 10.1111/j.1399-3062.2008.00329.x

17. Simon AK, Hollander GA, McMichael A. Evolution of the immune system in humans from infancy to old age. *Proc R Soc B*. (2015) 282:20143085. doi: 10.1098/rspb.2014.3085

18. Shaw ER, Su HC. The influence of immune immaturity on outcome after virus infections. *J Allergy Clin Immunol Pract*. (2021) 9:641–50. doi: 10.1016/j.jaip.2020.11.016

19. Díaz Fernández C, Gámez Arance M, de la Vega Bueno A, Frauca Remacha E. Trasplante hepático pediátrico: indicaciones, técnicas quirúrgicas, complicaciones y tratamiento. *Anales Pediatría*. (2004) 60:42–55. doi: 10.1016/S1695-4033(04)78216-8

20. Van Delden C, Stampf S, Hirsch HH, Manuel O, Meylan P, Cusini A, et al. Burden and timeline of infectious diseases in the first year after solid organ transplantation in the Swiss transplant cohort study. *Clin Infect Diseases*. (2020) 71:e159–69. doi: 10.1093/cid/ciz1113

21. Demetris AJ, Bellamy C, Hübscher SG, O'Leary J, Randhawa PS , Feng S, et al. 2016 Comprehensive update of the Banff working group on liver allograft pathology: introduction of antibody-mediated rejection. *Am J Transplant*. (2016) 16:2816–35. doi: 10.1111/ajt.13909

22. Shearer WT, Rosenblatt HM, Gelman RS, Oyomopito R, Plaeger S, Stiehm ER, et al. Lymphocyte subsets in healthy children from birth through 18 years of age. *J Allergy Clin Immunol*. (2003) 112:973–80. doi: 10.1016/j.jaci.2003.07.003

23. Rich RR, Fleisher TA, Schroeder HW, Weyand CM, Corry DB, Puck J eds. *Clinical immunology: principles and practice. Sixth edition*. Amsterdam, The Netherlands: Elsevier (2023). 1279 p.

24. Pawlowska J, Michalkiewicz J, Czubkowski P, Jankowska I, Teisseyre M, Socha P, et al. Reduction of naive CD4/CD45RA+ T cells in children with biliary atresia before and after liver transplantation. *Transplant Proc*. (2003) 35:3026–8. doi: 10.1016/j.transproceed.2003.10.088

25. Möhring T, Karch A, Falk CS, Laue T, D'Antiga L, Debray D, et al. Immune status in children before liver transplantation—A cross-sectional analysis within the chilsSFree multicentre cohort study. *Front Immunol*. (2019) 10:52. doi: 10.3389/fimmu.2019.00052

26. Lario M, Muñoz L, Ubeda M, Borrero MJ, Martínez J, Monserrat J, et al. Defective thymopoiesis and poor peripheral homeostatic replenishment of T-helper cells cause T-cell lymphopenia in cirrhosis. *J Hepatol*. (2013) 59:723–30. doi: 10.1016/j.jhep.2013.05.042

27. Mozer-Glassberg Y, Shamir R, Steinberg R, Kadmon G, Har-Lev E, Mor E, et al. Hypogammaglobulinemia in the early period after liver transplantation in children. *Clin Transplant*. (2013) 27:E289-294. doi: 10.1111/ctr.12116

28. Fernández-Ruiz M, López-Medrano F, Allende LM, Andrés A, García-Reyne A, Lumbreras C, et al. Kinetics of peripheral blood lymphocyte subpopulations predicts the occurrence of opportunistic infection after kidney transplantation. *Transpl Int*. (2014) 27:674–85. doi: 10.1111/tri.2014.27.issue-7

29. Garcia-Prat M, Álvarez-Sierra D, Aguiló-Cucurull A, Salgado-Perandrés S, Briongos-Sebastian S, Franco-Jarava C, et al. Extended immunophenotyping reference values in a healthy pediatric population. *Cytometry Part B Clinical*. (2019) 96:223–33. doi: 10.1002/cyto.b.21728

30. Martin SR, Atkison P, Anand R, Lindblad AS, SPLIT Research Group. Studies of Pediatric Liver Transplantation 2002: patient and graft survival and rejection in pediatric recipients of a first liver transplant in the United States and Canada. *Pediatr Transpl*. (2004) 8:273–83. doi: 10.1111/j.1399-3046.2004.00152.x

31. Goldschmidt I, Chichelnitskiy E, Rübsamen N, Jaeger VK, Karch A, D'Antiga L, et al. Diagnosing acute cellular rejection after paediatric liver transplantation—Is there room for interleukin profiles? *Children*. (2023) 10:128. doi: 10.3390/children10010128

32. Kerkar N, Yanni G. *De novo*" and "recurrent" autoimmune hepatitis after liver transplantation: A comprehensive review. *J Autoimmun*. (2016) 66:17–24. doi: 10.1016/j.jaut.2015.08.017

33. Liberal R, Vergani D, Mieli-Vergani G. Recurrence of autoimmune liver disease and inflammatory bowel disease after pediatric liver transplantation. *Liver Transpl*. (2016) 22:1275–83. doi: 10.1002/lt.24490

34. Taddei R, Riccardi N, Tiseo G, Galfo V, Biancofiore G. Early intra-abdominal bacterial infections after orthotopic liver transplantation: A narrative review for clinicians. *Antibiotics (Basel)*. (2023) 12:1316. doi: 10.3390/antibiotics12081316

35. Kim YJ, Kim SI, Wie SH, Kim YR, Hur JA, Choi JY, et al. Infectious complications in living-donor liver transplant recipients: a 9-year single-center experience. *Transpl Infect Dis*. (2008) 10:316–24. doi: 10.1111/j.1399-3062.2008.00315.x

36. Righi E. Management of bacterial and fungal infections in end stage liver disease and liver transplantation: Current options and future directions. *World J Gastroenterol*. (2018) 24:4311–29. doi: 10.3748/wjg.v24.i38.4311

37. Camacho PMP, Osorio VB, Cárdenas DFC, García MAA, Tarapués EM, Torres-Cánchala L, et al. Infectious complications in pediatric patients after liver transplantation in the first 3 months at the Fundación Valle del Lili, a Latin American transplant center. *J Liver Transplantation*. (2024) 15:100221. doi: 10.1016/j.liver.2024.100221

38. Lei H, Tian M, Zhang X, Liu X, Wang B, Wu R, et al. Expansion of double-negative T cells in patients before liver transplantation correlates with post-transplant infections. *JCM*. (2022) 11:3502. doi: 10.3390/jcm11123502

39. Fernández-Ruiz M, López-Medrano F, Romo EM, Allende LM, Meneu JC, Fundora-Suárez Y, et al. Pretransplant lymphocyte count predicts the incidence of infection during the first two years after liver transplantation: Pretransplant Lymphocyte Count and Infection. *Liver Transpl*. (2009) 15:1209–16. doi: 10.1002/lt.21833

40. Nierenberg NE, Poutsiaka DD, Chow JK, Cooper J, Price LL, Freeman RB, et al. Pretransplant Lymphopenia is a Novel Prognostic Factor in CMV and Non-CMV Invasive Infection After Liver Transplantation: Lymphopenia & infection after LT. *Liver Transpl*. (2014) 20:1497–507. doi: 10.1002/lt.23991

41. Matsushima H, Fujiki M, Sasaki K, Raj R, D'Amico G, Simioni A, et al. Biliary complications following split liver transplantation in adult recipients: a matched pair analysis on single-center experience. *Liver Transpl*. (2023) 29:279–89. doi: 10.1097/LVT.0000000000000058

42. Warny M, Helby J, Nordestgaard BG, Birgens H, Bojesen SE. Lymphopenia and risk of infection and infection-related death in 98,344 individuals from a prospective Danish population-based study. *PLoS Med*. (2018) 15:e1002685. doi: 10.1371/journal.pmed.1002685

43. Terrones-Campos C, Ledergerber B, Specht L, Vogelius IR, Helleberg M, Lundgren J. Risk of bacterial, viral, and fungal infections in patients with solid Malignant tumors treated with curative intent radiation therapy. *Adv Radiat Oncol*. (2022) 7:100950. doi: 10.1016/j.adro.2022.100950

44. Sood S, Haifer C, Yu L, Pavlovic J, Churilov L, Gow PJ, et al. A novel immune function biomarker identifies patients at risk of clinical events early following liver transplantation. *Liver Transpl*. (2017) 23:487–97. doi: 10.1002/lt.24730

frontiers | Frontiers in Immunology

TYPE Original Research
PUBLISHED 26 June 2025
DOI 10.3389/fimmu.2025.1551173

OPEN ACCESS

EDITED BY
Rita Maccario,
San Matteo Hospital Foundation (IRCCS), Italy

REVIEWED BY
Marcello Maestri,
University of Pavia, Italy
Donato Madalese,
A.O.R.N. Santobono-Pausilipon, Italy

*CORRESPONDENCE
Yang Zhou
zhouyang@ujs.edu.cn
Yu Wu
760020220423@xzhmu.edu.cn

†These authors have contributed equally to this work and share first authorship

RECEIVED 24 December 2024
ACCEPTED 02 June 2025
PUBLISHED 26 June 2025

CITATION
Haider CG, Sun B, Wang Y, Zhang Z, Cao C, Zhu Y, Abdelhak O, Huang H, Liu H, Jiang T, Dong X, Zhou Y and Wu Y (2025) Optimized multiplex PCR-NGS for comprehensive HLA genotyping in Chinese populations: resolving ambiguities at high resolution.
Front. Immunol. 16:1551173.
doi: 10.3389/fimmu.2025.1551173

Optimized multiplex PCR-NGS for comprehensive HLA genotyping in Chinese populations: resolving ambiguities at high resolution

Cuello Garcia Haider[1,2†], Binbin Sun[2†], Yinfeng Wang[1], Zhoufan Zhang[1], Changling Cao[3], Yiying Zhu[1], Ouzaouit Abdelhak[1], Huiqiang Huang[3], Haitao Liu[3], Tingya Jiang[3], Xueping Dong[4], Yang Zhou[1*] and Yu Wu[2*]

[1]School of Life Sciences, Jiangsu University, Zhenjiang, China, [2]Nephrology Department, The Affiliated Xuzhou Municipal Hospital of Xuzhou Medical University, Xuzhou, China, [3]Biostatistics, Research & Development (R&D), AlloDx Biotech (Shanghai), Co., Ltd, Shanghai, China, [4]Pediatrics Department, The Affiliated Xuzhou Municipal Hospital of Xuzhou Medical University, Xuzhou, China

Introduction: Accurate human leukocyte antigen (HLA) genotyping is critical for organ transplantation to ensure donor-recipient compatibility. Conventional methods, such as sequence-based typing (SBT), often face challenges in resolving allelic ambiguities, particularly in highly polymorphic regions of HLA loci. Therefore, this study aimed to develop 6 locus multiplex primers combined with Next-generation sequencing NGS for high-resolution of long sequenceshigh-resolution sequencing, focusing on improving sequencing depth and reducing costs.

Methods: Multiplex PCR primers targeting HLA-A, -B, -C, -DPB1, -DQB1, -DRB1 loci were designed using high-frequency alleles from public databases. PThe primers were optimized using as reference the sequencing depth across loci. The method was validated using SBT and probe capture-based targeted next-generation sequencing to evaluate its approach accuracy. Moreover, 770 samples from Chinese population were further studied to verify the allele frequency adding information about HLA types of this population.

Results: The optimized multiplex PCR-NGS sequencing showed depths within athe target range of 100-1000 with high accuracy determined in the 2ndtwo-digit ,and 4thfour-digit and six-digit HLA typing, with a reliability of ≥ 98%, ≥ 95% and ≥ 95% respectively in both methods.

Discussion: Allele digits in the HLA-class I and II loci. However, in the 6th digit of HLA-C, -DQB1, and -DRB1 the accuracy was 94.74%. The developed multiplex PCR-NGS method offers a reliable, cost-effective approach for high-resolution HLA genotyping, and may be particularly suitable for clinical studies, especially in donor-recipient matching during organ transplantation.

KEYWORDS

HLA matching, deep sequencing, next-generation sequencing, multilocus sequence typing, HLA alleles

1 Introduction

Human leukocyte antigen (HLA) genes exhibit high polymorphism across populations (1), making HLA genotyping critical for clinical research especially in organ transplantation (2, 3). Accurate HLA matching between donors and recipients is crucial to ensure optimal conditions for the recipient (4). Currently, techniques such as Sanger sequencing-based typing (SBT) (5), probe capture-based targeted next-generation sequencing (PCT-NGS) (6), and multiplex PCR-based next generation sequencing (MP-NGS) of HLA loci (7) are used for determining HLA alleles.

In HLA typing, the SBT method was considered the gold standard for HLA genotyping from 1996 until 2016 for the incorporation of next-generation sequencing (NGS) (8, 9); it was widely recognized for accurate matching. SBT has certain limitations, including ambiguity resulting from the combination of two or more different alleles (10); moreover, SBT is designed to amplify short targets of the genome, primarily focusing on exons (11, 12), excluding intron and non-coding regions both important in HLA classification. Additionally, HLA has different polymorphic regions that SBT cannot determine and could be identical in *cis* or *trans* sequencing (13). Thus, accurate HLA typing cannot be achieved in these cases. Prior to the development of more advanced techniques, other methods were designed to identify alleles for HLA loci such as PCR-based HLA typing using sequence-specific primers (SSP) and sequence-specific oligonucleotide probes (SSOP); nonetheless, SSP and SSOP are less detailed compared to SBT (14–16).

In 2011, NGS was considered a novel method for advancing immunogenetics (17); however, it was not until 2016 that researchers demonstrated the functionality and reliability of high-resolution sequencing, heralding the beginning of a new gold standard for HLA typing (8, 18). In recent years, however, PCT-NGS (19) and MP-NGS for HLA genotyping have become the focus of investigations due to their high resolution in HLA typing (20) and their ability to resolve the allelic ambiguity in polymorphic HLA regions. MP-NGS may study large genomic regions of HLA genes including exons, introns, and non-coding regions with high depth, reducing errors in the assignment of alleles conferring high precision and resolving ambiguous calls (21, 22), compared to SBT, SSP, and SSOP, which may ignore important information due to its reliance on short-range PCR. Current multiplex PCR kits designed to study HLA loci are tailored to cover each allele independently. Therefore, their primers cannot be mixed to amplify different loci in the same PCR mixture; in contrast, PCT-NGS has the advantage of probe coverage; moreover, it has been demonstrated to exhibit relatively low standards for DNA quality (19). Nevertheless, PCT-NGS needs a longer experimental process and furthermore requires higher DNA concentrations.

This study is valuable because it describes a stable PCR approach, capable of simultaneously amplifying HLA-A, -B, -C, -DQB1, -DRB1, and -DPB1 loci using a one-tube multiplex PCR setup. Therefore, we developed a high-resolution HLA genotyping assay integrating multiplex PCR and high-fidelity NGS, which markedly enhanced sequencing library efficiency. In addition, this process was initially carried out to optimize the sequencing time and the operation of the PCT-NGS method on the Illumina platform since it is costly and time-consuming. Consequently, MP-NGS has adopted this approach based on the available techniques to develop a better methodology and ensure a reliable amplification of HLA-A, -B, -C, -DQB1, -DRB1, and -DPB1 alleles for individual genotypes in Chinese samples.

2 Materials and method

2.1 Design of multiplex PCR primers

The aim of this experimental study was to design and apply specific primers in a multiplex PCR to amplify the HLA-A, -B, -C, -DRB1, -DQB1, and -DPB1 loci (Figure 1), which are important subtypes in the Chinese population (23). Therefore, the primers were designed to amplify samples with high stability, thus avoiding dimers. GenBank, EMBL, and DDBJ, as well as the genome

Abbreviations: HLA, human leukocyte antigen; MP-NGS, Multiplex PCR-based next-generation sequencing; PTC-NGS, probe capture-based targeted next-generation sequencing; SBT, sequence-based typing; SSP, sequence-specific primers; SSOP, sequence-specific oligonucleotide probes; NGS, next-generation sequencing; gDNA, genomic DNA; SNP, single nucleotide polymorphism; UTR, untranslated region.

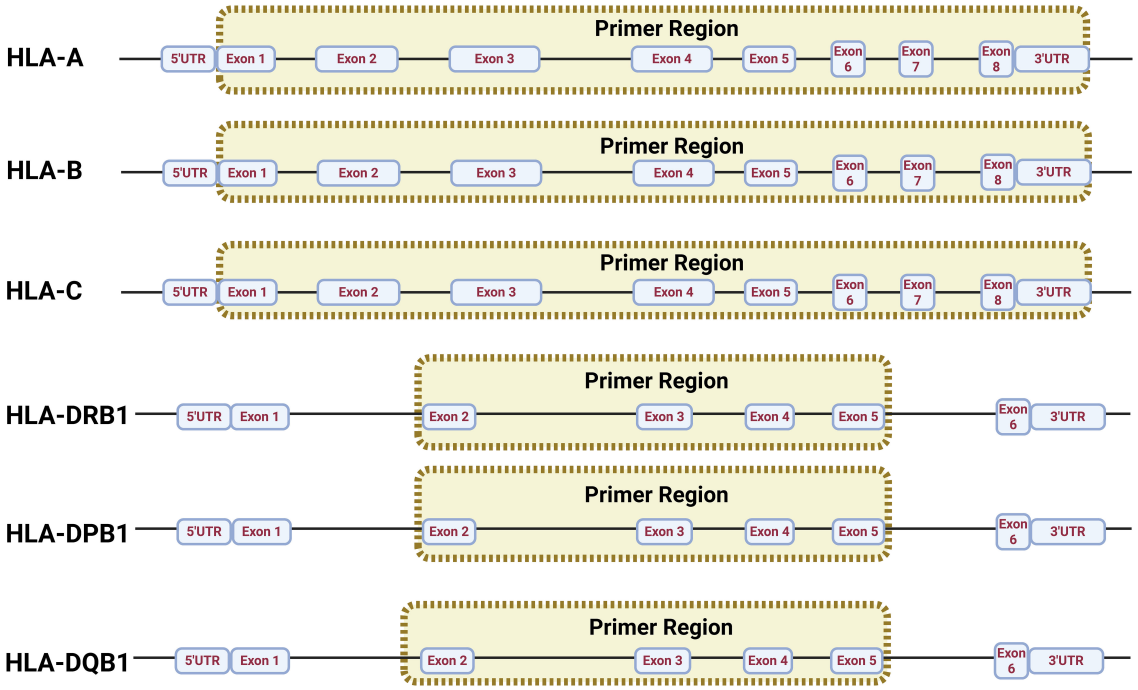

FIGURE 1
Multiplex PCR primer design principle in HLA loci.

sequence data published on the website (https://www.ebi.ac.uk/ipd/imgt/hla/), were employed to identify high-frequency HLA loci (Supplementary Table A). Subsequently, MEGA 11.0 was employed to align the loci and select primer cohorts that can match in high percentage the HLA loci reported for the Chinese population with a frequency of at least 98.5%. In addition, the resulting length designed for the target products was in the range of 2,000–6,000 bp.

2.2 Multiplex PCR and sequencing library creation

2.2.1 First step: amplification of HLA loci

The multiplex PCR amplification of target amplicons was performed using gDNA, and it was extracted using the QIAamp kit (QIAGEN, Hilden, Germany) according to the manufacturer's instruction (Figure 2A); Qubit 4.0 (Thermo Fisher Scientific, Waltham, Massachusetts, USA) was used to measure the sample DNA concentration. During the preparation of the DNA library (Figure 2B), 50 ng of DNA was employed in a 25-μL reaction system and was used to amplify the HLA regions adding 4 μL of the primer mix and 12.5 μL of NUHI® Pro NGS PCR Mix (Xinhai Biotechnology Co., Ltd, Suzhou, China). Primer sets covering HLA type I and HLA type II were mixed into a multiplex PCR primer pool with the following concentrations: HLA-A (0.04 μM), HLA-B (0.1 μM), HLA-C (0.15 μM), HLA-DQB1 (0.18 μM), HLA-DRB1 (0.07 μM), and HLA-DPB1 2-35 (0.04 μM), in accordance with a suitable depth ratio. Multiplex PCR parameters for the first round of target gene amplification were as follows: first step, 95°C for 10.5 min; second step, 98°C for 0.17 min at denaturation, 63°C for 1 min at hybridization, 72°C for 5 min for 30 cycles; third step, 72°C for 5 min at elongation; finally, the sample was maintained at 4°C for storage (Figure 2B1).

2.2.2 Second step: DNA fragmentation of HLA loci

After PCR, in a total volume of 30 μL, 40 ng of the PCR product was used in optimal concentration, and 5 μL of Hieff Smearase (YEASEN Biotech Co., Ltd, Shanghai, China) was employed to cleave and fragment the DNA (Figure 2B2). Moreover, the PCR conditions for this reaction were 4°C for 1 min, 30°C for 20 min, and 72°C for 20 min.

2.2.3 Third step: adapter ligation in DNA library preparation

The fragmented DNA product with a size of 250–350 bp was obtained, and it was linked with a specific adapter to identify the sample in the mixture during sequencing. Therefore, 15 μL of Rapid Ligation buffer, 2.5 μL of Rapid DNA Ligase, and 2.5 μL of adapter (all from YEASEN Biotech Co., Ltd, Shanghai, China) were added to the product of the second step. Moreover, the adapters were ligated using a temperature of 20°C for 20 min using the thermal cycler (Figure 2B3). After the ligation product, the DNA was purified using Hieff NGS® DNA Selection Beads, and thus, another PCR was performed in a total volume of 25 μL; 10 μL of the purified DNA was added to the 12.5 μL of 2× Canace Pro Amplification Mix from Hieff NGS DNA Library Prep Kit 2.0 (YEASEN Biotech Co., Ltd, Shanghai, China) and 2.5 μL of the PCR primer mix from the MGIEasy Universal DNA Library Conversion Kit (App-A) (MGI Tech Co., Ltd,

Shenzhen, China) (Figure 2B4). After PCR, it was necessary to purify the product again using magnetic beads, and then the concentration of the purified DNA was quantified to confirm the existence of DNA and thus mix the samples to produce the DNA library, considering a range of 6–10 ng/μL as the final concentration to sequence via NGS using the MGI sequencing platform (Figure 2B5) and finishing with genotyping (Figure 2C).

2.3 Evaluation of MP-NGS results

After sample sequencing, the result was filtered of low-quality and contaminated samples; moreover, sequencing junctions were removed using Cutadapt (https://cutadapt.readthedocs.io/en/stable/#cutadapt). These filtered reads were compared to an integrated genome (containing the human genome reference GRCh38, eight MHC

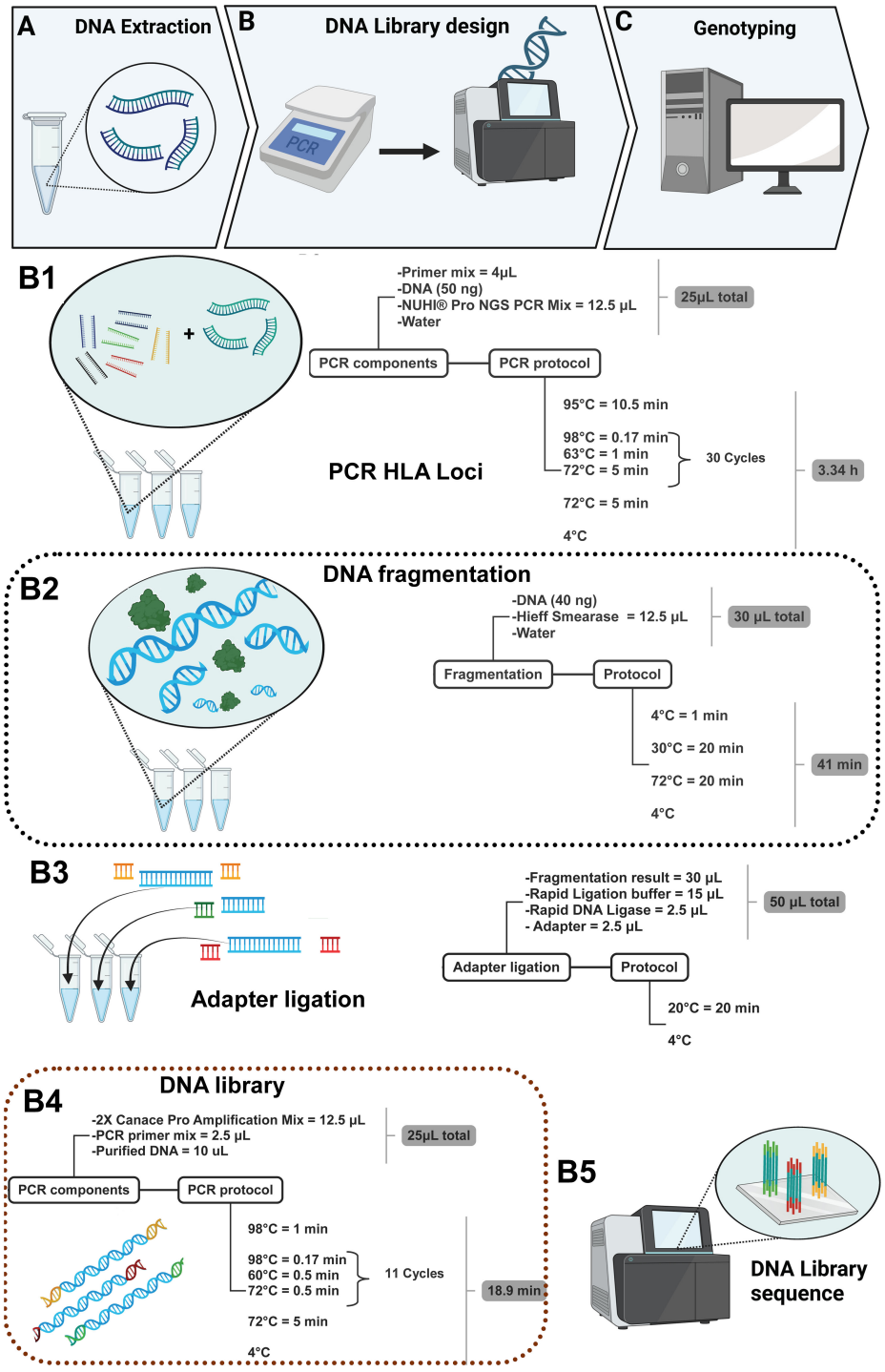

FIGURE 2
DNA library construction method for six loci in 770 samples.

haplotypes, and the human genome reference GRCh38) using BWA (http://bio-bwa.sourceforge.net) to order the fragmented amplicons to recover the original sequence amplified. The HLA-LA tool (24) was used for HLA genotyping using the database of HLA-alleles from IPD-IMGT/HLA (https://www.ebi.ac.uk/ipd/imgt/hla/) (24) for allele identification.

2.4 Optimization of multiplex PCR conditions and deep homogenization of NGS sequencing

For the purpose of obtaining sufficient information, each primer concentration was quantified automatically using the software HLA-LA by depth count (Equation 1), by genotyping the samples to establish a range of 100–1000× for an accurate assay. Therefore, prior to optimization, the concentration of each primer was 0.2 µM, and this was adjusted until an optimal depth count is achieved; the primer concentration was in the range of 0.04–0.5 µM based on the suggestions of Henegariu et al. (25) when performing a stable multiplex PCR. Therefore, higher depth was corrected by decreasing primer concentration, considering that using an identical primer concentration for amplicons of different lengths may introduce imbalances in the reaction.

$$Depth = \frac{Number\ \ of\ \ reads * Average\ \ reading\ \ length}{Length\ \ of\ \ the\ \ target\ \ region} \quad (1)$$

- Number of reads: HLA-LA reads the BAM file and counts how many aligned records are in the target region.
- Average read length: HLA-LA adds up each read in the target region measured in bp and then it is divided by the total number of aligned reads.
- Length of the target region: HLA-LA determines the beginning and end of the region and subtracts: Length = end − start + 1.

2.5 Evaluation of SBT

SBT analysis was performed for the purpose of evaluating the reliability of NGS for the genotyped samples. The analysis employs a PCR of HLA class I (A, B, and C) in exons 2 and 3, and of HLA class II (DR, DQ, and DP) in exon 2 (26, 27) of 70 samples. Moreover, Biopython was employed to align the database of IPD-IMGT/HLA with the correspondent sample analyzed. Furthermore, the SNP profile was also determined between the samples and the sequences of the database reference with fewer variations. However, it is necessary to use high-quality sequences to generate this procedure, since Sanger sequencing results with peaks at low levels of fluorescence can produce wrong results (28).

2.6 Evaluation of PCT-NGS

Hybridization capture was performed using the ProbeCap® system (Homgen Biotechnology, China), based on DNA probes developed for Illumina and MGI platforms. The same set of 70 samples previously used for the SBT study were applied to this PCT-NGS approach. Therefore, it was necessary for the capture to

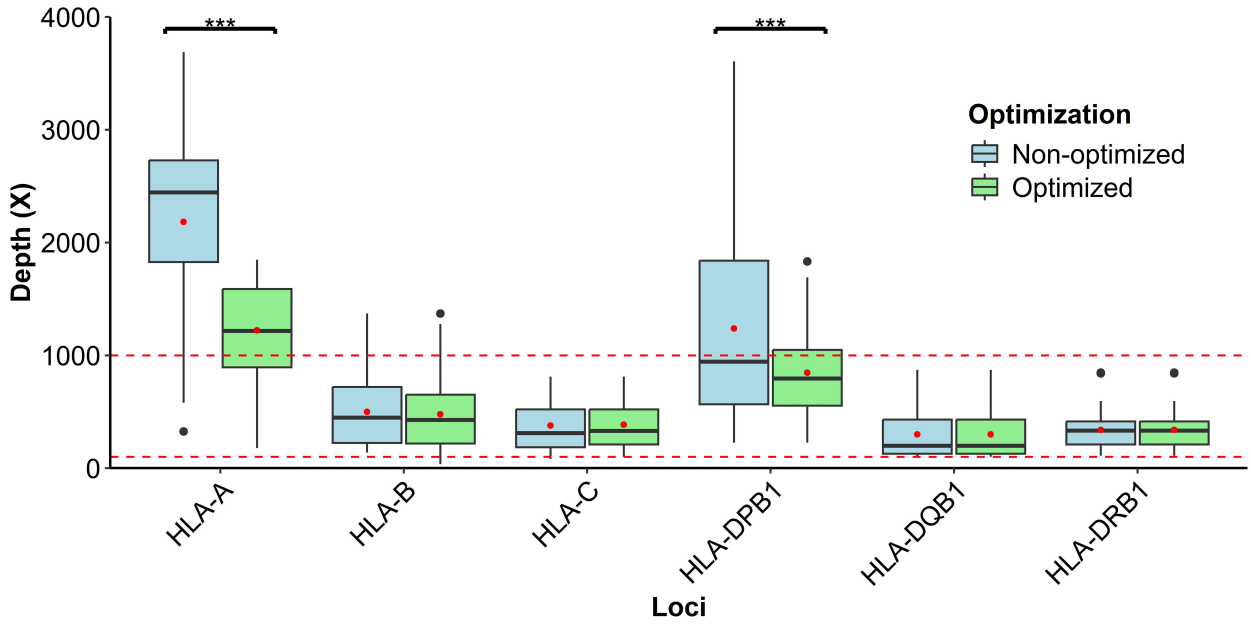

FIGURE 3
Depth distribution analysis of HLA primer optimization within the defined interval permissible of 100–1,000×, considering that each red point inside the box is the respective average study of loci; moreover, asterisks represent highly significant *p*-values ($p < 0.01$).

10.3389/fimmu.2025.1551173

employ 500 ng of each library, 5 μL of human cot-1 DNA, and 2 μL of MGI blocker; thereafter, this mix was evaporated at 55–60°C; each sample was resuspended in 10 μL of hybridization buffer (HYB-Buffer), 2 μL of enhancer, and 2 μL of probes thereafter; and water was added until a total volume of 16 μL was reached. The hybridization protocol was as follows: 95°C for denaturation for 5 min and then 65°C for 3 h for the respective hybridization.

When the hybridization protocol ended, it was necessary to add 16 μL of hybridization beads; thereafter, each sample was incubated at 65°C for 30 min with mixing every 10 min to capture the biotinylated probes hybridized to the target DNA. subsequently washing protocol was necessary to pre hot the Wl and S-W at 65°C, following 120 μL of WI was added for 10 s, later 150 μL of S-W for 5 min, thereafter 150 μL of WI , WII, WIII were added for 10 s, considering take each wash before adding the next respectively, and then resuspend the beads in 23 μL of ddwater. The product was amplified (POST-PCR) using 25 μL of 2× HIFI enzyme, 2 μL of adapters, and 23 μL of the microbeads suspended in dd water; thereafter, this mix was amplified using the PCR protocol of 98°C for 45 s, 98°C for 15 s, 50°C for 30 s, 72°C for 30 s for 12 cycles, and 72°C for 1 min, considering a 4°C hold. After PCR, it was necessary to perform a new purification using DNA clean beads by adding 25 μL of water to elute the sample from microbeads.

2.7 Statistics

R-statistics 4.4.3 was employed for statistical analysis using the depth count of the sequence to compare pre- and post-optimization, with each value obtained by the HLA-LA genotyping of MP-NGS; the Wilcoxon signed-rank test ($p < 0.05$) was used to study the significant differences of each locus of 40 random samples. Furthermore, ggplot2 version 3.5.1 was selected for illustrating a box-and-whisker plot to visualize their distribution. Moreover, the HLA class I and II loci frequencies were determined by counting via the same program using 770 patients requiring organ transplantation; in addition, samples were provided from the databank of AlloDx (Shanghai) Biotech Co., Ltd., and rare alleles were determined using the web site http://www.allelefrequencies.net, which includes HLA frequency data.

TABLE 1 Timing information for post-PCR to sequencing.

Processing time	Step	Time
Library Preparation	Multiplex PCR	3.5 h
	DNA fragmentation	0.75 h
	Native barcode ligation	0.42 h
	DNA purification	1 h
	Total library prep time	5.67 h
Sequencing and Analysis	Sequencing	24 h
	Base calling, demultiplexing, consensus, and genotyping	4 h
	Total sequencing and analysis time	28 h
Total Time		33.67 h

Furthermore, homozygosity and heterozygosity assessment was rigorously performed for all samples included in the frequency analysis. This was ensured by maintaining sufficient sequencing depth and high-quality thresholds to decrease allelic dropout and sequencing errors (29); in addition, Integrative Genomics Viewer (IGV) was used to validate the results of the invalidation set. Additionally, the accuracy of six-locus NGS genotyping was determined using Equation 2 with SBT and PCT-NGS results, and the reliability of the methodology has been verified using 70 randomly selected samples in parallel with MP-NGS.

$$Accuracy = \frac{number\ of\ concordant\ allele\ (MP-NGS = SBT\ or\ PCT-NGS)}{concordant\ allele + discordant\ allele} \quad (2)$$

3 Results

3.1 Multiplex PCR primers and experimental optimization

Prior to formal sample validation, we performed normalization adjustments to the sequencing depth through the primer concentrations in the multiplex PCR primer pool and the initial DNA input. The analysis of Wilcoxon signed-rank test demonstrated the influence of altering primer concentration on the measured values for HLA-A (2,444.04 vs. 1,215.59, p-value = $1.179e^{-05}$) and HLA-DPB1 (1,032.43 vs. 794.41, p-value = 0.00244). However, no significant differences were observed in the HLA-B (447.56 vs. 427.10, p-value = 0.4227), HLA-C (310.35 vs. 330.09, p-value = 0.83), HLA-DQB1 (198.12 vs. 196.12, p-value = 0.86), and HLA-DRB1 (332.17 vs. 334.171, p-value = 0.83) loci. Moreover, our result showed a depth range within 100–1,000 for the multiplex PCR (Figure 3). Therefore, post-optimization, a significant decrease in depth was observed in both HLA-A and HLA-DPB1 loci, although HLA-A was out of the established limit. On the other hand, the loci HLA-B, HLA-C, HLA-DQB1, and HLA-DRB1 remained similar before and after modification, and despite variations in primer concentration at loci B, C, DQB1, and DRB1, the sequencing depth remained within the optimal range for robust data analysis.

For the time employed to perform the HLA genotyping results, it was determined that for the library preparation, the time required was 5.67–6 h, while sequencing and bioinformatic analysis were generated at ~28 h. Consequently, the total time used to finish the experiment was 33.67–40 h (Table 1), considering that the requisite time depended on the sample size analyzed. Thus, this time lapse may faithfully explain a group of ~5 samples.

3.2 Comparison of MP-NGS results on PCT-NGS and SBT results

The comparison of 70 samples mapping using NGS vs. SBT and NGS vs. PCT-NGS determined the accuracy of HLA loci genotyped

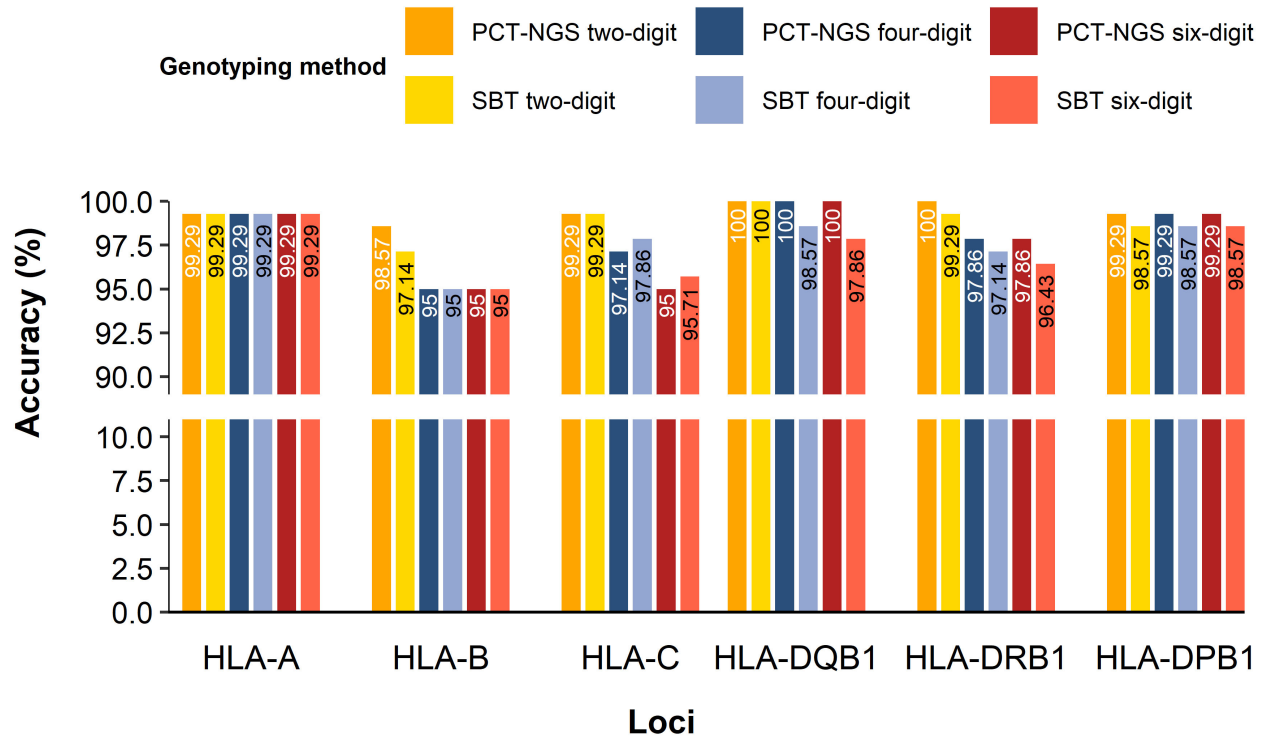

FIGURE 4
HLA class I and II accuracy for MP-NGS genotyping for two-digit, four-digit, and six-digit.

for MP-NGS methodology. HLA-A showed a concordance rate of 99.29% in both MP-NGS vs PTC-NGS and MP-PCR vs SBT comparisons, across two-digit, four-digit, and six-digit typing resolutions. HLA-B presented different accuracies in different methods; for PCT-NGS, the two-digit typing resolution showed 98.57% confidence. However, SBT reached 97.14%; moreover, at the four-digit HLA typing, both methods showed 95% accuracy, and the six-digit reliability remained at 95% for both methods. For HLA-C, two-digit accuracy was 99.29% for both methods, at the four-digit, PCT-NGS describes 97.14% of confidence, whereas SBT slightly outperformed it with 97.86%; in the six-digit, PCT-NGS showed 95% concordance and SBT showed 95.71%. In class II HLA loci, specifically HLA-DQB1, PCT-NGS showed 100% confidence in the two-digit, four-digit, and six-digit. Using the SBT method, the two-digit had 100% confidence, the four-digit had 98.57% confidence, and the six-digit had 97.86% confidence. For HLA-DRB1, the two-digit showed 100% matching using the PCT-NGS method; however, SBT results described 99.26% accuracy for the same digit; at the four-digit, accuracy was 97.86% using PCT-NGS and 97.14% using SBT, while the six-digit had an accuracy of 97.86% with PCT-NGS and 96.43% with SBT. For HLA-DPB1, 99.29% precision was found in two-digit, four-digit, and six-digit using PCT-NGS; moreover, the reliability of SBT for two-digit, four-digit, and six-digit showed 98.57% (Figure 4). These results confirm a high overall reliability of MP-NGS genotyping, with small variations between traditional SBT and PCT-NGS methods across loci and resolution levels.

Consequently, allele frequencies for PCT-NGS, SBT, and MP-NGS alleles were compared (Table 2), with few exceptions; NGS provided unambiguous allele assignments at the three-field level at high accuracy within the permitted limits. Ambiguities observed were among the highly polymorphic loci. At HLA-A, a single allele mismatch was observed. For HLA-B, six alleles differed using different methods; however, one allele observed was matched using PCT-NGS, but SBT showed an ambiguous result, with other alleles, analyzed by SBT, showing concordant alleles, but the alleles diverged using PCT-NGS. For HLA-C, six alleles had ambiguous NGS assignments; moreover, sample number 10 differed from SBT. However, its result matched with that of PCT-NGS, and sample number 12 typed with SBT and MP-NGS described a perfect match, but showed mismatch using PCT-NGS.

In the HLA-DQB1 locus, three ambiguous alleles were found, and although those ambiguous NGS assignments were confirmed in parallel with SBT, using the PCT-NGS method, the MP-NGS results matched. For HLA-DRB1, which is the most polymorphic of the class II group, there were five ambiguous NGS results; four alleles presented mismatches using SBT as reference; moreover, the allele at position 25 was different using both methods. For HLA-DPB1, two ambiguous mismatches were determined; the allele comparison at position 26 showed a mismatch using SBT; however, using PCT, it was possible to observe a respective match.

Upon analysis of the results, the observed ambiguities were attributed to the causes detailed in Table 3. For the HLA-A locus,

10.3389/fimmu.2025.1551173

TABLE 2 Alleles with differences between SBT, PCT-NGS, and MP-NGS analysis.

#	MP-NGS		SBT		PCT-NGS	
	Allele 1	Allele 2	Allele 3	Allele 4	Allele 5	Allele 6
1	A*33:03:01	A*30:13	A*33:03:01	A*68:18N	A*33:03:01	A*31:01:02
2	B*46:01:01	B*14:02:01	B*46:01:01	B*46:01:01	B*46:01:01	B*14:02:01
3	B*13:02:01	B*15:34	B*13:02:01	B*15:400N	B*13:02:01	B*15:01:01
4	B*18:01:01	B*40:83	B*18:01:01	B*07:02:01	B*18:01:01	B*40:06:01
5	B*35:01:01	B*35:01:01	B*35:01:01	B*40:256N	B*35:01:01	B*40:06:01
6	B*40:01:01	B*40:130:02	B*40:01:01	B*40:506N	B*40:01:01	B*40:06:01
7	B*13:01:01	B*13:01:01	B*13:01:01	B*40:506N	B*13:01:01	B*40:06:01
8	B*40:20	B*46:01:01	B*40:20	B*46:01:01	B*40:06:01	B*46:01:01
9	B*07:05:01	B*40:120	B*07:05:01	B*40:506N	B*07:05:01	B*40:06:01
10	C*01:02:01	C*01:02:01	C*01:02:01	C*01:02:02	C*01:02:01	C*01:02:01
11	C*02:02:03	C*03:04:01	C*02:02:02	C*03:04:01	C*02:02:02	C*03:04:01
12	C*03:04:26	C*14:02:01	C*03:04:26	C*14:02:01	C*03:04:01	C*14:02:01
13	C*03:02:01	C*03:151	C*03:02:01	C*03:316N	C*03:02:01	C*03:03:01
14	C*12:02:01	C*14:02:02	C*12:02:01	C*14:02:01	C*12:02:01	C*14:02:01
15	C*04:140	C*06:02:01	C*04:09N	C*06:02:01	C*06:02:01	C*06:02:01
16	C*01:67	C*03:04:01	C*07:02:01	C*03:04:01	C*01:02:01	C*03:04:01
17	C*01:67	C*08:03:01	C*01:67	C*08:03:01	C*01:02:01	C*08:03:01
18	DQB1*06:01:01	DQB1*06:02:01	DQB1*06:02:01	DQB1*06:02:01	DQB1*06:01:01	DQB1*06:02:01
19	DQB1*03:01:01	DQB1*03:03:02	DQB1*03:03:02	DQB1*03:03:02	DQB1*03:01:01	DQB1*03:03:02
20	DQB1*05:01:01	DQB1*05:03:01	DQB1*05:01:45	DQB1*05:03:01	DQB1*05:01:01	DQB1*05:03:01
21	DRB1*08:03:02	DRB1*12:02:01	DRB1*08:03:02	DRB1*12:02:02	DRB1*08:03:02	DRB1*12:02:01
22	DRB1*12:01:01	DRB1*12:02:01	DRB1*12:01:01	DRB1*12:01:01	DRB1*12:01:01	DRB1*12:02:01
23	DRB1*03:01:01	DRB1*04:09	DRB1*03:01:01	DRB1*04:20	DRB1*03:01:01	DRB1*04:05:01
24	DRB1*15:01:01	DRB1*15:02:01	DRB1*15:01:01	DRB1*04:20	DRB1*15:01:01	DRB1*15:01:01
25	DRB1*04:24	DRB1*09:01:02	DRB1*04:20	DRB1*09:01:02	DRB1*04:05:01	DRB1*09:01:02
26	DPB1*02:01:02	DPB1*05:01:01	DPB1*02:01:02	DPB1*02:01:02	DPB1*02:01:02	DPB1*05:01:01
27	DPB1*100:01	DPB1*02:01:02	DPB1*02:01:02	DPB1*02:01:02	DPB1*05:01:01	DPB1*02:01:02

ambiguities were associated with PCR-induced artifacts. In the case of HLA-B, the ambiguities resulted from inserted sequences detected in the SBT analysis, PCR-induced artifacts due to amplification cycles, allele-specific amplification bias, and erroneous allele calls. For the HLA-C locus, regions not covered by primers, particularly at the UTR boundaries, as well as PCR-induced artifacts and incorrect allele assignments were identified as contributing factors. At the HLA-DQB1 locus, discrepancies in SBT were attributed to SNPs likely introduced by PCR artifacts. For HLA-DRB1, both regions not covered by SBT and PCR-induced artifacts were observed. In the case of HLA-DPB1, ambiguities were also linked to coverage gaps and PCR-induced artifacts.

3.3 Frequencies in the Chinese population

3.3.1 Allelic frequency of HLA class I and II

Regarding the frequency analysis of 770 genotyped patients (Figure 5), a total of 13 alleles showed high frequency: 5 were identified for HLA class I and 8 for HLA class II. HLA-A presented three alleles with a frequency above 10%: A*24:02:01 at 16.36%, A*11:01:01 at 14.35%, and A*02:01:01 at 13.90%. Additionally, for HLA-C, two alleles were identified with a frequency above 10%: C*01:02:01 at 14.87% and C*07:02:01 at 12.34%; HLA-B was observed as the most polymorphic with 97 different allelic specificities, and the allele B*13:02:01 was the most frequent at 9.29%.

10.3389/fimmu.2025.1551173

TABLE 3 Differences analyzed in the ambiguous alleles of the 70 HLA samples.

#	MP-NGS	SBT	PCT-NGS	Affected region	Cause
1	A*30:13	A*68:18N	A*31:01:02	Exon 2	PCR-induced artifacts
2	B*14:02:01	B*46:01:01	B*14:02:01	Exon 2	Sequence insertion
3	B*15:34	B*15:400N	B*15:01:01	Exon 3	PCR-induced artifacts
4	B*40:83	B*07:02:01	B*40:06:01	Exons 2 and 3	PCR-induced artifacts
5	B*35:01:01	B*40:256N	B*40:06:01	Exons 2 and 3	Quantitative imbalance in multiplex PCR amplification
6	B*40:130:02	B*40:506N	B*40:06:01	Exon 3	PCR-induced artifacts
7	B*13:01:01	B*40:506N	B*40:06:01	Exon 2	PCR-induced artifacts
8	B*40:20	B*40:20	B*40:06:01	————	Erroneous allele call
9	B*40:120	B*40:506N	B*40:06:01	Exon 3	PCR-induced artifacts
10	C*01:02:01	C*01:02:02	C*01:02:01	Introns	Region not covered
11	C*02:02:03	C*02:02:02	C*02:02:02	Exon 3	PCR-induced artifacts
12	C*03:04:26	C*03:04:26	C*03:04:01	Intron 2	PCR-induced artifacts
13	C*03:151	C*03:316N	C*03:03:01	Exons 2 and 3	PCR-induced artifacts
14	C*14:02:02	C*14:02:01	C*14:02:01	Exon 3	PCR-induced artifacts
15	C*04:140	C*04:09N	C*06:02:01	Exon 2	PCR-induced artifacts
16	C*01:67	C*07:02:01	C*01:02:01	Exon 2	Erroneous allele call and PCR-induced artifacts
17	C*01:67	C*01:67	C*01:02:01	UTR	Region not covered
18	DQB1*06:01:01	DQB1*06:02:01	DQB1*06:01:01	Exon 2	PCR-induced artifacts
19	DQB1*03:01:01	DQB1*03:03:02	DQB1*03:01:01	Exon 2	PCR-induced artifacts
20	DQB1*05:01:01	DQB1*05:01:45	DQB1*05:01:01	Exon 2	PCR-induced artifacts
21	DRB1*12:02:01	DRB1*12:02:02	DRB1*12:02:01	Out Exon 2	Region not covered
22	DRB1*12:02:01	DRB1*12:01:01	DRB1*12:02:01	Out Exon 2	Region not covered
23	DRB1*04:09	DRB1*04:20	DRB1*04:05:01	Exon 2	PCR-induced artifacts
24	DRB1*15:02:01	DRB1*04:20	DRB1*15:01:01	Exon 2	PCR-induced artifacts
25	DRB1*04:24	DRB1*04:20	DRB1*04:05:01	Exon 2	PCR-induced artifacts
26	DPB1*05:01:01	DPB1*02:01:02	DPB1*05:01:01	Exon 2	PCR-induced artifacts
27	DPB1*100:01	DPB1*02:01:02	DPB1*05:01:01	Exon 2	PCR-induced artifacts and region not covered

In class II, the locus HLA-DPB1 showed two alleles with a frequency above 10%: DPB1*05:01:01 at 37.60% and DPB1*02:01:02 at 21.36%; notably, the allele DPB1*05:01:01 was the most frequent with 579 repetitions, and HLA-DQB1 showed three alleles with a frequency above 10%: DQB1*03:01:01 at 20.91%, DQB1*03:03:02 at 14.03%, and DQB1*02:01:01 at 13.90%. Additionally, HLA-DRB1 presented three alleles with a frequency above 10%: DRB1*09:01:02 at 13.70%, DRB1*12:02:01 at 10.78%, and DRB1*07:01:01 at 10.71%. Furthermore, there was evidence that 18 patient alleles for A*24:02:01, 14 patient alleles for C*01:02:01, 113 patient alleles for DPB1*05:01:01, 40 patient alleles for DQB1*03:01:01, and 28 patient alleles for DRB1*09:01:02 were homozygous carriers. A complete table with all of the HLA class I and II frequencies is given in the Supplementary Materials (Table B).

A rare allele study presented alleles A*24:260, C*03:151, C*03:231, C*04:140, C*06:143, and C*12:55, which were the most observed (Table 4); moreover, the HLA-C locus presented a more rare polymorphism with 26 different alleles, higher than that of HLA-B with 16 and HLA-A with 9, assuming that locus C includes a larger number of rare alleles.

The rare analysis described that the alleles DRB1*09:05 and DQB1*03:69 were the most frequent at 0.268% and 0.179%, respectively, considering that the DRB1 locus was the most polymorphic locus of HLA class II with 16 rare alleles, and DQB1 presented 10 different rare alleles (Table 5).

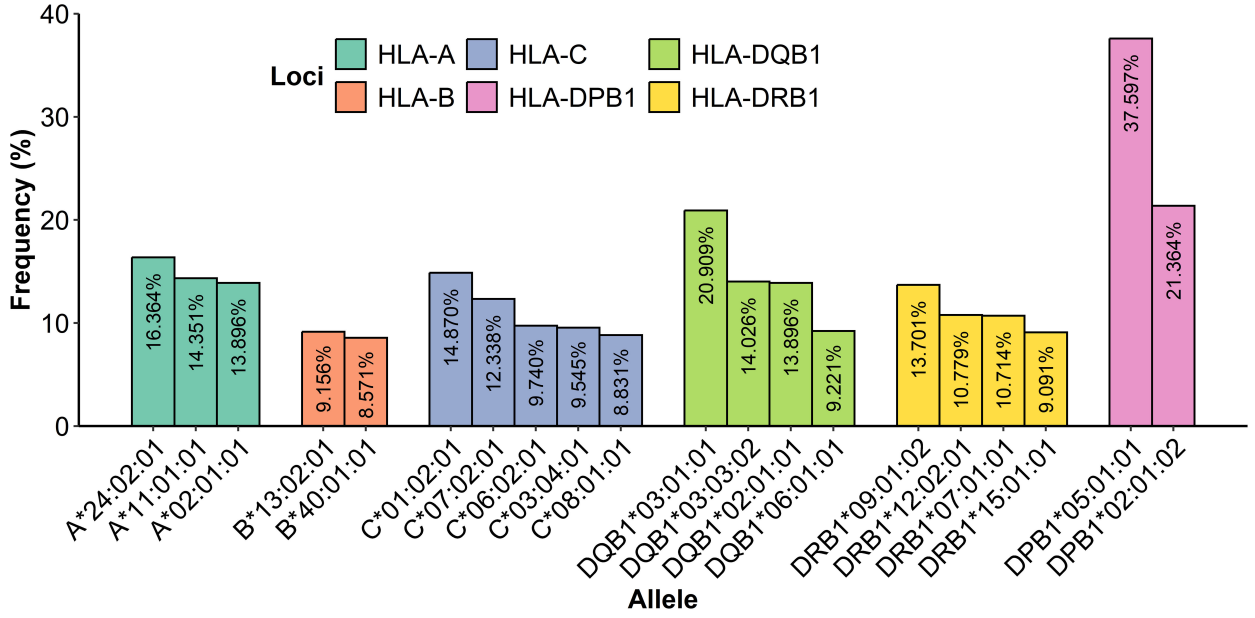

FIGURE 5
Frequency determination of alleles from HLA class I and class II most presented in 770 samples.

4 Discussion

NGS has been essential in the development of HLA genotyping in clinical histocompatibility due to its capacity to provide high-throughput and high-resolution genotypes, making it possible to reduce the time required to analyze a large number of samples and facilitate accurate studies. The multiplex long primer resolution can give determinant information to identify multiple existing alleles at low cost, compared to SBT, where screening different alleles requires preprograming multiplex PCR mixtures for only one locus. In addition, traditional methods such as SBT, SSP, and SSOP are often ambiguous in allele assignment, especially in heterozygotic samples, in contrast to NGS that can carry out precise allele assignment. Smith et al. described 21 novel sequences using NGS that were not detected by SSOP (30). Furthermore, long PCR amplification can cover significant targets of HLA loci; moreover, multiplex PCR permits the simultaneous amplification of multiple HLA loci in one mixture with a substantial reduction in production costs and processing times; this is particularly advantageous in clinical contexts, where meticulous and precise typing skills are paramount (31). Table 6 presents the advantages and limitations of MP-NGS, PCT-NGS, SBT, SSP, and SSOP. Compared to other studies, this approach validated MP-NGS using two different methods: one typically used in clinical settings as SBT (which was considered the gold standard), and PTC-NGS, which is used to avoid artifacts caused by PCR amplifications at high resolution (19). Moreover, this is the first large-scale study to perform MP-NGS covering HLA-A, -B, -C, -DPB1, -DRB1, and -DQB1, which are important for transplantation proceedings. It also provides additional information on HLA allele frequencies in the Chinese population, including rare alleles. On the other hand, Chinese HLA frequency studies using NGS have focused on screening either class I (32) or class II (33), but not both.

Based on our findings, optimizing HLA genotyping by adjusting primer concentrations in multiplex pools and verifying the read depth count of this modification using NGS sequencing can improve the accuracy of genotyping organ transplantation. Therefore, determining that 100–1,000× is suitable for accurate MP-NGS genotyping, read depth values below 100× in our study showed inconsistences due to low coverage. However, the 40 samples analyzed with the optimized primer concentration yielded consistent and reliable results, thereby ensuring suitability and compatibility between donor and recipient. Statistical analysis of the Wilcoxon test determined that HLA-A and HLA-DPB1 are sensitive to primer concentration variations. However, it was relatively tedious to handle the locus HLA-A since its reads were higher in the multiplex PCR. HLA genotyping findings have determined 100–500× as an accurate range for performing this genetic analysis (34, 35), though other research has suggested depth counts of above 53× (36), considering that exceeding this threshold may generate redundant information and increase analysis time. Furthermore, it is common to have difficulties in depth control when a long amplification multiplex PCR is ongoing since it may be affected by the respective structures of these loci. It is, however, widely recognized that HLA-A is often easy to amplify because this target is more exposed compared to other loci, in contrast to loci HLA-C and DRB1, which have been reported with lower read depth (31, 37). Therefore, this outcome is encouraging since their sequencing depth was within the limit suggested, thus determining reliable results and avoiding possible complications for less donor compatibility. Moreover, this experiment showed that the time required to perform this procedure was similar to other

10.3389/fimmu.2025.1551173

TABLE 4 Rare allele frequency determined in HLA class I.

#	HLA-A	%	HLA-B	%	HLA-C	%
1	A*24:260	0.1786	B*15:188	0.0893	C*03:151	0.1786
2	A*02:255	0.0893	B*27:05:14	0.0893	C*03:231	0.1786
3	A*02:543	0.0893	B*35:09:02	0.0893	C*04:140	0.1786
4	A*11:147	0.0893	B*35:197	0.0893	C*06:143	0.1786
5	A*11:88	0.0893	B*37:50	0.0893	C*12:55	0.1786
6	A*31:01:07	0.0893	B*46:12	0.0893	C*01:02:32	0.0893
7	A*02:112	0.0893	B*40:219	0.0893	C*01:102	0.0893
8	A*25:30	0.0893	B*51:157	0.0893	C*03:04:03	0.0893
9	A*30:11:02	0.0893	B*54:04	0.0893	C*03:04:38	0.0893
10			B*54:16	0.0893	C*03:116:01	0.0893
11			B*58:16:02	0.0893	C*03:99	0.0893
12			B*58:34	0.0893	C*03:132	0.0893
13			B*40:53	0.0893	C*04:178	0.0893
14			B*46:03	0.0893	C*06:02:43	0.0893
15			B*46:13:03	0.0893	C*06:132:01	0.0893
16			B*54:30	0.0893	C*06:147	0.0893
17					C*08:08:02	0.0893
18					C*08:16:01	0.0893
19					C*08:72:01	0.0893
20					C*12:49	0.0893
21					C*14:02:05	0.0893
22					C*14:09	0.0893
23					C*14:17	0.0893
24					C*14:18	0.0893
25					C*14:58	0.0893
26					C*14:69	0.8929

HLA genotyping reports (38) with the advantage of analyzing a large number of samples in multiple loci at high confidence; however, there are other NGS platforms that can decrease processing time.

The accuracy of NGS results showed that our method is reliable to identify clinical histocompatibility samples, since the percentage of matches at the two- and four-digit demonstrates high reliability. It is well known that the four-digit is important for transplantation compatibility, and it is usually employed in this procedure (39); therefore, this methodology meets the minimum standard for providing sufficient information in transplant procedures. A rigorous quality control pipeline for NGS genotyped was established; however, ambiguous results were observed across all three HLA typing methodologies. For instance, the sole ambiguous HLA-A result involved an insertion detected exclusively by Sanger-based sequencing (SBT). This insertion was not identified by either multiplex PCR (MP-PCR) or probe capture-based NGS (PCT-NGS). It is plausible that PCT-NGS lacked specific probes targeting this region. However, MP-PCR yielded the same result in exon 2, suggesting that the insertion might be an artifact introduced during SBT sequencing. Furthermore, the highest variability in genotyping was observed in SBT, which typically relies on exonic regions, and it is therefore more prone to incorrect allele assignments compared to MP-NGS and PCT-NGS that amplify long amplicons. PCT-NGS results are used in parallel with MP-NGS, exposing fewer mismatches than SBT. The few ambiguities identified by MP-PCR and PCT-NGS were attributed to software-related errors. Reanalysis using an alternative bioinformatics tool, HLA-HD, produced consistent results for both MP-PCR and PCT-NGS. Furthermore, in-depth examination using IGV confirmed the presence of these sequences, indicating that the discrepancies were likely due to initial software misassignments. A total of 15 ambiguous results were identified, 5 of which involved mismatches in the two-digit. Although our MP-NGS approach employs long amplicon for its genotyping, it is possible that these discrepancies come from DNA library processing, since it is well known that enzymatic fragmentation can exhibit sequence preference, potentially cleaving near important SNPs, inducing GC-containing bias, typically observed in MHC (40); another possibility is the presence of artifacts induced by the PCR reaction, which may introduce biases into the target sequence and lead to poor assignment in allele calls (41). However, the match percentage presented for the two-digit is acceptable since it is above 98%, which is considered reliable for HLA mapping. Moreover, reports described four-digit values ≥ 95% in unambiguous calls (42). Moreover, although six-digit resolution is not commonly determined through imputation; however, the values observed using this approach were ≥95%, which indicates robustness.

This methodology may be employed in HLA populations because of its versatility in the type of allele being studied; consequently, the study with 770 patients determined an important information about the Chinese population for HLA-A, -B, -C, -DPB1, -DQB1, and -DRB1. This finding can corroborate the existing frequency information, that is, the locus HLA-A frequency of allele A*24:02:01 at 0.164, which was similarly described in the Han population by Wang et al. (43). Alleles A*11:01:01 and A*02:01:01 are commonly found in China (43, 44) in the HLA-C locus; the allele C*01:02:01 is highly identified in the Chinese population, and is reported worldwide in HLA databases. The HLA-B locus was determined as the most polymorphic locus, considering its crucial role in immune system function through the presentation of diverse peptide antigens on the cell surface of $CD8^+$ T cells (45), providing genetic variability in the control of diseases. However, its variability makes transplantation search difficult for recipients and donors.

HLA class II showed a smaller number of polymorphisms where DPB1*05:01 was identified as more frequent in China (46); furthermore, studies confirm that this locus has a less polymorphic variation (47); additionally, the alleles DQB1*03:01:01 and DRB1*09:01:02 are highly reported in the Chinese population (48). Moreover, investigations on HLA-C polymorphisms across the entire gene and its flanking regions in the Chinese population have uncovered issues of significance for both clinical and evolutionary perspectives, making this allele the most

10.3389/fimmu.2025.1551173

TABLE 5 Rare allele frequency determined in HLA class II.

#	HLA-DPB1	%	HLA-DQB1	%	HLA-DRB1	%
1	DPB1*05:01:02	0.0893	DQB1*03:69	0.1786	DRB1*09:05	0.2679
2	DPB1*394:01	0.0893	DQB1*02:47	0.0893	DRB1*04:107	0.0893
3			DQB1*02:50	0.0893	DRB1*04:116	0.0893
4			DQB1*02:54	0.0893	DRB1*04:152	0.0893
5			DQB1*03:10:02	0.0893	DRB1*04:77	0.0893
6			DQB1*03:112	0.0893	DRB1*04:86	0.0893
7			DQB1*03:57	0.0893	DRB1*07:25	0.0893
8			DQB1*02:38	0.0893	DRB1*07:50	0.0893
9			DQB1*06:19:01	0.0893	DRB1*03:105	0.0893
10			DQB1*06:67	0.0893	DRB1*11:01:13	0.0893
11					DRB1*11:130	0.0893
12					DRB1*11:157	0.0893
13					DRB1*11:159	0.0893
14					DRB1*12:21	0.0893
15					DRB1*14:142	0.0893
16					DRB1*15:66:02	0.0893

TABLE 6 Advantages and limitations of MP-NGS, PCT-NGS, SBT, SSP, and SSOP.

Method	Advantage	Limitation
MP-NGS	• High resolution: it may identify alleles using exons and introns • Scalability: It may analyze multiple samples and genes simultaneously • New alleles detection: its high precision may describe new alleles not documented • Ambiguity reduction: it may determine complex haplotypes	• High initial cost of equipment • Experience in bioinformatic for the data analysis
PCT-NGS	• Low-quality DNA: Probe capture system can capture low-quality DNA targets • Long coverage: the system is designed to cover the most important regions of HLA loci	• Long time processing • High concentration of DNA • Pricessing costly per sample • High number of steps
SBT	• Precision: it may identify known alleles with high accuracy • It is high adopted in clinical laboratories	• Limited to specific regions (generally exons 2 and 3 in HLA class I) • Less capability identifying new alleles
SSP	• Rapid and easy: ideal for routine clinical applications • Low operating cost	• Low resolution: does not distinguish minimal differences between alleles • Limited to predefined alleles
SSOP	• High throughput: can analyze multiple samples simultaneously.	• Lower resolution: it cannot detect variations outside the designed probes • Cannot fully resolve phase ambiguities

polymorphic among rare alleles (49). However, further investigations are necessary to generate conclusions about HLA in the Chinese population; nevertheless, this methodology could be useful in this kind of research to provide additional information to the HLA database.

Standardization of depth of coverage is important to reduce analysis costs while still obtaining the necessary information for accurate HLA compatibility assessment. Moreover, minimizing the number of reaction mixtures per sample significantly decreases both time and cost, while the results demonstrated consistency despite the limited sample size in standardization and reliability analysis, and increasing the number of samples could yield additional insights. These six loci are the most useful when determining donor compatibility in kidney transplantation. While the initial validation was performed on a set of 70 random samples, which included both common and rare variants, the method was subsequently applied to a larger cohort of 770 individuals. Although no samples in this larger set were Sanger-sequenced due to logistical constraints, no novel alleles outside our primer coverage were observed. These results suggest that the method generalizes well to larger populations without introducing unanticipated issues. This MP-NGS opens the way for future

experiments to include other loci such as DQA and DPA to provide a better comprehensive donor–recipient HLA framework; moreover, this MP-NGS approach may provide information to identify new HLA alleles in the Chinese population and support broader validation across additional ethnic groups, providing sufficient read depth with lower cost, offering a reliable method in HLA genotyping experiments.

5 Conclusion

This study presents an optimized NGS-based multiplexing approach for HLA genotyping. Our HLA genotyping describes depths in the range of 100–1000× and, combined with strong agreement between MP-NGS, SBT, and PCT-NGS results, proves to be a reliable method in clinical, population, and evolutionary studies. Thus, our six-site multiplex PCR method is highly valuable in simplifying and reducing methodological costs. This six-site method offers phase-unambiguous genotyping data, even with a limited sample size, and has the potential to replace conventional methods for polymorphism discovery, paving the way for future studies in various HLA populations.

Data availability statement

The datasets generated for this study are not publicly available due to legal restrictions on data sharing imposed by the Chinese government. However, the data may be made available by the corresponding author upon reasonable request.

Author contributions

CH: Writing – original draft. BS: Methodology, Writing – review & editing. YFW: Investigation, Writing – review & editing. ZZ: Data curation, Writing – review & editing. CC: Validation, Writing – review & editing. YYZ: Conceptualization, Writing – review & editing. OA: Visualization, Writing – review & editing. HH: Formal analysis, Writing – review & editing. HL: Software, Writing – review & editing. TJ: Project administration, Writing – review & editing. XD: Resources, Writing – review & editing. YZ: Writing – review & editing, Supervision. YW: Funding acquisition, Writing – review & editing.

Funding

The author(s) declare that financial support was received for the research and/or publication of this article. This project was supported financially by the Collaborative Innovation Fund of Medicine and Education of Jiangsu University (JDY2023020), the Medical Science and Technology Innovation Project of Xuzhou Municipal Health Commission (XWKYHT20240005), the Xuzhou Medical University Affiliated Hospital Science and Technology Development Fund (XYFM202315), and the Clinical Medical Science and Technology Development Fund of Jiangsu University (JLY2021145 and JLY2021178).

Conflict of interest

Authors CC, HH, HL, and TJ were employed by the company AlloDx Shanghai Biotech Co, Ltd.

The remaining authors declare that the research was conducted in the absence of any commercial or financial relationships that could be construed as a potential conflict of interest.

Generative AI statement

The author(s) declare that no Generative AI was used in the creation of this manuscript.

Publisher's note

Supplementary material

The Supplementary Material for this article can be found online at: https://www.frontiersin.org/articles/10.3389/fimmu.2025.1551173/full#supplementary-material

References

1. Geng J, Raghavan M. Conformational sensing of major histocompatibility complex (MHC) class I molecules by immune receptors and intracellular assembly factors. *Curr Opin Immunol.* (2021) 70:67–74. doi: 10.1016/j.coi.2021.03.014

2. Gaykema LH, van Nieuwland RY, Lievers E, Moerkerk WBJ, de Klerk JA, Dumas SJ, et al. T-cell mediated immune rejection of beta-2-microglobulin knockout induced pluripotent stem cell-derived kidney organoids. *Stem Cells Transl Med.* (2024) 13:69–82. doi: 10.1093/stcltm/szad069

3. Matey-Hernandez ML, Brunak S, Izarzugaza JMG. Benchmarking the HLA typing performance of Polysolver and Optitype in 50 Danish parental trios. *BMC Bioinf.* (2018) 19:239. doi: 10.1186/s12859-018-2239-6

4. Ajith A, Mulloy LL, MdA M, Bravo-Egana V, Horuzsko DD, Gani I, et al. Humanized mouse model as a novel approach in the assessment of human allogeneic responses in organ transplantation. *Front Immunol.* (2021) 12:687715. doi: 10.3389/fimmu.2021.687715

5. Xin H, Li J, Sun H, Zhao N, Yao B, Zhong W, et al. Benchmarking of 5 algorithms for high-resolution genotyping of human leukocyte antigen class I genes from blood and tissue samples. *Ann Transl Med*. (2022) 10:633–3. doi: 10.21037/atm-22-875

6. Hogendorf A, Abel M, Wyka K, Bodalski J, Młynarski W. HLA-A gene variation modulates residual function of the pancreatic β-cells in children with type 1 diabetes. *Pediatr Endocrinol Diabetes Metab*. (2020) 26:73–8. doi: 10.5114/pedm.2020.95617

7. Liu C, Duffy BF, Weimer ET, Montgomery MC, Jennemann J-E, Hill R, et al. Performance of a multiplexed amplicon-based next-generation sequencing assay for HLA typing. *PloS One*. (2020) 15:e0232050. doi: 10.1371/journal.pone.0232050

8. Douillard V, Castelli EC, Mack SJ, Hollenbach JA, Gourraud P-A, Vince N, et al. Approaching genetics through the MHC lens: tools and methods for HLA research. *Front Genet*. (2021) 12:774916. doi: 10.3389/fgene.2021.774916

9. Weimer ET, Montgomery M, Petraroia R, Crawford J, Schmitz JL. Performance characteristics and validation of next-generation sequencing for human leucocyte antigen typing. *J Mol Diagnostics*. (2016) 18:668–75. doi: 10.1016/j.jmoldx.2016.03.009

10. Baek I-C, Choi E-J, Shin D-H, Kim H-J, Choi H, Kim T-G. Allele and haplotype frequencies of human leukocyte antigen-A, -B, -C, -DRB1, -DRB3/4/5, -DQA1, -DQB1, -DPA1, and -DPB1 by next generation sequencing-based typing in Koreans in South Korea. *PloS One*. (2021) 16:e0253619. doi: 10.1371/journal.pone.0253619

11. Erlich H. HLA DNA typing: Past, present, and future. *Tissue Antigens*. (2012) 80:1–11. doi: 10.1111/j.1399-0039.2012.01881.x

12. Lazaro A, Tu B, Yang R, Xiao Y, Kariyawasam K, Ng J, et al. "Human Leukocyte Antigen (HLA) Typing by DNA Sequencing," In: Zachary Andrea A, Leffell MS, editor. *Transplantation Immunology: Methods and Protocols* (2013), 161–95. doi: 10.1007/978-1-62703-493-7_9

13. Adams SD, Barracchini KC, Chen D, Robbins F, Wang L, Larsen P, et al. Ambiguous allele combinations in HLA Class I and Class II sequence-based typing: when precise nucleotide sequencing leads to imprecise allele identification. *J Transl Med*. (2004) 2:30. doi: 10.1186/1479-5876-2-30

14. Kishore A, Petrek M. Next-generation sequencing based HLA typing: deciphering immunogenetic aspects of sarcoidosis. *Front Genet*. (2018) 9:503. doi: 10.3389/fgene.2018.00503

15. Dunckley H. "HLA Typing by SSO and SSP Methods," In: Christiansen Frank T, Tait BD, editor. *Immunogenetics: Methods and Applications in Clinical Practice* (2012), 9–25. doi: 10.1007/978-1-61779-842-9_2

16. Li X-F, Zhang X, Chen Y, Zhang K-L, Liu X-J, Li J-P. An analysis of HLA-A, -B, and -DRB1 allele and haplotype frequencies of 21,918 residents living in liaoning, China. *PloS One*. (2014) 9:e93082. doi: 10.1371/journal.pone.0093082

17. Gabriel C, Stabentheiner S, Danzer M, Pröll J. What next? The next transit from biology to diagnostics: next generation sequencing for immunogenetics. *Transfusion Med Hemotherapy*. (2011) 38:308–17. doi: 10.1159/000332433

18. Hiho S, Bowman S, Hudson F, Sullivan L, Carroll R, Diviney M. Impact of assigning 2-field HLA alleles from real-time PCR on deceased donor assessments and conformance with high resolution alleles. *HLA*. (2023) 102:570–7. doi: 10.1111/tan.15083

19. Lai S-K, Luo AC, Chiu I-H, Chuang H-W, Chou T-H, Hung T-K, et al. A novel framework for human leukocyte antigen (HLA) genotyping using probe capture-based targeted next-generation sequencing and computational analysis. *Comput Struct Biotechnol J*. (2024) 23:1562–71. doi: 10.1016/j.csbj.2024.03.030

20. Yin Y, Lan JH, Nguyen D, Valenzuela N, Takemura P, Bolon Y-T, et al. Application of high-throughput next-generation sequencing for HLA typing on buccal extracted DNA: results from over 10,000 donor recruitment samples. *PloS One*. (2016) 11:e0165810. doi: 10.1371/journal.pone.0165810

21. Hosomichi K, Shiina T, Tajima A, Inoue I. The impact of next-generation sequencing technologies on HLA research. *J Hum Genet*. (2015) 60:665–73. doi: 10.1038/jhg.2015.102

22. Osoegawa K, Montero-Martín G, Mallempati KC, Bauer M, Milius RP, Maiers M, et al. Challenges for the standardized reporting of NGS HLA genotyping: Surveying gaps between clinical and research laboratories. *Hum Immunol*. (2021) 82:820–8. doi: 10.1016/j.humimm.2021.08.011

23. Xia L, Chen M, Zhang H, Zheng X, Bao J, Gao J, et al. Genome-wide association study of 7661 Chinese Han individuals and fine-mapping major histocompatibility complex identifies HLA-DRB1 as associated with IgA vasculitis. *J Clin Lab Anal*. (2022) 36:e24457. doi: 10.1002/jcla.24457

24. Dilthey AT, Mentzer AJ, Carapito R, Cutland C, Cereb N, Madhi SA, et al. HLA*LA—HLA typing from linearly projected graph alignments. *Bioinformatics*. (2019) 35:4394–6. doi: 10.1093/bioinformatics/btz235

25. Henegariu O, Heerema NA, Dlouhy SR, Vance GH, Vogt PH. Multiplex PCR: critical parameters and step-by-step protocol. *Biotechniques*. (1997) 23:504–11. doi: 10.2144/97233rr01

26. Perng CL, Chang LF, Chien WC, Lee TD, Chang JB. Effectiveness and limitations of resolving HLA class I and class II by heterozygous ambiguity resolving primers (HARPs)-a modified technique of sequence-based typing (SBT). *Clin Biochem*. (2012) 45:1471–8. doi: 10.1016/j.clinbiochem.2012.05.023

27. Jekarl DW, Lee GD, Bin YJ, JR K, Yu H, Yoo J, et al. -C, -DRB1 allele and haplotype frequencies of the Korean population and performance characteristics of HLA typing by next-generation sequencing. *HLA*. (2021) 97:188–97. doi: 10.1111/tan.14167

28. Nowak J, Mika-Witkowska R, Graczyk-Pol E. "Genetic Methods of HLA Typing," In: Witt Michal M, Dawidowska ST, editor. *Molecular Aspects of Hematologic Malignancies: Diagnostic Tools and Clinical Applications*. Berlin, Heidelberg: Springer Berlin Heidelberg (2012), 325–39. doi: 10.1007/978-3-642-29467-9_21

29. Broeckx BJG, Peelman L, Saunders JH, Deforce D, Clement L. Using variant databases for variant prioritization and to detect erroneous genotype-phenotype associations. *BMC Bioinf*. (2017) 18:535. doi: 10.1186/s12859-017-1951-y

30. Smith AG, Pereira S, Jaramillo A, Stoll ST, Khan FM, Berka N, et al. Comparison of sequence-specific oligonucleotide probe vs next generation sequencing for HLA-A, B, C, DRB1, DRB3/B4/B5, DQA1, DQB1, DPA1, and DPB1 typing: Toward single-pass high-resolution HLA typing in support of solid organ and hematopoietic cell transplant programs. *HLA*. (2019) 94:296–306. doi: 10.1111/tan.13619

31. Ozaki Y, Suzuki S, Kashiwase K, Shigenari A, Okudaira Y, Ito S, et al. Cost-efficient multiplex PCR for routine genotyping of up to nine classical HLA loci in a single analytical run of multiple samples by next generation sequencing. *BMC Genomics*. (2015) 16:318. doi: 10.1186/s12864-015-1514-4

32. He Y, Wang F, Wu Z, Zhang W, Zhu F. Establishment and application of a multiplex PCR NGS method for the genotyping of HLA-class I and HPA. *HLA*. (2024) 104:e15716. doi: 10.1111/tan.15716

33. Su-Qing G, Zhan-Rou Q, Yan-Ping Z, Hao C, Liu-Mei H, Hong-Yan Z, et al. The polymorphism analysis of HLA class II alleles based on next-generation sequencing and prevention strategy for allele dropout. *Zhongguo Shi Yan Xue Ye Xue Za Zhi*. (2024) 32:2024–56. doi: 10.19746/j.cnki.issn1009-2137.2024.02.042

34. Wu R, Li H, Peng D, Li R, Zhang Y, Hao B, et al. Revisiting the potential power of human leukocyte antigen (HLA) genes on relationship testing by massively parallel sequencing-based HLA typing in an extended family. *J Hum Genet*. (2019) 64:29–38. doi: 10.1038/s10038-018-0521-0

35. Erlich RL, Jia X, Anderson S, Banks E, Gao X, Carrington M, et al. Next-generation sequencing for HLA typing of class I loci. *BMC Genomics*. (2011) 12:42. doi: 10.1186/1471-2164-12-42

36. Baek I, Choi E, Kim H, Choi H, Kim T. Distributions of 11-loci HLA alleles typed by amplicon-based next-generation sequencing in South Koreans. *HLA*. (2023) 101:613–22. doi: 10.1111/tan.14981

37. Ehrenberg PK, Geretz A, Baldwin KM, Apps R, Polonis VR, Robb ML, et al. High-throughput multiplex HLA genotyping by next-generation sequencing using multi-locus individual tagging. *BMC Genomics*. (2014) 15:864. doi: 10.1186/1471-2164-15-864

38. Mosbruger TL, Dinou A, Duke JL, Ferriola D, Mehler H, Pagkrati I, et al. Utilizing nanopore sequencing technology for the rapid and comprehensive characterization of eleven HLA loci; addressing the need for deceased donor expedited HLA typing. *Hum Immunol*. (2020) 81:413–22. doi: 10.1016/j.humimm.2020.06.004

39. Szolek A, Schubert B, Mohr C, Sturm M, Feldhahn M, Kohlbacher O. OptiType: precision HLA typing from next-generation sequencing data. *Bioinformatics*. (2014) 30:3310–6. doi: 10.1093/bioinformatics/btu548

40. Zheng GXY, Terry JM, Belgrader P, Ryvkin P, Bent ZW, Wilson R, et al. Massively parallel digital transcriptional profiling of single cells. *Nat Commun*. (2017) 8:14049. doi: 10.1038/ncomms14049

41. Kong D, Lee N, Dela Cruz ID, Dames C, Maruthamuthu S, Golden T, et al. Concurrent typing of over 4000 samples by long-range PCR amplicon-based NGS and rSSO revealed the need to verify NGS typing for HLA allelic dropouts. *Hum Immunol*. (2021) 82:581–7. doi: 10.1016/j.humimm.2021.04.008

42. Zheng X, Shen J, Cox C, Wakefield JC, Ehm MG, Nelson MR, et al. HIBAG—HLA genotype imputation with attribute bagging. *Pharmacogenomics J*. (2014) 14:192–200. doi: 10.1038/tpj.2013.18

43. Wang F, Dong L, Wang W, Chen N, Zhang W, He J, et al. The polymorphism of HLA-A, -C, -B, -DRB3/4/5, -DRB1, -DQB1 loci in Zhejiang Han population, China using NGS technology. *Int J Immunogenet*. (2021) 48:485–9. doi: 10.1111/iji.12554

44. Hong W, Fu Y, Chen S, Wang F, Ren X, Xu A. Distributions of HLA class I alleles and haplotypes in Northern Han Chinese. *Tissue Antigens*. (2005) 66:297–304. doi: 10.1111/j.1399-0039.2005.00474.x

45. Olson E, Geng J, Raghavan M. Polymorphisms of HLA-B: influences on assembly and immunity. *Curr Opin Immunol*. (2020) 64:137–45. doi: 10.1016/j.coi.2020.05.008

46. Wu X-M, Wang C, Zhang K-N, Lin A-Y, Kira J, Hu G-Z, et al. Association of susceptibility to multiple sclerosis in Southern Han Chinese with HLA-DRB1, -DPB1 alleles and DRB1-DPB1 haplotypes: distinct from other populations. *Multiple Sclerosis J*. (2009) 15:1422–30. doi: 10.1177/1352458509345905

47. Jawdat D, Uyar FA, Alaskar A, Müller CR, Hajeer A. HLA-A, -B, -C, -DRB1, -DQB1, and -DPB1 allele and haplotype frequencies of 28,927 saudi stem cell donors typed by next-generation sequencing. *Front Immunol*. (2020) 11:544768. doi: 10.3389/fimmu.2020.544768

48. Hu W, Tang L, Wang J, Wang B, Li S, Yu H, et al. Polymorphism of HLA-DRB1, -DQB1 and -DPB1 genes in Bai ethnic group in southwestern China. *Tissue Antigens*. (2008) 72:474–7. doi: 10.1111/j.1399-0039.2008.01120.x

49. Xu Y, Deng Z, O'hUigin C, Wang D, Gao S, Zeng J, et al. Characterization and polymorphic analysis of 4.5 kb genomic full-length HLA-C in the Chinese Han population. *Tissue Antigens*. (2011) 78:102–14. doi: 10.1111/j.1399-0039.2011.01710.x

frontiers | Frontiers in Immunology

TYPE Opinion
PUBLISHED 03 July 2025
DOI 10.3389/fimmu.2025.1621252

OPEN ACCESS

EDITED BY
Luigi Nespoli,
University of Insubria, Italy

REVIEWED BY
Qingxiao Song,
Xinqiao Hospital, China
Everett Meyer,
Stanford University, United States

*CORRESPONDENCE
Annamaria Pasi
a.pasi@smatteo.pv.it

†These authors have contributed equally to this work

RECEIVED 30 April 2025
ACCEPTED 17 June 2025
PUBLISHED 03 July 2025

CITATION
Pasi A, Prezioso CT, Comoli P, Sbarsi I, Cacciatore R, Giorgiani G, Recupero S, Bergamaschi P, Torchio M, Taurino A, Losi G, Zerbi C, Bianchessi A, Defrancesco I, Polverelli N, Zecca M and Perotti CG (2025) Recipient-specific antibodies in HSCT: current knowledge and future perspectives. *Front. Immunol.* 16:1621252. doi: 10.3389/fimmu.2025.1621252

Recipient-specific antibodies in HSCT: current knowledge and future perspectives

Annamaria Pasi[1*†], Carmen Tania Prezioso[1†], Patrizia Comoli[2,3], Ilaria Sbarsi[1], Rosalia Cacciatore[1], Giovanna Giorgiani[2], Santina Recupero[2], Paola Bergamaschi[1], Margherita Torchio[1], Alessia Taurino[4], Giulia Losi[4], Caterina Zerbi[4], Antonio Bianchessi[4], Irene Defrancesco[4], Nicola Polverelli[4], Marco Zecca[2] and Cesare Giuseppe Perotti[1]

[1]Immunohematology and Transfusion Service, Fondazione IRCCS Policlinico San Matteo, Pavia, Italy, [2]Pediatric Hematology and Oncology, Fondazione IRCCS Policlinico San Matteo, Pavia, Italy, [3]Cell Factory and Pediatric Hematology/Oncology Unit, Department of Mother and Child Health, Fondazione IRCCS Policlinico San Matteo, Pavia, Italy, [4]Division of Hematology, Fondazione IRCCS Policlinico San Matteo, Pavia, Italy

KEYWORDS

hematopoietic stem cell transplantation, recipient-specific HLA antibodies, donor-specific anti-HLA antibodies, alloantigen-induced immune responses, complement-mediated endothelial injury, haploidentical stem cell transplantation, transplant immunology

1 Introduction

Allogeneic hematopoietic stem cell transplantation (HSCT) has significantly advanced the treatment of numerous hematological disorders. Advances in haploidentical transplantation have broadened access to this life-saving therapy, even for patients lacking fully matched donors (1–4). In this context, the role of donor-specific anti-HLA antibodies (DSA) in graft failure and delayed engraftment is well established, to the extent that pre-transplant screening for DSA has become standard practice in many centers (5–7). Conversely, considerably less attention has been devoted to another humoral immune factor: recipient-specific antibodies (RSA). Screening for DSA prior to transplantation—particularly those capable of complement fixation—is now standard practice and often guides interventions such as plasma exchange, administration of rituximab, and intensified immunosuppressive therapy in patients deemed at high immunological risk (8, 9). These practices underscore the clinical relevance of antibody-mediated complications in HSCT and offer a conceptual framework for evaluating the potential impact of RSA as well.

2 Clinical impact of Recipient-Specific Antibodies (RSAs)

2.1 Mechanisms of RSA-mediated damage

Recipient-specific antibodies (RSA) are antibodies present in the donor that recognize the recipient's HLA antigens. Their development is often associated with previous allo-sensitization events, such as pregnancy in multiparous female donors, blood transfusions, or previous transplants (10). Once transferred during HSCT, RSAs can bind to recipient tissues, activate complement, and contribute to endothelial injury and inflammatory responses. Mechanistically, RSAs could act similarly to DSAs by triggering antibody-dependent cellular cytotoxicity (ADCC) or complement-dependent cytotoxicity (CDC), resulting in endothelial cell activation, loss of vascular integrity, and the creation of a pro-inflammatory microenvironment (11–13).

2.2 Clinical evidence and potential implications

Although the clinical relevance of RSAs is not as well established as that of DSAs, emerging evidence suggests they may play a non-negligible role in immune modulation after transplantation. Delbos et al. (14) reported an increased incidence of acute and chronic GVHD in recipients of transplants from donors harboring class II anti-HLA antibodies. Sadowska-Klasa et al. (15) hypothesized that RSAs may mediate endothelial activation via complement pathways, contributing to complications such as veno-occlusive disease (VOD) and transplant-associated thrombotic microangiopathy (TA-TMA). Post-transplant complications, such as engraftment syndrome (ES), cytokine release syndrome (CRS) in haploidentical transplantation with cyclophosphamide-based GVHD prophylaxis, cardiotoxicity, TA-TMA, and veno-occlusive disease/sinusoidal obstruction syndrome (VOD/SOS), share a common pathogenic mechanism centered on endothelial injury. This injury originates from a subclinical baseline condition, which is exacerbated by pro-inflammatory and pro-thrombotic events, including cytokine release (e.g., TNF-α, IL-6), complement cascade activation, reduced nitric oxide (NO) bioavailability, and elevated levels of angiopoietin-2, von Willebrand factor (vWF), and high mobility group box 1, potentially resulting in multiorgan failure (16–18). To date, TA-TMA remains the only syndrome with a clearly demonstrated association with recipient-specific antibodies (RSA) (15), as RSA may activate complement and directly damage the endothelium. Although direct evidence linking RSA to other endothelial complications is currently lacking, their shared endothelial pathophysiology supports the hypothesis that RSA could similarly contribute to these syndromes, warranting further targeted research. Additionally, Ciurea et al. described a haploidentical transplantation case in which RSA transfer was associated with early endothelial injury and adverse outcomes (19).

This relative omission in clinical practice may stem from various factors: the perception of low RSA levels, the lack of routine testing on donor samples, or the hypothesis that their impact might be less significant compared to that of DSAs. Recent reviews (20) have mainly emphasized the need to start considering the potential clinical role of RSAs and to investigate possible management parallels with DSAs, as current evidence is still too limited to draw definitive conclusions.

2.3 Immunologic modulation and RSA pathogenicity

One possibility is that RSAs contribute to the creation of a pro-inflammatory environment in the period immediately following transplantation, amplifying tissue damage triggered by conditioning regimens or subclinical allogeneic reactivity. In particular, RSAs capable of binding complement may have greater pathogenic potential, suggesting the use of functional assays, such as the C1q binding test, to identify clinically relevant cases. RSAs could thus act more as immunological "modulators" rather than direct barriers to engraftment, influencing the threshold for the development of GVHD, endothelial dysfunction, or chronic graft failure.

2.4 NIMA tolerance and maternal alloimmunization: a dual immunological legacy in haploidentical transplantation

In haploidentical transplantation, the mismatched donor haplotypes are referred to as non-inherited maternal antigens (NIMA) or non-inherited paternal antigens (NIPA). Due to fetal exposure to maternal HLA antigens during pregnancy, which may induce partial immunological tolerance, grafts from NIMA-mismatched donors are generally considered less immunogenic than those from NIPA-mismatched donors. Accordingly, several studies have demonstrated that NIMA-mismatched haplo-HSCT is associated with a significantly lower incidence of acute graft-versus-host disease (aGVHD) compared to NIPA-mismatched transplants. Although this evidence supports a tolerogenic effect induced during gestation, it is important to note that a substantial proportion of pregnant women develop HLA antibodies against paternal antigens. The mother encounters inherited paternal antigens (IPA) during adulthood, when her immune system is fully mature and immunocompetent. During pregnancy, she has approximately a 50% probability of mounting both humoral and cellular immune responses against the IPA haplotype.

In this context, the development of recipient-specific antibodies (RSAs) in multiparous mothers against the child's IPA haplotype may adversely affect transplant outcomes, potentially negating the immunological advantage often attributed to maternal donors (21–23) (Figure 1). Future studies could be useful to clarify the interplay between NIMA-induced tolerance and maternal RSA formation against paternal antigens, and how these mechanisms impact donor selection and post-transplant outcomes (Figure 1).

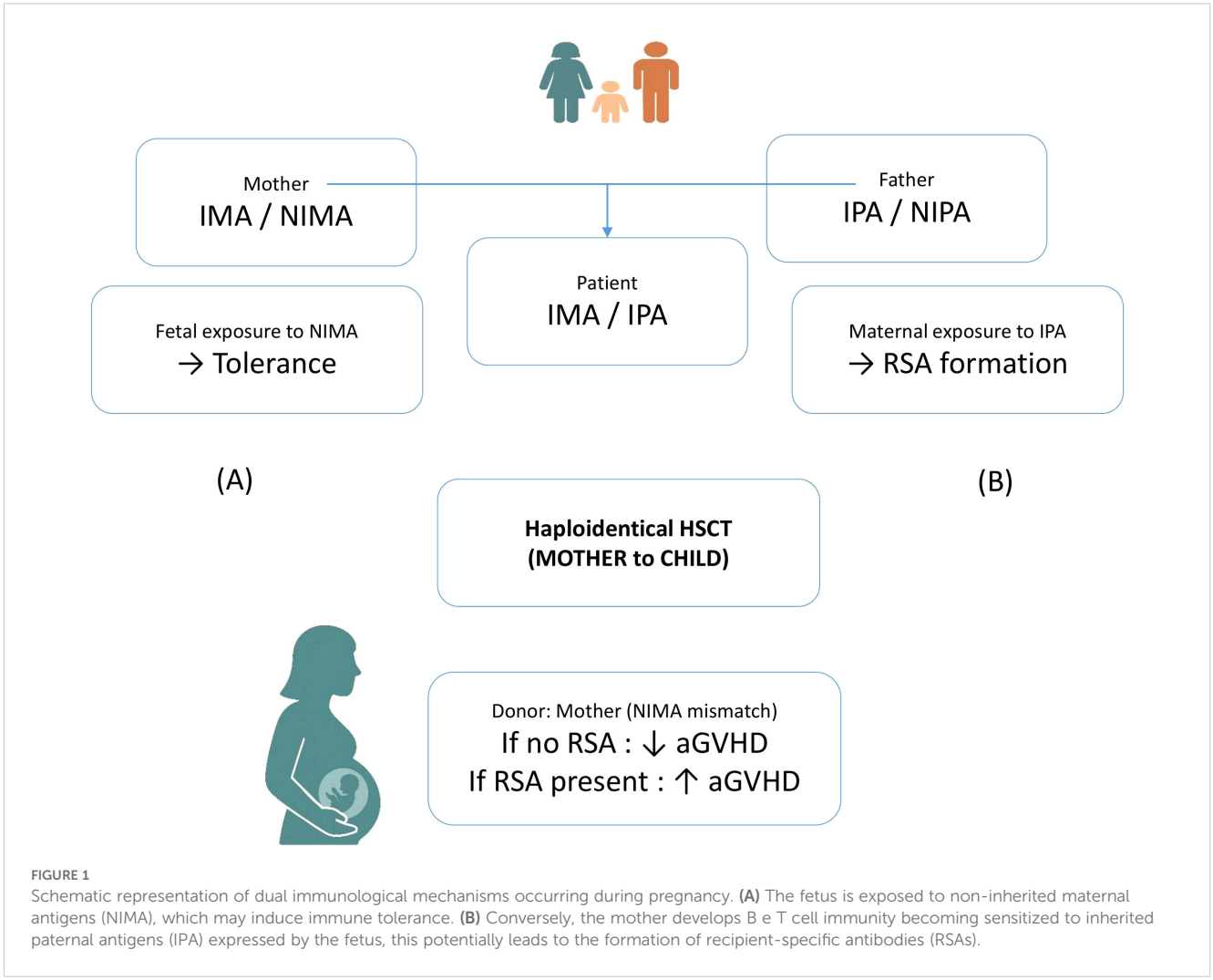

FIGURE 1
Schematic representation of dual immunological mechanisms occurring during pregnancy. **(A)** The fetus is exposed to non-inherited maternal antigens (NIMA), which may induce immune tolerance. **(B)** Conversely, the mother develops B e T cell immunity becoming sensitized to inherited paternal antigens (IPA) expressed by the fetus, this potentially leads to the formation of recipient-specific antibodies (RSAs).

2.5 Gender and reproductive history as risk factors

Gender-related and reproductive history–related immunologic sensitization is therefore a critical area that warrants further investigation. Should the clinical relevance of RSAs be confirmed, integrating targeted clinical strategies to mitigate the effects of prior sensitization could prove useful and might lead to modifications in current donor screening protocols and risk management approaches.

2.6 Technological advances in RSA detection

Defining clinically significant thresholds for RSAs would be crucial to standardizing diagnostic and therapeutic protocols at an international level, potentially promoting greater uniformity in the management of patients undergoing HSCT from haploidentical or partially matched donors (24).

Luminex technology has represented a significant methodological advance, enabling precise identification and quantification of RSAs thanks to its high sensitivity and specificity (25, 26). It has greatly facilitated the investigation of correlations between the presence and intensity of RSAs (measured by MFI) and post-transplant clinical outcomes. Although no validated thresholds currently exist for RSA interpretation, mean fluorescence intensity (MFI) values commonly used for DSA, typically >1,000 to indicate low-level sensitization and >5,000 for antibodies with clinical relevance, could serve as a preliminary reference. These values are supported by EBMT consensus guidelines (6). Aligning RSA interpretation with established DSA criteria may support more consistent risk assessment and guide future standardization efforts. Complement-binding functional assays, such as the C1q binding test, provide additional valuable information on the pathogenic potential of these antibodies.

2.7 Future perspectives on RSA screening and management

From a clinical perspective, the selective integration of RSA screening could represent a rational strategy. It could be especially considered for donors with a history of multiple pregnancies, and possibly for those with prior transfusion events, in whom the

identification of significant RSAs might guide targeted therapeutic choices or influence donor selection.

However, the lack of large prospective studies makes it difficult to draw definitive conclusions about the clinical need for RSA screening. Prospective multicenter studies with harmonized methodologies and functional characterization of RSAs would be useful to assess whether integrating RSA screening into clinical practice is appropriate. In parallel, the development of therapeutic strategies to mitigate the effects of pathogenic RSAs—such as plasmapheresis, immunoadsorption, or complement inhibition—could offer new therapeutic options.

3 Discussion

In conclusion, recipient-specific antibodies represent a fascinating yet still underexplored aspect of transplant immunology. Preliminary evidence suggests that they may contribute to shaping the immune environment after HSCT, influencing the risk of GVHD, endothelial injury, and long-term transplant success. In contrast to donor-specific antibodies (DSAs), which are more clearly associated with graft rejection and engraftment failure, RSAs may play a distinct pathogenic role, particularly in the context of GVHD and immune modulation. Recognizing these differences could help to refine risk stratification and to outline new strategies for donor evaluation. RSAs should be considered as a potential piece of the complex mosaic of immune reactivity in HSCT. As research in this field progresses, integrating RSAs into a broader vision of transplant immunology could, in our opinion, broaden horizons for improving clinical outcomes.

Author contributions

AP: Conceptualization, Writing – original draft. CTP: Conceptualization, Writing – original draft. PC: Writing – review & editing, Supervision. IS: Supervision, Writing – review & editing. RC: Writing – review & editing, Visualization. GG: Writing – review & editing. SR: Writing – review & editing. PB: Writing – review & editing, Visualization. MT: Writing – review & editing, Supervision. AT: Writing – review & editing. GL: Writing – review & editing. CZ: Writing – review & editing. AB: Writing – review & editing. ID: Writing – review & editing. NP: Writing – review & editing, Supervision. MZ: Writing – review & editing. CGP: Writing – review & editing, Supervision.

Funding

The author(s) declare that financial support was received for the research and/or publication of this article. The publication costs of this article were supported by institutional current research funds from the Italian Ministry of Health.

Conflict of interest

The authors declare that the research was conducted in the absence of any commercial or financial relationships that could be construed as a potential conflict of interest.

Generative AI statement

The author(s) declare that no Generative AI was used in the creation of this manuscript.

Publisher's note

References

1. Passweg JR, Baldomero H, Bader P, Bonini C, Duarte RF, Dufour C, et al. Use of haploidentical stem cell transplantation continues to increase: the 2015 European Society for Blood and Marrow Transplant activity survey report. *Bone Marrow Transplant*. (2017) 52:811–7. doi: 10.1038/bmt.2017.34

2. Fuchs EJ. Haploidentical transplantation for hematologic Malignancies: where do we stand? *Hematol Am Soc Hematol Educ Program*. (2012) 2012:230–6. doi: 10.1182/asheducation-2012.1.230

3. Kongtim P, Ciurea SO. Who is the best donor for haploidentical stem cell transplantation? *Semin Hematol*. (2019) 56:194–200. doi: 10.1053/j.seminhematol.2018.08.003

4. Chang YJ, Luznik L, Fuchs EJ, Huang XJ. How do we choose the best donor for T-cell-replete, HLA-haploidentical transplantation? *J Hematol Oncol*. (2016) 9:35. doi: 10.1186/s13045-016-0265-2

5. Gladstone DE, Bettinotti MP. HLA donor-specific antibodies in allogeneic hematopoietic stem cell transplantation: challenges and opportunities. *Hematol Am Soc Hematol Educ Program*. (2017) 2017:645–50. doi: 10.1182/asheducation-2017.1.645

6. Ciurea SO, Cao K, Fernandez-Vina M, Kongtim P, Al Malki M, Fuchs E, et al. The european society for blood and marrow transplantation (EBMT) consensus guidelines for the detection and treatment of donor-specific anti-HLA antibodies (DSA) in haploidentical hematopoietic cell transplantation. *Bone Marrow Transplant*. (2018) 53:521–30. doi: 10.1038/s41409-017-0062-8

7. Gladstone DE, Zachary AA, Fuchs EJ, Luznik L, Kasamon YL, King KE, et al. Partially mismatched transplantation and human leukocyte antigen donor-specific antibodies. *Biol Blood Marrow Transplant*. (2013) 19:647–52. doi: 10.1016/j.bbmt.2013.01.016

8. File B, Huang Y, Peedin A, Gergis U. The impact of HLA donor-specific antibodies on engraftment and the evolving desensitization strategies. *Bone Marrow Transplant*. (2022) 57:526–31. doi: 10.1038/s41409-022-01578-w

9. Zhang R, He Y, Yang D, Jiang E, Ma Q, Pang A, et al. Combination treatment of rituximab and donor platelets infusion to reduce donor-specific anti-HLA antibodies for stem cells engraftment in haploidentical transplantation. *J Clin Lab Anal*. (2020) 34:e23261. doi: 10.1002/jcla.23261

10. McCaughan J, Xu Q, Tinckam K. Detecting donor-specific antibodies: the importance of sorting the wheat from the chaff. *Hepatobiliary Surg Nutr*. (2019) 8:37–52. doi: 10.21037/hbsn.2019.01.01

11. Ciurea SO, Thall PF, Milton DR, Barnes TH, Kongtim P, Carmazzi Y, et al. Complement-binding donor-specific anti-HLA antibodies and risk of primary graft

failure in hematopoietic stem cell transplantation. *Biol Blood Marrow Transplant*. (2015) 21:1392–8. doi: 10.1016/j.bbmt.2015.05.001

12. Picascia A, Grimaldi V, Napoli C. From HLA typing to anti-HLA antibody detection and beyond: The road ahead. *Transplant Rev (Orlando)*. (2016) 30:187–94. doi: 10.1016/j.trre.2016.07.007

13. Morin-Zorman S, Loiseau P, Taupin JL, Caillat-Zucman S. Donor-specific anti-HLA antibodies in allogeneic hematopoietic stem cell transplantation. *Front Immunol*. (2016) 7:307. doi: 10.3389/fimmu.2016.00307

14. Delbos F, Barhoumi W, Cabanne L, Beckerich F, Robin C, Redjoul R, et al. Donor immunization against human leukocyte class II antigens is a risk factor for graft-versus-host disease. *Biol Blood Marrow Transplant*. (2016) 22:292–9. doi: 10.1016/j.bbmt.2015.09.027

15. Sadowska-Klasa A, Dukat-Mazurek A, Zielińska H, Dębska-Zielkowska J, Piekarska A, Moszkowska G, et al. Incidence and role of recipient-specific antibodies in allogeneic hematopoietic cell transplantation from mismatched related donors. *Transplant Cell Ther*. (2024) 30:99.e1–99.e10. doi: 10.1016/j.jtct.2023.10.015

16. Milone G, Bellofiore C, Leotta S, Milone GA, Cupri A, Duminuco A, et al. Endothelial dysfunction after hematopoietic stem cell transplantation: a review based on physiopathology. *J Clin Med*. (2022) 11:623. doi: 10.3390/jcm11030623

17. Hildebrandt GC, Chao N. Endothelial cell function and endothelial-related disorders following hematopoietic cell transplantation. *Br J Hematol*. (2020) 190:508–19. doi: 10.1111/bjh.16621

18. Baumeister SHC, Mohan GS, Elhaddad A, Lehmann L. Cytokine release syndrome and associated acute toxicities in pediatric patients undergoing immune effector cell therapy or hematopoietic cell transplantation. *Front Oncol*. (2022) 12:841117. doi: 10.3389/fonc.2022.841117

19. Ciurea SO, Cao K, Zou J. Donor-specific anti-HLA antibodies and … recipient-specific anti-HLA antibodies? The conundrum on pregnancy in transplantation. *Am J Hematol*. (2020) 95:E112–4. doi: 10.1002/ajh.25762

20. Little AM. HLA antibodies in hematopoietic stem cell transplantation. *HLA*. (2019) 94:21–4. doi: 10.1111/tan.13741

21. van Rood JJ, Roelen DL, Claas FHJ. The effect of noninherited maternal antigens in allogeneic transplantation. *Semin Hematol*. (2005) 42:104–11. doi: 10.1053/j.seminhematol.2005.01.008

22. van Rood JJ, Loberiza FR Jr, Zhang MJ, Oudshoorn M, Claas FH, Cairo MS, et al. Effect of tolerance to noninherited maternal antigens on the occurrence of graft-versus-host disease after bone marrow transplantation from a parent or an HLA-haploidentical sibling. *Blood*. (2002) 99:1572–7. doi: 10.1182/blood.V99.5.1572

23. Bracamonte-Baran W, Burlingham W. Non-inherited maternal antigens, pregnancy, and allotolerance. *BioMed J*. (2015) 38:39–51. doi: 10.4103/2319-4170.143498

24. Kiernan JJ, Ellison CA, Tinckam KJ. Measuring alloantibodies: a matter of quantity and quality. *Curr Opin Organ Transplant*. (2019) 24:20–30. doi: 10.1097/MOT.0000000000000593

25. Ellis TM. Interpretation of HLA single antigen bead assays. *Transplant Rev (Orlando)*. (2013) 27:108–11. doi: 10.1016/j.trre.2013.07.001

26. Taniguchi K, Yoshihara S, Maruya E, Ikegame K, Kaida K, Hayashi K, et al. Donor-derived HLA antibody production in patients undergoing SCT from HLA antibody-positive donors. *Bone Marrow Transplant*. (2012) 47:1338–42. doi: 10.1038/bmt.2012.28

Frontiers in Immunology

Explores novel approaches and diagnoses to treat immune disorders.

The official journal of the International Union of Immunological Societies (IUIS) and the most cited in its field, leading the way for research across basic, translational and clinical immunology.

Discover the latest Research Topics

See more →

Frontiers

Avenue du Tribunal-Fédéral 34
1005 Lausanne, Switzerland
frontiersin.org

Contact us

+41 (0)21 510 17 00
frontiersin.org/about/contact